Structural Modelling of Suspension Bridges with Particular Reference to the Humber Bridge.

A thesis submitted for the degree of Doctor of Philosophy

by

R Karuna

B.Sc. (Hon), M.Sc.

Department of Mechanical Engineering, Brunel University
Uxbridge, UB8 3PH, UK.

April 2002

Abstract

The purpose of this research was to investigate the parameters that influence the structural behaviour of a specific suspension bridge, The Humber Bridge.

Three finite element computer models of increasing complexity were created for the analyses. They were validated against field measurements for both static and dynamic loading, and good correlation was obtained.

The programs were used to

a) assess the integrity of the bridge as a whole were there failures of certain individual elements, such as a hanger failing under vehicle impact;

b) determine the influence of the sizing of individual components, such as deck plate thickness or main cable diameter, on overall behaviour;

c) ascertain the capability of the structure to cope with loading (traffic, wind or thermal), above the original design values; and

d) consider the performance of the bridge had other configurations of hangers been adopted in the original design.

From the results of this work, recommendations are made which could influence the future design of long-span suspension bridges.

Acknowledgements

It gives me great pleasure to express my deepest gratitude to C. J Brown and Professor A. Yettram for their guidance, suggestions, help and encouragement throughout this work.

I am grateful to Dr M. S. Yao for arranging this project with the Humber Bridge Board and his supervision in its initial stages.

I am particularly grateful to R. Evans, Bridgemaster and Engineer, Humber Bridge Board for his financial assistance, providing technical information, encouragement and support throughout this project.

I like to thank the Head of the Mechanical Engineering Department, Professor N. Ladommatos for financial assistance and the provision of supporting resources.

I like to give my gratitude to D. Binns, Dr S. Luke, S. Godman and especially to Dr J. Hodgson, Mouchel Consulting Ltd. for their friendly advice, discussion, encouragement and patience throughout this work.

I would also like to thank to my wife, Siva, for her support and devotion, and my sons, Varshan and Logan, throughout the writing. Last, but not least, I want to thank to my father, in-laws, brothers and sister who have always been supportive to my endeavours. Finally I have devoted this thesis to my late mother Sakundala Deavi.

CONTENTS

Chapter 1

Introduction

This research was sponsored by both the Humber Bridge Board and the Department of Mechanical Engineering at Brunel University. The Humber Bridge Board is responsible for the operational safety of the Humber Bridge on which the research was undertaken. The Bridge Board staff inspect and maintain the bridge either directly or by using contractors or consultants.

The original design calculations are used as a maintenance tool but, having been prepared at a time when computer-based design was in its infancy, they consist mainly of hand calculations. Consequently they can be unwieldy to use, are of limited value for investigating the consequences of revised Highway Loading Standards and are not suitable for assessing the effects either of unforeseen service loads or of structural damage. For example, removal of a component (a hanger bracket connection) due to an accident might take a long calculation time to reassess the structure under the worst loading scenario. Similarly the structure has to be assessed due to increasing traffic intensity over the period of time. It would take a long time to understand the previous design calculations and to replace with the newly found loading values.

To overcome these issues a Finite Element (FE) approach was used with available computer capacity for the calculations. Finite element computer models can now be prepared at reasonable cost, run efficiently on a PC and are relatively user-friendly. Such a model will facilitate rapid structural appraisal after accidents, allow investigation of various "what if" scenarios and assist with decisions regarding traffic management in unusual circumstances, as well as being an important maintenance tool. Carrying out numerical modelling will provide an enhanced management tool for the existing system and enable the Humber Bridge Board to determine the effects of accidental loading and allow them to plan for other events at various locations along the bridge. Due to the increasing traffic situation, from time to time the Humber Bridge Board has to reassess its traffic loading. This research enables them to assess the bridge structural components against the new loading values.

The Bridge operator currently uses the FE models developed as part of this research to understand the effect of modified or updated bridge loading. Each model has been validated against field measurements under static and dynamic conditions.

The following sets of test results were used to validated the models;

1) Displacement measurements for the passage of single lorry load and free vibration measurements carried out by Bristol University and the Humber Bridge Board (Brownjohn, 1986 & 1994).
2) GPS (Global Positioning System) monitoring (displacement) system with passage of five 32 tonnes lorry loads carried out by Brunel University, Nottingham University and the Humber Bridge Board (Brown, 1999).

Good correlation was obtained under static and dynamic conditions between measured and model predicted values. This gave confidence to the authority to rely on models especially under maintenance work. Replacements of hangers without requiring expensive and obtrusive traffic management and resurfacing on the deck and lane closure with appropriate traffic management are good examples.

Sensitivity analyses on suspension bridge components were performed. These will enable the components to be graded according to their sensitiveness. For example this grading process will help the suspension bridge designer and finite element analyst at the early design stage to give higher concentration on particular components and their parameters. Also it would give an indication to the maintenance team about the important sensitive structural components. In addition, this form of analysis will give an early indication of structural behaviour due to deterioration of particular components.

Hanger force variation under uniformly distributed and point load (at various locations) conditions of the Humber Bridge (existing system) was analysed. Extreme hanger force changes between adjacent hangers on the existing system lead to the introduction of other hanger systems. A number of alternative hanger systems such as vertical, vertical with inclined and, inclined with horizontal link were suggested and analysed. Hanger force variation and natural frequency values of these system were compared with the existing Humber Bridge system. Out of these systems considered, a feasible solution was suggested in terms of hanger force changes and lesser closure period of the bridge.

Chapter 2

Purpose and Outline of the Thesis

General

This research has been carried out to develop our understanding of the load carrying behaviour of cable suspended long span suspension bridges. This understanding has been utilised in the production of numerical models and advice notes for the Humber Bridge Board to assist them in their maintenance and traffic management activities. These models have been validated against field measurements under dead, static and dynamic loading conditions. Models have also been used to assess the structure after possible future accidents. This is a user-friendly tool for maintenance purposes for the Humber Bridge Board. Using this model a study has been performed to identify the degree of sensitivity of each component of the bridge under the self-weight condition. A parametric study has been performed to understand the structural behaviour with the introduction of different hanger system patterns. Finite element modelling, validation, analysis, identification of sensitive components of the bridge and, advantages and disadvantages of the hanger system styles are described chapter by chapter.

Outline of the Thesis

Chapter 1 briefly describes the purpose of the sponsorship from the Humber Bridge Board.

Chapter 2 describes the purpose of the thesis and gives a brief description of each chapter.

Chapter 3 describes the historical development of suspension bridges and also gives a comparison between cable stayed and suspension bridges.

Chapter 4 gives the basic theory behind the design of suspension bridges.

Chapter 5 describes the structural components and dimensions of the Humber Bridge and its maximum design load requirements.

Chapter 6 describes briefly the finite element method and also describes different types of analysis such as linear and non-linear analysis (with stress stiffening and large deformation effects), application of initial strain to the cables and the dynamic analysis adapted to this research work.

Chapter 7 describes the type of elements used for the 2-D and the 3-D modelling of the Humber Bridge. In addition to that it describes the modelling technique of the structural components and the boundary conditions of the bridge. This chapter also describes the needs for the use of different types of models and their advantages and disadvantages.

Chapter 8 describes a sensitivity study on structural components of the Humber Bridge model. Structural components have been graded according to their influence.

Chapter 9 describes the validation of the models under static and dynamic load conditions against field measurements. Also a comparison was done with the created models under dead load condition with the Humber Bridge designers' analysis results.

Chapter 10 describes the usage of the created models. Structural behaviour under different critical design loading and newly assessed Bridge Specific Assessment Live Loading are discussed. Some load cases are also created to obtain the maximum tensile and compressive forces of the A-Frames to be compared with the design values. In addition to the above, structural behaviour has been analysed for a selections of possible "what if" scenarios.

Chapter 11 describes the advantages and disadvantages of different hanger system patterns with respect to the hanger force fluctuation under uniformly distributed load and moving point load conditions. Also it describes a comparison of these models under dynamic loading conditions.

Chapter 12 gives some conclusions to the research work and points to possible future investigations.

Chapter 3

1) Historical Introduction

Introduction to cable assisted bridges

General

The idea of a slab bridge might have developed from a tree (Pugsley, 1958) fallen across a chasm or a creek. Similarly the idea of piers might have developed from rocks jutting out of shallow streams, which were used as abutment stones. As the depth of the water rose during the rainy season larger rocks were needed to serve as abutment stones. When people realized that walking was more convenient than hopping from abutment stone to abutment stone or abutment stone to pier stone for individuals and cattle, they created the slab. Slabs of stone were laid across the abutment stone to pier stone and then emerged as a multiple-span bridge. This development was associated with the growth of civilization where commerce became more important.

Developments of longer span bridges using twisted vines (now called cable-assisted bridges) are described in the following sections. Although methods of structural analysis were not known until the seventeenth century, bridges of three basic forms (beam, arch, and cantilever) were used very early in human history.
The only building materials that are available in nature and known since the beginning of history are stone, timber and some other organic products. Manufactured materials like plain, reinforced, and pre-stressed concrete and cast iron, wrought iron and steel were introduced gradually, mostly within the last two centuries. Use of these stronger and varied materials led to different forms of bridges and increasingly longer spans. The history of development of bridges is thus related to the introduction of stronger materials. In reality deficiencies in the materials, such as tensile and compressive strength, density and stiffness restricted the builders to expand the bridge span.

Improving construction technique (like cable stayed, suspension, combined cable stayed and suspension system) helps the builders to expand the length of bridge spans with available material properties.

i) Origin of the suspension bridge

The earliest form of suspension bridge used creepers, vines or other trailing plants as ropes, because these were the available materials at that time. As a kind of bridge used by primitive man, it originated in areas like South East Asia, South America and Equatorial Africa. History shows that Tibetans constructed the first purpose built rope suspension bridge across the Indus River near Swat and was erected in AD 400 (Geographical journal, 1942). However, a different historical source (Navier, 1823) states that the first iron chain bridge over the Pan-Po river in China was erected by a Chinese General in AD 65. It is known as the bridge of iron.

ii) Ancient development of suspension bridge construction and materials used

Early bridges in northeast India (Assam), generally built between trees using them as towers, were constructed of bamboo and comprised one or two main cables from which a footway of transverse canes was suspended by vertical rods. Similar bridges in the Himalayas and Burma were built using twisted osier or vine cables. The most primitive arrangement of suspension bridge was probably most common in Europe. It consists of two cables, one above the other, the lower was used to walk on and the upper to steady oneself whilst so doing (Robins, 1948). This technique is still used by elements of the armed forces.

In South America, suspension bridges were used as long ago as during the reign of the Incas. The cables were built of aloe or of twisted osiers, the towers were on natural rock, and anchorages were provided by attaching the cable to heavy timber cross beams held fast by rocks. Different kinds of creepers were used in Africa for their suspension bridges.

The transformation of these preliminary suspension bridges, built from natural ropes, into metal ropes first occurred in China. Iron chains with links measuring approximately inch in diameter began to be used instead of ropes to form some early Tibetan bridges. At the same time the towers sometimes were constructed from masonry. A 200 ft bridge built over the Hwa Kiang River in approximately 1632 is still standing. It contains iron chains with sixteen links. Many of the historical details outlined above have been abstracted from Pugsley (1958).

iii) Further development of suspension bridges

The Western world began using suspension bridges once they had developed wrought iron. This progressive development is associated with the knowledge of material science. Application of iron first appeared in China with the form of chains. The first metal suspension bridge in England was the Winch Bridge, a 2 ft wide pedestrian bridge suspended on iron chains spanning 70 ft over the river Tees. Erected in 1741, it collapsed under loading in 1802 due to corrosion of its chains.
The first iron chain suspension bridge in the USA was built by James Finely, who built his first chain bridge of 70 ft span across Jacob's Creek, Pennsylvania, in 1796. It was made from two chains consisting of wrought iron bars with a centre to centre distance of 13 ft. It broke under the weight of a six-horse team load in 1825.

Another chain suspension bridge was built in 1807 over the river Humber at Hookstow with the span of 130 ft with stone towers. The history of this bridge is unknown. The next suspension bridge known as Union Bridge was built in 1820 over the river Tweed with the span of 449ft and the roadway width of 12ft. Here the eye-bars were used for the chain for the first time. Unfortunately it was blown down during a storm after only six months period in service. Most of these chain bridges suffered heavily due to wind and collapsed as a result.

The first book on suspension bridges appeared in 1823 following Navier's tour from France to England in 1821. Theoretical work on the behaviour of suspension bridges began to develop during this first quarter of the nineteenth century.
Thomas Telford built the first great Suspension Bridge and the first bridge over the Menai Strait. Its 580 ft span and 28ft of total deck width was the world record at the time and opened to the public in 1826. Oscillation of the bridge deck and chains due to storm has occurred from time to time and some damage has been found. After installation of transverse bracing and a number of replacements of suspension rods and iron cables, the bridge is still in a satisfactory service condition.

iv) Development of suspension bridge theory

In the second quarter of the 19th century, suspension bridge theory advanced in England as a result of the large amount of experimental research carried out and much of this work was directed towards examining the effect of stiffening suspension bridges (Dredge, 1843).
By the second half of the century Rankine produced (Rankine, 1858) his approximate theory for two and three hinged stiffening girders. This work has been used extensively ever since despite its simplistic nature. By assuming that the girder spread any concentrated load uniformly across the whole span on to the cables, he produced the first theory of the interaction of cable and girder.

After the completion of the 1596 ft span Brooklyn Bridge in 1883, two major suspension bridge theories, "elastic" and "deflection" were developed. Melan (Melan, 1906) developed the first non-linear theory of suspension bridges in 1888, which he developed further and published in 1906. The fact that the behaviour of a heavy suspension cable, without any significant girder, under a concentrated load is non-linear was well known in the first half of the nineteenth century. Steinman (Steinman, 1913) translated Melan's paper on elastic theory in 1913. Alongside this, further development has produced the more accurate deflection theory (Timoshenko, 1928 and Atkinson, 1939).

Moisseiff (Moisseiff, 1932) presented an interesting development considering lateral forces on suspension bridges in 1932. It was an extension of deflection theory where the inclination of the cable plane caused by the lateral deflection was taken into account for the calculation of the moment and shear forces of the horizontal wind truss.

In 1939 Southwell (Southwell, 1940) showed how his relaxation process could treat the differential equation of the deflection theory. At the same time he drew attention to the fact that by his process allowance could be made, for the first time, for the horizontal actions introduced by any displacements from the vertical, of the suspension rods.

A major turning point on suspension bridge design occurred after the collapse of Tacoma Narrows Bridge in 1940. The importance of aerodynamic effects on decks was realized as a result of this collapse. This led to the introduction of deep box deck sections and deep stiffened girder bridges. The following section describes the Tacoma disaster under three sub headings such as the design review of the Tacoma Narrows Bridge, possible reasons for the collapse of the bridge and improvements of suspension bridge design after the collapse.

v) Failure of the Tacoma Narrows Bridge

a) General

The failure of the 2800-ft span slender Tacoma Narrows Bridge on November 7, 1940 (Goller, 1965) represented a significant milestone in the theoretical development of this form of structure. The bridge, the third longest suspension span in the world at the time (total width 39 ft, two lanes and depth 8 ft), cost $6,559,000. This bridge oscillated both in flexure and torsion, due to only moderate wind loading. Finally after a life of only a few months, it collapsed as a result of excessive oscillations in a transverse wind of only about 40 m.p.h. Oscillations became sufficiently large to break the hangers at the central main span which producing an unbalanced loading condition that created severe torsional oscillations which eventually led to the bridge's collapse.

In 1950, the new Tacoma Narrows Bridge was opened (cost $18,000,000) on the site of the first Tacoma Narrows Bridge (Koughan, 1996). Wind tunnel tests were performed at the University of Washington. The new bridge has four-lanes with a total width of 60 ft. Its 25 ft deep stiffening trusses form a box design that resists torsional forces. Hydraulic dampers at the towers and at the main span control the self-excitation on the structure. Using the same piers as the original bridge, the new structure was evidence that the lessons learned about the collapse were being rigorously applied to new design.

b) Design review on Tacoma Narrows Bridge

Immediately after the collapse of the bridge, a team of experts called Federal Works Agency (FWA) (Ammann, 1941), reviewed the design. The team (FWA) found that even with the higher loading, all stresses were within safe limits. When the structure underwent certain torsional mode shapes, the load was distributed in such a fashion as to produce maximum torsional deflection due to lack of stiffness. This happened on a day (November 7) where the main cables, hangers, towers, and various members of the bridge deck were subjected to stresses well above the design limits of these components at several locations which caused the failure to occur. It was found that the steel members had reached yield stress. Apart from the proper static design, there were no fault on the materials used and also no defects created during assembling the structure (Ross, 1984).

The team (FWA) agreed that the transition from relatively safe vertical motion to destructive torsional motion occurred. Due to this action, the concrete roadway experienced torsional stresses that exceeded the ultimate strength of the material. It happened near the centreline of the roadbed, where the maximum torsional stresses were to be expected. This collapse of the main span left the towers with very high unbalanced loading, supporting the full weight of the side spans without the balance of the main span. As a result the tower moved over 12 times the maximum design deflection. The side spans remained unaffected with the cable sagging 60 ft at the mid-point as a result of the tower deflection.

The fundamental reason for the failure of the bridge was its extreme flexibility, both vertically and in torsion. The bridge's narrowness, based on economic factors and transportation studies, made the structure extremely sensitive to torsional motions created by aerodynamic forces. Several methods were introduced to reduce the motions of the bridge before collapse, but none of them worked to avoid the disaster. The first one involved the attachment of tie-down cables to the plate girders and anchoring them into heavy concrete blocks on the shore. This failed as the cables snapped shortly after installation. The second one attempted adding a pair of inclined cable stays to connect the main cables and the deck at the mid-span. These remained in place until the collapse but were also inefficient in reducing the structural vibrations. The third technique was to equip with hydraulic buffers installed between the towers and the floor system of the deck to damp longitudinal motion of the main span. The effectiveness of the hydraulic dampers was nullified due to the seals of the unit being damaged (Schlager, 1994).

c) Possible reasons for the collapse on Tacoma Narrows Bridge

The team (FWA) (Ammann, 1941) came out with three possibilities of dynamic actions such as:

(i) aerodynamic instability producing self-induced vibrations in the structure,

(ii) eddy formations which might be periodic in nature and,

(iii) random effects of turbulence due to random fluctuations in velocity and direction of the wind.

The FWA team considered each case separately in seeking the causes of the vertical and torsional oscillations. The team appeared to have identified the leading possible contributors to the destructive oscillation.

d) Improvements after the collapse of the Tacoma Narrows Bridge

The need for practising engineers to have a complete understanding of nature's interaction with their designs has generated new problem solving methods. Thus design engineers start to look not only at static loads but also review the implications of aerodynamic effects of their structures. A preliminary design nowadays includes at least a two-dimensional wind tunnel analysis of the structure. The wind tunnel testing at the initial design stages may be avoided if a sufficiently aerodynamically similar bridge deck is used. Knowledge from wind tunnel testing on bridge deck section models has led to information on flutter response characteristics of various deck shapes (Scanlan, 1990). This information guides the bridge design engineer to understanding the general behaviour of a shape under various flow conditions.

Case studies on Bridge design demonstrate (Sibly, 1977) the need for engineers to acknowledge the design history of the structures they create. In the early structural design form, the aerodynamic force analysis was of secondary importance. Over time design engineers extended the limits where the aerodynamic factors became of prime importance.

vi) Development of aerodynamic measures

After the collapse of Tacoma Narrows Bridge a great deal of research was directed towards understanding the nature of this bridge's dynamic performance and to learn how to cope with it. Large-scale model experiments have been made in England (Frazer, 1952) and America (Farquharson, 1949). Also several advanced tentative theories (Bleich, 1950) were put forward. As a result, it has been found that higher oscillation can be largely prevented by proper aerodynamic measures applied to the deck and girder of the bridge. Engineers, with safety in mind rather than economy, returned to using bolted truss and aerodynamically stable closed box girders. Unlike previously built truss bridges which were designed for static load only, these new bridges were known to be aerodynamically stable over the expected range of wind speeds.

vii) Development in British Bridge design

Due consideration of aerodynamic effects were first adopted in Great Britain in the design of the Tamar and Forth bridges. In both bridges, open lattice stiffening girders were used and the deck structures of high torsional stiffness were achieved by wind bracing at the top and bottom of these girders.

The Tamar Bridge was opened to traffic in 1961. This suspension bridge has concrete towers (37 m high) and a deep steel truss (4.9 m) that supports the roadway. The central span is 335 m with side spans each of 114m. Consultants Mott, Hay and Anderson designed the original structure.

The Forth Bridge was opened to traffic in 1964. This bridge has cross-braced steel towers (191 m high) and a stiffening truss system of 8.4 m in depth. The main span is 1006 m and the side spans are 408 m. Messrs Freeman Fox & Partners designed this structure.

In the case of the Severn and Humber, the deck structure became a shallow plate box with a cross-section chosen to minimize the formation of eddies in a lateral wind. The measures were taken for ensuring its stability, and as a result, the cross section

of the decks become much more like those regularly adopted for aeroplane wings. As with the Forth Bridge, the design of the Severn Bridge and the Humber Bridge was carried out by Messrs Freeman Fox & Partners.
The Severn Bridge was opened to the public in 1966. This bridge has an inclined hanger system and steel towers with the height of 136 m. The depth of the plate box deck section is 3 m and the width is 11.5 m. It has four lanes with cantilevered footpath in both sides (width of 4.4 m). This bridge has the central span of 988 m and the side spans of 305 m.

Outside of the United Kingdom, Messrs Freeman Fox & Partners (British designer) carried out the major design project in Turkey. This suspension bridge is called the Bosporus Bridge, and opened to public in 1973. This is similar to the Severn Bridge having an inclined hanger system, steel towers and an aerodynamic box deck section. The total width of the section is 34.4 m. The main span has a length of 1074 m and the side spans lengths of 255 m and 231 m.

Experience gained in the previous bridges brought British designers back into the forefront of suspension bridge design. Contribution of this knowledge gained by Messrs Freeman Fox & Partners was put forward to the design of the Humber Bridge.

viii) Dimensions and details of the Humber bridge

The Humber Bridge was opened to traffic in 1981. The bridge, with its main span of 1410 m, was the longest operational single span suspension bridge in the world. Because of the topological and geological conditions there is a marked inequality in the lengths of the two side spans, being 530 m and 280 m respectively, which is a special feature compared to other suspension bridges (Humber Bridge Board, 1981). The deck is a slim, streamlined, steel box suspended from inclined hanger ropes. Three suspension bridges namely Humber, Severn and Bosporus have the inclined hanger system. The function and design requirements of each Humber Bridge component are described extensively with figures in Chapter 5.

ix) Further development after the construction of Humber Suspension Bridge

Further development (after the introduction of a streamline box deck section and wind tunnel test) started with increasing the length of the span and the studies on long span suspension bridges under the action of fast running trains, earthquake and high typhoon wind. The problems related to fatigue in the components subjected to railway loading have been investigated both theoretically and experimentally.
Development including increasing the length of 1377 m double deck Tsing Ma Bridge in Hong Kong, 1624 m Great Belt Bridge in Denmark, 1990 m Akashi Kaikyo Bridge in Japan and 3300 m Messina Strait Bridge in Italy (under planning) are some good examples.

x) Current development on suspension bridges

Current developments appear to be directed towards extending the length of the main span of each newly proposed structure. World wide recent development on length of main span shows the confidence existing in suspension bridge design and construction. Questions arising among the designers are: how far does the main span go, and what type of lesser weight materials can be used for the deck? This is because the main cables carry 80% of their load from self-weight. If the self-weight of the bridge can be reduced then extension of the main span will be possible. Introduction of new materials with a more favourable strength to density ratio than the present steel might give economically feasible solutions. As discussed in previous sections, development in bridge engineering proceeds along the line of finding a structural form that suits the available material. While new or improved materials are being developed, the situation is that of finding the most effective way of creating the available type of bridges. Ultimately the development of new or improved materials leads to the evolution of new structural forms and so the above process is continuous. Lightweight carbon fibre composites for the construction of the deck might be an answer for future development but cost is the questionable factor.

2) Design aspect of cable assisted bridges (Cable stayed & Suspension bridges)

i) Introduction

The design philosophy of suspended bridge structures is to use cables to provide global support for the bridge deck. The deck is therefore required only to support itself locally (i.e. between consecutive cable attachment positions). The cable-stayed bridge differs from the suspension bridge in the way that the deck is supported. This causes each form of structure to exhibit unique characteristics.

In suspension bridges the deck is supported from main cables with vertical or inclined hangers, but in cable-stayed bridges the deck is supported directly from the towers with stay cables. This causes the cable-stayed bridge to be significantly stiffer than the corresponding suspension bridge. It also results in a cable stayed bridge having higher wind resistance and increased lateral stiffness due to the self-anchored system where the horizontal component of the cable force is transferred to the stiffening deck girder.

ii) Comparison of span

On a comparison of relative cost and efficiency of material usage, cable-stayed bridges are suitable for main spans less than 1000 m. Gimsing (Gimsing, 1983) compared suspension bridges with fan system cable-stayed bridges in which all stay cables radiate from top of the pylon for 1000 m and 2000 m spans. The comparison was carried out considering equal loads, materials and type of stiffening girder. The 1000 m span bridges in both types contained approximately an equal quantity of structural steel. For a 2000 m span, a cable-stayed bridge contains approximately 70% more structural steel than that contained within the equivalent suspension bridge.

Considering a three-span structure having a main span of 1000 m, under both symmetrical and asymmetrical loading over half the length of the main span, the suspension bridge has the greater mid span deflection than the cable-stayed bridge.

For a main span of 2000 m, cable-stayed bridges have higher mid span deflection than the suspension bridge. This is an indication of a main span length restriction in the case of a cable-stayed bridge.

Another example (Gimsing, 1983) is for a structure having a main span of approximately 3200 m. This is the maximum expected length for the main span (for the proposed Messina Strait Bridge in Italy) so far with the height-to-span sag ratio of 0.1. The quantity-based cost of a self-anchored cable-stayed bridge will be more than three times larger than for an earth anchored suspension bridge. The excessive cost of the cable-stayed bridge is primarily due to the increase of the girder sections required to transmit the axial forces. The total amount of structural steel that would be required in the stiffening girder would be almost ten times larger in the cable-stayed bridge than in the suspension bridge.

iii) Comparison of the deck and the anchorage

A comparison of the performance of the deck of a cable stayed bridge with that of a suspension bridge reveals that they exhibit very similar behaviour. The suspension bridge needs more bending and torsional stiffness, while the cable-stayed bridge needs more steel area to withstand the thrust induced within it from the cables.
The outstanding advantage of a cable-stayed bridge is that it does not require a cable anchorage that is as large or as heavy as that of a suspension bridge. This is because the anchor forces at the ends of the cable-stayed bridge act only vertically and can usually be balanced by the weight of the pier and its foundation. Any additional cost incurred, as a result of having to provide additional resistance against bending effects is usually small.

iv) Comparison of material efficiency using a classical approach

Croll (Croll, 1997) compared the material efficiency of suspension and cable-stayed bridges using a classical approach (Appendix 1). For convenience, loading was restricted to uniformly distributed load acting upon the main span. All things being equal (such as span length, tower height, spacing of hangers and cross sectional area of these components), the relative efficiencies of the side spans would be closely related to those of the central span. It was assumed that the local bending stiffness of the deck girder would need to be similar in each case. More complex aspects of behaviour such as aeroelastic interaction, non-linear dynamics and economies arising from differences in fabrication techniques are not considered. The material efficiency between those two bridges can be given for the tower height of h above the deck level and the main span length of L with the assumption of σc (compressive strength of concrete) = $\frac{2}{3}\sigma t$ (tensile strength of steel). If $L/h > 4$ the suspension bridge is more efficient and if $L/h < 4$ the cable-stayed bridge is more efficient (Figure 3a). For a longer (> 800 m) main span, suspension bridges are a feasible solution and for the main span length of less than 800 m cable-stayed bridges are feasible.

v) Comparison of material efficiency using Maxwell's Lemma approach

French (French, 1997) compared the material efficiency by using Maxwell's Lemma. For completeness this is also reproduced in Appendix 1. The product of axial (member) force by length for a member is a measure of the structural task it performs, and the summation of the absolute values of such products is a measure of the structural economy. PERT is the sum of all such products for the tension members in the structure and PERC is similarly for compression members. The PER is defined by PERT-PERC, Clark Maxwell (Maxwell, 1964) showed that for a given set of loads, PER is a constant. For an optimum structure the value of PERT + PERC is minimal. For an inefficient structure the values of PERT and PERC are large compared with PER.

PERC is less at the cable-stayed tower as load is applied roughly uniformly throughout the tower height h, whereas in the suspension bridge it is all applied at the top, making twice as much PERC. On the other hand, part of the deck of the cable-stayed bridge is in compression, increasing the PERC, whereas there is no corresponding element in the suspension bridge.

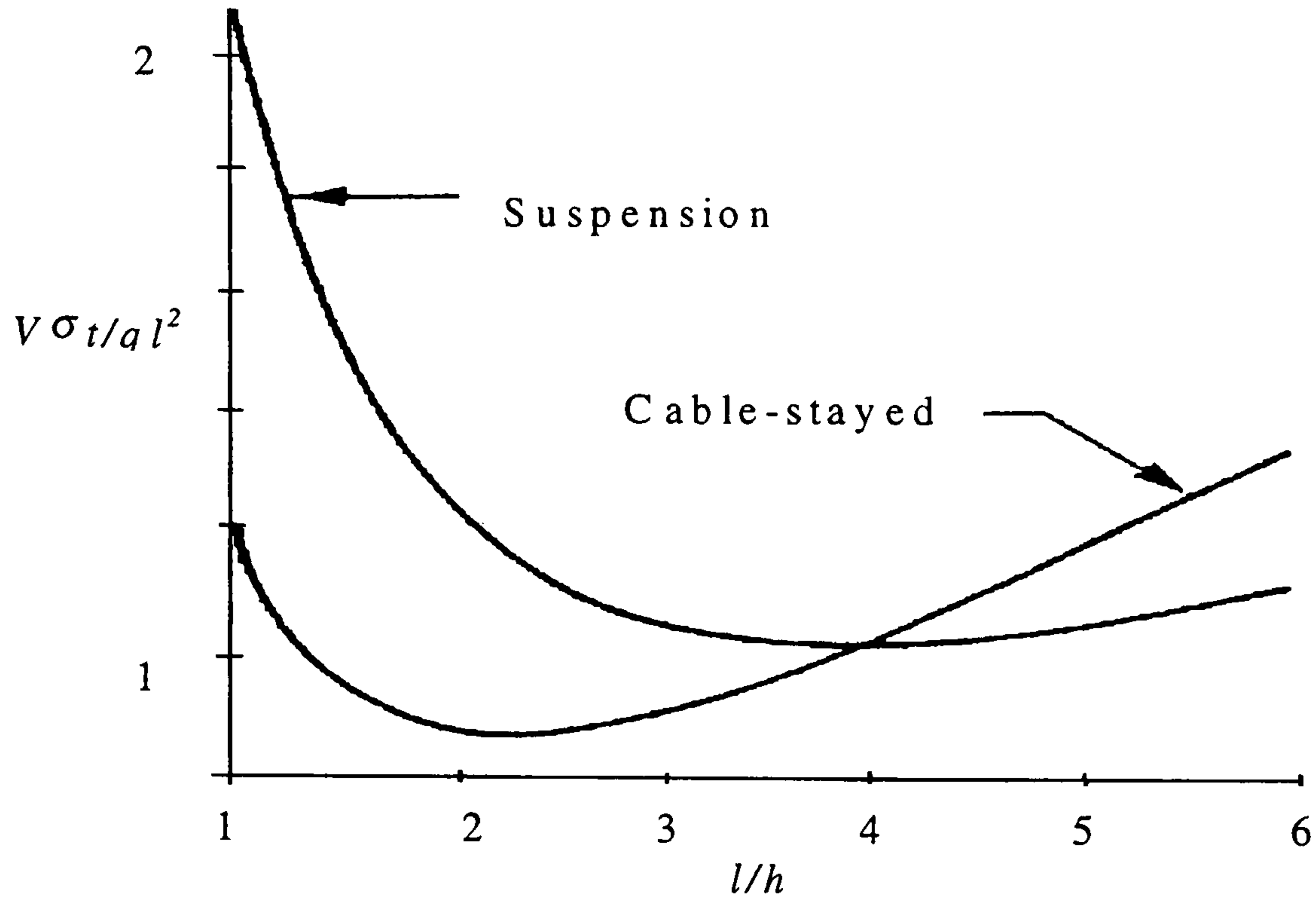

Figure 3a (from Croll (1997))

At some value of main span length of L, as shown in the above figure ($L/h = 4$), these opposing effects will balance each other out. The PERC will be the same for both, and both will exhibit the same economy, at the intersection of two hyperbolas shown in the above Figure 3a.

It can be concluded that the main span length is the major factor that influences designers selecting an economical design. Most cable-stayed bridges have the main span less than 900 m. The selection of a suspension bridge for Humber was therefore an economical solution.

3) About the Humber Bridge

i) Background information

The river Humber, which is located on the east coast of England, has long been a barrier to trade and development between the two banks of the river, and local interests campaigned for a bridge or a tunnel across the estuary for more than 100 years. Improved communications would enable Humberside to realize its potential as an area ripe for industrial and commercial development. With the coming of the bridge, the distance between the major towns in the region was cut down by approximately 80 km. The bridge, together with its approach roads, forms a vital element of the integrated road system linking Humberside as a whole with the national motorway network (Humber Bridge Board, 1981). This gave a big improvement to commercial and transport facilities between Hull and London. Structural components of the Humber Bridge are briefly outlined here (Humber Bridge, Tender drawings, 1973). More details about the Humber Bridge and its functions with figures are described in Chapter 5.

a) The towers & tower saddles

The two towers at Hessle and Barton, each 155.5 m high, are heavily reinforced with high concrete quality (concrete class of 37.5). It is constructed with slender, slightly tapered (1:100) and hollow legs with one leg in each tower containing a service lift for maintenance purposes. The foundation on the Hessle side is sited on the high water line with the concrete slab area of 44 m x 16 m and a depth of 11.5 m. On the Barton side, the tower is supported on a 16 m deep concrete pier which is resting on twin hollow 24 m diameter circular caissons. Tower saddles direct the main cables passing from Hessle to Barton anchorages. Due to high friction between the main cable and the tower saddle, the tower tops move with the main cable.

b) The deck

The main deck is a slim, streamlined, steel box structure suspended from inclined hanger ropes. The upper flange of the box is covered with mastic asphalt to a depth of 40 mm to provide the roadway surface. The cross-section of the deck was designed so that its strength and stability were maximized whilst trying to minimize the loading imposed on it due to wind. The boxes were assembled, each 140 tonnes, and welded into 124 boxes, generally 18.1 m long. These formed sections of the deck 22 m wide and 4.5 m deep; 3.25 m wide panels cantilevering from each side carry the walkways.

c) The main cables, anchorages & splay saddles

The main cables are formed from 14948 wires (each 5mm diameter) and in addition 800 wires are used for the Hessle side due to its steep slope, which gives higher tensile force. Each wire terminates in concrete gravity anchorages founded on the Kimmeridge clay of Barton, and the chalk rock at Hessle. The design and construction of the foundations of the Humber towers and of the anchorages were dictated by the geology of the site, which differs greatly between the north and south sides of the estuary. On the north side (Hessle) a deep bed of chalk comes to the surface and resolves the foundation problems. The anchorage on the Hessle side is 65.5 m long by 36 m high and 21 m below the ground level. The total weight of the Hessle side anchorage is 190,000 tonnes. On the south side, however, the chalk has been eroded by glacial action, leaving a 30 m deep bed of boulder clay (gravel saturated alluvium) overlying a thick bed of over-consolidated Kimmeridge clay. The foundations for both the tower and anchorage had to be taken down into the Kimmeridge clay. It was necessary to design and construct the foundation, taking note of the slurry action of the clay when it contacts water. The Barton side anchorage is 72 m long, wedge-shape in plan with the average width of 41.5 m and founded 35 m below the ground level in the Kimmeridge clay. The total weight of the Barton anchorage is 300,000 tonnes. The main cable is connected to the anchorages through splay saddles. The main cable is divided into a number of strands beyond the splay saddle and bolted with the anchorage block. The splay saddles move with the main cable.

d) The A-frames

Long-span bridges are very flexible structures, subject to very large movements arising from strain due to external (traffic and wind) load and from temperature effects. To accommodate these movements A-frames are introduced at each end of the span. These A-frames are categorized into two types. The A-frame legs mounted on the ground (platform) at the far ends of the north and south are called A-frame type 1. A-frame legs mounted on the tower cross beams are called A-frame type 2. Functions of these A-frames are described with figures in chapter 5. The deck is discontinuous at the towers and the deck movements are accommodated by a system of "rolling-leaf" expansion joints and A-frames. The A-frames also provide restraint against vertical, lateral and torsional loads. Consultants Freeman Fox and Partners designed the bridge on the basis of their experience gained on the first crossings of the Severn (England) and the Bosporus (Turkey), both of which were conceptually similar.

e) The hangers

Only three bridges including Humber, Severn and Bosporus have the inclined hanger system. Humber was the last one to introduce this inclined system.

The bridge designer Messrs Freeman Fox & Partners believed that the inclined hanger system gave extra stiffness to the structure. The inclined hangers apply some constraint on longitudinal movement of the deck. The resulting strain energy generated in each hanger by any movement is dissipated by the hysteresis characteristics of the wire ropes. These are spiral wound and dampen out oscillation.

f) The carriageway

The bridge accommodates dual two-lane carriageways, with footpath/ cycle tracks on both sides, wide enough for maintenance and road vehicle access, giving a total width of 28.5 m and a 4.5 m depth of the deck. Total width of the carriageway is 22 m and each lane is 5.5 m wide. Each footpath/ cycle track is 3.25 m wide.

The bridge was designed (BS 153 Part 3A 1954) according to the requirement of the time including a capacity for a 180 tonnes single vehicle and resistance to wind of 47 m/s on the deck and up to 66 m/s at the top of the towers. Since its opening more than 70 million vehicles of different types have used it.

g) Present development

The aerodynamic stability of a suspension bridge is an important issue to be carefully considered during its design and construction. The awareness of this issue greatly increased as a result of the collapse of the Tacoma Narrows Bridge in the 1940's. To overcome aerodynamic instability engineers have needed to investigate several alternative arrangements of the cross section. This leads to the change of deck section from plate to truss or trapezoidal box section. Because of the availability of computer facilities, bridge finite element models can now be prepared at different design stages, and provide an efficient tool for designers to solve complex problems. Also these facilities encourage designers to produce different types (number of spans, different shape of deck sections, different hanger patterns) of suspension bridges with solutions. In future, development and submission of a computer model of the bridge structure, with their design calculation, might be a requirement from the client. Introduction of lower weight materials for the deck will allow longer main spans in future.

Conclusion on Historical Introduction

History of suspension bridges started with using natural rope, and over the period of time it has been replaced by metal rope. Theoretical work on the behaviour of suspension bridges started during the first quarter of the nineteenth century. Melan developed the first non-linear theory on suspension bridges in 1888. Further development continued till 1940, this all based on vertical and lateral deflection, stiffness and static analysis.

A turning point on suspension bridge design occurred after the collapse of Tacoma Narrow Bridge. This disaster led to the design engineers considering the implication of aerodynamic forces on their structures. Wind tunnel tests on bridge deck section models were seriously considered. These tests led to information on flutter response characteristics of various deck shapes and give guidance to the design engineer about general behaviour of a shape under various flow conditions. It was concluded that proper aerodynamic measures applied to the deck section prevent higher oscillations of the bridge. As a result open lattice girders and box deck sections were introduced instead of simple plate sections for the design of the deck.

Further development of suspension bridge construction focused on self-weight of the suspended structure. Increasing the size of the deck section (single or double deck) considerably increases the main cable force resulting in a high volume of anchorage block, higher main cable diameter and high cross section area of the tower. Similar effects occur with increasing the span of the suspension bridge. Here the strength to density ratio plays a considerable role and depends on the development of material science knowledge. At present suspension bridges are being constructed with available materials for the required spans, the configuration and size of the components are dependent on the ability of the design engineer. Changing the material properties (strength to density ratio) in the future might introduce different configurations and sizes of structural components for previously built similar span bridges. Relatively lower weight materials will enable the design engineer to extend the spans of bridges in the future.

Chapter 4

Classical theory of suspension bridges

General

A single flexible cable suspended between two fixed points is the basic formation of a suspension bridge. The initial problem is to find the cable tension force at a particular point on the cable under its own weight. The solution of this problem provides a starting point for the consideration of the effects upon a suspended cable of different applied forces arising from the live loads on a practical suspension bridge. Here two types of cable elevation, catenary and parabolic, are described. Load distribution on a parabolic cable is closer to the suspension bridge under its self-weight as the weight is uniformly distributed across the span.

The catenary cable

A frictionless uniform chain, or a perfectly flexible uniform cable, hanging freely suspended between two fixed points, is represented as a catenary where the cable is also incapable of carrying any loads save by means of tension directed along its length. The weight per unit length along the cable w' is constant. This defines the classical problem of the common catenary, which was first solved by geometry by James Bernouilli in 1691. Tension on the catenary cable is given in terms of cable length, y co-ordinate and catenary parameter.

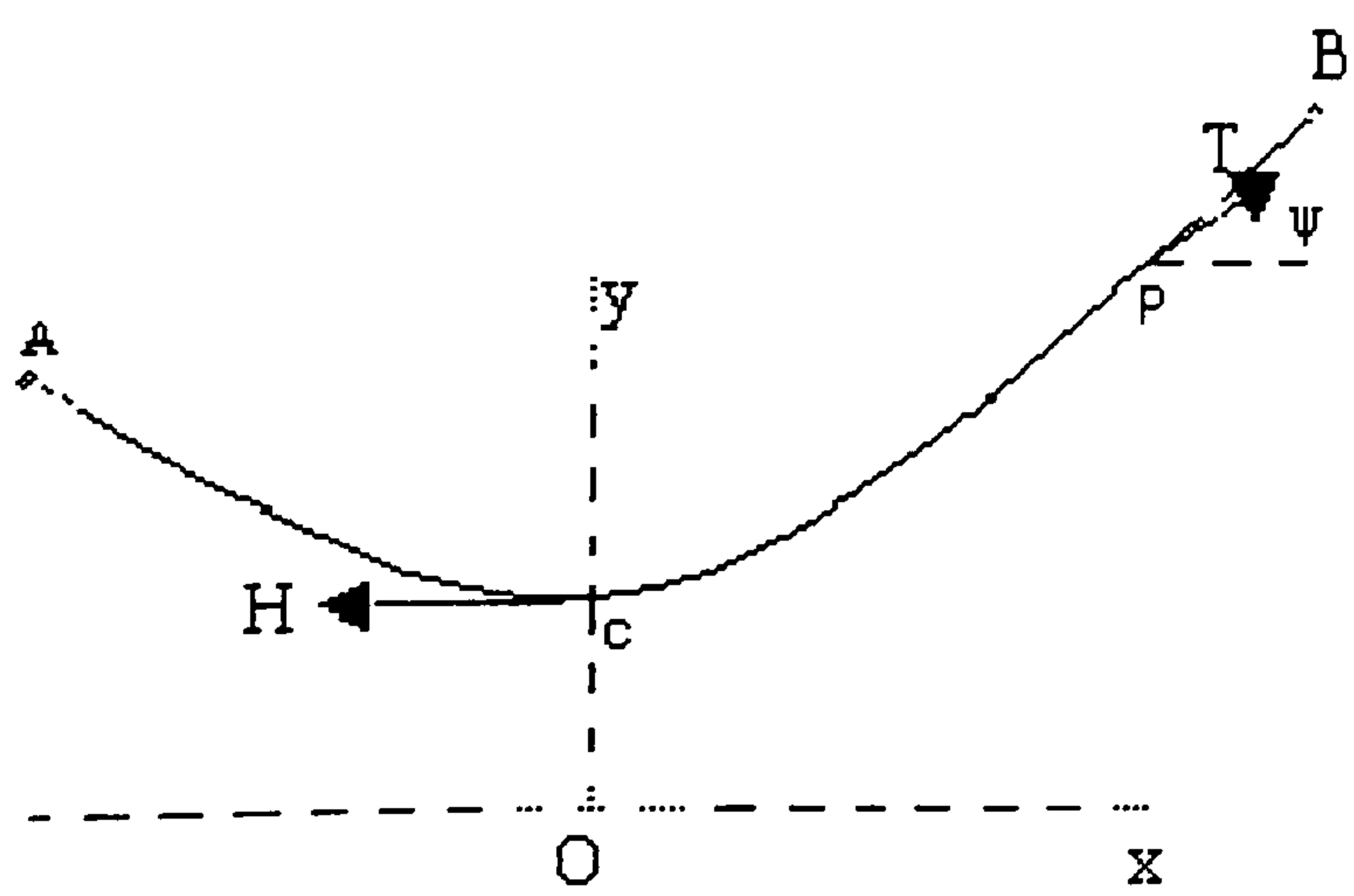

Figure 4a

The following notation is used for the introduction of classical theories.

c	the lowest point
s	length of the cable measured from c to p (arbitrary point on the cable)
ψ	inclination angle of cable (at a particular point)
T	tension in the cable
H	horizontal force on the cable
L	span length
l	cable length
h	horizontal force increment on the cable
v	vertical displacement
A	cross section area of cable
E	young modules of the cable
d	dip of the cable
w	weight per unit length of cable along the span
w'	weight per unit length along the cable

From horizontal equilibrium of the cable

$$T\cos\psi = H \qquad \text{Eq. 4.1}$$

From vertical equilibrium of the cable

$$T\sin\psi = w's \qquad \text{Eq. 4.2}$$

Defining the catenary parameter C *as*

$$C=\frac{H}{w'} \qquad \text{Eq.4.3}$$

Then combining equations 4.1-4.3 gives:

$$s = C\tan\psi$$

$$C\frac{dy}{dx} = s \qquad \text{Eq.4.4}$$

Differentiation of equation 4.4 brings:

$$C\frac{d^2y}{dx^2} = \frac{ds}{dx} = \left\{1+\left(\frac{dy}{dx}\right)^2\right\}^{\frac{1}{2}}$$

Integration of the above w.r.t. x gives

$$C\sinh^{-1}\frac{dy}{dx} = x + A$$

Applying the boundary condition that where x=0 , dy/dx=0 gives A=0, so that the above equation becomes

$$\frac{dy}{dx} = \sinh\frac{x}{C}$$

Integration of the above and applying the boundary conditions (at x=0, y = C) gives

$$y = C\cosh\frac{x}{C} \qquad \textit{Eq.4.5}$$

Combining equations 4.4 and 4.5 gives

$$s = C\sinh\frac{x}{C} \qquad \textit{Eq.4.6}$$

Squaring equations 4.1 and 4.2 gives

$$T^2 = H^2 + w'^2 s^2 \qquad \textit{Eq4.7}$$

Combining equations 4.5, 4.6 with 4.7 gives

T in terms of y, $T = w'y$

Results from the analysis show:

Horizontal component of T (i.e. H) is constant, equal to $w'C$

Vertical component of T at any point P equal to $w's$

The resultant tension T equal to $w'y$

All the above results depend on the catenary parameter C.

The parabolic cable

In many suspension bridges the total dead weight of the bridge is uniformly distributed across the span rather than along the cable. This is of course of more practical importance than the common catenary cable. If w' is the weight along the cable length, for a parabolic cable $w'\sec\psi$ is a constant and for a catenary cable w' is a constant. Consider the cable as perfectly flexible and in-extensible. Tension on the cable is given in terms of uniformly distributed load along the span w, length of span L and the central dip d.

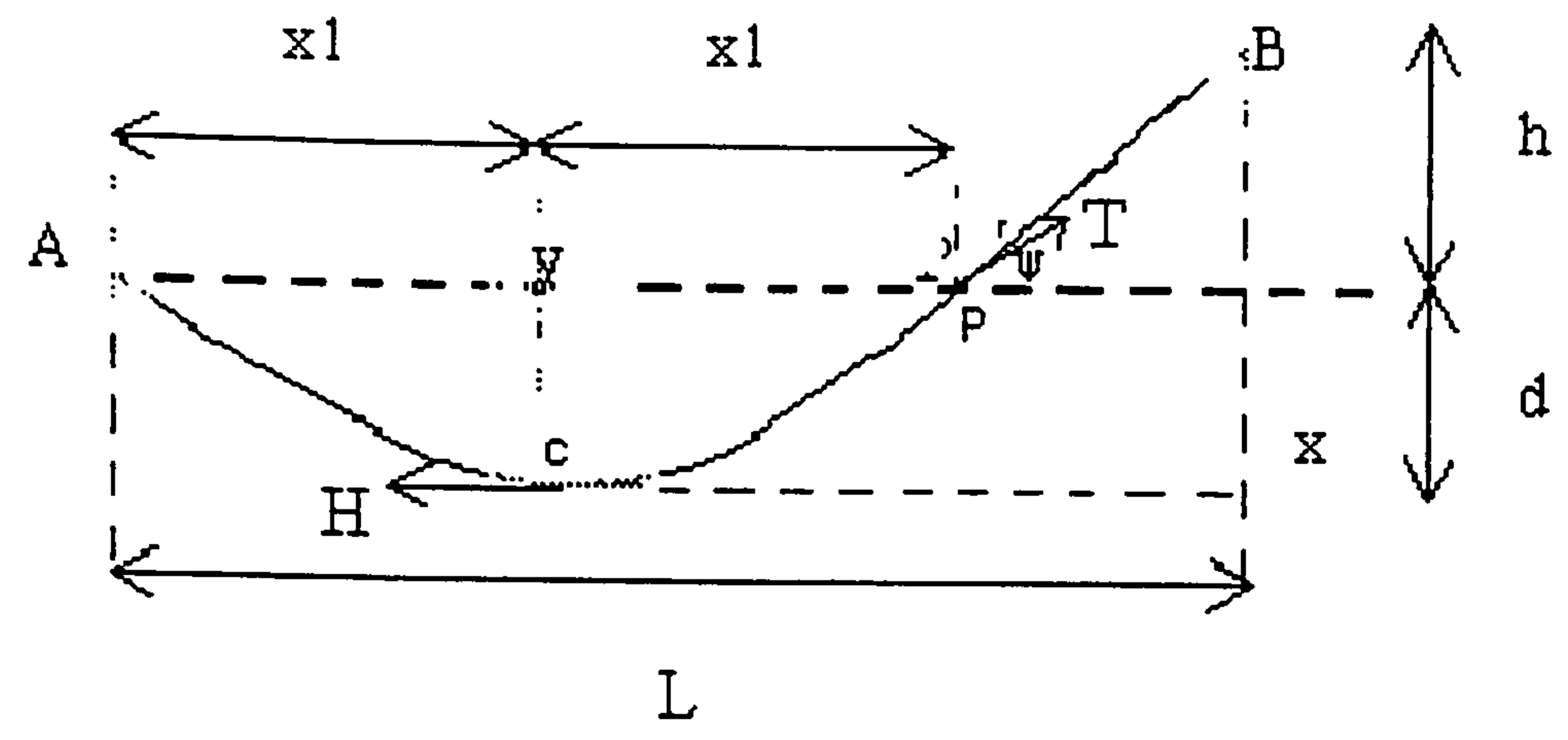

Figure 4b

Horizontal equilibrium of the cable gives

$T\cos\psi = H$ *Eq.4.8*

Vertical equilibrium of the cable gives

$T\sin\psi = wx$ *Eq.4.9*

Combining equations 4.8 and 4.9 gives

$$\tan\psi = \frac{wx}{H}$$ *Eq.4.10*

Integrating the above and applying boundary conditions (at x=0, y=0) gives the parabolic equation; $y = \frac{1}{2}\frac{w}{H}x^2$ *Eq.4.11*

Equation 4.8 can be written as

$$T = H\frac{ds}{dx} = H\left\{1+\left(\frac{dy}{dx}\right)^2\right\}^{\frac{1}{2}}$$

Combining the above with the equation 4.10 gives

The tension T at any point P can be written as: $T = H\left[1+\frac{w^2}{H^2}x^2\right]^{\frac{1}{2}}$ *Eq.4.12*

For a parabola where both ends are not on the same level as shown in figure 4b;

$$x_1 = \frac{L}{h}\left[\sqrt{d(d+h)} - d\right]$$

From equation 4.11 the horizontal force $H = w\frac{1}{2d}x_1^{\,2}$

From equation 4.12 the tension $T = H\left[1+4d^2\frac{1}{x_1^{\,4}}x^2\right]^{\frac{1}{2}}$

For most suspension bridges, both cable ends are at the same level;

From equation 4.11 at $x_1 = L/2$ the horizontal force $H = \dfrac{wL^2}{8d}$

And the cable tension $T = H\left[1+\dfrac{64x^2d^2}{L^4}\right]^{\frac{1}{2}}$

The maximum value of Tension occurs at $x=L/2$, $T = H\left[1+\dfrac{16d^2}{L^2}\right]^{\frac{1}{2}}$

The total length of the cable $= 2\int_0^{\frac{L}{2}}\left\{1+\dfrac{64x^2d^2}{L^4}\right\}^{\frac{1}{2}}dx$

$$=\frac{L}{2}\left(1+\frac{16d^2}{L^2}\right)^{\frac{1}{2}}+\frac{L^2}{8d}\log_e\left\{\frac{4d}{L}+\left(1+\frac{16d^2}{L^2}\right)^{\frac{1}{2}}\right\}$$

For small $\dfrac{d}{L}$ ratios and more practical purposes;

$$l = L\left\{1+\frac{8}{3}\left(\frac{d}{L}\right)^2\right\} \qquad \textit{Eq.4.13}$$

For more general cases where both ends are not on the same level;

$$l = L\left\{1+\frac{8}{3}\left(\frac{d}{L}\right)^2+\frac{1}{2}\tan^2\alpha\right\} \qquad \textit{Eq.4.14}$$

These equations were taken from Pugsley (1958).

Changes of cable length

Changes of length of the cable due to the tensions acting on it introduce a change of the cable dip if the ends of the cable are fixed. The small change of cable length Δl gives a change on the dip d. Calculation of change in dip Δd leads to construct the new parabola adopted by the cable. Changes of cable length due to elasticity (changing of deflection), temperature and span length L are described. Again, the relevant equations are taken from Pugsley (1958).

i) Due to change of dip

Simplified form related to the change in length Δl to the change of dip Δd for a constant span L;

$$\Delta l = \frac{16}{15}\frac{d}{L}\left\{5 - 24\frac{d^2}{L^2} + \ldots\right\}\Delta d \qquad \textit{Eq.4.15}$$

ii) Due to tension

If the change in length Δl is due to elasticity of the cable then it can be given as,

$$\Delta l = \int_0^l \frac{Tds}{AE}$$

then, $\Delta l = \dfrac{Hl}{AE}\left(1 + \dfrac{16}{3}\dfrac{d^2}{L^2}\right)$ *Eq.4.16*

iii) Due to temperature

If Δl arises from change of temperature t and α is the coefficient of linear expansion of the cable, then

$\Delta l = \alpha\, t\, l$

iv) Due to change in span

When the span L changes while there are no changes in the cable length l, the effect on ΔL on the cable dip d is given as;

$$\Delta L = \left[\frac{16\frac{d}{L}(5 - 24\frac{d^2}{L^2})^{\frac{1}{2}}}{15 - 40\frac{d^2}{L^2} + 288\frac{d^4}{L^4}}\right]\Delta d \qquad \textit{Eq.4.17}$$

Deflection theory

Melan introduced a more advanced theory in 1888 in terms of the differential equations of the cable and stiffening girder. There are other approaches Rankine (Rankine, 1858) and Elastic (Pippard, 1936), and this theory is commonly used with the following assumptions.

It is applicable to a single span with hangers transmitting vertical force only between the cable and the deck. Also no stresses exist on the deck in the dead load condition and deformation of the tower and extension of the hangers and the cable is negligible.

Consider the initial shape of the stiffening girder as that under dead loading condition and measure the deflection wholly due to the live loading p and the induced suspension rod loading q. Assuming the ordinary theory of bending to apply, flexure of the girder can be written as;

$$EI\frac{d^4v}{dx^4} = p - q \qquad \textit{Eq.4.18}$$

Consider equilibrium of the cable vertically, w' is the loading on the cable:

$$d(T\sin\theta) + w'dx = 0$$

In other form, vertical forces can be written as; $T\sin\theta = H\tan\theta$

As H is constant this will become; $H\frac{d^2y}{dx^2} = -w'$ *Eq.4.19*

For the dead load condition; $H\frac{d^2y}{dx^2} = -w$

As the load w' involves with the loading of w and q provided by the suspension rods and the ordinates y have, due to q, increased to $(y + v)$ and H increased to $(H + h)$, the equation for the live load condition can be written as:

$$(H+h)\frac{d^2}{dx^2}(y+v) = -w - q$$

From these above equations eliminate q and the fundamental suspension bridge equation can be written with unknown h and v:

$$EI.\frac{d^4v}{dx^4} - (H+h)\frac{d^2v}{dx^2} = p + h\frac{d^2y}{dx^2} \qquad \textit{Eq.4.20}$$

The theories and equations described above are applicable to single span cable and deck with vertical hangers. Developing analytical equations for more complex problems like a three span cable and deck with inclined hangers, gives more complicated equations and causes difficulties in solving. For this type of situation adopting numerical method is more appropriate. Throughout this project a numerical method (finite element analysis) is used to understand the structural behaviour of the bridge. Theories based on this numerical method are described in chapter 6.

Chapter 5

Configuration and design requirements of the Humber Bridge

i) Configuration of the bridge

The Humber estuary is in the north-east of England, and the bridge runs north (Hessle) - south (Barton). The main span is 1410 m, currently the third longest span in the world. The Hessle side span is 280 m and the Barton side span is 530m (Figure 5a). The two towers, each 155.5 m high (above water level), are concrete, while the main deck is a slim, streamlined, steel box suspended from inclined hanger ropes. The deck is discontinuous at the towers, with deck movements accommodated by a system of rolling-leaf expansion joints and A-frames. The A-frames also provide restraint against vertical, lateral and torsional loads.
The design stresses were calculated using a 2-dimensional frame analysis.

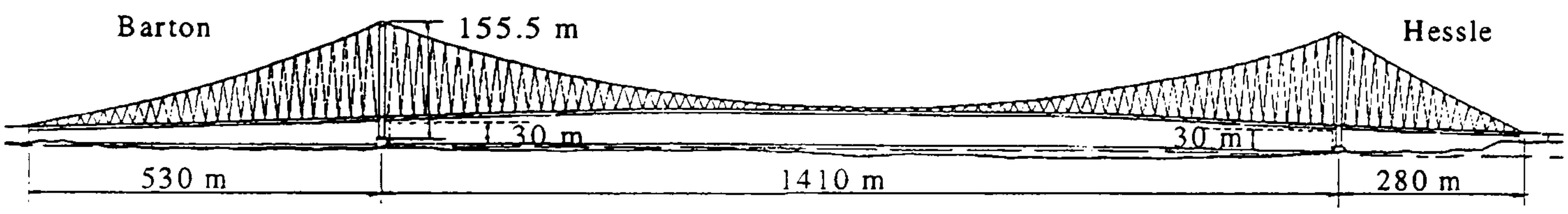

Figure 5a: View of Bridge looking upstream (courtesy Humber Bridge Board (1973)).

ii) Arrangement of structural elements

a) The main cables

The deck is suspended from the main cables by inclined hanger cables formed from spirally wound, high tensile, galvanised steel wires. The main cables were erected by the traditional method for long span suspension bridges called 'aerial spinning'. The cable wire is mounted above the final location of the cable and carries a spinning wheel. The number of wires from the reel with the moving spinning wheel form the strands (number (404) of wires) between the anchorages at both ends. The towers had to be pulled back at the top before the cables could be erected. The dead weight of the superstructure, after final completion, brought the towers back into the vertical. At the top of each tower, the cables pass through cast steel saddles built into the concrete. High levels of friction between the cable wires and the saddles prevent the cables from moving relative to the towers. Movements of the saddles along the axis of the bridge are achieved by flexure of the towers. Figure 5b shows the elevation of the saddle on the tower and Figure 5c shows the cross section of the side elevation with the cable trough of the tower saddle.

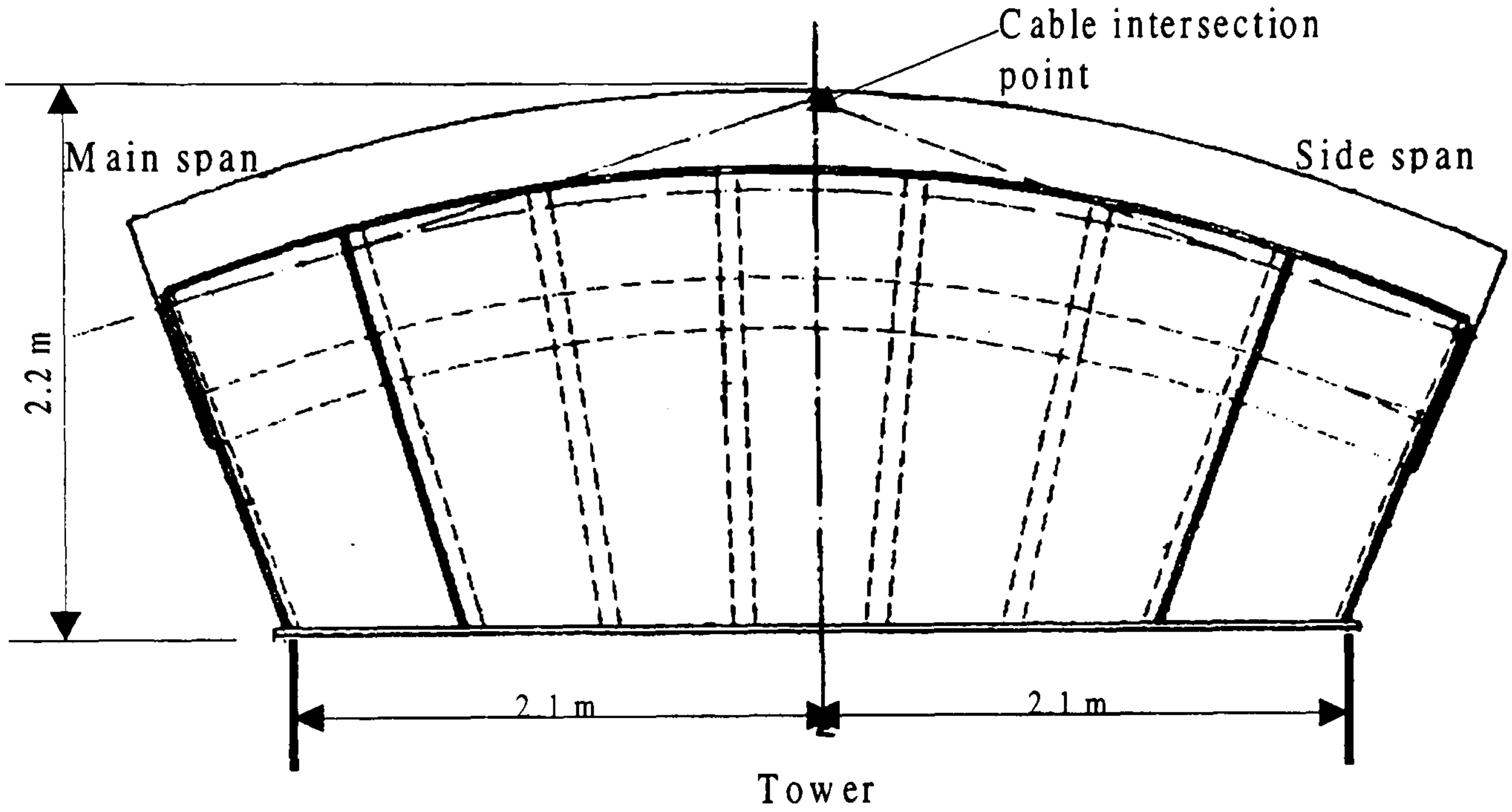

Figure 5b: Elevation of the tower saddle (courtesy Humber Bridge (1973)).

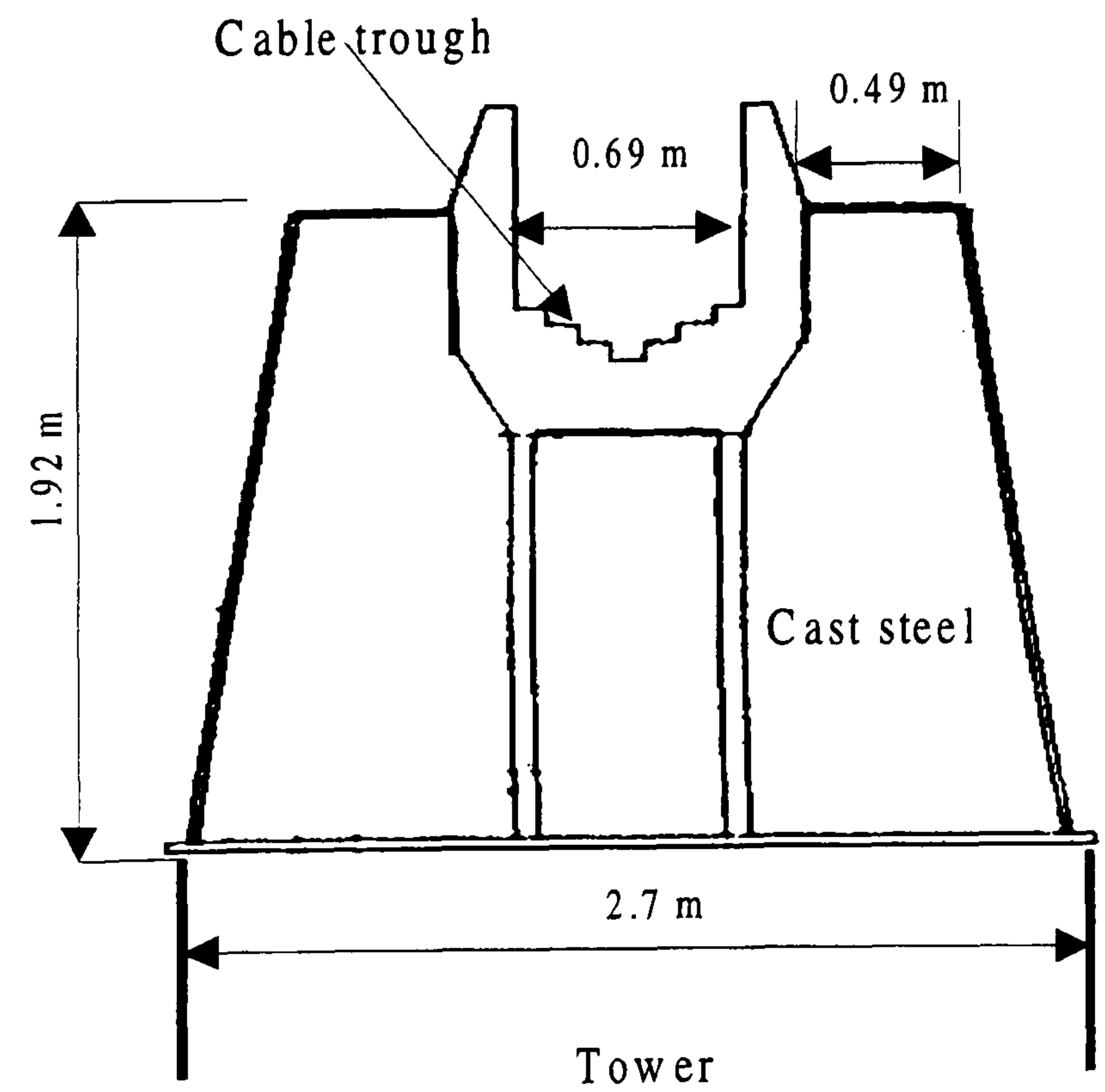

Figure 5c: Cross section of the side elevation of the tower saddle (courtesy Humber Bridge Board (1973)).

Each cable consists of 37 "strands" each made up of 404 high tensile, galvanised, parallel wires of 5mm diameter, making 14948 wires in total. For the Hessle side span, due to the steep slope and consequent greater tension, four additional strands of 200 wires each were introduced. At each end of the bridge the vertical and horizontal components of the main cable force are transferred to massive concrete anchor blocks and then to the soil. Figure 5d illustrates the layout of the anchorage block with pre-stressing tendons.

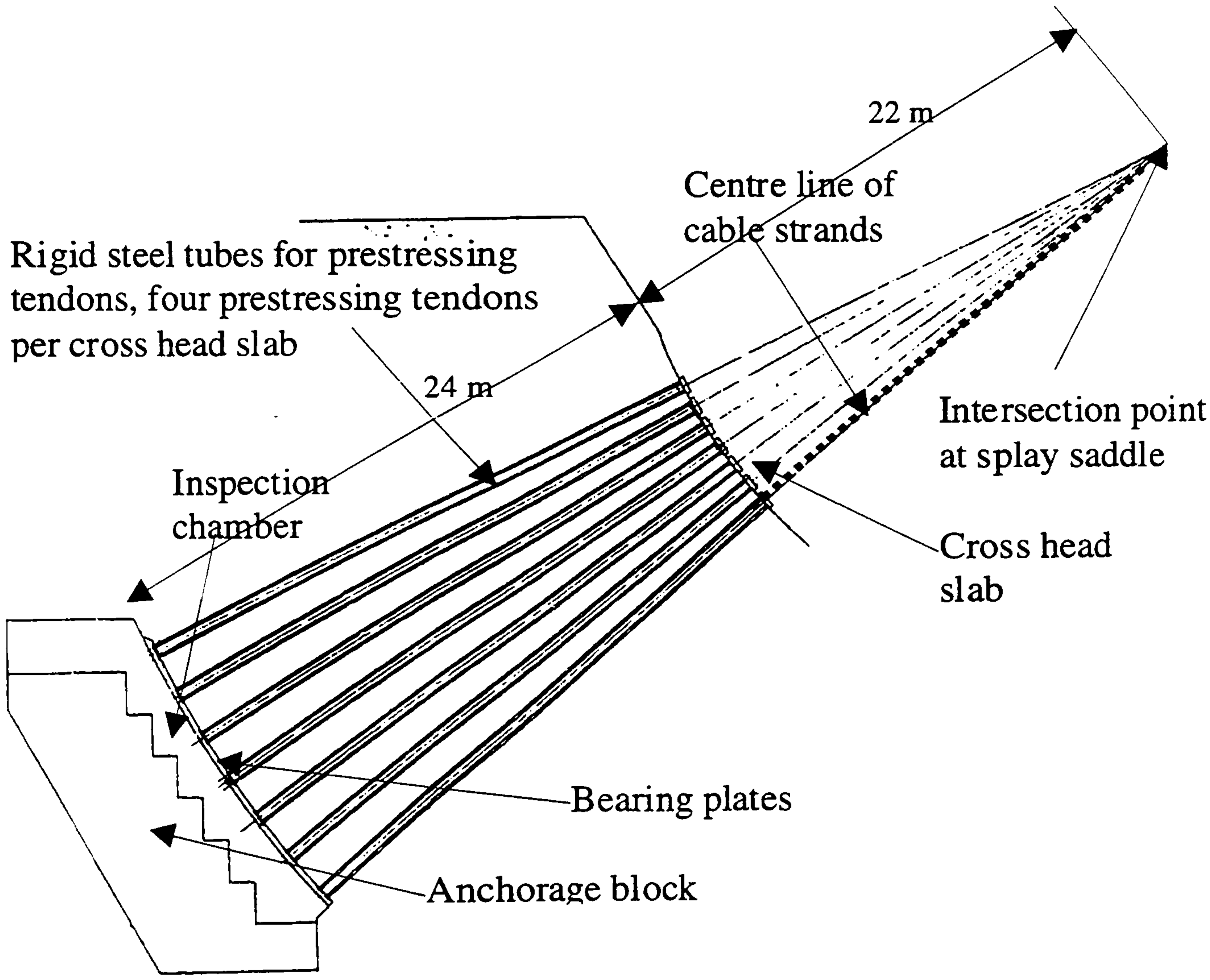

Figure 5d: Layout of the anchorage block with pre-stressing tendons (courtesy Humber Bridge Board (1973)).

The main cables separate into their individual strands as they pass through "splay saddles" just inside the anchor blocks. Figure 5e shows the elevation of the splay saddle at the Barton anchorage and Figure 5f shows the cross section (through A-A) of the splay saddle. Force transmission from the main cable to the anchor blocks is established by anchoring the individual strands to the concrete of the block.

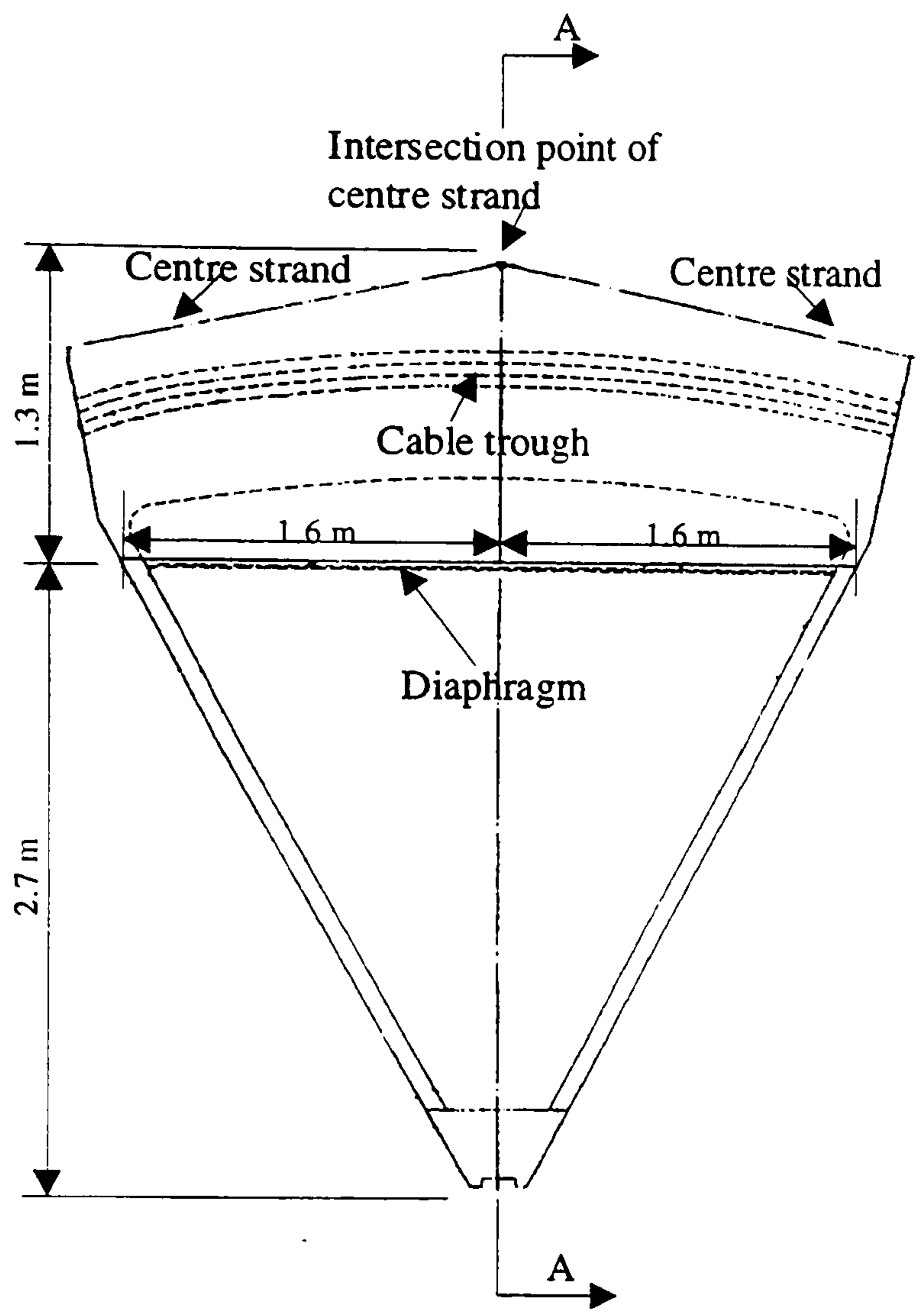

Figure 5e: Elevation of the splay saddle at Barton anchorage (courtesy Humber Bridge Board (1973)).

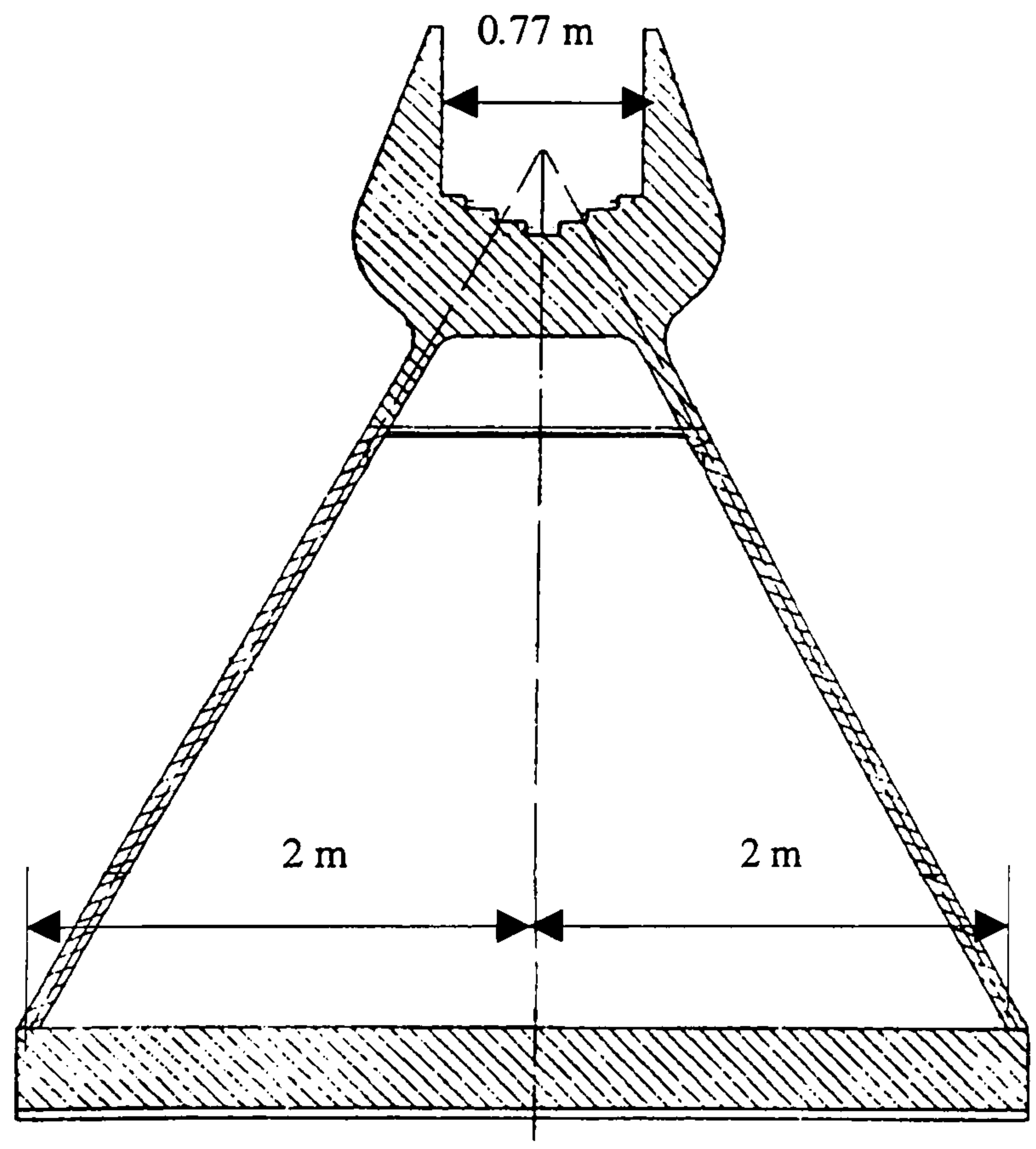

Figure 5f: Cross section (through A-A) of the splay saddle (courtesy Humber Bridge Board (1973)).

b) The deck

The deck is formed from streamlined hollow box sections and the upper flange (running surface) is covered with mastic asphalt to provide the roadway. The boxes are built up from 18.1 m long stiffened plate panels. The box sections are 22 m wide and 4.5 m deep to give a main span to depth ratio of 300 to 1. Five panels each 3.25m wide are cantilevered outward along each side of the box deck to carry the footpaths. The dimensions of the deck and positions of A-frames are shown in Figure 5g.

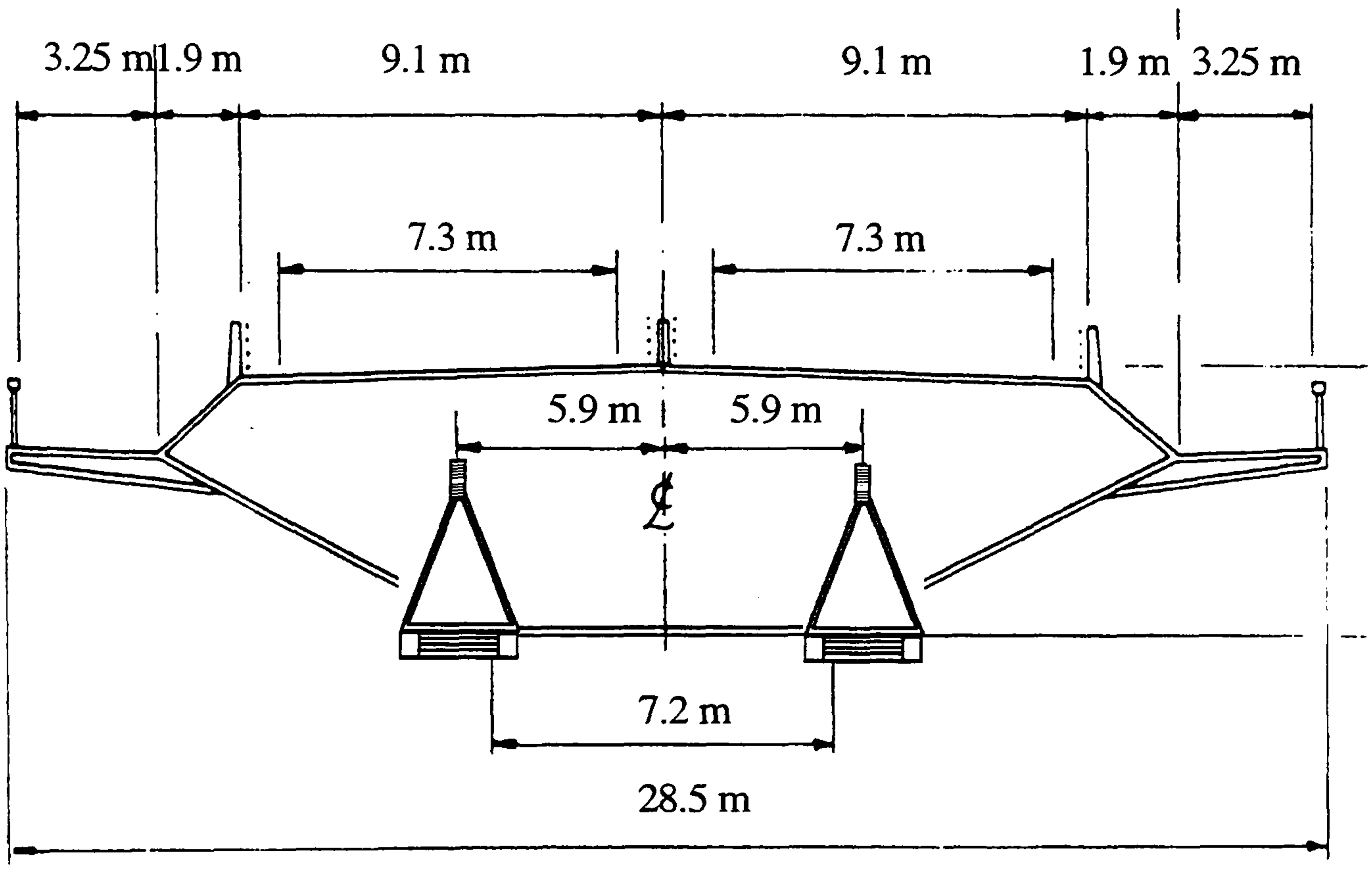

Figure 5g: Cross section of the box deck with A-frame arrangement (courtesy Humber Bridge Board (1973)).

The bridge accommodates dual two lane carriageways with footpath/cycle tracks wide enough for maintenance and road vehicle access, a combination of 124 boxes with each approximately 170 tonnes in weight. The box deck is composed of 18.1 m long prefabricated sections each having four equip-spaced bulkheads to improve torsional stiffness, and longitudinal stringers stiffening the roadway plate. Figure 5h shows the lateral stiffeners on the deck spaced in 4.5 m intervals. Figure 5i shows the longitudinal stiffeners and the footway cantilever (spaced in 4.5 m intervals).

Figure 5h: Lateral stiffeners placed inside the deck, top plate has been removed (courtesy Humber Bridge Board (1973)).

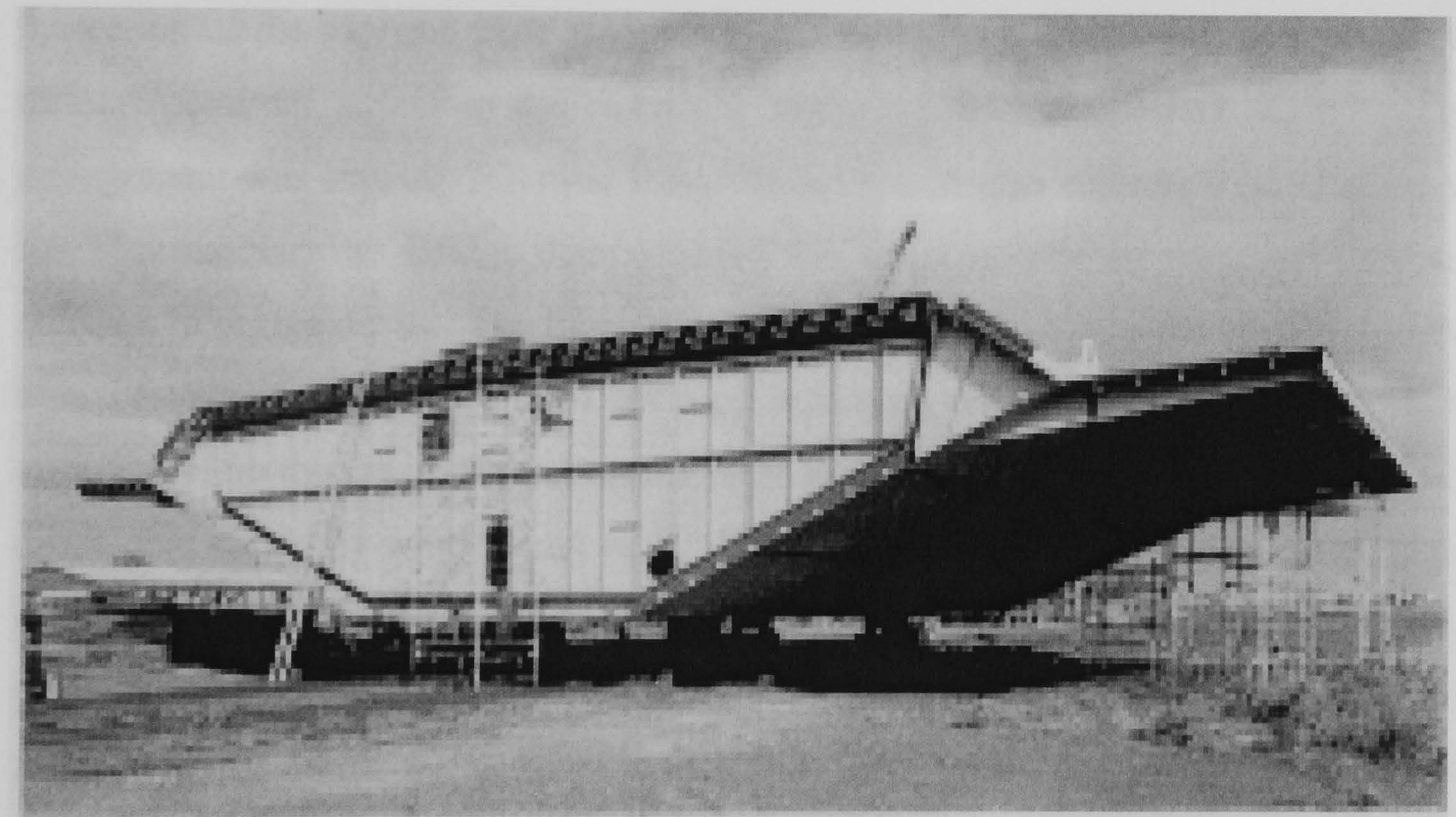

Figure 5i: Longitudinal stiffeners and the footway cantilever of the deck (courtesy Humber Bridge Board (1973)).

Many advantages are obtained with the box girder as compared with the classical lattice type stiffening truss. Less steel is required for the box section; the depth of the box section is only 4.5 m. This is less than the depth that would be required if a lattice truss were used. This is because torsional stiffness is greater in the closed section than in an open lattice truss of the same depth. For example the following bridges have shorter main spans and total span lengths than the Humber Bridge and they have lattice truss arrangements for their decks. The Golden Gate Bridge has the truss depth of 7.6 m, Second Tacoma Bridge has the truss depth of 10.0 m and Forth Bridge has the truss depth of 8.4 m. In addition to the depth, the presence of numbers of bracing and stiffeners increases the weight (and the cost) of the deck per unit length compared with the box deck section. Also the trusses have to be bolted with each other at the required angle, which will again increase the cost of the lattice truss arrangement. This action (reduction of the deck weight) reduces the size and therefore weight of the cables and hence towers, anchorages and foundations. The streamlined shape reduces the direct load arising from the wind thereby relieving the towers of very considerable lateral forces with consequent further economy. Deck box section construction permits shop fabrication of the stiffened panels and off-site assembly of the boxes, and facilitates erection into the bridge structure. Corrosion protection of the external plate surfaces is easier than for a complex latticework of trusses. Internal access to the box deck is easier for maintenance work. This arrangement was actually followed from the Severn Bridge construction. Failure of the Tacoma Narrows Bridge demonstrated the need to provide adequate torsional stiffness in bridge decks. The inherent torsional stiffness of a deep box girder, wind tunnel tested, obviated the need to use deep stiffening trusses to achieve aerodynamic stability. Here the shape of the Tacoma plate girders were replaced by a streamlined shape determined by wind tunnel tests. The large torsional stiffness of a box girder reduces the possibility of failure due to insignificant torsional rigidity. Powered painting gantries carried from the deck provide access to the exterior of the box girder itself. These advantages of the box girder lead to lower costs against alternative forms of structure.

c) The A-frames

Steel A-frame rockers that permit rotation about a lateral axis (east-west) and longitudinal movements, support the ends of all three spans but constrain the lateral movements. These have been categorised into two types with the same functions.
A-frame type 1 is mounted on the anchorage block and A-frame type 2 is mounted on the tower cross-beam. Figure 5j shows the diagram of the A-frame.

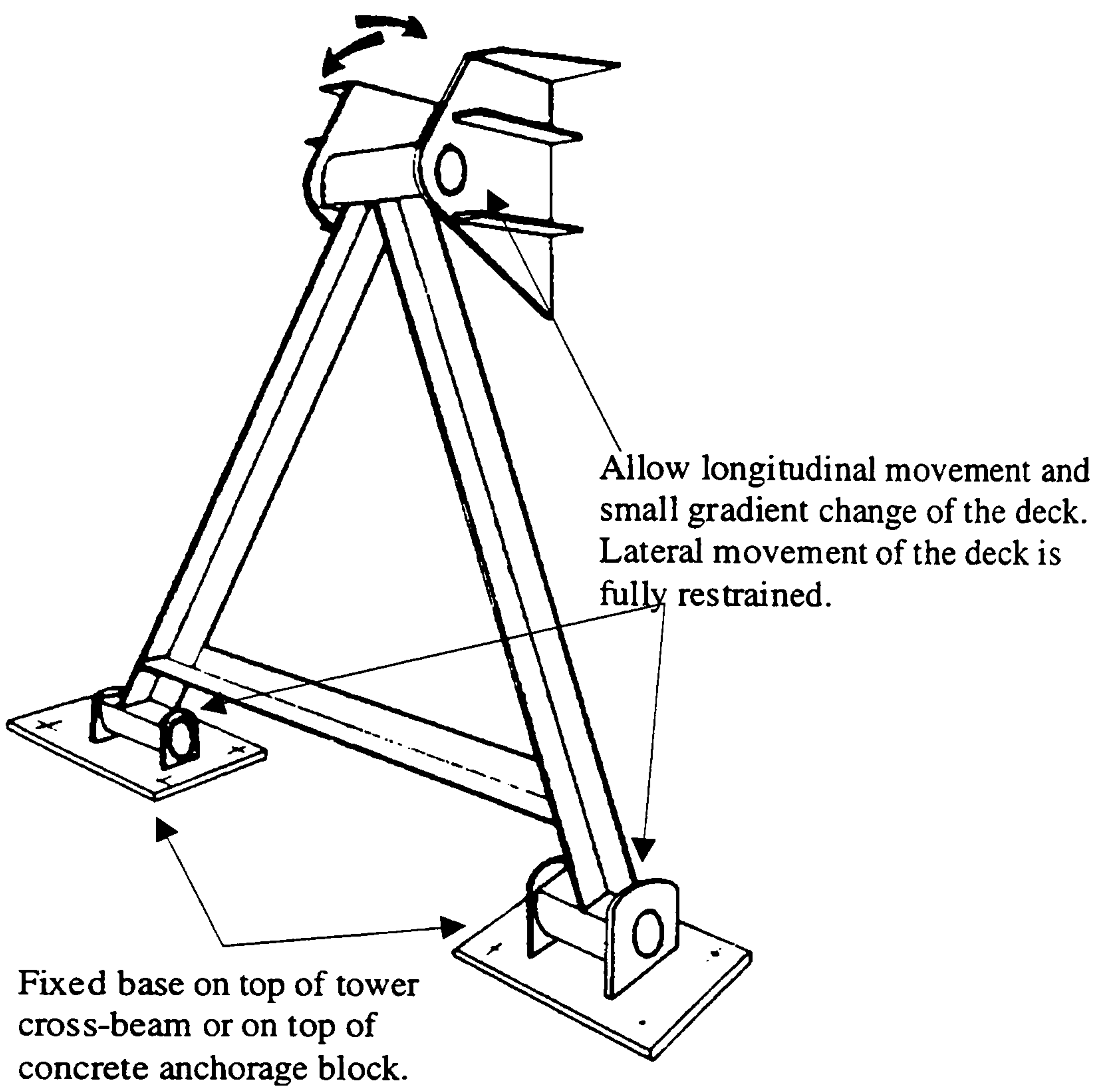

Figure 5j: Diagram of the A-frame (courtesy Humber Bridge Board (1973)).

At the towers, considerable longitudinal movements have to be accommodated. The continuity of the roadway surface is provided by a special arrangement of 'rolling leaf' type expansion joints. The arrangement of a rolling leaf type expansion joint with A-frames (type 2) at the tower is illustrated in Figure 5k. The cross section at the tower with A-frame (type 2) is shown in Figure 5l.

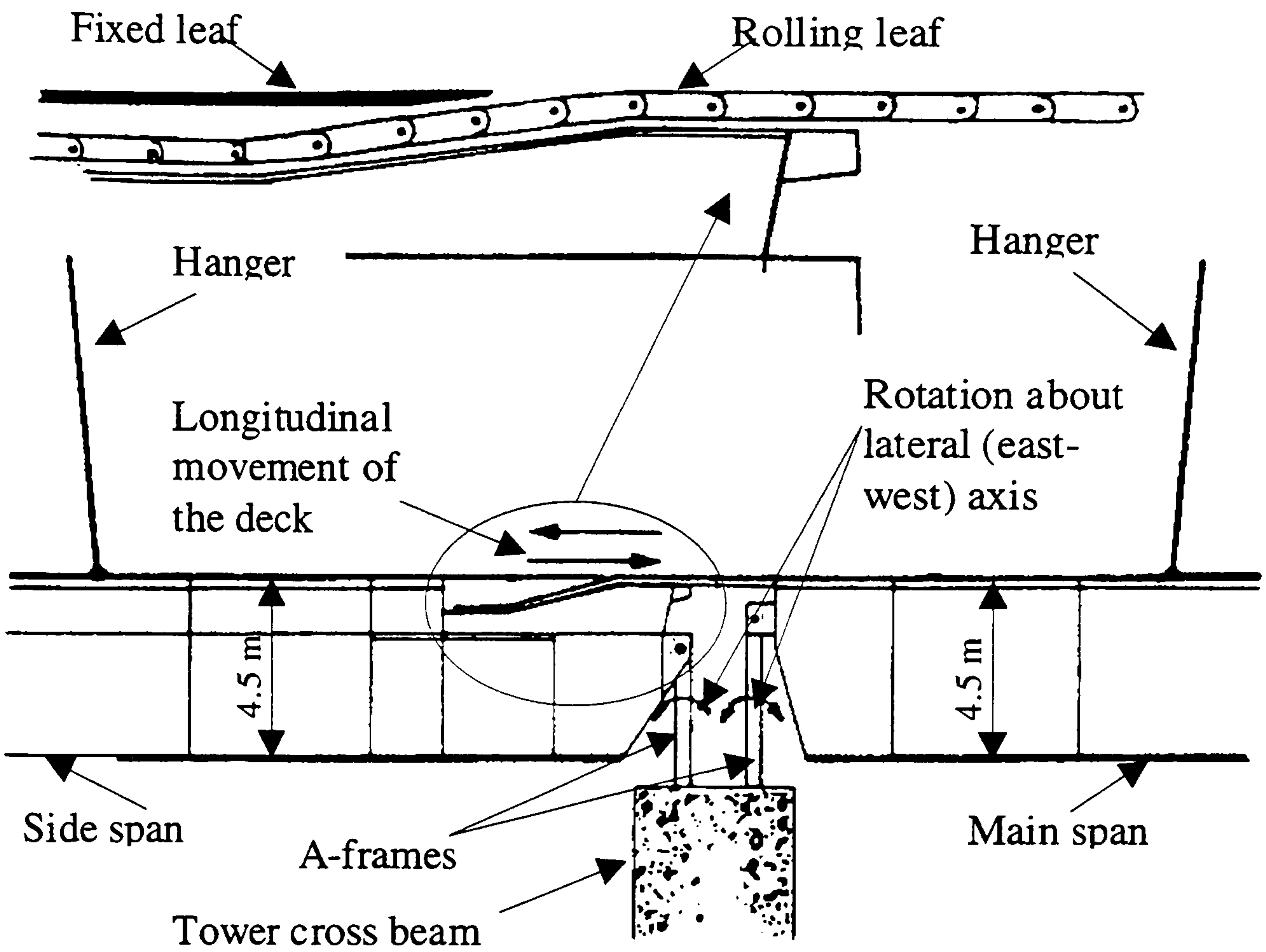

Figure 5k: Longitudinal section of the bridge with A-frame type 2 at the tower (courtesy Humber Bridge Board (1973)).

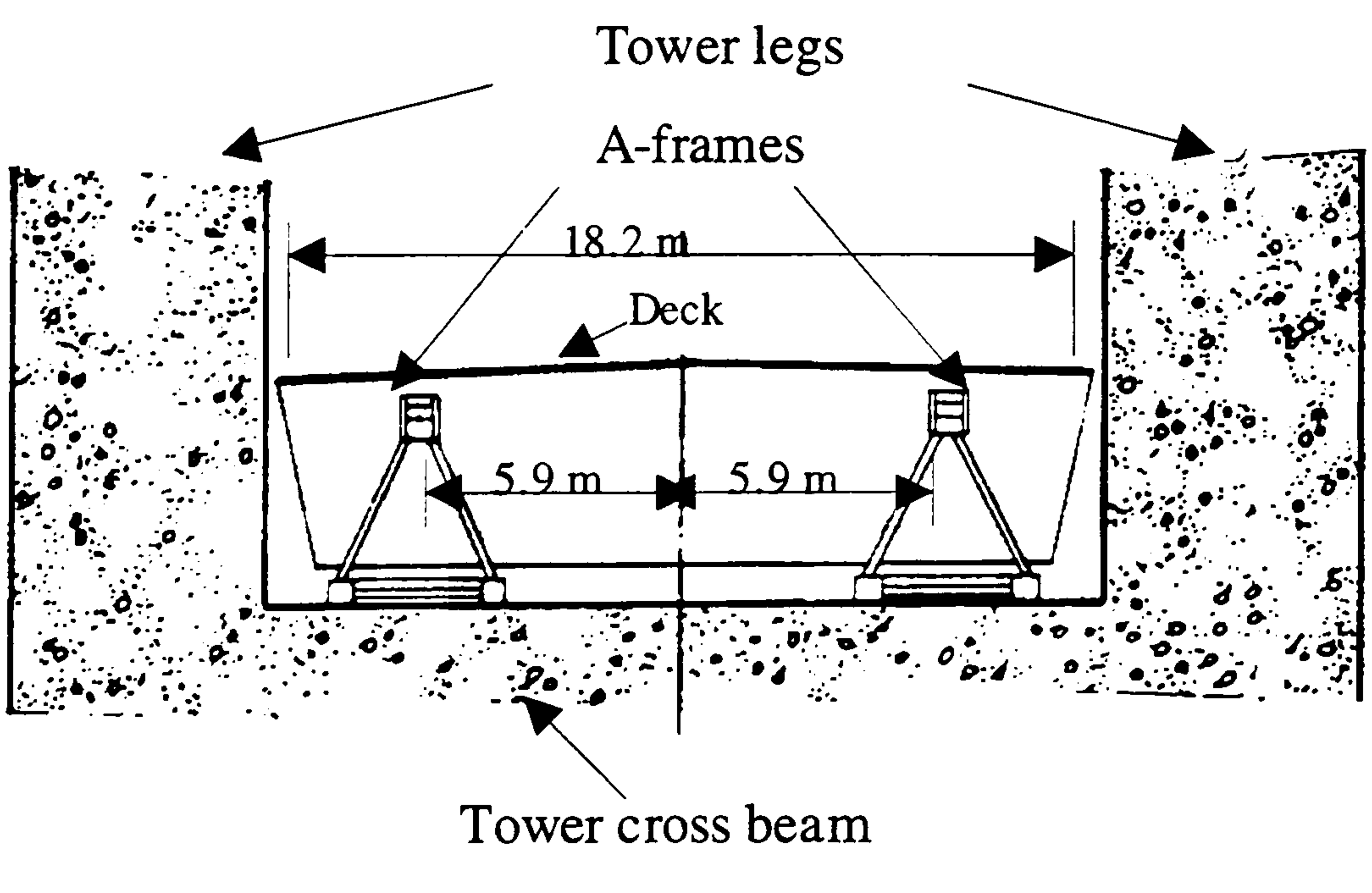

Figure 5l: Cross section at the tower with the A-frame type 2 (courtesy Humber Bridge Board (1973)).

The A-frame bases are placed on top of the cross-beams which connect the east and west legs of the towers. At the Barton tower the joint can cope with the maximum longitudinal movement of 2.8 m caused partly by the traffic loading and temperature. At the anchorages special rubber joints allow for movements whilst maintaining road continuity. Here the A-frames (type 1) are placed on the front of the massive concrete anchor blocks and function in a similar way to those on the towers.

d) The towers

Each tower is a heavily reinforced (ratio of area of reinforcement to concrete area of 6 %) concrete slender (flexible) structure with a height of 155.5 m from the water level and having four cross-beams to connect east and west tower legs. Tower legs are fully fixed within a massive concrete foundation. The main cables pass continuously from north to south through the tower saddles at the tower tops. The tower legs are slightly tapered (at the base 6m x 6m and at the top 4.75m x 4.5m), hollow and one leg in each tower contains a service lift for maintenance purposes. Figure 5m illustrates the general arrangements of the tower.

Lateral loads due to wind and traffic (unsymmetrical loading) at the level of the stiffening deck are transferred by shear and bending into the legs and the cross-beams. The towers with the legs in the vertical plane perpendicular to the bridge axis are relatively flexible in the longitudinal direction. This is favourable for the main cable movement in the longitudinal direction due to different loading conditions. The flexible tower top can move longitudinally up to 725 mm due to traffic, wind and temperature or the combination of those loads.

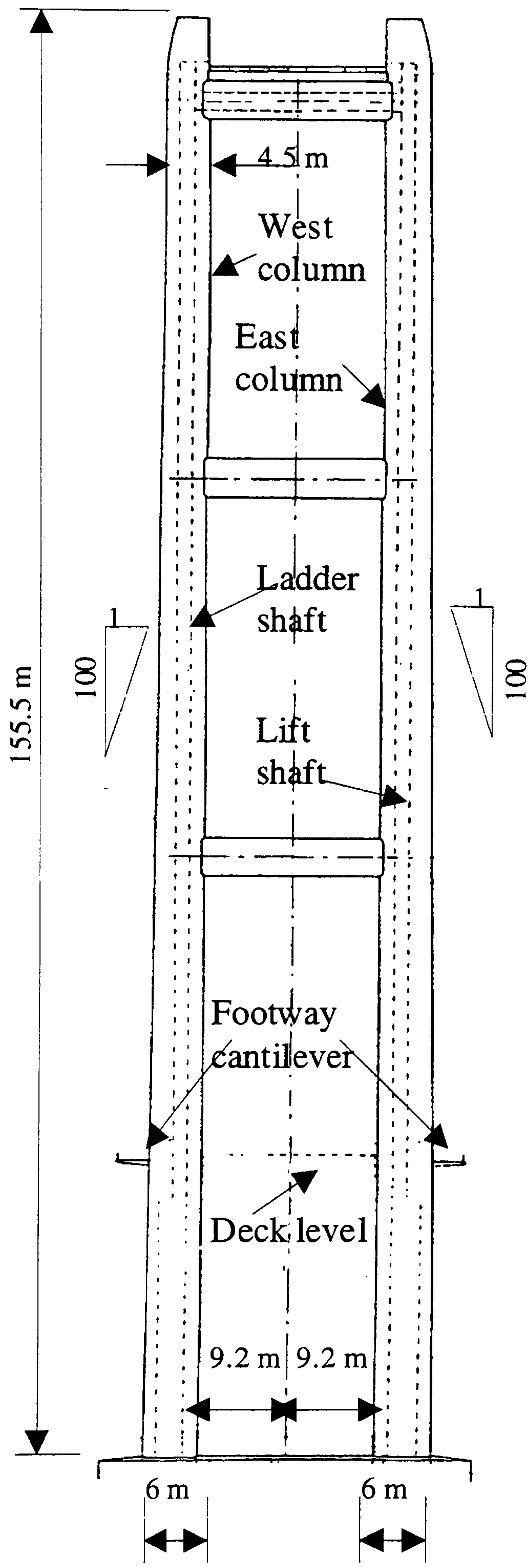

Figure 5m: General arrangements of the tower (courtesy Humber Bridge Board (1973)).

e) The hangers

The hangers play a main role as they transfer vertical, lateral and longitudinal loads from the deck to the main cable. Each hanger has a combination of 6 mm diameter wires in spiral form with the overall diameter of 62 mm. The Humber Bridge has an inclined hanger system, which is one of its special features. The hangers are connected to the cable band using an open socket i.e. the hanger has a socket at the upper end and is pin connected to the cable band. Again open sockets with pin connections have been used between inclined hangers and the stiffened deck. Figure 5n shows the inclined hanger arrangement at the centre of the main span area, where only one hanger is connected to a bracket. This pattern of hanger arrangement (24 pair of hangers) is followed at the centre of the main span area over a longitudinal length of 486 m. Also this figure (Figure 5n) shows the type of pin connection of hanger member with the main cable and the deck. Elsewhere two hangers (towards and away from the centre of the span) are connected to a bracket (refer Figure 5o). The type of hanger connection with the main cable is the same everywhere on the bridge, as shown in Figure 5n.

Some vertical hangers were introduced (with double the cross section area of the other hangers) at the beginning (entrance) and end (exit) of the bridge. At the Barton side three vertical hangers and at the Hessle side two vertical hangers were placed.

Use of an inclined hanger system forms a zigzag net between the main cable and the deck allowing the hysteresis of the helical ropes forming the hangers to contribute to damping out oscillations. Actually damping is a process of energy dissipation in a vibrating system. This is a combination of viscous damping, coulomb (dry-friction) damping and hysteresis damping. For analysis it is customary to adopt viscous damping (though it is not strictly correct), and to select an appropriate amount that will yield the same dissipation of energy per cycle as that produced by the actual damping mechanism. In addition, it is easy to express it in mathematical form as it is in direct proportion to the velocity. Hysteresis damping occurs when materials are cyclically stressed. Energy is dissipated within the material itself, primarily due to internal friction of particles within the material as it is in the process of being stretched and unstretched. During this process there is a lag between the cyclic damping force and the corresponding deformation. The created area (difference between damping forces and corresponding difference between deformation) due to this effect is given as loss of energy by this hysteresis damping effect. This effect is defined in terms of energy loss per cycle and therefore a non-linear function of displacement. Therefore it is not readily taken into account for the analysis. However for convenience it can be expressed as an equivalent viscous damping. For this the energy loss due to the selected viscous damping coefficient is equal to that produced by the hysteresis damping. The zigzag formation of inclined hangers might be considered to provide an effective hysteresis damping to the suspension bridge structure (Brownjohn, 1994). This was the main reason at that time for the introduction of an inclined hanger system. The advantages and disadvantages of the inclined system and alternative arrangements are described more extensively in Chapter 11.

Figure 5n: Type of pin connection of hanger member with the main cable and the deck, where single hanger is connected to the bracket (courtesy Humber Bridge Board (1973)).

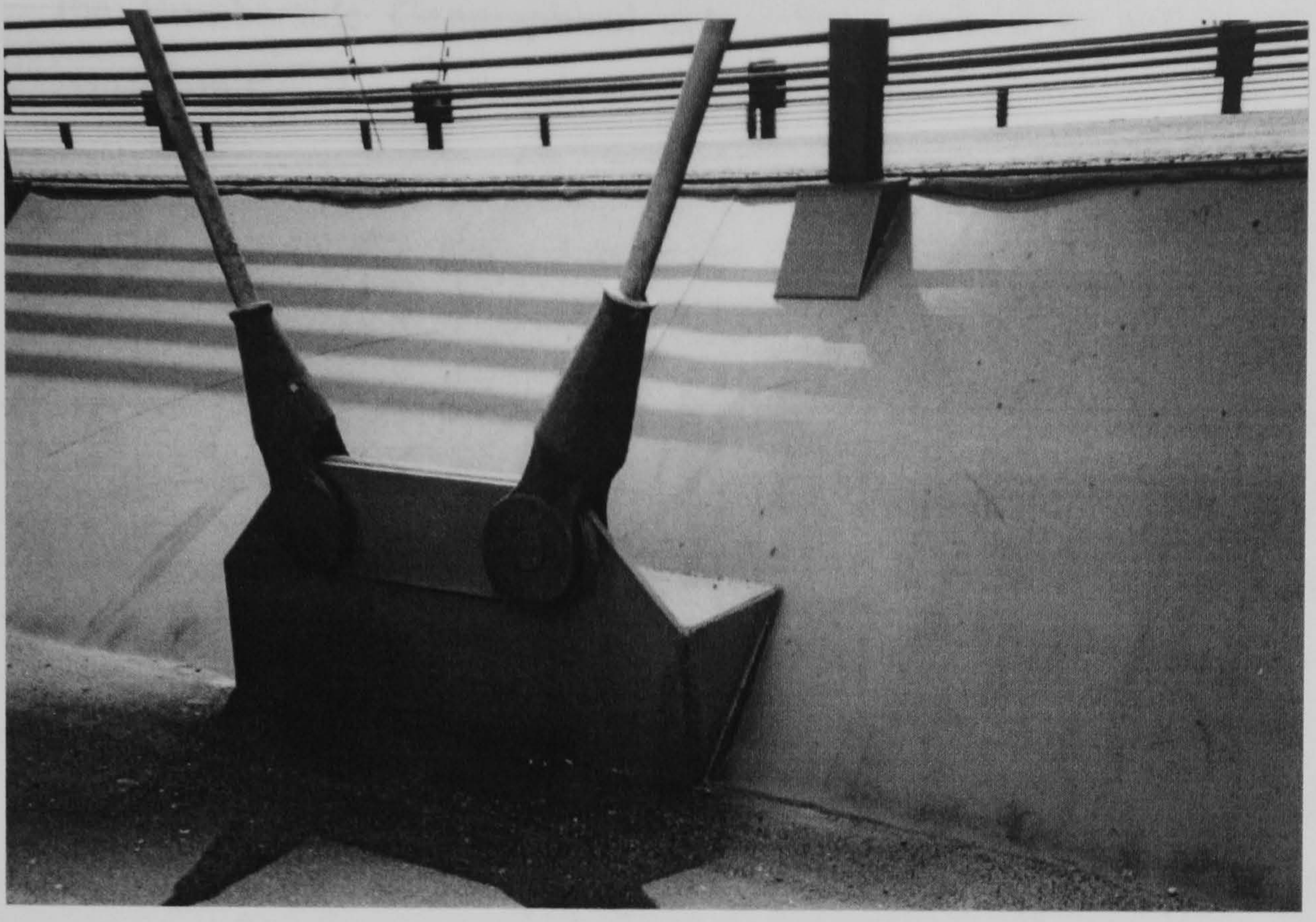

Figure 5o: Type of pin connection of hangers with the bracket, where two hangers are connected to the bracket (courtesy Humber Bridge Board (1973)).

iii) Design loading

The bridge was originally designed to carry highway loading according to BS 153 Part 3A 1954, but the minimum lane load was increased by 50 % over the design period due to increasing traffic intensity (from 5.84 kN/m to 8.76 kN/m). The lane load applied to short loaded lengths was 30.0 kN/m. In addition the bridge can accommodate the maximum HB (Highway "B" loading) special vehicle loading of 180 tonnes. Different traffic patterns and combinations of loading were considered for the design of bridge components. Wind loading is a major consideration for this type of long span flexible structure. Maximum wind speeds of 47 m/sec at the deck level and 66 m/sec at the tower top level have been found in the Humberside area and were used for the design calculations. Wind velocity has been transferred to wind load acting on the deck surface, tower and the main cable. The uplift coefficient, drag coefficient, dynamic factor and design wind speed factors (to be used later) were taken for each component from the Humber Bridge design book. These enable transfer of the wind velocity into wind load acting on each specified component on the bridge structure. In addition to the above loading, thermal loads due to a change in temperature between –20° C and + 50° C were considered from the Humberside Geographical data. Solar gain does not appear to have been considered.

iv) Historic traffic usage data at the Humber Bridge

Annual traffic figures (passage of vehicles) since opening of the bridge (last 20 years) is shown in Figure 5p (The Humber Bridge Board, 2001). To date, 90 million vehicles in different categories have passed over the bridge. The figures show the increment of traffic volume over the years and the necessity of assessment of the bridge against the present traffic intensity. Traffic is categorised into three types as motorcycles, cars & light vans, and heavy goods vehicles. Traffic volume of categorised types (vehicles) are considered for each year and compared with the corresponding volume in the Humber Bridge opening year, 1981. Passage of traffic is calculated in percentage terms and given in graphical form for the total traffic volume (Figures 5p), cars & light vans (Figure 5q) and heavy goods vehicles (Figure 5r). Increasing the passage of heavy goods vehicles gives significant changes in the initially used traffic loading condition. The weight of these heavy vehicles range from 7.5 tonnes to 41 tonnes with the length ranging from 6 m to 11m.

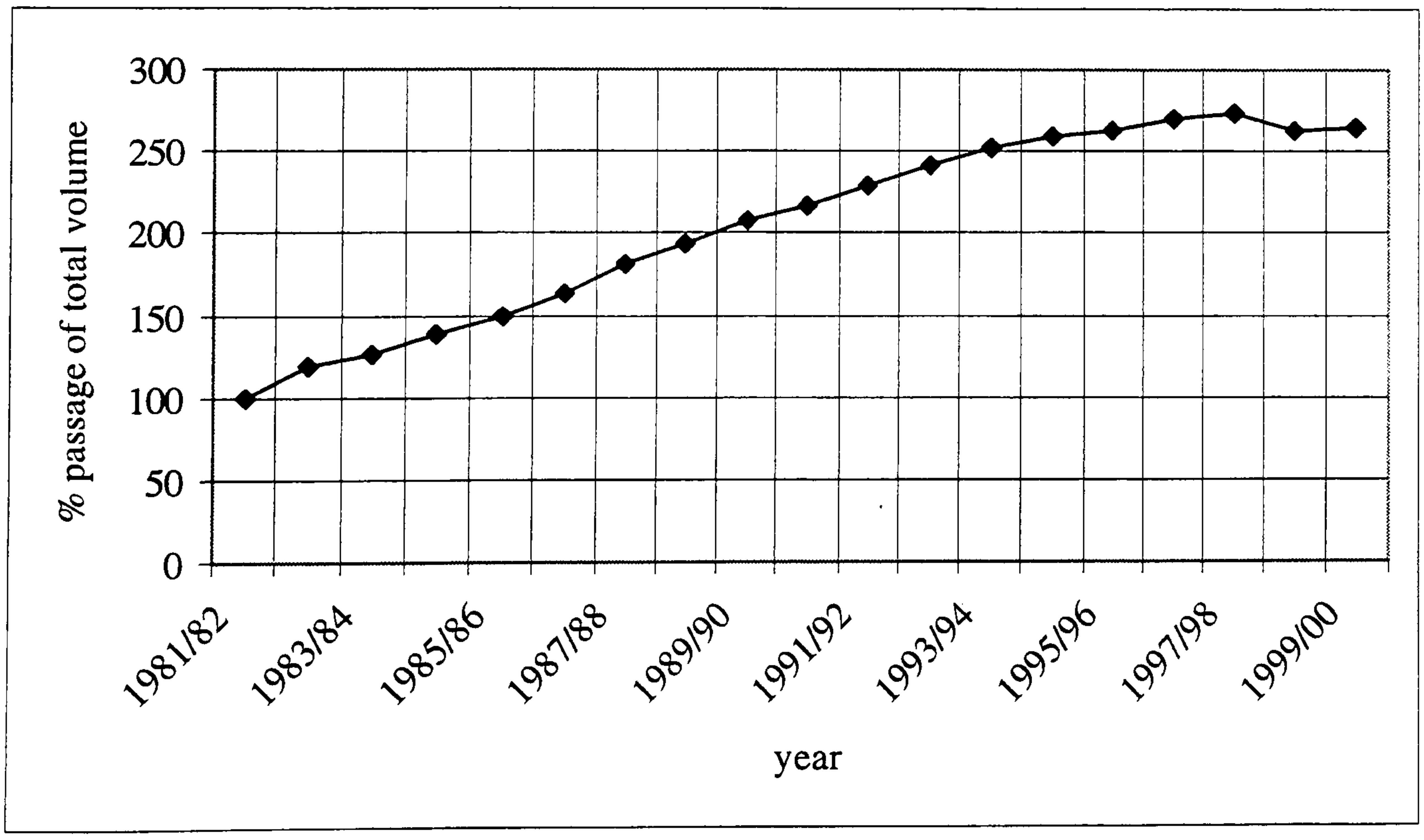

Figure 5p: Passage of total traffic volume in percentage over the last 20 years.

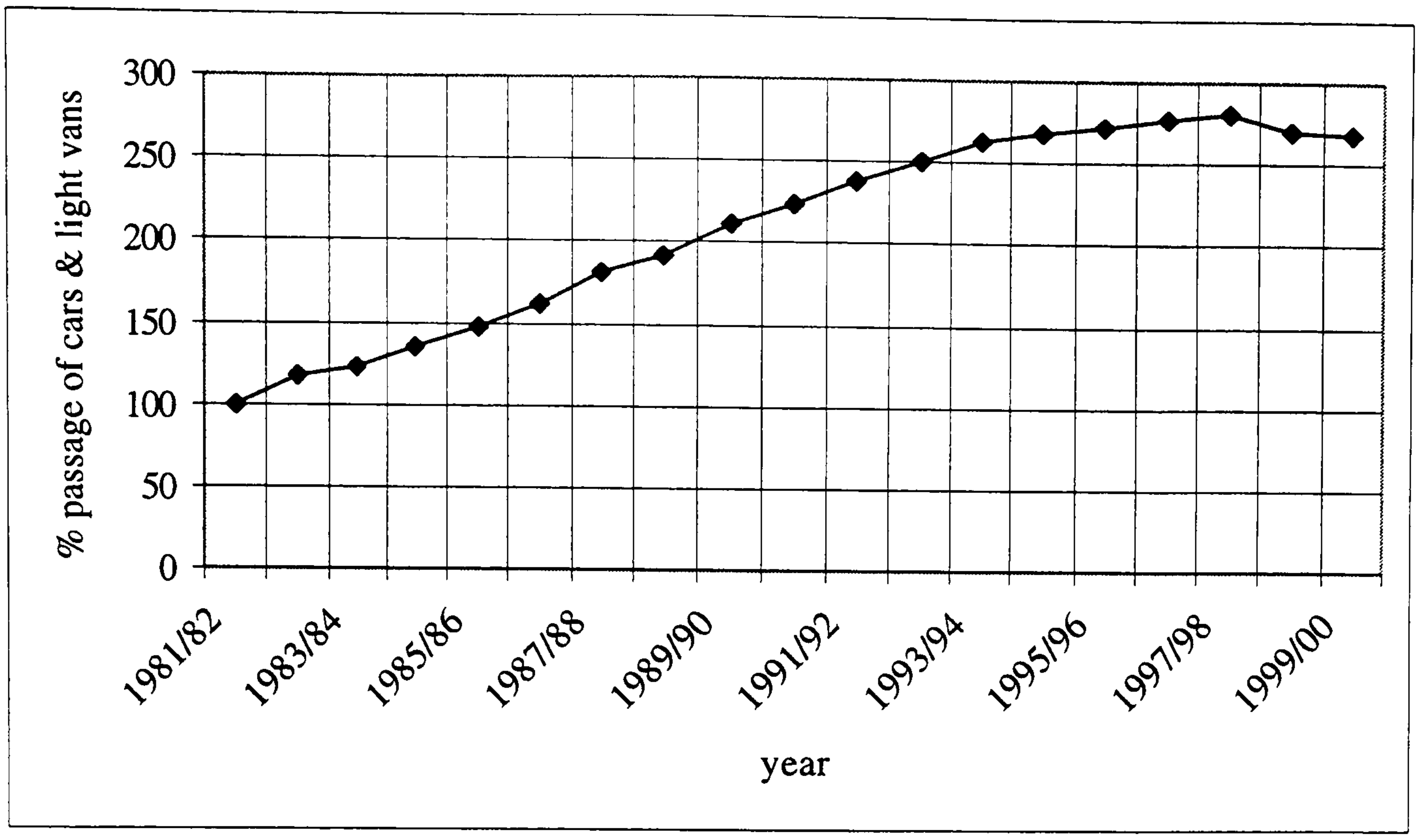

Figure 5q: Passage of cars & light vans in percentage over the last 20 years.

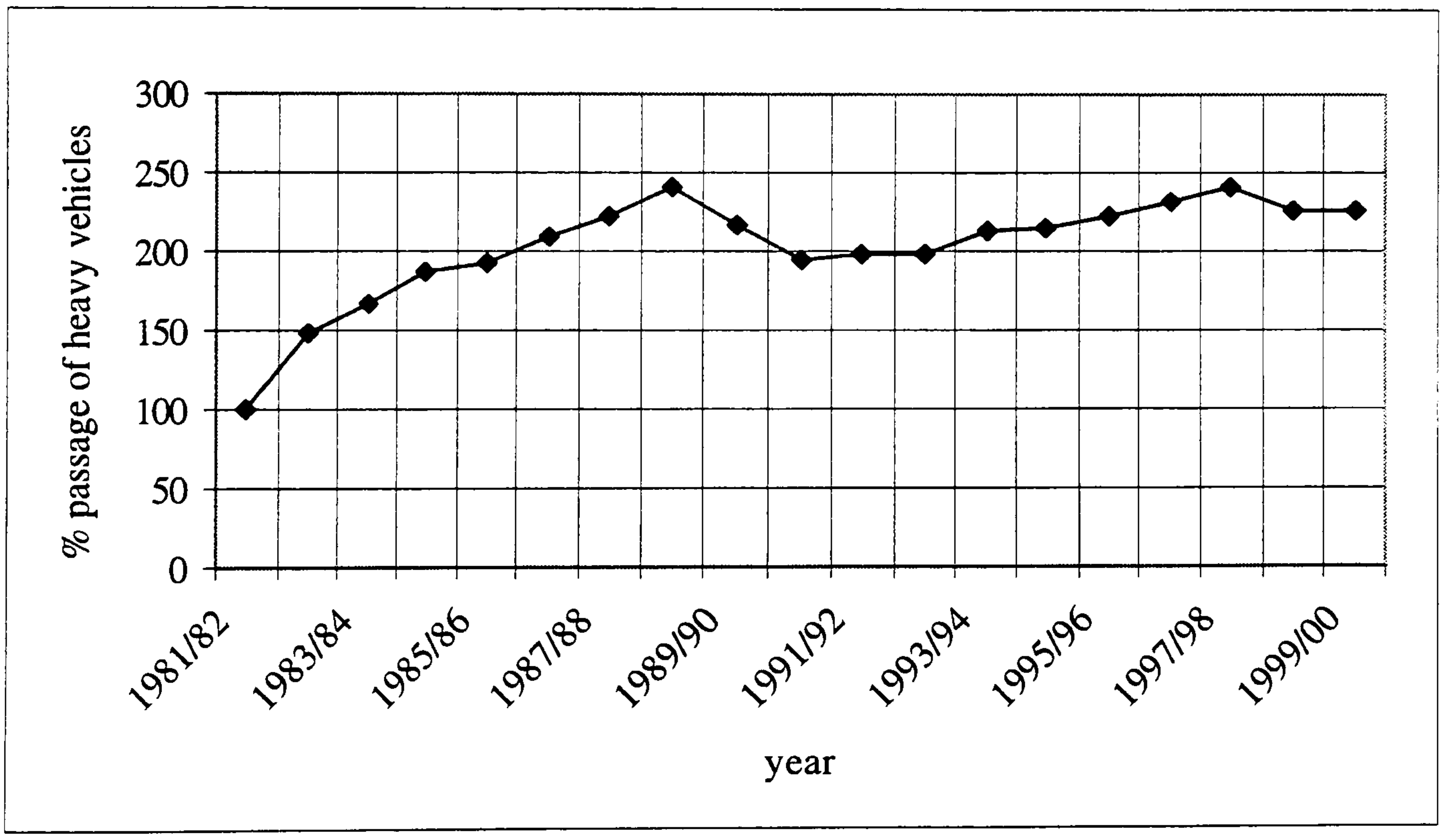

Figure 5r: Passage of heavy goods vehicles in percentage over the last 20 years.

Total traffic volume has increased to 275 % of its original value since opening. Passage of cars & light vans increased to 280 %. The volume of heavy goods vehicle increased to 240 %. Load effect from the heavy goods vehicles gives changes in the calculated traffic loading on the bridge. This effect, 2.4 times the increment of traffic volume with the maximum weight of 41 tonnes per vehicle, leads to a necessity to calculate revised traffic loading on the bridge. This is known as "Bridge Specific Assessment Live Loading" (BSALL) for this particular Humber Bridge. Fairhust & Partners performed a three weeks survey and calculated the new traffic loading (BSALL) condition for the Humber Bridge in 1995. Assessment of the bridge against this loading, and the results, are described in Chapter 10. The finite element models (with validation) created for this research will be useful to the Humber Bridge Board to carry out an assessment of varying traffic loading, from time to time.

Chapter 6

Finite Element Analysis

General

Basic suspension bridge theories are described briefly in Chapter 4. In addition the real need for finite element (FE) analysis is explained in this chapter. The finite element method is a numerical solution technique applicable to a wide range of physical problems. The variables in this analysis can be correlated in the form of algebraic, differential or integral equations. This technique allows dividing a region into number of sub-regions (elements). The solution within each sub-region can be represented by a function to reflect its behaviour. Thus the behaviour of each sub-region can be readily described under different physical (loading) conditions. The sub-regions are joined together, making sure their boundary conditions are compatible with adjacent sub-regions. This method became the most powerful numerical tool available in structural engineering analysis to solve complex problems. Continuity in geometry of the structure, material properties and loading provides accuracy in results. Discontinuities in any of these quantities may be dealt with by smoothed distribution of properties in adjacent members, and hence the results may not be as precise.

The basic steps involved in finite element analysis can be illustrated by the following. Defining the domain physically and geometrically, discretization, and solution are the three primary sources of approximation in the finite element method. The approximation used in defining the physical characteristics of different regions of the domain are very much problem oriented. The process starts by defining the physical nature of the problem (e.g. solid-mechanics, heat-transfer etc). Mathematical description of this physical problem (e.g. deformation of an elastic body) leads to inclusion of a conservation principle (equilibrium of forces), state variables (forces or displacement), material constants (Young's modulus, Poisson ratio, etc.), sources of forces (body forces, surface forces, etc.) and constitutive equations (e.g. Hooke's law). This mathematical interpretation will be formulated into a set of differential equations. The procedure then involves establishing the co-ordinate system where the local (element) and global axes will be defined, after which it is necessary to construct approximate functions for the elements based on the state variable (physical condition) and the shape of the element (geometrical condition). This will lead to formulating the element matrices and equations, and co-ordinate transformation of physical entities in the form of vectors and matrices. Next all the element equations are assembled into an overall equation into which the boundary conditions to the system are introduced.

Structures such as suspension bridges can be modelled and analysed precisely using this finite element technique with geometrically and materially linear and non-linear behaviour. In this research a powerful commercially available package called ANSYS (version 5.3) has been used. Two types of analysis, static and modal have been performed.

i) Virtual work principle

The governing equations of finite element analysis are based on the virtual work principle. This states that for any system in equilibrium a virtual change in the internal strain energy must be equal to the change in external work done by the loads applied to the system.

It can be written as, $\varepsilon^T \sigma \, d(vol) = \delta u^T P_e$

Here the external force P_e and the stress σ are in equilibrium, and the displacement δu and the internal strain ε are in geometrical compatibility. This virtual work principle is applied to each element in the finite element model.

ii) Shape function on element

The displacement of an element relative to the displacements of its nodal points can be given by a shape function. This displacement field is assumed for the most widely used elements. It contributes to form a stiffness matrix, which represents the relationship between force and displacement of each element individually. This can be assembled to form an overall stiffness matrix.

In general terms the displacement function can be written for an element 'e' as $u = \Sigma N_i a_i^e$, where u represents the movement of a typical point within the element in x, y and z directions separately and a_i gives the corresponding displacements of a node i in x, y and z directions. N represents the shape function, its components (say N_i, N_j, etc.) give the shape function relative to each node on the element.

Thus the shape function varies with element shapes such as 2-D quadrilaterals or triangles, and 3-D solid, tetrahedrons etc. Also the shape function depends on the number of nodes on the element. Increasing the number of nodes for the element gives a complex shape function and increases the computer running time. Increasing the number of nodes along a side of an element enable one to model curved sides accurately.

iii) Non-linear analysis

In this analysis geometrical non-linearity only is considered, material properties are assumed as constant. Basically this non-linearity refers to the changes in stiffness of the structure due to the deformation of elements through change in shape and change in orientation. Non-linearity is always present within a structure, but depending on its effect (magnitude) it may be neglected.

A non-linear problem can be resolved by a number of approaches.

The purely incremental approach divides the load into a number of load steps and replaces each into linear analysis. At completion of each incremental solution it creates a new stiffness matrix to reflect the non-linear changes. This approach accumulates error with each load increment and may cause the final results to be out of equilibrium.

The better approach can be described as an iterative process, named the Newton - Raphson method, and drives the solution to equilibrium convergence at the end of each load increment (load sub-step). It brings the difference between the applied load and the restoring loads corresponding to the element internal loads to within a given tolerance. This method evaluates the difference between the restoring forces and the applied loads before making each solution, and then performs a linear solution using this force difference and checks for convergence. If the convergence criterion is not satisfied, it re-calculates the force difference and updates the stiffness matrix (iterative process) and obtains the new solution for convergence. This process is continuous until the problem converges. In summary the non-linear analysis performed using this approach can be described by the following;

a) Defining the number of load steps for a given load case.
b) Within each load step allowing the program to perform a number of sub-steps where the load is applied gradually.
c) At each sub-step performing a number of equilibrium iterations to obtain a converged solution. This convergence depends on the tolerance, which can be set by the user. A lower tolerance produces more accurate results but the computer running time may increase.

Within the Newton-Raphson method a number of approaches are available for obtaining convergence. One approach updates the stiffness matrix at every iteration so that the stiffness of the structure is always based on the tangent of the load-deflection curve at a particular point. In this method additional work is required for repeatedly formulating the revised stiffness matrix. An alternative approach keeps the initial stiffness and does not update the stiffness matrix. Stiffness of the structure during each subsequent iteration is based on the tangent to the load-deflection curve at the beginning of the sub-step. More equilibrium iterations are required in this approach.

iv) Static analysis

Static analysis can be performed with geometric linearity or non-linearity.
Geometric non-linear analysis can be performed with stress stiffening and large deformation effects, which are ANSYS terms described below in the next two sub-headings. In the geometric linear case, e.g. small deflection with small strain analysis, the resulting stiffness changes are insignificant and the stiffness is based on the original geometry. Geometric non-linear analysis with the effect of stress stiffening caters for large strain and / or large deflection effects, where the element shape and orientation are changing respectively. These changes affect element

stiffness and the contribution of element stiffness to global components. Also due to the deformation the points of application of the loads change.

a) Stress stiffening effect

This effect is the stiffening or otherwise of a structure due to its stress state. It couples the in-plane and transverse displacements. This effect has to be considered seriously for thin structures where the bending stiffness is very small compared to the axial stiffness. This effect needs to be included in order to give the total stiffness matrix along with the regular non-linear stiffness matrix produced by large strain or large deflection effects. The stress-stiffening matrix is computed based on the stress-state of the previous equilibrium iteration, so to handle a stress-stiffening problem at least two iterations are required. The first iteration is used to determine the stress-state. Then it will be used to generate the stress stiffness matrix for the second iteration. The number of iterations needed varies depending on how the additional stiffness affects the stresses to get a converged solution.

As these bridge models contain strained cables and a thin plate box deck the out-of-plane stiffness of the cable and the deck elements can be significantly affected by the in-plane stress in the structure. Adding stress-stiffening characteristics (i.e. introducing coupling between in plane stress and transverse stiffness) is essential for this type of structure.

b) Large deformation effect

Large deformations can occur due to a large strain or a large deflection effect.

The changing geometry due to excessive strain is known as the large strain effect. If the rotations are large but the mechanical strains are small (e.g. long slender bar under bending) then it can be identified as a large deflection effect. Due to the large strain effect an element's nodes undergo displacement and this will contribute to the overall stiffness of the structure. It can happen by two ways. They are changes of element shape (element local stiffness changes) and changes of element orientation (transformation of its local stiffness into global component changes). A large deflection effect can create a large rotation, which gives a contribution of element stiffness to the global component through transformation of its local stiffness.

c) Initial strains

The term initial strain is quite often used in this analysis, as the main cables and the hangers are strained in the dead load situation. The strained co-ordinates of the bridge are used for this analysis and are compatible with initial strain values for the main cable and the hanger. In mathematical terms it can be given as $\varepsilon=(1/E)*\sigma + \eta$, where η is the initial strain value, given by $\delta/L0$. The element length L is defined from the node I and J locations and L0 is the zero strain length. The length δ is given by L-L0 and σ is the stress due to the live loads.

In simple terms, the main cables and the hangers are strained on the suspension bridge even under dead load (self-weight) condition. It can be said that there is a value of η always present in the main cable and the hangers. Finding the appropriate initial strain value (η) for the main cable and the hangers depends on the strained (under self-weight) and notional unstrained lengths, L and L0. For a typical design of a cable assisted bridge, calculation through a preliminary analysis produces approximate initial strain values. These initial strains are used in a FE analysis under self-weight condition only. By analysing the results of the deflected shape of the deck and the main cable profile, the initial strain values for the next iteration of the analysis can be obtained. This is a trial and error procedure for finding initial strain values until the required deflected profiles of the deck and the main cable are obtained. The initial strain in the main cables and the hangers are the prime factors in deciding the profile of the newly built bridge under its self-weight.

For an as-built bridge, the final co-ordinates have been fixed under its self-weight. When modelling these types of structures with the final co-ordinates and with unknown initial strain values, the only way of finding the initial strain values of the main cables and the hangers is to bring the deflected form of the structure to its as-built condition from its initial position. This analysis has to be done under the dead load condition and the final results can be achieved by a number of trial and error iterations of initial strain values.

For the FE modelling of the Humber Bridge the initial strain values for the first iteration were taken from the strained (under dead load condition) and unstrained lengths of the main cables and the hangers found in the Humber Bridge Design book. These strain values were always positive, which represents the extension of the main cables and the hangers. The estimated as-built co-ordinates (called the strained co-ordinates) of the bridge were input for the initial analysis. Static analysis was performed under dead load condition and the deflected profile of the structure was noted. The aim of this exercise was to bring the deflected form of the deck and the main cable profile back to zero displacement from its initially assumed position. This was achieved by trial and error with the small changes in the initial strain values. Getting the deflected profile with ideally zero displacement is practically impossible. Fine-tuning of initial strain values of the main cables and the hangers gave the maximum deflection of 47mm on the main span of the deck. This value is negligible compared with the span length of 1410m. The applied (fine-tuned) initial strain values for the main cables and the hangers are compatible with the newly deformed profile.

Working backwards will explain the process in a simplified way. The above mentioned deformed profile (under the dead load condition) gives the new co-ordinates, inputting these co-ordinates with the above fine-tuned initial strain values produces a new model. Performing static analyses on this new model under dead load condition produces the new deflected profile. The new deflected profile gives zero displacement from its initial (new model) position. This reflects that the initial strains of the main cables and the hangers are compatible with the new model co-ordinates under dead load condition. So the conclusion can be made that the initial strain for the main cables and the hangers has been fixed for the new model and also is the appropriate datum level for further analysis. Under this situation there are no unstrained elements on the structure. Applying further loads on the bridge structure will change the strain from its applied initial strain value. The main cable, which is carrying the higher force on the structure, has 80% of its allowable design force from this dead load condition, so that the decision on finding a main cable initial strain value has to be precise. Small changes will produce different main cable force and different deck and main cable profile.

An example has been carried out in Appendix 2 to understand what is initial strain and how it will affect the main cable and the deck profile. A beam simply supported at both ends and connected at a number of points through vertical hangers to the main cable, where the main cable is supported at two points at the same level. Effects on applying different initial strain values to the main cable are extensively discussed.

v) Modal analysis

This analysis provides an understanding of the dynamic behaviour of the structure. The structure will respond in a dynamic manner to different loading conditions such as seismic, wind, traffic movement, blast etc.

The determination of natural frequencies is important in order to avoid resonance. This phenomenon occurs when the frequency of the applied loading corresponds with the natural frequency of the structure. Resonance magnifies the amplitude of the forced vibration of a structure but it also depends on the damping value. Hence it is important to avoid any possible resonance on the structure under dynamic loading. Carrying out a modal analysis on the F.E model and correlating it with experimental data provides a good validation of the dynamic model, which can then be used to carry out further dynamic response analyses more efficiently.

This modal analysis is a characteristic of the system itself and does not depend on the external forces. These characteristics of the system are purely a function of stiffness (elastic properties), mass (inertia properties) and boundary conditions (constraints to the natural behaviour). Eigenvalues and eigenvectors mathematically represent the natural frequencies and mode shapes. Formulating the stiffness and mass matrices using finite elements of the model to represent its behaviour and solving this eigenvalue problem produces the natural frequency values and mode shapes.

Here modal analysis has been performed on the bridge models to determine natural frequencies and mode shapes of the structure. It is a linear analysis and any form of non-linearity will be ignored. A subspace mode extraction method has been used to get the results. For the large set of equations this method is preferable. Eigenvalues and eigenvectors are found using the full, uncondensed equations rather than using condensed techniques such as Guyan reduction. Hence this method is highly accurate and the full stiffness matrix and the mass matrix have been used. It is comparatively slower than the reduction method. Comparisons of natural frequency values with field measurements are described in Chapter 9. These comparisons only confirm the stiffness, mass and boundary condition of the models. The stresses, moments and magnitude of deformation for a particular mode shape have no real meaning. To get the dynamic response of the system i.e. the dynamic stresses, moments and displacements, the dynamic forces have to apply externally. This analysis is called a forced vibration analysis.

Chapter 7

Geometric Modelling of the Humber Bridge

General

The Humber Bridge is a large, expensive and complex 3-D structure. It is important that an accurate method of analysis is developed that can efficiently predict its in-service performance. Also it is important to give maintenance guidelines (such as replacement of hangers, close down of lanes, resurfacing of deck surface etc.) and continuing safety under revised loading conditions.

For this purpose finite element models can be used as a powerful tool to accurately model the bridge behaviour under different loading conditions. Finite element analysis is now a commonly used predictive design tool. While in some mechanical engineering applications prototyping might be feasible, in most civil engineering designs extensive physical modelling is not possible. The assessment of as-built or large important structures therefore requires a somewhat different approach to *ab initio* design processes. Real behaviour represents 'accuracy', and models must be assessed against that criterion.

a) Necessity of different type of models

Three numerical models were developed to assist in the investigation of the behaviour of the Humber Bridge. These were:

1) 2-D simplified model
2) 3-D plate formulation model
3) 3-D box formulation model

Geometrically non-linear large deformation finite element analyses (which are explained in the next section) have been performed to assess the deflected shape, main cable force, hanger force, A-Frame force and stress levels on the deck of the bridge. A model incorporating initial conditions is used to predict natural frequencies and associated mode shapes of the structure. The 2-D model was used for rapid determination of symmetrical load effects. It also produced vertical mode shapes and associated natural frequencies of the bridge. The 3-D plate deck formulation model is a simplified version of the 3-D box deck formulation model. It can accommodate symmetric and unsymmetrical loading conditions, and is appropriate for rapid determination of the effect of unsymmetrical loading cases such as torsion. Vertical and lateral mode shapes and associated natural frequencies are also obtained. The 3-D box formulation model, in addition to the above capabilities, was used to predict the stress levels on the deck and also to give more accurate information about the torsional and wind induced behaviour of the bridge.

b) Geometric non-linearity

As mentioned in Chapter 6 section iv (a), stress stiffening is important as the bridge model contains strained cables and a thin plate box deck, where the out-of-plane stiffness of a structure can be significantly affected by the in-plane stress in the structure. This stress stiffening is a form of non-linear effect where the overall stiffness matrix is changing (by adding the new stiffness matrix due to stress stiffening) and the number of iterations in the solution procedure depend on how the additional stiffness affects the stress to get a converged solution. Therefore the stress stiffening is most pronounced in thin and highly stressed structures.

With this effect the small deformation and large deformation analysis results (vertical displacement of the deck) are compared. Under its self-weight, 1.04 % difference was obtained. The point load condition where the 170 tonnes load is at mid-span gave only 0.3 % difference in results. The uniformly distributed load over half the main span gave 2.7 % difference in results. The large deformation effect becomes necessary in analysis, as the present measurement system called GPS described in Chapter 9 can measure the deflection at a point up to 2-3 mm in accuracy. The Bridge Specific Assessment Live Loading (BSALL) for this particular Humber Bridge, which is described in Chapters 5 and 10 produces up to 3.2 m vertical displacement at the centre of the main span. This will give a difference in results of 86 mm, which is measurable. So this is clearly showing the effectiveness of considering the large deformation effect in this analysis.

c) Modelling of the bridge components

i) Modelling of the main cable

A spar (cable) element, which does not accommodate bending stiffness, is used to represent the main cable in each model. The main cable was constructed with a number of 6mm diameter wires. The bending stiffness due to the combination of these wires is ignored in this modelling. This is reasonable because it is an extremely long continuous cable and its contribution of bending stiffness to the structure is negligible.

Both ends (Hessle and Barton side) of the main cables are connected to the anchorage chambers through tower saddles and splay saddles (described in Figure 5f *et seq.* above). The anchorage chamber and the splay saddle are situated close to each other. The main cables are divided into number of separate strands as they pass through the splay saddle and are bolted with the anchorage chamber. In modelling, the main cable movement has been restrained in x, y and z directions at the anchorage chamber. At the splay saddle, the main cable movement due to slipping has been ignored, as it is negligible. The main cable movement at this point is dependent on the movement of the vertex of the splay saddle. It can move longitudinally (x direction). The lateral movement (z direction) is fully restrained (refer Figure 7a). At the tower saddle, the main cable has a pin connection with the tower top. Thus the tower top movement due to flexibility and the main cable movement at that point are compatible with each other.

For the 2-D model a spar element type has been used throughout (Link1, Ansys manual 1995). It is a uniaxial tension-compression element with two translational degrees of freedom at each node, translations in the x and y directions. This element accommodates stress stiffening and large deflection capabilities. It also has the facility to accommodate the initial strain value. The main cable is under pre-tension at its initial stage (i.e. under self-weight condition). Therefore the introduction of an initial strain value to the spar element is necessary. The main cable will remain in tension during any loading condition so it is appropriate to use this 2-D spar element. Figure 7a shows constraint details and the splay saddle arrangement at the main cable end.

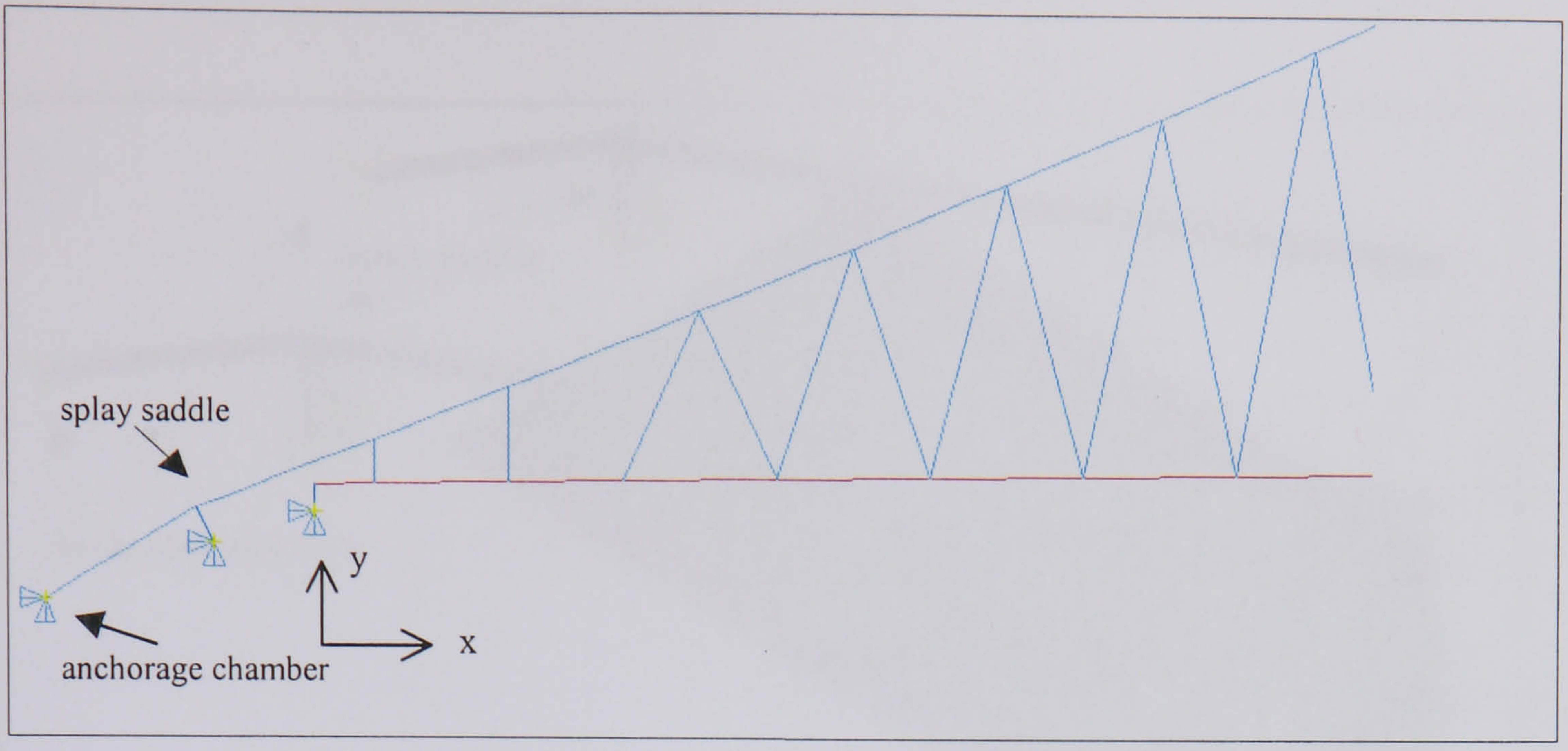

Figure 7a: Constraint and splay saddles details of the 2-D model at the main cable (Hessle) end

For 3-D models a spar element type has been used for the main cable (Link8, Ansys manual 1995). This element has stress stiffening and large deflection capabilities. Link8 is also a uniaxial tension-compression element with three degrees of freedom at each node. They have translations in the nodal x, y and z directions. This also has the facility to accommodate the initial strain value. As mentioned before, the main cable is always under tension so it is an appropriate element to use. Figure 7b shows constraint details and splay saddles arrangement of both 3-D models at the main cable end.

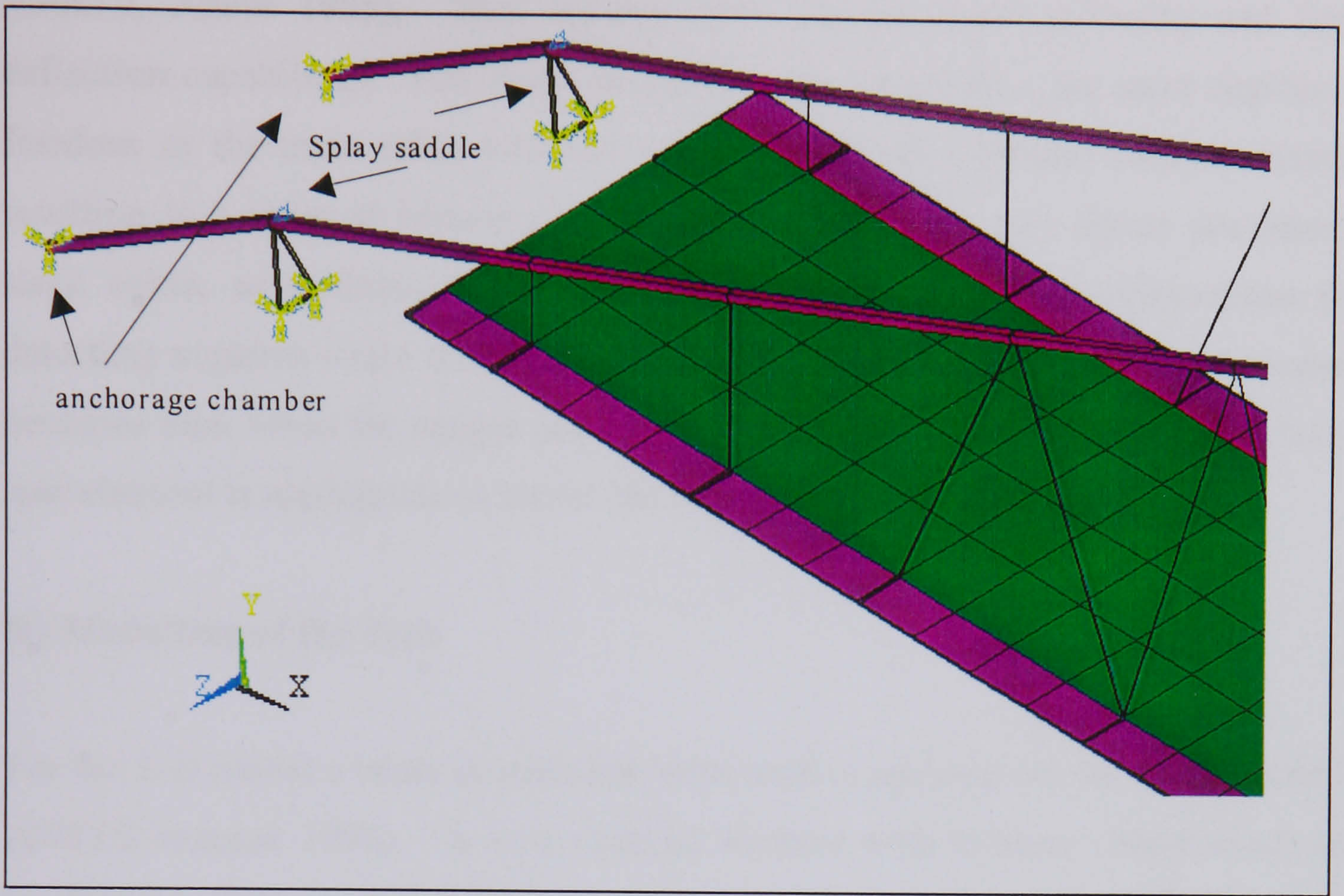

Figure 7b: Constraint and splay saddles details of the 3-D model at the main cable end

ii) Modelling of the hanger

Hangers are connected to both the deck and the main cable using a pinned connection. The load on the deck is transferred through the hanger to the main cable. There are no unstrained hangers in the structure even under its own weight.

For the 2-D model a spar element (Link1), has been used to represent the hangers. The introduction of an initial strain to this element is necessary because the hanger is under tension at its initial state i.e. under only self-weight.

Since this element possesses stiffness in either tension or compression it will predict compression when in reality the hanger would be slack. However, this is not a major deficiency since hangers seldom go slack. Nevertheless it is theoretically possible such a situation may arise when a heavily loaded vehicle moves along the bridge during a high wind-loading situation, and analyses using this 2-D model should be checked to ensure no compressive loads result. If compression results, a further iteration will be necessary.

For the 3-D model a spar element type has been used to represent the hanger (Link10, Ansys 1995). This element also has the stress stiffening and large deflection capabilities. The elements used for the hanger have the same degrees of freedom as the main cable with the unique feature of a bilinear stiffness matrix, resulting in a uniaxial tension only element. The tension only option simulates a slack cable, as stiffness is removed if the element goes into compression (by detecting negative strain on the element), so the tension force value of the element becomes zero when the hanger gets slack. Unlike the 2-D spar element the Link10 spar element is appropriate to model the hanger in the 3-D situation.

iii) Modelling of the deck

For the 2-D model a beam element has been used to represent the box deck (Beam3, ANSYS manual 1995). It is a uniaxial element with tension, compression and bending capabilities. It has three degrees of freedom at each node, translations in the local x and y direction and rotation about the local z-axis. It also has the stress stiffening and large deflection capabilities. The box deck is represented by a beam with the actual cross sectional area and the actual second moment of area for vertical bending.

For the 3-D models the box deck is represented by four noded shell elements (Shell63, ANSYS manual 1995). They have both bending and membrane capabilities and also have the stress stiffening and large deflection capabilities. The element has six degrees of freedom at each node, translations in the x, y, and z directions and rotations about the x, y, and z-axes.

In the simplified 3-D model the whole box deck is idealised by a set of flat shell elements. The following procedure is adopted: the thickness of the deck plate has been found according to the actual second moment of area about the major axis (Iyy).

The actual Iyy of the deck is 37.07 m^4 and the width of the deck plate in the model is 28.5 m. Thus the effective thickness of the deck plate (t) in the model is 0.0192 m.

According to the thickness t (0.0192 m) and the width 28.5 m, the second moment of area about the minor axis for the deck plate in the model has been calculated, which is 1.681e-5 m^4. This second moment of area value is called as Ip_{xx} which is related to the element local co-ordinate system, refer Figure 7c. The actual second moment of area about the major axis (Ixx) of the deck is found as 1.94 m^4. This actual value has been given to the model by introducing the RMI value. The RMI value is the ratio of second moment of area between the actual deck (I_{ZZ} = 1.94 m^4) and the deck plate (Ip_{xx} =1.681e-5 m^4), which is 115407.6. The weight per unit length of the deck has been adjusted by introducing the suitable density value as the width and the thickness of the deck plate has already been fixed.

The 22 m wide highway is meshed into four to represent the 5.5 m width of lanes. Both side 3.25 m footways are also modelled with the same element type.

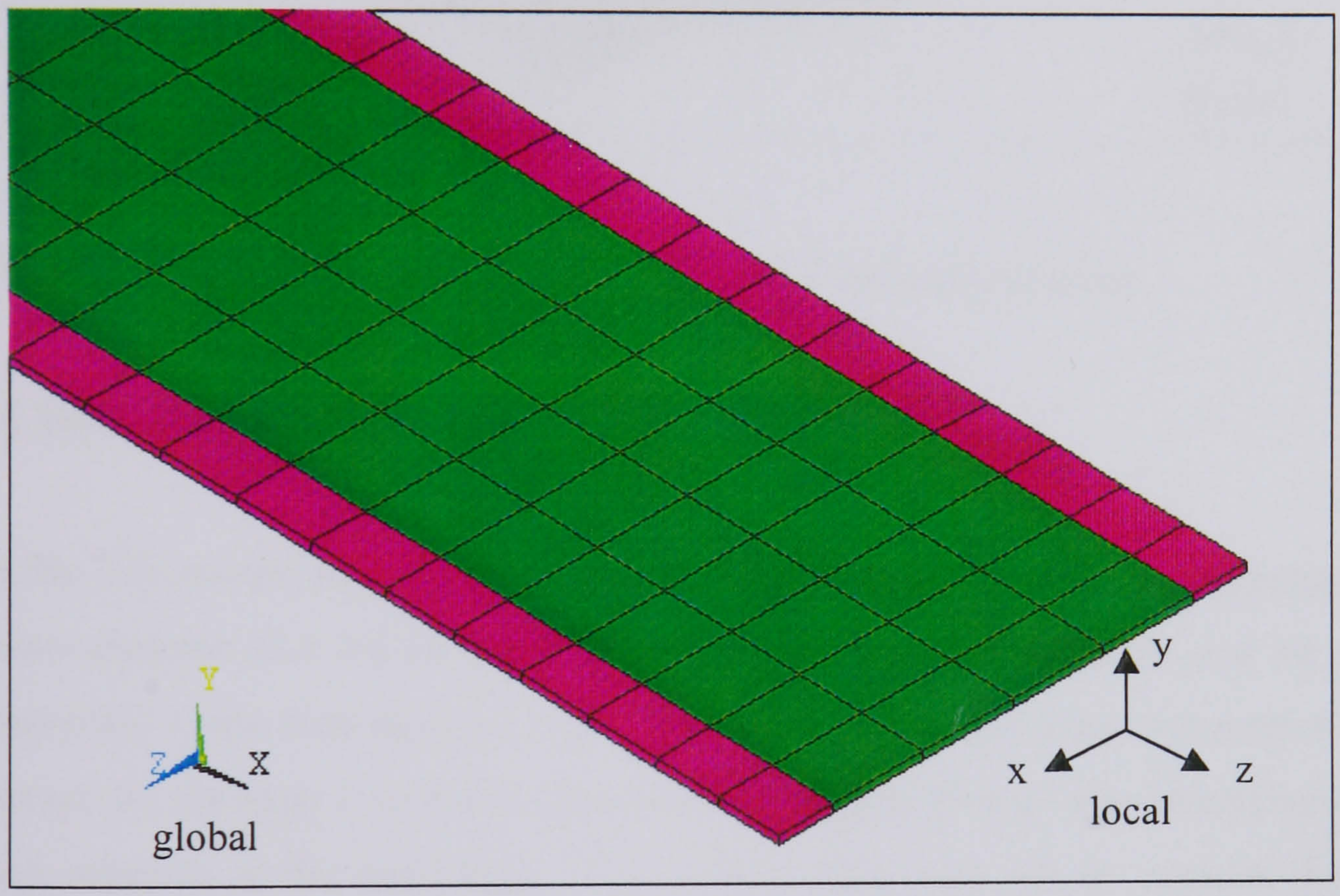

Figure 7c: Simplified plate deck with footpath in both sides

In the 3-D box formulation model, the deck is modelled in more detail. As the top plate, side plate, bottom plate and diaphragm of the box have stiffeners in both directions (refer chapter 5: Figure 5h & 5i on page 36), these are idealised as mentioned above with the equivalent thickness and the second moment of area values. Figure 7d shows one-deck component which is 18.1 m long and 28.5 m wide where the top plate has been removed to see the diaphragm arrangements.

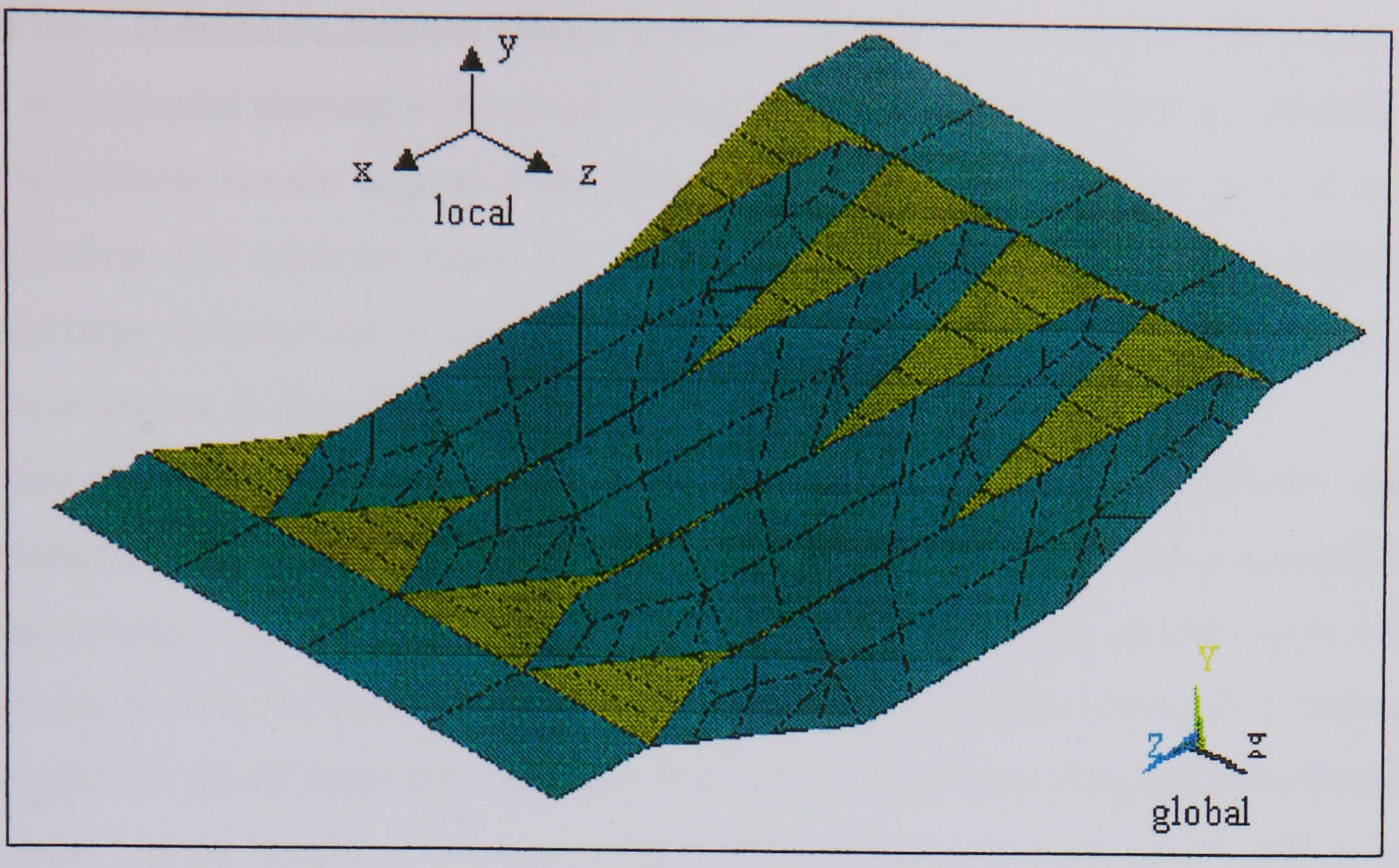

Figure 7d: Deck component where the top plate has been removed

iv) Modelling of the A-Frame

In the 2-D model, the A-frame is modelled with Beam3 and Link1 elements. The beam element (0.3 m) of the A-frame is connected to the deck, and the pin is connected to the link element. The link element then has a pin connection to the ground for the type 1 A-frames (described in chapter 5) that were identified as side span supports at the anchorage. The A-frame base only allows rotation about the global z-axis, which in turn allows longitudinal movement along the x-axis and slight vertical movement in the y direction of the deck. The A-frames closer to the tower (that is, type 2 described in chapter 5) were identified as side span support at the tower or the main span support. The type 2 A-frames are situated on the tower cross beams, so that the A-frame base is coupled with the tower cross beam as shown below. The behaviour described above will model the A-frame mechanism. This spar element can carry tensile and compressive forces depending on the loading condition.

In the 3-D models a Beam44 (Ansys manual 1995) element is used for the A-frame. It is a uniaxial element with tension, compression, torsion, and bending capabilities. The element has six degrees of freedom at each node: translations in the x, y, and z directions and rotations about the x, y, and z-axes. It also has the stress stiffening and large deformation capabilities. In addition to these it has the facility to release the rotational degree of freedom at nodes.

Here the A-frame is modelled with a 0.3 m length of vertical rigid beam and a triangular part. For the type 1, as mentioned before, the A-frame base is supported to the ground. For the type 2, the A-Frame bases are supported on the tower cross-beams, so that the A-Frame base nodes are coupled to have freedoms of identical magnitude (in all directions and rotations) with the corresponding tower cross-beam nodes. As the bottom of the legs of the A-frame (triangular part) are pinned i.e. only allowing rotation about the z-axis (the deck can only move longitudinally along the x-axis and have slight vertical movement in y direction) the rotational constraint about the z-axis has been released. Thus for the vertical rigid beam, the lower end rotation has been allowed to rotate freely about the z-axis.

From the above modelling arrangement on the deck end, longitudinal movement in the x direction, slight vertical movement in the y direction and rotation about the z-axis (transverse) is possible. The lateral movement at the deck end is completely restrained. These arrangements will satisfy the function of the A-frame. Figure 7e & 7f show the A-frame arrangement of the 3-D model.

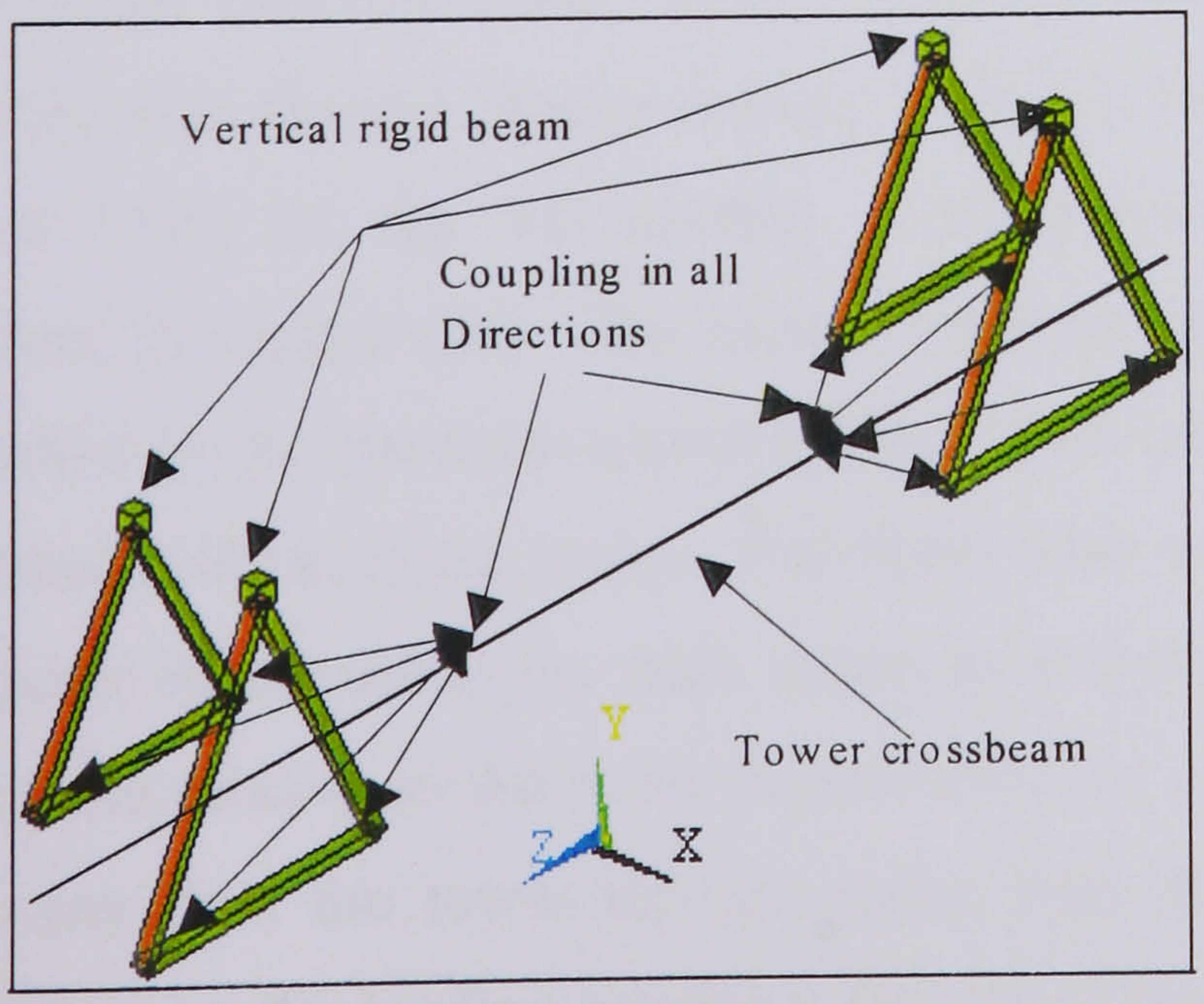

Figure 7e: A-frame models (type 2, side span support at tower cross beam)

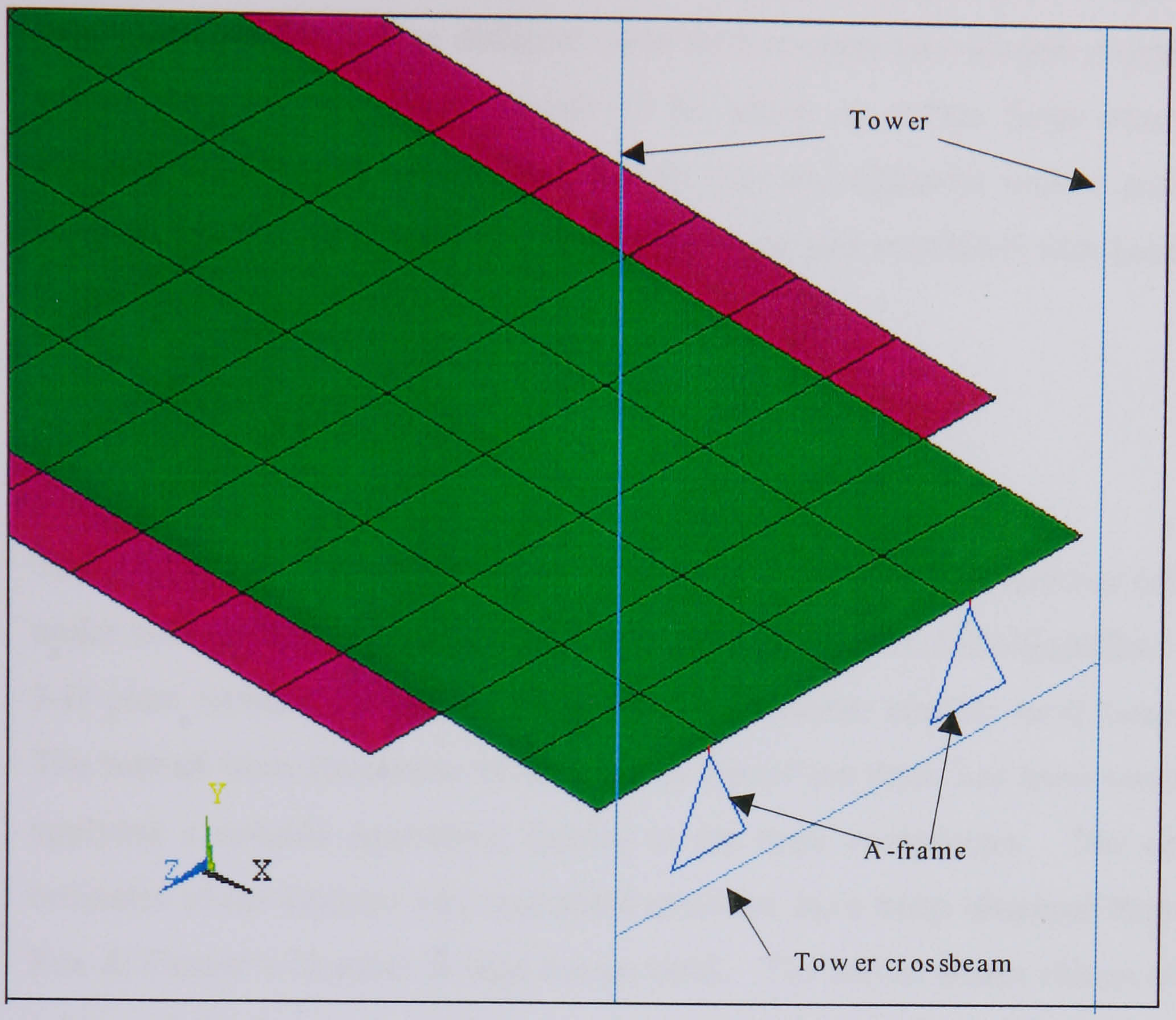

Figure 7f: A-frame model arrangement (type 2, side span support at tower cross beam)

v) Modelling of the tower

The slender, concrete tower, with a hollow section for each leg for lift access is modelled with Beam3 (Ansys manual 1995) for the 2-D model and Beam4 (Ansys manual 1995) for the 3-D models. Capabilities of Beam3 elements have been described in section (iii). The Beam4 element has similar capabilities as Beam44 (described in the previous section), but it does not have the facility to release the rotational stiffness at the nodes. The tower base is completely fixed. The tower top is directly connected to the main cable, as it is assumed that the movement of the main cable relative to the tower is prevented by a high level of friction. Since the tower can flex, the tower top can move with the movement of the main cable. Depending on the loading condition the tower top can move 'inward' or 'outward' relative to the main span. As the tower legs are tapered (at the tower base 6 x 6 m and at the tower top 4.5 x 4.75 m) averaged cross section area and second moment of area values are used. Five different cross section areas and second moments of area values are used through the height of the tower as it has three cross beams at different levels which are connecting both legs and different hollow areas between the deck level to the ground. The crossbeams are also modelled with beam elements in the same way as the tower.

d) Modelling of the full bridge

The structure has been fully modelled to analyse the global behaviour of the bridge under different loading conditions. Three types of models, 2-D simplified 3-D plate formulation and 3-D box deck formulation models have been prepared. The asphalt layer (thickness of 40 mm) on top of the deck has been represented by applying a suitable equivalent density to the deck component. The original co-ordinates of the strained and unstrained structure have been obtained from Freeman Fox & Partner's Humber Bridge design book. The initial strain values of the main cable and the hanger at different locations have been calculated from these given unstrained and strained co-ordinate values. It has been noted that the hangers closer to the towers and at both the Hessle and the Barton deck ends, have higher (at least twice the value of middle span) initial strain values. This is because pulling the deck upward (under self-weight condition) reduces the compressive force acting on the A-frames. The main cables have a slightly higher (at least 10 % higher than at middle span) initial strain value at tower tops. This is due to a steeper slope of the main cable on the side spans than for the main span. There is clearly no unstrained position for the bridge, as the self-weight is such a significant proportion of the total load. Application of gravity loading gave a deflected form which was required to match the given initial strain data. This process cannot be validated until the geometry of the final as-built structure is known. There were some trial-and-error iterations carried out with minor adjustments on the main cables and the hangers' initial strain values to get an acceptable deformed profile of the deck and the main cables. Degree of freedom constraints are applied as mentioned previously at the tower bases, main cable ends and at the A-frames.

The total weight of the structure (76158.2 tonnes) has been calculated from the Humber Bridge design book (internal). These results were compared with the

ANSYS vertical reaction force (76150.6 tones) values (total) for each model under self-weight loading. Good agreement was obtained; all three models gave approximately 0.01 % (7.6 tones) difference in results.

i) 2-D simplified model

The 2-D simplified model (Figure 7g & Figure 7h) has 745 nodes, 981 elements and 1725 d.o.f., and it is appropriate for the rapid determination of some of the principal forces and vertical mode shapes and associated natural frequency values. Only symmetric load cases along the longitudinal axis can be applied to the structure. Obviously it is easy and quicker to model, with no need to deal with meshing of areas or shell elements and less computational time and capacity to get the output results.

Figure 7g: Enlarged view on 2D model at Hessle tower

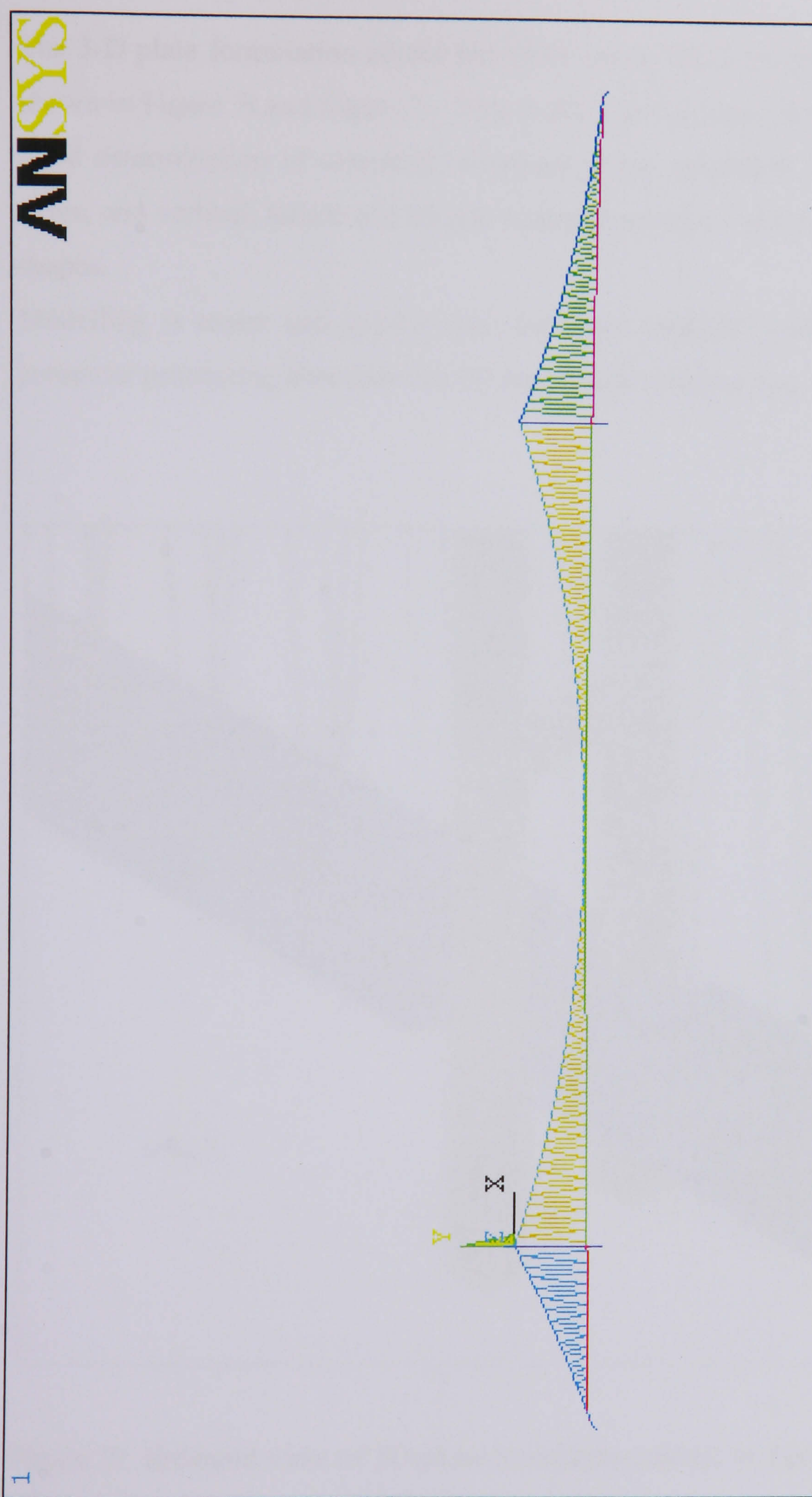

Figure 7h: 2D model of the Humber Bridge

ii) 3-D plate formulation model

The 3-D plate formulation model has 3949 nodes, 5676 elements and 22000 d.o.f., shown in Figure 7i and Figure 7j. This model can be used, unlike the 2D model, for rapid determination of structural behaviour under symmetric and asymmetric load cases, and vertical, lateral and hanger natural frequency values and associated mode shapes.

Modelling is easier and quicker than the more detailed model but it needs more computer processing time than the 2D model as it involves area meshing.

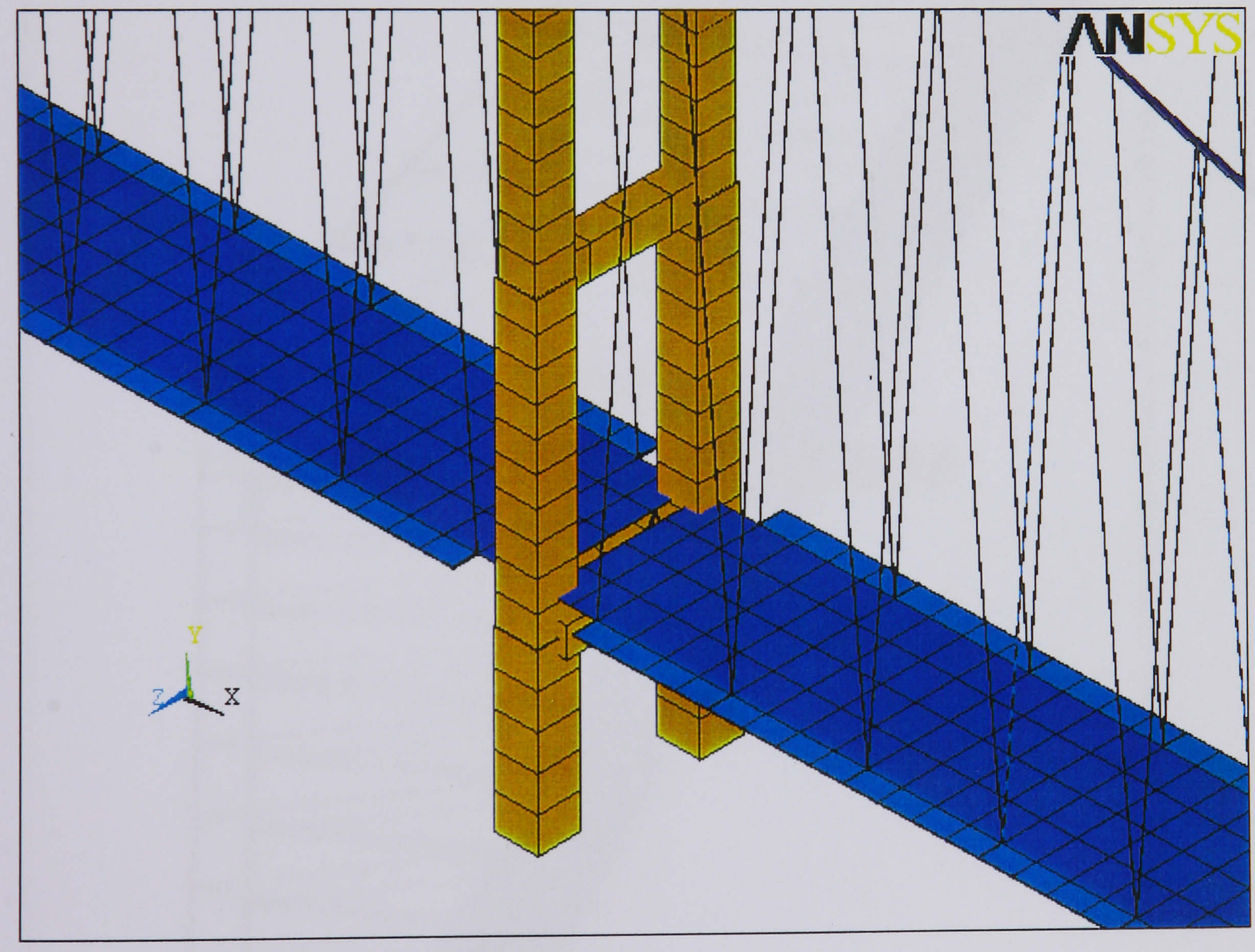

Figure 7i: Enlarged view of 3D-plate formulation model at the Hessle tower (Note: the tower is actually modelled using beam elements)

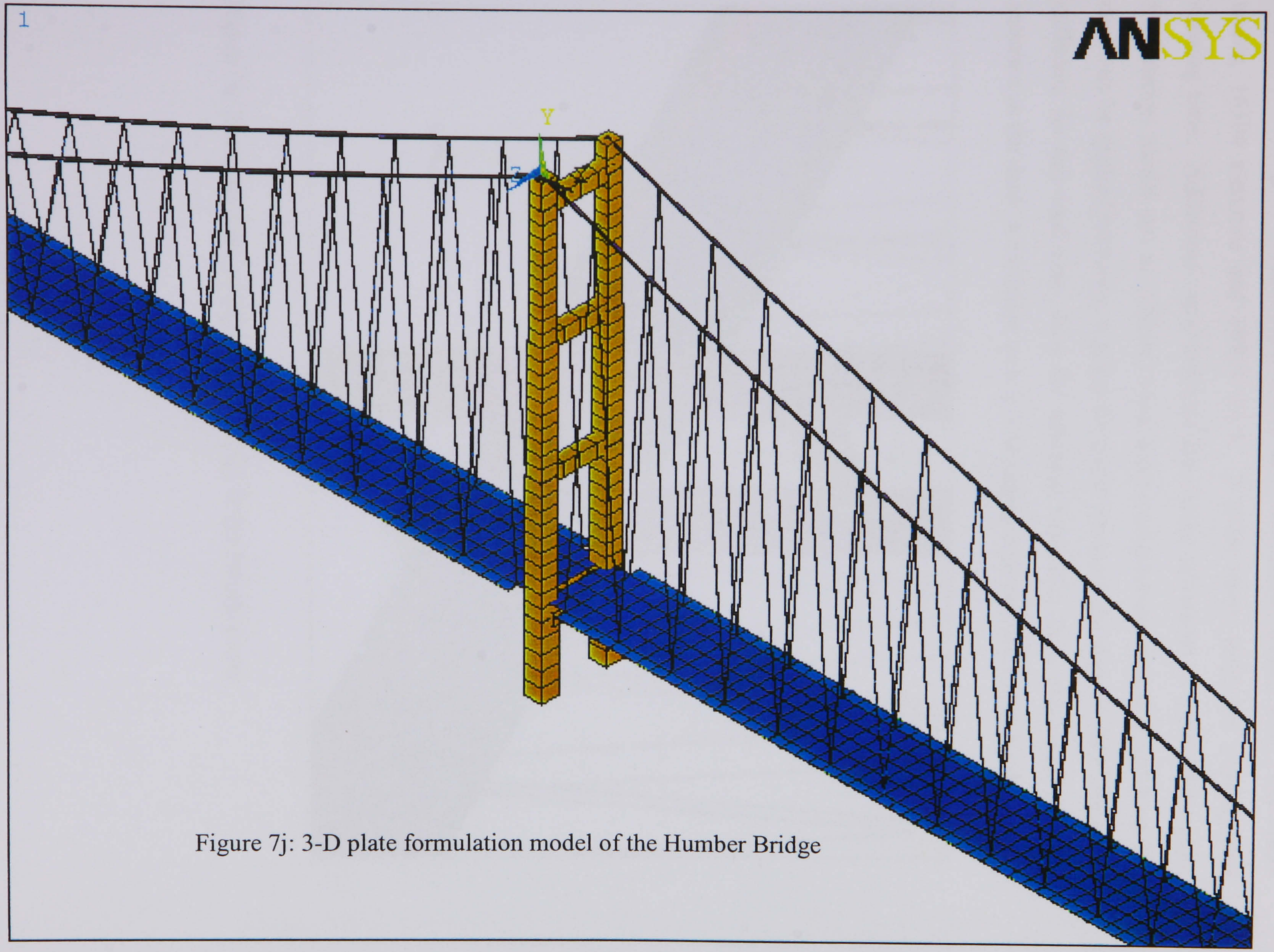

Figure 7j: 3-D plate formulation model of the Humber Bridge

iii) 3-D box deck formulation model

Figure 7k and Figure 7l show the 3-D box deck formulation model, which has 11659 nodes, 16304 elements and 68924 d.o.f. It takes more computer capacity and running time. Additional capabilities of this model compared to those of the plate formulation model are as follows; wind force components, drag and uplift on the deck can be applied precisely, it gives the stress levels on the deck surface and in the stiffeners for any load case. Also the torsional behaviour from this model is more accurate as the deck is modelled as it is with trapezoidal box section and stiffeners.

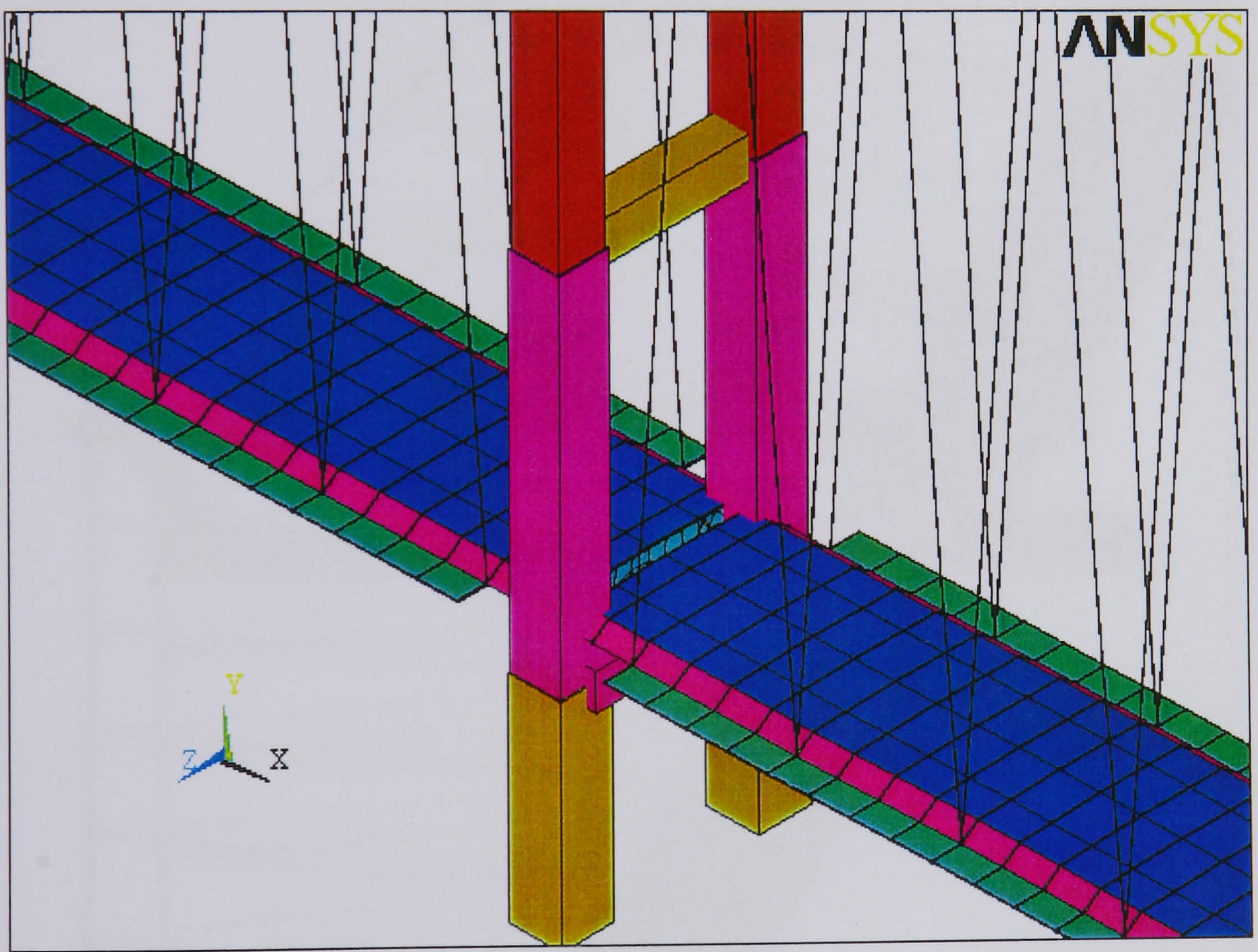

Figure 7k: Zoom up view of 3D detailed model at the Hessle tower

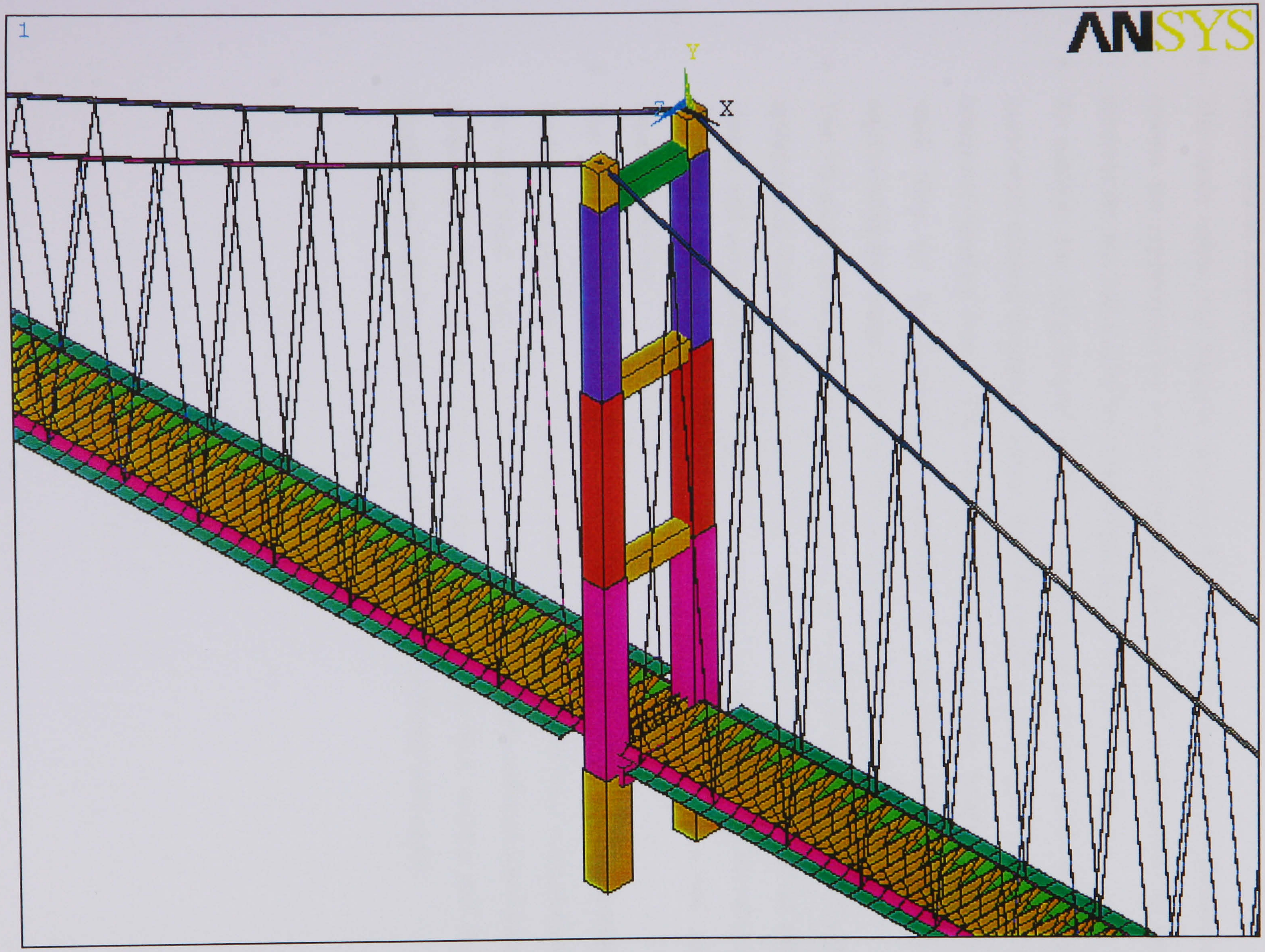

Figure 71: 3-D box formulation model (the top deck plate has been removed) of the Humber bridge

Summary of findings

- 2-D, 3-D plate formulation and 3-D box formulation models have been created, and according to the loading arrangement and computer capacity the required model can be selected.
- The main cable and hangers are represented by spar elements. A-frames and towers are represented by beam elements and the deck is represented by beam element for the 2-D model and shell elements for the 3-D models.
- To analyse for symmetrical loading conditions and vertical mode shapes and associated natural frequency values, the 2D model is preferable, as it will save computer-running time. The only limitation is that when hangers want to go slack they act as compressive members, as the Link1 element, which is representing the hanger, does not have the tension-only capability.
- The 3D-plate formulation model is one step up on the 2D model. This will allow symmetrical and asymmetrical loading, and produce vertical and lateral mode shapes and associated natural frequency values. As the element representing the hanger has tension only capability, it will detect any slack hangers and make them ineffective.
- The 3D box formulation model will accommodate symmetrical and asymmetrical loading. In addition, it will accommodate the drag and lift force components of the wind load. Also it will produce torsional mode shapes and associated natural frequency values of the bridge. Stress levels on the deck surface and in the diaphragm stiffeners can be produced precisely for different load cases.

Chapter 8

Sensitivity Study on the Model

General

These analyses are carried out in order to understand how the behaviour of the bridge model changes with variation of important parameters. The following are the principal reasons for carrying out such a study:

i) To study the effects of maintenance/ repair/ replacement schemes in which engineered changes to the structure are made either through temporary removal of members or the addition of materials. In some cases minor changes in the model will cause significant change in its modelled structural behaviour.

ii) To study the changes of modelled structural behaviour of the bridge with long term effects, such as possible deterioration and relaxation of the main cables and the hangers (changes of initial strain and effective diameter), and corrosion and cracks on the deck (changes of stiffness and cross sectional area).

iii) It guides the design engineer at the initial stage of suspension bridge design, where the sensitive components have been identified. This will enable them to concentrate on particular components and reduce time on trial and error activities.

iv) To give an indication on importance of maintenance on sensitive components to the maintenance team.

v) It is a guide to getting information on behaviour of the structure with replacement of materials such as replacement of asphalt layer on the carriageway and the footpath.

From this study justification can be made for the sensitivity of each parameter with respect to the modelled structural behaviour of the Humber Bridge. Resulting from this, the behavioural pattern of suspension bridges in general can be identified. A wide range of parameter variation from -30% to +30% was selected so that effects could be exaggerated and easily observed. This selected wider range was somewhat arbitrary, but enabled detection of the behaviour of hangers, especially when they were slack. It is not meant to be representative to a change in the structure but of a change in the model.

Throughout this study the gravity load case has been used to establish the sensitivity of the various parameters. This is because the main cables, which are carrying the bridge, have 80 % of this load from self-weight. For this study the 3-D plate formulation model has been used as it has the facility to detect slack hangers. Also this model can give quicker results with less computer resources than the detailed 3-D deck formulation model. In this study all the main cable, hanger and A-frame elements are considered. The maximum and minimum values of the forces are plotted regardless of the position where they occur, and corresponding positions are marked on the graph itself. The tower top and, middle and quarter span deck movements are also plotted.

The following definitions are used through out this chapter;

The "concave effect" of the deck refers to the deck moving downward from the datum. The "convex effect" refers to the deck moving upward from the datum level.

The maximum and minimum main cable, hanger and A-Frame forces on the graphs define the maximum tensile (+ ve) and compressive (-ve), minimum tensile (+ve) and compressive (-ve) force respectively, in that particular component of the structure. Figure 8.1 shows the general key locations of the deck along the bridge. Figure 8.2 shows the key location along the main cable, Figure 8.3 shows the key location of the hangers and Figure 8.4 shows the A-frame locations. These figures (Figure 8.2, 8.3 and 8.4) are repeatedly plotted wherever necessary for easy reading. The first (capital) letter indicates the location and the second (lower case) letter indicates the element (e.g.h=hanger, c=cable, a=A-frame.)

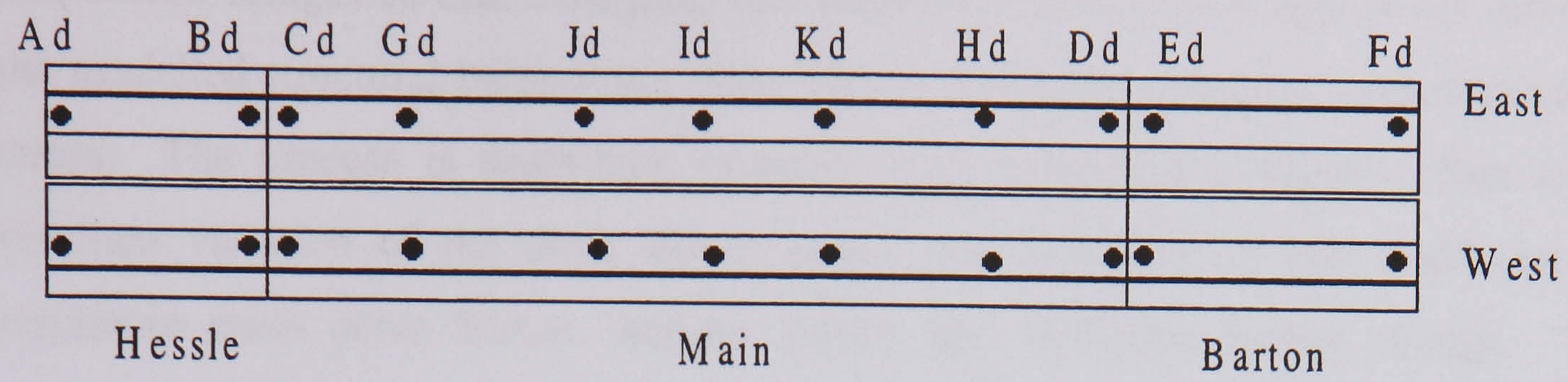

Figure 8.1: Key locations of the deck along the bridge.

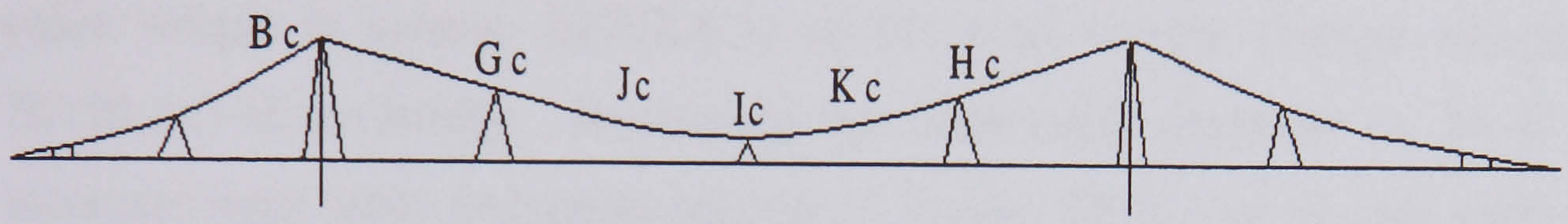

Figure 8.2: Figure shows the key main cable locations

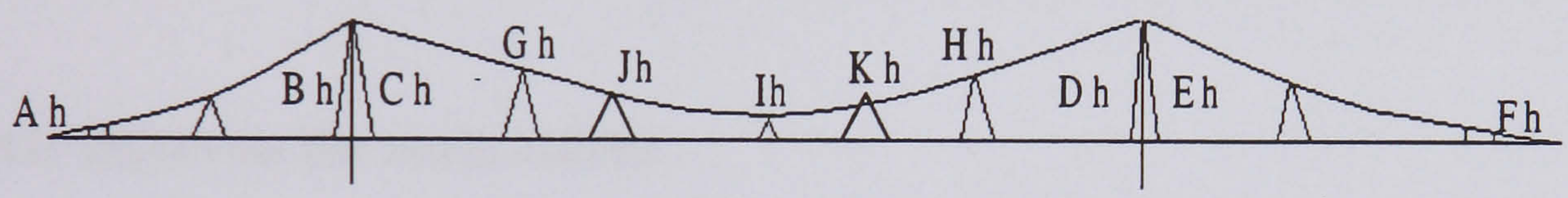

Figure 8.3: Figure shows the key hanger locations

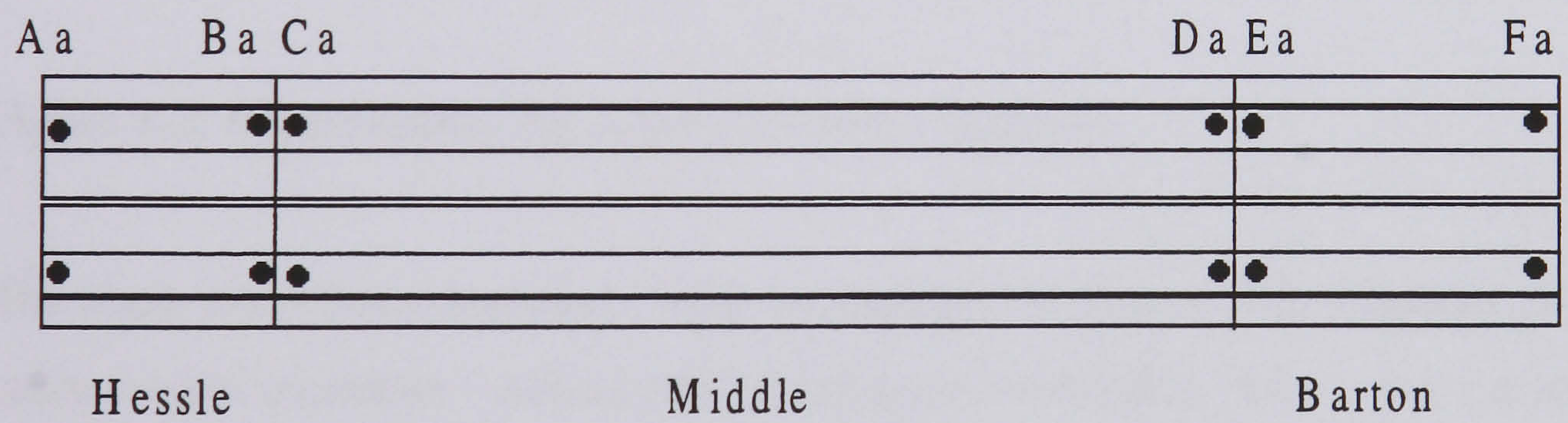

Figure 8.4: Figure shows the A-Frame locations

a) Changing the main cable diameter

Changing the main cable diameter on the model gives significant changes in both the main cable and the deck profile. Also this assumes that there are no changes in the initial strain applied to the main cable, and it is the same as its initially assumed (self-weight condition) value. The main cable is the primary structural element on suspension bridges so that changing this parameter value has a significant effect on the modelled structural behaviour. This occurs due to the changes in the main cable stress. The process is described extensively in section a i) below. Due to the resultant variation of the deck displacement, the locations of the maximum and minimum main cable forces, hanger forces and A-Frame forces change. This variation is illustrated in graphical representation with colour plots from Figure 8a1 to Figure 8a10.

Assuming all other features remain the same, the main cable contributes 17 % (main cable weight in tonnes, 12932.8 t) of the total weight (bridge weight in tonnes, 76158.2 t) of the bridge. Increasing the main cable diameter by 30 % gives 69 % increase (main cable weight increment in tonnes, 8924 t) of its own cable weight and therefore 9 % increase of the total bridge weight. Decreasing the main cable diameter by 30 % gives 51 % (main cable weight reduction in tonnes, 6595 t) reduction of its own cable weight and 8 % reduction of the total bridge weight.

a1) Effect on the main cables

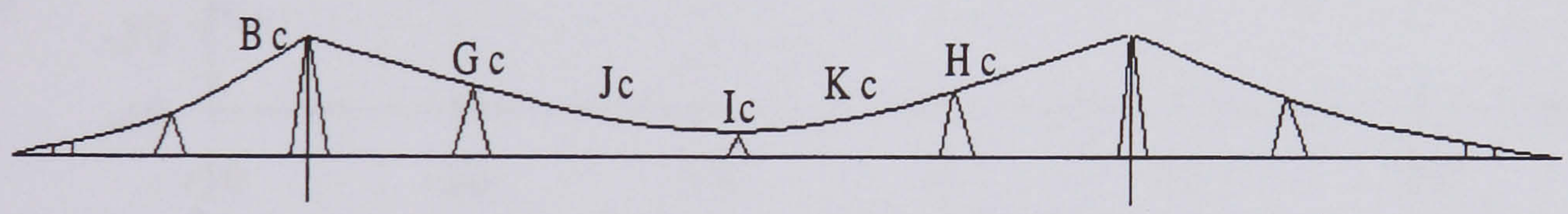

Figure 8.2: Figure shows the key main cable locations

The main cable force increases with increasing the main cable diameter as the main cable weight increases. Always the maximum main cable force occurs at main cable position Bc (as with the initially assumed main cable diameter). This is because of the steep slope of the main cable at the Hessle side. The minimum main cable force occurs at positions Ic (as with the initially assumed main cable diameter). It happens due to the fact that the resultant hanger force on this node at the main cable is less than at other nodes. In other words it can be said that the change of slope of the main cable profile reduces on those positions. For decreasing the main cable diameter the minimum main cable forces occur at position Jc and Kc. As mentioned above the resultant hanger force is less than at the other nodes on the main cable or the change of slope of the main cable profile reduces at that position.

Increasing the main cable diameter by 30 % (increment of bridge weight in tonnes, 8924 t) gives 30 % increment in the maximum (increment of maximum main cable force in tonnes, 5235 t) or minimum (increment of minimum main cable force in tonnes, 4696 t) main cable force (refer Figure 8a1). Increasing the main cable diameter by 30 % gives 69 % increase in the main cable cross sectional area. Meanwhile the maximum main cable force increases only by 30 %. Hence a reduction of main cable stress occurs with increasing the main cable diameter. Increasing the main cable diameter by 30 % gives 23 % reduction in the main cable stress at positions Gc and Hc (refer Figure 8a2).

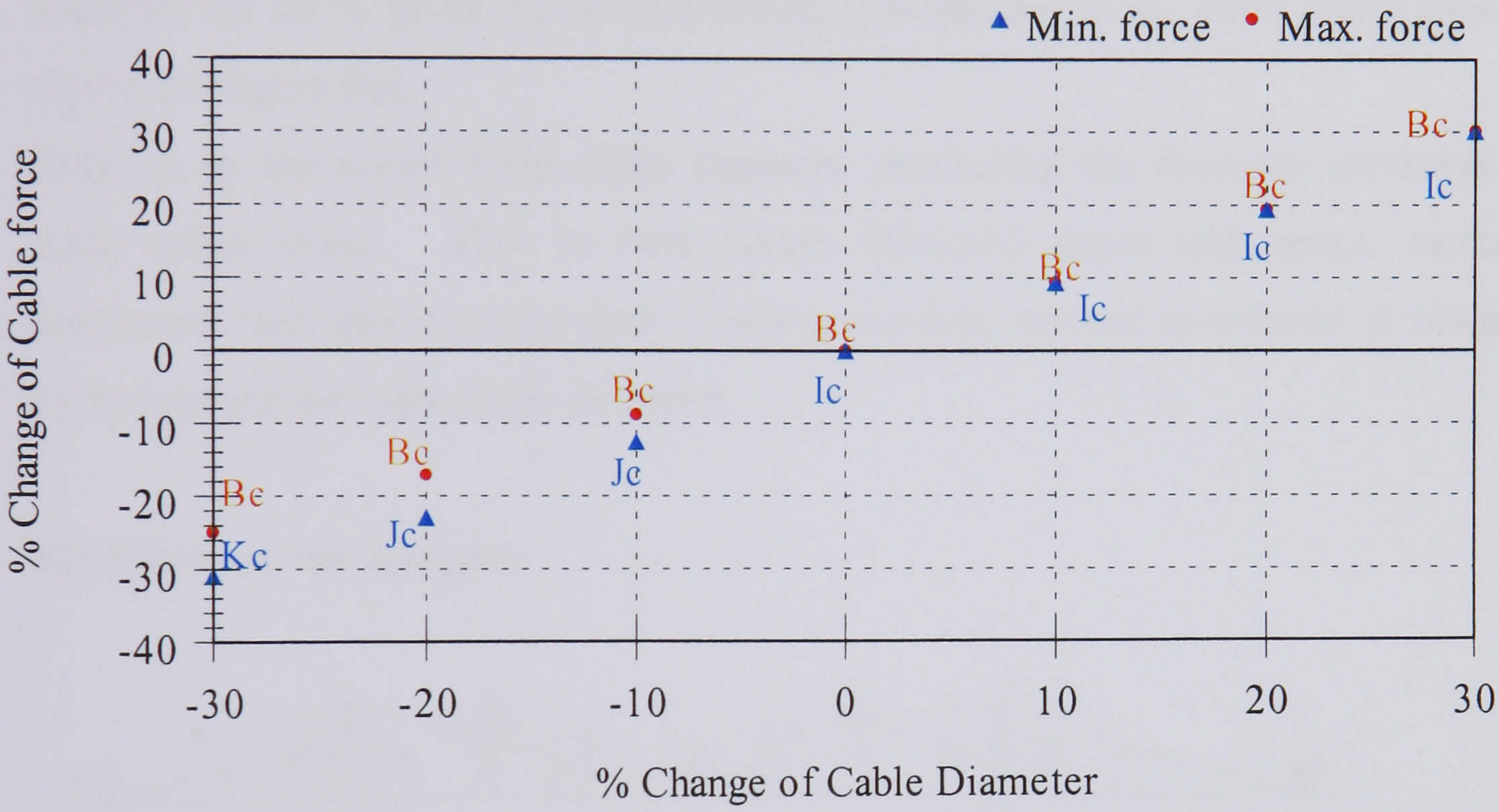

Figure 8a1: Change of main cable forces with the change of main cable diameter

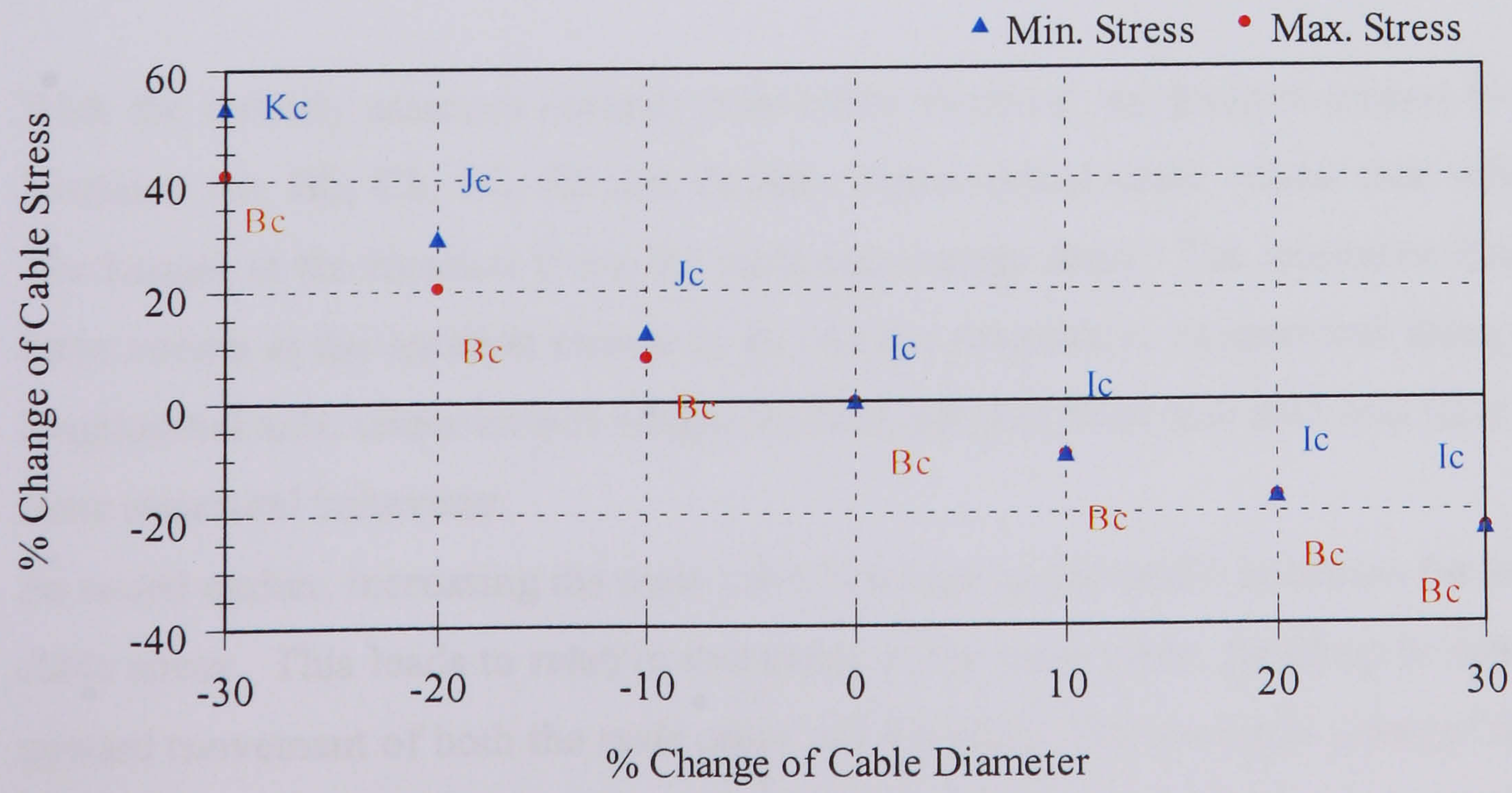

Figure 8a2: Change of main cable stresses with the change of main cable diameter

Decreasing the main cable diameter by 30 % (reduction of bridge weight in tonnes, 6595 t) gives 25 % (reduction of maximum main cable force in tonnes, 4320 t) reduction in the maximum main cable force. Also it gives 30 % (reduction of minimum main cable force in tonnes, 4803 t) reduction in the minimum main cable force as shown in Figure 8a1. The main cable stress increases with decreasing the main cable diameter. Reduction of the main cable diameter by 30 % gives 51 % reduction in the main cable cross sectional area; meanwhile the maximum main cable force reduces by 25 %. This shows that the increase of main cable stress occurs with decreasing of the main cable diameter. Reduction of the main cable diameter by 30 % gives 53 % (at position I) increment in the main cable stress as shown in Figure 8a2.

Relative to the actual main cable diameter, decreasing the diameter increases the main cable stress. This in turn causes increased strain and hence increases downward movement of the deck, while conversely upward movement is obtained by increasing the main cable diameter.

a2) Effect on the hangers

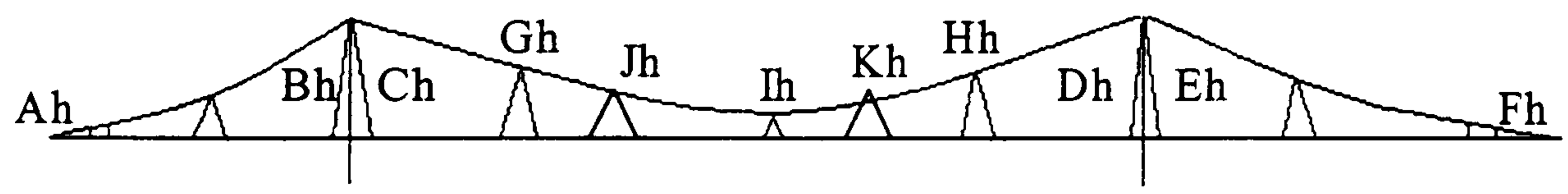

Figure 8.3: Figure shows the key hanger locations

With the initially assumed (actual) main cable diameter, the hangers closest to the locations Ah, Bh, Ch, Dh, Eh and Fh have higher initial strain values than others. The hanger at the location E has the maximum hanger force. The minimum hanger force occurs at the location closest to Ih. As the structure is symmetrical along the longitudinal axis, under its self-weight the East side and West side elements have the same structural behaviour.

As stated earlier, increasing the main cable diameter in the model decreases the main cable stress. This leads to relative shortening of the main cable, resulting in relative upward movement of both the main cable and the deck. The maximum hanger force position remains at location Eh. The minimum hanger force moves to a position between Jh and Kh (an element away from the mid-point whose bottom node is closer to the mid-point than the top node).

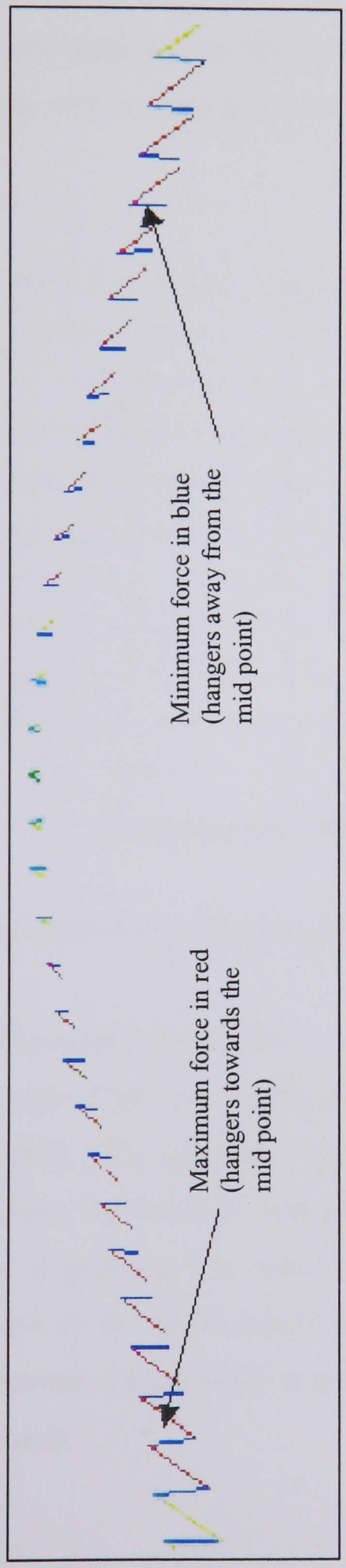

Figure 8a3: Hanger forces with increased main cable diameter (from its initially assumed diameter)

Increasing the main cable diameter gives a convex (i.e. the deck is moving upward from the datum) effect on the main and side spans of the deck. This effect increases the hanger strain on elements towards (element's top node is closer to the mid-point than the bottom node) the mid-point of the span (refer Figure 8a3). Also it decreases on elements away from the mid-point of the span (element's bottom node is closer to the mid-point than the top node) relative to the initially assumed main cable diameter. As a result the maximum hanger force value increases and the minimum hanger force value decreases with increasing the main cable diameter, refer Figure 8a4.

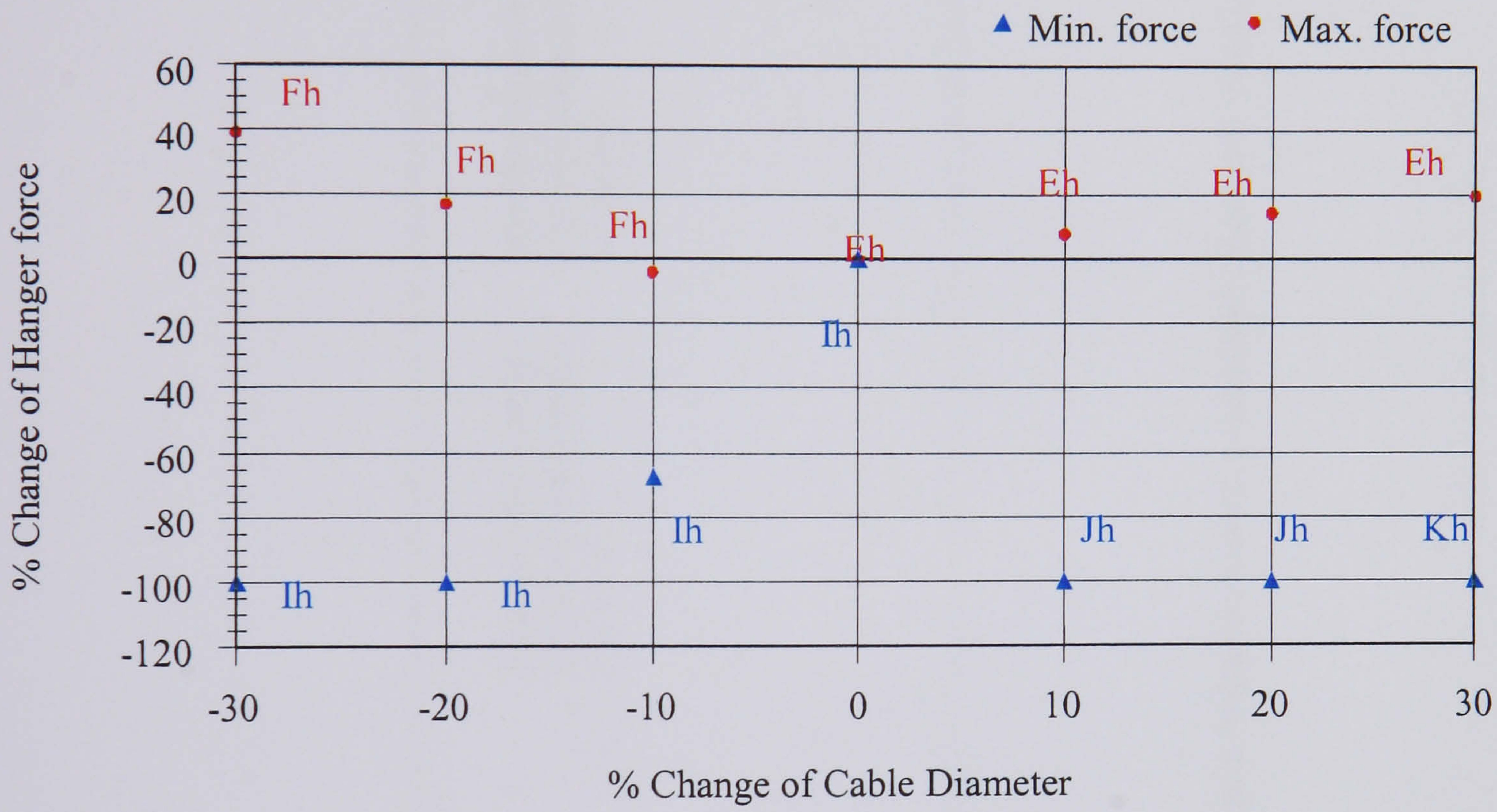

Figure 8a4: Change of hanger forces with the change of main cable diameter

Decreasing the main cable diameter in the model increases the main cable stress. This leads to relative extension of the main cable and causes downward movement of the main cable and the deck. The maximum hanger force value increases with increasing main cable diameter; the location changes from position Eh to position Fh. This happens because at position F a vertical hanger (there are no inclined hangers) gets more force due to its newly deformed position (from the increased main cable force). The minimum hanger force position is still closer to location Ih (element towards the mid-point).

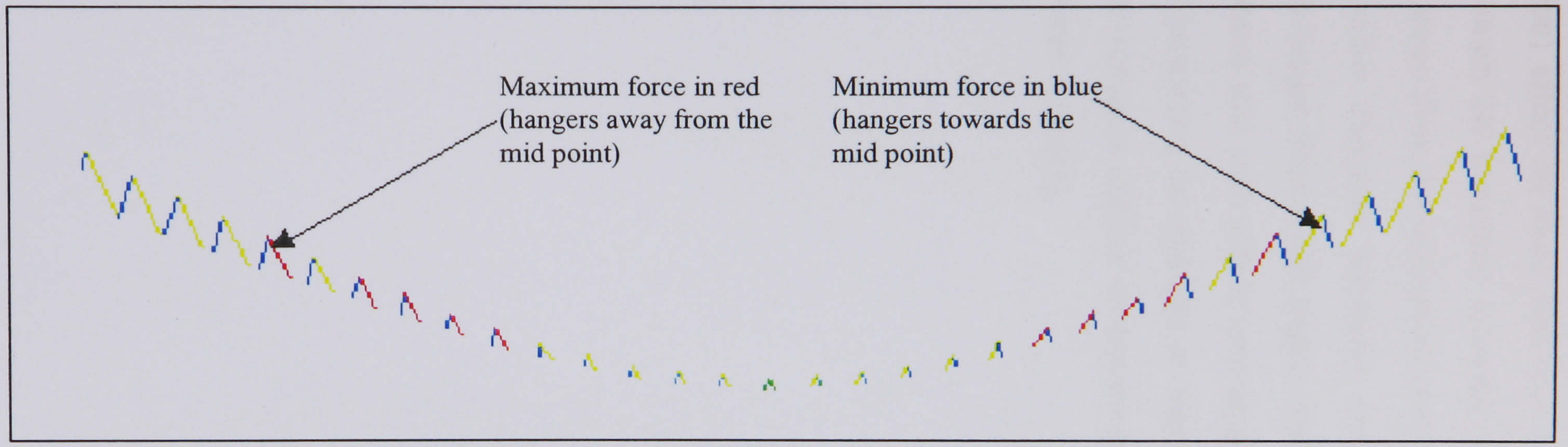

Figure 8a5: Hanger forces with decreased main cable diameter (from its initially assumed diameter)

Decreasing the main cable diameter gives a concave (i.e. the deck moves downward from the datum position) effect on main and side spans of the deck. This effect increases the hanger strain on elements towards the mid-point of the span and decreases on elements away from the mid point of the span (refer Figure 8a5). Thus decreasing the main cable diameter increases the maximum hanger force and decreases the minimum hanger force (refer Figure 8a4).

As a result it can be stated that with either increasing or decreasing the main cable diameter in the model (assuming no changes in main cable initial strain value), the maximum hanger force increases and the minimum hanger force decreases, but with the location of these forces changing.

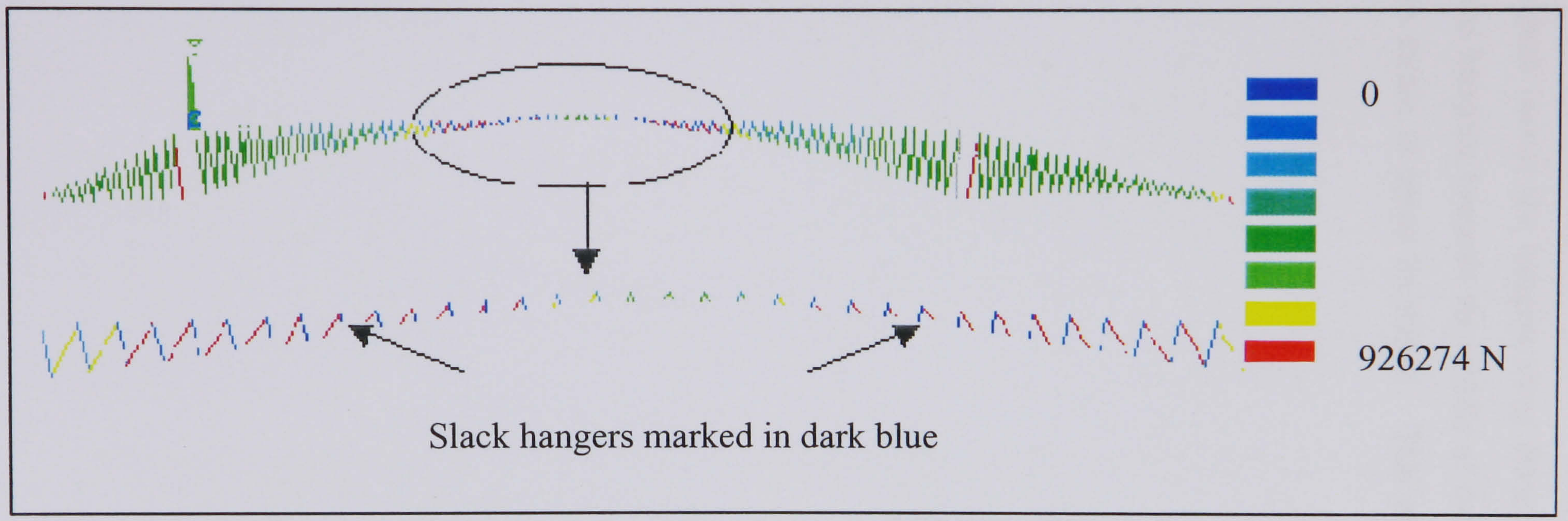

Figure 8a6: Hanger force (N) diagram (slack hangers found with zero tension value) with increased main cable diameter by 10%.

Slackening of hangers occurs with approximately a 10 % increase of the main cable diameter and beyond a 20 % decrease of the main cable diameter. As shown in Figure 8a6, hangers start to slacken at the middle of main span region for the 10 % increment of the main cable diameter. The relative upward deflected form of the main cable and the deck leaves the hangers away from the middle of the main span to strain more and the hangers towards the middle of the main span to reduce strain, ending up with zero strain at some locations. This effect starts to produce slack hangers.

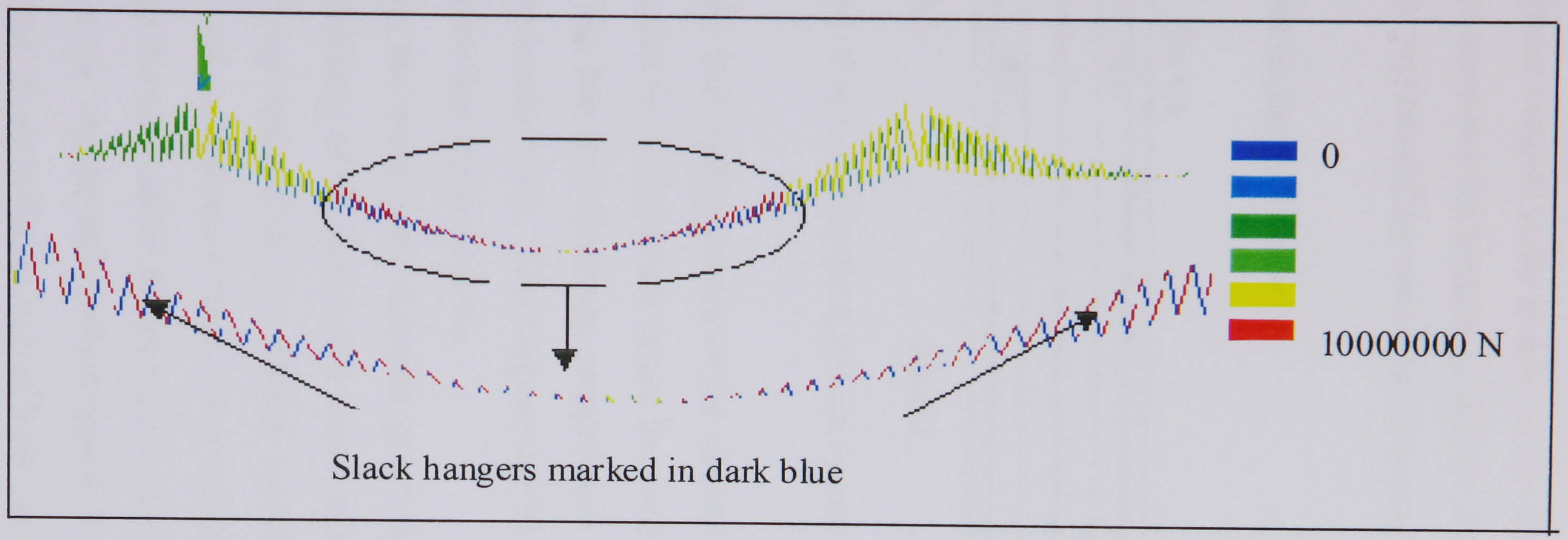

Figure 8a7: Hanger force diagram (slack hangers found with zero tension value) with decreasing of main cable diameter by 20%.

As shown above in Figure 8a7, the relative downward movement of the deck and the main cables causes the hangers away form the middle of the main span to strain more and the hangers towards the middle of main span to reduce strain. This leads to zero strain hangers at the middle of the main span area. The tension only element is used to represent the hangers so that the slack hanger elements become ineffective. These are represented by zero force elements with blue colour.

a3) Effect on the A-Frames

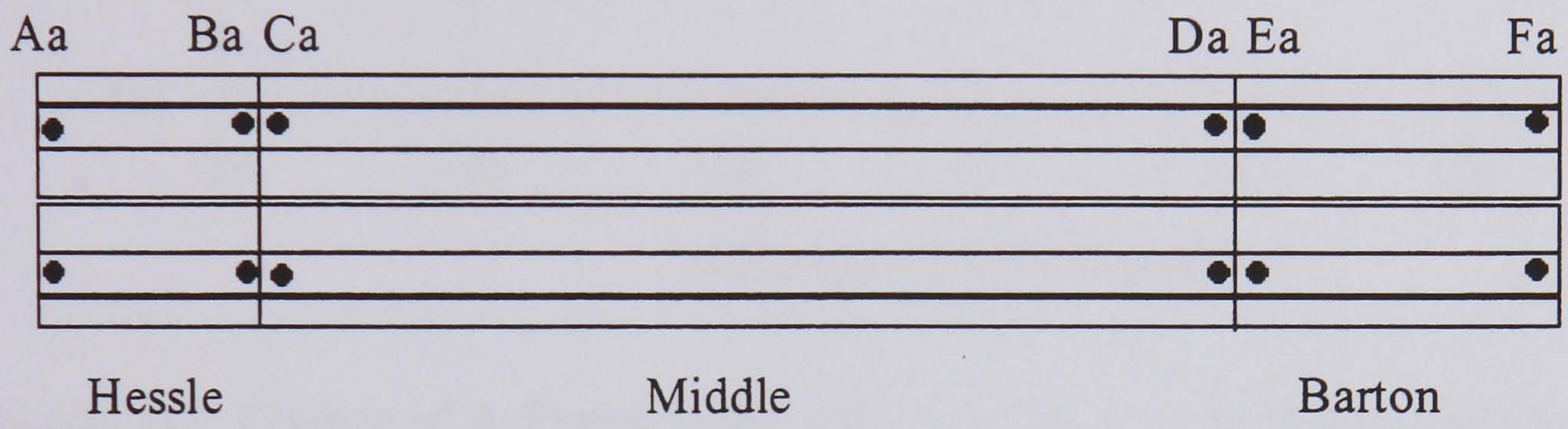

Figure 8.4: Figure shows the A-Frame locations

Due to the deflected geometry of the structure with its initially assumed main cable diameter and the initial strain values for the main cable and hangers, the A-Frame at location Aa has the maximum compressive force and that at location Ea has the maximum tensile force. This happens due to hangers at location Ea having a higher tensile force than those do at Aa.

Increasing the main cable diameter gives decreases in the main cable stress that cause shortening of the main cable which in turn cause the main cable and the deck to deflect upwards relatively. Hence tensile force (+ve) values on the A-Frame increase and compressive force (-ve) values decrease as shown in Figure 8a8. Increasing the main cable diameter gives the maximum compressive A-Frame force at location Aa. As the deck deflects upward with increasing diameter, the maximum tensile force on an A-Frame moves from location Ea to location Fa. Increasing the main cable diameter gives greatest longitudinal movement in the A-Frame at location Fa. Hence a higher strain value obtains at the A-frame members resulting in greater tensile force in the A-Frame.

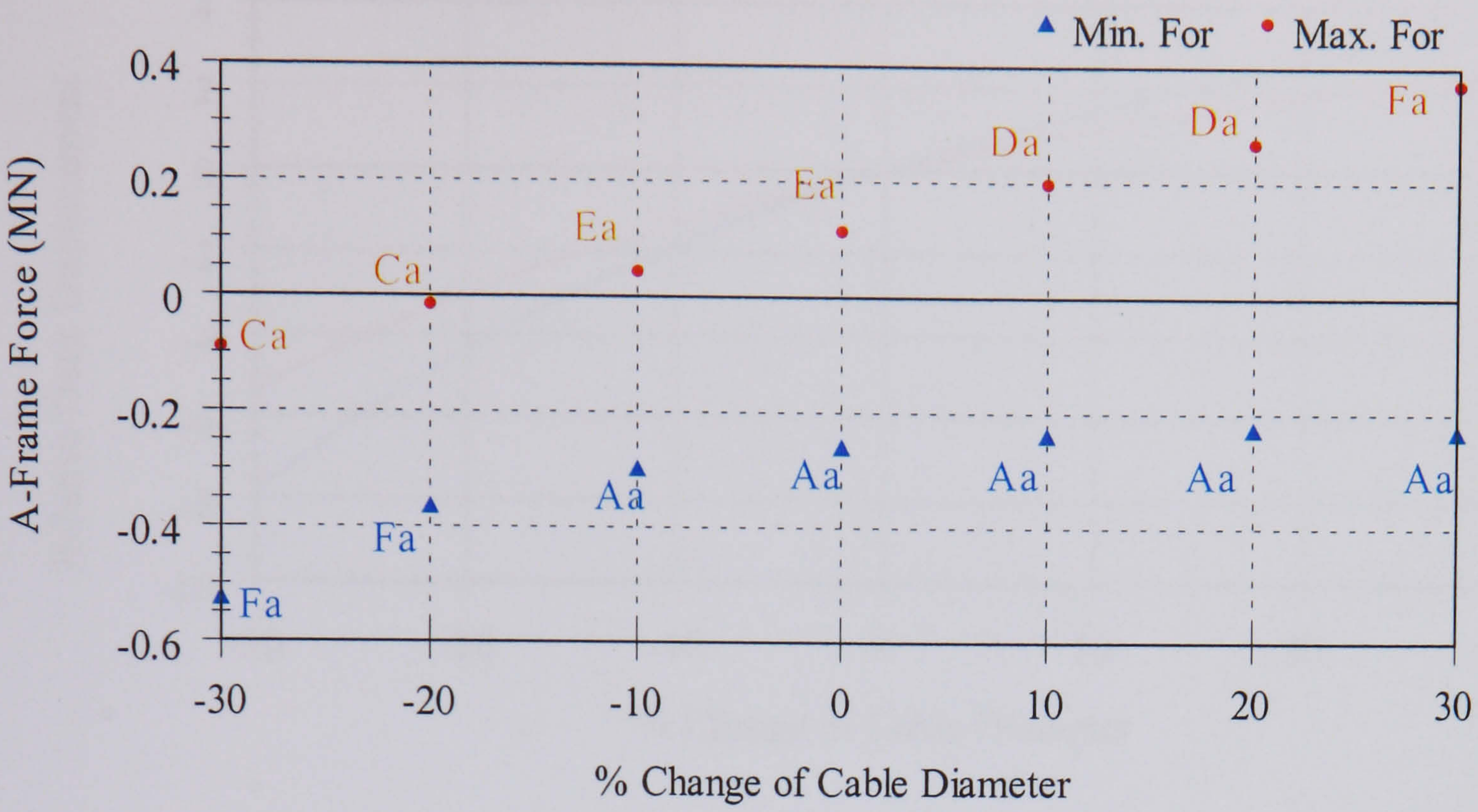

Figure 8a8: Change of A-Frame forces with the change of main cable diameter

The A-Frame force changes to compressive with reduction of the main cable diameter, i.e. the main cable stress increases which expands the main cable, and as a result the main cable and the deck deflect relatively downward. With reduction of the main cable diameter, the A-Frame members at location Fa shorten more, hence resulting in a greater compressive force (refer Figure 8a8).

a4) Effect on the deck

Changes in the main cable diameter, give changes in the main cable stress that cause expansion or shortening of the main cable resulting in significant changes in the main cable and the deck displacement, (refer Figure 8a9).

Increasing the main cable diameter by 30 % gives a relatively upward mid-point deck displacement of 3.5 m and at quarter point displacement of 2.5 m.

Decreasing the cable diameter by 30 % gives a relatively downward mid point deck displacement of 8 m and at quarter point displacement of 5.5 m.

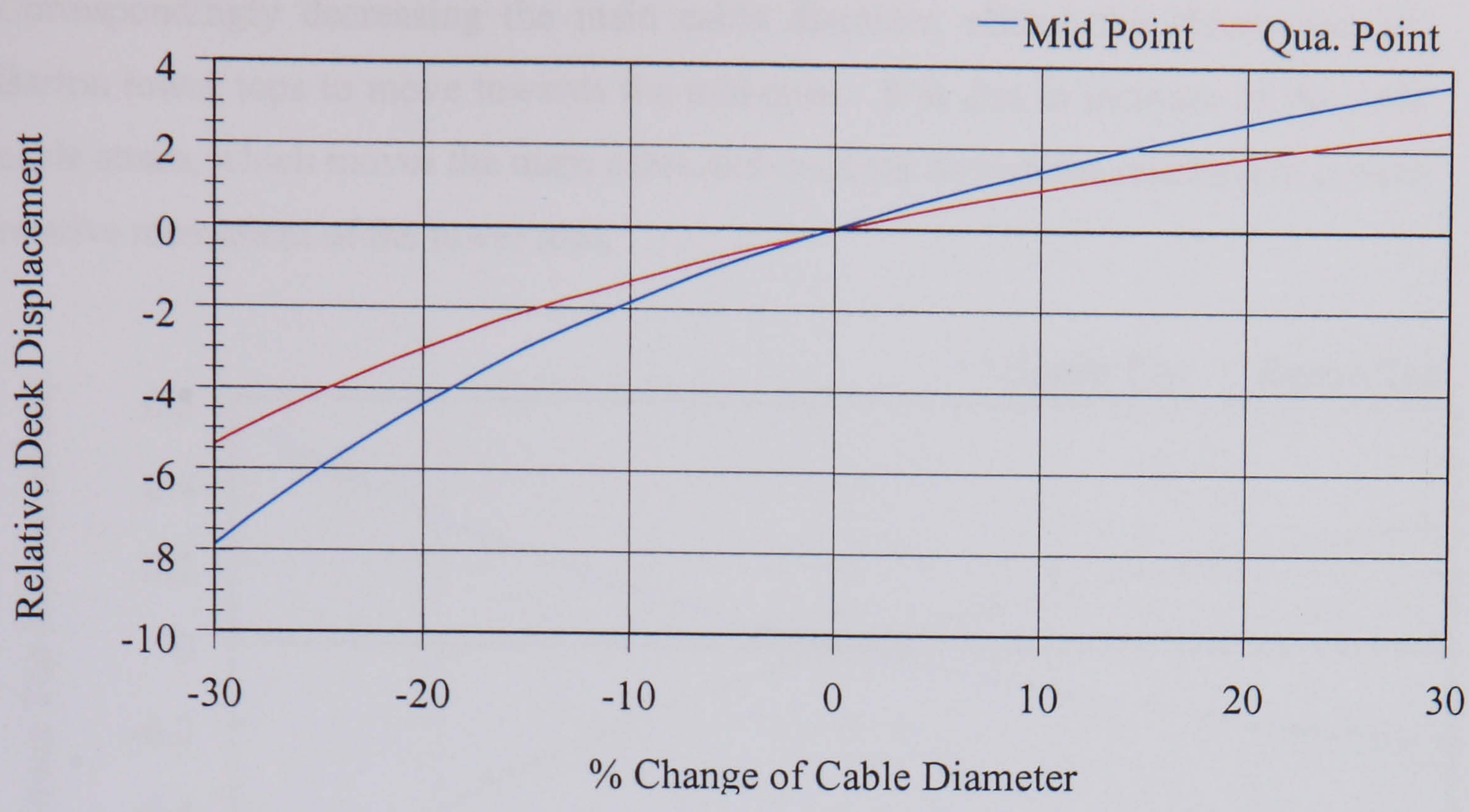

Figure 8a9: Change of deck vertical displacement with the change of main cable diameter

As discussed in section a 1), increasing the main cable diameter decreases the main cable stress and decreasing the main cable diameter increases the main cable stress. The change of main cable stress due to increase of main cable diameter is lower compared with decreasing the main cable diameter, (refer Figure 8a2). Hence the shortening length of the main cable is less than the expansion length. These results give higher magnitude of relative downward deck displacement due to decrease of main cable diameter, compared with the upward deck displacement due to increase of the main cable diameter.

a5) Effect on the towers

Barton and Hessle tower top movements due to change in main cable diameter are given in Figure 8a10.

With increasing the main cable diameter the Hessle and the Barton tower tops move away from the centre span. This happens because increasing the cable diameter (i.e. decreasing the main cable stress, shortening the main cable length) moves the main cable and the deck relatively upwards, which allow both towers to deflect relatively away from the mid-span.

Correspondingly decreasing the main cable diameter, allows the Hessle and the Barton tower tops to move towards the mid-span. It is due to increase of the main cable strain, which moves the main cable and the deck downward resulting in inward relative movement of the tower tops.

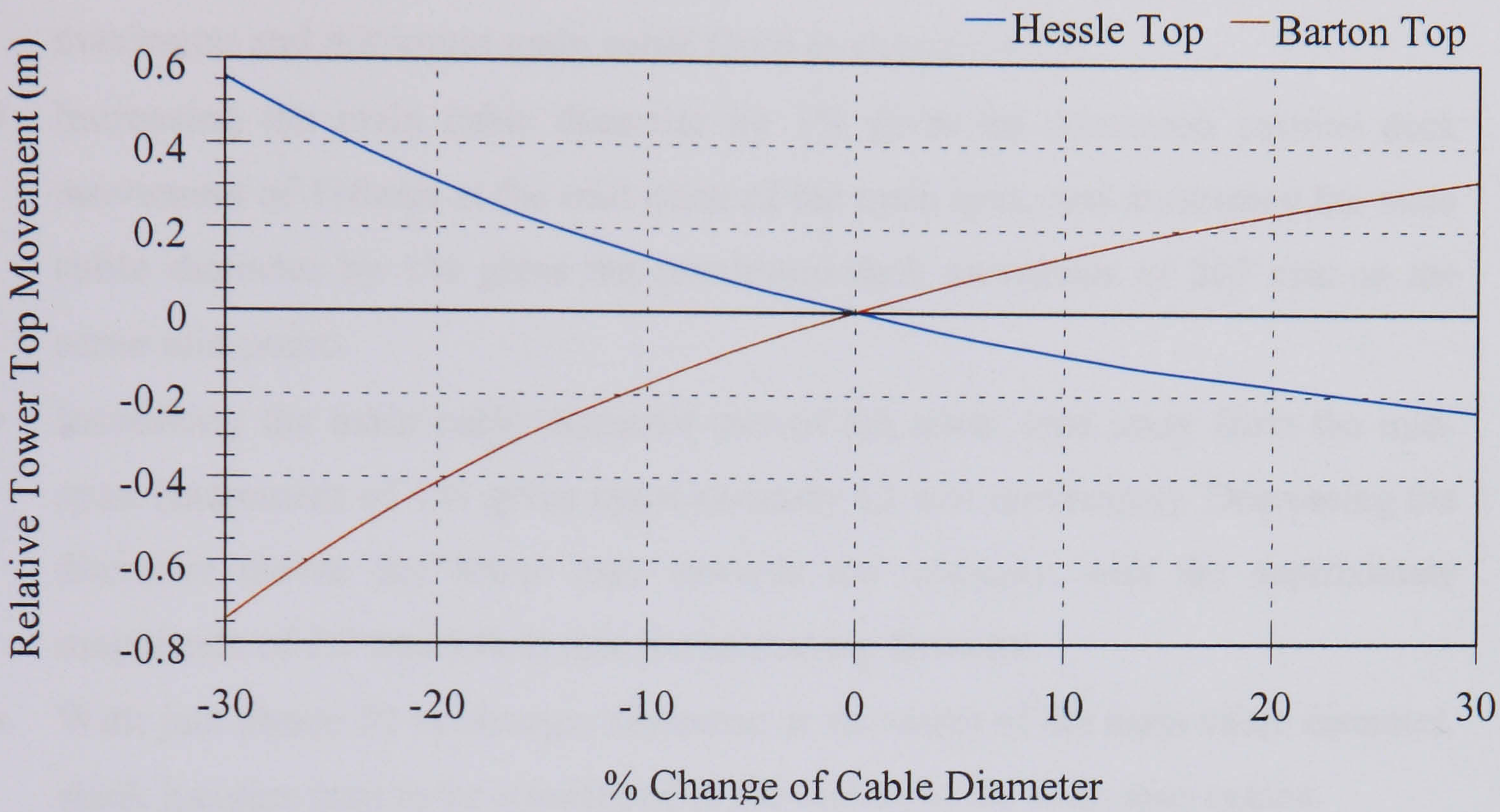

Figure 8a10: Change of tower movement with the change of main cable diameter

The Barton tower top moves by 0.320 m and the Hessle tower top moves by 0.239 m with the main cable diameter increases to 30 %. Similarly the Barton tower top moves by 0.743 m and the Hessle tower top moves by 0.557 m with the main cable diameter decreases to 30 %. The reason for the different tower top movement for increasing and decreasing of the main cable diameter is discussed in section a 1).

a6) Conclusion on change of main cable diameter

- The main cable diameter is the most sensitive parameter with regards to bridge behaviour.
- Decreasing the main cable diameter has more effect on the main cable and deck relative displacement, and both tower top movements (at least 2.3 times for the change of 30 %) than does increasing the main cable diameter.

- In other words during the modelling stage, applying a lower diameter value than the actual value has more effect in structural response compared with applying a higher diameter value (with the same magnitude) than the actual value.
- The maximum and minimum main cable forces have approximately linear variation with changing the main cable diameter. Changes of 1% cause the maximum and minimum main cable force to change by 1%.
- Increasing the main cable diameter by 1% gives the maximum relative deck movement of 116mm at the mid point of the main span, and decreasing the main cable diameter by 1% gives the maximum deck movement of 267 mm on the same mid point.
- Increasing the main cable diameter moves the tower tops away from the mid-span (increment of 1% gives approximately 12 mm movement). Decreasing the diameter moves the tower tops towards the mid-span with the approximate magnitude of 2.2 times than that for increasing diameter.
- With just above 10 % changes (increase or decrease) of the main cable diameter, slack hangers start to be introduced at the middle of the main span region.
- A long-term deterioration, which might cause a minor reduction (say 1%) in diameter of the main cable, could give considerable change in structural behaviour such as deck movement, tower top movement and main cable force compared to that with the actual value.

b) Changing the main cable initial strain value

Another important parameter on modelling the main cable is initial strain, which is defined as the strain of the main cable at its initial stage (under self-weight loading condition). It is a significant factor as the bridge is strained under its own weight. There is no unstrained element on the bridge under the dead load condition. The main cables and the hangers are used as important tools to maintain the appropriate curvature of the bridge deck between the supports. Introducing suitable pulling force (pre-stressing force) or in other words introducing acceptable initial strain value to the main cables and hangers is how this is achieved. The initial strain values of the main cables and the hangers are always positive. Increasing or decreasing a percentage of the initial strain value from the initial stage (self-weight condition) will increase or decrease the pulling forces on the main cables and the hangers, and these forces are always in tension. Changes in initial strain value used on the model (main cable) give significant changes in pre-stressing force on the main cable and changes on the main cable and the deck profile.

Reduction of the initial strain values reduces the initial pre-stressing force on the main cable. Meanwhile there are no changes in the dead weight of the structure. These effects give relative downward movement of the main cable and the deck. Increasing the initial strain value increases the initial pre-stressing force on the main cable while there is no change in the dead weight of the structure. This causes relative upward movement of the main cable and the deck.

b1) Effect on the main cables

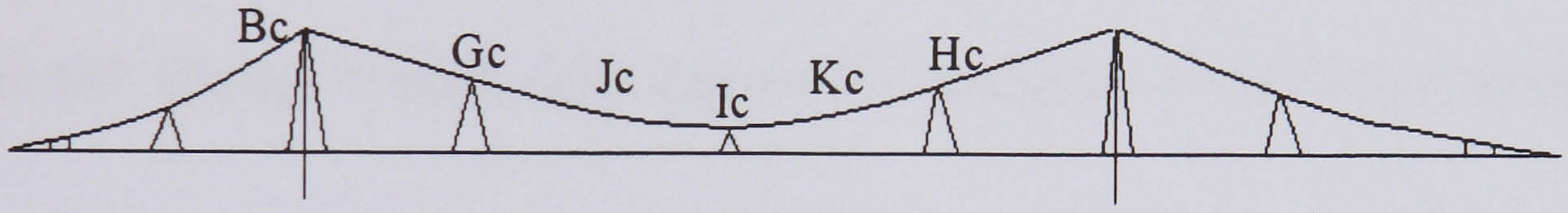

Figure 8.2: Figure shows the key main cable locations

Effects on the main cable due to its change of initial strain value are given in Figure 8b1. The maximum main cable force occurs always at position Bc as mentioned before, because of the steep slope of the main cable at the Hessle side. The minimum main cable force occurs at positions Jc and Kc for increasing the main cable initial strain value. As mentioned before it happens because the resultant hanger force on the node at the main cable is less than other nodes. In other words it can be said that the change of slope of the main cable profile reduces at those positions. For decreasing main cable diameter the minimum main cable forces occur at position Ic (as with the initially assumed main cable diameter). As mentioned earlier the resultant hanger force is less than at the other nodes on the main cable or the change of slope of the main cable profile reduces at that position.

Increasing the main cable initial strain value increases the pre-stressing force on the main cable while there is no change in the dead weight. Increasing the initial strain by 30 % (0.00087) gives 4 % increase in the maximum (increase of main cable force in tonnes, 689 t) and minimum (increase of main cable force in tonnes, 636 t) main cable forces. This leads to upward movement of the main cable mid-point by 4.1 m.

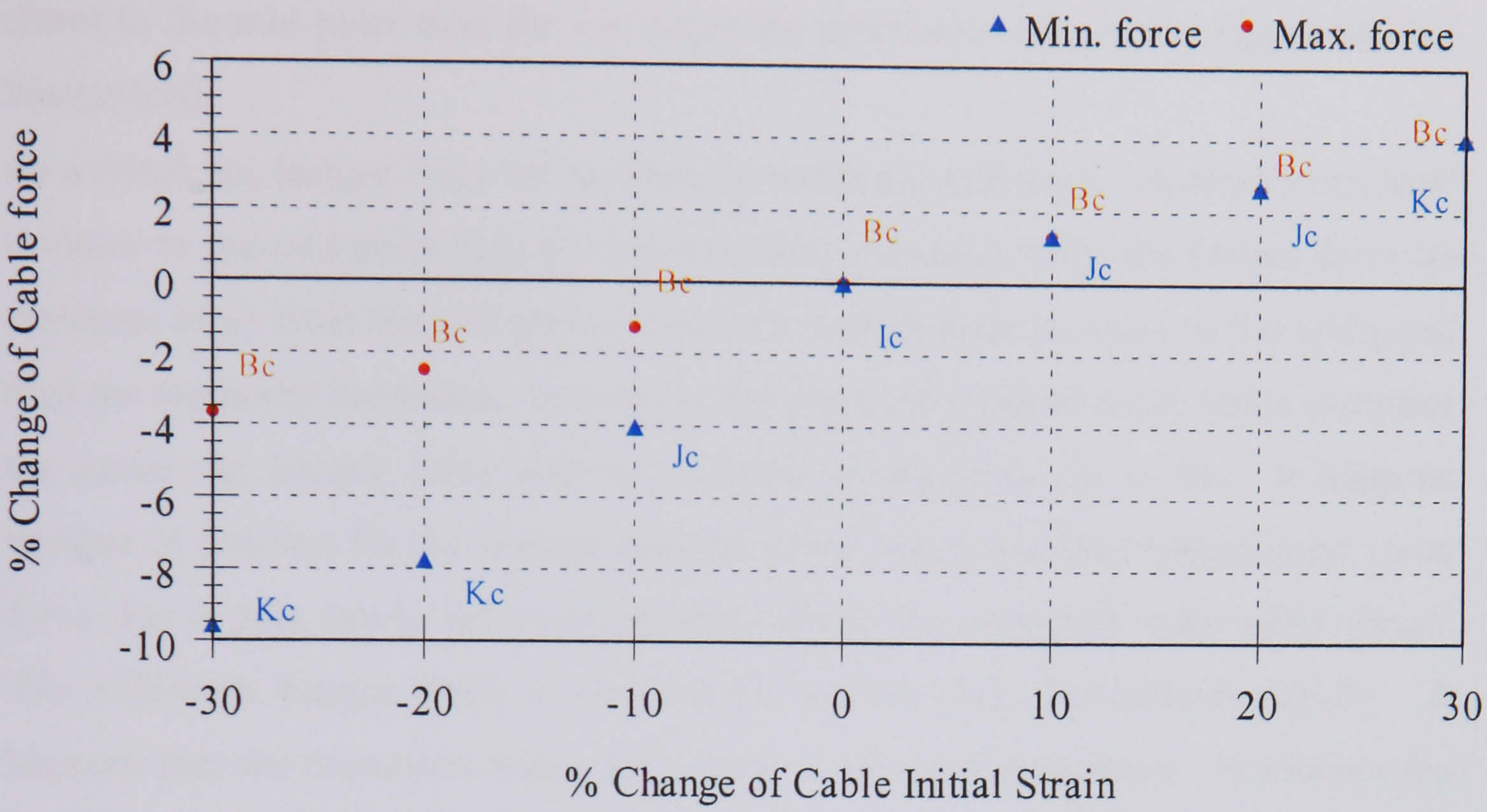

Figure 8b1: Change of main cable forces with the change of main cable initial strain

Decreasing the initial strain value of the main cable reduces the pre-stressing force on the main cable. Reduction of initial strain by 30 % (0.00087) gives 3.6 % (decrease of main cable force in tonnes, 637 t) decreases in the maximum main cable force and 9.5 % (decrease of main cable force in tonnes, 1488 t) decreases in the minimum main cable force. This leads to downward movement of the main cable mid-point by 4 m.

b2) Effect on the hangers

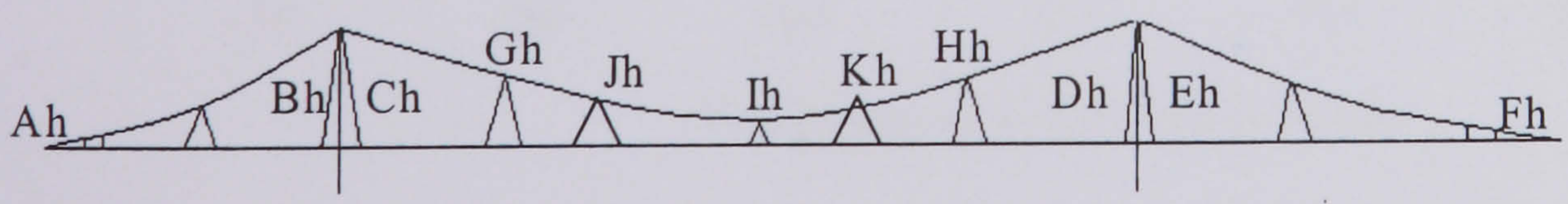

Figure 8.3: Figure shows the key hanger locations

Increasing the main cable initial strain value moves the main cable and the deck (positions at middle and side span) relatively upwards, and the maximum hanger force value moves from location Eh to location Fh (refer Figure 8.1). Due to the convex effect on the deck and the main cable, strain on hanger members towards the mid-point (element's top node is closer to the mid-point than the bottom node) increases. Also for members away from the mid-point (element's bottom node is closer to the mid-point than the top node) the strain decreases (refer Figure 8a3 for illustration).

As a result, the hanger force on members towards the mid-point (element's top node is closer to the mid-point than the bottom node) increases while the hanger force on members away from the mid point (element's bottom node is closer to the mid-point than the top node) decreases. Increasing the main cable initial strain value increases the maximum hanger force and the location moves from Eh to Fh. It happens because at position Fh the vertical hangers (there are no inclined hangers) get more force due to this newly deformed position (from the increased main cable force). The minimum hanger force at location Jh (moves from Ih) reduces rapidly. It happens that the minimum main cable force occurs at that position. Increasing the convex effect causes slacking beyond 14 % increment of the initial strain value of the main cable, refer Figure 8b2.

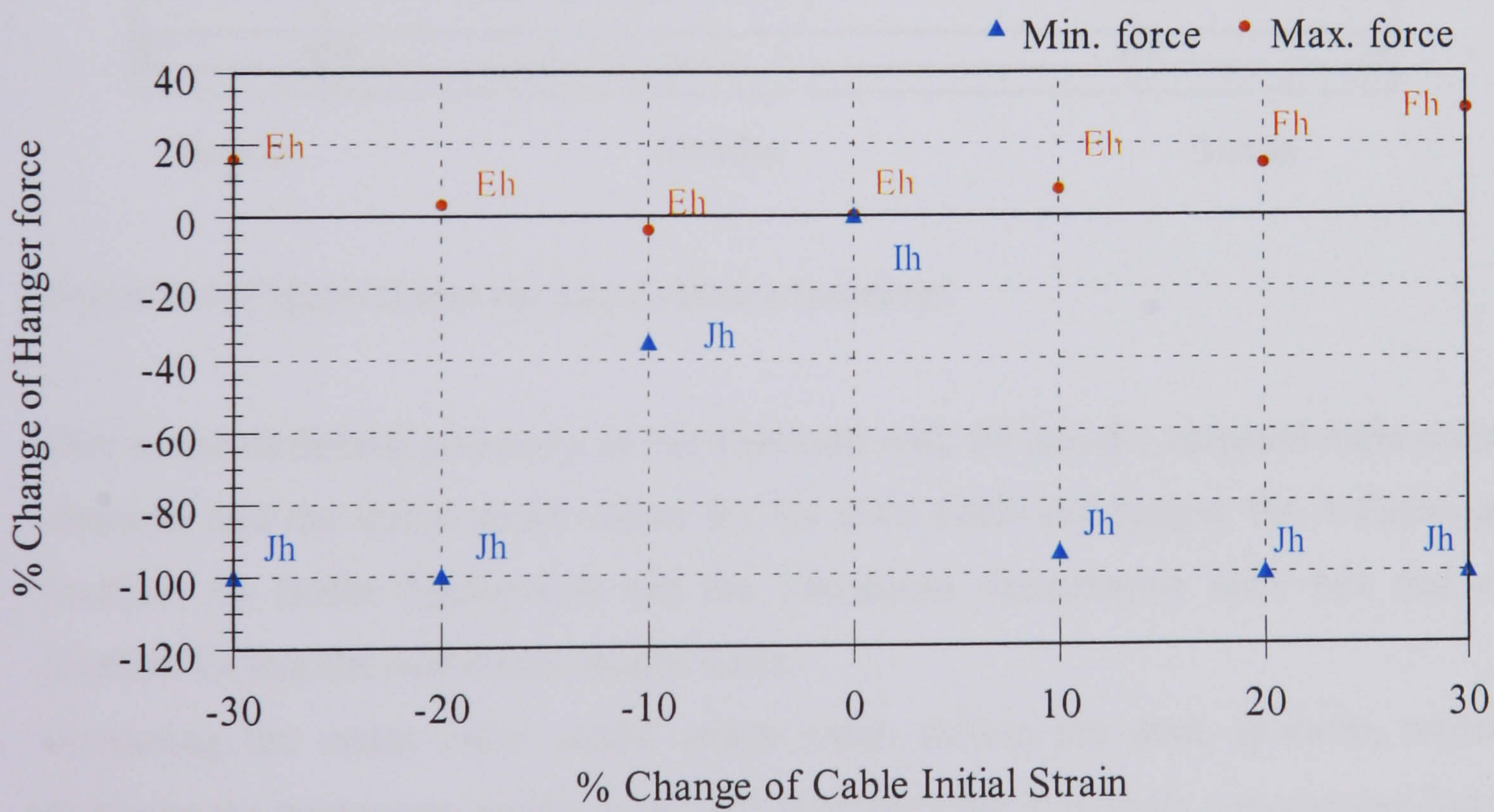

Figure 8b2: Change of hanger forces with the change of main cable initial strain

Decreasing the main cable initial strain value causes downward movement of the main cable and the deck. Due to the concave effect on the deck and the main cable, the strain on hanger members away (element's bottom node is closer to the mid point than the top node) from the mid-point increases. Also the strain on hanger members towards (element's top node is closer to the mid-point than the bottom node) the mid-point decreases. As a result the hanger force on members away from the mid-point increases and the hanger force towards the mid-point decreases (refer Figure 8a5 for illustration). As shown in Figure 8b2 the minimum hanger force at location Jh (element towards the mid-point) reduces with decreasing the main cable initial-strain value up to 20 % then due to the increasing of the concave effect slacking of the hangers occurs.

Slacking of hangers occurs beyond 20 % decrease and 14 % increase of the main cable initial strain values. This is due to an increasing convex or concave effect of the deck.

b3) Effect on the A-Frames

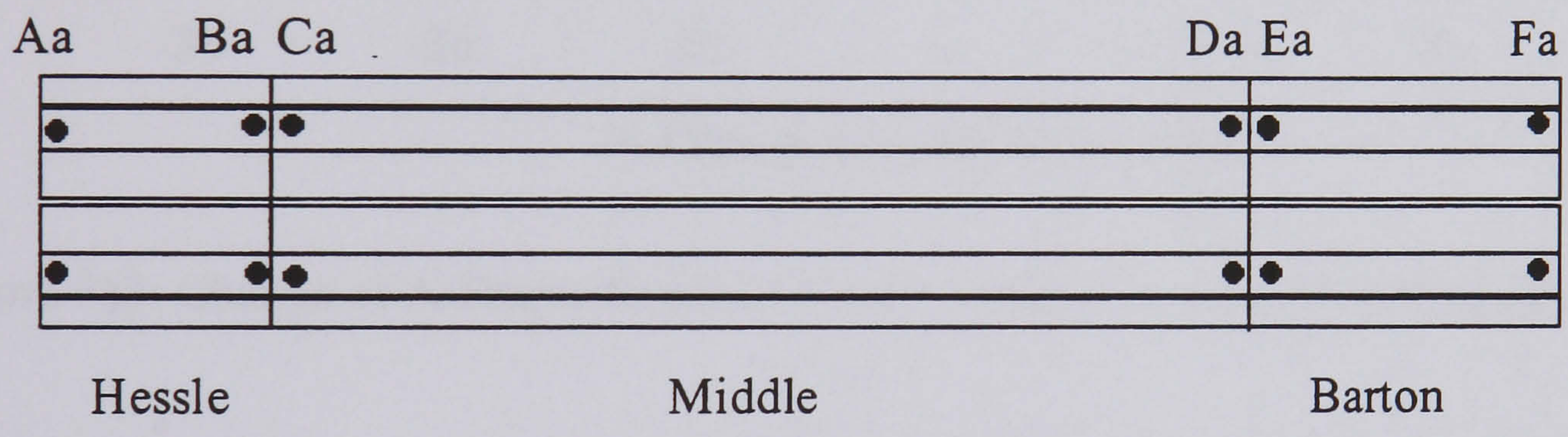

Figure 8.4: Figure shows the key A-Frame locations

Due to the deflected geometry of the structure with its initially assumed main cable diameter and the initial strain values for the main cable and hanger, the A-Frame at location Aa (refer Figure 8.4) has the maximum compressive force and that at location Ea has the maximum tensile force.

Increasing the main cable initial strain value moves the deck upwards, which increases the maximum tensile force and decreases the maximum compressive force on the A-Frame as shown in Figure 8b3.

With increasing the initial strain value, the location of the maximum tensile force on the A-Frame moves from location Ea to location Fa and the magnitude increases. This is because increasing the hanger force at location Fa pulls the deck upwards, thus increasing the A-frame tensile force.

Location of the maximum compressive force on the A-Frame at location Aa does not change as the magnitude decreases. It happens because increasing the hanger force at the same location Aa, which pulls the deck upwards, gives a reduction in compressive force.

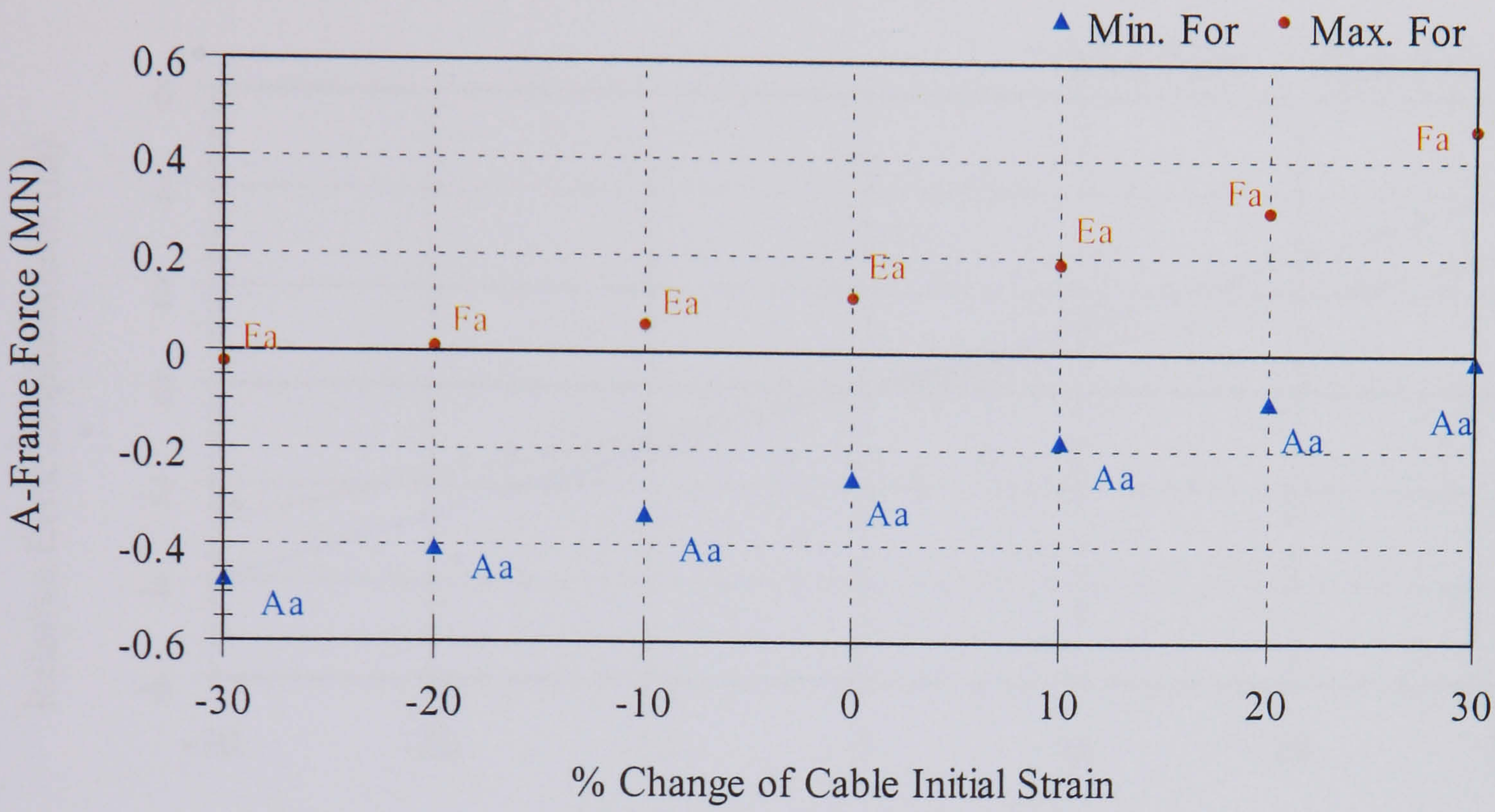

Figure 8b3: Change of A-Frame forces with the change of main cable initial strain

Decreasing the main cable initial strain value moves the deck downward which decreases the maximum tensile force and increases the maximum compressive force (refer Figure 8b3).

With decreasing the initial strain value, the location of the maximum tensile force in the A-Frame moves from location Ea to location Fa and the magnitude decreases, as a result of decreasing hanger force on that location.

Location of the maximum compressive force on the A-Frame at location Aa does not change but the magnitude increases because of reduction in hanger force at that location.

b4) Effect on the deck

Changes in the main cable initial strain value give significant changes in the deck displacement (refer Figure 8b4).

Increasing the main cable initial strain value increases the pre-stressing force on the main cable while there is no change in the dead weight of the structure. As a result it pulls the deck by means of the hangers. Thus the initial position of the deck moves upwards. Increasing the initial strain value by 30 % gives the deck mid-point upward deflection of 4.1 m and the deck quarter point upward deflection of 2.8 m.

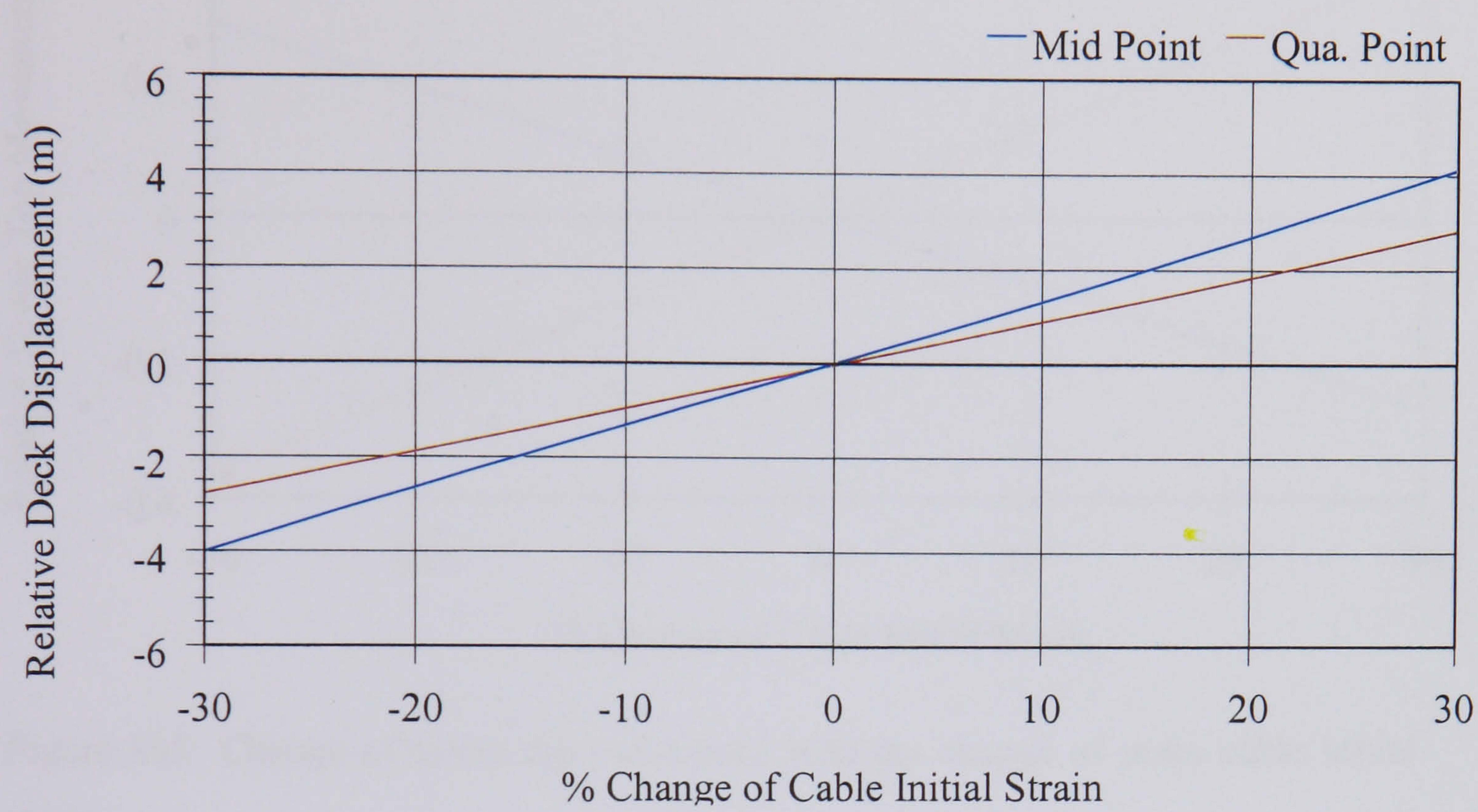

Figure 8b4: Change of deck displacement with the change of main cable initial strain

Decreasing the initial strain value of the main cable decreases the pre-stressing force on the main cable that deflects the deck downward.

Decreasing the initial strain value by 30 % gives the deck mid-point a downward displacement of 4 m and the deck quarter point a downward displacement of 2.8 m. Changing strain by 1 % gives 133 mm vertical movement at the mid-point of the main span for the main cable and the deck. Comparatively this is a higher value, as the deck under dead load condition only has 0.047 mm deformation.

b5) Effect on the towers

Increasing the main cable initial strain value increases the pre-stressing force that moves the main cable and the deck upward and also moves both tower tops away from the main span. In other words due to increasing the main cable initial strain value, the main cable on the main span expands more than the side spans. As a result the tower tops move outward from the main span, refer Figure 8b5. Increasing the initial strain value by 30 % gives the Hessle tower top a movement of 0.28 m and the Barton tower top a greater movement of 0.38 m because of the longer side span.

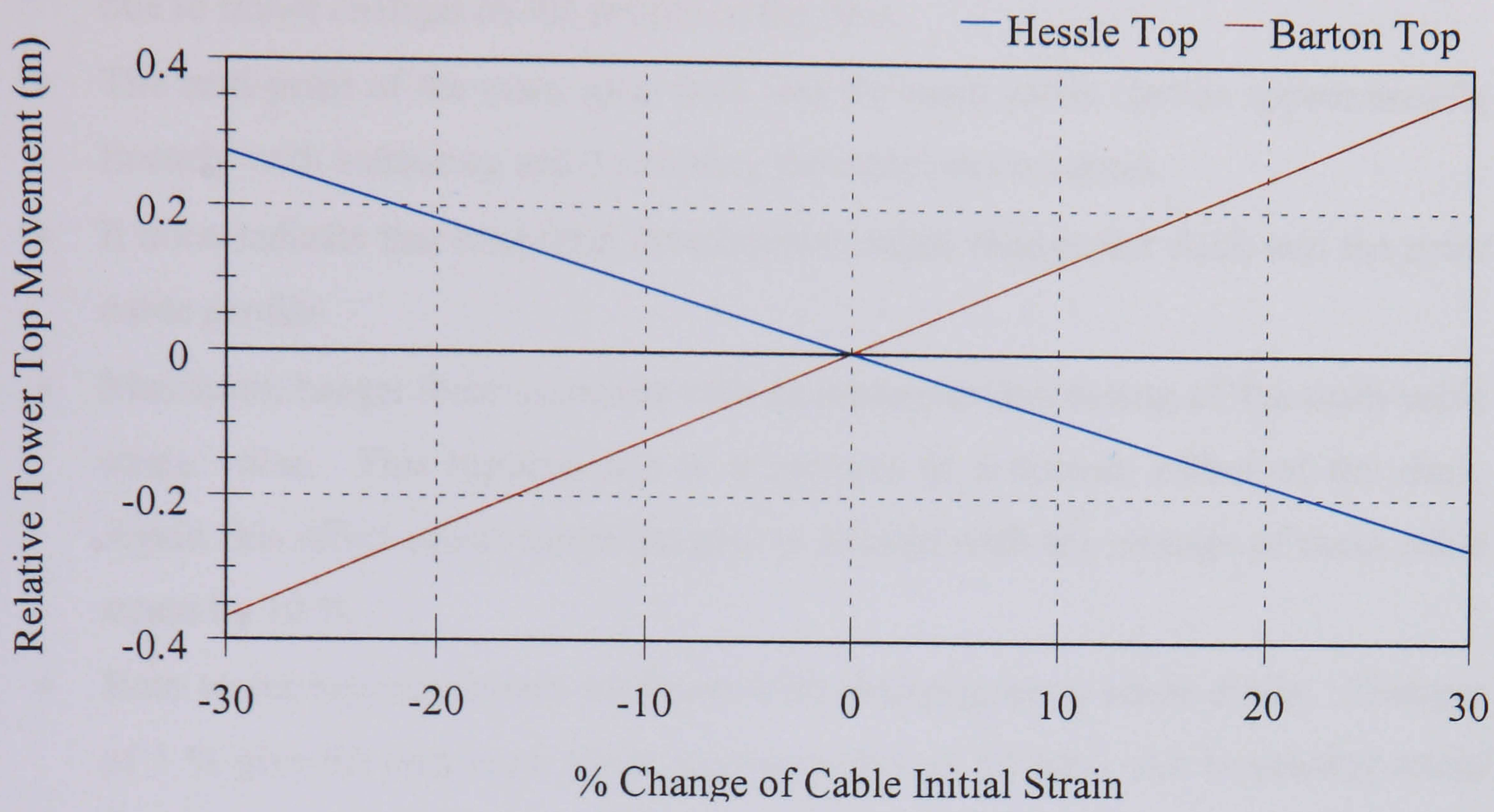

Figure 8b5: Change of tower top movement with the change of main cable initial strain

Decreasing the main cable initial strain value decreases the pre-stressing force that moves the main cable and the deck downward and pulls both tower tops towards the main span. In other words decreasing the main cable initial strain value, shortening the main cable on the main span more than the side spans, gives the tower tops movement towards the main span as shown in Figure 8b5. Decreasing the initial strain value by 30 % gives the Hessle tower top a movement of 0.27 m and the Barton tower top a movement of 0.36 m.

b6) Conclusion from changing main cable initial strain

- As for the main cable diameter, strain on the main cable at its initial stage is also sensitive, as it is a major deciding factor for the deck and the main cable profiles.
- In addition to that, hangers start to slacken just above 10 % change of the main cable strain.

- Increasing or decreasing of initial strain gives an approximately linear variation of the maximum main cable force This always occurs at the location Bc.
- The minimum main cable force changes within the middle of main span region, due to minor changes on the profile of the deck.
- The mid-point of the main span deck and the main cable moves approximately linearly with increasing and decreasing the initial strain values.
- It does indicate that long-term deterioration might change the deck and the main cable profile.
- Maximum hanger force increases with increasing or decreasing of the main cable strain value. This happens due to a concave or a convex effect of the deck. Again this effect causes some hangers to slacken with the change of main cable strain by 10 %.
- Both tower top movements are linear with changing main cable strain. Changes of 1 % give the maximum tower top movement of 13 mm. An increasing strain value move the tower tops away from the main span and a decreasing strain value moves the tower tops towards the main span.

c) Changing the hanger diameter

The hanger weight is only 0.7 % (hanger weight in tonnes, 507 t) of the total bridge weight. Increasing the hanger diameter by 30 % gives 1.12 % of total bridge weight and decreasing the hanger diameter by 30 % gives 0.3 % of the total bridge weight. Also increasing the hanger diameter decreases the maximum and minimum hanger stresses and decreasing the hanger diameter increases the maximum and minimum hanger stresses. As before the maximum and minimum forces for the main cable and hanger are plotted regardless of position.

c1) Effect on the main cables

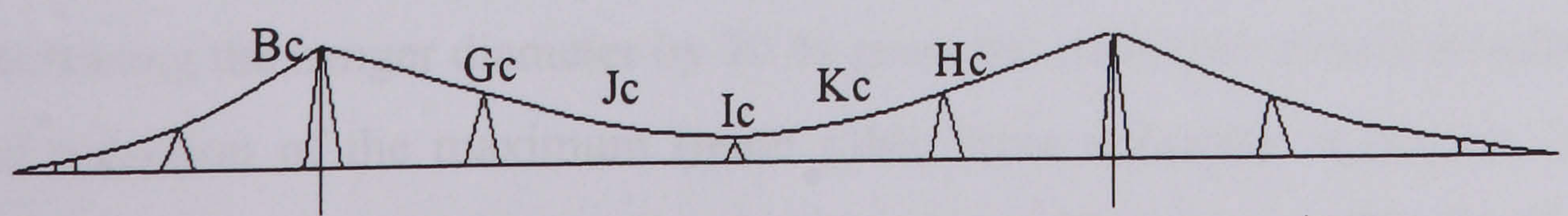

Figure 8.2: Figure shows the key main cable locations

Increasing the hanger diameter on the model increases the self-weight of the structure, which increases the main cable force on the model, but the increment of self-weight is very little. Due to increasing the hanger diameter, the maximum main cable force always occurs at location Bc. It happens because of sudden slope on the main cable at the Hessle span. The minimum main cable force always occurs at location Ic, as the change of slope is less at that location. Also the minimum hanger force (from both inclined hangers) occurs at that point.

Increasing the hanger diameter on the model by 30 % gives 1.12 % increase of total bridge weight. The maximum main cable force increases by 0.75 % (main cable force increment in tonnes, 125 t) and the minimum main cable force increases by 0.6 % (main cable force increment in tones, 95 t), refer Figure 8c1.

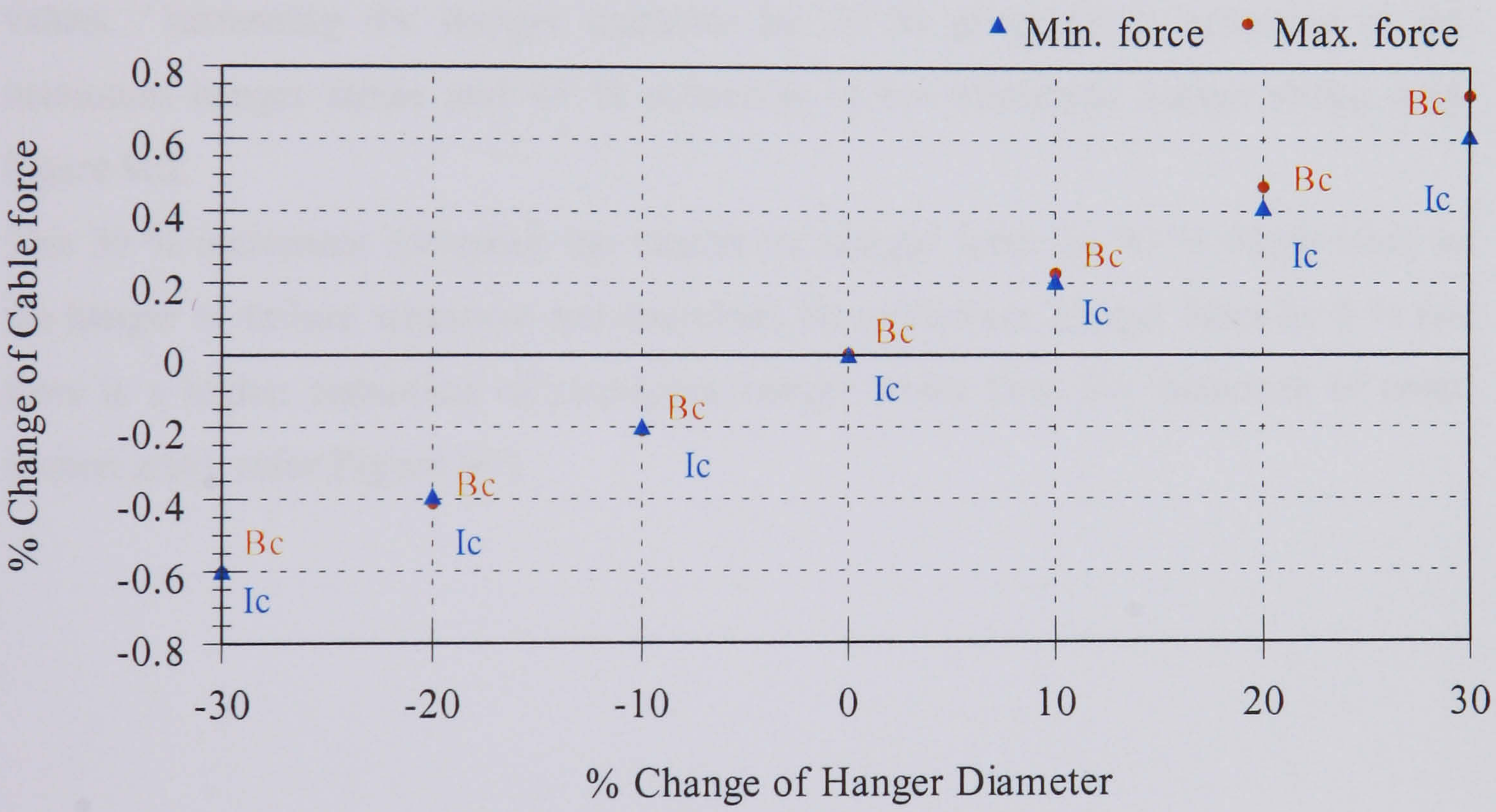

Figure 8c1: Change of main cable forces with the change of hanger diameter

Decreasing the hanger diameter on the model decreases the self-weight of the structure, which decreases the main cable force. As before the maximum main cable force occurs at location Bc and the minimum main cable force occurs at location Ic.

Decreasing the hanger diameter by 30 % gives the reduction of self-weight by 0.3 % and reduction of the maximum (main cable force reduction in tonnes, 105 t) and minimum (main cable force reduction in tonnes, 93 t) main cable force by 0.6 % (Figure 8c1). Therefore increasing or decreasing the hanger diameter does not have a significant effect on the main cable force.

c2) Effect on the hangers

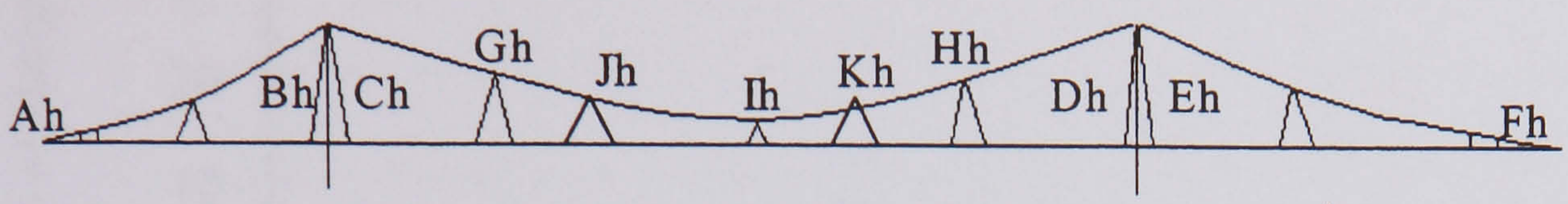

Figure 8.3: Figure shows the key hanger locations

Increasing the hanger diameter gives the maximum hanger force at location Eh and the minimum hanger force at location Ih. This increment does not give significant changes to the main cable and the deck profiles.

Increasing the hanger diameter decreases the maximum and minimum hanger stress values. Increasing the hanger diameter by 30 % gives 18 % reduction in the maximum hanger stress and 45 % reduction in the minimum hanger stress, refer Figure 8c2.

This 30 % increment increases the maximum hanger force by 43 % which leads to the hanger to failure situation and decreases the minimum hanger force by 8 % (as there is a higher reduction of minimum hanger stress than the increment of cross section area), refer Figure 8c3.

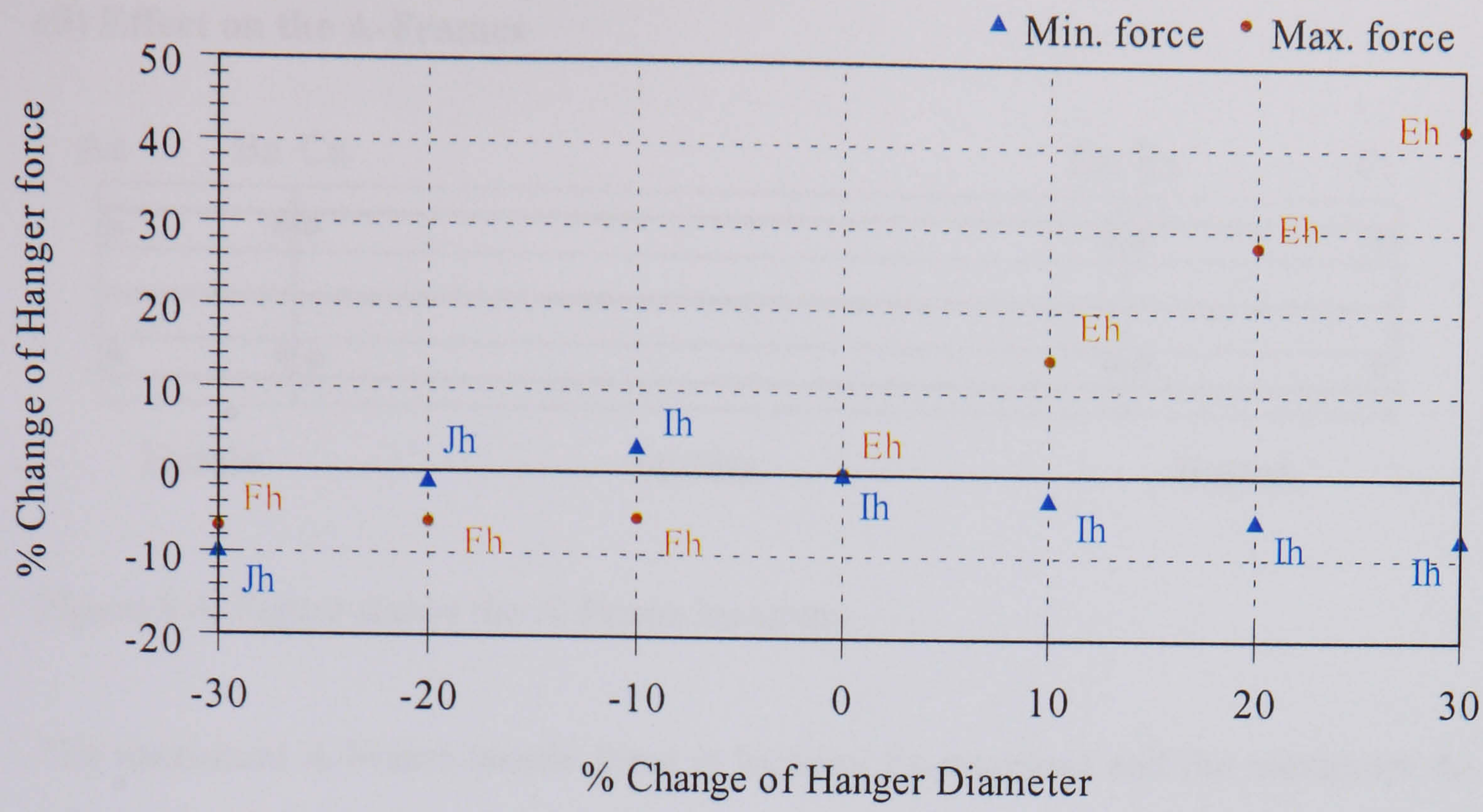

Figure 8c2: Change of hanger stress with the change of hanger diameter

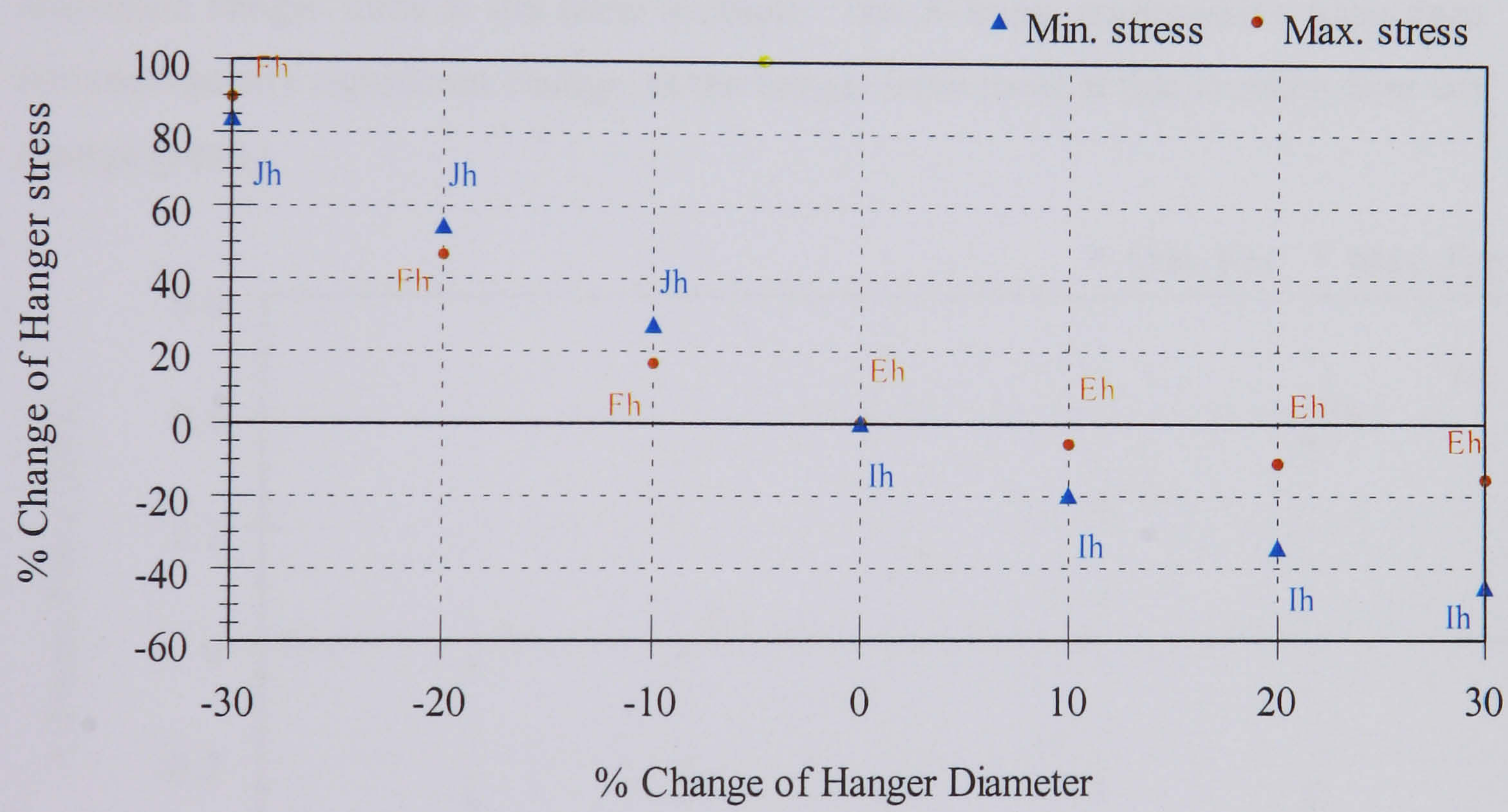

Figure 8c3: Change of hanger force with the change of hanger diameter

Decreasing the hanger diameter increases the maximum and minimum hanger stress values. The reduction of hanger diameter by 30 % gives 91 % increase of maximum stress and 84 % increase of minimum stress, refer Figures 8c3.

This 30% reduction reduces the maximum and minimum hanger forces approximately by 10 %, refer Figures 8c2.

No slackening of any hanger occurs over the selected range of hanger diameter.

c3) Effect on the A-Frames

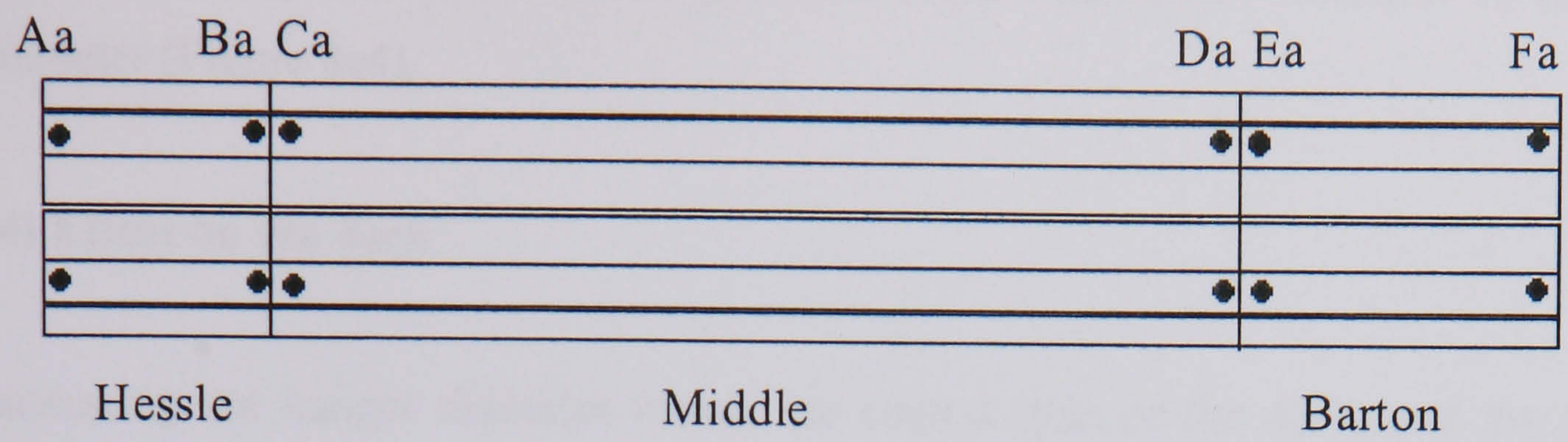

Figure 8.4: Figure shows the A-Frame locations

The maximum A-Frame tensile force at location Ea increases and the maximum A-Frame compressive force at location Aa has no change with increasing the hanger diameter. The increment of maximum tensile force occurs due to increasing the maximum hanger force at the same location. The A-frame compressive force does not undergo any significant change, as the hanger force itself at that location does not change greatly.

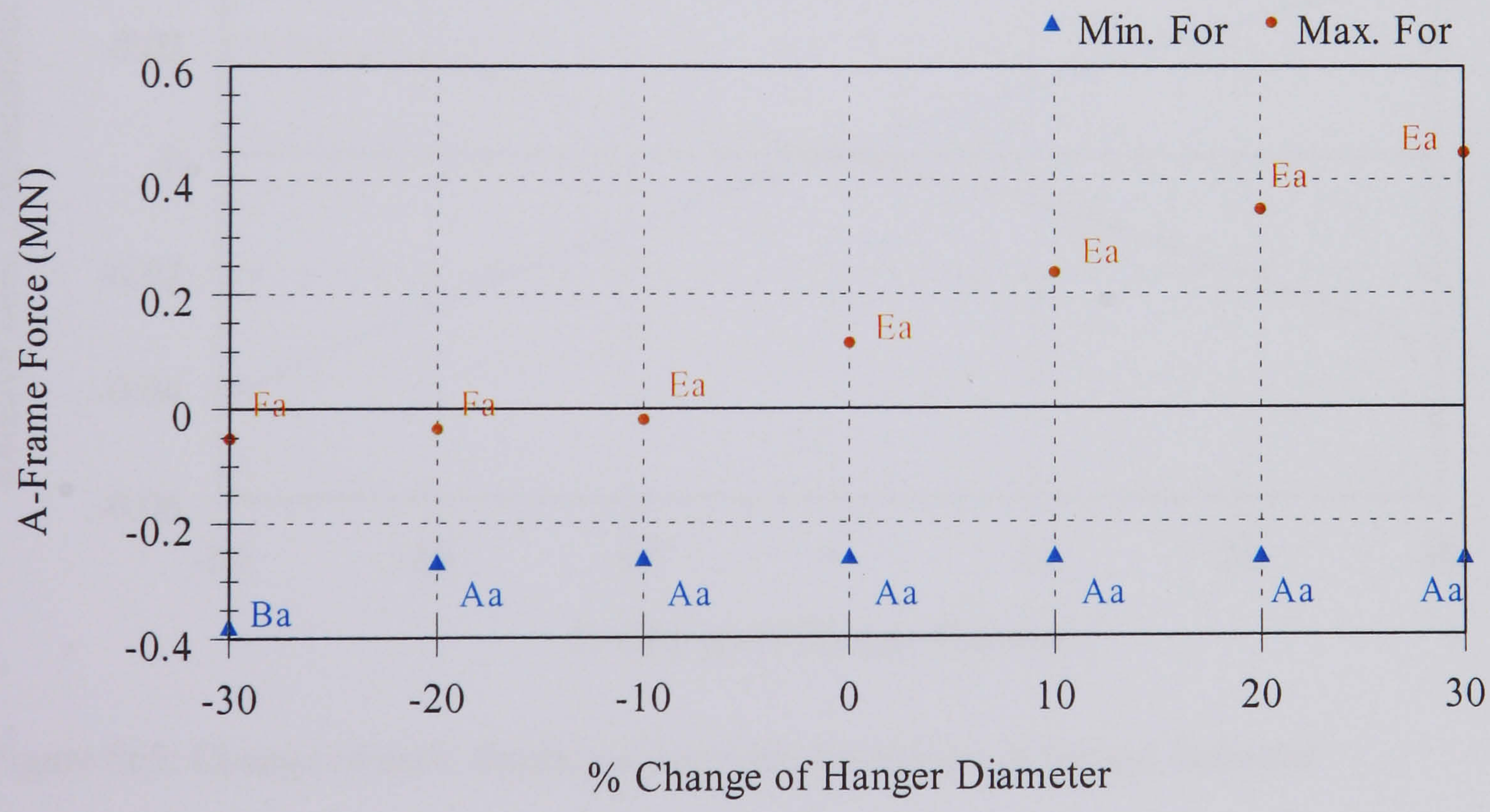

Figure 8c4: Change of A-Frame forces with the change of hanger diameter

Decreasing the hanger diameter up to 10 % decreases the maximum A-Frame tensile force. Then further reduction of the hanger diameter gives no change in the maximum A-Frame tensile force. This happens due to the decrease of the maximum hanger force at the same location up to a decreasing of hanger diameter of 10 % after which no changes in maximum hanger force occur with further reduction of hanger diameter (Figure 8c4).

c4) Effect on the deck

Increasing the hanger diameter moves the central span of the deck, and the main cable mid points relatively upward, and the quarter points relatively downward (refer Figures 8c5 and 8c6). The minimum hanger stress appears at the middle of the central span, which decreases with increasing hanger diameter. This decrease of stress decreases the strain, which then moves the deck mid point relatively upward.
At the central span quarter point the deck moves relatively downward due to shortening of the hanger being less at the quarter point of the central span than at the middle of the central span.

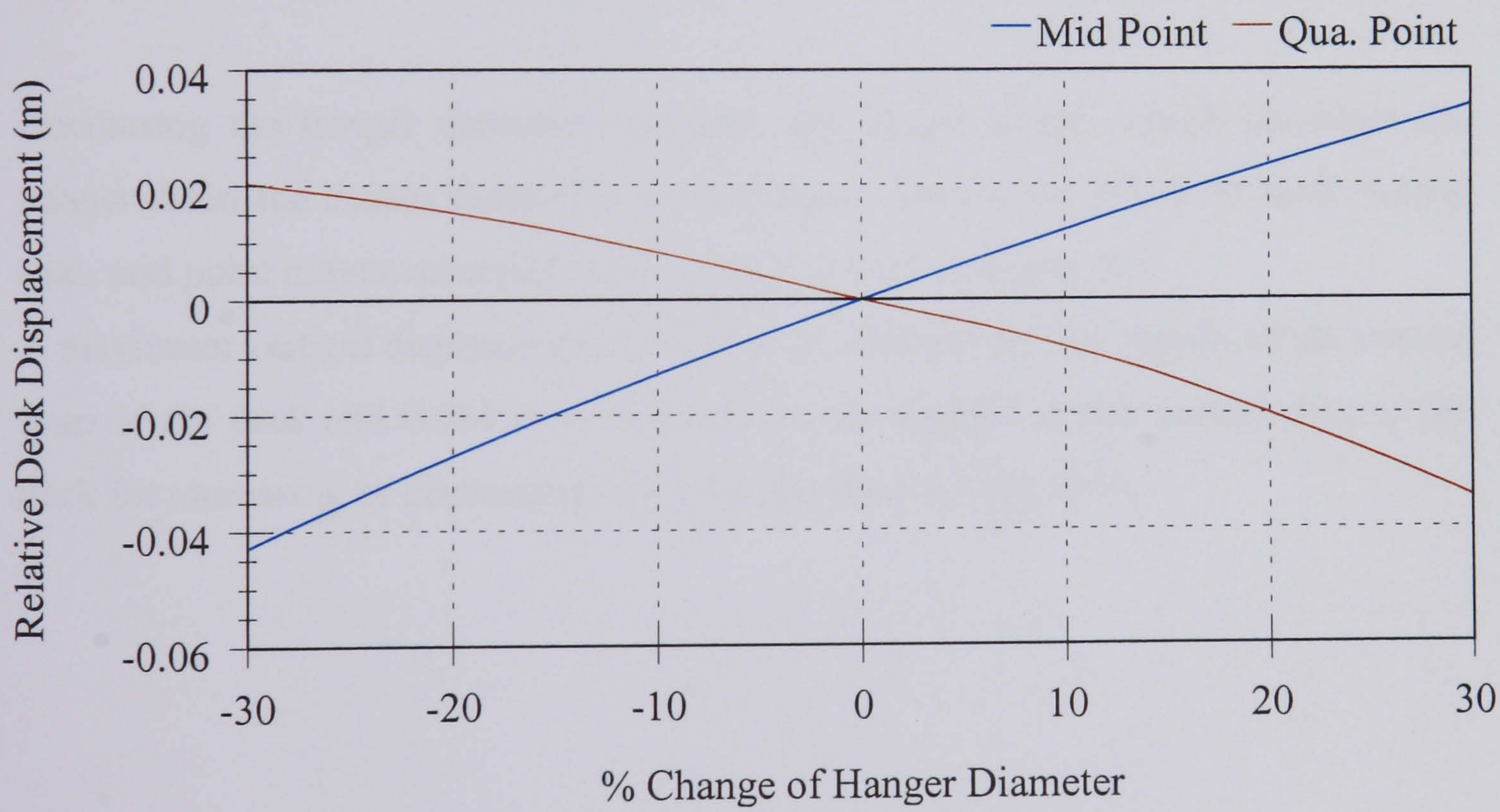

Figure 8c5: Change of deck displacements with the change of hanger diameter

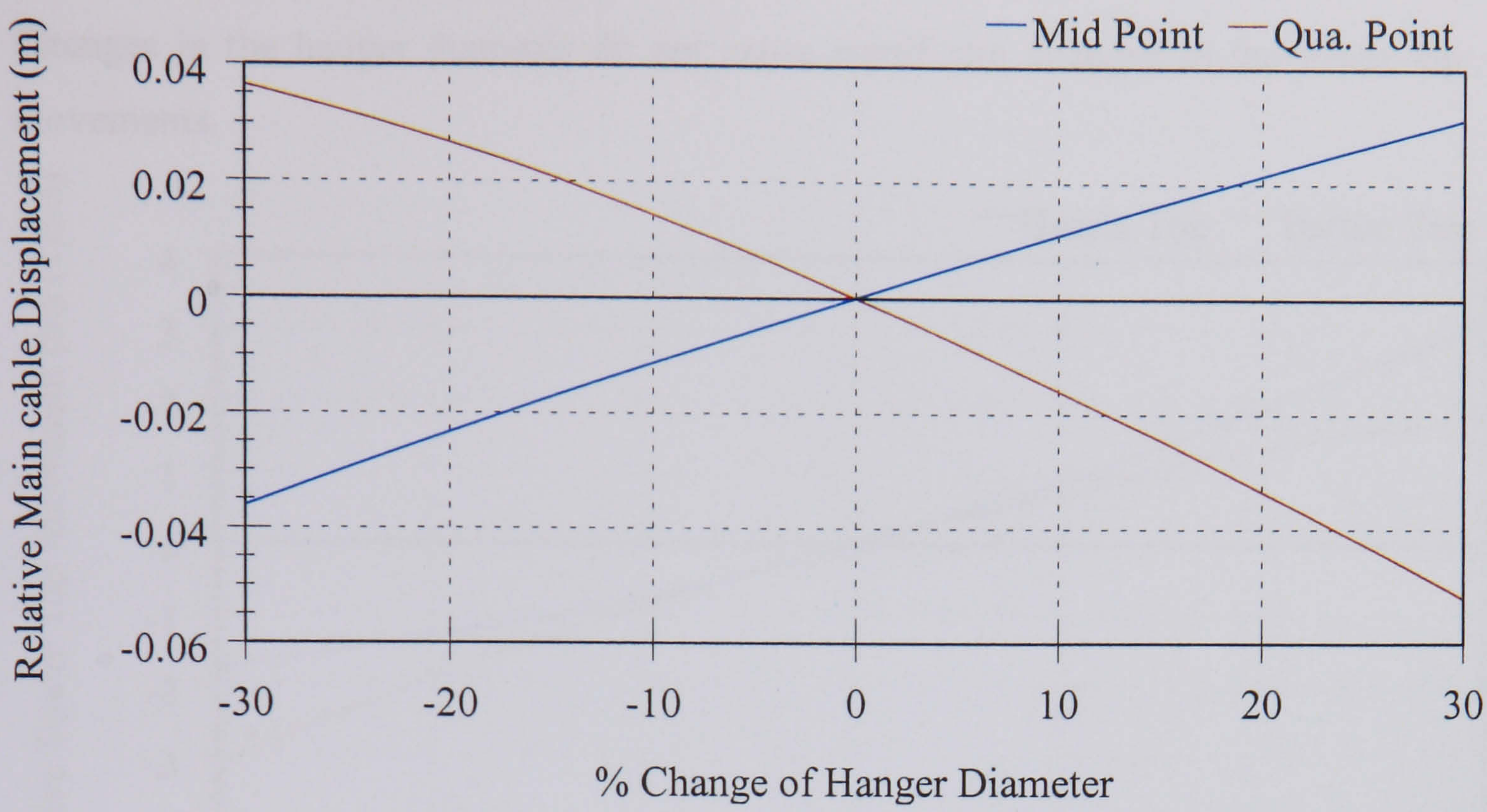

Figure 8c6: Change of main cable displacements with the change of hanger diameter

Decreasing the hanger diameter increases the hanger stress, which increases the hanger strain and causes elongation of the hanger. Due to this effect the deck central span mid point moves relatively downward as shown in Figure 8c5.

A maximum vertical displacement of 0.05 m is obtained for the middle of the central span of the deck and 0.035 m is obtained for the quarter of the central span of the deck for increasing or decreasing of the hanger diameter by 30 %.

c5) Effect on the towers

Changes in the hanger diameter do not cause significant changes in the tower top movements.

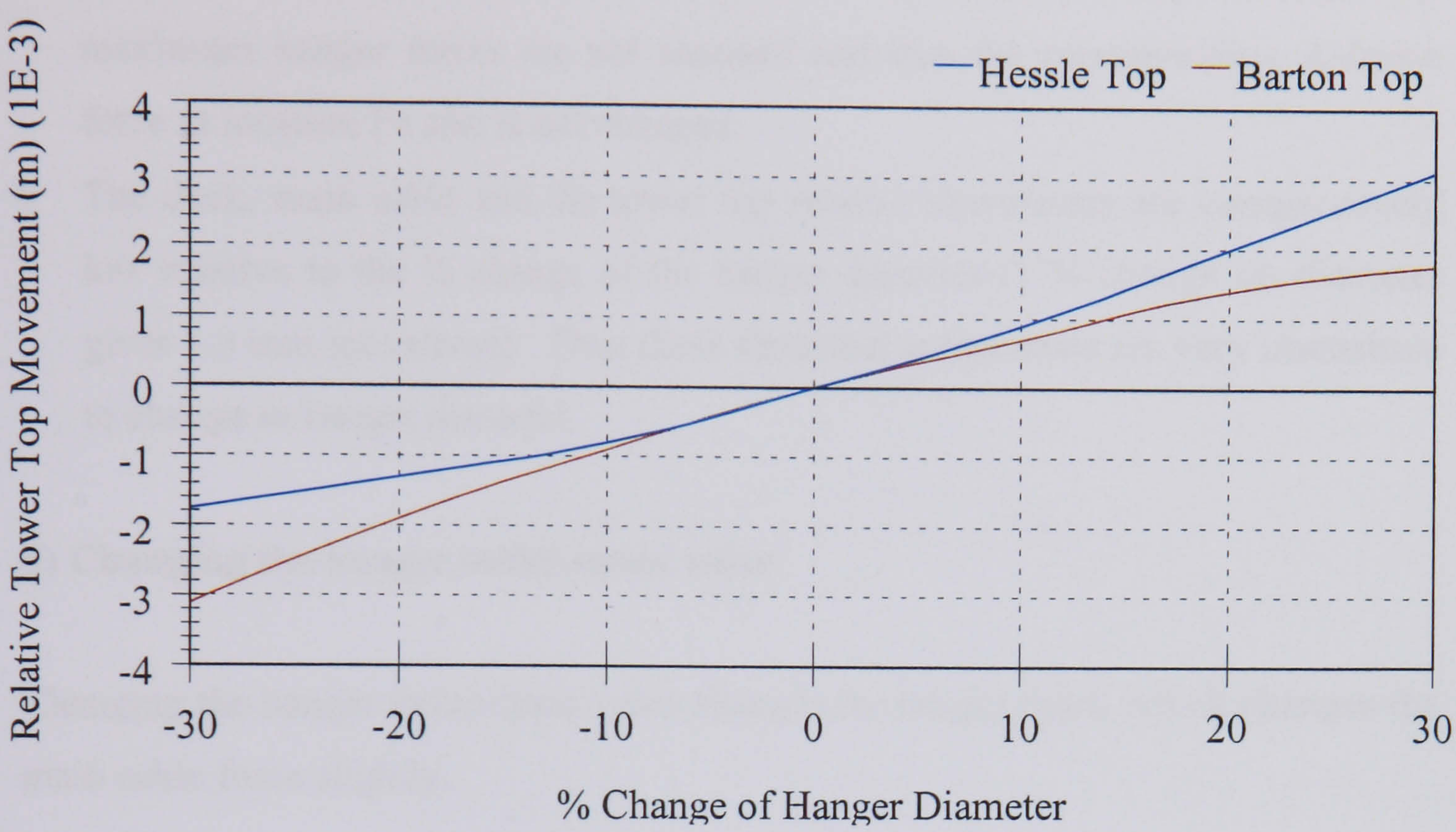

Figure 8c7: Change of tower top movement with the change of hanger diameter

c6) Conclusion on changing hanger diameter

- Sensitivity on changing the hanger diameter is less compared with changing parameters related to the main cables.
- Maximum and minimum main cable force has quite a linear variation (changes of diameter by 1% gives only 0.02 % changes in main cable force) with changing hanger diameter.
- There are no slack hangers found within the selected range. Increasing hanger diameter increases the hanger force steadily (at location Eh with the rate of 1.3% for 1% change in diameter) due to the changes on deck profile, but decreasing hanger diameter keeps the maximum hanger force (at Fh) as constant. The minimum hanger force stays at the middle of the main span region with the change of 0.33 % for 1 % change on the diameter. The maximum hanger force, and hence the maximum strain, occurs at Barton tower and at the end of the

Barton side span deck. Thus the changes do not have significant effect on the structural components.

- The tensile force on the A-frame at location Ea increases as the hanger at that particular location increases in diameter. For the decreasing diameter the maximum hanger forces are not changed and thus the corresponding A-frame force at location Fa also is not changed.
- The deck, main cable and the tower top relative movements are comparatively low relative to the % change of the hanger diameter (1 % change on diameter gives 1.3 mm movement). Thus those structural components are very insensitive to change in hanger diameter.

d) Changing the hanger initial strain value

Changing the hanger initial strain value changes the hanger force, which changes the main cable force slightly.

d1) Effect on the main cables

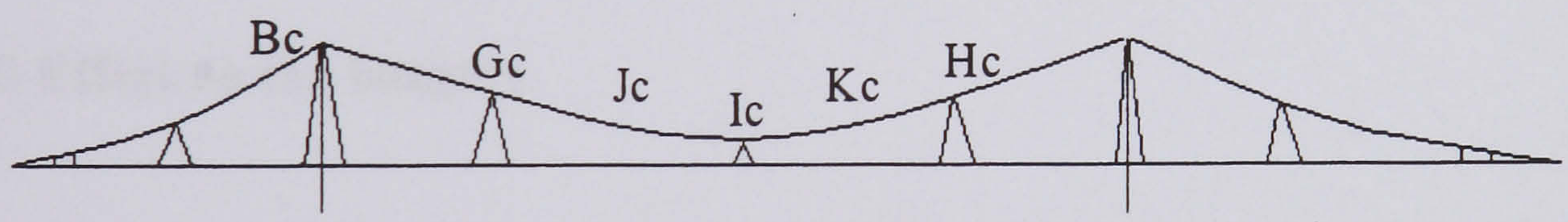

Figure 8.2: Figure shows the key main cable locations

The maximum main cable force increases slightly with increasing the hanger initial strain value, refer Figure 8d1. Increasing the hanger strain increases the maximum force on that hanger element which increases the maximum main cable force (at location Bc, refer Figure 8.1) due to the equilibrium at that main cable -hanger connection. The minimum hanger force at location Ic (Figure 8.1) does not change with increasing the strain value, which in turn gives no significant changes in the minimum main cable force at the same location.

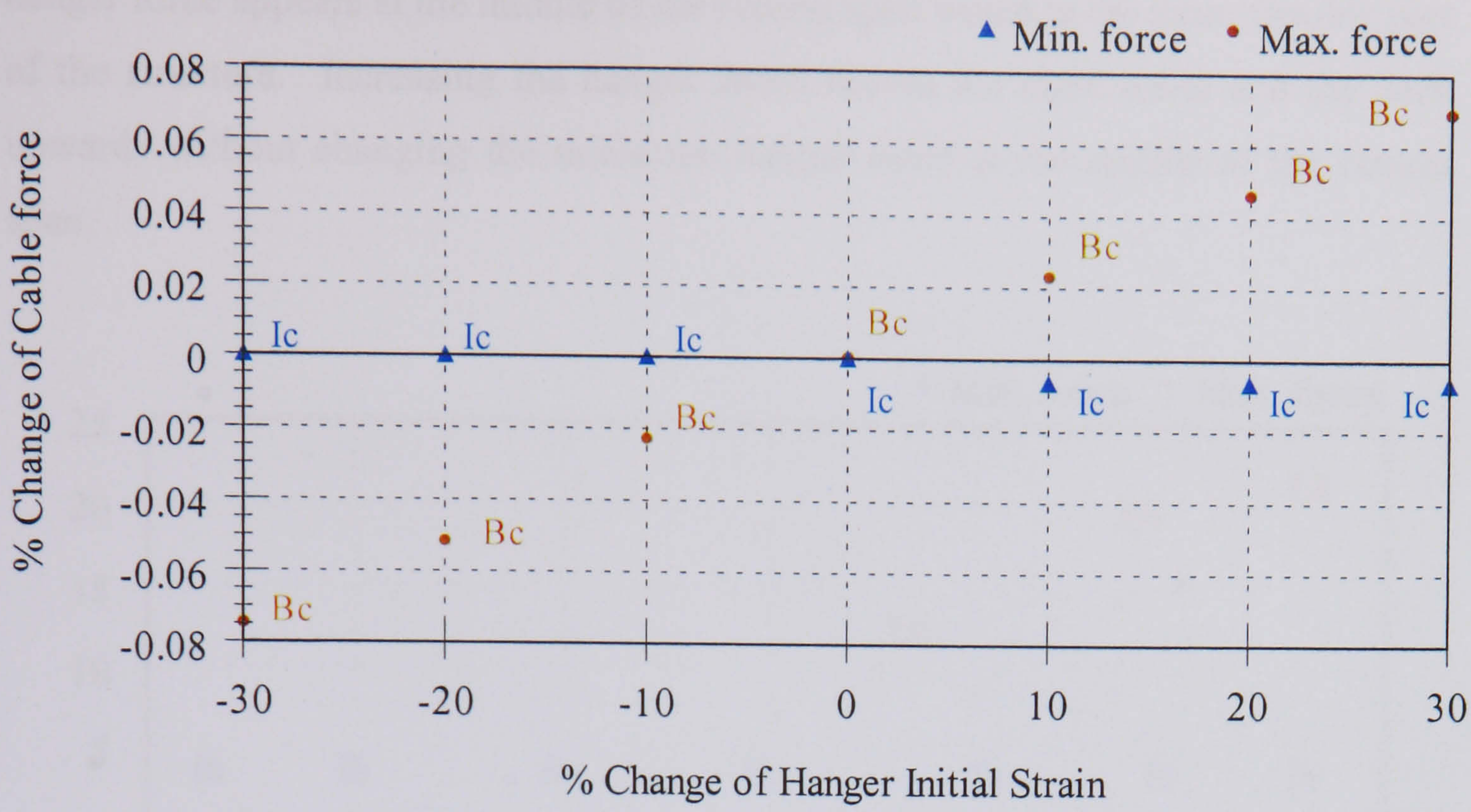

Figure 8d1: Change of main cable forces with the change of hanger initial strain

Decreasing the hanger initial strain value decreases the maximum hanger force, which decreases the maximum main cable force at location Bc. The minimum hanger force does not change with decreasing the strain value, which in turn gives no changes in the minimum main cable force (at location Ic).

d2) Effect on the hangers

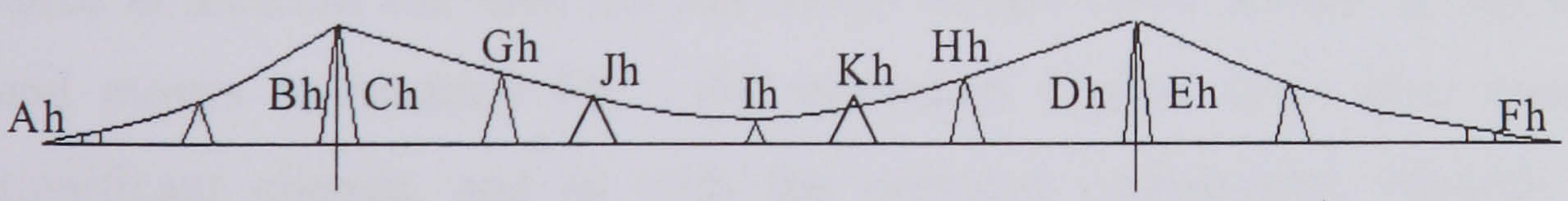

Figure 8.3: Figure shows the key hanger locations

With the initially assumed hanger initial strain value, the hangers closest to the location Ah, Bh, Ch, Dh, Eh and Fh (refer Figure 8.1) have higher initial strain value than others. The hanger closest to the location Eh has the maximum hanger force. Increasing the hanger initial strain increases the maximum hanger force at the above-mentioned location Eh pulling the deck upwards. An increase of initial strain by 30% gives 23% increase in the maximum hanger force. There is no significant change in the minimum hanger force at location Ih (refer Figure 8d2). This minimum hanger force appears at the middle of the central span which is the more flexible part of the structure. Increasing the hanger strain moves the main cable and the deck upwards without changing the minimum hanger force at the middle of the central span.

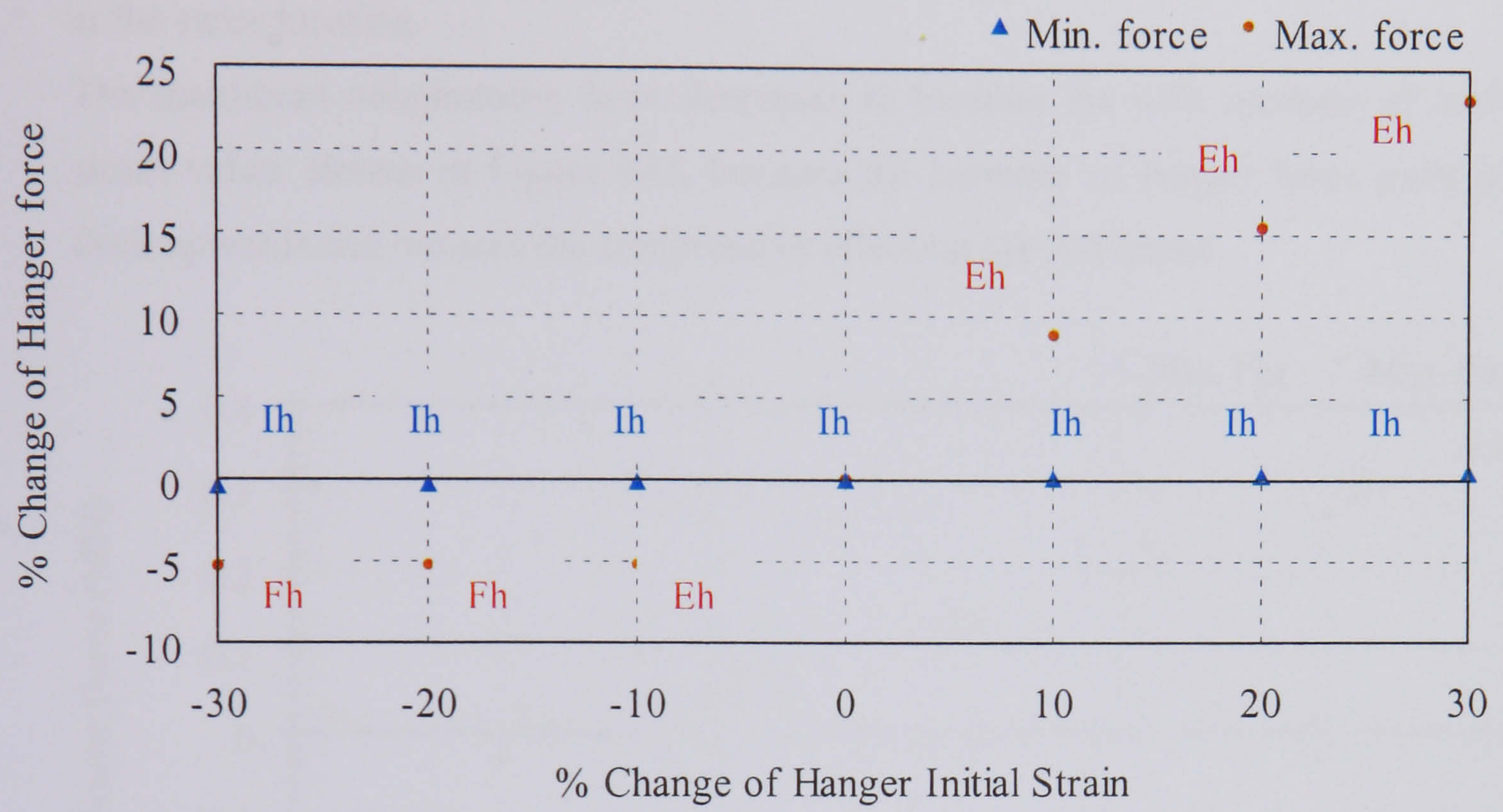

Figure 8d2: Change of hanger forces with the change of hanger initial strain

Decreasing the initial strain value by up to 10 % decreases the maximum hanger force at location Eh; then the maximum hanger force suffers no significant change and moves to location Fh. The minimum hanger force also does not have a significant change, and as with the previous explanation, remains at the same location Ih (Figure 8d2).

d3) Effect on the A-Frames

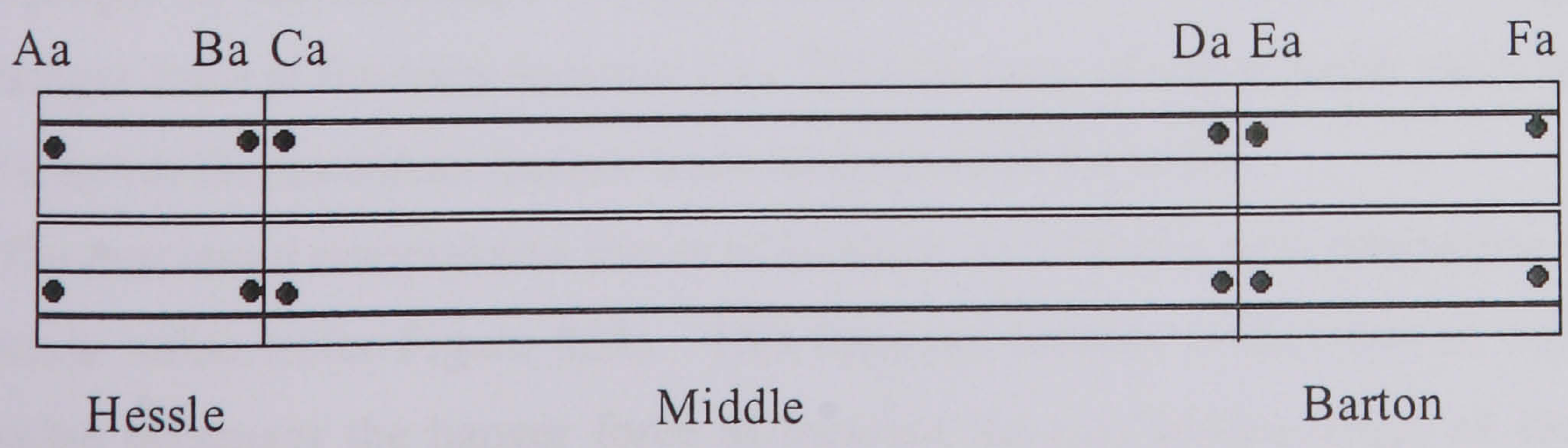

Figure 8.4: Figure shows the key A-Frame locations

Due to the deflected geometry of the structure with its initially assumed hanger initial strain values, the A-Frame at location Aa has the maximum compressive force and that at location Ea has the maximum tensile force, refer Figure 8d3.

Increasing the hanger initial strain value increases the maximum A-Frame tensile force at location Ea, because of the resulting increase of the maximum hanger force at the same location.

The maximum compressive force decreases at location Aa with increase of initial strain value, shown in Figure 8d3, because the increase of hanger force pulls the deck upwards and reduces the compressive effect on the A-Frames.

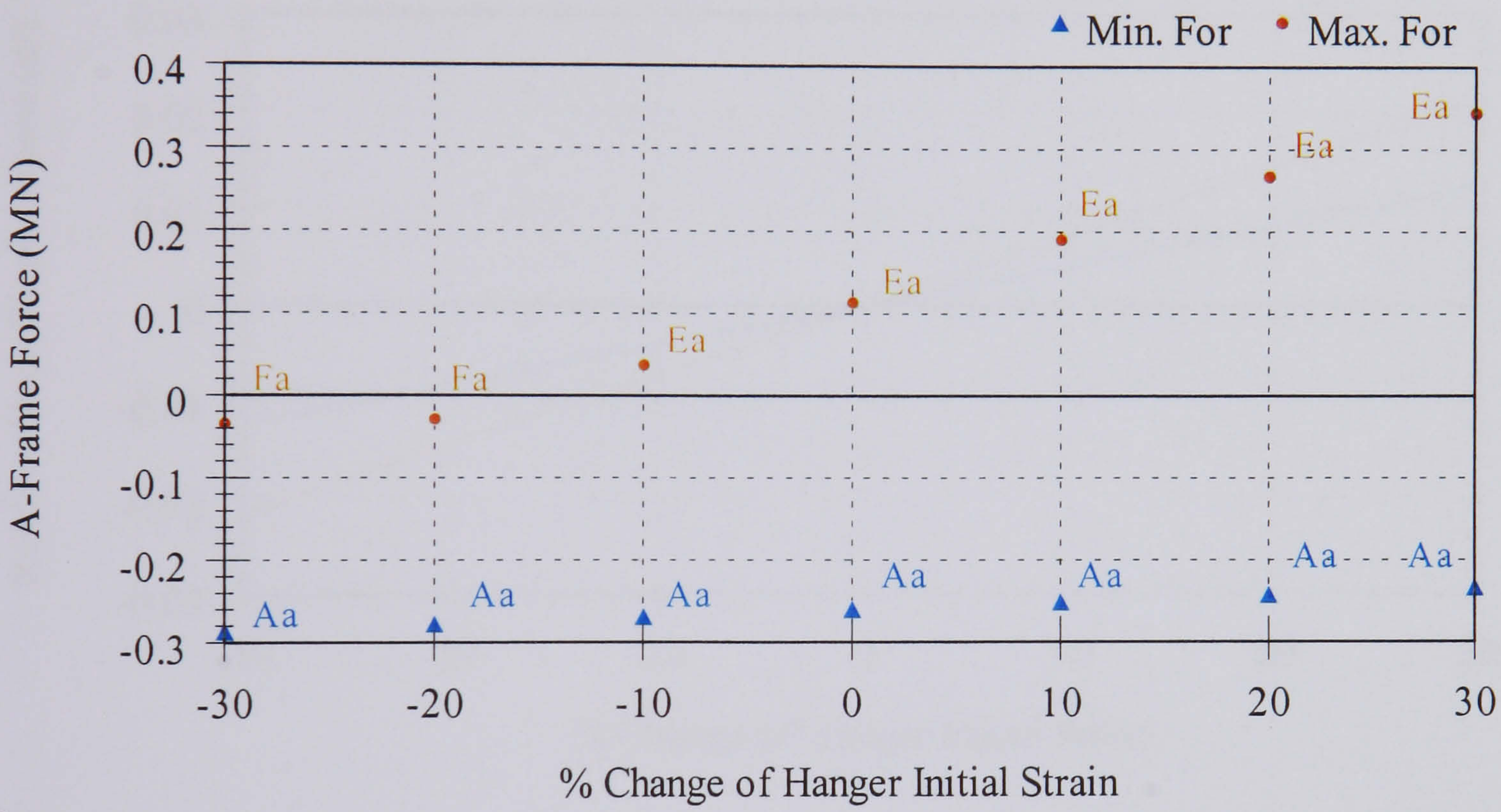

Figure 8d3: Change of A-Frame forces with the change of hanger initial strain

Decreasing the initial strain value decreases the maximum A-Frame force as the maximum hanger force on the same location Ea decreases. There are no significant changes in the maximum A-Frame force beyond 20 % due to no changes in the hanger force at the same location Ea. This decrease of initial strain value beyond 20 % moves the maximum hanger force location from Ea to Fa.

The maximum compressive forces at location Aa increase with decreasing the initial strain value (refer Figure 8d3). This happens because a decrease of initial strain value decreases the hanger force at location Aa (i.e. pulling force of the deck at location Aa decreases).

d4) Effect on the deck

The deck central span's mid point and quarter point both move upward with increasing hanger initial strain value. The increment of hanger force at a quarter point is higher than at the mid-point, which therefore moves the deck quarter point more than the mid-point.

Increasing strain by 30 % moves the mid point upward by 0.013 m and quarter point by 0.022 m relative to the initially assumed position, refer Figure 8d4.

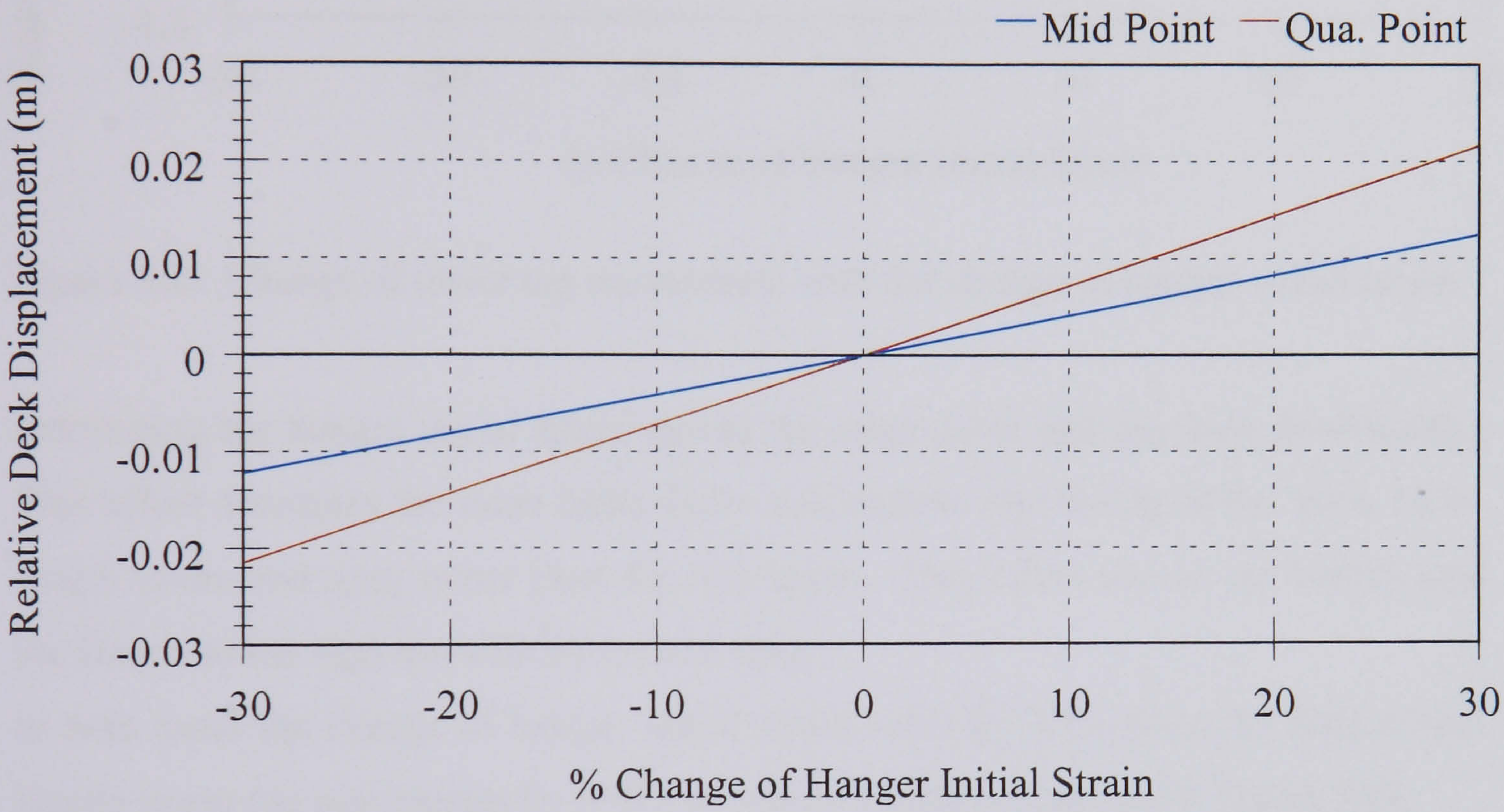

Figure 8d4: Change of deck displacements with the change of hanger initial strain

Similarly decreasing the hanger initial strain moves the deck quarter and mid point downward. Again the quarter point moves more than the mid-point. Decreasing strain by 30 % moves the mid point downward by 0.012 m and quarter point by 0.022 m relative to the initial position.

d5) Effect on the towers

Increasing the hanger initial strain moves the main cable and the deck upwards. As mentioned before the main cable force increases which leads to elongation of the main cable at mid span rather than the side spans. This effect moves the Barton and the Hessle tower tops away from the central span.

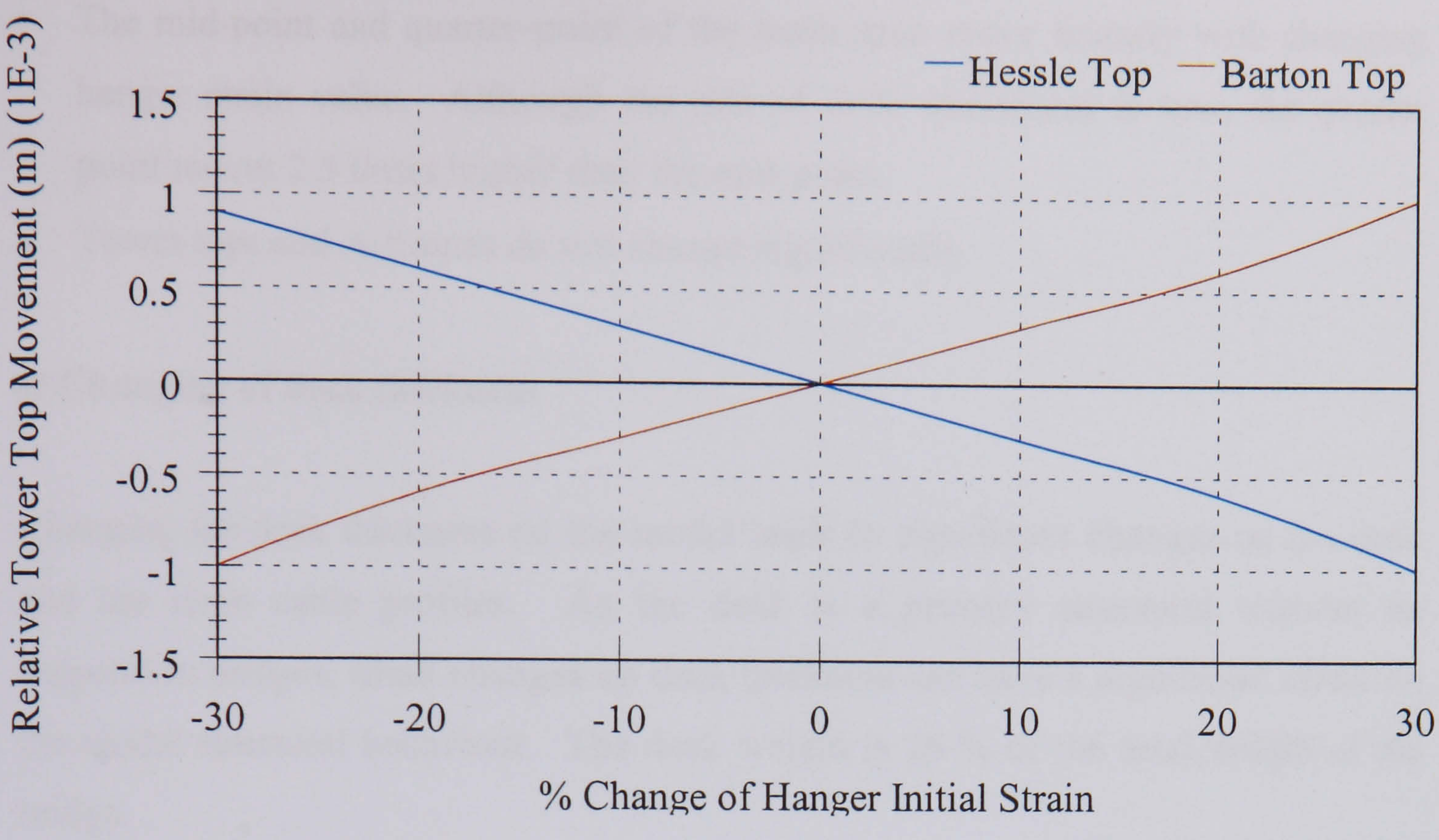

Figure 8d5: Change of tower top movements with the change of hanger initial strain

Decreasing the hanger initial strain moves the main cable and the deck downwards. This effect decreases the main cable force and leads to shortening of the main cable length at the mid span rather than the side spans. This effect moves the Barton and the Hessle tower tops towards the central span.

In both cases the change of hanger initial strain value by 30% gives the Barton and Hessle tower top movements by 0.001 m which is insignificant (refer Figure 8d5).

d6) Conclusion on changes of hanger initial strain

- Changes of hanger initial strain (introducing extra pulling force to the hangers) are more sensitive than the changes of the hanger diameter, as this strain is a factor for (minor) adjustment of the deck and the main cable profiles.
- The main cable force does not change significantly as it is in the order of 1000 times the hanger force.
- Hangers start to slacken just above 10 % change of the initial strain value. Increasing or decreasing of the initial strain value increases the maximum hanger force and decreases the minimum hanger force.

- The mid-point and quarter-point of the main span move linearly with changing hanger strain value. Although the rate of deck movement is low, the quarter point moves 2.5 times higher than the mid-point.
- Tower tops and A-frames do not change significantly.

e) Changing of deck thickness

Changing the deck thickness on the model leads to significant changes on the deck and the main cable profiles. As the deck is a primary structural element on suspension bridges, small changes on deck thickness can have a significant effect on the model structural behaviour. The deck weight is 26 % of the total weight of the bridge.
Increasing the deck thickness by 30 % gives 7 % increase in the total bridge weight and decreasing the deck thickness by 30 % gives 8 % decrease in the total bridge weight. Here the moment of inertia about the major and minor axis were kept as constant, so that the changing deck thickness does not affect the flexural stiffness.

e1) Effect on the main cables

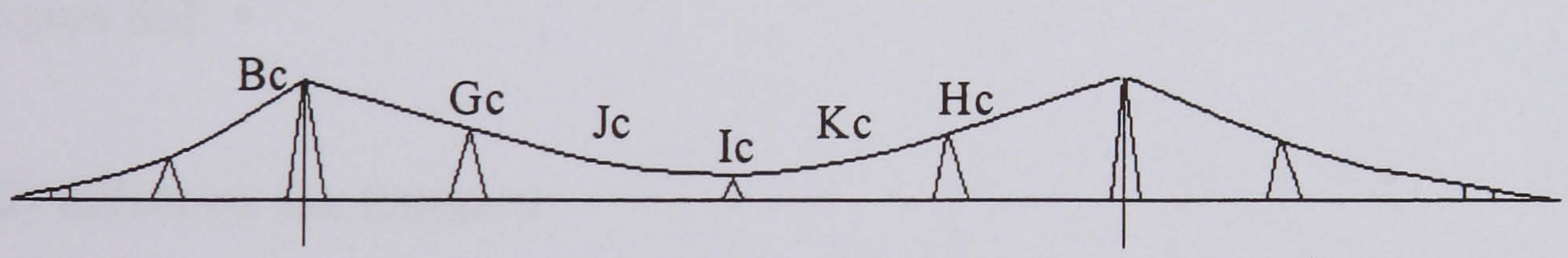

Figure 8.2: Figure shows the key main cable locations

Increasing the deck thickness on the model increases the total weight of the bridge model, which increases the main cable force on the structure. This increases the main cable strain, which expands the main cable and leads to downward movement of the deck and the main cable profile. Increasing the deck thickness by 30 % gives a 15 % increment in the maximum main cable force, refer Figure 8e1.

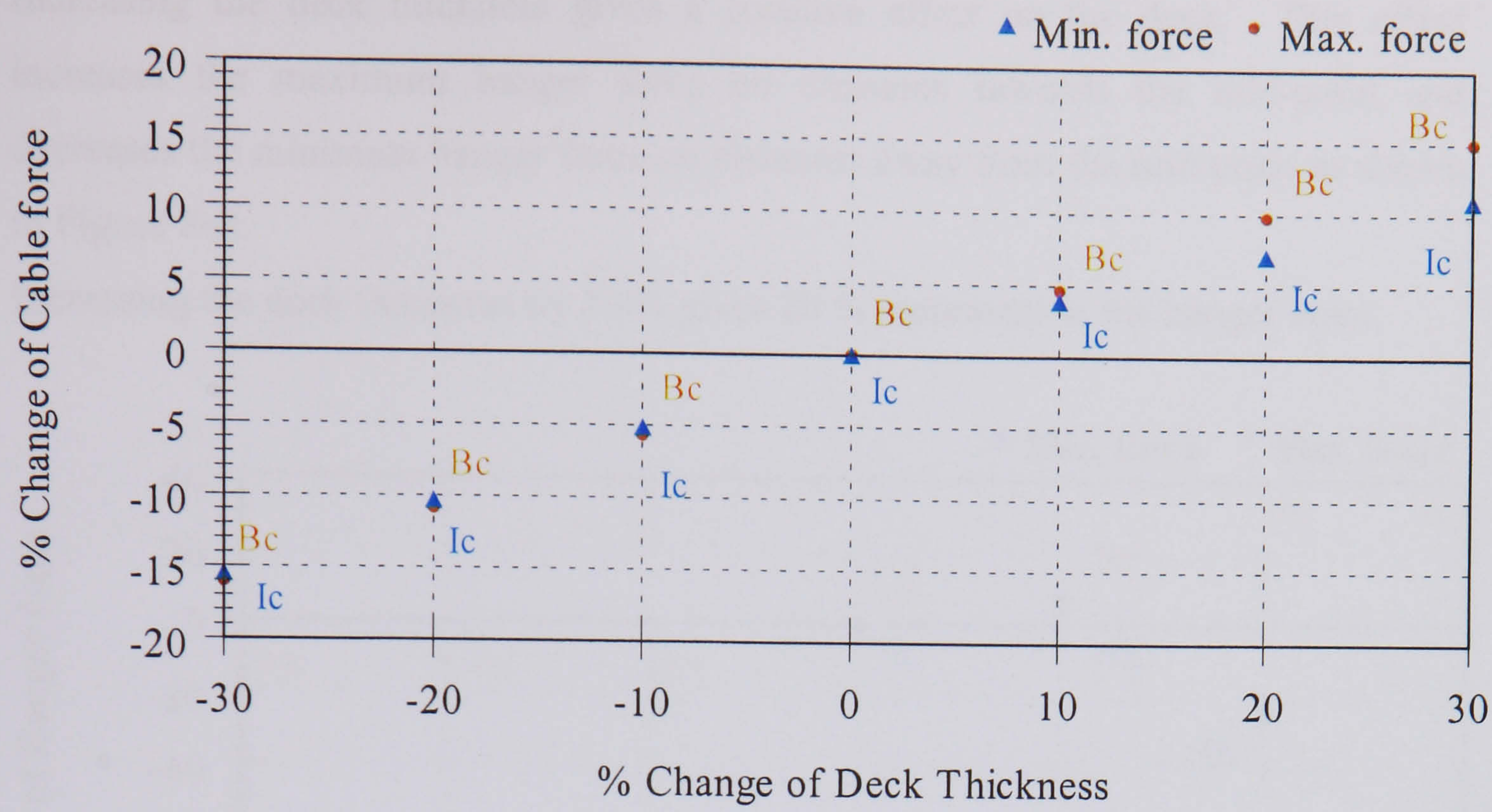

Figure 8e1: Change of main cable forces with the change of deck thickness

Decreasing the deck thickness decreases the main cable force, which decreases the main cable strain. As a result shortening of the main cable and relatively upward movement of the deck and the main cable profile occur. Decreasing the deck thickness by 30 % gives 16 % reduction in the maximum main cable force, refer Figure 8e1.

e2) Effect on the hangers

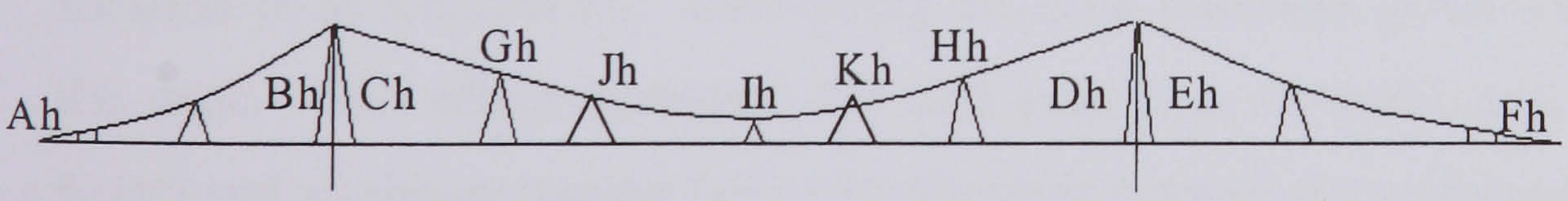

Figure 8.3: Figure shows the key hanger locations

With the initially assumed deck thickness, the hangers closest to the location Ah, Bh, Ch, Dh, Eh and Fh have higher initial strain value than others. This gives higher force value on those hangers than the others and the hanger closest to the location Eh has the maximum hanger force.

Increasing the deck thickness moves the maximum hanger force from location Eh to location Fh and the minimum hanger force moves from location Ih to location Hh.

Increasing the deck thickness gives a concave effect on the deck. This effect increases the maximum hanger force on elements towards the mid-point and decreases the minimum hanger force on elements away from the mid-point as shown in Figure 8e2.

Increasing the deck thickness by 30 % gives 20 % increment in the hanger force.

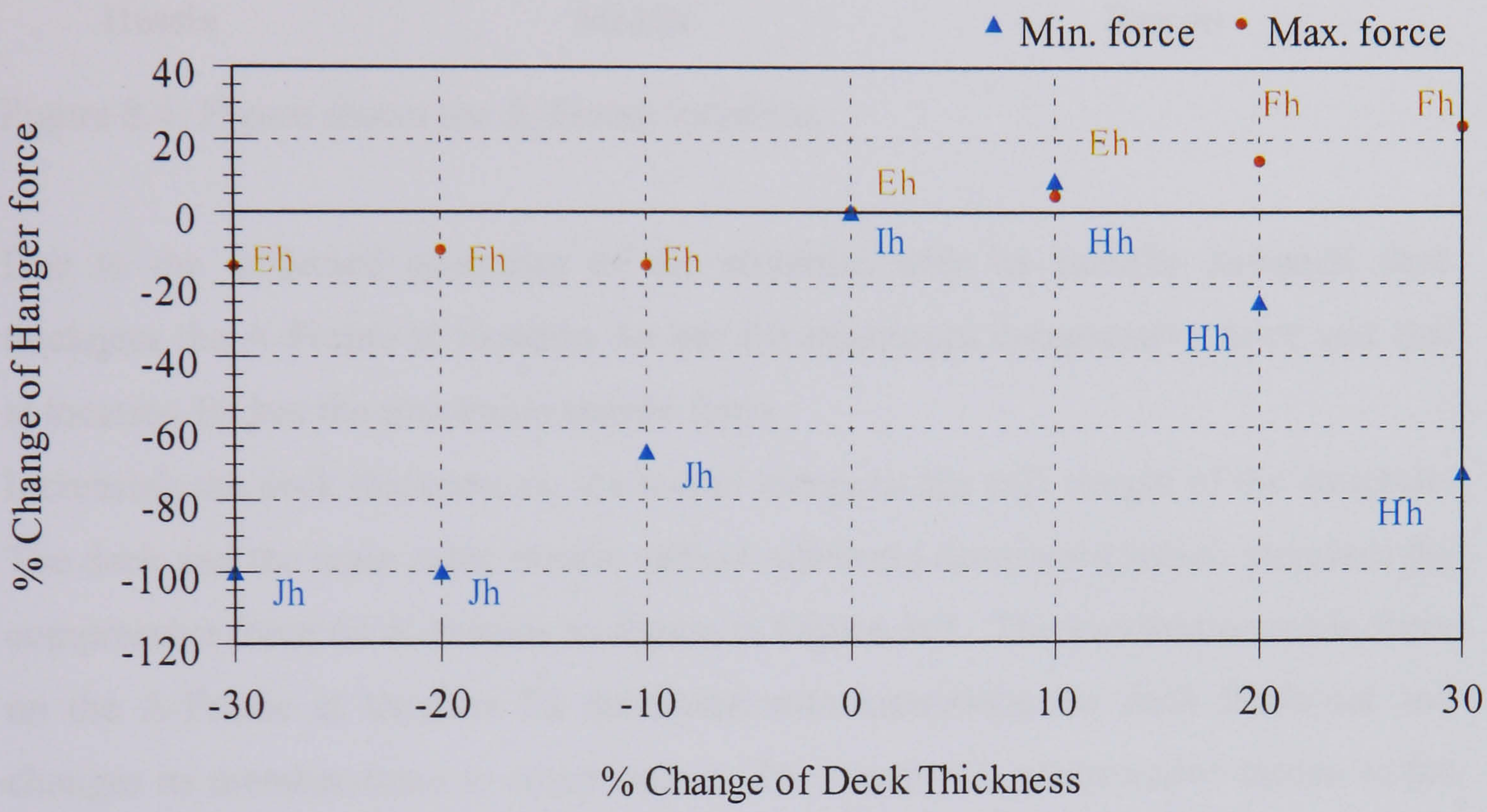

Figure 8e2: Change of hanger forces with the change of deck thickness

Decreasing the deck thickness moves the maximum hanger force from location Eh to location Fh then back to location Eh and the minimum hanger force moves from location Ih to location Fh. Decreasing the deck thickness gives a convex effect on the deck. This effect decreases the maximum (on elements away from the mid-point) and minimum hanger force (on elements towards the mid-point) values.

Decreasing the deck thickness by 30 % also gives 20 % reduction in the hanger force. Slackening of hanger occurs beyond decreasing the deck thickness by 20%, refer Figure 8e2.

e3) Effect on the A-Frames

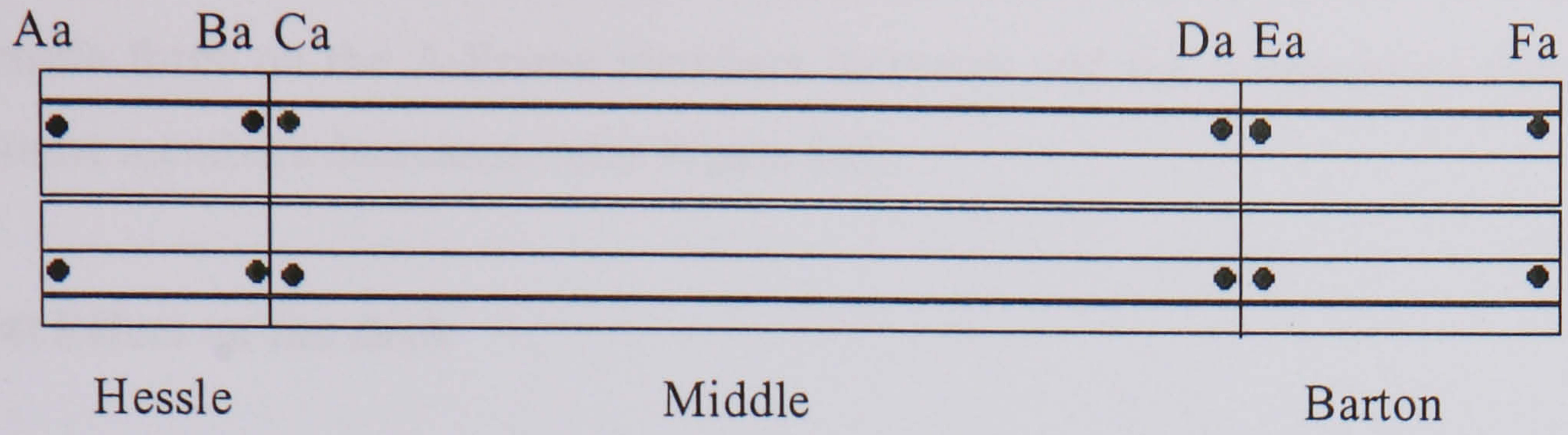

Figure 8.4: Figure shows the A-Frame locations

Due to the deflected geometry of the structure with its initially assumed deck thickness the A-Frame at location Aa has the maximum compressive force and that at location Ea has the maximum tensile force.

Increasing the deck thickness on the model increases the self-weight of the structure. The deck and the main cable profile deflect relatively downward which increases the compressive force on A-Frames as shown in Figure 8e3. The maximum tensile force on the A-Frame at location Fa decreases with increasing the deck thickness and changes its member force to compressive. The maximum compressive forces on the A-Frame at location Aa increases with increasing the deck thickness.

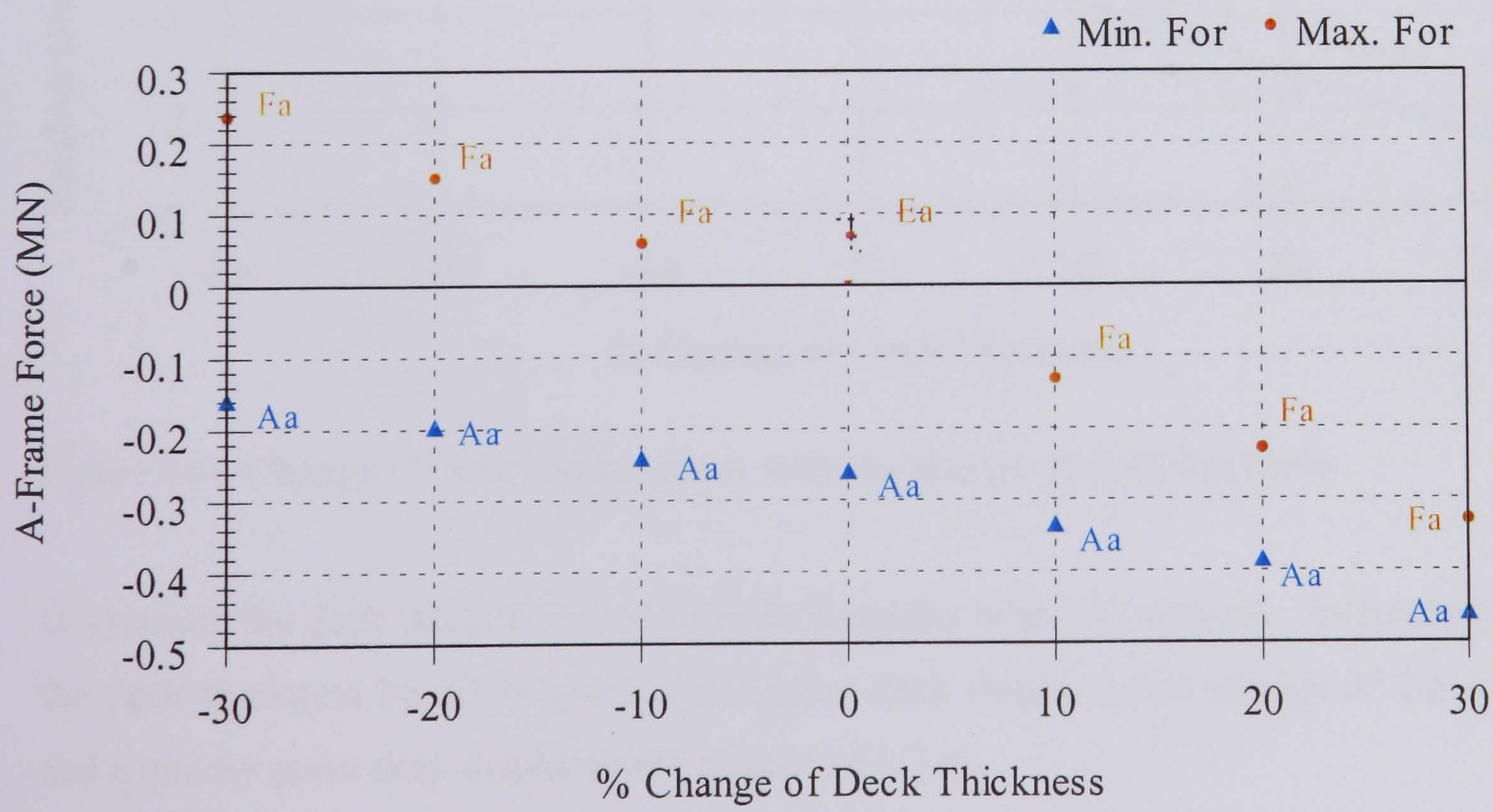

Figure 8e3: Change of A-Frame forces with the change of deck thickness

Decreasing the deck thickness on the model decreases the self-weight of the structure and moves the deck and the main cable profile relatively upwards. As a result the tensile force on the A-Frame members increases and the compressive force on A-Frame members decreases, refer Figure 8e3.

e4) Effect on the deck

The deck displacement changes significantly with changing the deck thickness as shown in Figure 8e4.

Increasing the deck thickness moves the deck profile downward due to increasing its self-weight. Increasing the deck thickness by 30% gives the mid-point deck displacement a change of 2.4 m and the quarter point deck displacement a change of 1.7 m.

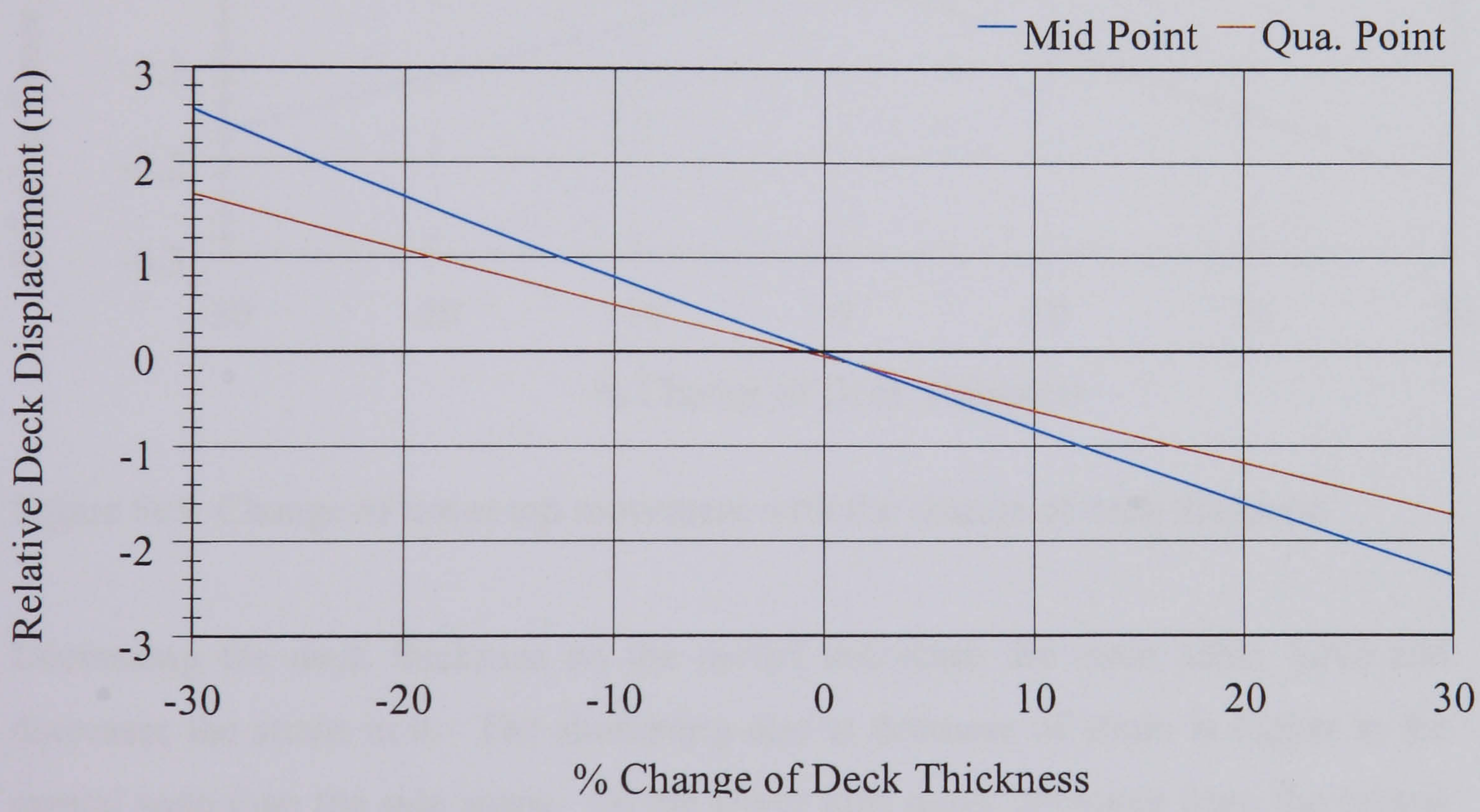

Figure 8e4: Change of deck displacement with the change of deck thickness

Decreasing the deck thickness moves the deck profile relatively upward. Decreasing the deck thickness by 30 % gives a mid-point deck displacement change of 2.6 m and a quarter point deck displacement change of 1.7 m.

e5) Effect on the towers

Increasing the deck thickness on the model increases the main cable force on the structure, which increases the strain on the main cable. The elongation on the main cable due to increasing strain is higher at the central span than the side spans. This difference in elongation pulls the tower tops towards the central span.
Increasing the deck thickness by 30 % gives Barton tower top movement of 0.23 m and Hessle tower top movement of 0.17 m as shown in Figure 8e5.

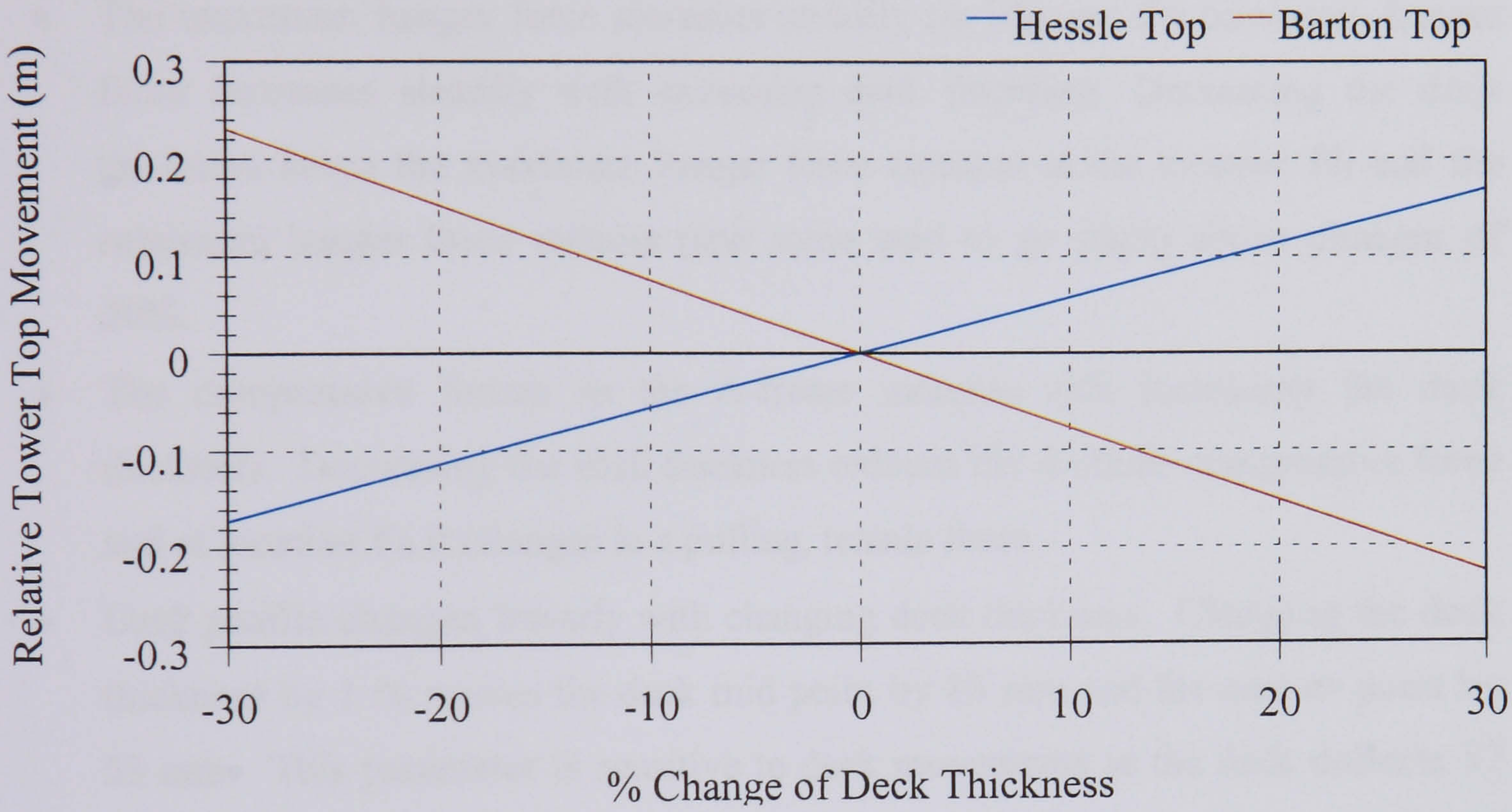

Figure 8e5: Change of tower top movement with the change of deck thickness

Decreasing the deck thickness on the model decreases the main cable force and decreases the strain in it. The shortening due to decrease of strain is higher at the central span than the side spans. So the tower tops move outwards from the central span.
Decreasing the deck thickness by 30 % gives Barton tower top movement of 0.23 m and Hessle tower top movement of 0.17 m, refer Figure 8e5.

e6) Conclusion on changing deck thickness

- As with the main cable, the deck is another structural component on suspension bridges which has a very significant effect on the overall structural behaviour. The basic deck contributes 25 % of the total bridge weight.
- The maximum and minimum main cable force changes approximately linearly (change of deck thickness by 1 % gives 0.5 % change in the main cable force) with increasing or decreasing deck thickness.
- The maximum hanger force increases steadily (at Eh) and the minimum hanger force decreases steadily with increasing deck thickness. Decreasing the deck thickness keeps the maximum hanger force constant at the location Fh and the minimum hanger force reduces (and some start to go slack) above changes of 20%.
- The compressive forces on the A-frame increase with increasing the deck thickness. Decreasing the deck thickness reduces the A-frame compressive force and at location Fa it changes to a pulling, tensile force.
- Deck profile changes linearly with changing deck thickness. Changing the deck thickness by 1 % moves the deck mid point by 83 mm and the quarter point by 53 mm. This parameter is sensitive to deck movements as the deck deflects 57 mm under the bridge self weight.
- Tower tops move linearly with changing deck thickness. Changes of 1 % give 8mm movement on the tower top. Increasing the deck thickness moves the tower tops towards the main span and decreasing the deck thickness moves the tower tops away from the main span.

f) Changing of the deck stiffness

Introducing stiffeners while there is no change in the total weight of the deck can change deck stiffness on the model. Introducing different I-values without changing the deck cross sectional area can be affected by this procedure. As a result there is no change in the total weight. This I-value change does not have significant effect on the model structural member forces.

f1) Effect on the main cables

Changing the deck stiffness does not have any significant change in the main cable force. This happens due to there being no change in the self-weight of the model structure.

f2) Effect on the hangers

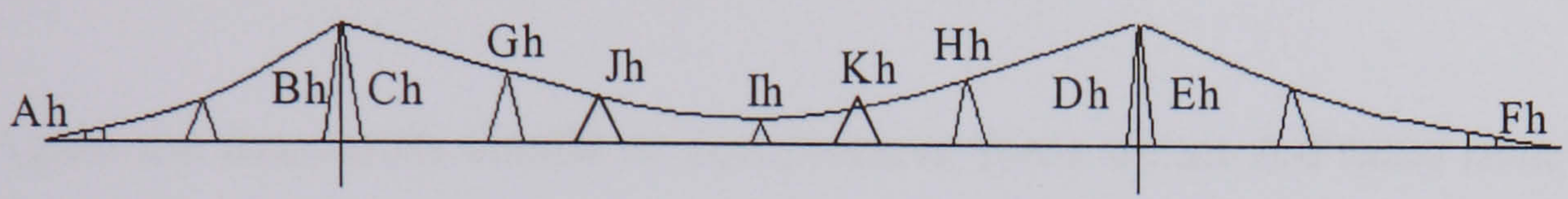

Figure 8.3: Figure shows the key hanger locations

Changing the deck stiffness does not have any significant effect on the maximum and the minimum hanger force on the model. No considerable changes in the hanger force occur due to the constant self-weight of the structure.

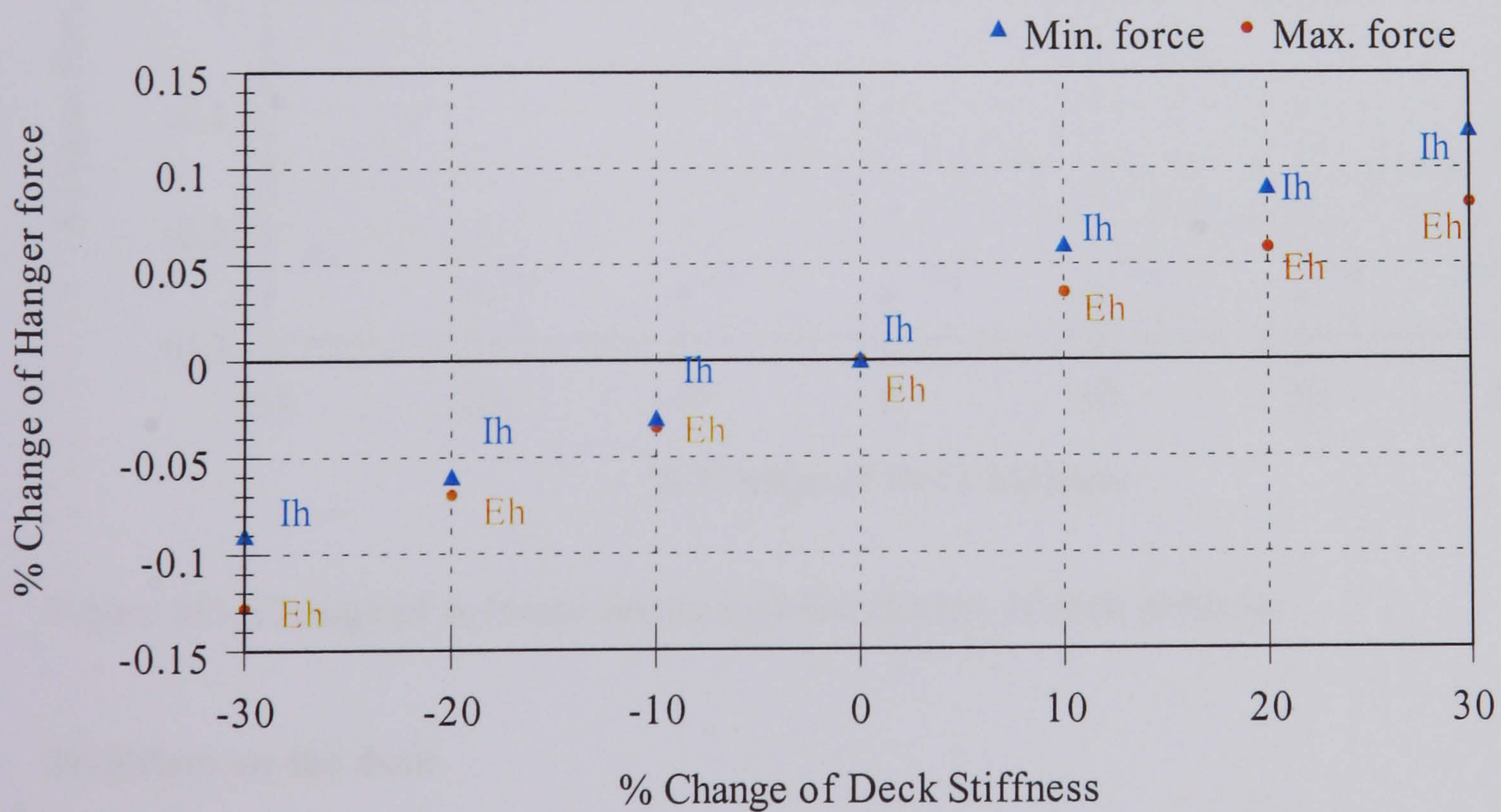

Figure 8f2: Change of hanger forces with the change of deck stiffness

Increasing or decreasing of the deck stiffness up to 30 % gives the maximum hanger force change of 0.13 %, which is insignificant (refer Figure 8f2).

f3) Effect on the A-Frames

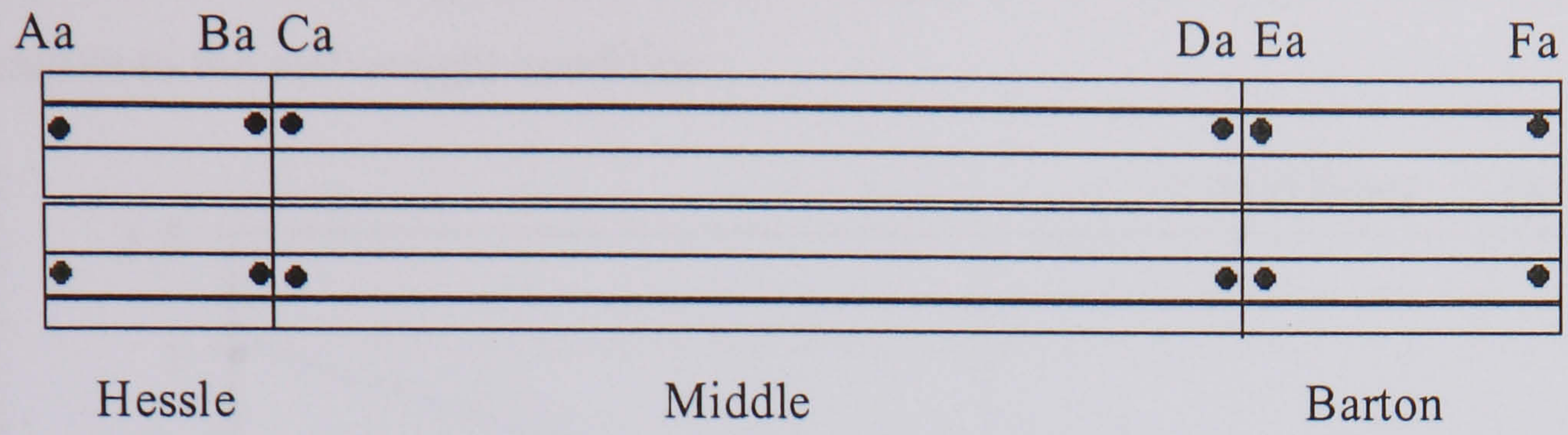

Figure 8.4: Figure shows the A-Frame locations

Again the maximum tensile or compressive force on an A-Frame member does not change significantly due to there being no changes of the bridge self weight (refer Figure 8f3).

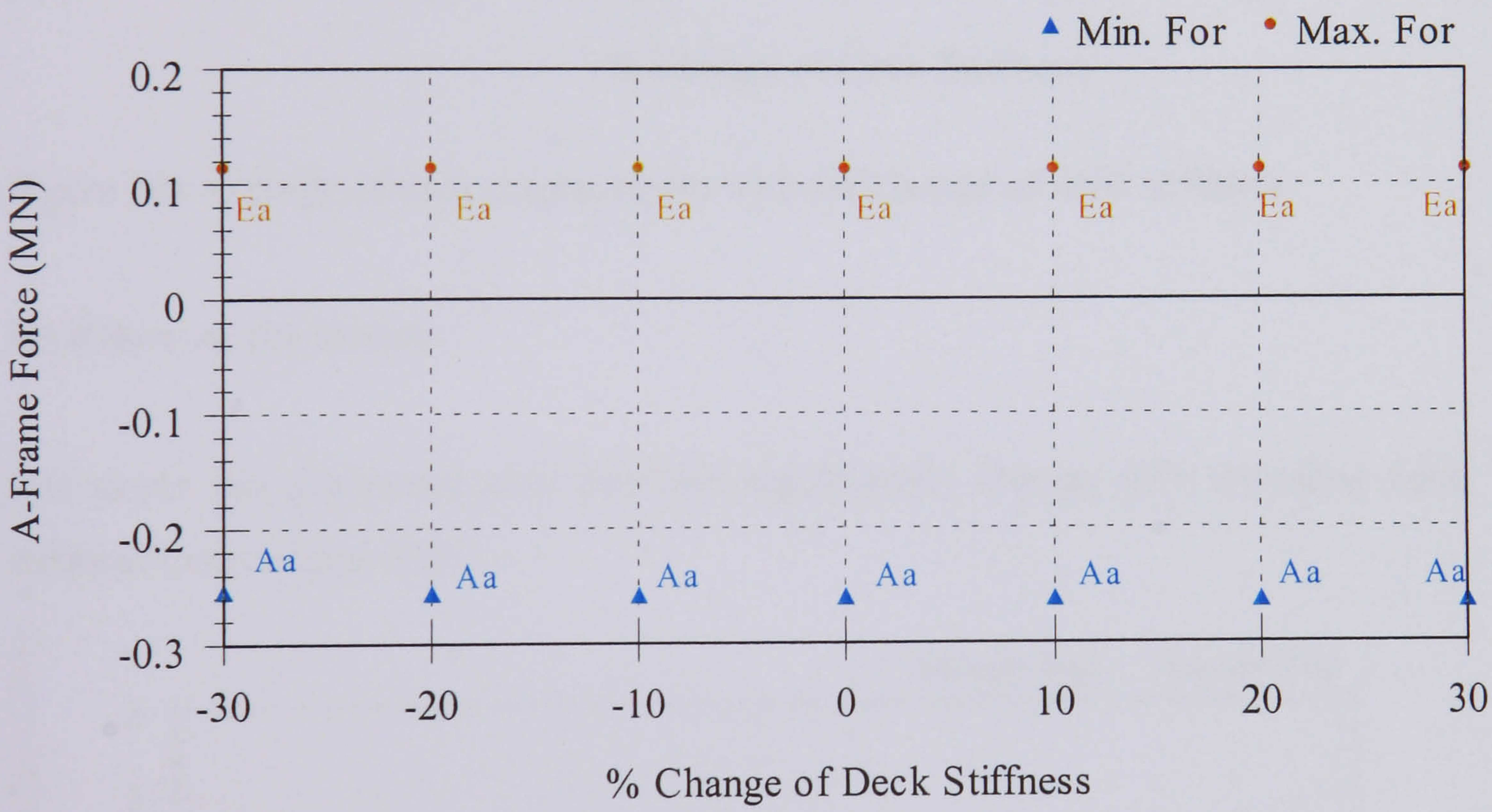

Figure 8f3: Change of A-Frame forces with the change of deck stiffness

f4) Effect on the deck

The deck displacement at mid and quarter span positions only undergoes a small change with changes of the deck stiffness (refer Figure 8f4). Although the deck stiffness is an important parameter in defining the deck profile, here the self-weight of the main cable and the deck are predominant. This is mainly due to the flexibility of the structure. As the middle of the main span has higher flexibility than at the quarter point, changes of stiffness by 30 % gives 5.2 % changes in vertical displacement at mid point and 0.3 % changes at quarter point of the main span relative to the self-weight condition.

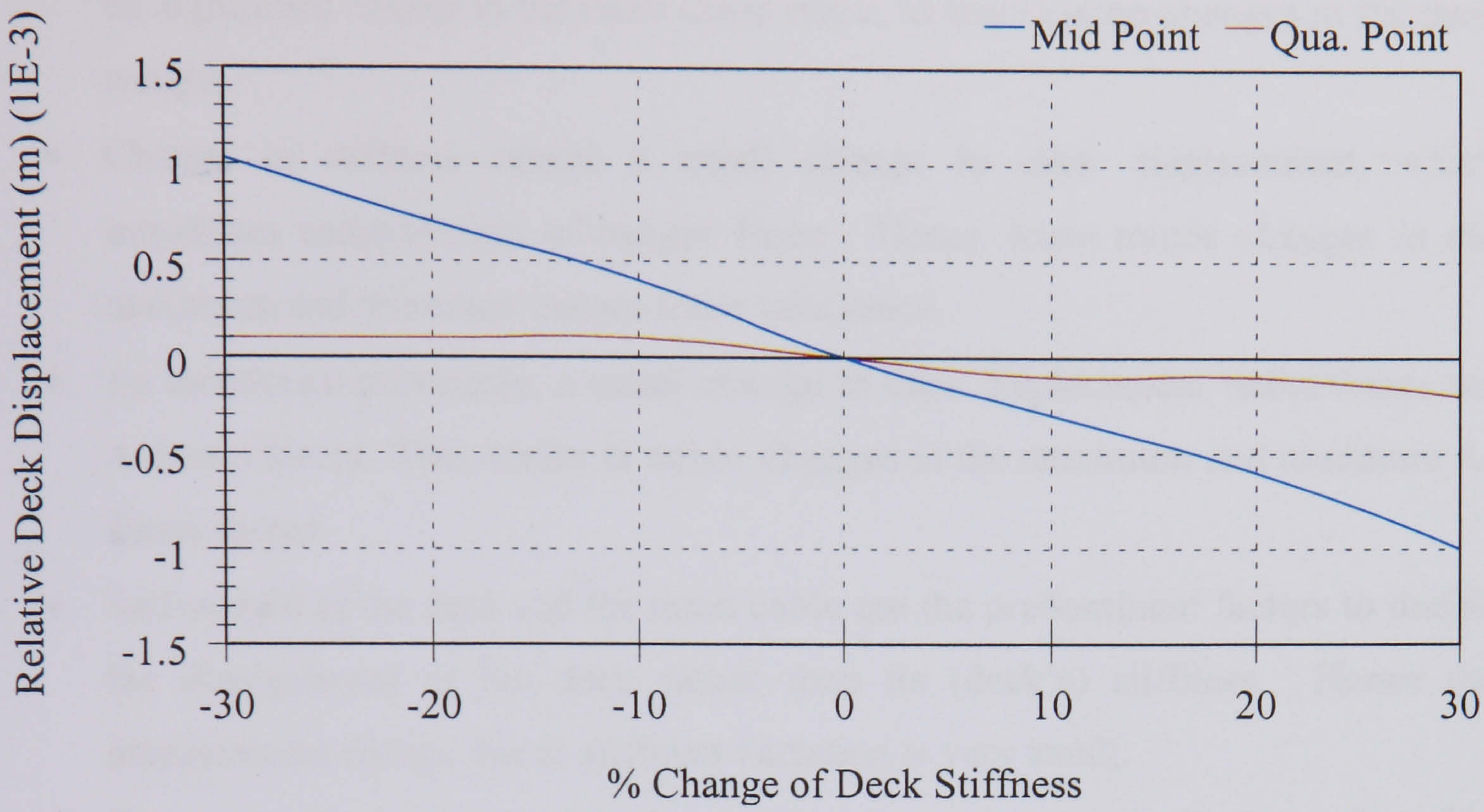

Figure 8f4: Change of deck displacement with the change of deck stiffness

f5) Effect on the towers

The tower top movement also does not significantly change with changing deck stiffness (refer Figure 8f5).

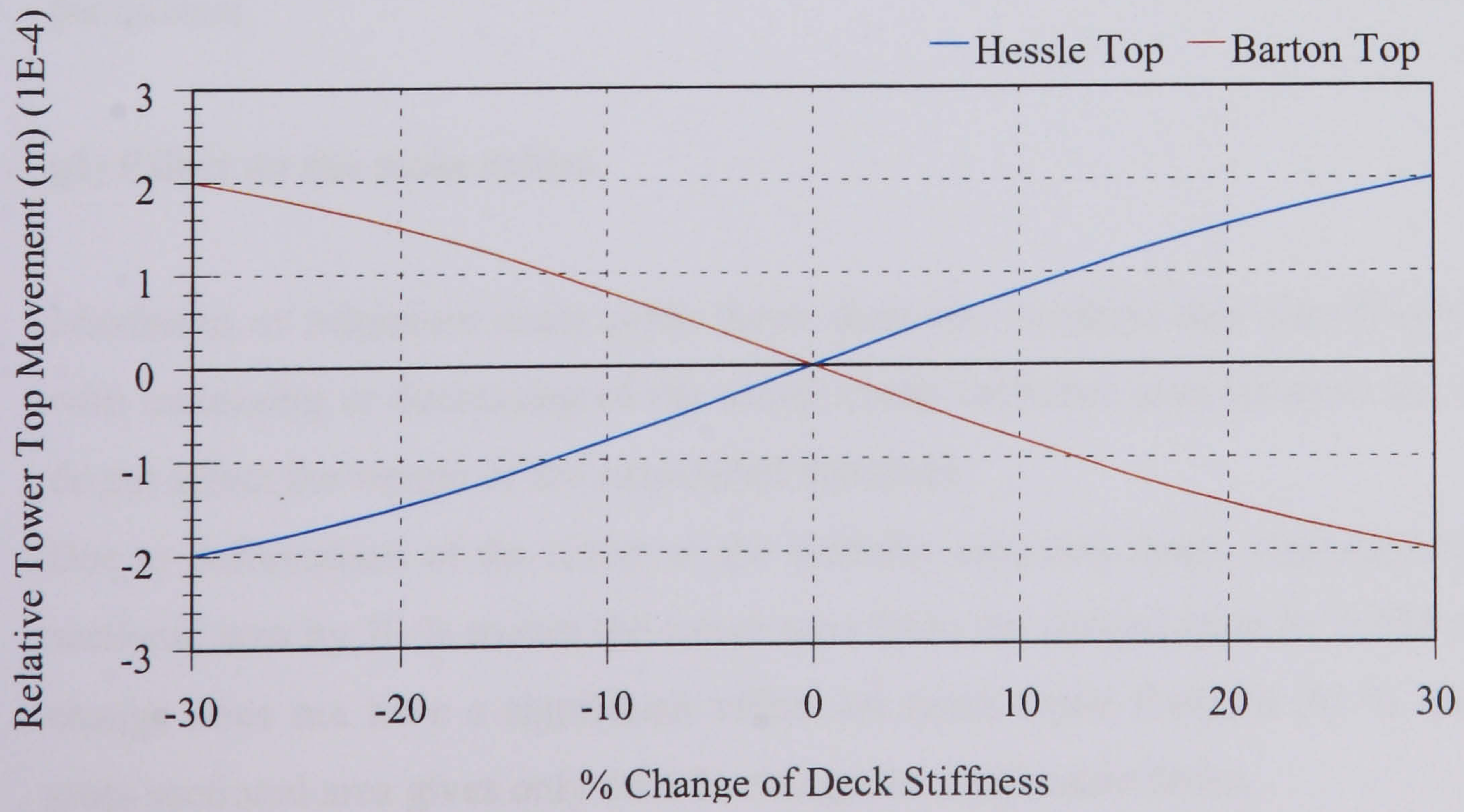

Figure 8f5: Change of tower top movements with the change of deck stiffness

f6) Conclusion on changing deck stiffness

- Change in deck stiffness without changing the deck cross sectional area causes no significant change in the main cable force, as there are no changes in the deck weight.
- Change in stiffness causes a small change in deck displacement, which introduces redistribution of hanger force. Hence some minor changes in the maximum and minimum hanger force take place.
- As mentioned previously, a small change in deck displacement redistributes the A-frame forces. This results in minor changes in the maximum and minimum A-frame forces.
- Self-weight of the deck and the main cable are the predominant factors to decide the displacement of the deck rather than its (deck's) stiffness. Hence the displacement change due to stiffness variation is very small.
- Tower top displacements are also negligible, as the change in the main cable force is negligible.

g) Changing the tower cross section area

With the initially assumed tower cross section area, the towers have some initial deformation. Increasing or decreasing tower dimensions has little effect on other parameters.

g1) Effect on the main cables

Maximum or minimum main cable force does not undergo any significant change with increasing or decreasing of the tower cross sectional area because the changes do not affect the weight of the suspended structure.

Due to deformation of the tower at the initially assumed stage, changing the cross sectional area by 30 % moves the tower tops from the central span by 0.005 m. This change does not have a significant effect on main cable force; a 30 % change of cross sectional area gives only 0.06 % change in main cable force.

g2) Effect on the hangers

Although there is no change in the weight of the suspended structure, changing the tower cross section area slightly changes the hanger force due to the movement of the tower top. This causes slight movement of the main cable. Increase of the tower cross section area by 30 % gives 0.9 % increase in the maximum hanger force, and no change in the minimum hanger force.

The maximum hanger force reduces by 1.7 % when reducing the tower cross section area by 30 % and there are no changes in the minimum hanger force

g3) Effect on the A-Frames

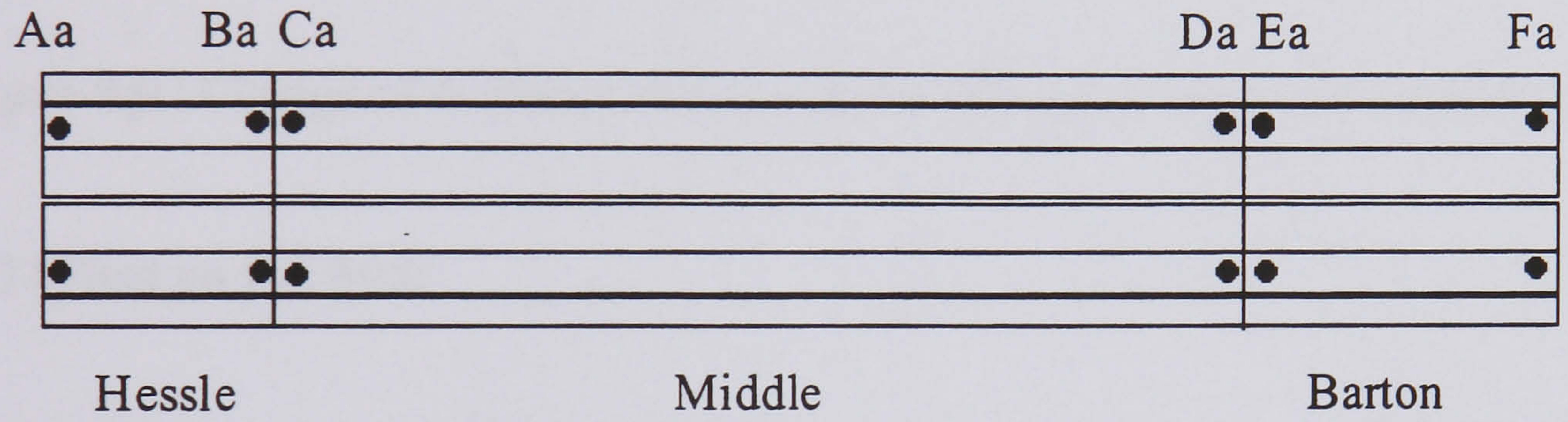

Figure 8.3: Figure shows the A-Frame locations

The A-frame force does not significantly change with increasing or decreasing the tower cross section area, as there is no change in the weight of the suspended structure (refer Figure 8g1).

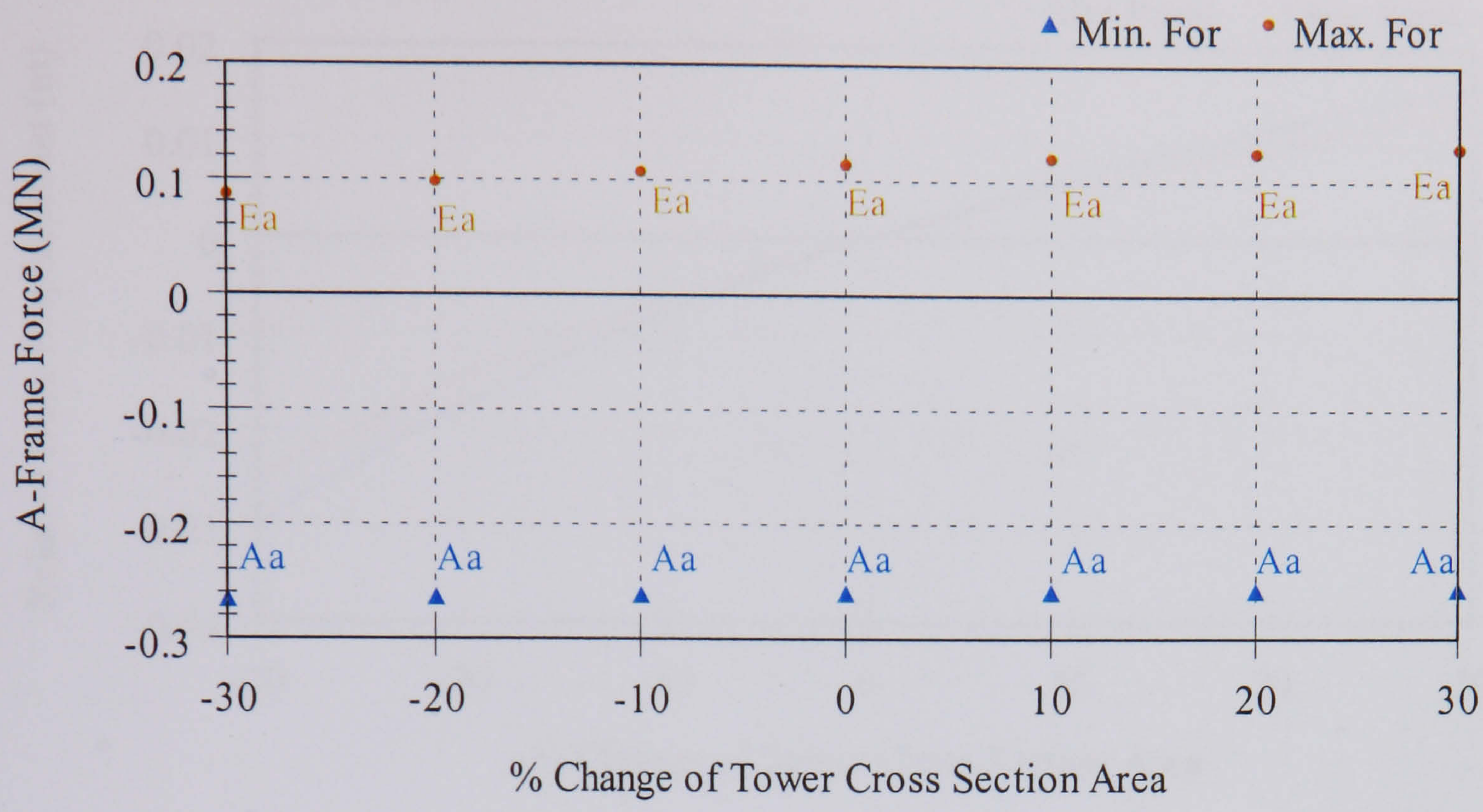

Figure 8g1: Change of A-Frame forces with the change of tower cross section area

g4) Effect on the deck

Increasing the tower cross section area moves the tower tops away from the mid-span. Hence the main cable moves relatively upwards. This causes the deck mid point and the quarter points to move slightly relatively upwards, 30 % increases gives the mid-point deck relative displacement and the quarter-point deck relative displacement both of 0.015 m.

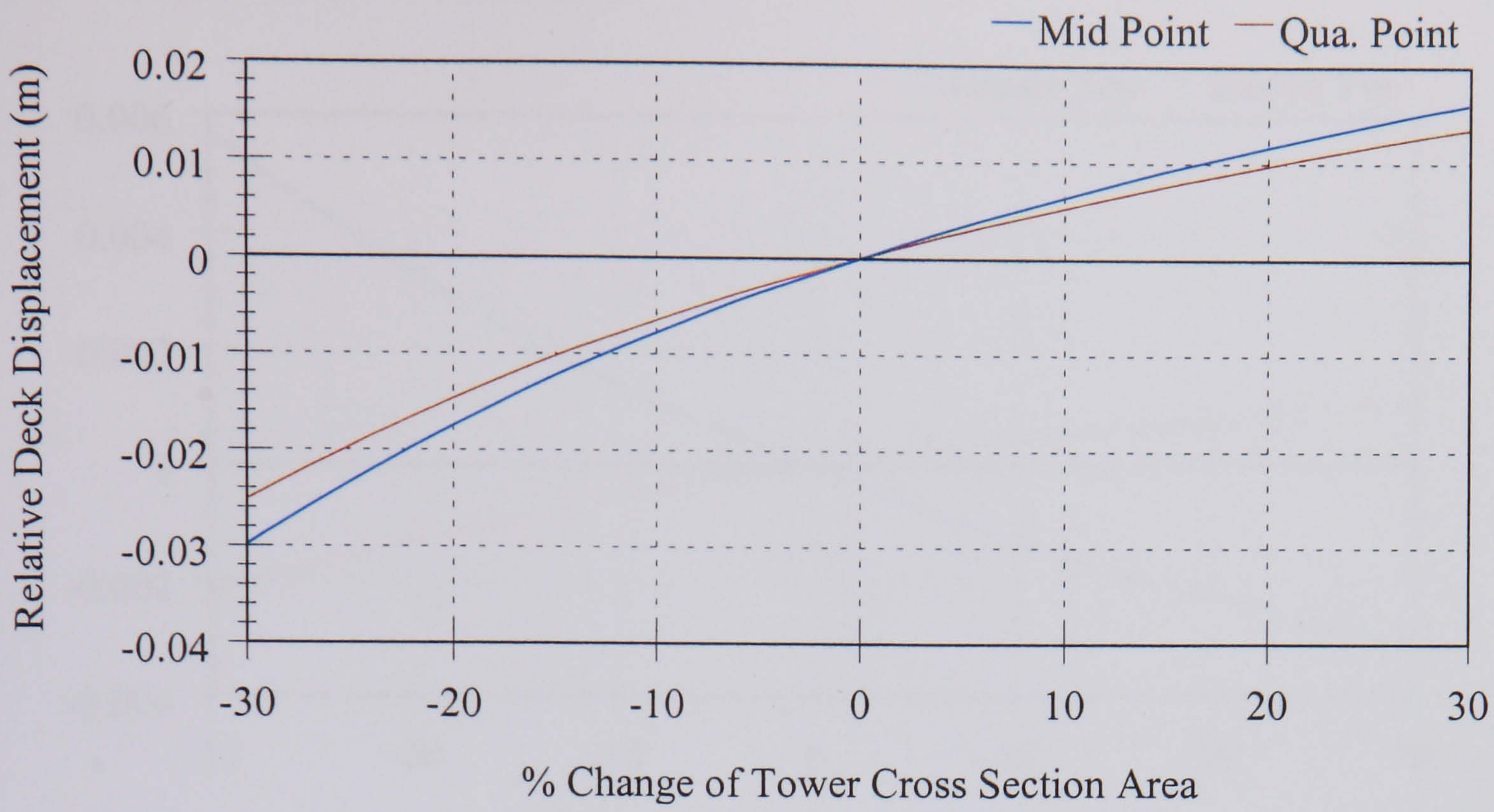

Figure 8g2: Change of deck displacements with the change of tower cross section area

Reduction of the tower cross section area by 30 % gives the downward mid point deck relative displacement of 0.03 m and the quarter point deck relative displacement of 0.025 m, refer Figure 8g2.

g5) Effect on the towers

The Hessle and the Barton tower top move away from the central span by 0.001 m and 0.003 m respectively with increasing the tower cross section area by 30 %. Decreasing the tower cross section area by 30 % moves the Hessle and the Barton tower top move towards the central span by 0.0056 m and 0.0023 m respectively as shown in Figure 8g3.

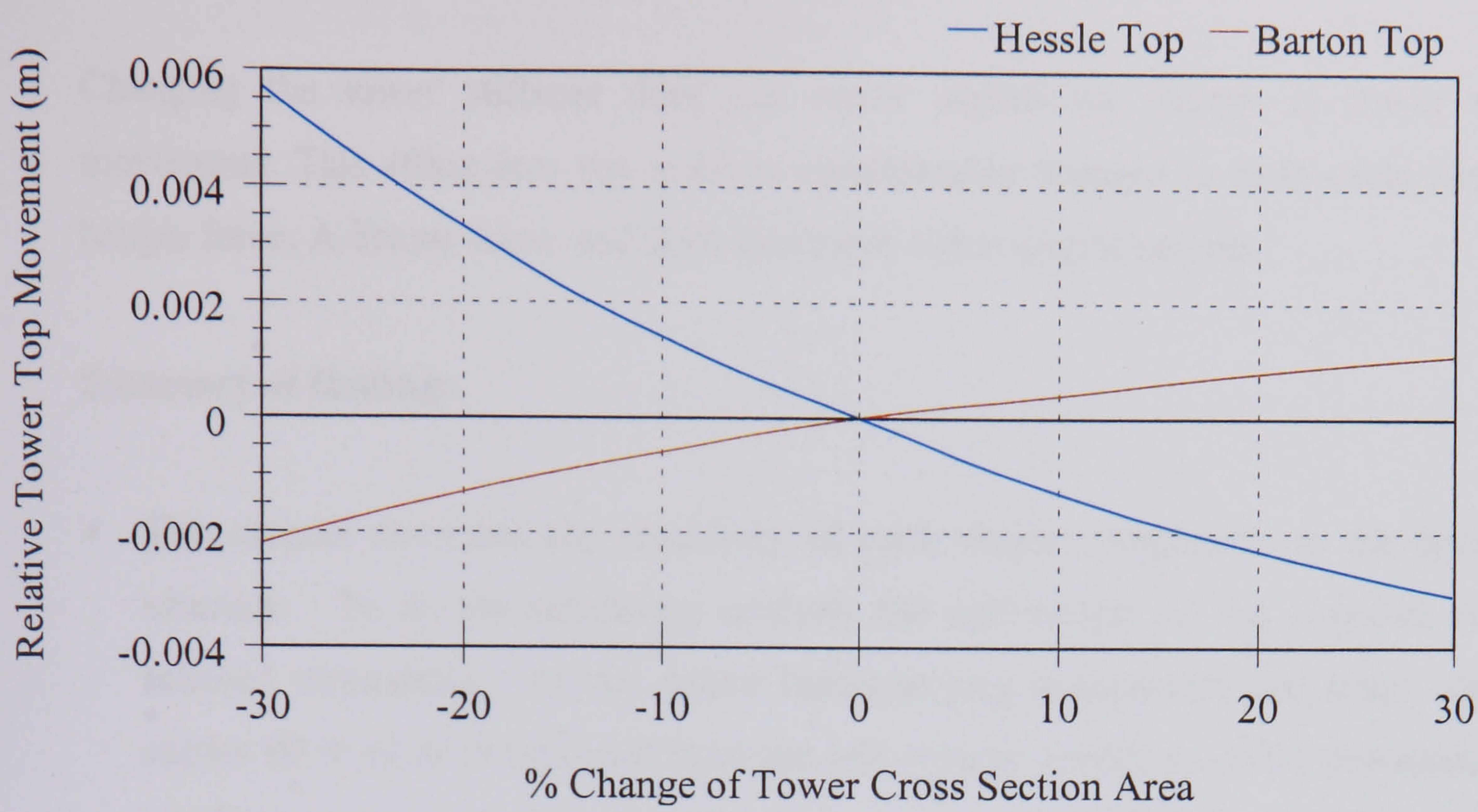

Figure 8g3: Change of tower top movements with the change of tower cross section area

g6) Conclusion on changing tower cross sectional area

- Changing the tower cross sectional area does not have any significant effect on most of the structural components. This is because the suspended weight of the structure has not changed.
- Main cable force and hanger forces undergo negligible changes (0.06 % for 1 % change in tower cross sectional area) on account of this factor.
- Maximum deck movement at the mid-point of the deck is 1mm for the change of the tower cross section area by 1 %. Thus it is not a sensitive factor.
- Tower top movements and A-frame forces also do not show any significant changes.
- In general, the tower cross sectional area is not a sensitive parameter compared to the main cable and deck sizes.

h) Changing the tower stiffness

Changing the tower stiffness does not cause significant change in tower top movements. This effect does not result in considerable changes in main cable force, hanger force, A-Frame force, and deck and main cable displacements.

Summary of findings

- This chapter describes the sensitivity of each major component on the bridge structure. To do the sensitivity analysis the self-weight of the structure was selected throughout. As the major load-carrying component, the main cable carries 80 % of its design load from the self-weight condition. Also this loading condition gives a better general view on component sensitivity than for a particular point load or uniformly distributed load.
- The main cable diameter and the deck weight are the most sensitive structural parameters. These components greatly affect the profile of the structure, which leads to change of behaviour of other components such as the hangers, towers and A-frames.
- By considering these two major components, the main cable diameter is the more sensitive parameter. Then follows the main cable initial strain and thirdly the deck thickness.
- Decreasing the main cable diameter has 2.3 times higher effect on the deck and the main cable profile than does increasing the main cable diameter by the same percentage.
- Decreasing the main cable diameter by 1 % gives 267 mm extra downward movement of the main cable and the deck at mid span. Next is the main cable initial strain, which gives 133 mm movement on the same point for a change of initial strain value of 1 %. Increasing the main cable diameter by 1 % gives 116 mm movement on the deck and the main cable at mid span. Finally the change of deck thickness by 1 % gives 83 mm movement on the same point at the main cable and the deck profile.
- A sensitivity rating based on the changing deck and the main cable profiles follows: decreasing the main cable diameter is first then comes the main cable

initial strain, and third is increasing the main cable diameter and finally the deck thickness. The changes on the hanger and the tower parameters do not have much effect on the profile.

- A sensitivity rating based on the movement of the tower top is of the same order as changing the profile of the main cable and the deck. Again changing hanger and tower parameters does not have a significant effect on tower top movements.
- Moving the main cable profile upward from its initial position gives outward movement of the tower tops from the main span. Downward movement of the main cable profile from its initial position gives inward movement of the tower tops with respect to the main span.
- A sensitivity rating considered based on whether or not slack hangers occur, results in changing of the main cable diameter, the main cable initial strain and the deck thickness being the significant parameters to consider. Increasing or decreasing any one of these parameter values beyond 20 % from its initially assumed value starts to produce slack hangers.
- The hanger initial strain then the hanger diameter are the next sensitive parameters in order.
- The tower cross sectional area and the stiffness of the tower are the least sensitive parameters under the assumed self-weight only condition.

Chapter 9

Assessment and validation of different type of model – 2D, 3D plate formulation and 3D box formulation models

General

The validation of the computer models described in Chapter 7 is described in this chapter. Validation has been carried out by comparing the prediction of the model with the behaviour of the real structure. To demonstrate this, a number of checks have been made to ensure the mass and stiffness distribution of the model closely resembles that of the actual structure. Both the dynamic and static behaviour of each model is compared with the corresponding behaviour of the structure using field measurements. Additional validation is carried out by comparing the prediction made using the above computer models with the frame analysis carried out by Freeman Fox & Partners (the designer's of the Humber Bridge), although this could only be carried out under dead load.

The deflection of the deck at certain points was monitored under a known live load situation. The live load took the form of a heavy lorry load moving slowly from one end of the bridge to the other. Similar loads were applied to the models and the displacement of the deck at corresponding points was noted. The results were compared as a means of checking the stiffness of the models.

Two separate tests were carried out under this live load condition. In the first test a single heavy load of 170 tonnes (but see below) was moved at a speed of 4m/sec from one end to the other. In the second test case five lorry loads of each 32 tonnes were moved in different combinations at a speed of 7.5 m/sec. The reason for the two separate tests is explained in the following sections.

The stiffness of the models was verified as being acceptably accurate by carrying out a modal analysis. Each mode shape and associated natural frequency was compared with bridge specific properties (with available field measurements).

Under the dead load situation the total weight of the structure has been compared with the total vertical reaction force on the model. The main cable force and hanger forces are compared at certain places along the bridge, which will test the mass distribution of the structure. Under this condition the maximum deflection of the deck and the main cable of the models have been monitored. Smooth deflected shapes and the maximum magnitude of deflection of the deck and the main cable have been noted. This will test the applied initial strain value to the main cable and the hanger, and also mass and stiffness distribution of the structure.

i) Models under dead load condition

a) Deflection of the models under dead load condition

The deflected shape of the structure under dead load will be used for future reference (used as datum for further numerical analysis). Under this load condition, the deflected shape of the deck and its maximum deflection as well as that of the main cable were observed. As shown in Figure 9a, the maximum deflection was predicted to be 47 mm. This occurs at the quarter points of the main span. Ideally this deflection should be zero. However due to small inaccuracies in the application of initial strain within the main cables (as described in Chapter 8, Figure 8b4, where 1 % change in main cable initial strain gives 80mm deck displacement at the quarter span) there is a small non-zero deflection. As described in Chapter 7, the initial strain values of the main cable and the hanger are calculated from its strained and unstrained lengths, which is from the Humber Bridge Design Report (internal). As an exercise, a number of "trials and errors" with different initial strains have been performed to bring about the acceptable deflected form. This deflection is negligible compared with the length of the main span. This deflection value and the deflected shape are the same for all three models. Here the deflected shape of the 3-D box formulation model has been plotted, Figure 9a.

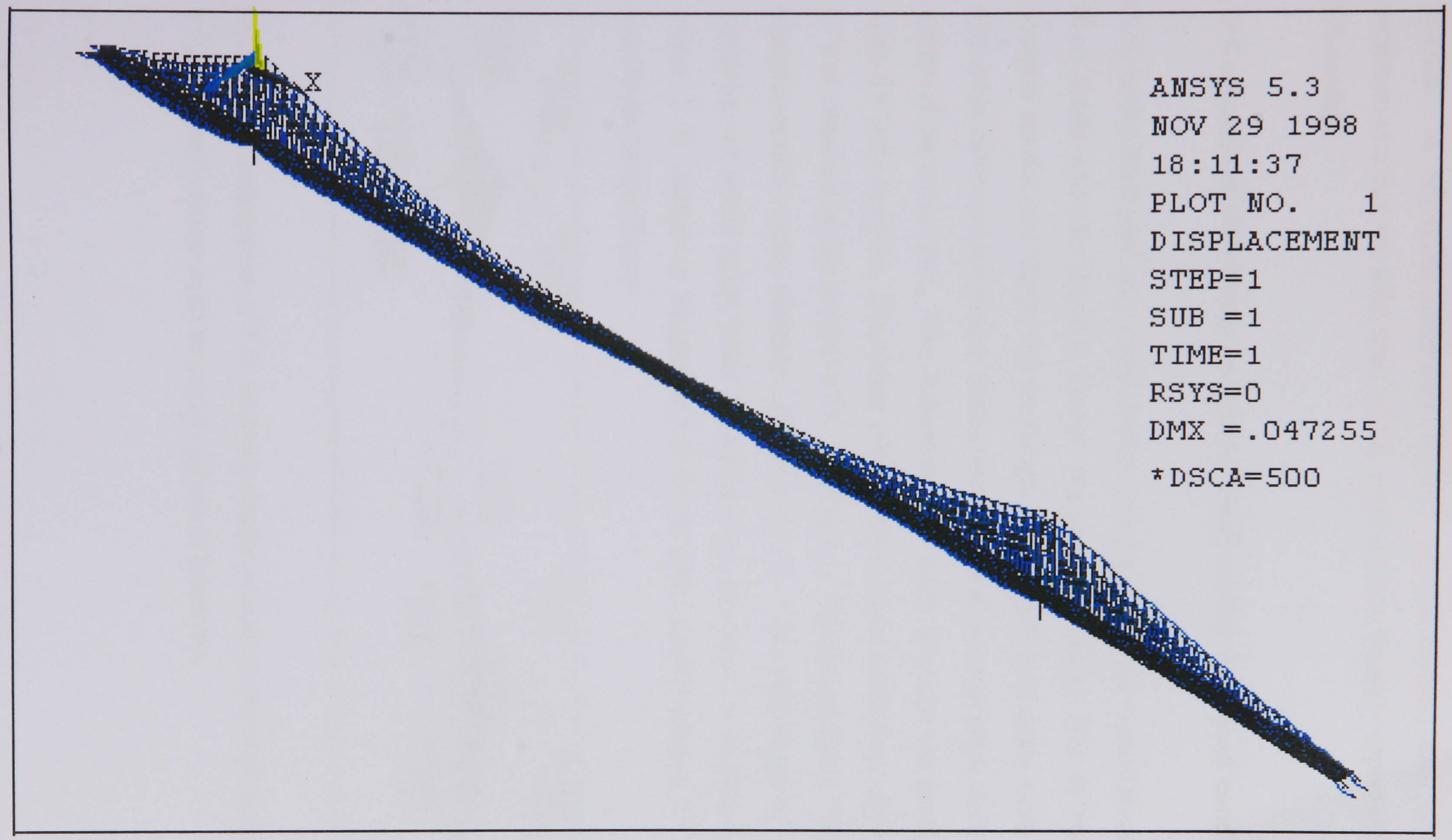

Figure 9a: Deflected shape of the model under its self-weight, and the maximum predicted deflection of 0.047 m.

Under dead load only the total weight of the structure calculated manually has been compared with the total vertical reaction forces calculated using the computer models. A negligible difference of 0.01 % (7.6 tonnes) was obtained. This demonstrated that the total mass of the structure is accurately represented within the FE models.

b) Comparison with bridge designers' results under dead load condition

Also under dead load only comparisons, using the 3-D box formulation model, have been made with the Humber Bridge designers' (Freeman Fox & Partners) frame analysis results (see figure 9b) for hanger forces (HF) and main cable forces (CF). The main cable and the hanger forces were obtained at tower tops, deck ends and the centre of the main span. The maximum main cable forces at the tower tops are the same for both analyses. Elsewhere the maximum main cable force difference of -0.7 % was obtained at the centre of the main span. The hanger force value from both analysis results varies between -6.0 and 4.5 %. The difference is due to small variations of initial strain value on hangers (as described in chapter 8, Figure 8d2 where 1 % change in hanger initial strain gives approximately 1 % change in maximum hanger force).

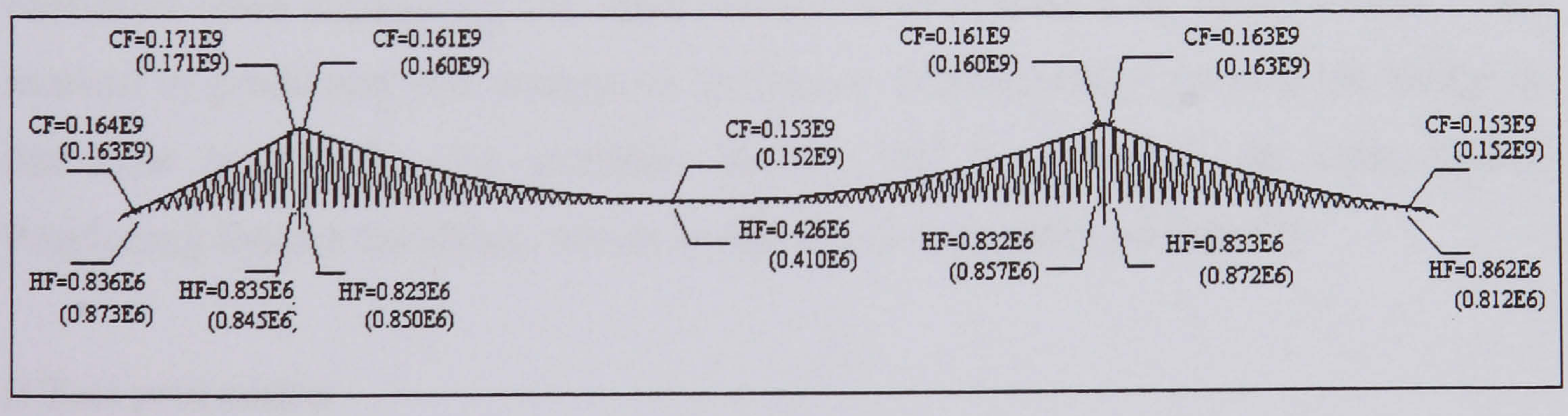

Figure 9b: Comparisons of F.E. analysis results of main cable and hanger forces (N) with designer's frame analysis results (given in brackets).

ii) Validation of models under static live (quasi-static) load condition

a) Single lorry load, displacement measured by optometer

General

A number of tests (Brownjohn, 1994) have been performed on the Humber Bridge to determine the behaviour of the structure under different loading situations. In this test the bridge was closed to allow a single heavy vehicle (170 tonnes) to traverse it. The displacement of the structure at various points was then measured using an optometer. This instrument is used for long term monitoring of large structures like bridges, dams etc. Using this the necessary information (like deck displacement, wind speed and direction, hanger acceleration and main cable temperature) can be taken under real operating conditions that is useful for the assessment of actual behaviour. It will perform automatic and continuous measurement of the target displacements in an assigned direction on the plane orthogonal to the optical axis. The magnitude of loading applied to this test was doubtful, as there was no facility at that time to measure such a heavy load at the Humber Bridge Board, so it could not be confirmed independently that the vehicle was of weight 170 tonnes. This leads to confusion when comparing the field measurement results with model results. This resulted in predicting the weight of the heavy vehicle which crossed the bridge at that time (to clarify this problem another test was carried out using Global Positioning System facilities, which is described in the next section (b).

i) Test procedure

Optical systems were installed to record vertical displacements at two points on the main span to determine the quasi-static response on the deck. These were at the centre of the main span and at the north quarter point of the main span. A heavy load assumed to be 170 tonnes was then moved slowly (in the second lane) across the bridge from the south side (Barton) to the north side (Hessle). The bridge was closed during the passage of the heavy load. The 3-D plate formulation model was selected for the purpose of analysing the behaviour of the structure when loaded in this way because it can accommodate unsymmetrical loading. The load due to a heavy lorry of 170 tonnes was applied as a pressure distributed over an area of 10 m x 5.5 m.

ii) Different modelling approach

Figures 9c and 9d show a comparison (analysis and measured values) of the vertical displacements at centre and quarter of the main span for lorry loads of 120 and 170 tonnes. It can be seen that the calculated values differ from the measured values.
To check whether this discrepancy was due to features of the modelling the main cable was represented by beam elements instead of link elements, but no significant changes in vertical displacements were obtained. In another model, wind pressure corresponding to 24 m/s wind speed was applied (uplift and drag forces) as the test was carried out at that wind speed. Again no significant changes in vertical displacements (i.e. the difference in vertical displacement with and without the lorry load while the wind load is applied) were obtained. As the 170 tonnes load follows the same curve pattern (from the model results), it was decided to apply different magnitudes of load by trial and error to match with the field measurement results. From this a load of 120 tonnes could well have been the actual test vehicle weight, as it gave a good agreement against measured values for both mid and quarter-span vertical displacements.

iii) Validation of measured and computer model results

From Figures 9c & 9d, it is clear that both measured and predicted graphs follows the same curve pattern. From Figure 9c the maximum upward movement of 112.5 mm was obtained at the centre of the main span when the 120 tonnes lorry load was in the Barton span. Although the decks are not continuous this happens due to upward movement of the main cable. Note that the main cable is continuous throughout the bridge. Increasing tensile force on the Barton side main cable moves the Barton tower top away from the main span. This will move the main cable upward in the main span, and result in upward movement of the deck.

Figure 9d gives the maximum upward movement of 115.3 mm at the quarter point on the main span. This happened when the 120 tonne lorry load was on the main span 350 m away from the Barton tower. Due to the flexibility of the main cable and the deck, at the load position the main cable and the deck move downward which induces the upward main cable and the deck movement at the quarter point on the main span.

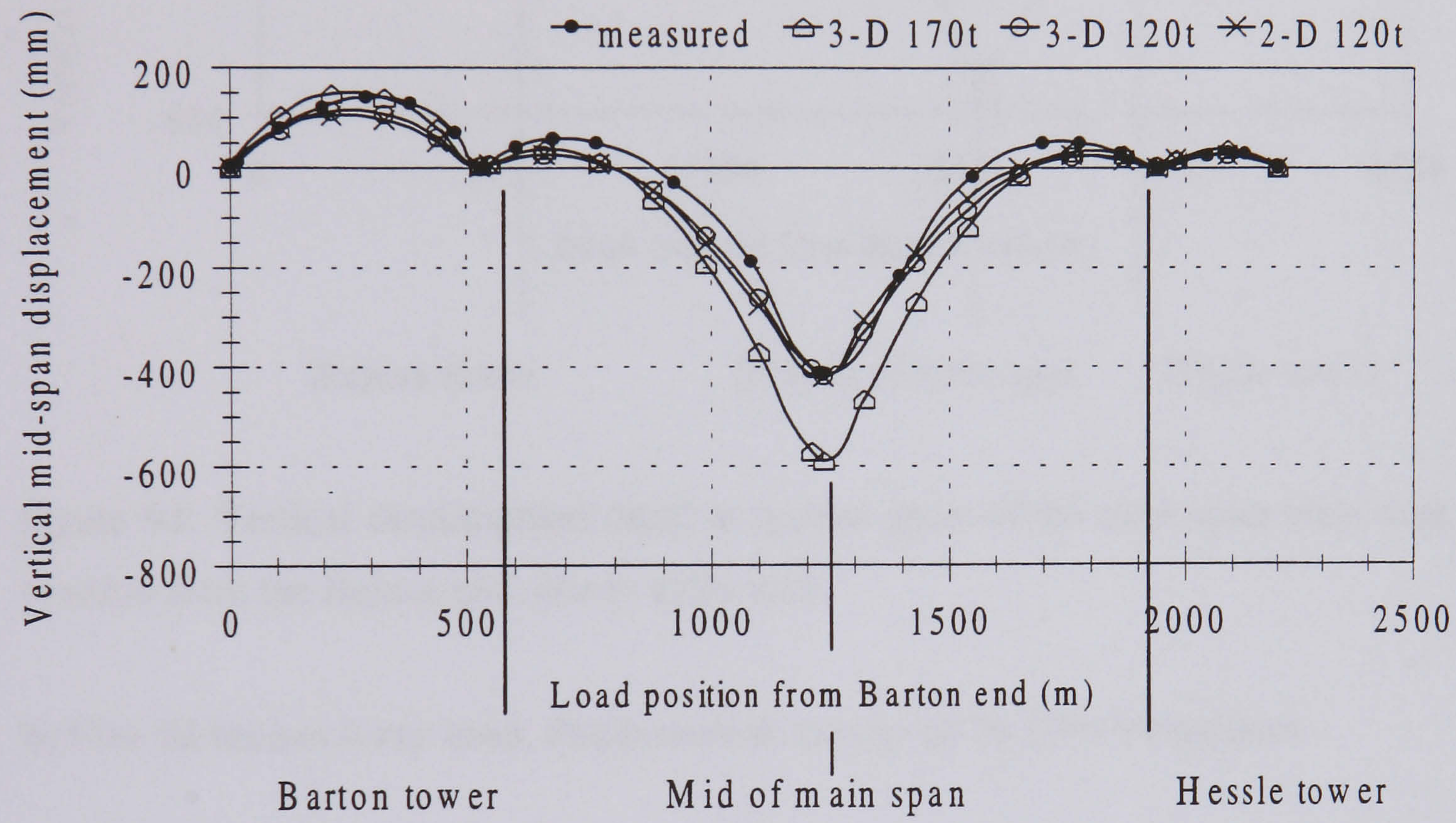

Figure 9c: Vertical displacement (mm) at mid point of the main span with load position from the Barton end, due to a live load.

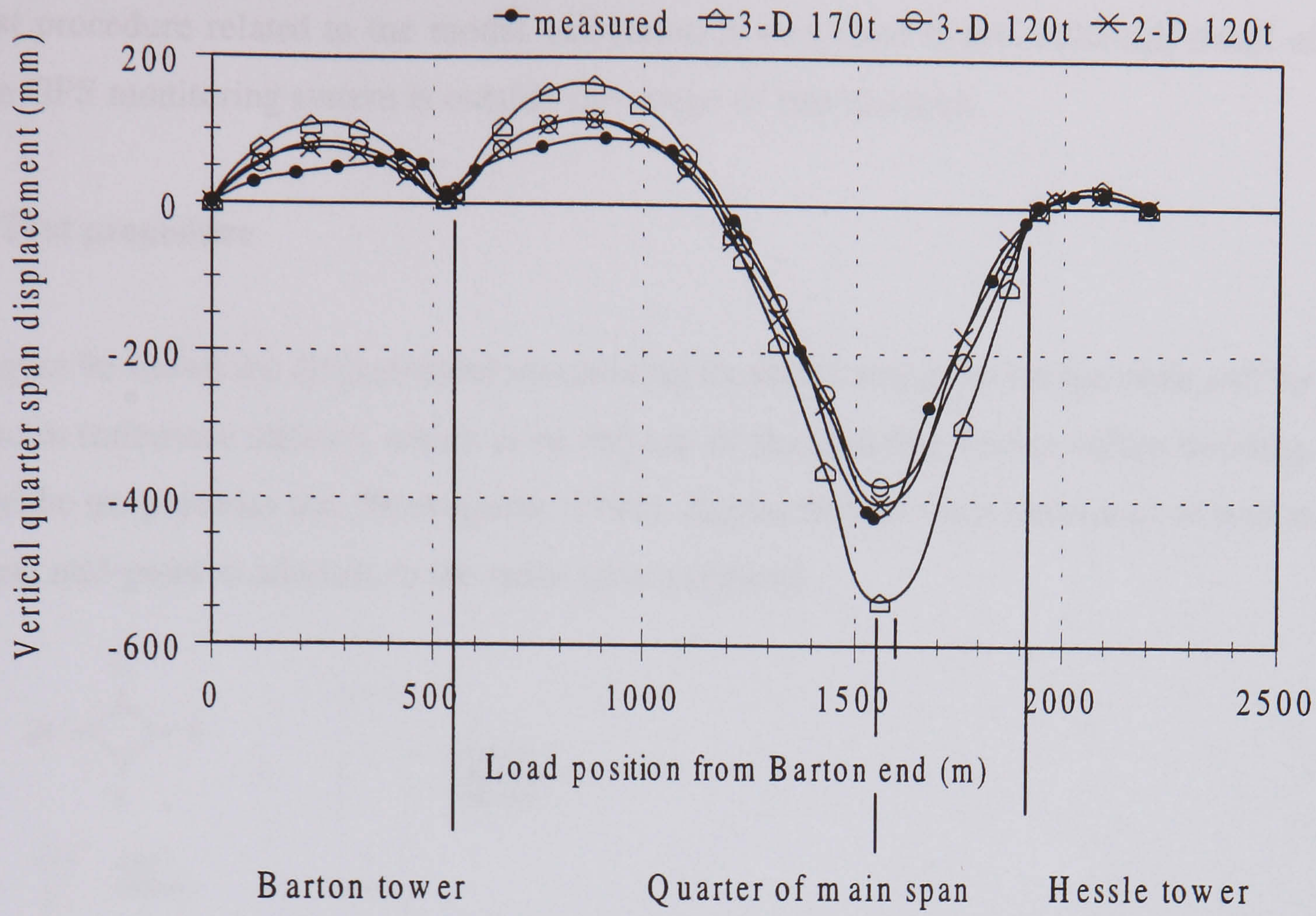

Figure 9d: Vertical displacement (mm) at quarter point of the main span with load position from the Barton end, due to a live load.

b) Five 32 tonnes lorry load, displacement measured by GPS techniques

General

The results from previous field measurements (Brownjohn, 1994) are less reliable as the lorry load was not precisely known. This matter causes confusion to the Humber Bridge Board and to the research work, as these validations are the key issue for getting confidence with the model and for further predictions. So each and every prediction should have real physical meaning. Models matched well with the measured natural frequencies and associated mode shapes (described in the next section); this was a necessary but not sufficient condition for validation of the models. The distribution of mass along the structure has to be satisfied and also the stiffness of the structure has to be modelled precisely.

The displacement of the bridge due to a specific lorry load has been monitored using the relatively new technique of Global Positioning System (Brown *et al,* 1999). The test procedure related to the model validation is described below although detail of the GPS monitoring system is outside the scope of this research.

i) Test procedure

Figure 9e shows the displacement monitoring locations along the bridge deck and the datum (reference station), which is on the top of the Humber Bridge office building. Unlike the previous test (Brownjohn, 1994), displacements were measured at Barton span mid-point in addition to the main span positions.

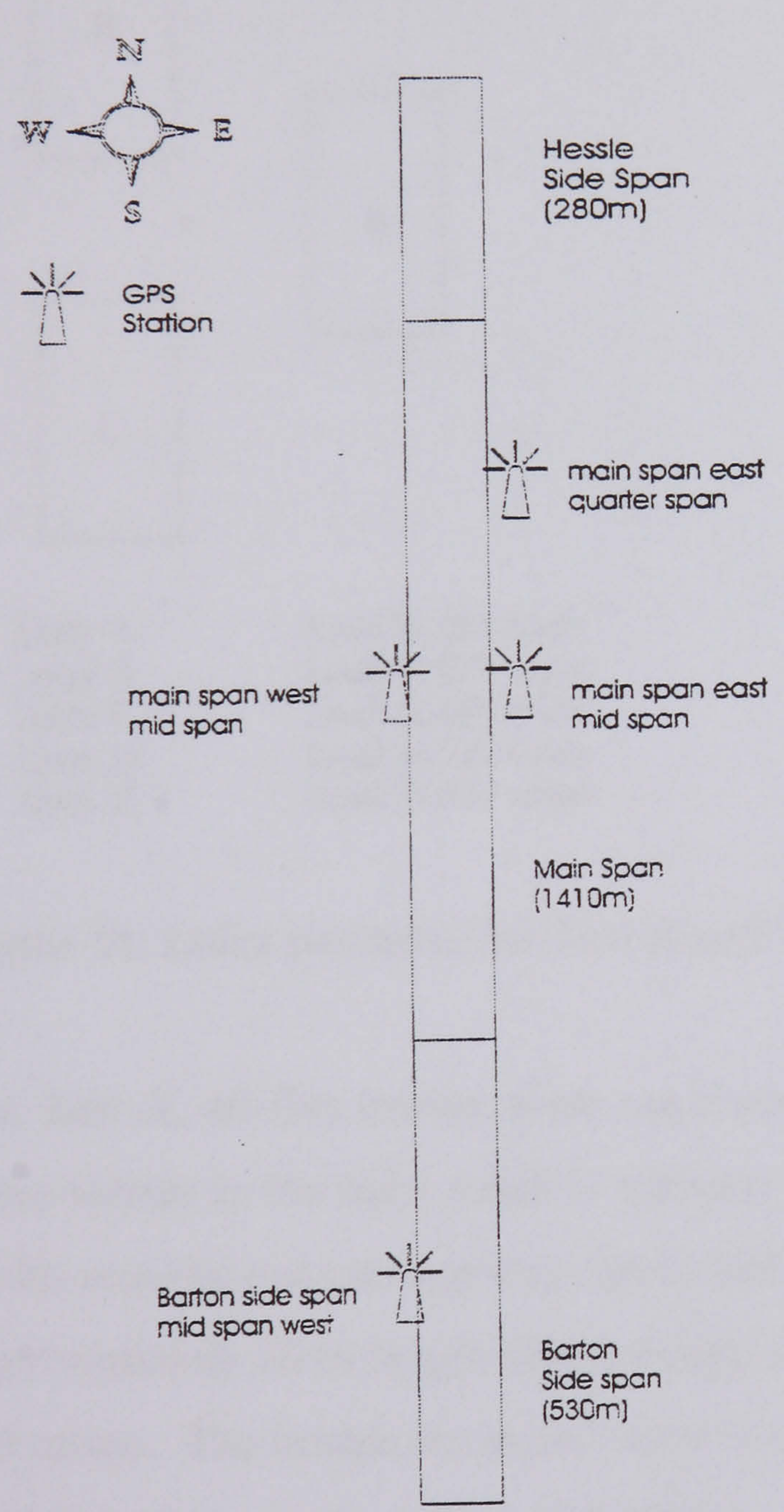

Figure 9e: Displacement monitoring locations along the bridge deck

Three tests were performed, these will be referred to as Tests A, B & C. Lorry positions for Test A and Test B are shown in Figure 9f.

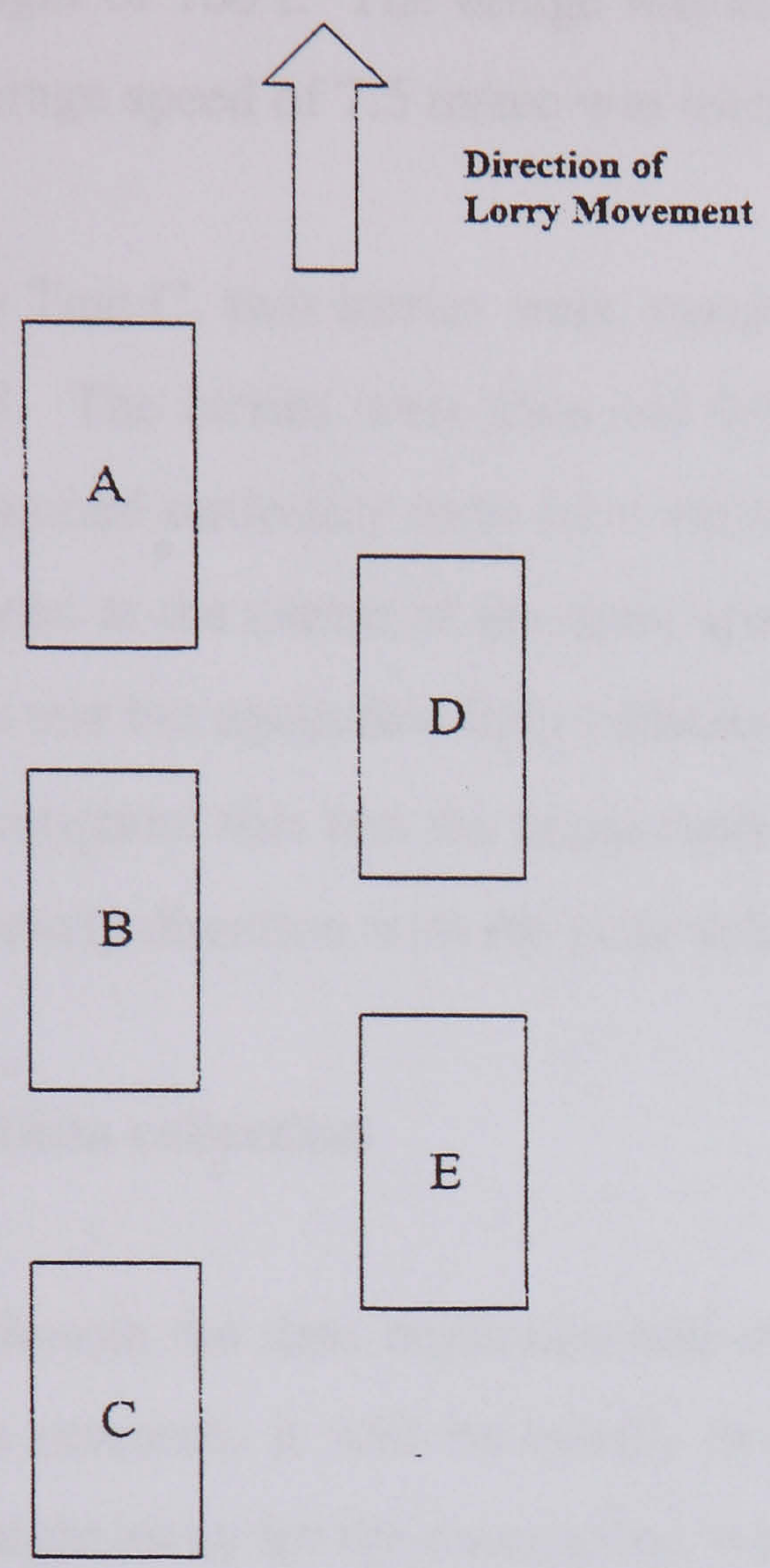

Lorry A	Load 31.080 tonne
Lorry B	Load 30.270 tonne
Lorry C	Load 32.680 tonne
Lorry D	Load 33.790 tonne
Lorry E	Load 31.920 tonne

Figure 9f: Lorry positions for Test A and Test B

For Test A, all five lorries were run from Hessle to Barton, in a group. There were three lorries in the most easterly running carriageway (outer lane) and the other two in the southbound carriageway (inner lane). The compact group of lorries occupying approximately 50 m length (total weight of 159.74 t) travelled with uniform speed of 7.5 m/sec. The bridge remained open to other traffic for this test but only a few light vehicles (three cars) crossed at that time.

For Test B, the lorry group was turned around at the Barton end, and this time they ran from the Barton end to the Hessle end (south to north). The same configuration i.e. three lorries in the outer lane and the two in the inner lane with approximate total weight of 160 t. The bridge was closed to all other traffic for this test. The vehicle average speed of 7.5 m/sec was maintained.

For Test C, two lorries were started from the Barton end and two from the Hessle end. The lorries were then run from the ends to the centre of the main span, and remained stationary there for a while, so that a static load of approximately 128 t was placed at the centre of the main span. The bridge remained open to other traffic for this test but again few light vehicles crossed at that time.

Throughout this test the temperature dropped to 9°C, and the wind was from south-westerly direction with the peak velocity of 19.6 m/sec.

ii) Data collection

Although the data collection and digital signal processing are outside the scope of this research, it will be briefly described as these filtered plotted data were used straight away for the comparison with model results.

The measurement stations are shown in Figure 9e. The data were obtained in terms of the global-positioning co-ordinate system and subsequently converted to displacement data relative to local (bridge) co-ordinate system. The Institute of Engineering Surveying and Space Geodesy developed this co-ordinate transformation software at Nottingham University (Brown *et al,* 1999). A typical data set is shown in Figure 9g for the vertical displacement at the centre of main span on the easterly pedestrian walkway, where the axis of 0.2 sec is used to represent each data point at 5 Hz. Similar plots were produced for all the other displacements measured. From these results it is readily apparent that this form of the data is difficult for engineering use and it needs processing (filtering), which is explained in the next section.

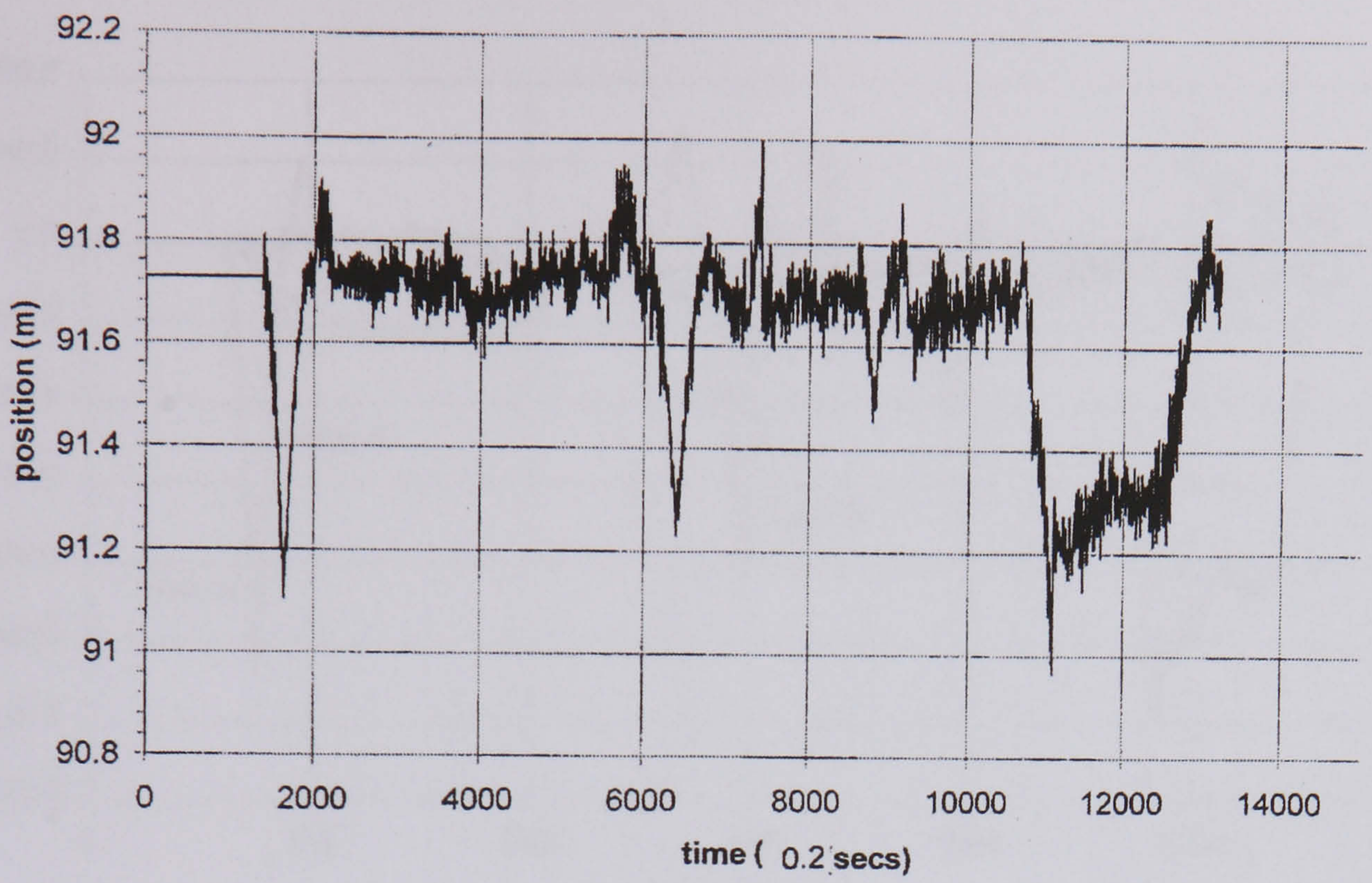

Figure 9g: A typical data for the vertical displacement at the centre of main span on the easterly pedestrian walkway

iii) Data filtering

The data were processed using standard spreadsheet techniques. The data were examined using a simple filtering technique in which they were averaged over a period longer than the observed frequency. It is a standard procedure in many other data acquisition applications (Munch-Andersen, 1998). For the data presented here an averaging period of 100 s was adopted. Using this filtering process reduces the maximum value observed by approximately 2 % for these data.

iv) Data analysis

The filtered data were plotted as displacement against time. The averaged longitudinal, lateral and vertical displacements at each measuring station are plotted separately, shown in following Figures (9h-9k). Figure 9h & 9i shows the displacements at the centre of main span for both eastern and western carriageways.

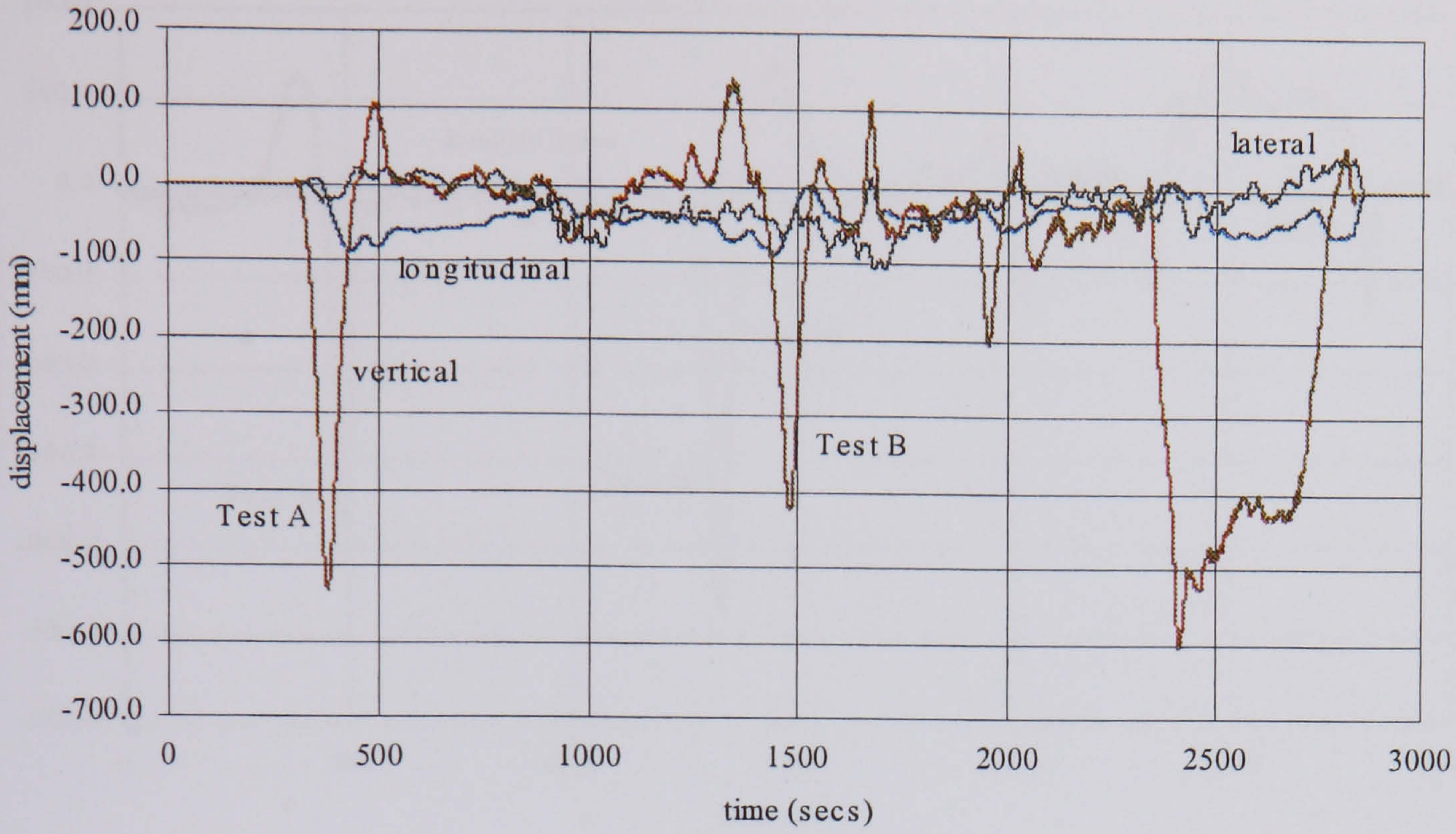

Figure 9h: Displacements at the centre of main span for the eastern carriageway

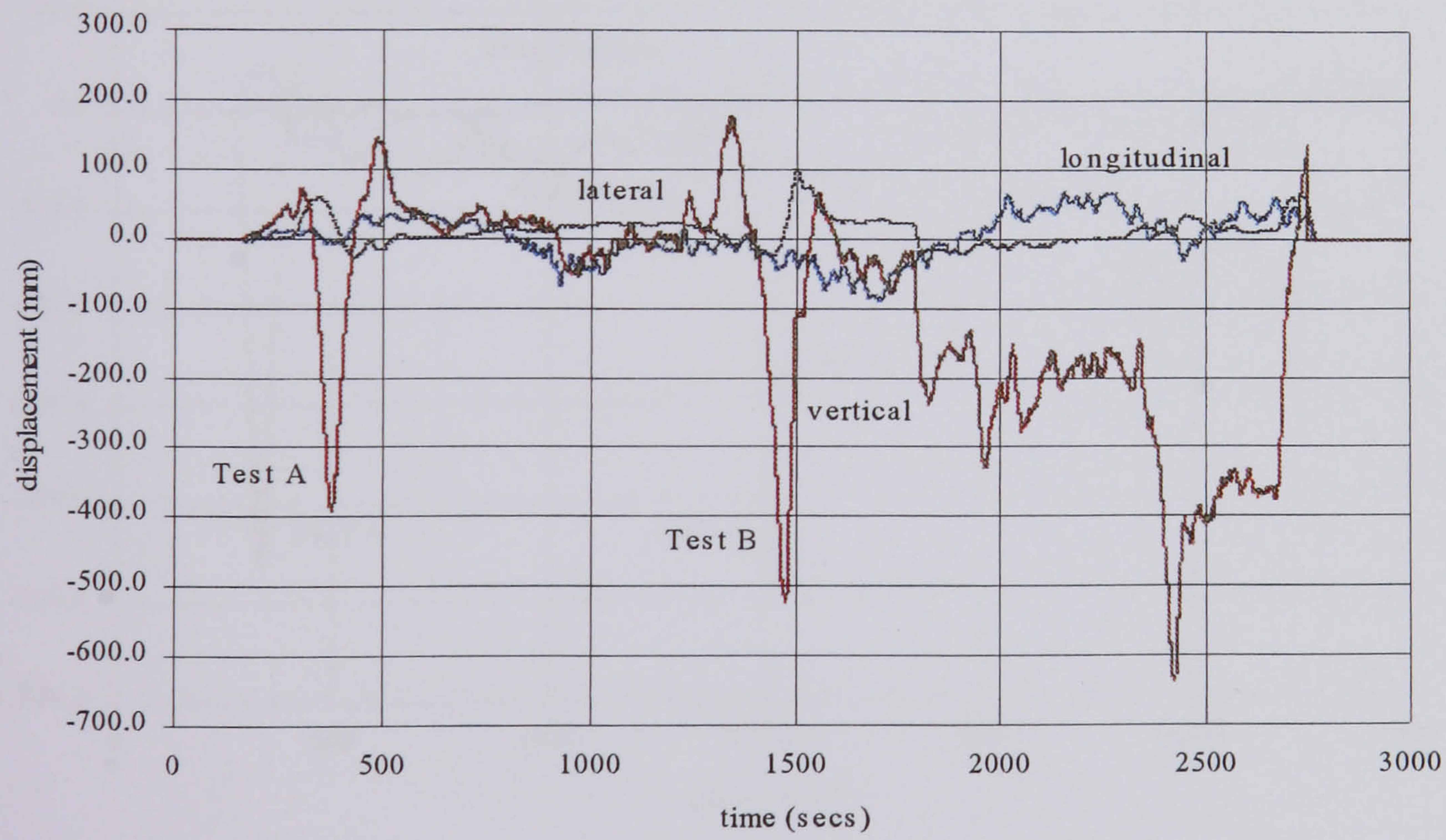

Figure 9i: Displacements at the centre of main span for the western carriageway

Figure 9j shows the displacements at the centre of the Barton side span western carriageway. Figure 9k shows the displacements at the quarter point of the main span towards the Hessle side.

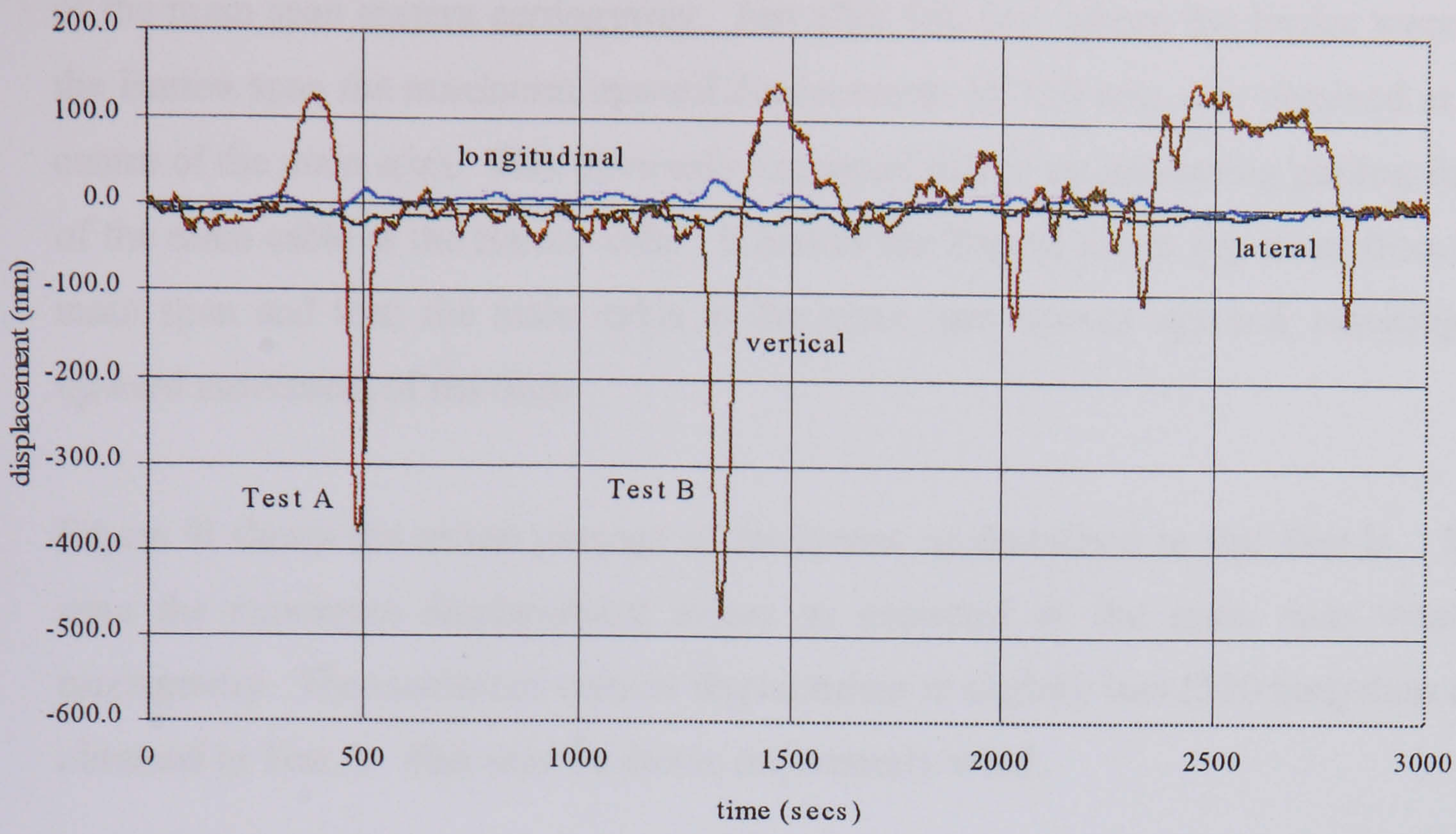

Figure 9j: Displacements at the centre of the Barton side span western carriageway

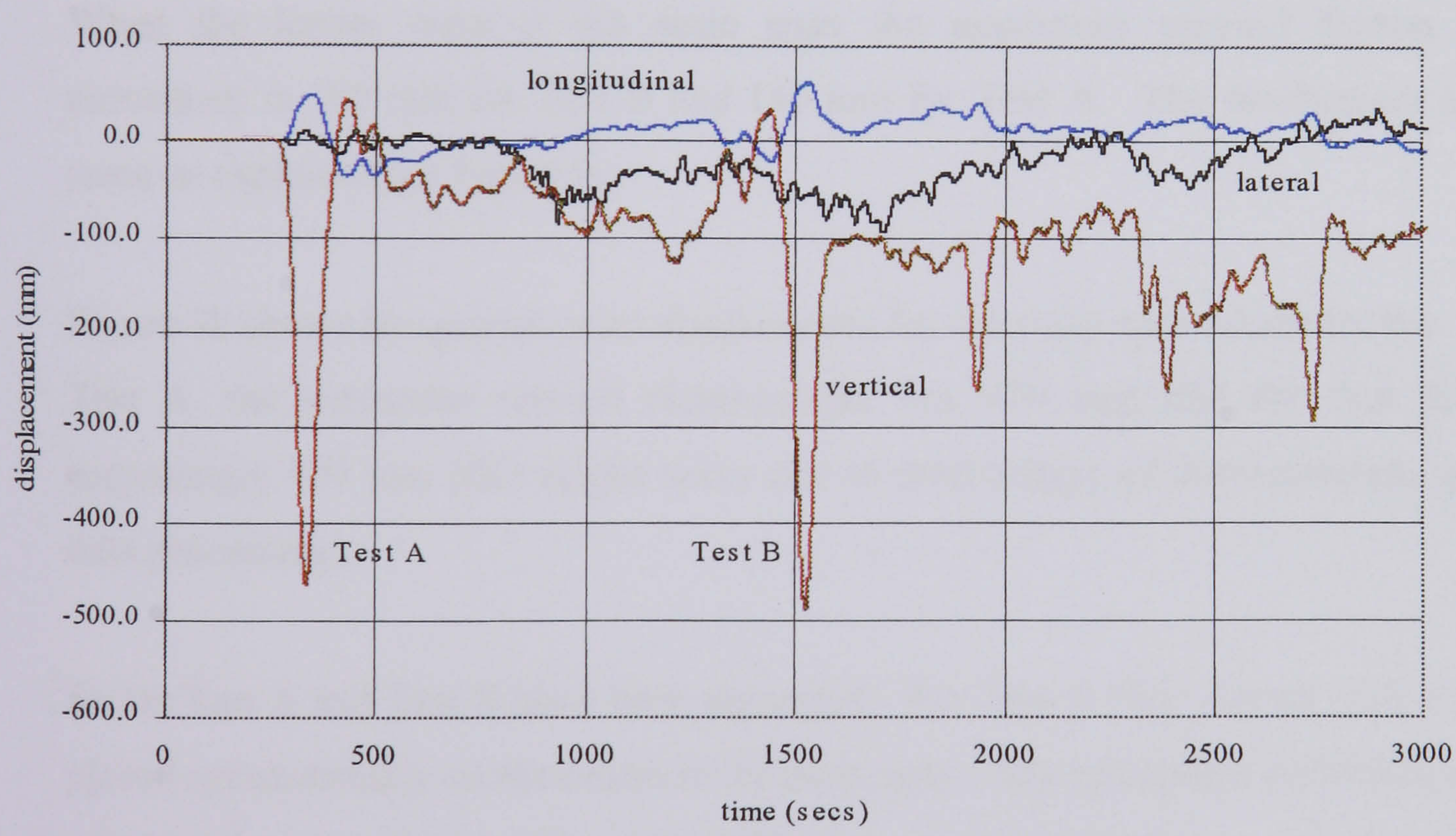

Figure 9k: Displacements at the quarter point of the main span towards the Hessle side

These results were compared with the model-predicted results. From Figure 9h the major displacement occurs approximately 350 sec. after the first station was switched on and represent the five lorries travelling along the bridge as described in

Test A. The maximum vertical displacement of 530 mm was obtained at the centre of the main span eastern carriageway. Just after 500 sec. where the lorries were on the Barton span the maximum upward displacement of 120 mm was obtained at the centre of the main span. This obviously happened due to an increasing pulling force of the main cable at the Barton side. It moves the Barton tower top away from the main span and then the main cable at the main span moves upward, resulting in upward movement of the deck.

Figure 9i shows the return passage of the lorries as described in the Test B. This time the maximum displacement occurs as expected at the main span western carriageway. The maximum vertical displacement is slightly less (520 mm) than that obtained in Test A. This may be due to the westerly wind.

As expected, in Figure 9j the maximum vertical displacement of 460 mm was obtained in the Barton span for Test B and is higher than for Test A (400 mm).
When the lorries were at the main span the maximum upward Barton span movement is 160 mm for Test B and 140 mm for Test A. The mechanism is the same as explained for Figure 9i.

Figure 9k shows the quarter point displacement for the main span where for the Test A, the maximum vertical displacement was 470 mm and for Test B was surprisingly 490 mm (this might occur due to interchange of measurements at the data processing).

So far Test A and Test B have been discussed. For Test C four lorries (128 t) were placed symmetrically on the centre of the main span. The maximum deflection at the centre point was found with some difficulties in interpretation. At the western carriageway the deflection of 420 mm was estimated and for the eastern carriageway it was 430 mm.

Figure 9l shows the sequence of data acquisition and the first lorry passage (Test A). The duration of lorry traverse (180 sec.) agrees with the measured time. The maximum peak occurs at the data acquisition locations, first at the quarter-span point on the Hessle end (480 mm) then at the main span (530 mm) and finally at the Barton side span (400 mm)

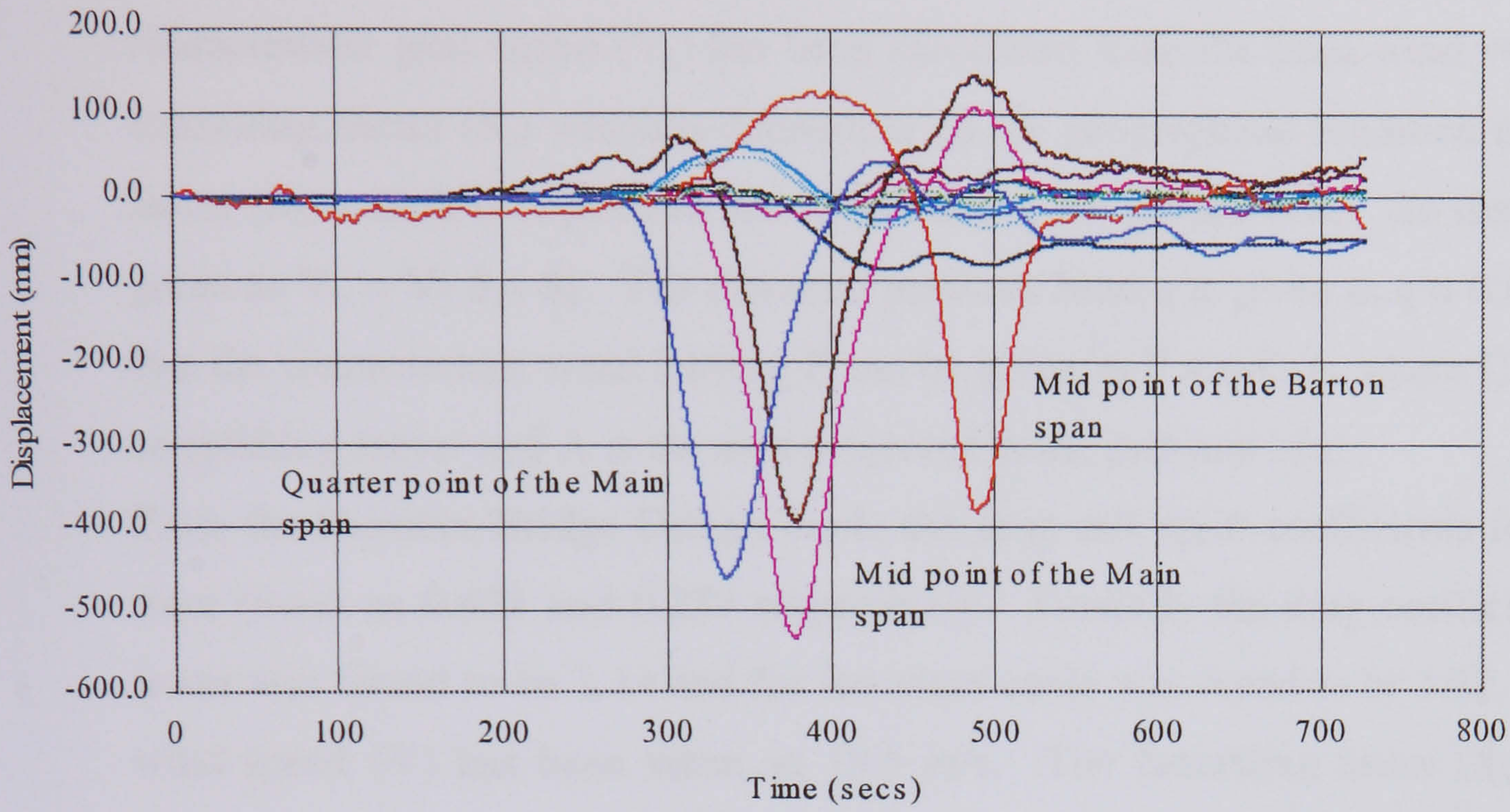

Figure 9l: Filtered displacement data for all channels for Test A

v) Model prediction for the GPS monitoring exercise

As described for the single lorry load displacement, the total lorry load of 160 tonnes was applied as surface pressure on the plate deck. As before, the 3-D box formulation model was used for the predictions. For the outer lane 30 m and for the inner lane 20 m loaded lengths were used along the deck. This arrangement satisfies the Test A and Test B requirements.

a) Application of load to the model

The model prediction was given at the centre of the deck for the main span mid point data receivers. The model first predicts the vertical deflection without any traffic loads. Gravity, wind velocity of 19.5 m/sec and the atmospheric temperature at that time of 9°C were applied together (refer Figure 9m for the loading applied to the model). The detailed model has been used, as the loading arrangement is unsymmetrical. The wind load is applied as drag and uplift pressure over the deck.

For the main cables and the towers, the pressure load has been applied as horizontal beam pressure.

The following methodology has been adopted according to British standard code for wind loading (CP3: chapter V, part2, 1972) to calculate the wind pressure. The characteristic gust speed (V_c) has been calculated from the basic wind velocity (V), funnelling factor (S_1) which is depending on the geographical condition and the gust factor (S_2) which is depend on the height above the ground level. So that V_c can be given as $V_c = V * S_1 * S_2$. The dynamic pressure head q is given as $q = 0.613 * V_c^2$, so that the characteristic wind loading F can be given as $F = q*C*A$. where C is the drag or uplifting factor and A is the area projected to the pressure load.

From the Humber Bridge Design book, the drag and uplift coefficients for the deck were found as 0.493 and 0.259 respectively. Similarly the drag coefficient for the tower was found to be 1.14 and for the main cable was found to be 1.22. The basic wind speed (V) has been taken as 19.5 m/s. The funnelling factor (S_1) has been taken as 1, which is the value for an open space. The gust factor (S_2) has been taken at the deck level as 1.53 and the tower top level as 2.07. The load file for the wind load analysis has been attached as Appendix 4.

The thermal load is applied with the reference temperature of 20°C and the uniform body (structure) temperature of 9°C. The solar gain was not considered as the test was carried out at night time (2 am). This produces a vertical upward deflection of 0.4076 m at the data receiving location at mid of eastward footpath on the main span. The Figure 9n shows the vertical deflection of the structure where the maximum upward value of 0.4097 m occurs at the centre point of the mid-span on the deck, meantime the overall deflection by considering the vertical, lateral and longitudinal movement is given by DMX, which is 0.8772 m.

Then it predicts the vertical deflection with the additional lorry load of 160 tonnes. This produces the vertical downward deflection of 0.1121 m at the same location (mid of eastward footpath on the main span). The Figure 9o shows the plot of vertical deflection of the structure where the maximum downward value of 0.1783 m occurs, while the overall deflection DMX is 0.7840 m. The difference between both readings (net) at the data receiving location at mid of eastward footpath on the main span gives the prediction for the 160 tonnes load, which is 0.5197 m (0.1121 m + 0.4076 m).

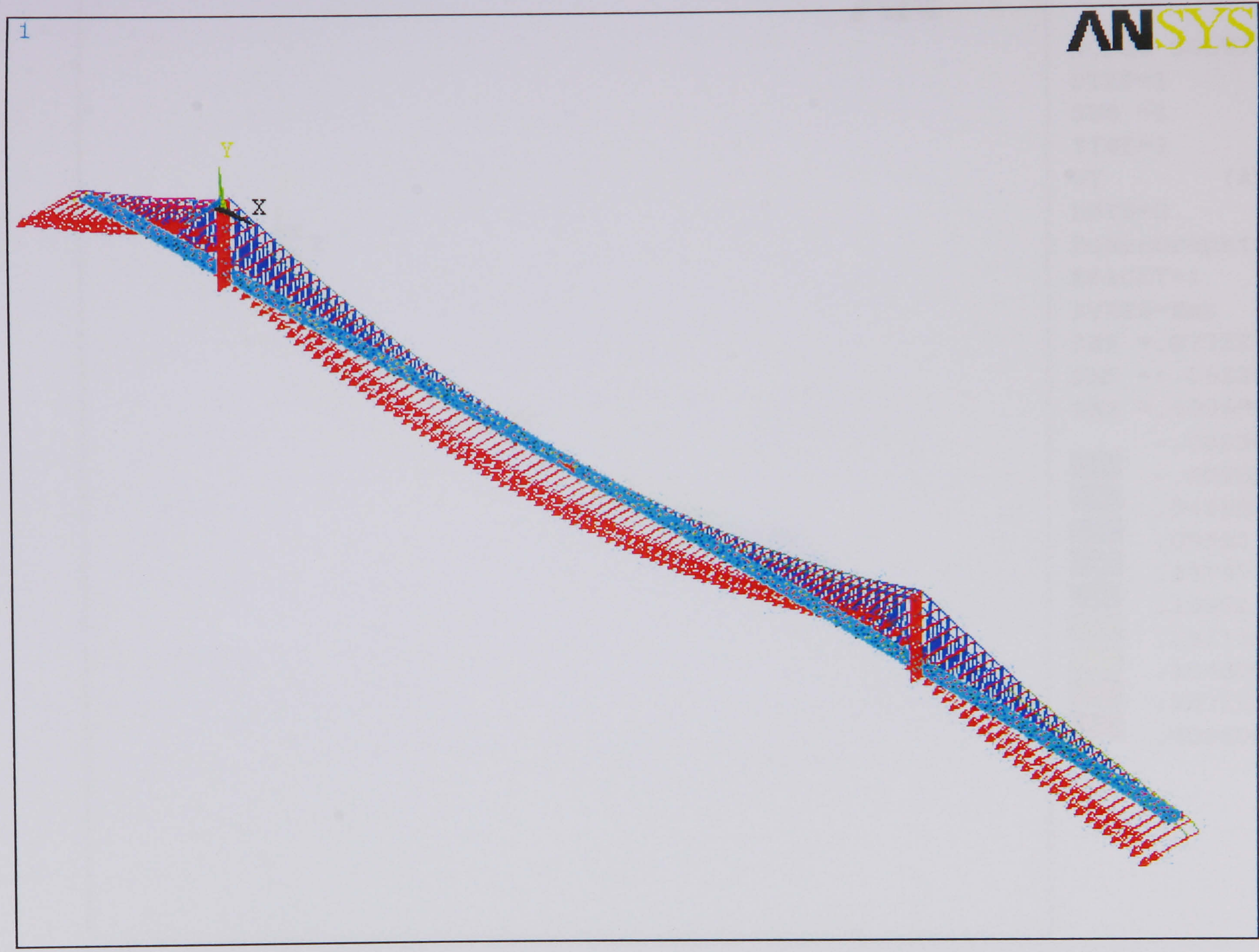

Figure 9m: Wind load applied on the main cable, tower and the deck of the model

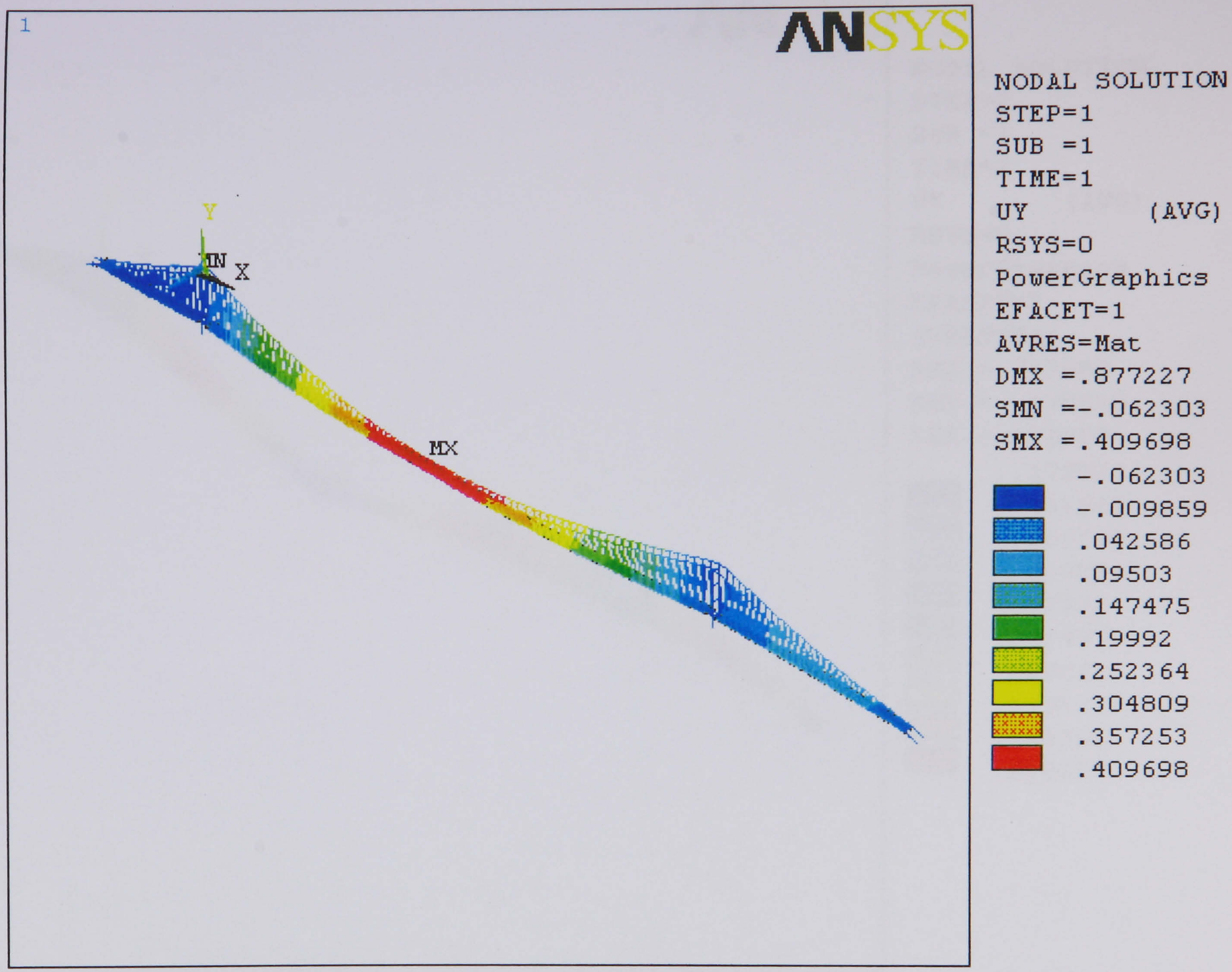

Figure 9n: Vertical deflection (m) due to self-weight, wind and atmospheric temperature of 9°C.

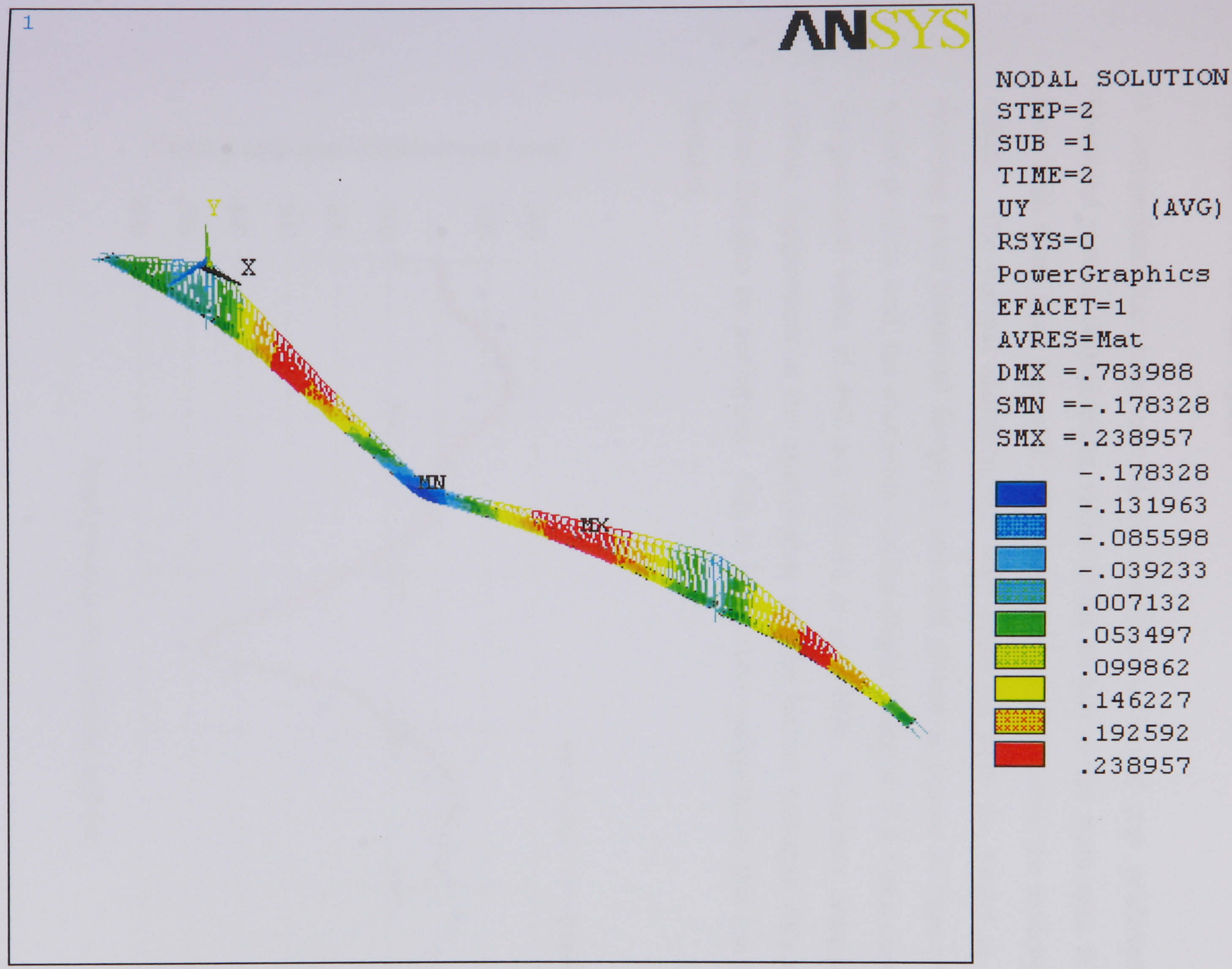

Figure 9o: Vertical deflection (m) due to self-weight, wind, atmospheric temperature of 9°C and 160 tonnes load at the centre of the main span.

b) Validation of results for 160 tonnes lorry load

1) Middle of the main span

A comparison has been carried out between measured and predicted values. Measured vertical displacement values at the middle of the main span for Test A have been taken from figure 9l. This has been compared with the model-predicted values. The vertical displacements were predicted from the model at the data receiving point (eastward footpath), and then plotted as shown in Figure 9p. The model predicts well, the maximum vertical displacement of 518.7 mm compared to the measured value of 490 mm (Brown *et al,* 1999). Similarly comparison for vertical displacement at the quarter-span and the Barton mid-span data receiving points can also be performed. Due to heavy data manipulation this has not been included

Figure 9p: Comparison of measured and model prediction of the vertical displacement at mid point of the main span with load position from the Barton end

2) Quarter of the main span

There is only one data receiving location for the main span quarter point (east). The vertical displacement for Test A and Test B are predicted at the required location and averaged, then plotted as shown in Figure 9q for the quarter point of the main span. This figure predicts the maximum net vertical displacement of 482.4 mm which agrees well with the average measured value of 480 mm.

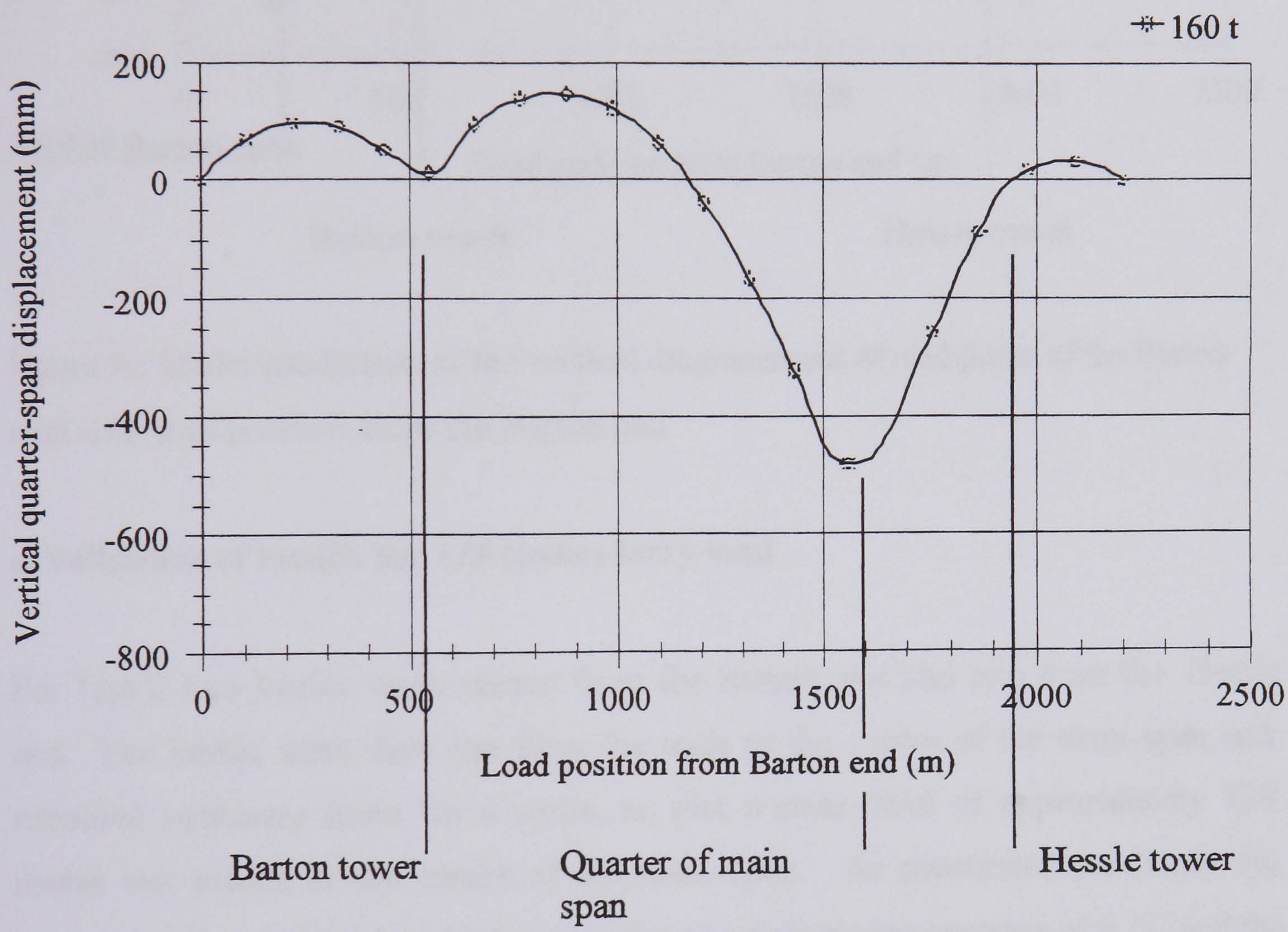

Figure 9q: Model prediction of the vertical displacement at quarter point of main span with load position from the Barton end

3) Middle of the Barton span

As with the quarter point of the main span there is only one receiving location for the Barton span mid-point (west). So the vertical displacements predicted at the above mentioned location for the Test A and Test B are averaged and plotted on Figure 9r. This figure predicts the maximum net vertical displacement of 425.2 mm which agrees well with the average measured value of 430 mm.

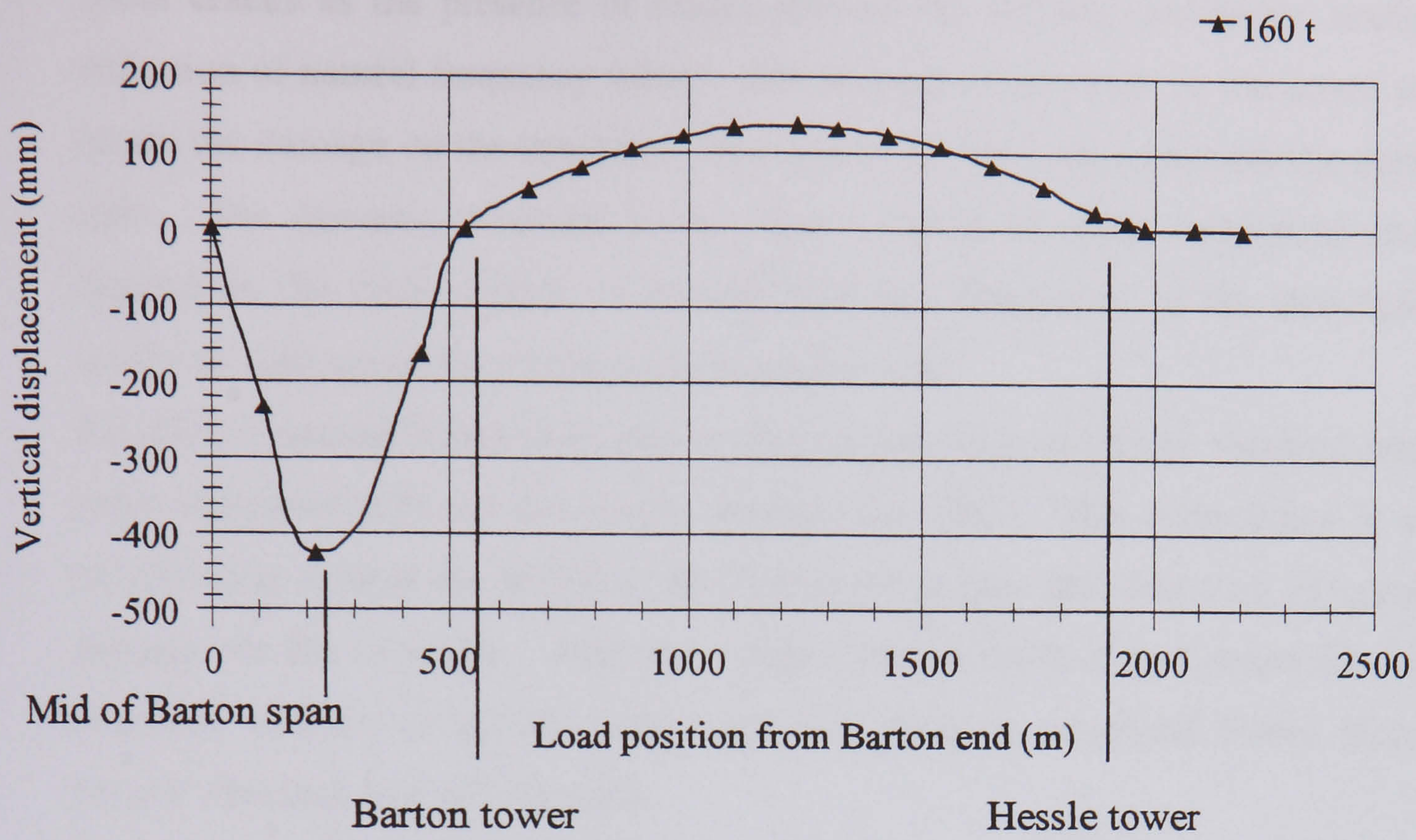

Figure 9r: Model prediction of the vertical displacement at mid point of the Barton span with load position from the Barton end

c) Validation of results for 128 tonnes lorry load

For Test C two lorries were started from the Barton end and two from the Hessle end. The lorries were then run from the ends to the centre of the main span and remained stationary there for a while, so that a static load of approximately 128 tonnes was placed at the centre of the main span. As mentioned previously (in section A), the wind load of 19.5 m/sec, the atmospheric temperature of 9 °C and the gravity loads were applied. The model predicts the net value of 440 mm at the centre of the main span, which gives the close agreement with the average measured value of 425 mm.

iii) Validation of models under dynamic condition

Validation against modal analysis gives confidence about the dynamic model and enables the subsequent response analysis to be carried out. These dynamic parameters (natural frequencies and associated mode shapes) are directly related to the stiffness of a structure. Dynamic analysis gives a general indication on structures about cracks as the presence of cracks reduces the stiffness and hence leads to a reduction of natural frequency values. The changes of curvature in the mode shapes locate the damage on the structure. Also newly formed cracks increase the damping ratio. The dynamic structural forces from a forced vibration (response) analysis depend on the mode shapes, so accurate stiffness distribution of the structure and cracks or damage on the structure plays a major role.

Results of natural frequencies and modal shapes from the finite element analysis were compared with site test results (Brownjohn, 1986). This comparison is a way of checking against the stiffness, distribution of masses and detection of cracks or damage on the structure. Also this comparison on mode shapes helps for further response analysis to get the right (expected) dynamic structural forces from the forced vibration dynamic analysis.

In addition to that, the GPS monitoring system (Brown *et al,* 1999) gave first vertical and lateral oscillation natural frequency values. The value of the frequency at which oscillation occurs was determined using a readily available computer-based numerical analysis package called MATLAB. The approach followed within this program called Fast-Fourier-Transform based power-spectral density analysis. However the methodology used is outside the scope of this research.

Examination of the modal shapes predicted by 2-D (vertical modes only), 3-D plate and 3-D box formulation finite element models shows that the measured mode shapes are being predicted well by numerical simulations. The present GPS monitoring system also gave good agreement with predicted and measured values. Comparison of the first two vertical and torsional vibration frequencies with laboratory test results (performed by National Physical Laboratory and British Maritime Technology) gave good agreement.

The GPS monitoring system and the field measurement gave the same first vertical and lateral natural frequency values of 0.116 Hz and 0.052 Hz respectively.

Table 9a shows the natural frequency values up to 0.32 Hz for vertical and lateral modes, and up to 0.53 Hz for the torsional mode obtained from both measurements and numerical analysis. Figure 9s and Figure 9t show the first lateral and second torsional mode shapes of the 3-D box formulation model respectively.

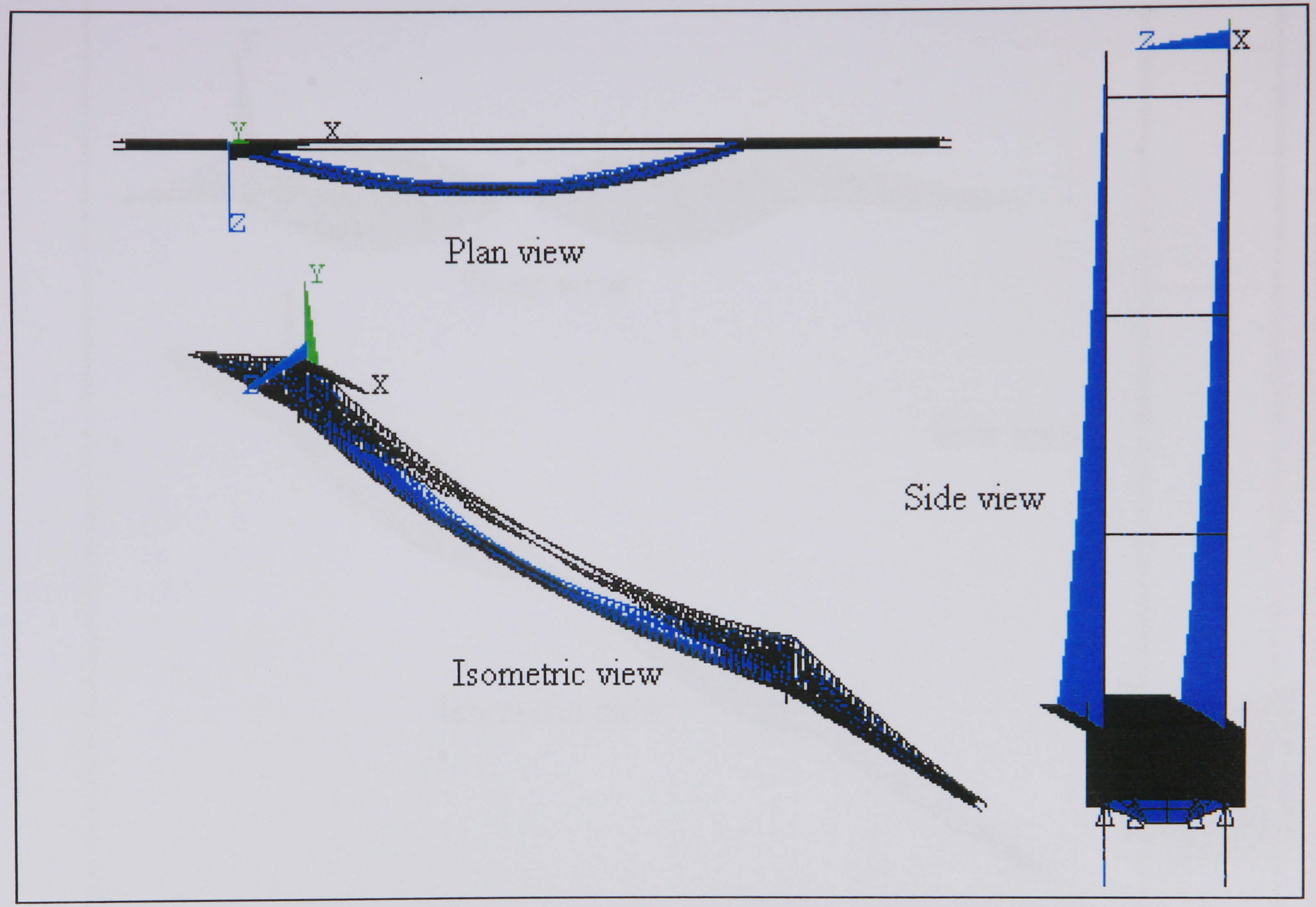

Figure 9s: First lateral mode shape of the 3-D box formulation model.

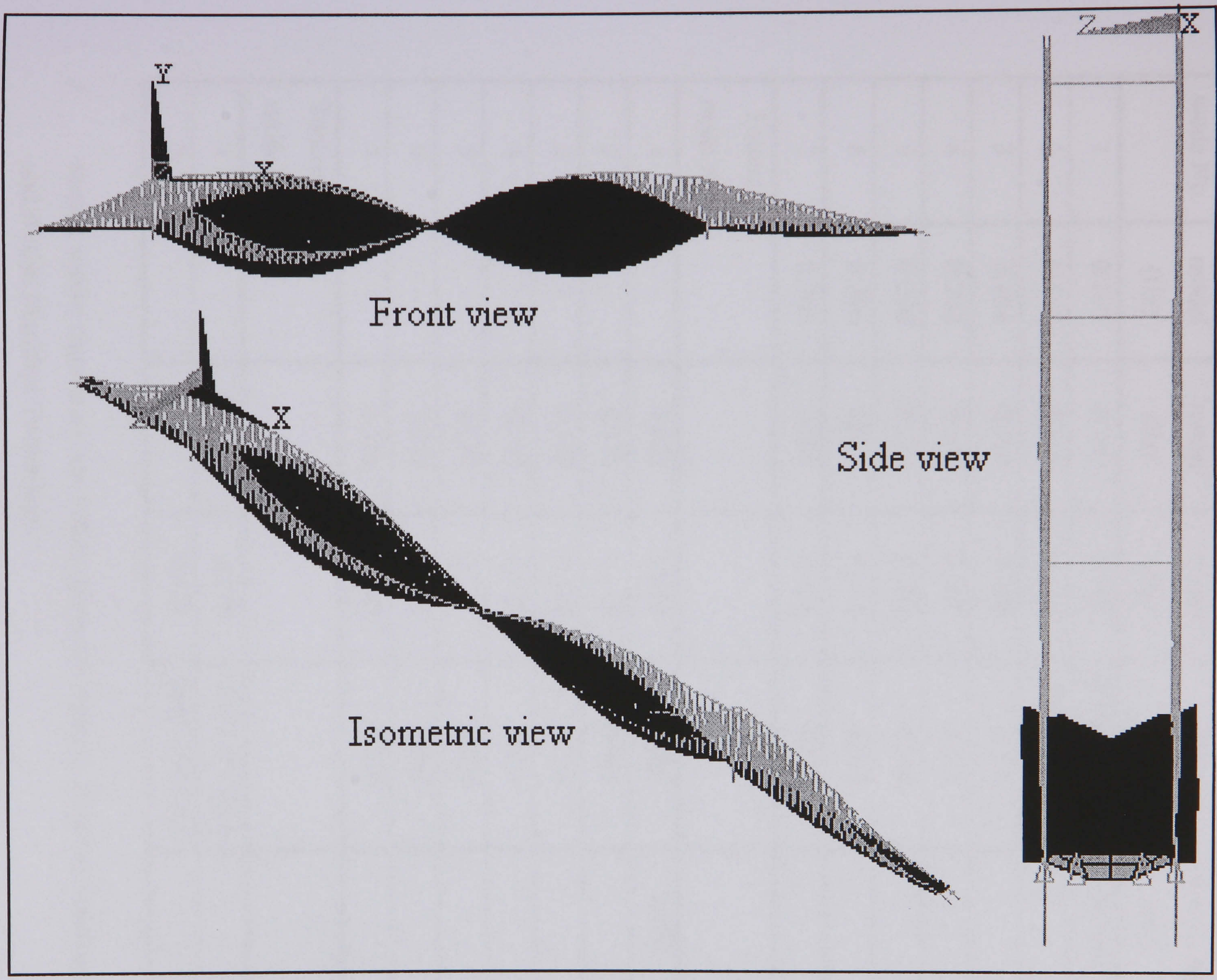

Figure 9t: Second torsional mode shape of the 3-D box formulation model.

Vertical mode No.	2-D model (Hz)	3-D plate model (Hz)	3-D box model (Hz)	Measured (Hz)	GPS Monitoring (Hz)
1	0.107	0.107	0.108	0.116 (*0.104)	0.116
2	0.113	0.113	0.116	0.154 (*0.107)	
3	0.164	0.164	0.169	0.177	
4	0.202	0.202	0.207	0.218	
5	0.236	0.236	0.241	0.240	
6	0.296	0.304	0.314	0.310	
7	0.306	0.306	0.316	0.317	
Lateral mode No.					
1	-	0.052	0.054	0.056	0.052
2	-	0.110	0.119	0.143	
3	-	0.159	0.178	0.218	
4	-	0.195	0.225	0.239	
5	-	0.230	0.232	0.239	
6	-	0.239	0.243	0.260	
7	-	0.255	0.262	0.276	
Torsional mode No					
1	-	0.301	0.318	0.311 (*0.300)	
2	-	-	0.524	0.482 (*0.519)	

* Scaled modal laboratory test values given by National Physical Laboratory and British Maritime Technology

Table 9: Natural frequency values from F.E. analysis and measurements

Summary of findings

- Created models have been validated under dead load condition where acceptable deflected profiles were obtained. A maximum deflection of 47 mm was found at the main span, which is negligible (1:29800) compared with the span of 1410 m.
- Under the same dead load condition the main cable and the hanger forces at key locations were compared with the Humber Bridge Designer's calculation report. The range of difference of 0 % to –0.7 % for the main cable force and –6.0 to 4.5% for hanger force were found. It shows that the models are not far away from the designer's predictions.
- As mentioned in chapter 8, changes of main cable initial strain by 1 % give 133-mm movement on the main cable and the deck. This gives considerable changes on the hanger force due to the relative movement of the main cable and the deck. Minor inaccuracies on the initial strain might cause the difference in hanger forces.
- The first load test (single lorry load displacement measurement on the site) gives the same pattern of displacement vs. time curves at the middle and quarter span location for the measured and FE analysis results. Adjusting the applied lorry load from 170 tonnes to 120 tonnes on the model produces the same magnitude as field measurement. This might imply that the load of the single lorry passage was 120 tonnes.
- The second load test (passage of five 32 tonnes lorry loads, GPS measurements) gives very close agreement on deflection vs. time curves at three locations including mid and quarter of the main span and the mid of Barton span. This gives confidence on distribution of stiffness and mass along the bridge structure.
- Finally the natural frequency values and the associated mode shapes give good correlation with measured and FE analysis results. The vertical, lateral and torsional mode shapes and the natural frequency values of the field measurement compared well with the corresponding FE analysis results. This is confirming that the vertical, lateral and torsional stiffness distribution on the structure, in addition to the mass distribution along the structure, are realistic.

Chapter 10

Application of the models

General

Models have been built to assist in understanding the structural behaviour of the Humber Bridge under different loading conditions. It is the primary application of these models in this research and is also a requirement of the Humber Bridge Board. These models can also be used to determine the structural behaviour should any elements ever be removed from the structure. Using the computer models it will be possible to prepare a useful table with say, wind loading, or removal of number of hangers against maximum traffic loading. This will enable the practical engineer to make decisions as to whether to allow the traffic at a windy day or while maintenance work is on process.
A wide range of other applications of these models could include the following;
Understanding the sensitivity of structural components; effects due to deterioration of structural components; design of other bridges in terms of the required dimensions of particular structural components, as have been extensively discussed in Chapter 8.
Another application of the models is to understand the advantages and disadvantages of the existing hanger system. This has been studied and compared with the introduction of different hanger system patterns and additional problems due to new hanger systems are extensively described in Chapter 11.

The Humber Bridge design check was based on the loading requirements given in BS 5400, Part 2 (1978). Due to increasing traffic density in recent years the Humber Bridge Authority has decided to assess the current loading situation. Fairhurst & Partners in April 1995 carried out a structural assessment. A three weeks continuous traffic survey was carried out to calculate the Bridge Specific Assessment Live Loading (BSALL) for the Humber Bridge, which is described in section two below. The computer models are important tools for understanding the structural behaviour of the Humber Bridge under this recently assessed (revised, BSALL) loading condition.

Predictions are given with confidence as the models have been validated against field measurements. Models are selected for use depending on the requirements and the loading conditions. Here the traffic load is applied as surface pressure on the deck elements for 3-D models. On the 2-D model it is applied as uniformly distributed load.

For the application of wind load, the 3-D box formulation model is used to withstand the drag and uplift forces on the box deck. The wind load on the main cable is applied as point loads on the series of nodes. On the tower it is applied as uniformly distributed load.

1) Predictions under critical loading

The bridge is currently operating in a perfectly acceptable way with no known problems. However, the number of vehicles travelling across the bridge has risen sharply over the last few years. Therefore it has become necessary to carry out further structural analysis to ensure continuing safety under conditions different to those anticipated in the original design, and to provide maintenance guidelines for the bridge. Sets of possible critical case studies have been created and are described below to understand the structural behaviour.

Some critical basic load cases like maximum wind speed, maximum temperature differences and HB loading (which is the abnormal vehicle unit loading in Great Britain) have been considered and the results compared with the designer's allowable values. Although these critical basic load cases were considered at the time of design, these cases have also been applied to the current models and the results compared with the original allowable design values.

The new loading conditions called BD 37/88 for bridges introduced by the department of transport in 1988 were also applied to the bridge model and the results are compared with the allowable design values. The original design load or the BSALL load (3.0 tonnes/m) is significantly less than the BD 37/88 loading (3.4 tonnes/m) values. For the purpose of assessment 30m loaded length of BD 37/88 value, which is the most critical loading value is applied to one lane of the bridge carriageway. This is a repetition of the original design where the 30m loaded length value (3.0 tonnes/m) from BS 5400, Part 2 (1978) was used.

Freeman Fox & Partners, through discussion with Department of Transport, decided to design the structure using HA loading but conservatively selected a load case based on the above loaded length. This loading condition (loaded length) was specified by the client as an acceptable design basis.

For this type of structure (span above 1600m according to BD37/88) BSALL is the substitute for the standard HA loading, which is a formula loading representing normal traffic in Great Britain. The load cases, which are to be considered, relate both to the bridge carrying only BSALL and to the bridge carrying abnormally heavy vehicles (45 units as defined in BD37/88) combined with the BSALL.

Combination of loading like fully span loaded BSALL condition and/or HB loading with temperature rise and wind is also applied and the results are checked against allowable design values.

In addition to the above loading conditions some selected critical BSALL load cases combined with HB loading have been applied to create the worst tensile and compressive forces on the A-Frames. The results have been tabulated and checked against the allowable design values.

a) Thermal effect

The expected temperature changes over a 120 year period have been predicted to be between -30°C to +30°C with ambient temperature 20°C. These values are from a geographical survey of the Humberside area (Humber Bridge Design Data, internal). Hence the structural responses at the two extremes -10°C and +50°C have been considered. The 3-D plate formulation model has been used for this analysis. Deflected forms of the structure models are shown in Figure 10a and 10b.

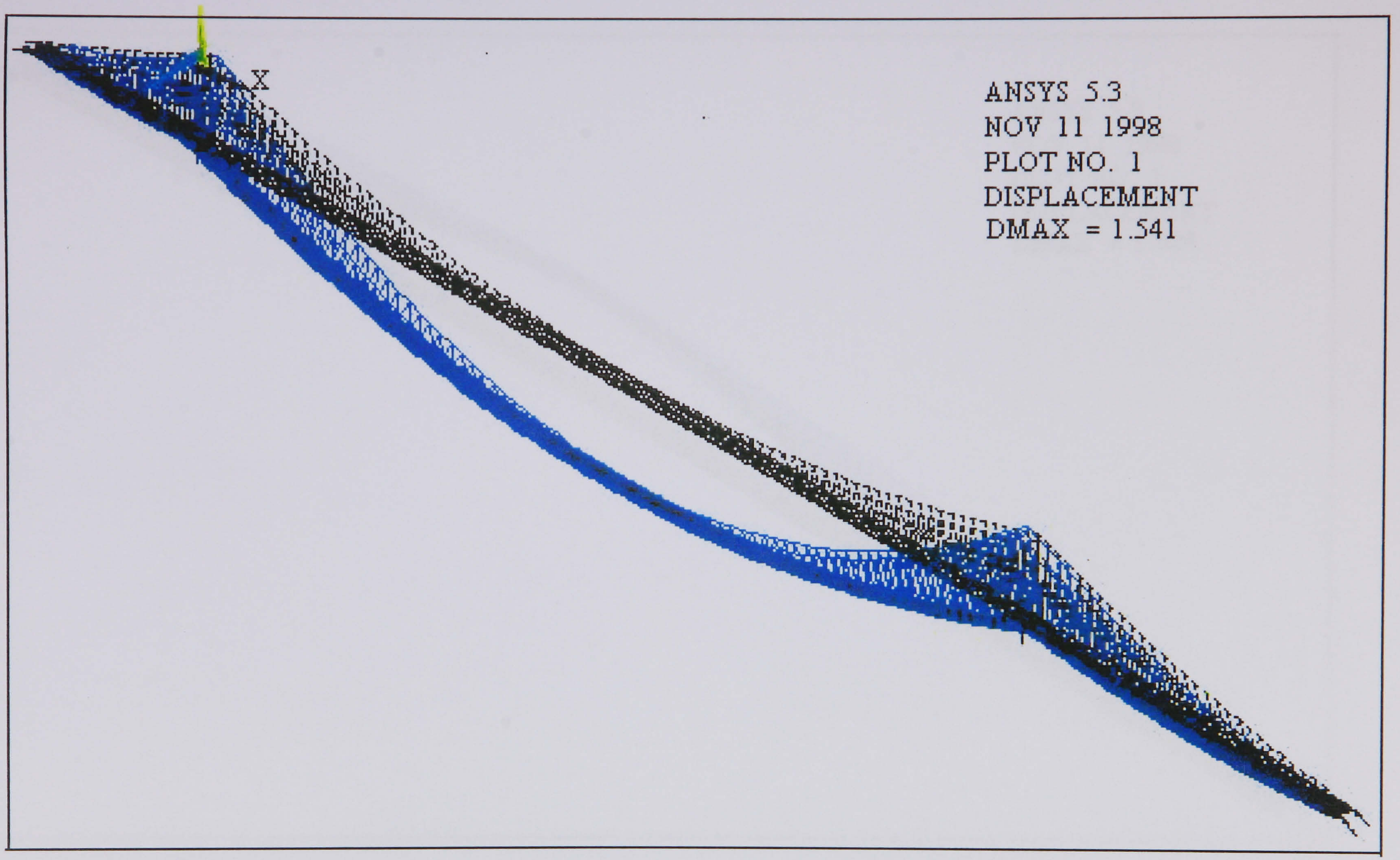

Figure 10a: Deflected shape for +50°C thermal load (maximum deflection 1.541 m). (In this plot the displacement is magnified by 100 times.)

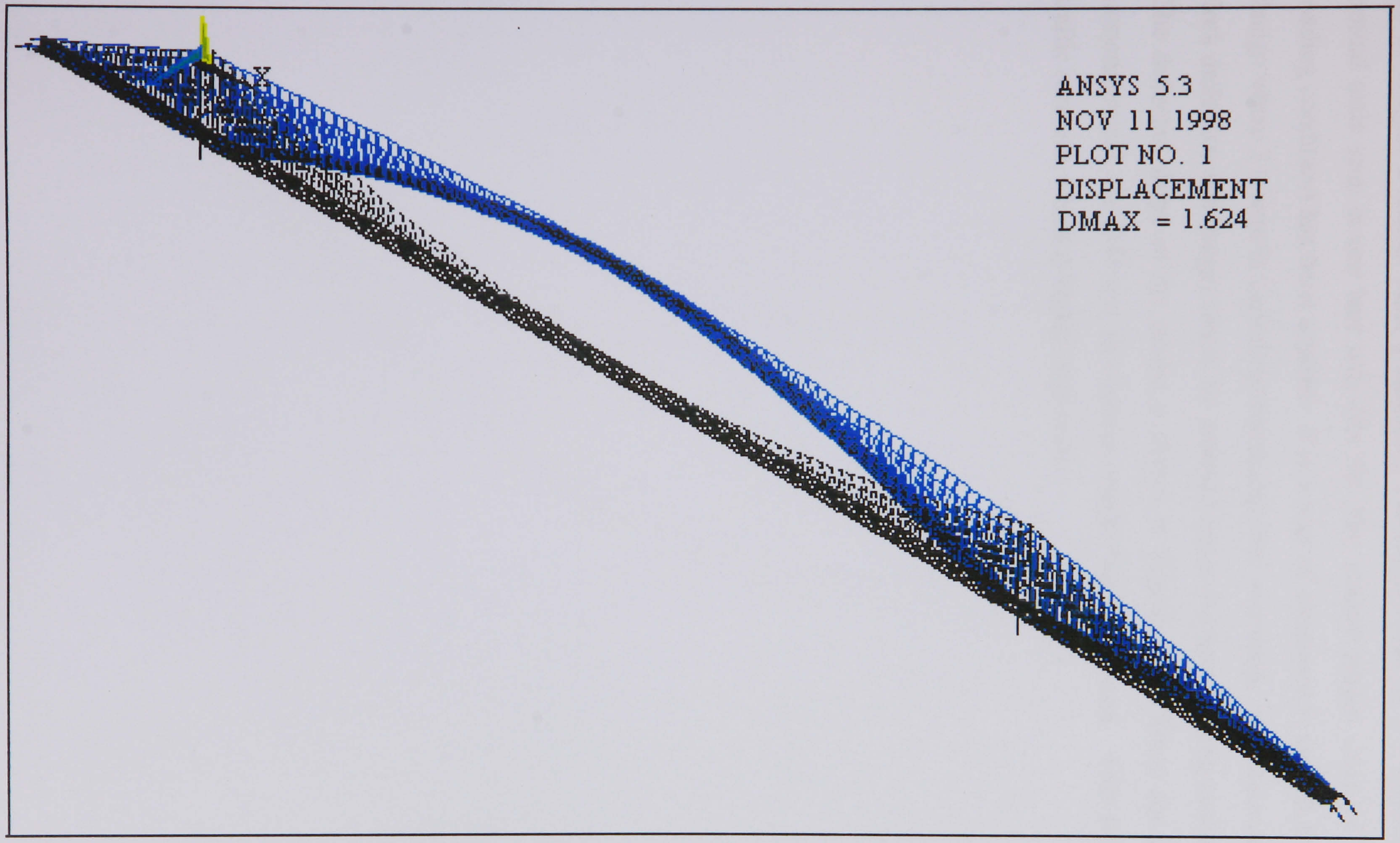

Figure 10b: Deflected shape for -10°C thermal load (maximum deflection 1.624 m). (In this plot the displacement is magnified by 100 times.)

b) BD 37/88 loading condition

To investigate a critical case, a uniformly distributed load of 3.4 tonnes/m on the central main span in one lane only (for the 30m loaded length value of BD 37/88 loading condition) has been applied. It is a way of assessment against the original design where 3 tonnes/m uniformly distributed load was used. The main cable force, deck deflection and hanger forces are assessed under the new loading condition.

The deflected shape of the model is shown in Figure 10c. Since the loading is unsymmetrical, the 3-D box formulation model has been used. This is the worst traffic scenario, which is highly improbable.

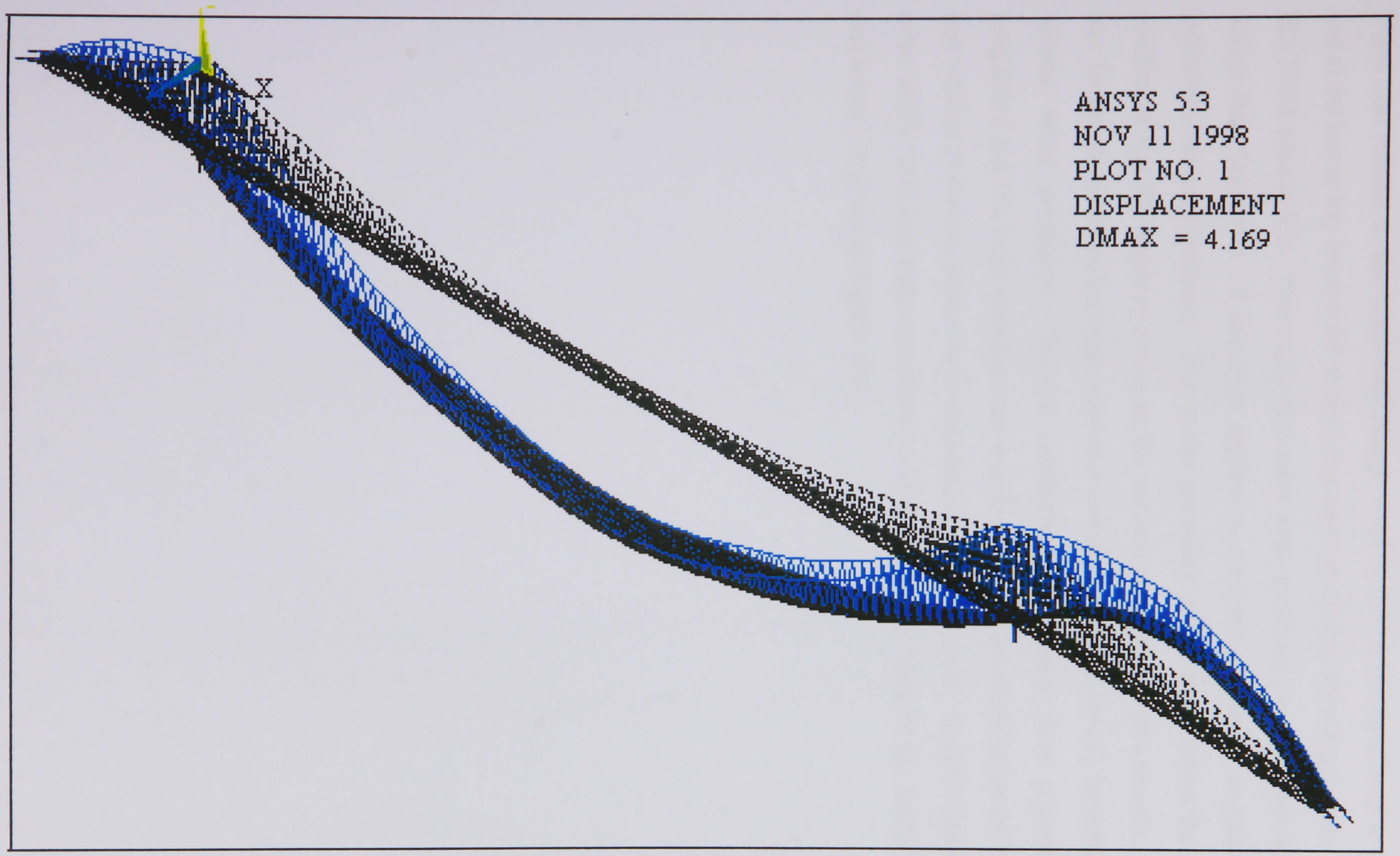

Figure 10c: Deflected shape for BD 37/88 traffic load (maximum deflection 4.169 m). (In this plot the displacement is magnified by 50 times.)

c) Maximum design wind speed

Wind load related to the maximum design wind speed (at the deck level is 48 m/sec. and at the tower top level is 66 m/sec.) has been applied in accordance with BD 37/88 clause 5.3. This wind data have been gathered from the Humber Bridge design data (internal). It has been applied as transverse (lateral), longitudinal and uplifting (vertical) pressure. Due to the geometry of the deck section the uplifting coefficient has the negative value, so the vertical pressure acts downwards. The 3-D box formulation model has been used as it can accommodate lateral, longitudinal and vertical wind pressures. Several combinations of these three pressures were considered but the most onerous case was found to be the combination of transverse and vertical pressure, others were consequently not reported. At this wind speed no other traffic load has been considered and the deflected form of the model (vertical and lateral) is given in Figure 10d.

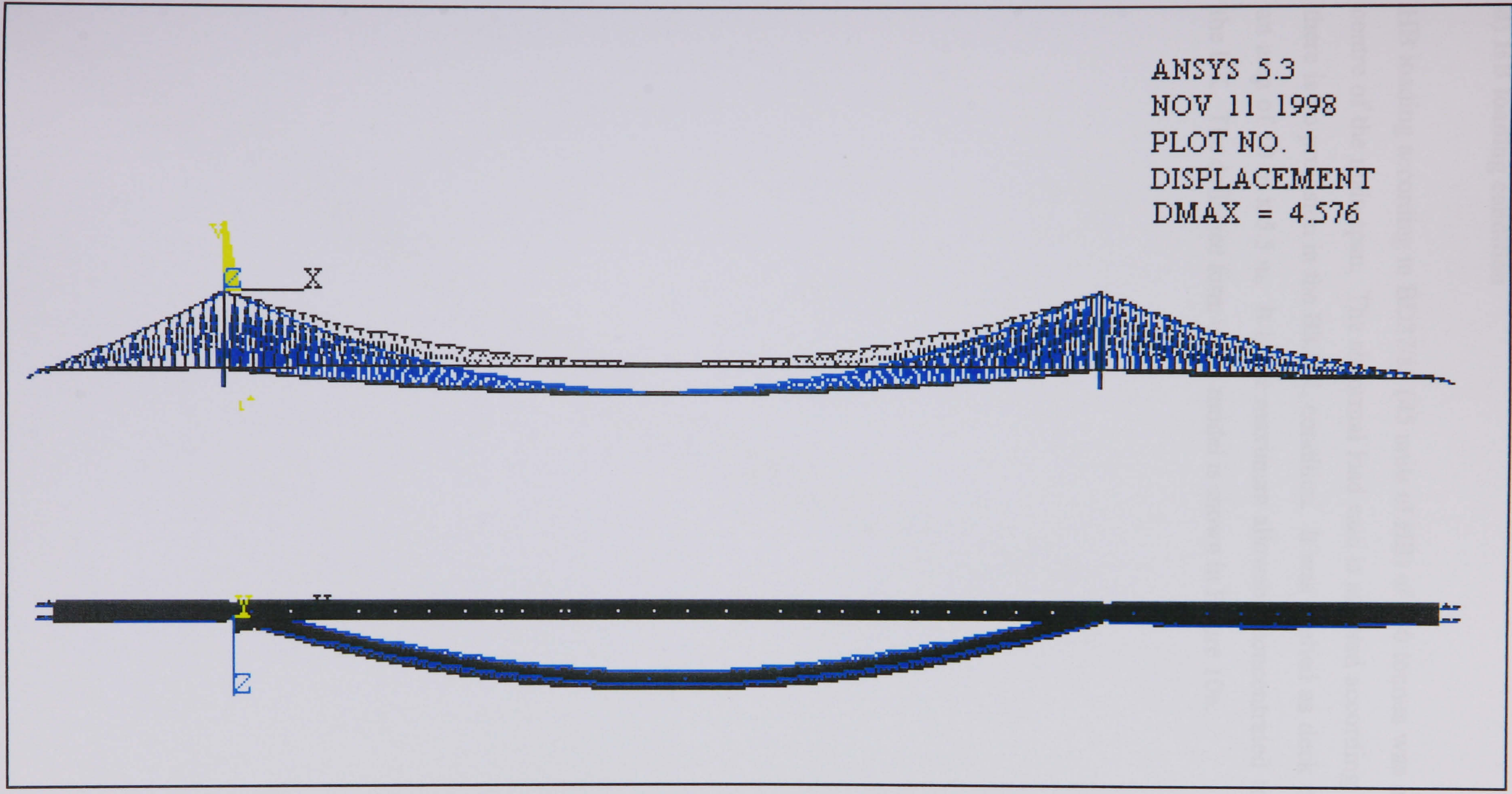

Figure 10d: Deflected shape for design wind load (maximum lateral deflection of 4.467 m and maximum vertical deflection 0.992 m). (In this plot the vertical and the lateral displacements are magnified by 100 times.)

d) HB loading condition

HB loading according to BD37/88 (45 units of HB) of 180 tonnes was applied at the centre of the main span. The abnormal load case is adopted according to BD37/88, there is no provision in the BSALL condition. It was applied as deck pressure over an area of 10 m x 5.5 m. It is the maximum allowable concentrated traffic load in the UK. The deflected form of the model is shown in Figure 10e.

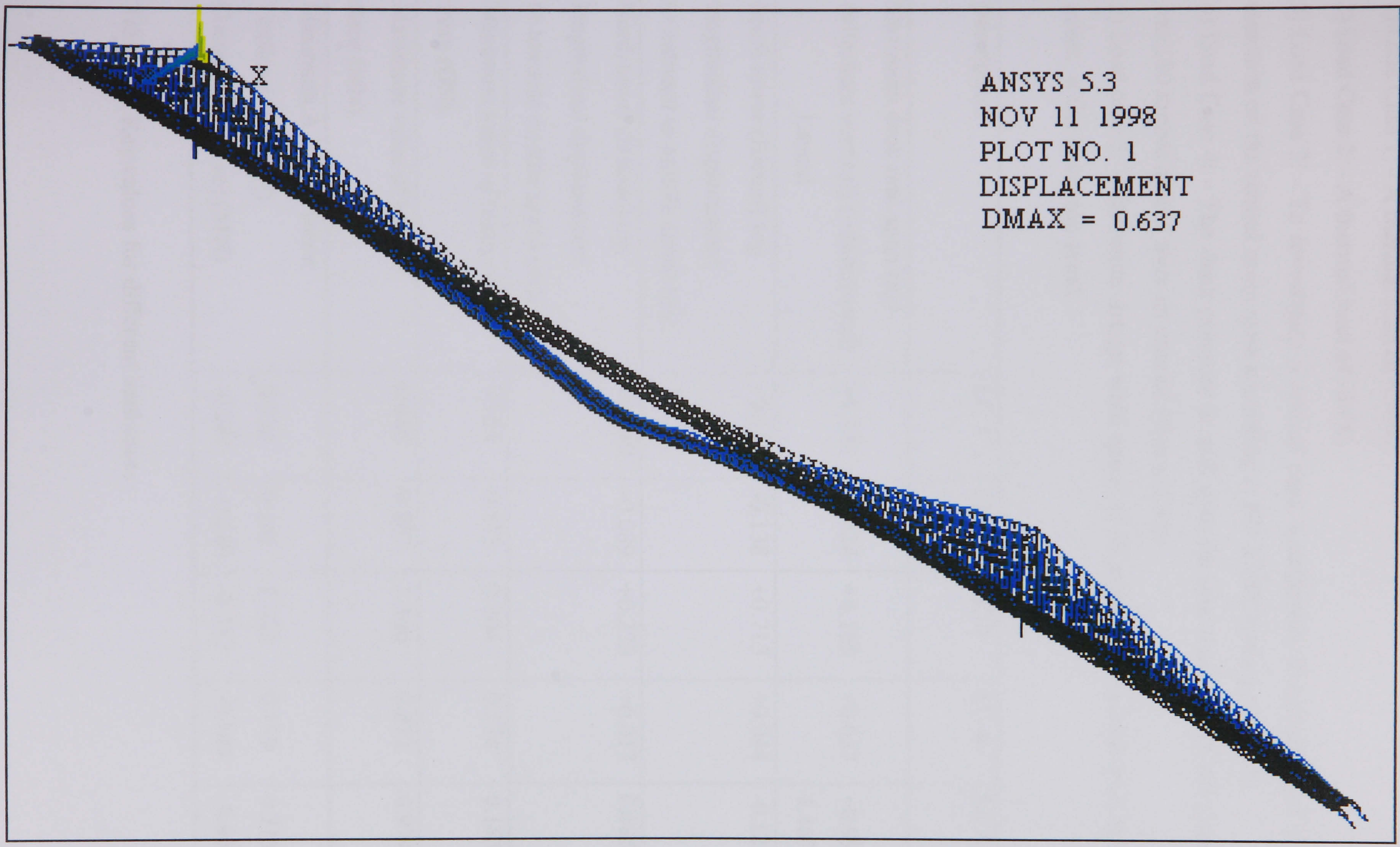

Figure 10e: Deflected shape for HB loading (maximum deflection 0.637 m). (In this plot the displacement is magnified by 100 times.)

The above mentioned load cases and key results are given in table 10a.

1) Load Case 1: - A thermal load of +30°C.

2) Load Case 2: - A thermal load of -30°C.

3) Load Case 3: - To investigate a critical case, a uniformly distributed load of 3.4 tonnes/m on the central main span according to BD 37/88 loading condition.

4) Load Case 4: - The deck pressure at mid span (in one lane), under HB loading, was 180 tonnes spread over an area of 10 m x 5.5 m.

5) Load case 5: -Maximum design wind speed of 48 m/sec. at the deck level and 66 m/sec. at the tower top level.

Description	LC 1	LC 2	LC 3	LC 4	LC 5	Design value
Maximum deck mid-span (m) deflection: vertical) (+downward) Lateral	+1.541	-1.624	+4.169	+0.637	+0.992 4.467	4.310 4.510
South tower (Barton) top longitudinal displacement (+ outward to middle span) (m).	+0.139	-0.138	+0.713	+0.044	-0.122	0.723
North tower (Hessle) top longitudinal displacement (+ towards middle span) (m).	+0.089	-0.089	+0.273	+0.017	0.095	0.723
Maximum value of main cable force (GN).	0.169	0.173	0.204	0.174	0.185	0.210
Maximum value of hanger force (MN).	0.846	0.887	1.360	0.872	0.974	1.450
Maximum A-Frame force: Tension (+ve)(MN) Compression (- ve) (MN)	 0.056 -0.281	 0.161 -0.149	 2.922 -3.757	 0.119 -0.144	 0.319 -0.462	 9.500 8.200

Table 10a: Key values for different load cases

The worst load case for the deck vertical displacement, main cable force and hanger force was found to arise when the bridge was subjected to a uniformly distributed load of 3.4 tonnes/m on the central main span at lane 1 (load case 3). These values are just satisfying the allowable design requirement for the deck vertical displacement of 4.310 m, main cable force of 0.21GN and for the hanger force of 1.45 MN.

Stress levels (Von Mises value) on the deck under wind load (load case 5) were calculated. This particular loading was selected as it has the vertical (uplift) and lateral (drag) pressure components. Due to this loading the maximum stress on the main span deck occurs at the A-frame supports. The deck top plate (Figure 10f) has the maximum stress value of 0.20 GPa and the diaphragm stiffeners (Figure 10g) have the maximum value of 0.124 GPa. These values are well within the design limit of 0.29 GPa. The maximum stresses occur at the main span Hessle tower end as the deck deflects laterally and higher stress concentration occurs at the A-frame support.

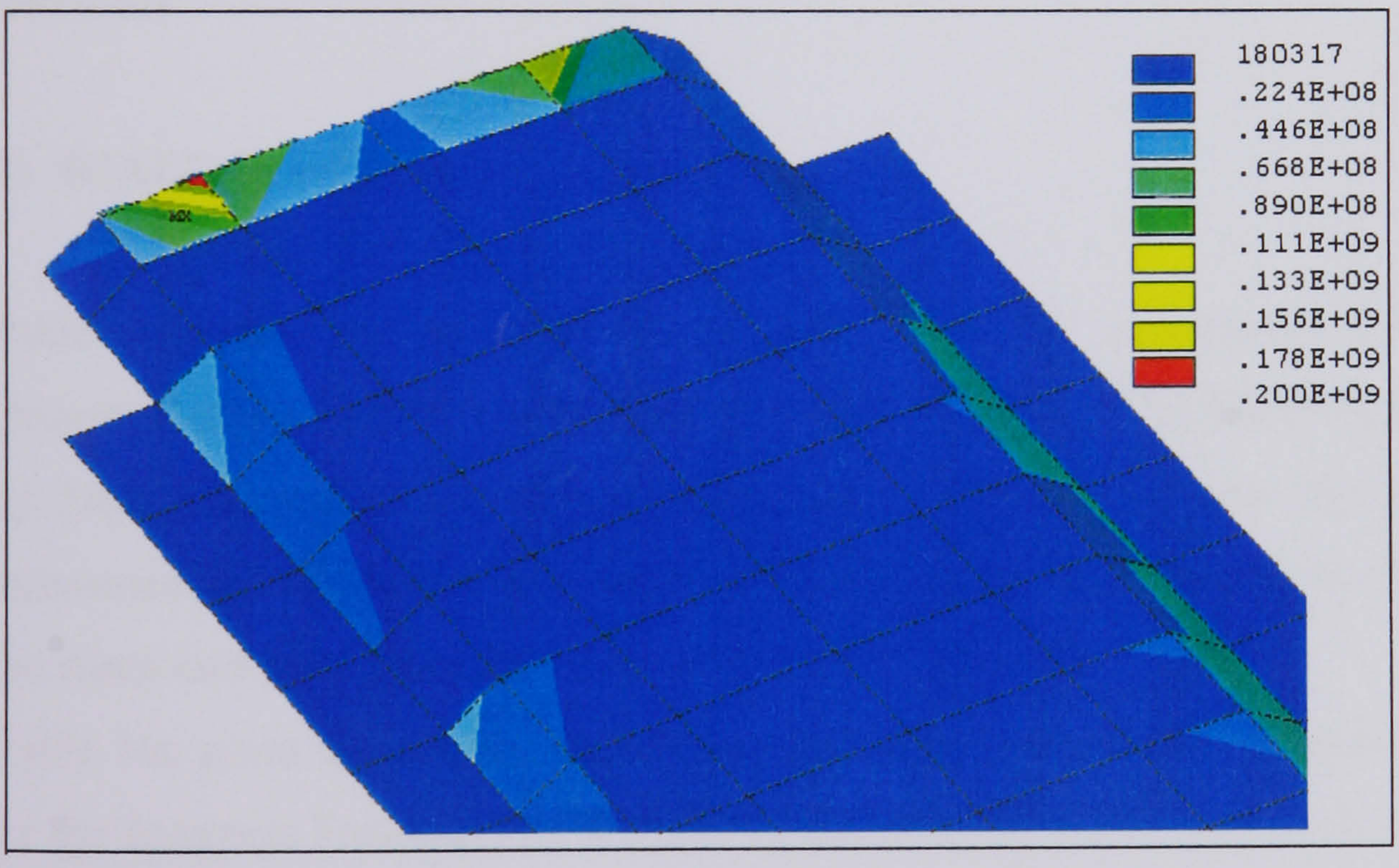

Figure 10f: Stress levels on the main span deck under load case 5

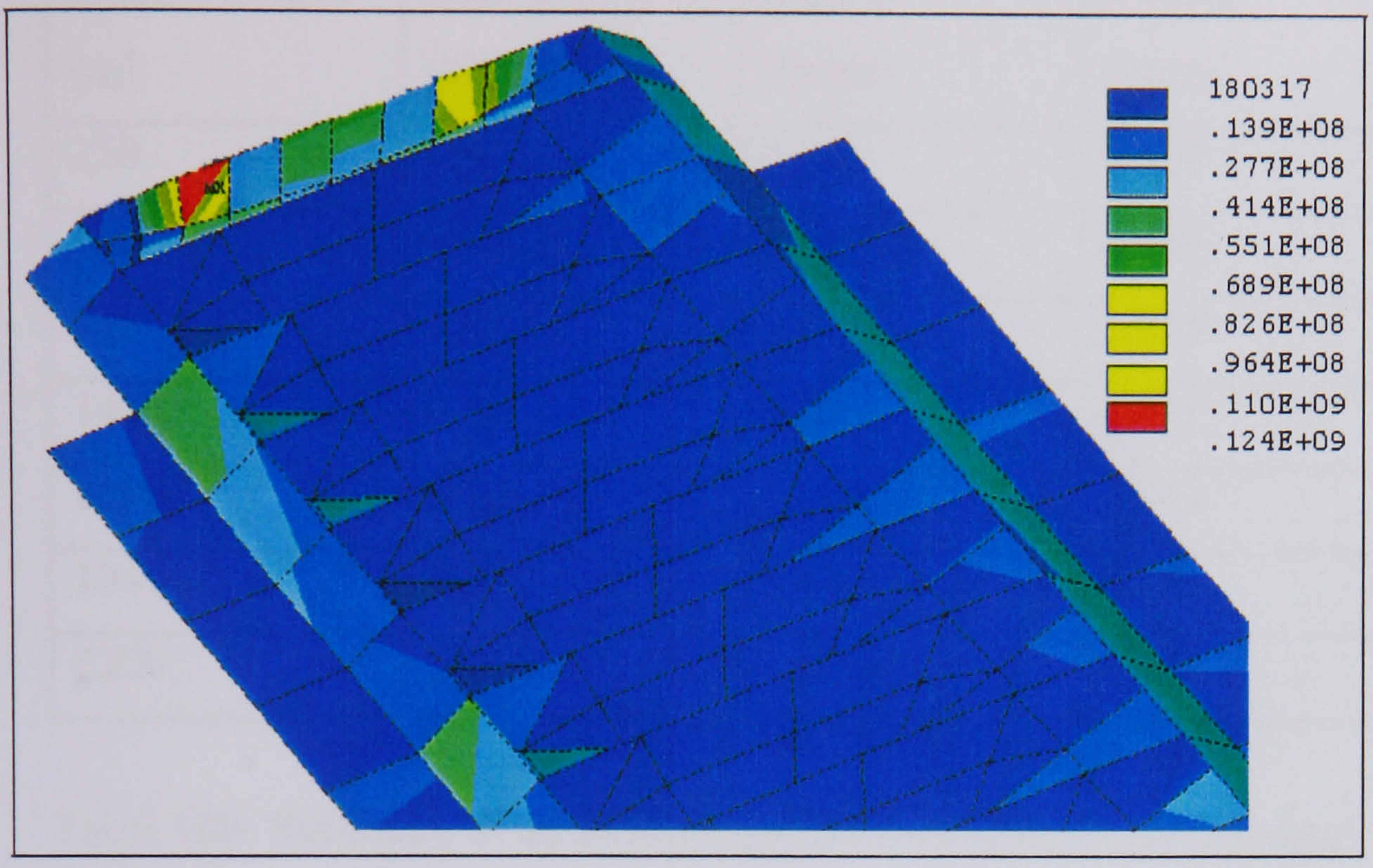

Figure 10g: Stress levels on the main span deck under load case 5 (top plate has been removed)

2) BSALL Condition

Table 10b gives the summary of the Bridge Specific Assessment Live Loading (Nominal values) which was performed by W.A Fairhurst and Partners and checked by Mott MacDonald Ltd (Mott MacDonald, 1997). This was the latest traffic assessment data from the Humber Bridge Board, (refer to Figure 5p in Chapter 5 for the sharp increase of number of vehicles over the period of time).

Table 10c gives the original design live loading (nominal values) which was taken by the designers Freeman Fox & Partners based on BS 5400, Part 2 (1978), (Humber Bridge Design Data, internal). At the start of the Humber Bridge design in 1970s the assessment code was BS 153, Part 3A (1954). The loading was updated with the arrival of BS 5400, Part 2 (1978).

Loaded length (m)	Lane 1 (kN/m)	Lane 2 Factor	Lane 3 Factor	Lane 4 Factor
250	15.06	0.568	0.320	0.246
470	13.33	0.614	0.360	0.275
705	12.72	0.619	0.378	0.288
1410	8.76	1.000	0.333	0.333
1690	8.76	1.000	0.333	0.333
1940	8.76	1.000	0.333	0.333
2200	8.76	1.000	0.333	0.333

Table 10b: Summary of the Bridge Specific Assessment Live Loading

Loaded length (m)	Lane 1 (kN/m)	Lane 2 Factor	Lane 3 Factor	Lane 4 Factor
250	11.70	1.000	0.333	0.333
470	8.76	1.000	0.333	0.333
705	8.76	1.000	0.333	0.333
1410	8.76	1.000	0.333	0.333
1690	8.76	1.000	0.333	0.333
1940	8.76	1.000	0.333	0.333
2200	8.76	1.000	0.333	0.333

Table 10c: Summary of the Original Design Live Loading

The lanes closer to the footpath are defined as lane 1 and 2, the other two lanes away from the footpath are defined as lane 3 and lane 4.

It has been noticed that from the above Tables for the loaded length of 1410 m or more the BSALL has the same lane 1 value and load factors as the original design loading.

a) Main span loaded with BSALL

A further study has been performed using the Humber Bridge "Bridge Specific Assessment Live Loading (1996)" condition. It is the newly updated loading criterion, which accommodates increasing traffic situations. The central main span has been fully loaded according to this loading condition. As a result, the maximum hanger force of 1.16 MN and the maximum main cable force of 0.196 GN were obtained. The maximum A-Frame vertical tensile force of 2.014 MN and the maximum vertical compressive force of 2.538 MN were found. The maximum vertical deck deflection of 3.216 m was also obtained. These values are well below the design limits as tabulated in Table 10a.

b) BSALL with Wind load and Temperature rise

An extreme load case was studied by using the 3-D box formulation model. In this case the bridge was subjected to a fully loaded condition according to the revised Bridge Specific Assessment of Live Loads (BSALL). In addition to that the design wind velocity of 48 m/s at deck level and 66 m/s at tower top level together with a temperature rise of 10°C were applied. This gave the maximum lateral deflection of 4.353 m, maximum vertical deflection of 1.256 m, maximum deck (top) stress of 0.270 GPa, maximum main cable force of 0.178 GN and maximum hanger force of 0.933 MN. The maximum A-Frame tensile force was found to be 1.961 MN and the maximum compressive force was found to be 5.074 MN. These values were within the design limit (refer table 10a) of 4.510 m for lateral deflection, 4.310 m for vertical deflection, 0.290 GPa for deck stress, 0.210 GN for main cable force, 1.45 MN for hanger force, 9.5 MN for A-Frame tensile force and 8.2 MN for A-Frame compressive force. This on-going traffic situation with high wind speed is highly unlikely.

c) A-Frame forces

In addition to the above predictions, the A-Frame forces were noted under different loading conditions. Schematic layouts of A-Frames on the structure are shown in Figure 10h. The aim is to create the maximum tensile and compressive forces on different A-Frame locations under BSALL condition with the knife-edge loading of 120kN/lane and combined with abnormal HB loading. The HB loading of 1800kN is spread over a length of 10m above one compressed rocker and a 35m length of BSALL load is removed from the deck end. Some suggested load cases and HB load positions (shown in Figure 10i) are selected as of interest to the Humber Bridge Board and these cases are the most likely traffic situation to create the maximum A-Frame forces. The results are compared with the allowable design compressive and tensile values. There are numbers of other load cases including wind and temperature might change the A-Frame forces but those are not considered here.

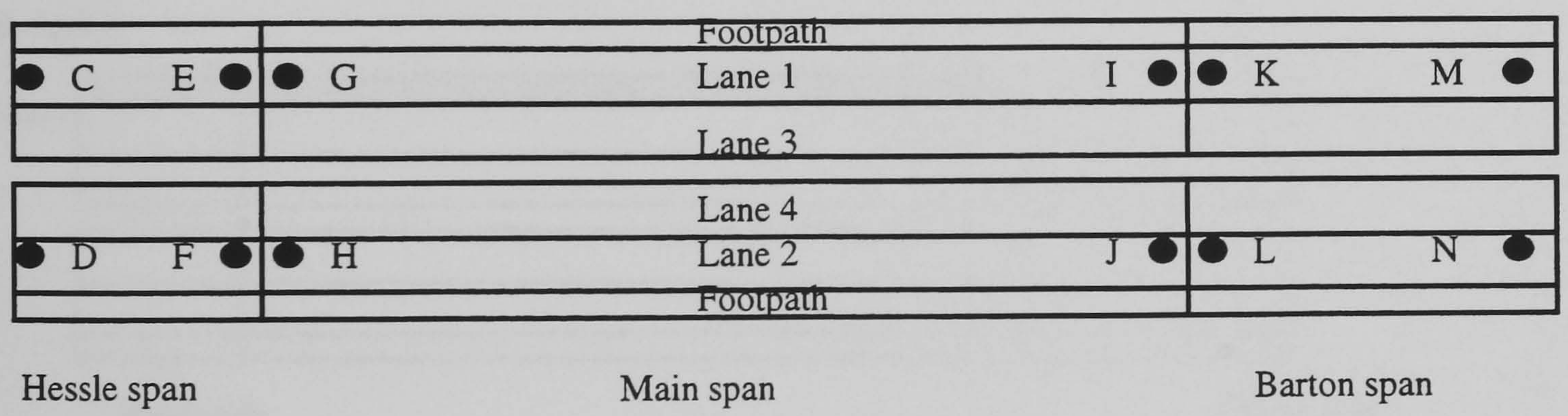

Figure 10h: Schematic layout of A-Frames on the structure

BSALL cases for the A-Frame forces (Figure 10i)

Load case 1

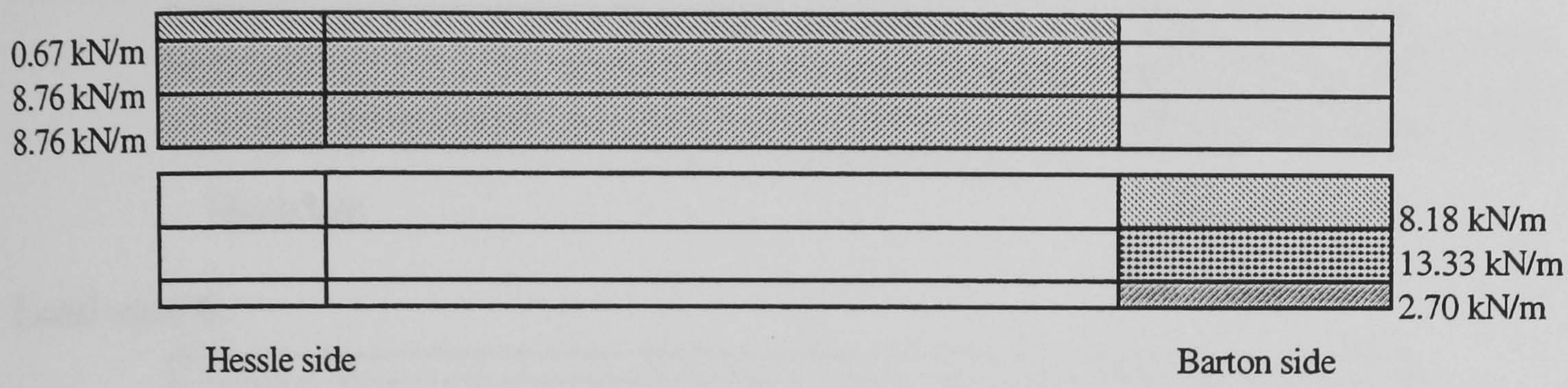

Load case 2

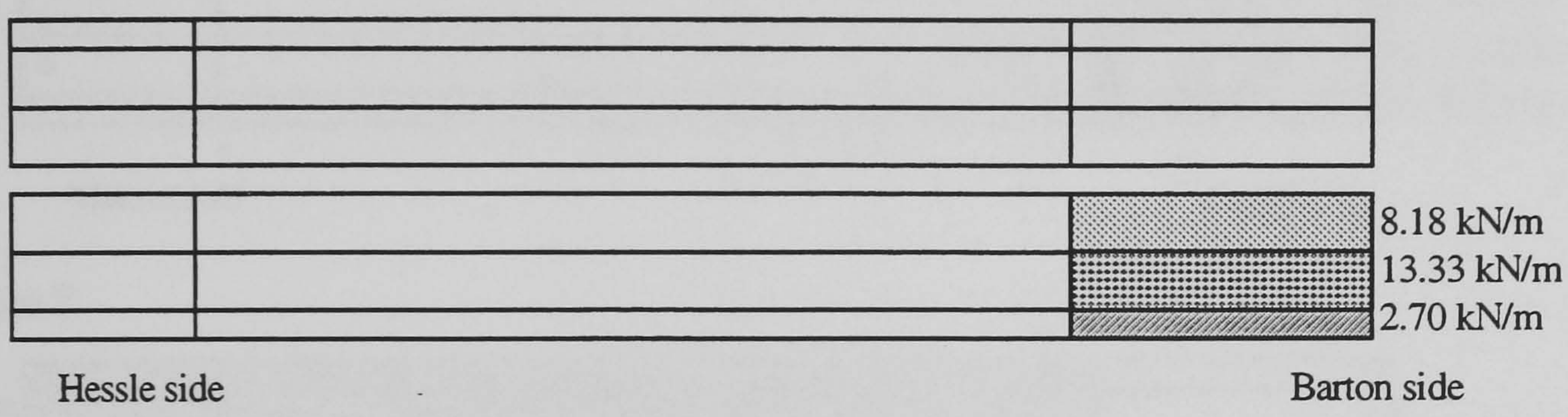

Load case 3

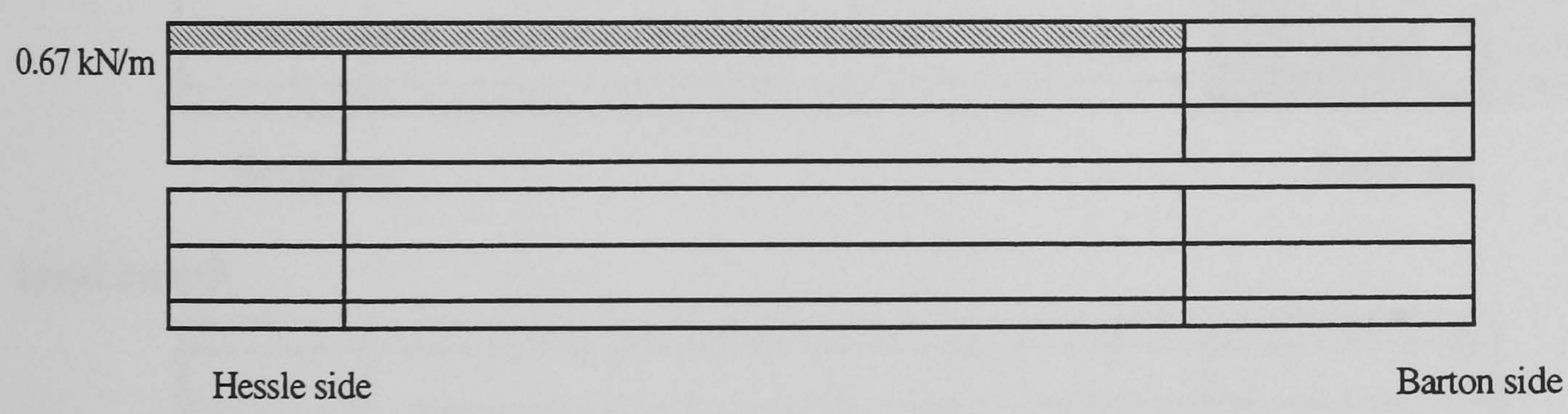

Load case 4

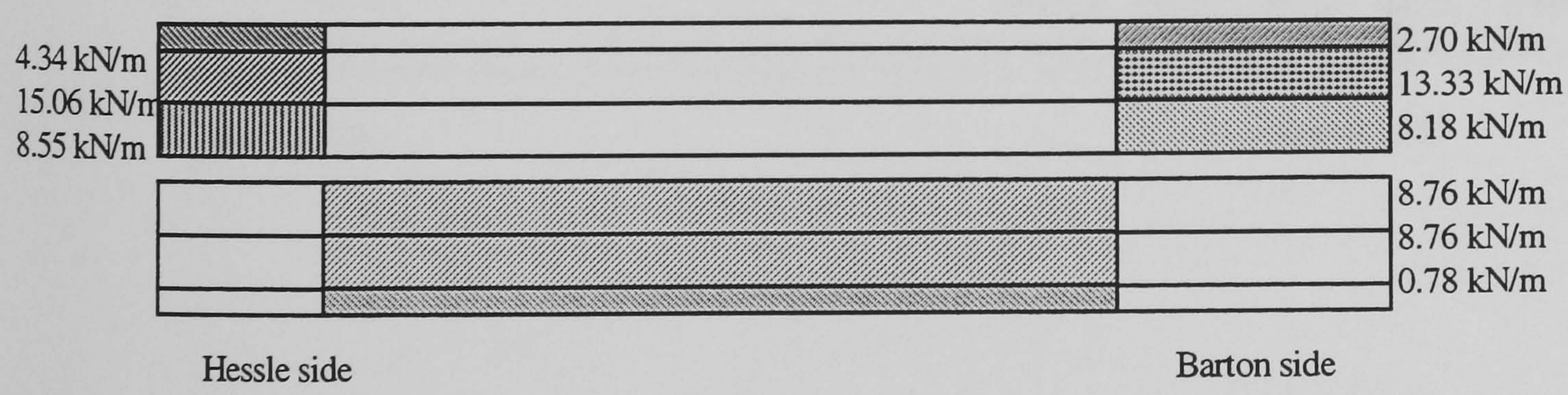

Load case 5

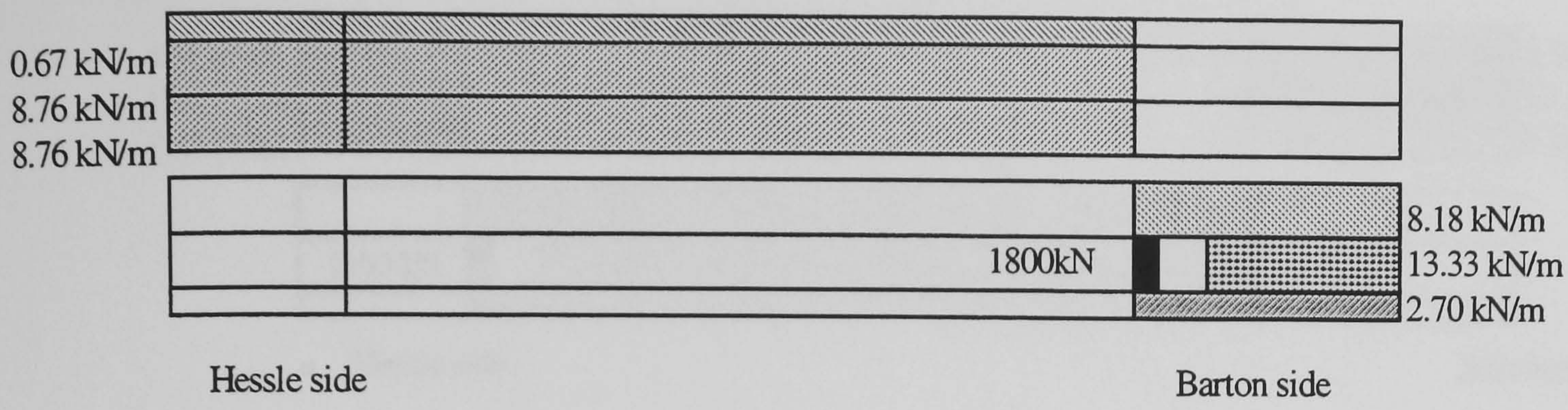

Load case 6

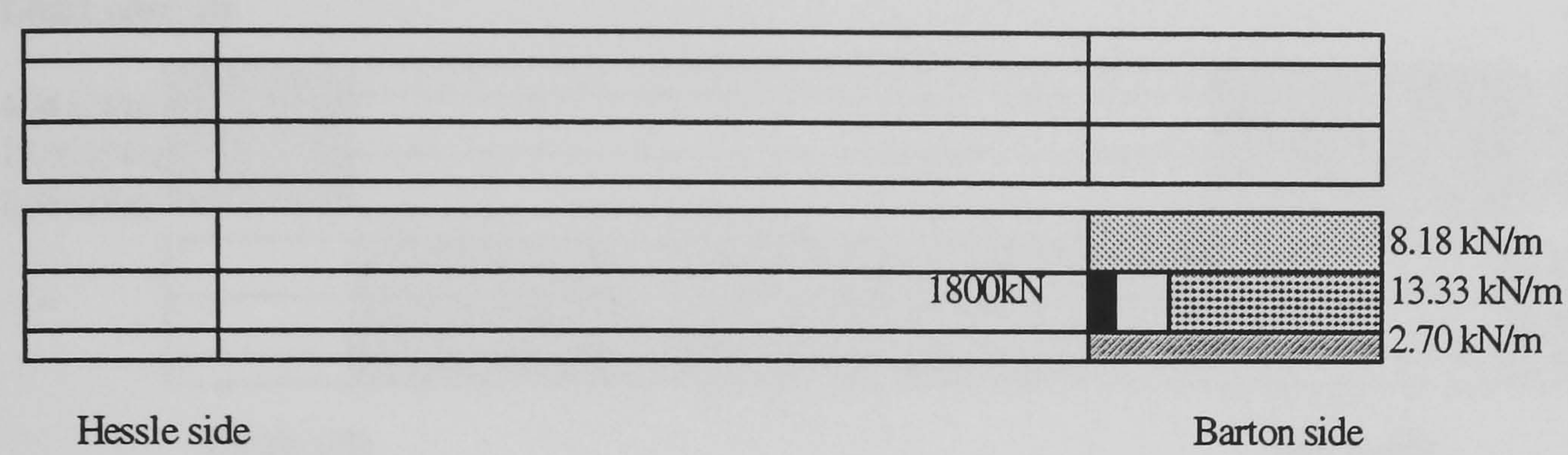

Load case 7

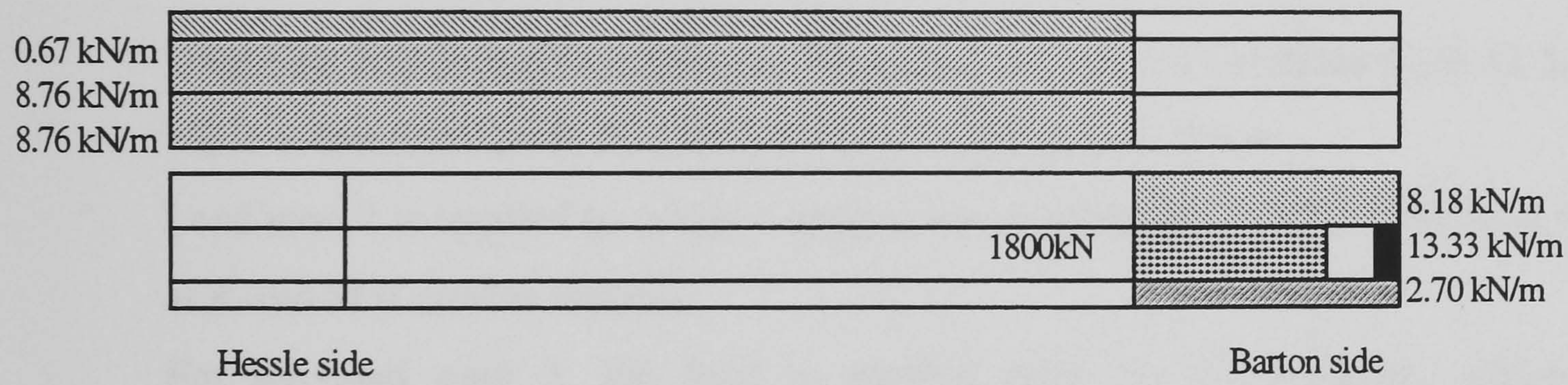

Load case 8

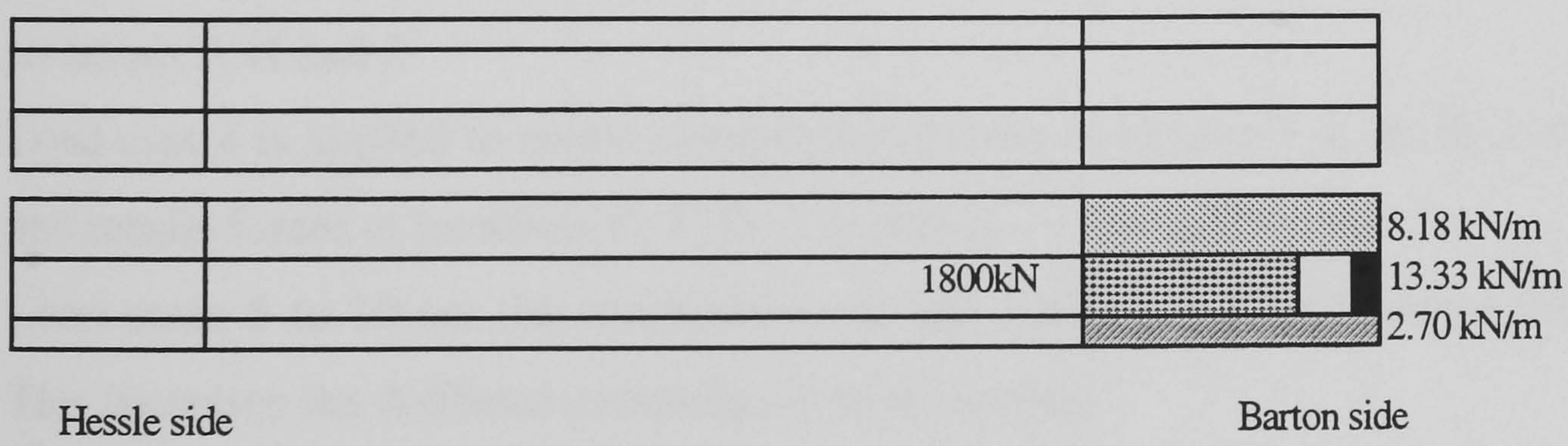

Load case 9

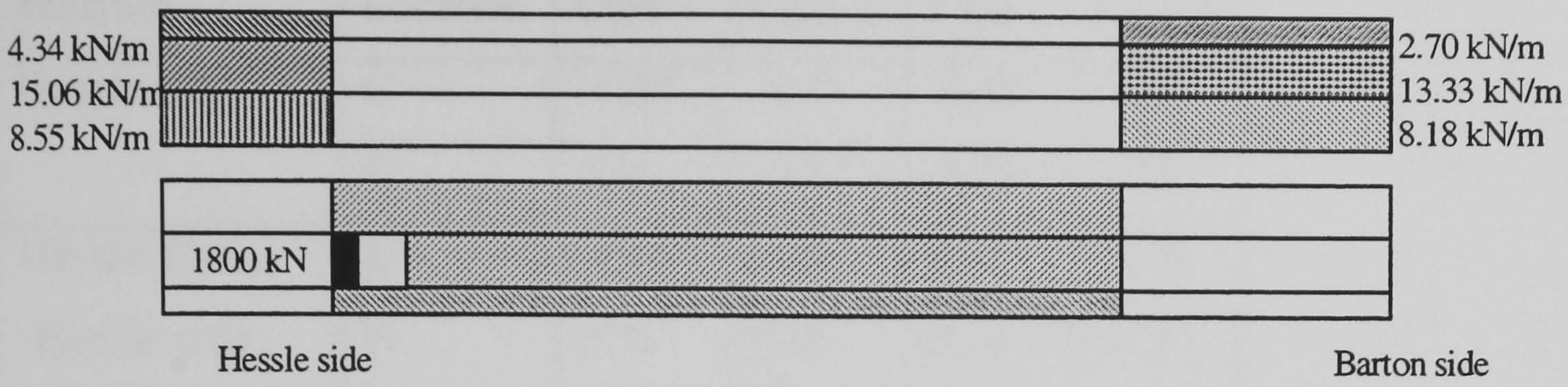

Load case 10

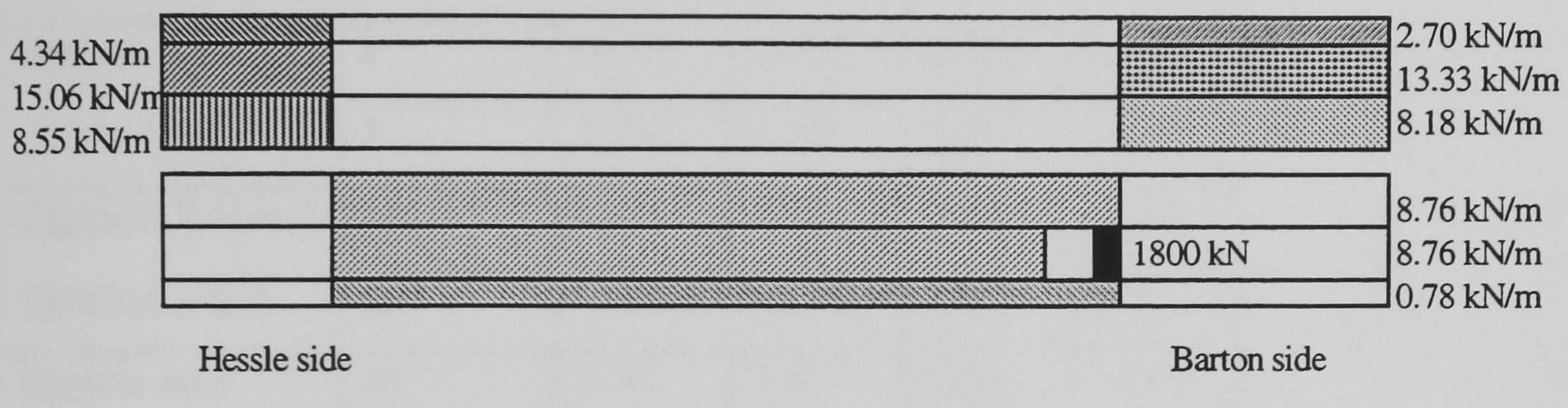

Load case 1 is applied to create the compressive force at locations C, E, G, L N and I while at locations D, F, H, J, K and M it creates tensile force.

Load case 2 is applied to create compression at locations L and N while at locations at K and M it creates tension.

For the load case 3, the load is applied only to the footpath, which creates compressive force at locations C, E, G and I, while it creates tensile force at locations F, H and J.

Load case 4 is applied to create compressive forces at locations C, E, H, J, K and M, and tensile forces at locations D, F, G, I, L and N.

Load cases 5 to 10 are the combination of HB loading with the above load cases. This increases the A-Frame compressive force sharply.

As the 3-D box formulation model accommodates symmetric and asymmetric loading, it has been selected for these predictions. The results are given for load cases 1 to 4 in Table 10d and load cases 5 to 10 are given in Table 10e. Predicted values are well within the allowable vertical compressive force value of 8.2 MN and the allowable vertical tensile force value of 9.5 MN.

Position	Location	Case 1	Case 2	Case 3	Case 4
Hessle End	C	-1.20	-0.23	-0.35	-3.30
	D	0.46	-0.23	-0.21	1.72
Hessle Tower	E	-1.00	0.09	0.01	-2.74
(Hessle side)	F	0.79	0.09	0.14	2.13
Hessle Tower	G	-3.85	0.08	-0.22	3.67
(Main side)	H	3.55	0.18	0.37	-3.96
Barton Tower	I	-4.02	-0.03	-0.22	3.82
(Main side)	J	3.76	0.29	0.39	-4.09
(Barton Tower)	K	3.37	2.70	0.14	-3.89
(Barton side)	L	-3.88	-3.77	0.08	3.38
Barton end	M	3.03	1.89	0.03	-4.42
	N	-4.42	-4.73	-0.04	3.05

Table 10d: Vertical A-Frame member forces (MN) for cases 1 to 4.

Position	Location	Case 5	Case 6	Case 7	Case 8	Case 9	Case 10
Hessle End	C	-1.20	-0.23	-1.20	-0.23	-3.31	-3.31
	D	0.46	-0.23	0.46	-0.23	1.72	1.72
Hessle Tower	E	-1.00	0.09	-1.00	0.09	-2.74	-2.74
(Hessle side)	F	0.79	0.09	0.79	0.09	2.13	2.13
Hessle Tower	G	-3.85	0.07	-3.85	0.07	3.98	3.67
(Main side)	H	3.56	0.17	3.55	0.17	-5.66	-3.97
Barton Tower	I	-4.03	-0.04	-4.03	-0.04	3.83	4.14
(Main side)	J	3.76	0.30	3.76	0.30	-4.09	-5.79
(Barton Tower)	K	3.63	2.95	3.39	2.72	-3.89	-3.89
(Barton side)	L	-5.41	-5.30	-3.90	-3.80	3.38	3.38
Barton end	M	3.05	1.91	3.27	2.16	-4.42	-4.42
	N	-4.45	-4.77	-5.95	-6.30	3.05	3.05

Table 10e: Vertical A-Frame member forces (MN) for cases 5 to 10.

3) Hanger forces

Hanger force variations under different loading conditions including uniformly distributed and point load are plotted (Chapter 11, Figures 11i & 11n). The maximum force on the hanger is observed to be well within the design limit. Some hangers might go slack when the traffic load is applied along with the wind load. This loading is highly unlikely in the real situation as less traffic is on the bridge on a very windy day. The slack hanger condition is possible (Figure 11i on Chapter 11) for the fully span loaded BSALL condition. At a distance of 150 m on both sides from the centre of the main span a minimum hanger force of 12 kN was found. This hanger force value will become zero with the application of wind load. This occurs as the vertical force on the deck due to wind acts downward. It is because the deck has the negative value for the uplifting coefficient so that the pressure acts downward. It is the fluctuation of forces observed on the hanger that leads to investigation of different hanger systems for the suspension bridges. This is extensively discussed in Chapter 11.

4) "What if" Scenarios

The removal of structural components due to vehicle accident on the carriageway, unexpected minor blast, etc. might cause damage to the hanger - deck connection, ending up with the loss of hanger elements. This scenario has been analysed with fully span loaded, HB loading and wind loading conditions.

a) Removal of hanger with BSALL & HB loading

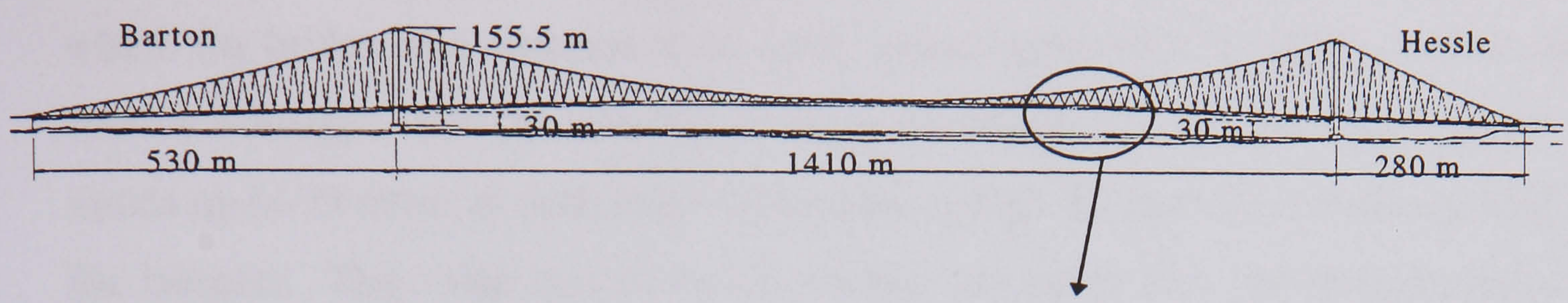

Figure 10j - Bridge Elevation

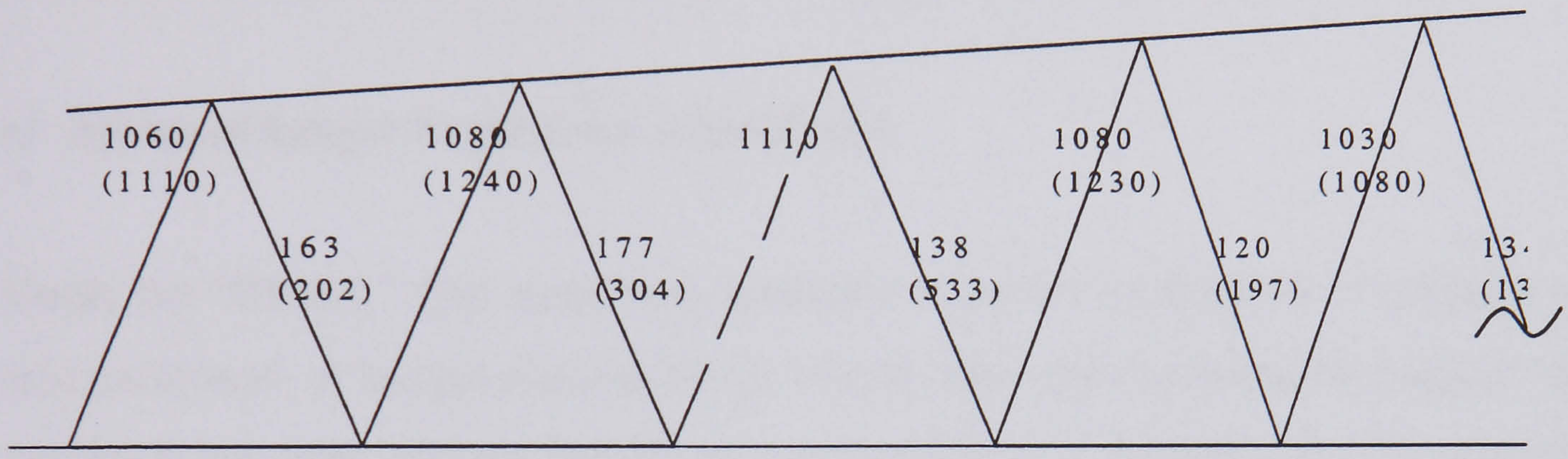

Figure 10k - Hanger Forces (kN) under BSALL and Special Vehicle loading (figures in brackets with Hanger removed)

To get a general view on the loss of a hanger, a hanger element has been chosen at random - not highest or least loaded. Removal of a hanger in the model indicated in Figure 10j leads to the change in hanger forces shown in Figure 10k. Removal of the critical hanger is described in the following section. The loading used has been a case from BSALL - Bridge Specific Assessment Live Loading (used to assess the bridge in line with national UK guidelines), and subsequently a Special Vehicle Load of 180 tonnes. The bridge operator is able to assess the integrity of the structure under possible combinations of maintenance and exceptional load conditions, and in the case shown, the hanger loads remain within design values (1450 kN).

b) Removal of hangers with BSALL & wind load

An alternative example could involve the determination of maximum wind speeds in which the bridge may continue to be used, again combined with BSALL loads and loss of a hanger. For the removal of the same hanger, the bridge may operate in winds up to 33 m/sec at deck level without exceeding the permitted working load in the hangers. This value was found by the trial and error with the consideration of different wind speeds. The full design wind speed is 48m/sec. Other structural elements can be considered in the same way under this, or any other loading.

c) Series of hanger breakdown with BSALL

Under the "BSALL" (full span) load condition, a sudden breakdown of a hanger was also examined. A hanger element on the central main span carrying the biggest force has been removed, and the maximum hanger force of 1.22 MN and the maximum main cable force of 0.196 GN were found. It is important to note that the hanger forces and the main cable forces remain within the allowable design limit.
Additionally the adjacent hanger element 7 m towards the Hessle side which is carrying the biggest force has also been removed. The maximum hanger force of 1.38 MN and the maximum main cable force of 0.196 GN were obtained, and again the hanger forces (allowable 1.45 MN) and the main cable forces (allowable 2.10 GN) were within the allowable design limit. Further removal of hangers leads to a series of failures. At the beginning this starts on the same side then it moves to the other side as well.

5) Other possible uses of models

- The structure can be assessed rapidly in connection with revised loading codes in the future.
- Assessing special or abnormal vehicles can be performed rapidly with revised magnitude of loading.
- Structural assessment after accidents is possible as mentioned above, regarding the loss of hanger or hanger bracket situation.

- Modifications can be made on the model to investigate the viability of maintenance or repair procedures.
- Assisting with the development of traffic management procedures by applying different magnitude of loading at different positions on the deck to find the stresses and make sure that all are well within the allowable limit.
- By introducing appropriate displacement and rotational constraints on the model, can help to assess the stress developed due to foundation movements.
- Vehicle on fire might affect the deck surface. Assessment can be performed on the structure with the modification on the model.

Summary of findings

- Models have been used to assess the structure under different critical loading conditions. Also some specified load cases were created according to Humber Bridge Board's requirement to assess the A-frame capabilities.
- In addition to that the models can be used as a traffic management tool where any maintenance work can be done with greater confidence.
- Removal of hangers was analysed for a number of loading situations. Stability of the structure is ensured with maximum possible removal of hangers.
- The reviewed loading (BSALL) condition has been applied to the bridge model and the structural components have been assessed and the stability of the structure is ensured. There were no slack hangers found under this loading condition.
- The application of 3 tonnes/m load at the main span in a single lane was followed as mentioned in the original design with the BS5400, Part 2 (1978). This work was repeated with the BD 37/88 for bridges introduced by the Department of Transport with the load of 3.4 tonnes/m. The main cable, hanger and A-frame forces were within the allowable design limit, and the deck and the tower top movements were also within the limit. However, a few (ten hanger elements) slack hangers were found at the middle of the main span.
- As in the original design, the wind and temperature loads are applied to the bridge model and the forces and displacements are found. These values are within the limit as expected.

- To assess the A-frame members, specified load cases were applied to get the maximum compressive and tensile forces according to BSALL uniformly distributed loaded condition and combination of BSALL and BD37/88 HB loaded condition. Results are found to be well within the design limit.
- Possible numbers of hanger removals were found with the all span loaded BSALL case. To get a failure envelope, the hanger carrying the maximum force was removed and then the adjacent hanger which carries the maximum force was removed. The results indicate that a maximum of two hangers can be removed anywhere in the bridge structure while still ensuring its safety under the mentioned all span loaded BSALL condition.

Chapter 11

Performance of different hanger systems

General

The hanger configuration is a key feature in the design of long span suspension bridges. Depending on the hanger system the magnitude of the hanger force and the hanger force fluctuations will vary for a particular loading condition. In addition to that, the contribution of stiffness to the deck will also vary (for example due to an inclined hanger system forming a zigzag between the main cable and the deck), so it is necessary to identify the different hanger patterns and their advantages and disadvantages.

To do these exercises the validated existing (inclined hanger system) model has been used. Instead of the existing inclined hanger system different hanger patterns are introduced to the validated model and the changes in structural performance have been noted.

This parametric study has been performed with five different hanger systems (including the existing one).

Due to a moving load, the existing hanger system Figure 11a has a high fluctuation of force at any hanger. Thus it is interesting to analyse the cause for the fluctuation and to find an alternative hanger system arrangement to avoid the variation of forces.

Out of these four different hanger systems (described below), Figure 11e can be introduced easily with small modification from the existing system. This can be done by the introduction of a link between the hangers from the adjacent brackets. Also this system is comparatively more cost effective than the other systems in terms of material and man-days.

Background

Three long span suspension bridges, Severn (1966), Bosporus (1973) and Humber (1981) have an inclined hanger system arrangement. Earlier suspension bridges have always used vertical hanger systems. The erection procedure highlights the major difference between conventional vertical hangers and inclined hanger bridges.

The inclined hanger system gives an increased hanger material requirement and a more complicated construction procedure, as instead of one vertical hanger element at a junction two inclined hangers have to be used. The increase in hanger material, which would be required for an inclined hanger system, can be up to 200% when compared with a vertical hanger system. Since the cost of the hangers for a suspension bridge is only a small percentage of the total cost, this increment may not be critical.

A stated advantage (Homberg, 1982) of inclined hangers is that the stiffness of the deck can be reduced, and hence this reduces the dead load. Consequently, this reduces the main cable force and results in a smaller cross sectional area of the main cable. This could also result in more slender towers and reduction in anchorage chambers.

The Severn Suspension Bridge hangers were showing signs of distress after eight years of their lifetime (Miller, 1988). Broken wires in the hanger ropes were found normal to the longitudinal plane (along the cross sectional direction). Slackening of particular hangers led to localised bending which was suggested for their failure.

The Humber Bridge system has performed very well since its opening. There has been no change in the hangers or broken wires in the whole hanger system. The change in hanger force at hangers due to its zigzag form was found to be common on suspension bridges having inclined hanger systems.

Introduction

Bridges have been subject to increasing traffic densities in recent years. For example the Severn Bridge design was based on BS 153, Part 3A (1954), and under fully span loaded condition (according to BS 5400, Part 2 (1978)), slackening of some hangers was observed.

A 50 % increase in load intensity was the reason. These increases of load intensity increase the tension in one hanger and decrease the tension within the other hanger on the same hanger bracket; a further increment of load results in slack of one hanger and high tension in the other hanger on the same hanger bracket.

The Humber Bridge design was based on the BS 153, Part 3A (1954) loading system. A traffic survey was carried out by Fairhurst and Partners to assess the present traffic loading situation. This traffic calculation was presented as the Bridge Specific Assessment Live Loading (BSALL) for the Humber Bridge. Under the BSALL fully span loaded condition there were no slack hangers found. The reason was that there is no change in the BSALL value from the original design value for the loaded length of 1410 m or more. There were no slack hangers found at the time of design check of the bridge under the BS 5400, Part 2 (1978) loading condition (according to Humber Bridge Design Report).

Obviously reducing the hanger force difference between adjacent hangers under dead or uniformly distributed load condition and maintaining a steady hanger force on a hanger with moving live load will ensure the long survival of hangers. Of course changing magnitude (where it is going up and down from its initial dead load value) of the hanger forces due to vehicular movement causes a long term fatigue problem on the hangers and the hanger brackets, although the maximum hanger force is well below the allowable design value.

Configuration of hangers

Fluctuation (change) of hanger force is found on suspension bridges having inclined hanger systems. The live load will invariably cause greater deck and main cable curvature in the region directly above the applied load. The increased tension in the main cable will tend to straighten it out in the region above the deck where there is no live load. This will cause significant horizontal and vertical relative movements of both the deck and the main cable. These vertical movements tend to be dominant in the determination of the specific distribution of forces in the inclined hanger system. In practice some hangers attract more than their share of additional load relative to adjacent hangers, and this causes uneven distribution of forces in the system. The worst situation, slackening of inclined hangers, is caused by the relative longitudinal movement between the points of connection of the hangers with the main cable and the deck.

Introduction of different hanger system styles

The following hanger system models shown in Figures 11a to 11e are selected for the parametric study. Figure 11a is the existing hanger system model and Figure 11b is the vertical hanger system model. Figure 11c and 11d are the combination of vertical and inclined hanger systems. Figure 11e is the combination of the existing hanger system with a horizontal link connecting two hangers from the adjacent hanger brackets. Figure 11a1 to 11e1 shows the dimension of the bridge, hanger spacing and hanger lengths. All these models have the same hanger cross sectional area and the same hanger initial strain value as the existing model. These models are compared with each other under dynamic and different static loading conditions. The following conditions are considered;

a) Hanger force distribution along all three spans of the bridge under uniformly distributed load; dead, BSALL and wind loading conditions are observed.

b) Similarly for the moving quasi-static point load condition, mid hanger (from middle of span) is selected from each span and the hanger force variation is observed.

c) For the same moving quasi-static point load condition, mid and quarter position of the deck vertical displacement has been observed.

d) Free vibration (modal or no external means of force) analysis has been performed to compare the vertical, lateral and torsional natural frequency values among different hanger system patterns.

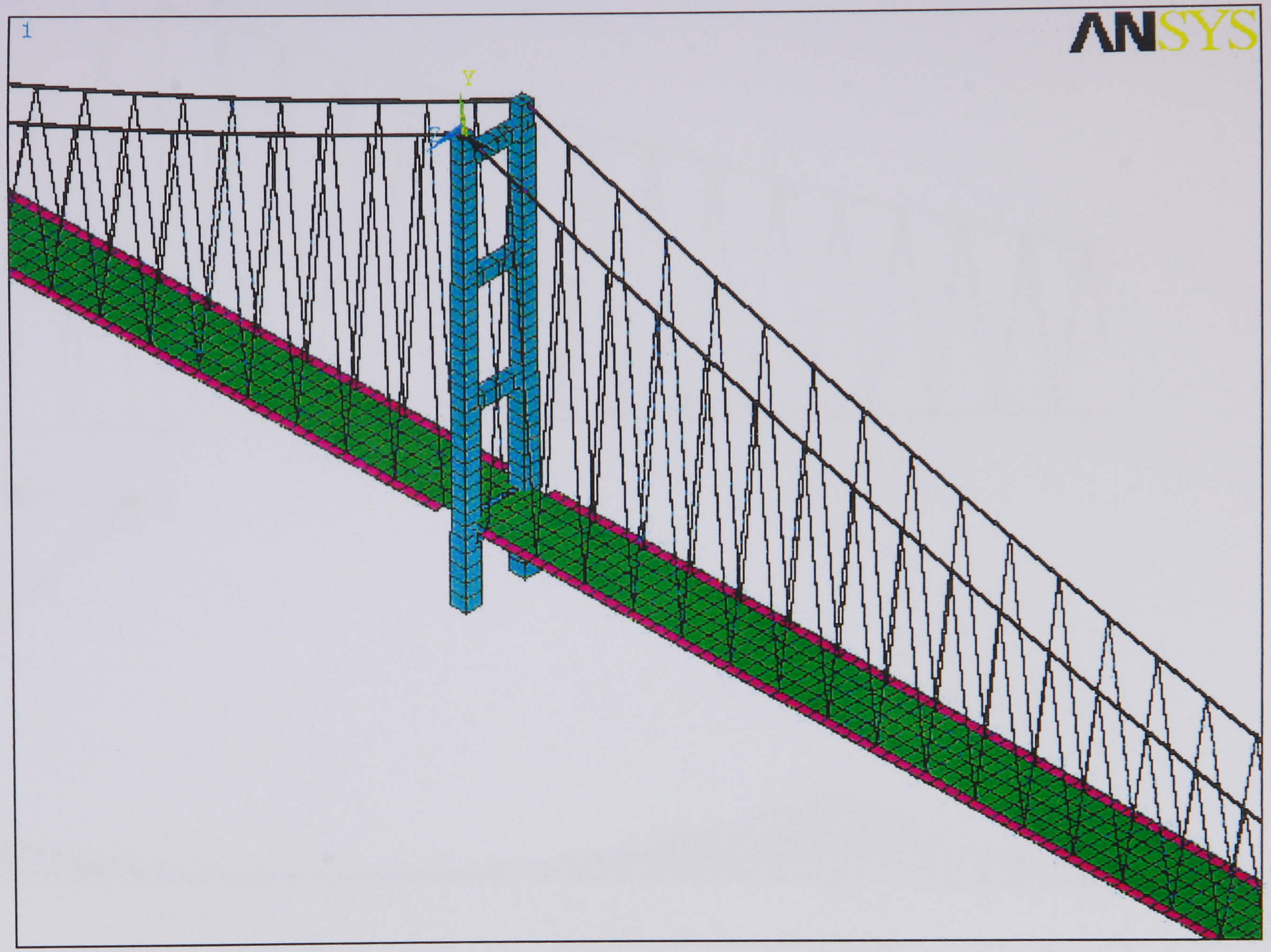

Figure 11a: Existing hanger system

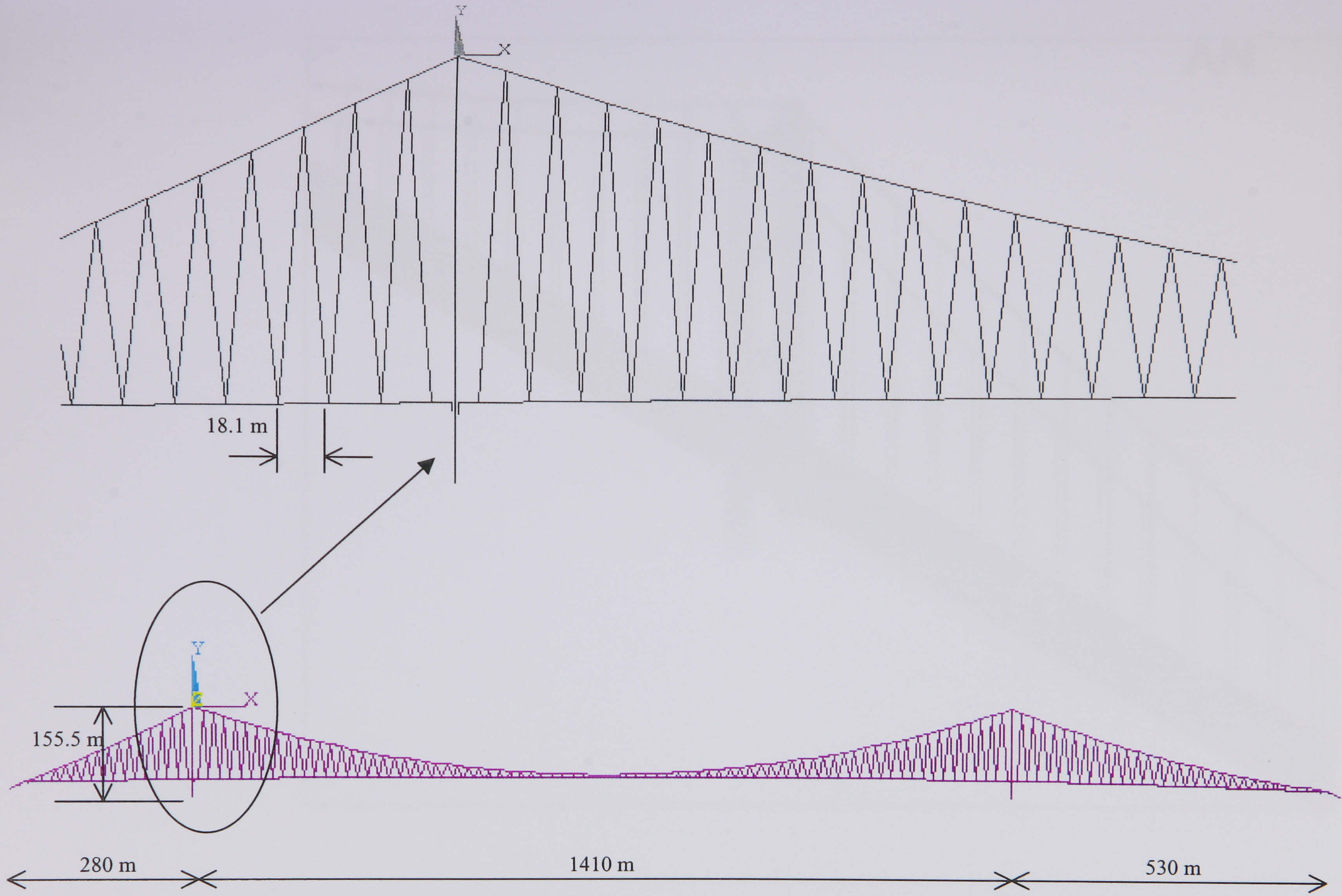

Figure 11a1: Dimension of the Existing hanger system

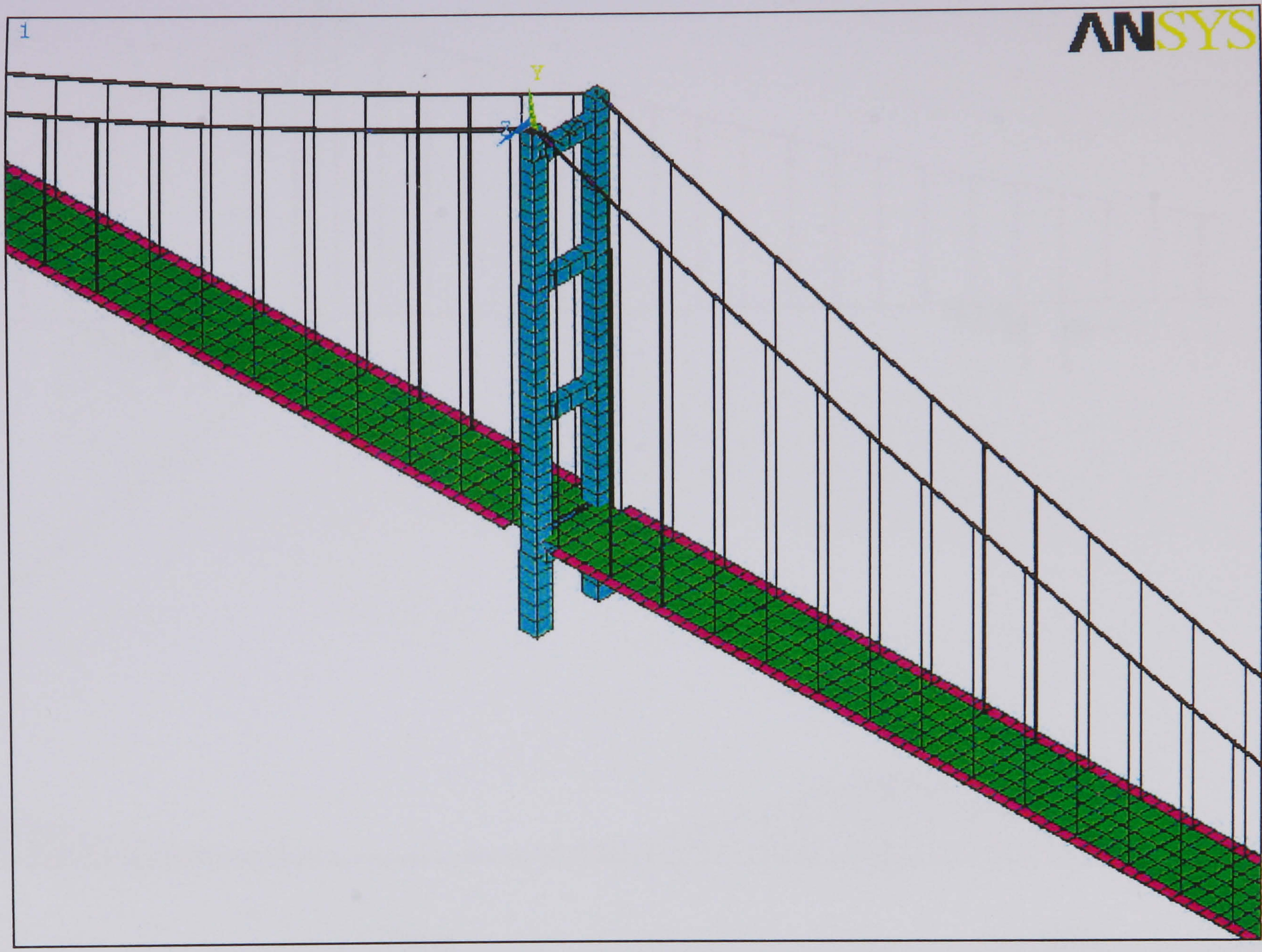

Figure 11b: Vertical hanger system

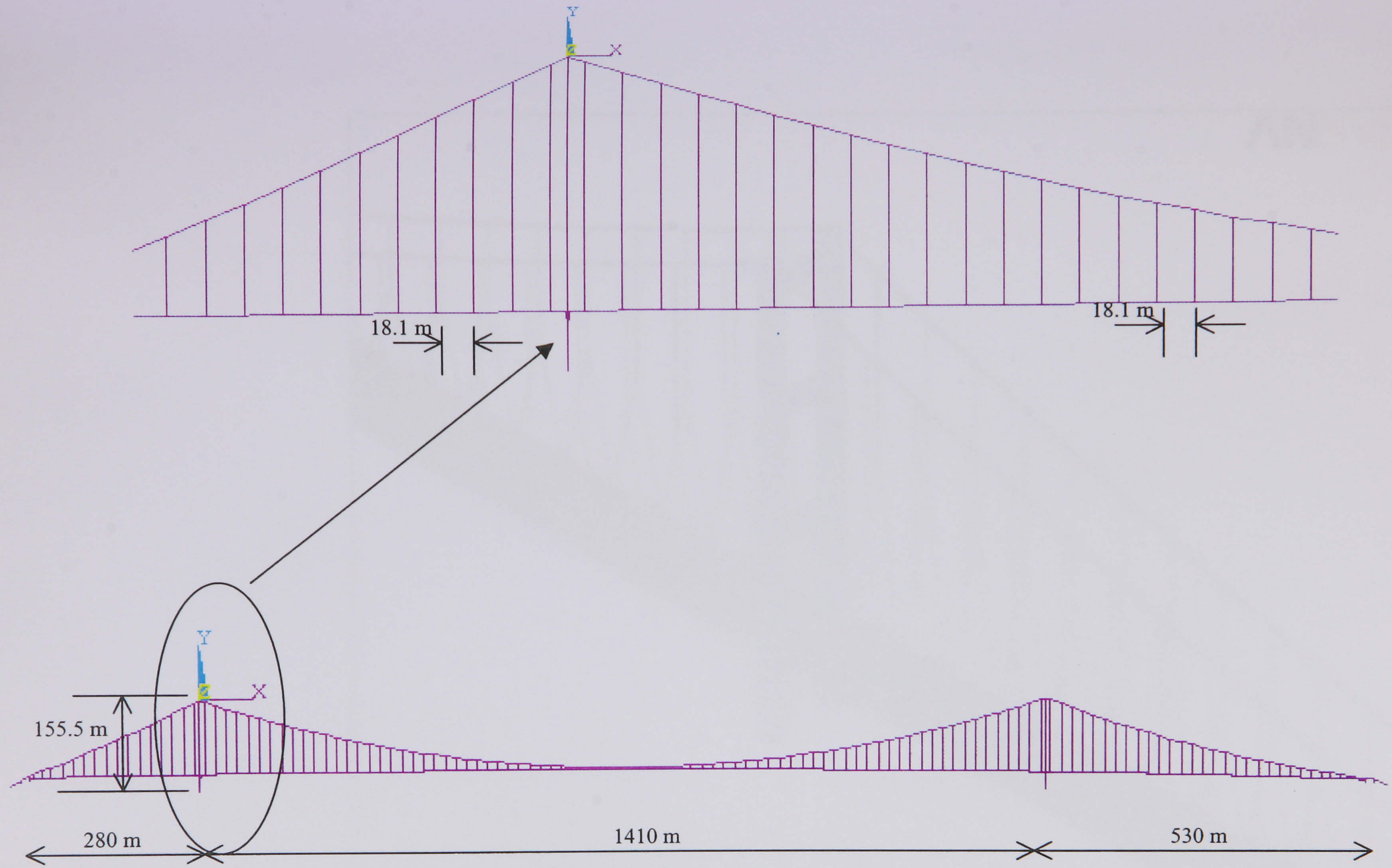

Figure 11b1: Dimension of the Vertical hanger system

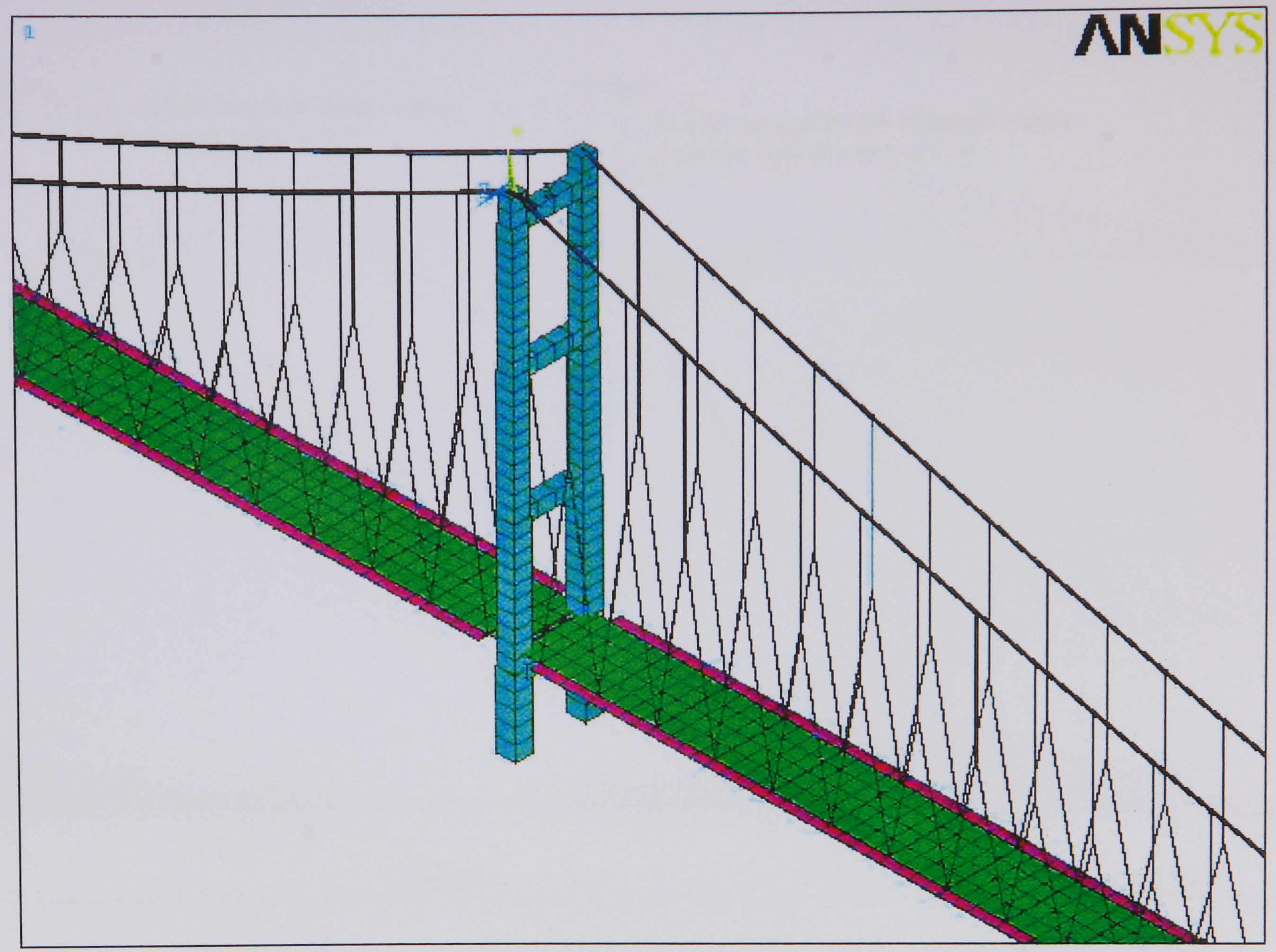

Figure 11c: Mod 1 hanger system

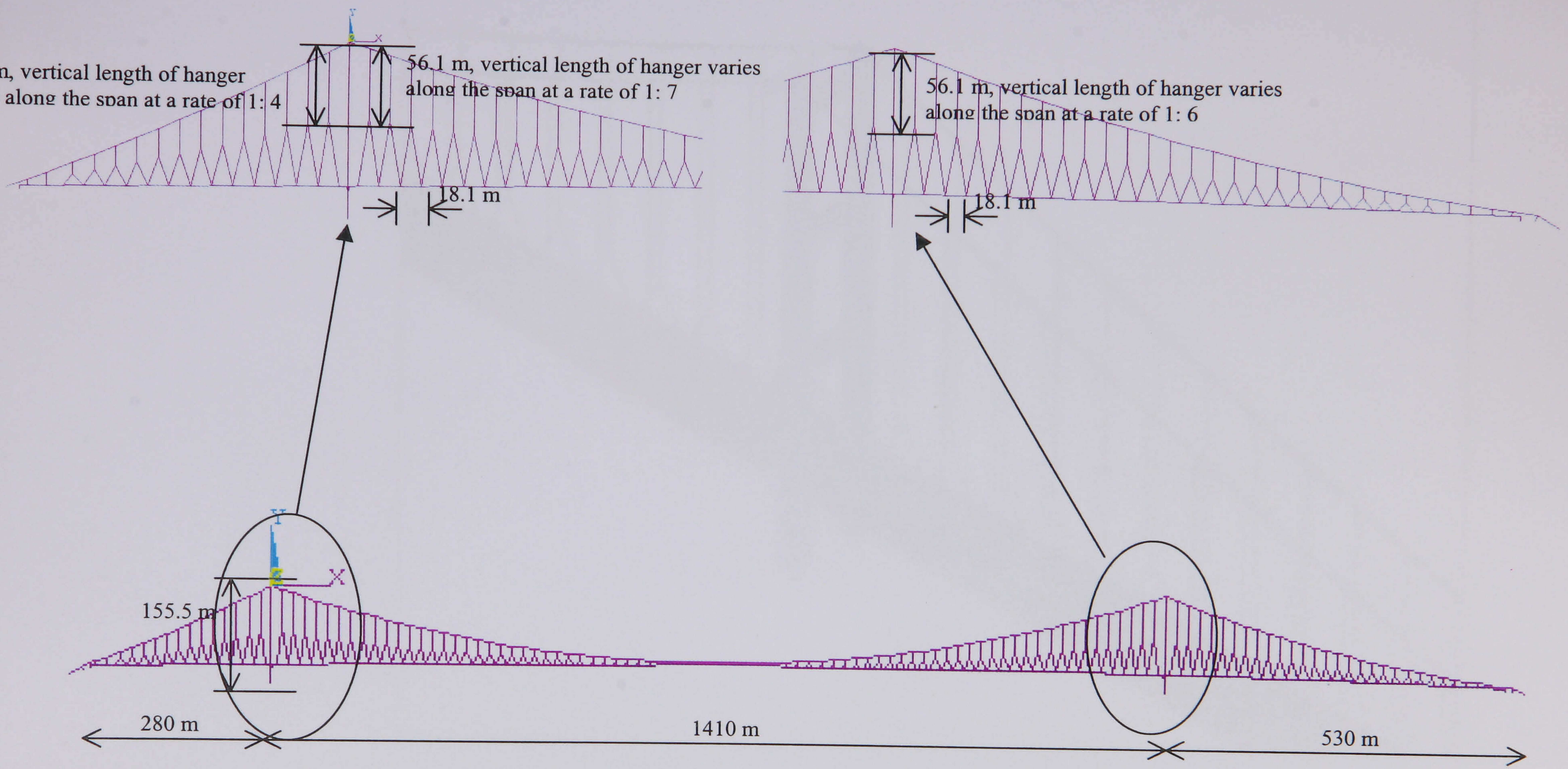

Figure 11c1: Dimension for the Mod 1 hanger system

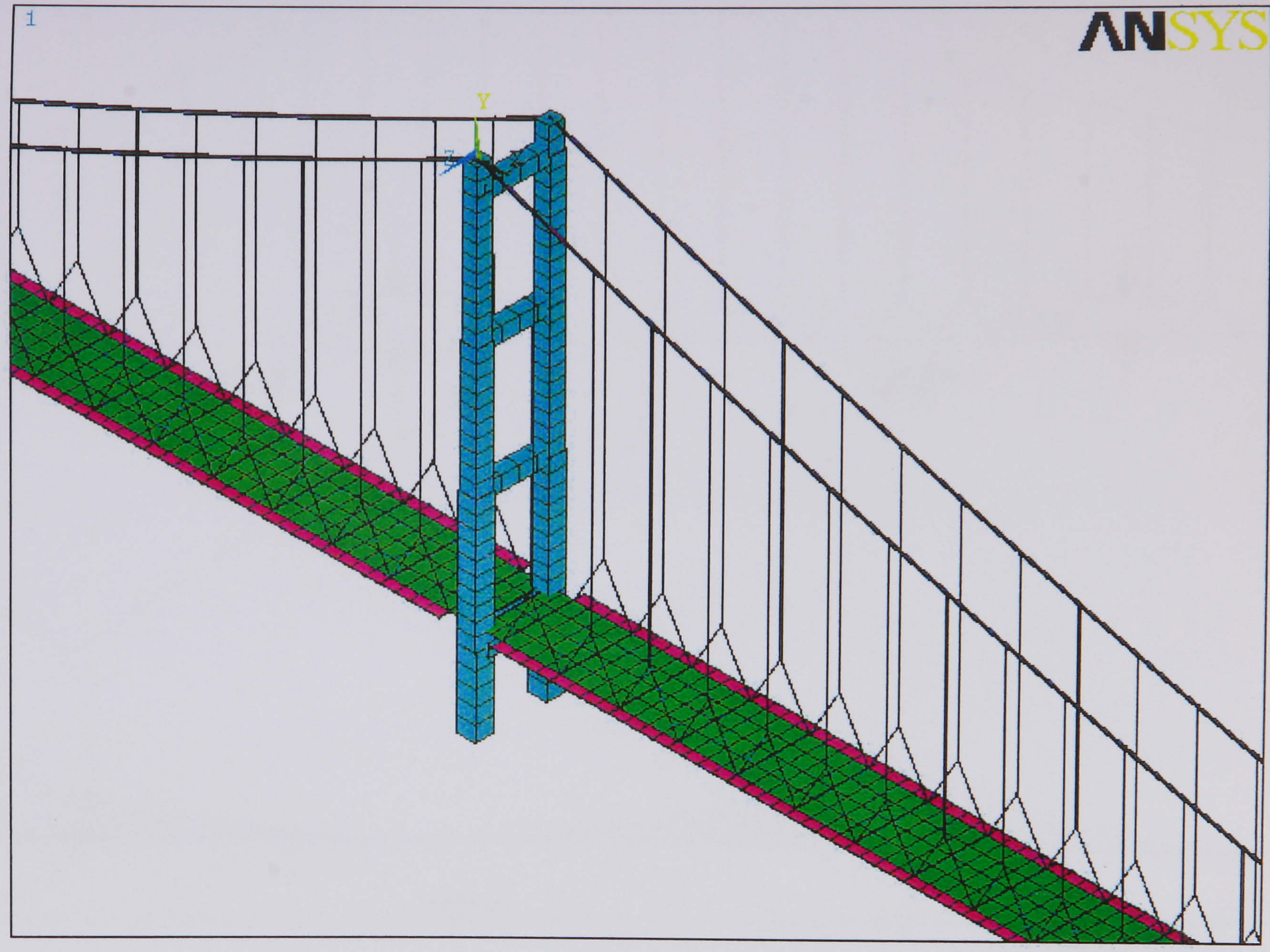

Figure 11d: Mod 2 hanger system

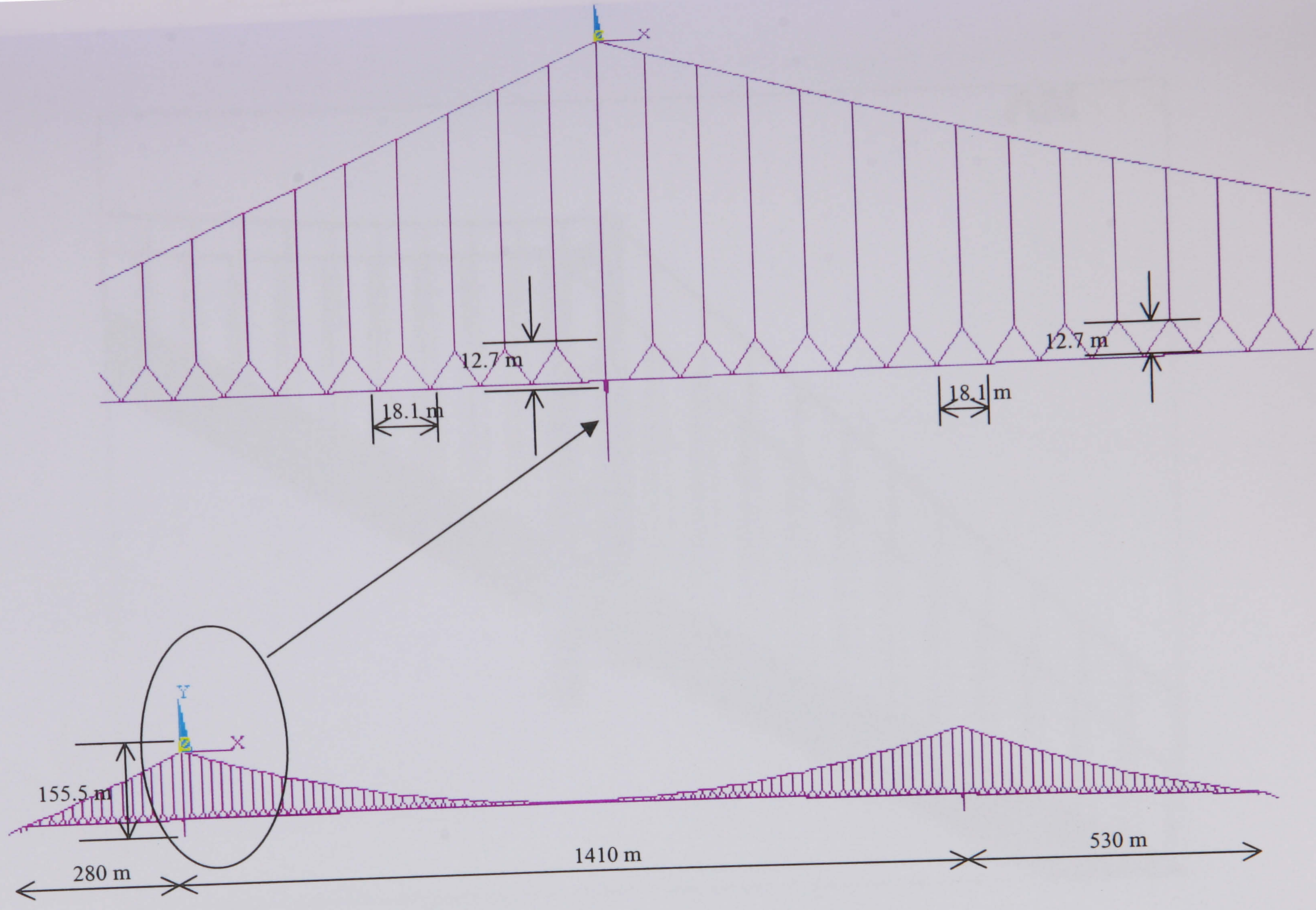

Figure 11d1: Dimension of the Mod 2 hanger system

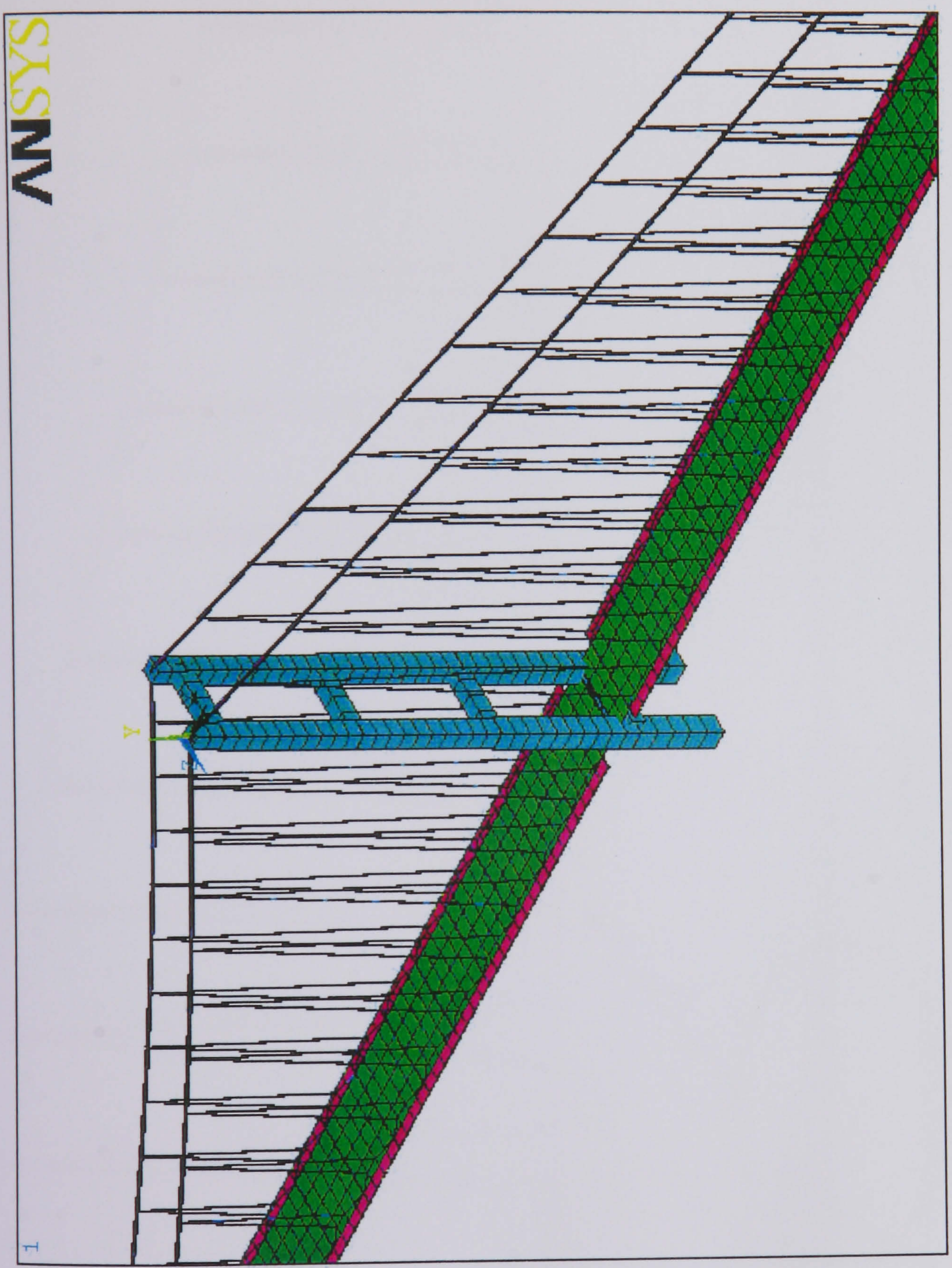

Figure 11e: Mod 3 hanger system

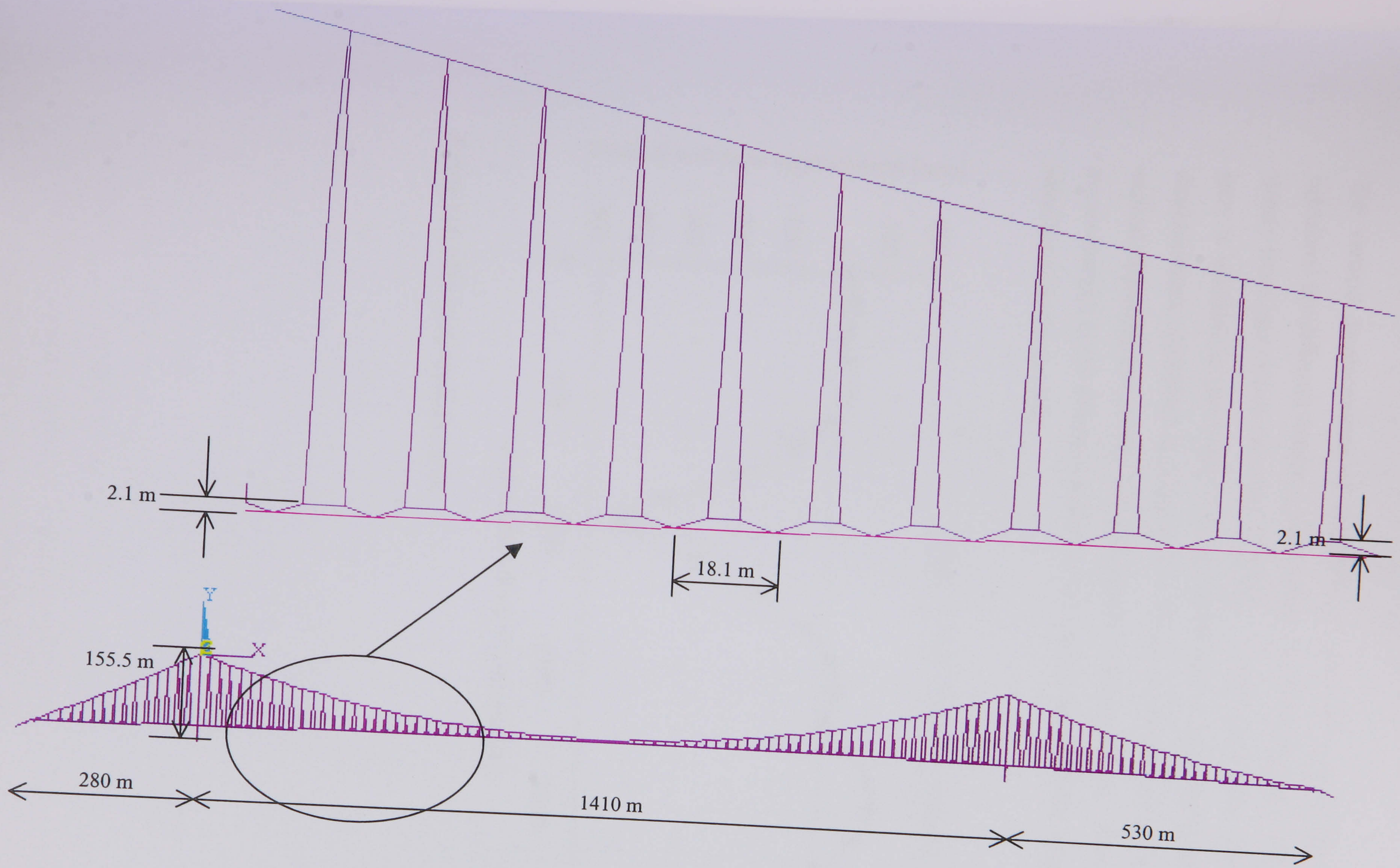

Figure 11e1: Dimension of the Mod 3 hanger system

Comparison of mid and quarter span vertical displacements

The vertical displacements of the deck at mid and quarter span positions were calculated for different hanger system under the condition of a 120t vehicle moving slowly from one end to the other (Figures 11f and 11g). The above weight of the lorry is selected as previously for the validation at mid and quarter span vertical displacements, described in Chapter 9. There is no significant change found in vertical displacements among different hanger system patterns. This is because there are no changes in the effective hanger cross section area and the hanger initial strain value between the models.

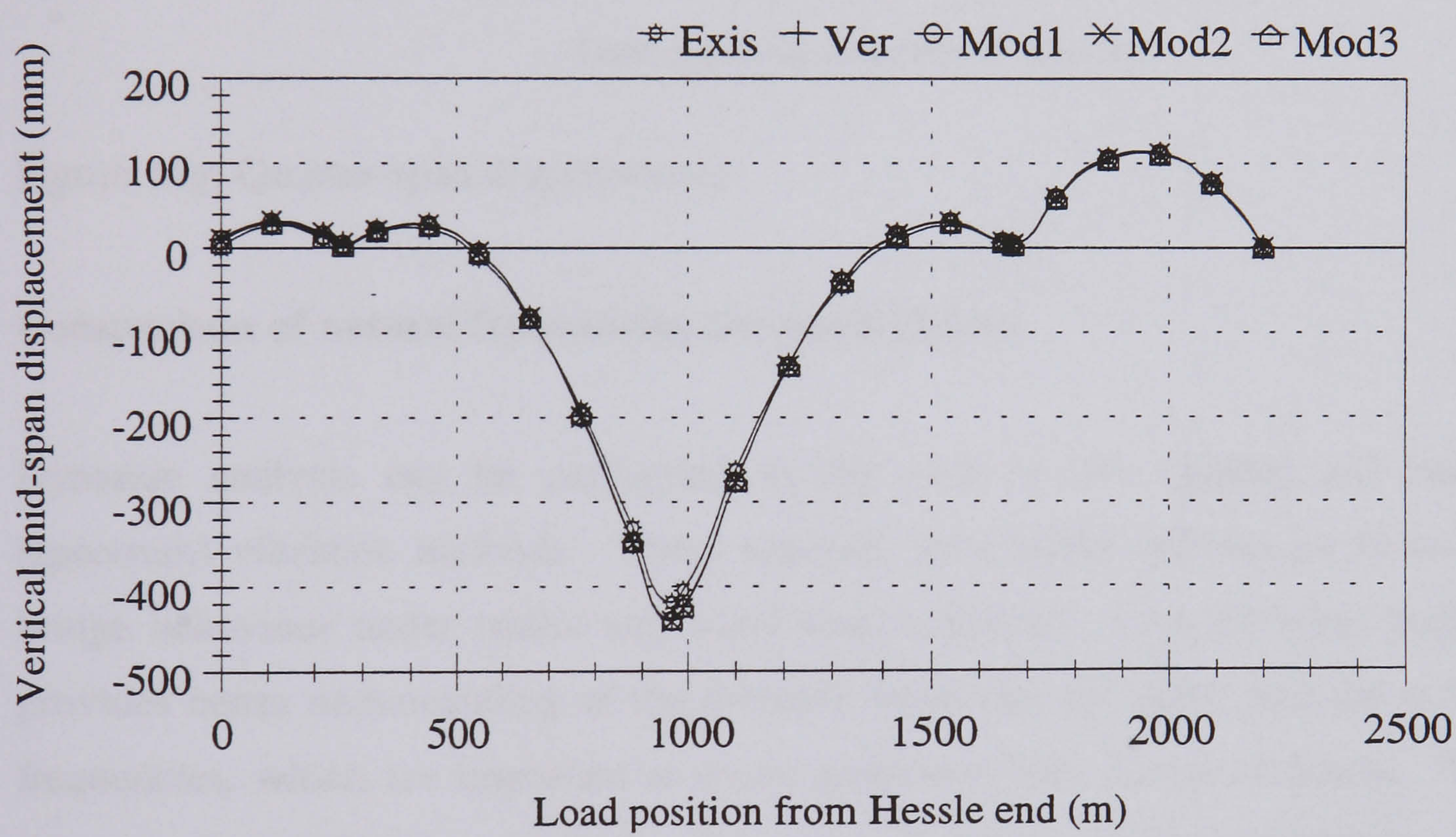

Figure 11f: Mid-span displacements

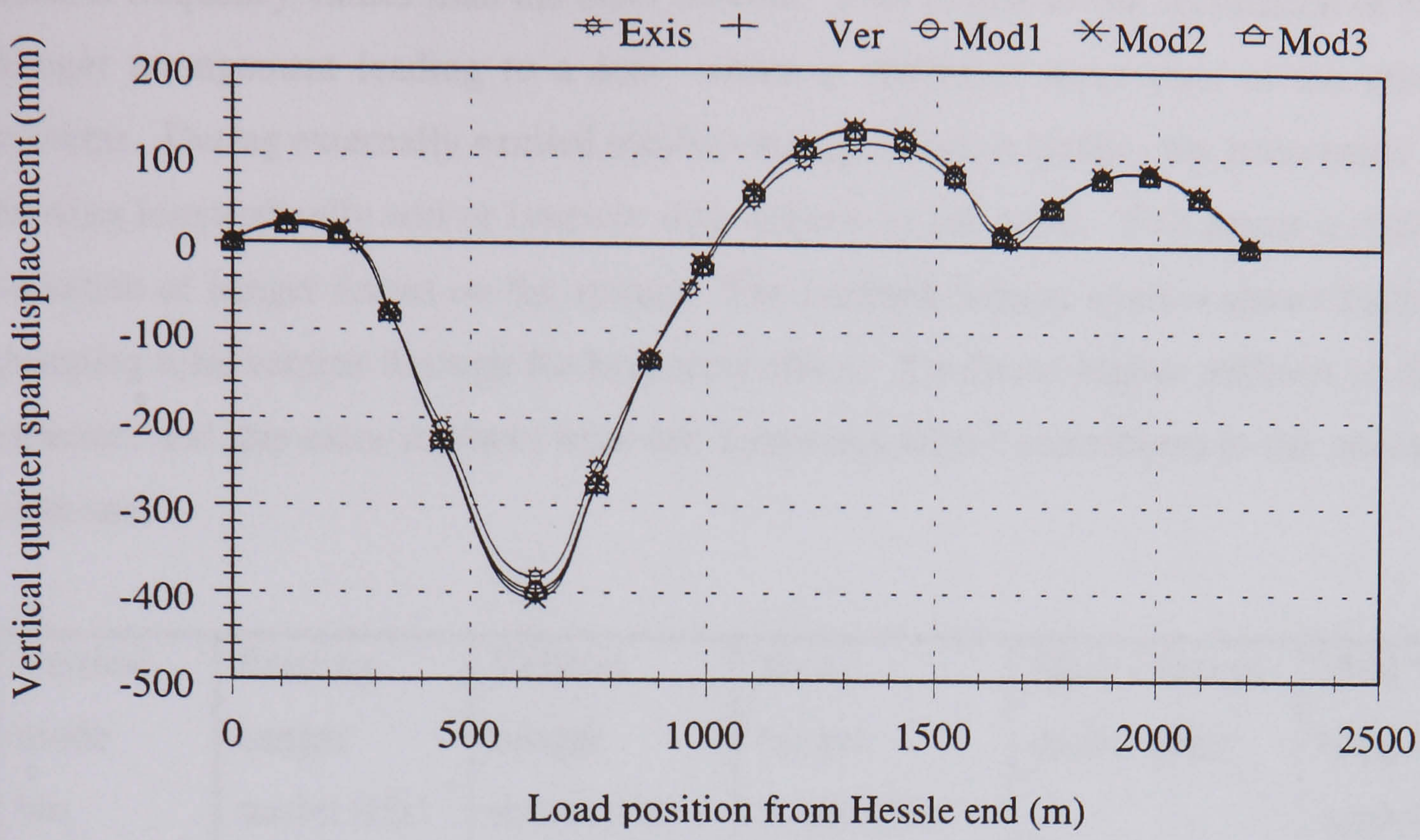

Figure 11g: Quarter-span displacements

Comparison of natural frequencies and mode shapes

Dynamic analysis can be performed in the form of free (modal) and forced (spectrum) vibration methods. These analyses yield useful information about the bridge behaviour under traffic and wind load conditions. Free vibration analysis provides better understanding of the dynamic behaviour and determines the natural frequencies, which are important to avoid resonance from forced excitation. This resonance magnifies the amplitude of the forced vibration of the components. The magnification is heavily dependent on the damping, but an understanding of natural frequency values will avoid any possible resonance on the structure. Force vibration could be due to dynamic loads including earthquake loads, wind loads, wave loads, blast loads etc. These are commonly defined in the form of a time history or a response spectrum. This dynamic response is characterised by amplitude, a deflected mode shape, a resonant frequency and damping associated with the structure. The response to these loads is calculated in terms of displacements, velocities and accelerations and these are subsequently used to derive strains, and then finally provide forces and moments for the assessment of the structure.

In this research natural frequencies and mode shapes of the different models are compared and given in Table 11a. The existing inclined hanger system has higher natural frequency values than the other models. This is due to the inclination of the hanger arrangement leading to a deck, which is stiffened more than in the other systems. During externally excited oscillation (e.g. wind or traffic) the main cable is moving longitudinally and/or laterally with respect to the deck. This forms a cyclic variation of hanger forces on the system. The inclined hanger system shows higher damping achievement through the hysteresis effect. It reflects higher stiffness to the structure and this extra stiffness from this hysteresis effect contributes to the overall structure.

Vertical mode No.	Existing hanger model (Hz)	Vertical hanger model (Hz)	Mod 1 hanger model (Hz)	Mod 2 hanger model (Hz)	Mod 3 hanger model (Hz)
1	0.107	0.099	0.097	0.087	0.100
2	0.113	0.107	0.107	0.090	0.107
3	0.164	0.153	0.136	0.139	0.154
4	0.202	0.176	0.156	0.155	0.190
5	0.236	0.195	0.192	0.188	0.216
6	0.304	0.216	0.216	0.221	0.230
7	0.306	0.276	0.276	0.273	0.276
Lateral mode No.					
1	0.055	0.054	0.053	.0605	0.061
2	0.129	0.126	0.122	0.115	-
3	0.198	-	0.190	0.180	0.141
4	0.217	0.229	0.195	0.193	0.216
5	0.218	0.231	0.200	0.215	0.217
6	0.246	0.241	0.234	0.225	0.225
7	0.249	0.242	0.243	0.258	0.259
Torsional mode No					
1	0.303	0.296	0.298	0.299	0.299

Table 11a: Natural frequency values for different models

Comparison of main cable forces

The main cables are loaded mainly due to the self-weight of the bridge. The fluctuation of main cable forces due to traffic does not exceed 15.6 %. Introducing a different hanger system pattern will not significantly change the main cable forces. For completeness Figure 11h shows the magnitude of main cable force under self-weight condition along the longitudinal length of the bridge. This is applicable for all hanger configurations.

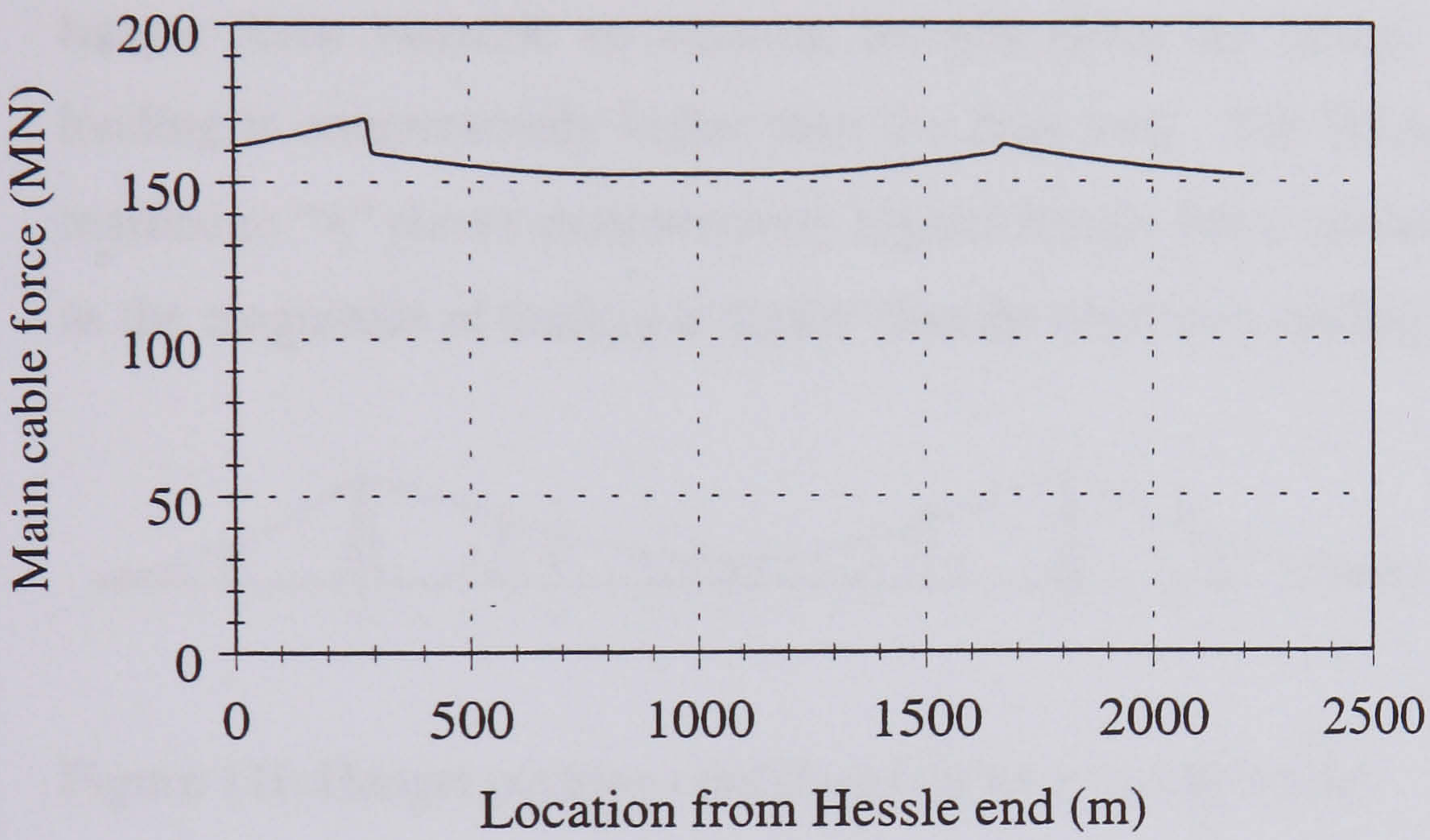

Figure 11h: Main cable force variation along the bridge under self-weight condition

Comparison of hanger forces under uniformly distributed load condition

In suspension bridges, hangers are subjected to a greater percentage of load fluctuations (changes) than the main cable. Hanger forces on each model were compared separately under dead, BSALL load and wind load condition. Results are presented in graphical form in Figures 11i – 11m. The uniformly distributed load condition BSALL, which is the worst case among the three systems, is used. The existing inclined system gave a higher force variation of 11 kN and 1110 kN among adjacent hanger brackets, (refer Figure 11i).

i) Existing inclined hanger system

Three loading conditions dead, BSALL load and design wind loading were used to understand the variation of hanger forces under uniformly distributed loading. To carry out this process four hanger positions were selected as shown below in Figure 11i. The dead load condition marked in "•" shows (below in Figure 11i1) how the hanger force on adjacent hangers (e.g. position 1-2 and 3-4) varies approximately 550 m in the middle span. The wind loading condition marked in "°" shows the hanger force variation on adjacent hangers along the bridge as the magnitude of loading is comparatively higher than the dead load. The BSALL loading condition marked in "×" shows comparatively highest hanger force variation (described below) as the magnitude of loading is higher than the other two loading.

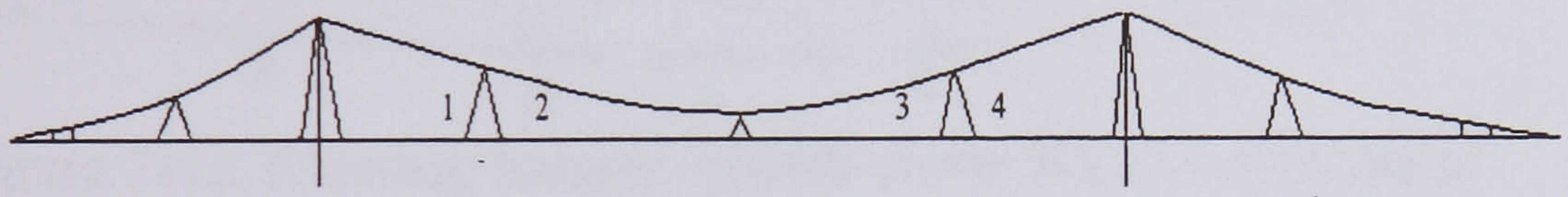

Figure 11i: Hanger position considered on the existing model

The Figure 11i1 shows the hanger position for the graph on Figure 11i. The hanger position 2 and 3 strained more and carries higher tensile force (maximum 100 times) than the hanger position 1 and 4 under BSALL condition.

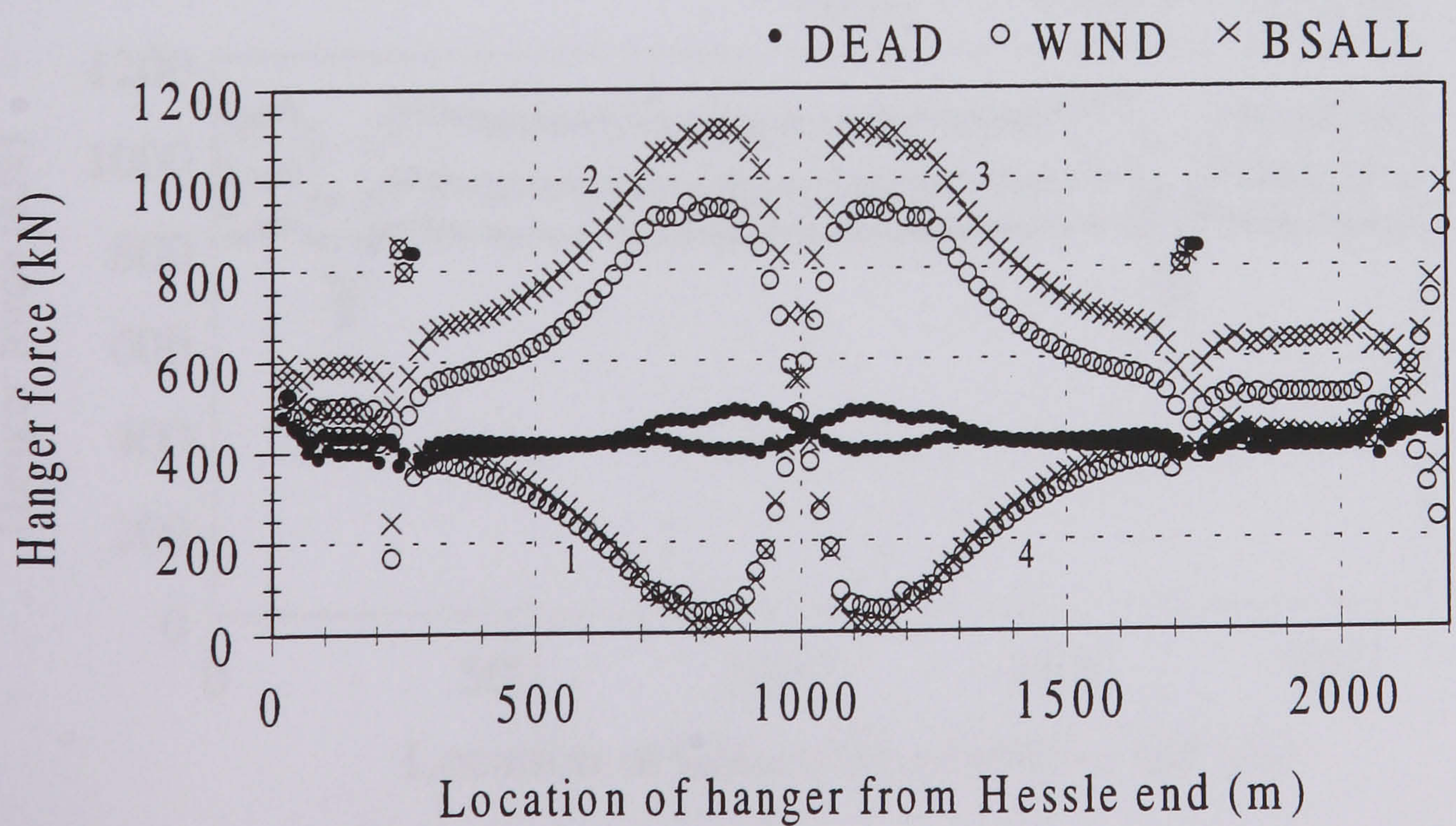

Figure 11i1: Hanger forces on the existing hanger system model

As shown in Figure 11i2, hangers (AC and DE) towards the mid of main span (at O) are strained more than the hangers away from the mid span (AB and DF) under BSALL uniformly distributed loading condition. Considering the hangers from the adjacent brackets (AB and AC), the hanger AC has higher force value at its new position A^1C^1. Similarly the hanger DE has higher force value at its new position D^1E^1. These differences in hanger force among adjacent hanger brackets depend on the deflection of main cable and the deck (relative movement between the main cable and the deck at the corresponding hanger nodes). This deflection depends on the loading condition. This force variation between adjacent hangers leads to change in the distributions of stress in the hanger bracket.

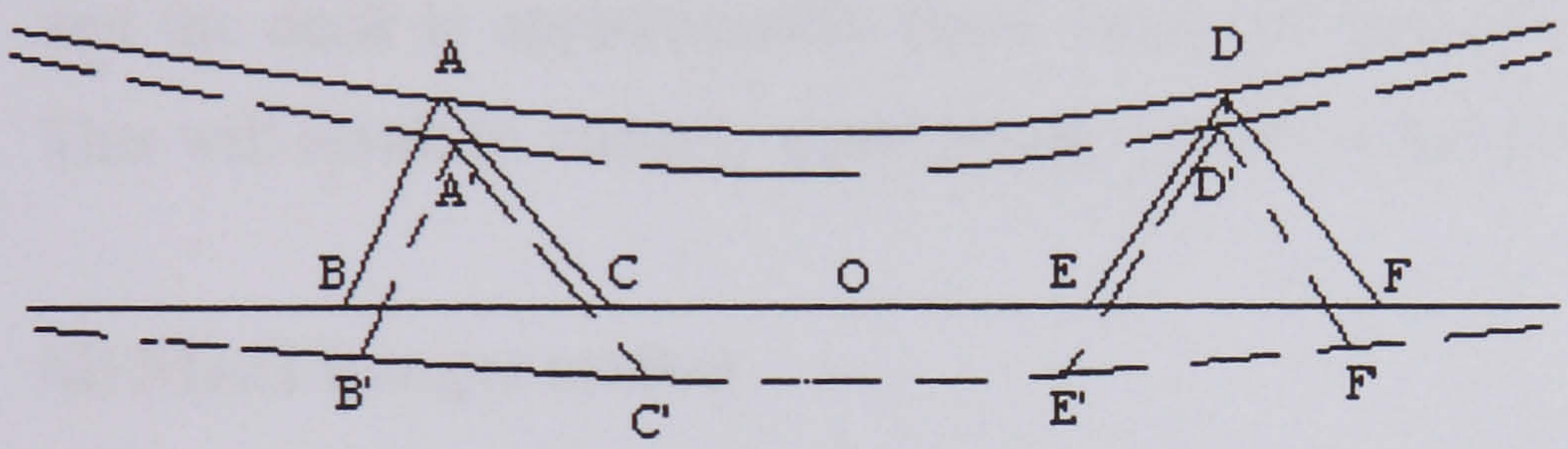

Figure 11i2: Existing hanger system under BSALL condition

ii) Vertical hanger system

Under the same load condition the vertical hanger model gave a maximum hanger force of 1100 kN at each span (refer Figure 11j). No considerable force differences were found between adjacent hangers.

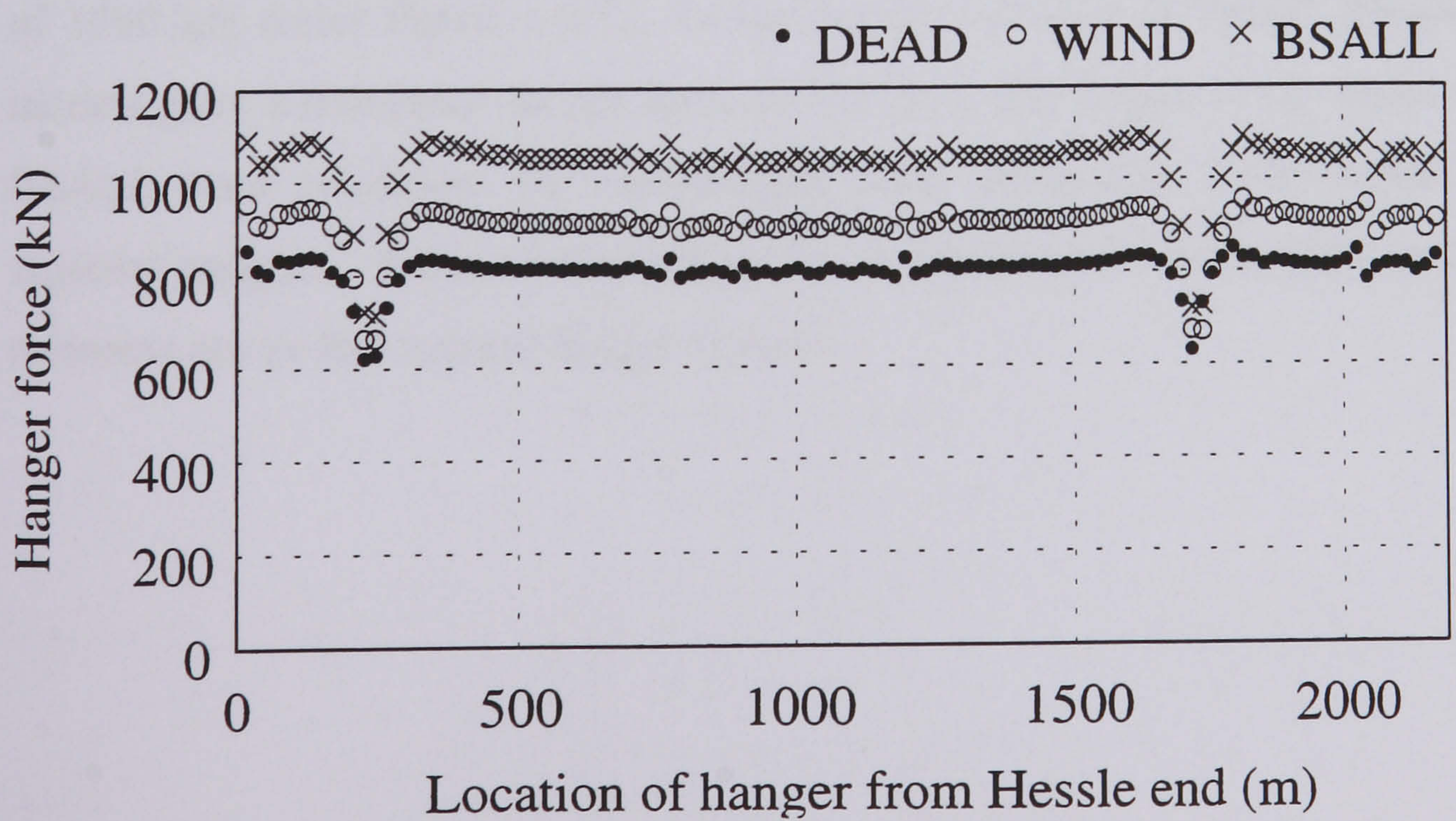

Figure11j: Hanger forces on the vertical hanger system model

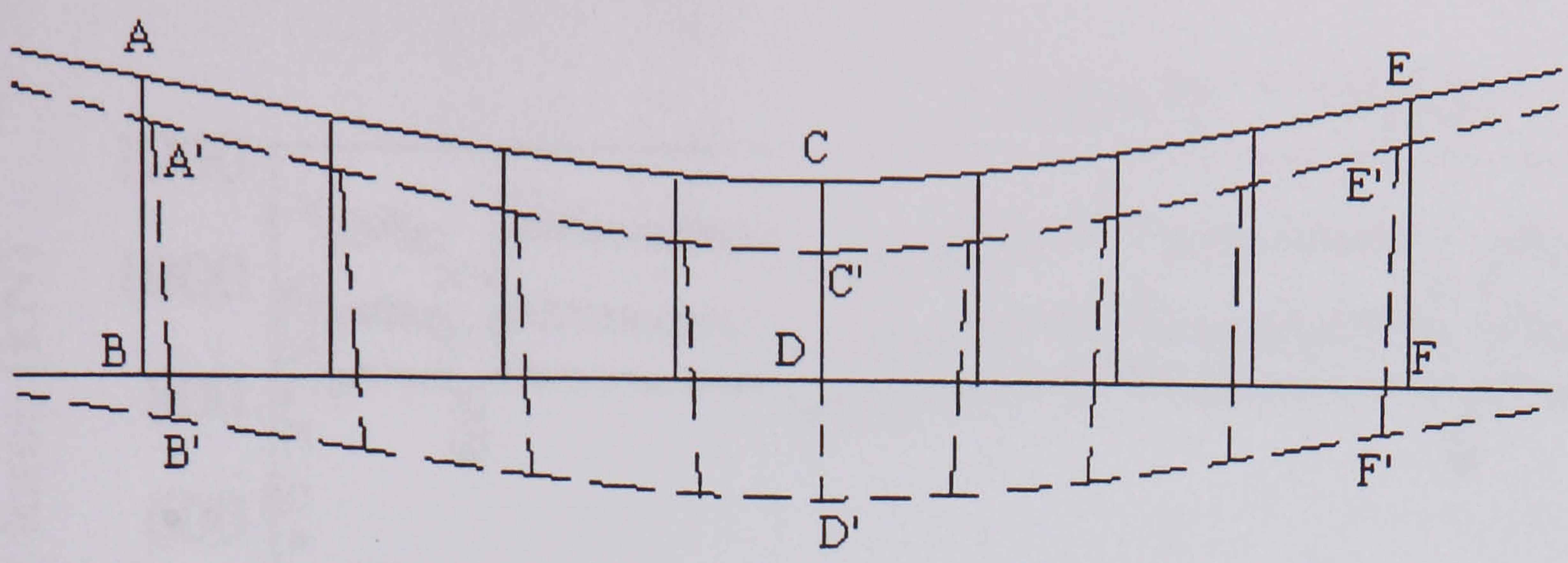

Figure 11j1: Vertical hanger system under BSALL condition

As shown in Figure 11j1, strain on the hangers due to deflection of the main cable and the deck is approximately equal along the longitudinal direction of the bridge. This will result in virtually equal hanger forces on the structure.

iii) Mod1 hanger system

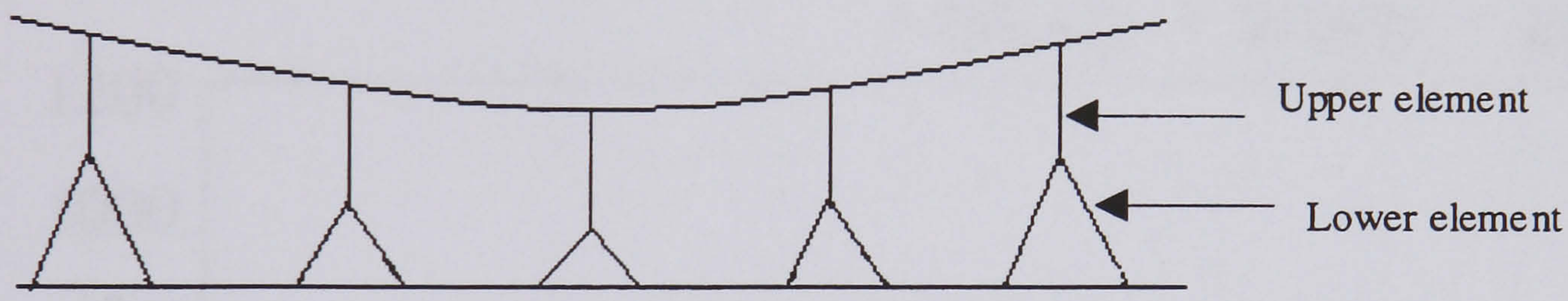

Upper hanger elements in Mod1 hanger system model gave maximum hanger forces of 1090 kN (refer Figure 11k1). Lower hanger elements on Mod1 hanger system models gave a maximum hanger force of 749 kN (refer Figure 11k2) under the same BSALL load condition. No considerable force differences were found between adjacent hangers. The maximum force and the hanger force distribution on the upper elements are as like vertical hanger system.

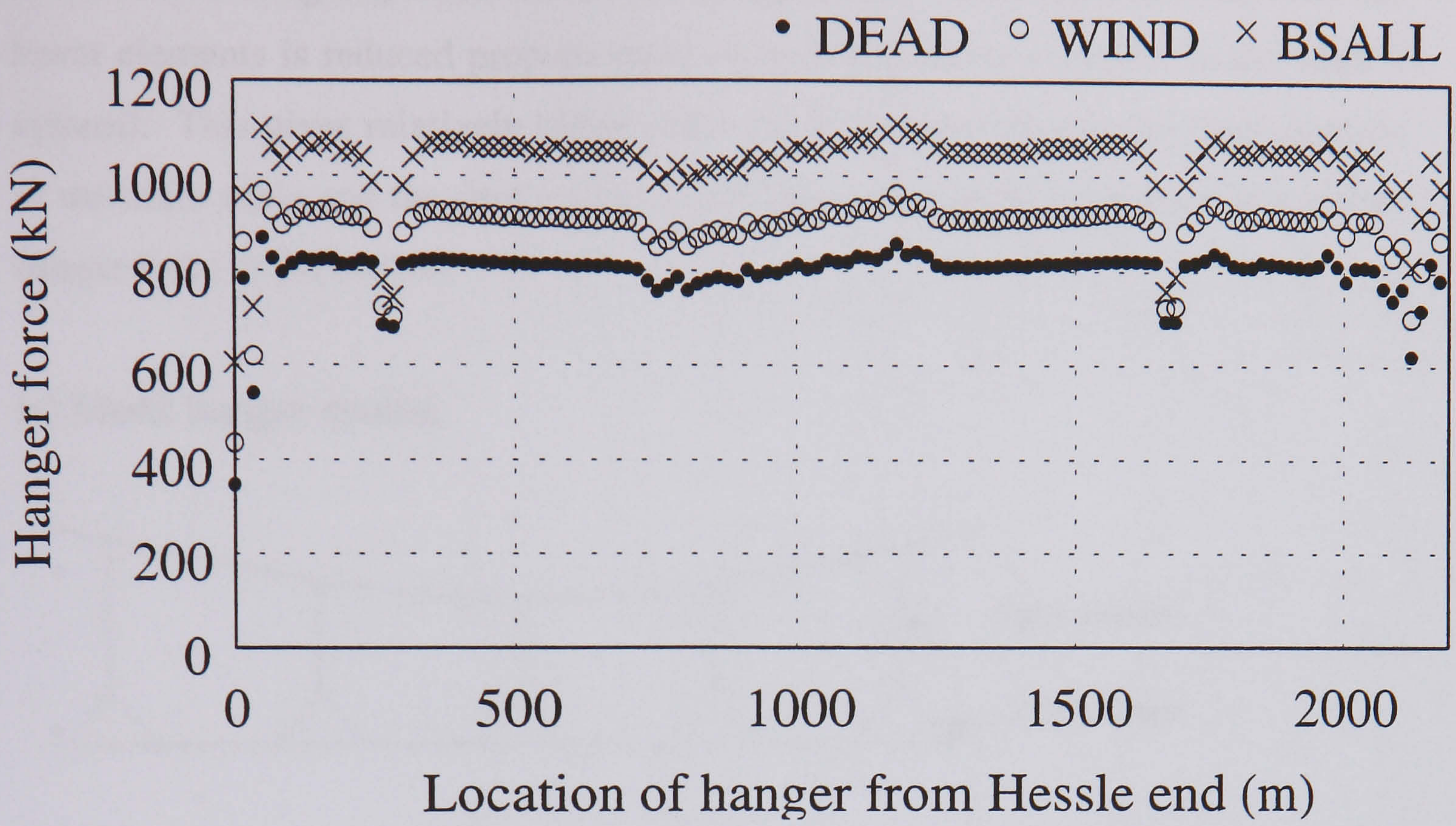

Figure 11k1: Hanger forces on the Mod 1 hanger system model (upper element)

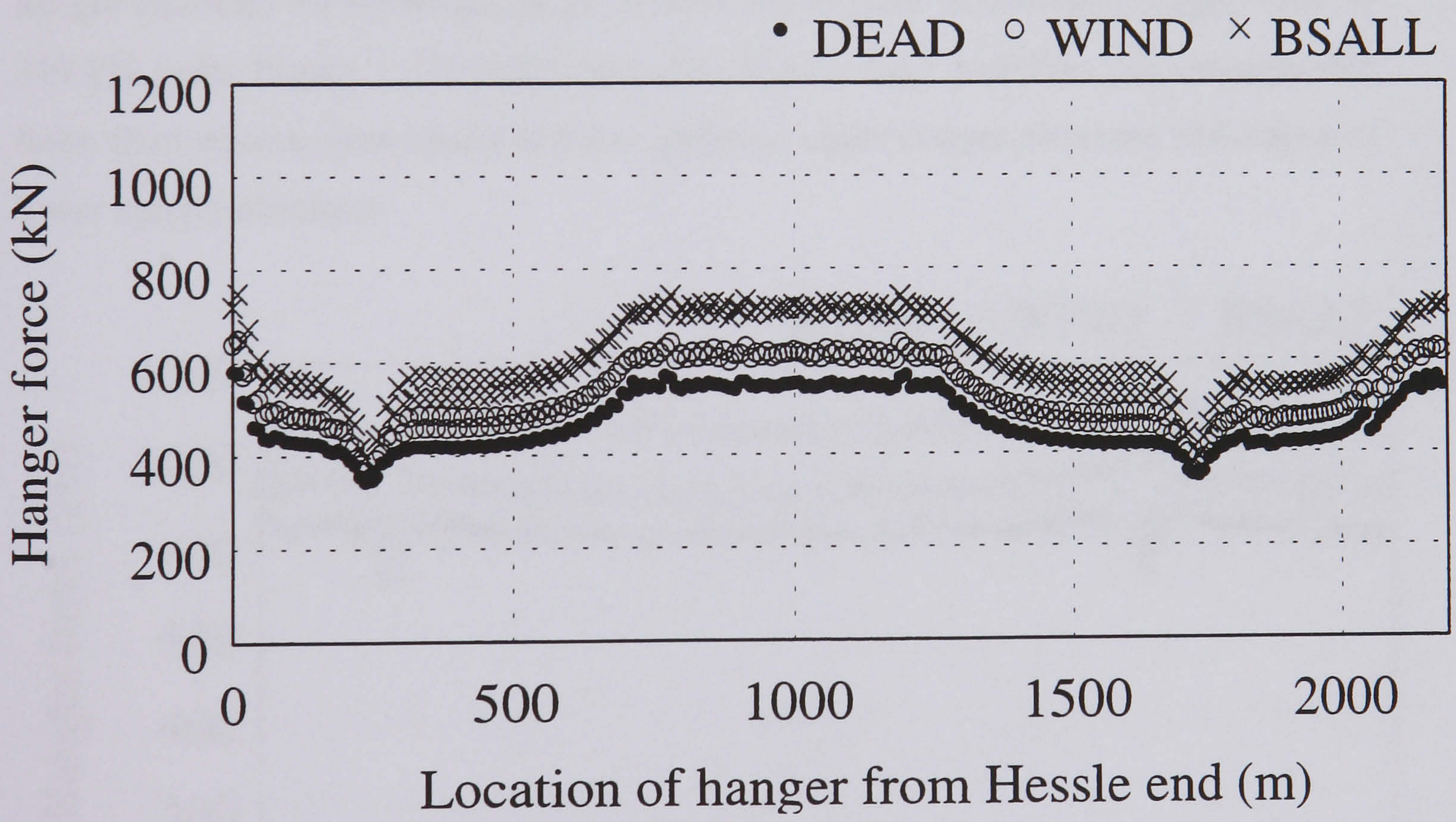

Figure 11k2: Hanger forces on the Mod 1 hanger system model (lower element)

In the Mod 1 hanger systems due to the arrangement of the hangers, the length of the lower elements is reduced proportionally towards the centre (compare to the Mod 2 system). This gives relatively higher strain on the hangers (due to the displacement of the main cable and the deck) at the centre than at the ends. Thus there is a higher hanger force at the centre.

iv) Mod2 hanger system

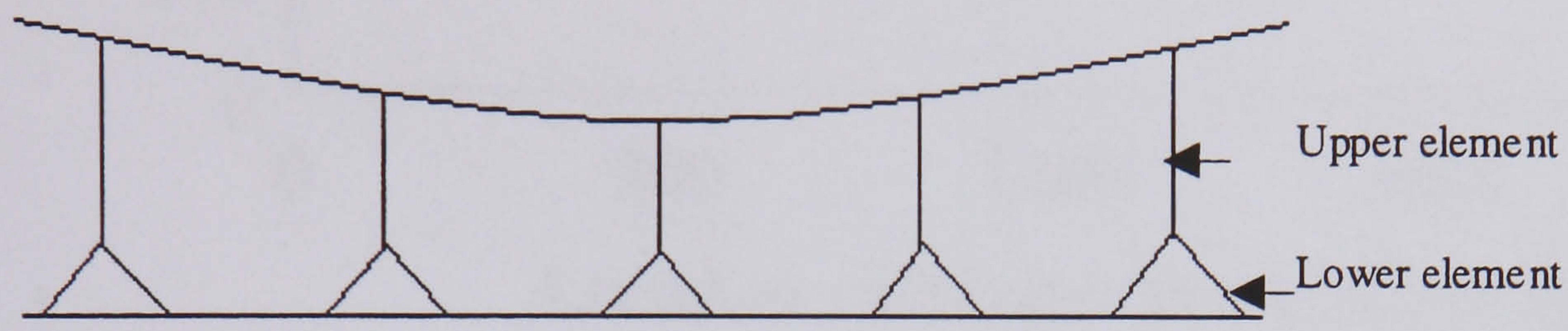

As with the Mod1 system, the upper hanger elements in the Mod2 hanger system model also gave the maximum hanger forces of 1090 kN (refer Figure 1111). Lower hanger elements on the Mod2 hanger system model gave a maximum hanger force of 749 kN (refer Figure 1112) under the same BSALL load condition. No considerable force fluctuations were found between adjacent upper hanger elements and adjacent lower hanger elements.

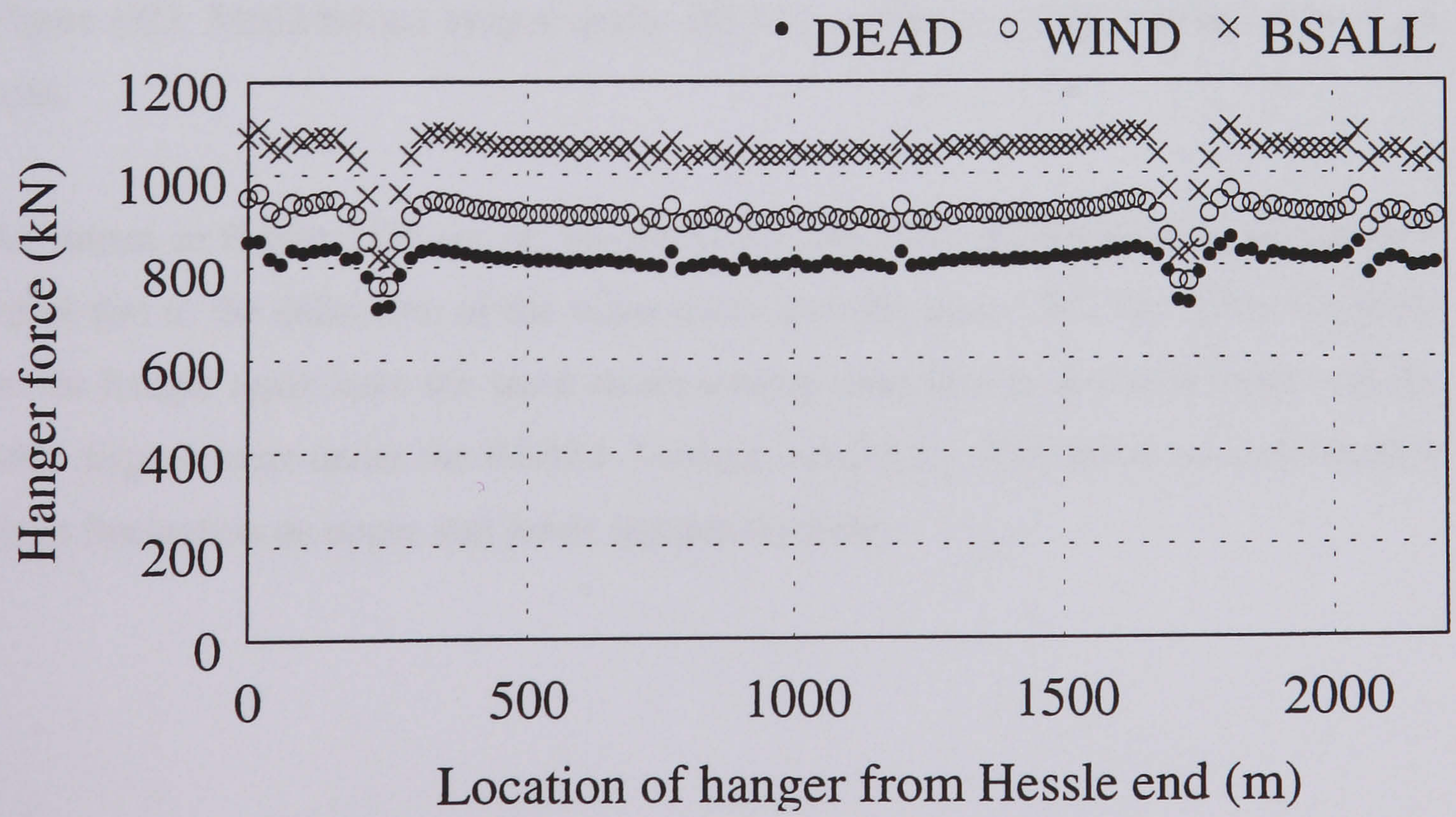

Figure 1111: Hanger forces on the Mod 2 hanger system model (upper element)

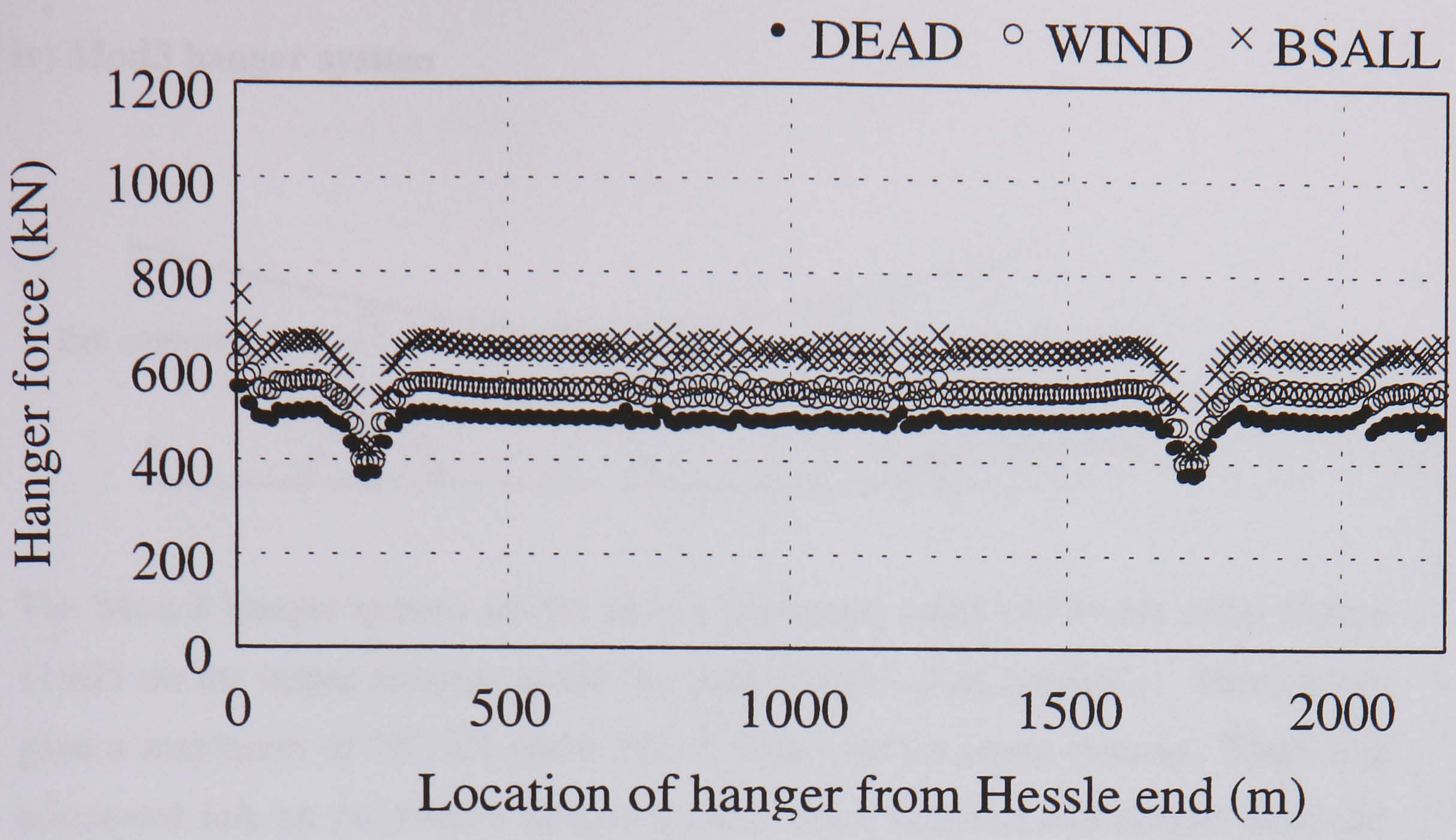

Figure 11l2: Hanger forces on the Mod 2 hanger system model (lower element)

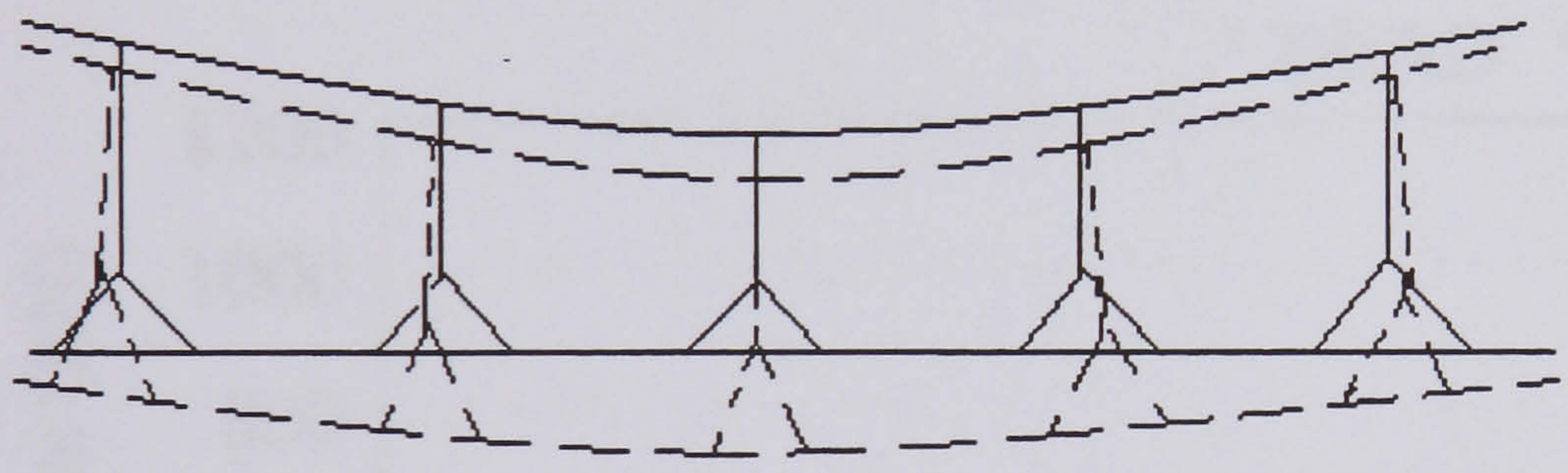

Figure 11l3: Mod2 hanger system under BSALL condition at the middle of the main span

As shown in Figure 11l3 above, the strain on the upper elements is approximately equal due to the deflection of the main cable and the deck. For the lower elements on the hanger again have the same strain among them due to the main cable and the deck displacement under the BSALL loading condition. This gives no considerable force fluctuation on upper and lower hanger elements.

iv) Mod3 hanger system

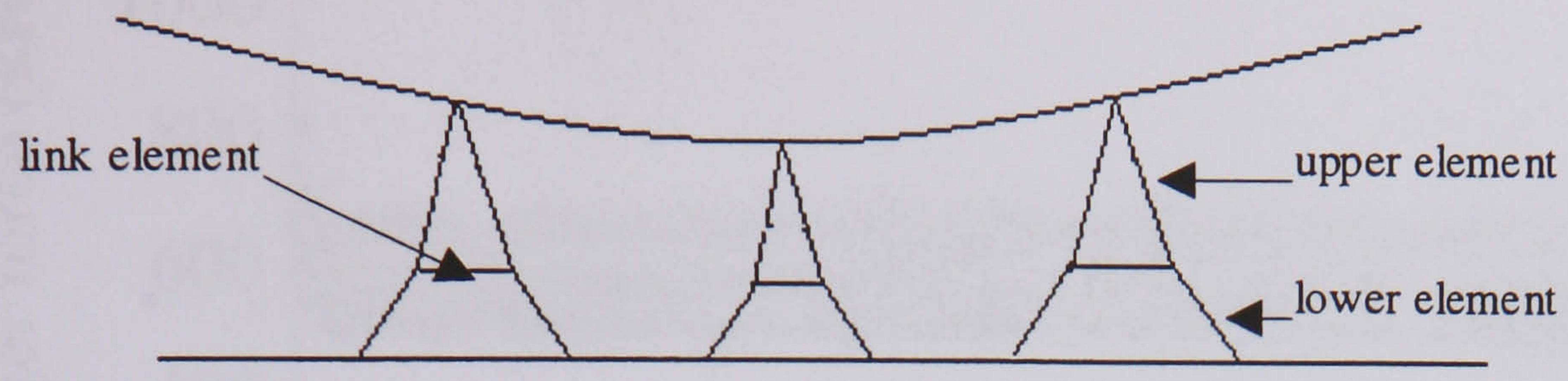

The Mod 3 hanger system model gave a maximum value of 664 kN (refer Figure 11m2) on the upper element under the same BSALL load condition. This system gave a maximum of 787 kN (refer Figure 11m1) on the lower element. There is a horizontal link on the Mod 3 hanger system, which connects two hangers from the adjacent hanger brackets with a maximum force of 390 kN (refer Figure 11m3). No considerable force fluctuations were found between adjacent hangers.

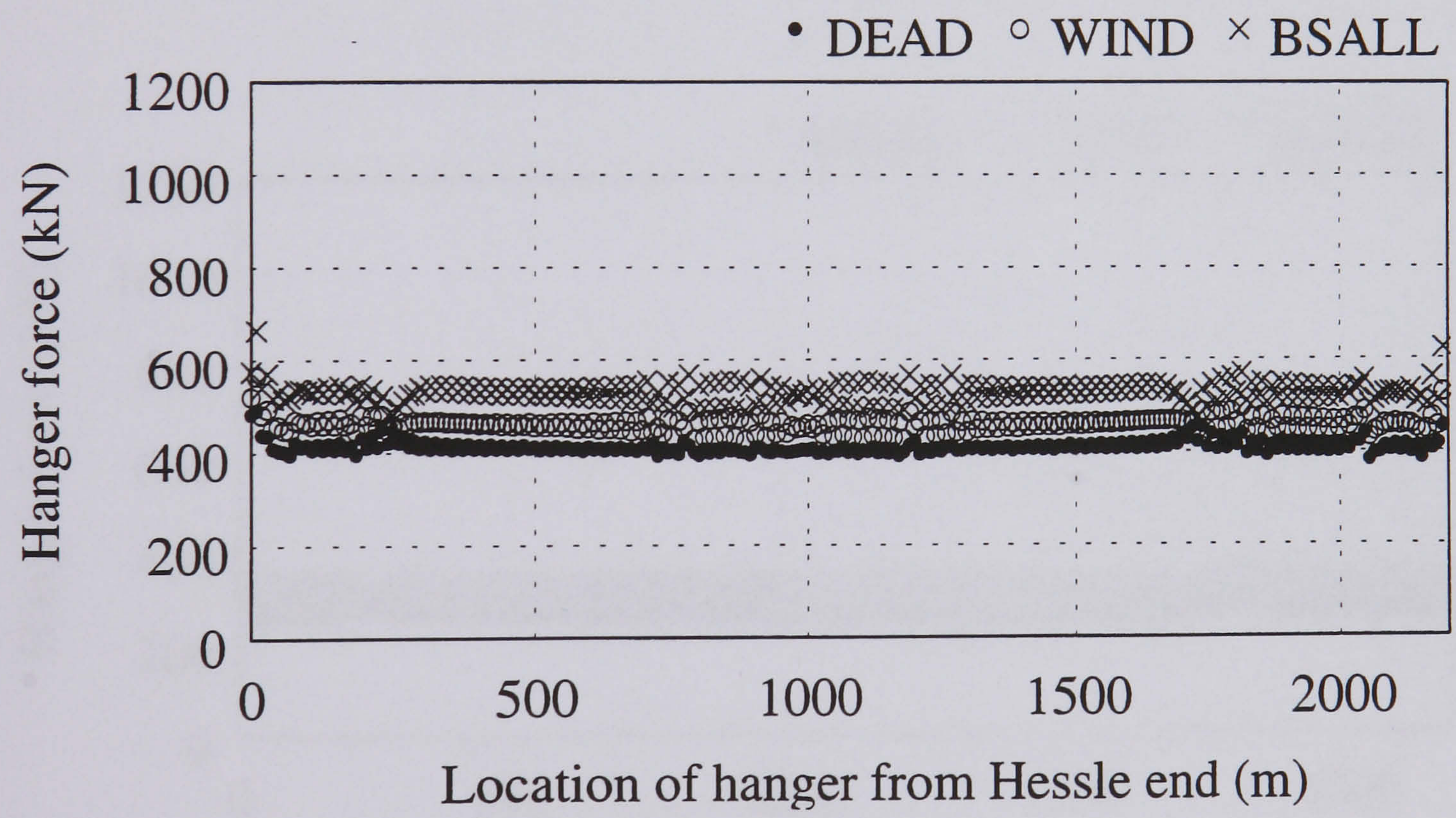

Figure 11m1: Hanger forces on the Mod 3 hanger system model (upper element)

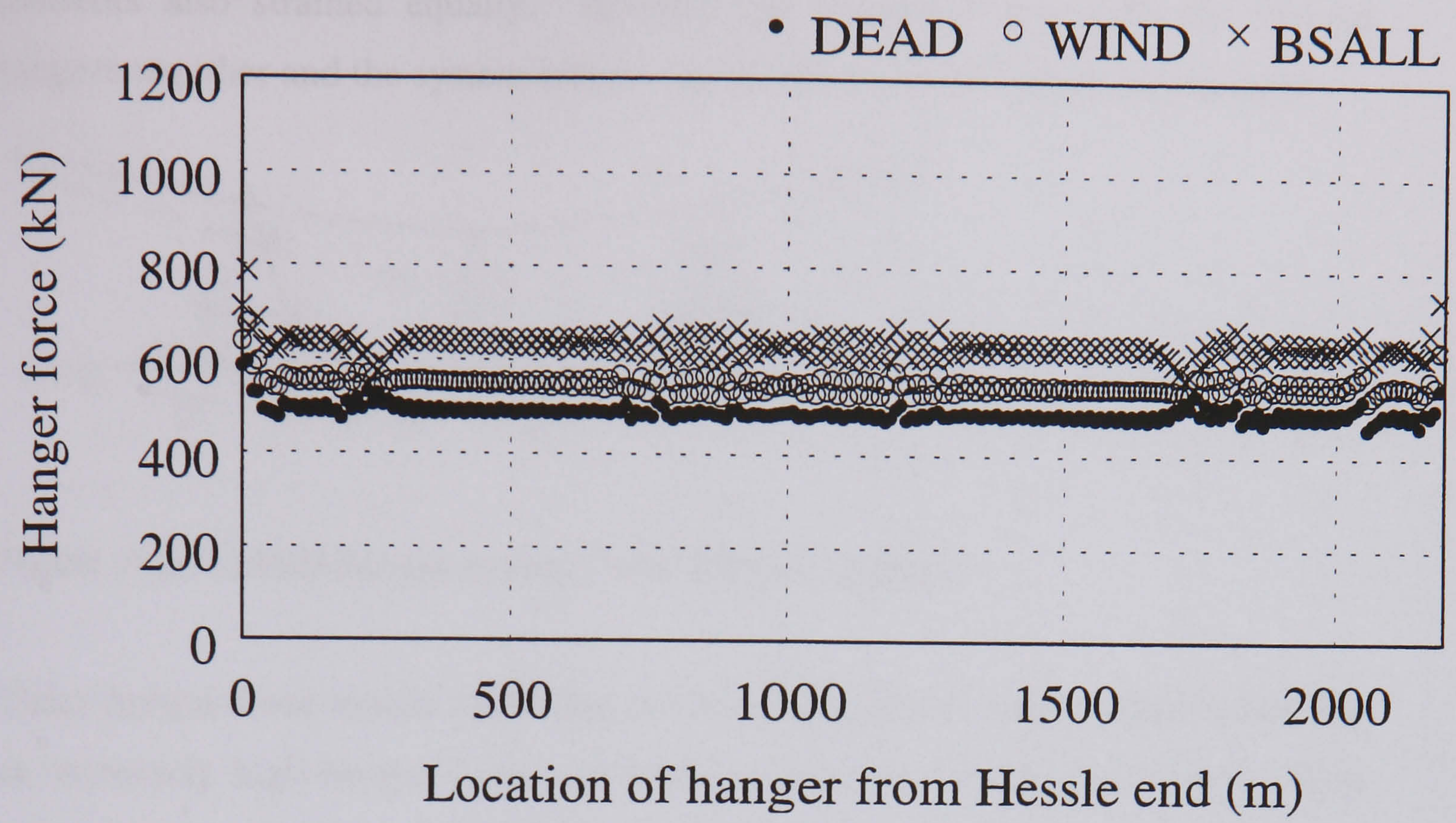

Figure 11m2: Hanger forces on the Mod 3 hanger system model (lower element)

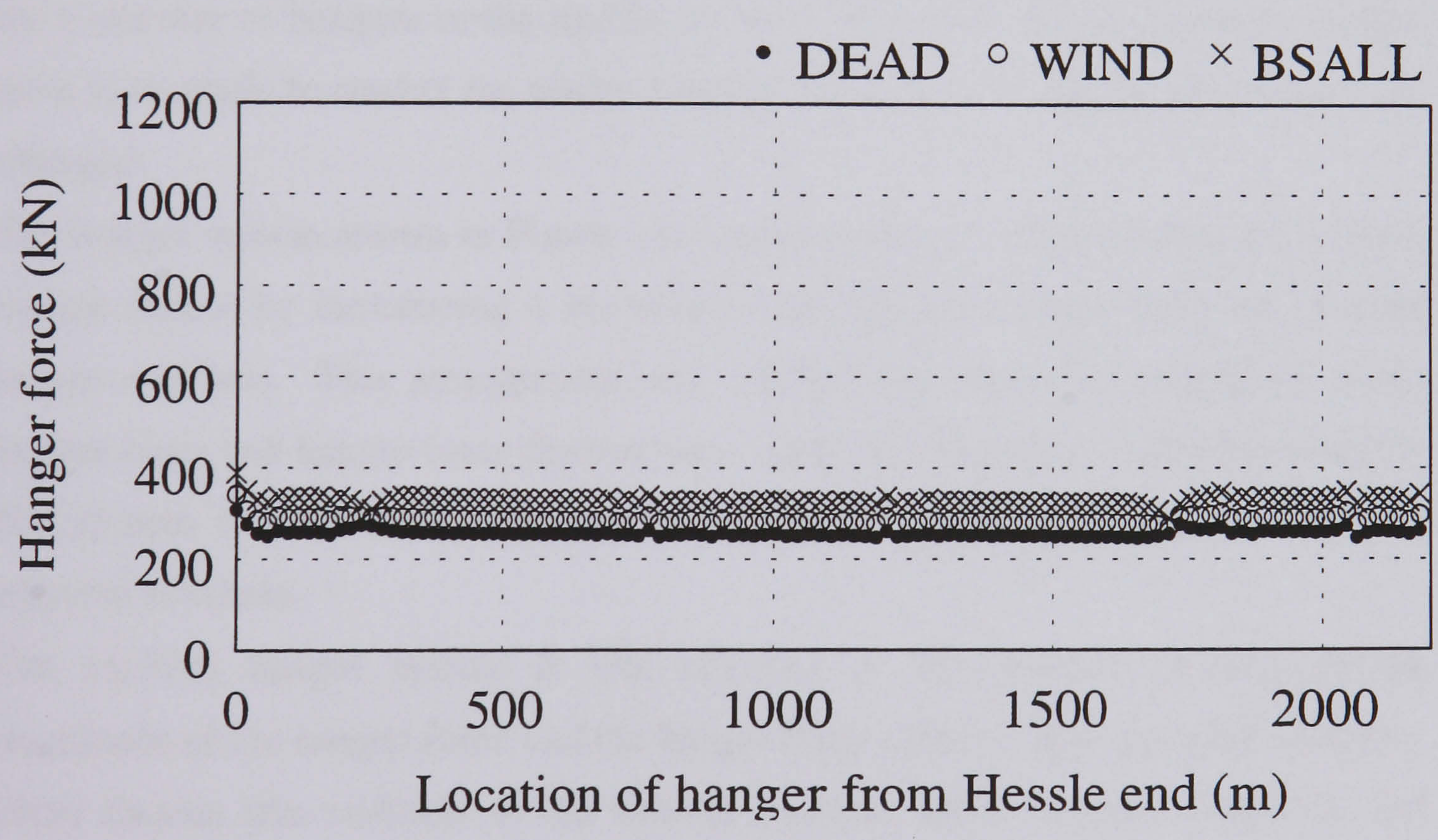

Figure 11m3: Hanger forces on the Mod 3 hanger system model (link element)

The Figure 11m4 below shows the deflected shape of the structure under BSALL condition. The strain on the hangers depends on the main cable and the deck deformations. Unlike the existing system, due to the link between the adjacent hangers, upper elements are strained approximately equally. Similarly lower elements also strained equally. Actually the introduced link pulls the inclined hangers together and the system behaves more like a vertical hanger arrangement.

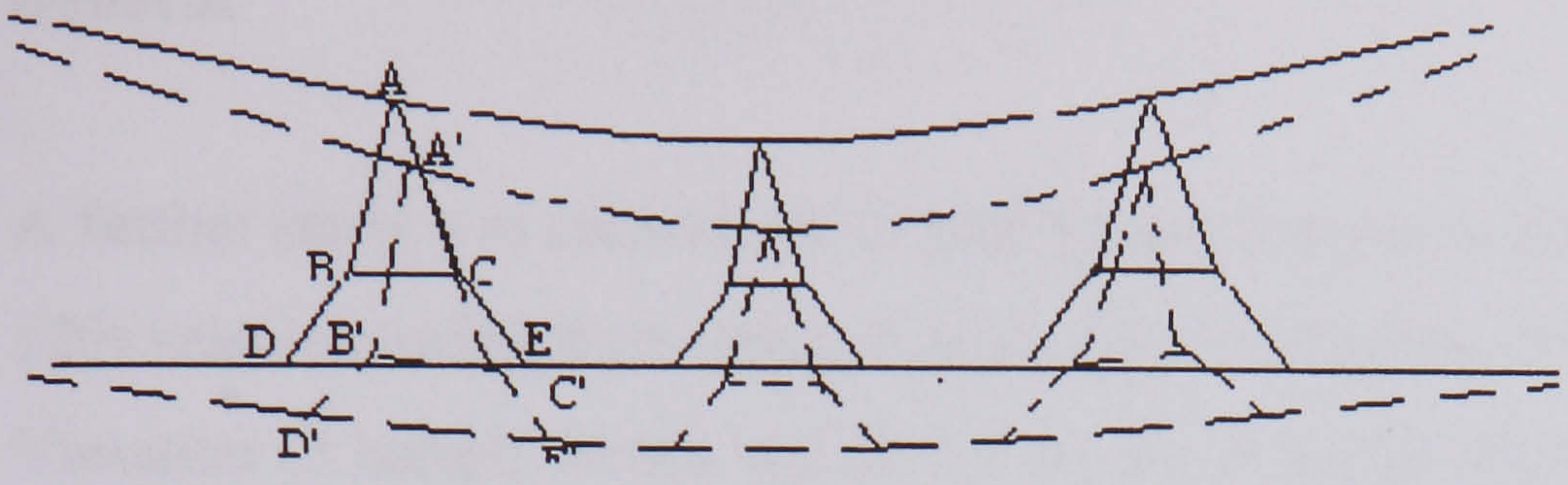

Figure 11m4: Mod3 hanger system under BSALL condition

These hanger force results show that the existing inclined hanger system model has an extremely high hanger force variation between adjacent hangers than the other hanger system models. From Figure 11i it is clear that increasing the fully span loaded BSALL value beyond the present limit will cause some hangers to slacken. Increasing the traffic intensity beyond this present limit will be a problem in future for a number of hangers in the middle of main span area. Future recommendations have to be made to control the traffic intensity or, the hanger system pattern has to be changed.

The hanger system shown in Figure 11e is easy to modify from the existing inclined hanger model by introducing a horizontal link between hangers from the adjacent hanger brackets. This arrangement will considerably reduce the magnitude of the hanger force and hanger force fluctuations. There is a need for an extended study on this system at both ends of the link, which is connecting the hangers from the adjacent brackets.

The existing hanger system is less effective in this situation in reducing the magnitude of the hanger force and the hanger force variation than the other systems. Other factors like stiffness of the overall structure under dynamic condition, and longitudinal, lateral and torsional behaviour of the deck ends under different loading conditions have to be analysed. The change of deck and tower dimensions due to change of stiffness also have to be considered before taking the next step to introduce the different hanger system patterns.

Comparison of hanger forces under point load condition

General

A further study was carried out to find hanger forces on the models in the case of a 120t vehicle moving from one end to the other end of the bridge.
Variation of hanger forces was found on the selected elements at the centre of the middle (Cen-mid) and side spans (Hes-mid, Bar-mid). These results were plotted for each model (Figures 11n- 11s). Symbol (R) and (L) represents the right side and left side hanger on the hanger set respectively. The performance (hanger force) of the selected hangers for the moving load is analysed and plotted against the load position. The existing system clearly gave higher variation of hanger force than the other systems.

i) Existing inclined hanger system

The moving live load gave the maximum change of hanger force on the existing inclined hanger model. The maximum fluctuation of 230 kN (refer Figure 11n) was obtained at a hanger in the centre of the middle span. Relatively higher flexibility at the centre causes the deck and the main cable to move comparatively greater than other places. This gives relatively higher difference in hanger forces at the centre of the main span (580 kN and 350 kN) for particular hanger elements. This is due to higher and lower relative deck and main cable movement on the hanger nodes. At the centre of the side spans the relative movement between the deck and the main cable is comparatively less. Resulted lower variation of hanger force either increases or decreases at the centre of the side span than the centre of the main span. This gives less fluctuation in hanger force than at the centre of the main span.

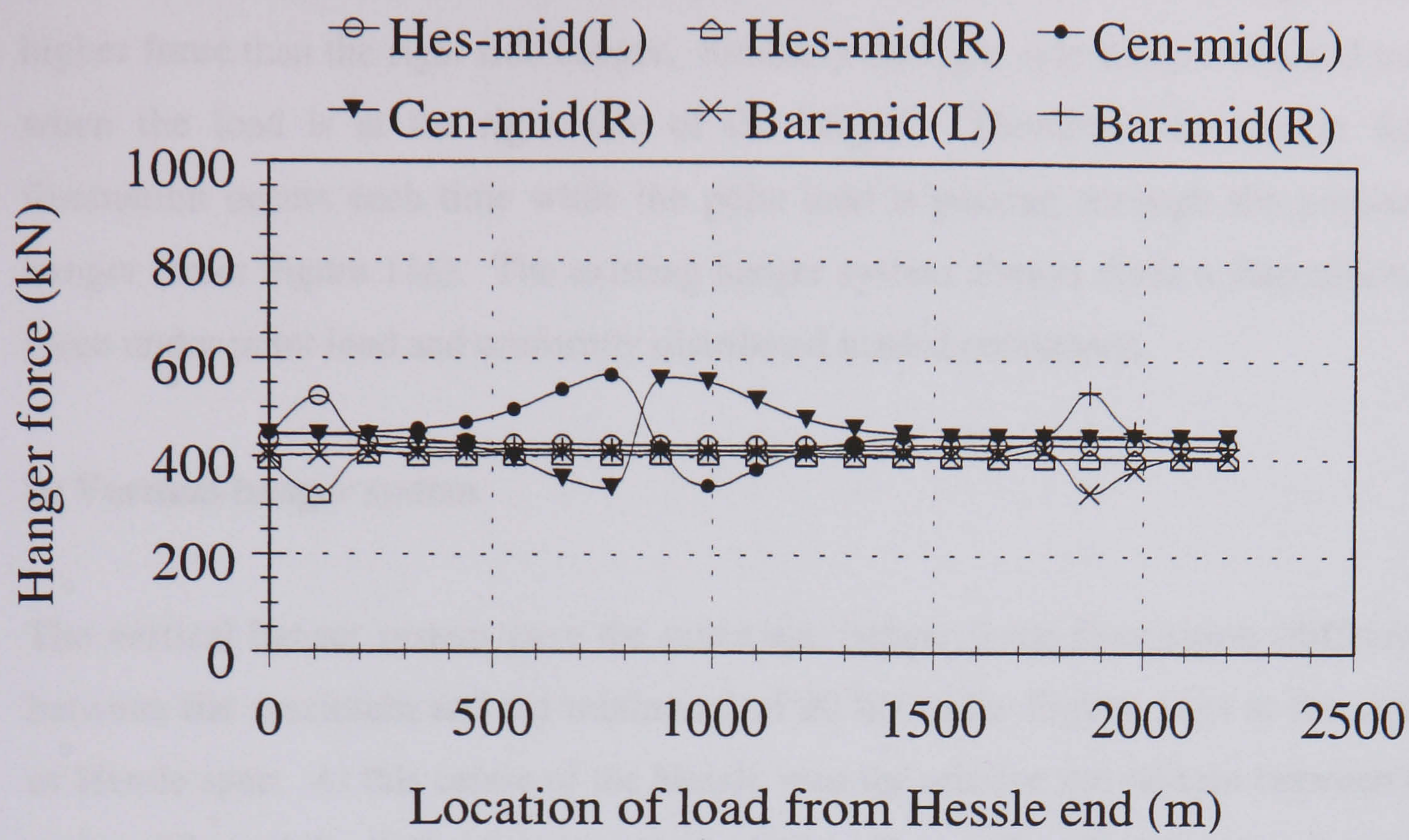

Figure 11n: Hanger force on an element for the existing hanger system model

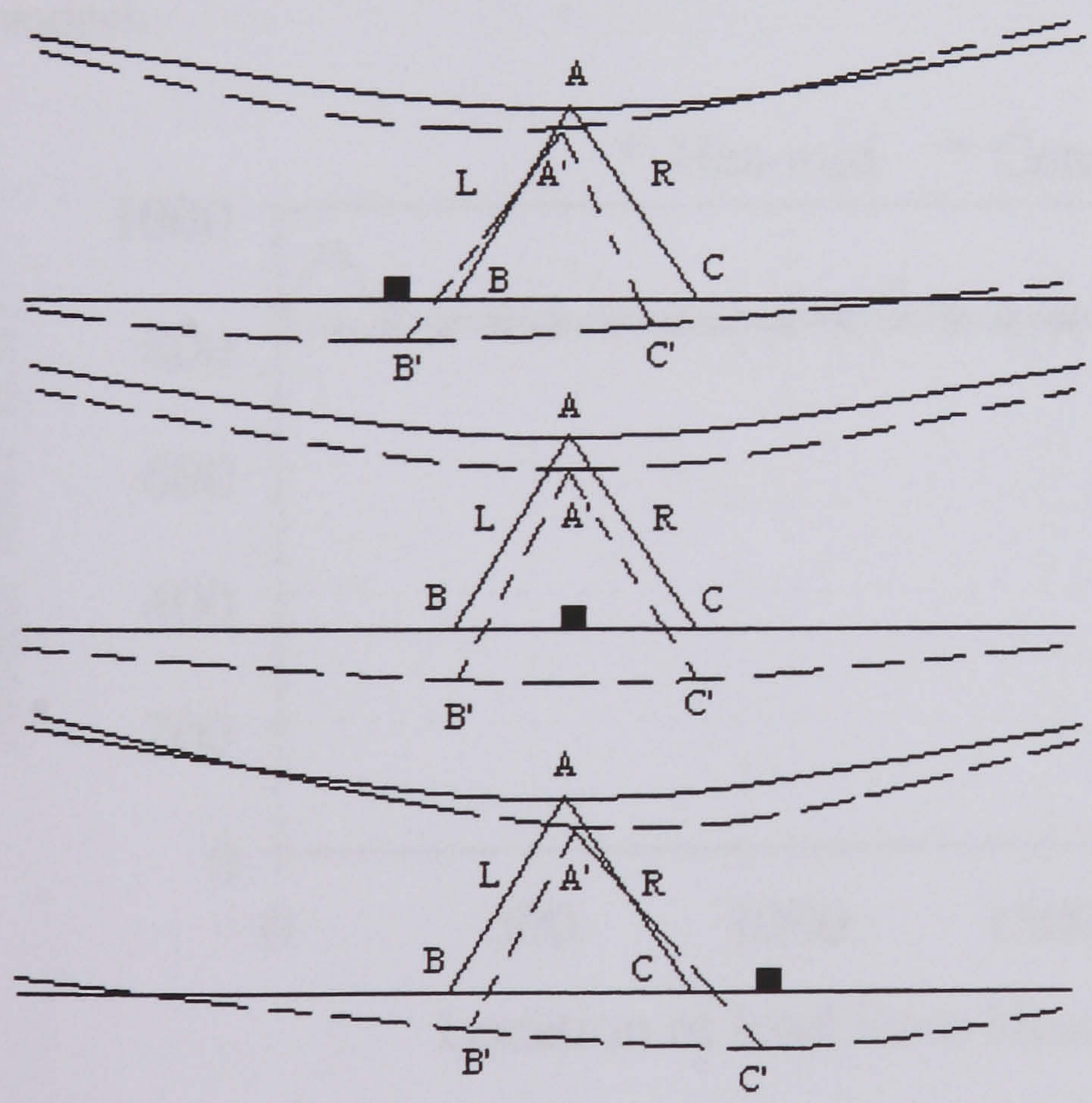

Figure 11n1: Existing system under point load condition

Figure 11n1 shows the hanger at the centre of main span where the point load is moving from left to right. L and R represent the left and right side of the hangers respectively. When the load is at the left side of the hanger, due to the main cable and the deck movement the left side hanger strained more (A^1B^1) and the right side one shortened (A^1C^1) from its initial position. Thus the left side hanger carries higher force than the right side hanger. Similarly the right side hanger strained more when the load is at the right side of the hanger. Therefore the hanger force fluctuation occurs each time while the point load is passing through the particular hanger (refer Figure 11n). The existing hanger system always feels a fluctuation of force under point load and uniformly distributed loaded conditions.

ii) Vertical hanger system

The vertical hanger system gave the maximum hanger force fluctuation (difference between the maximum and the minimum) of 90 kN (refer Figure 11p) at the centre of Hessle span. At this centre of the Hessle span the relative movement between the main cable and the deck is comparatively high. Due to the shorter span, the main cable is comparatively stiffer so that the relative movement between the deck and the main cable is higher (the deck moves more than the main cable between the hanger nodes).

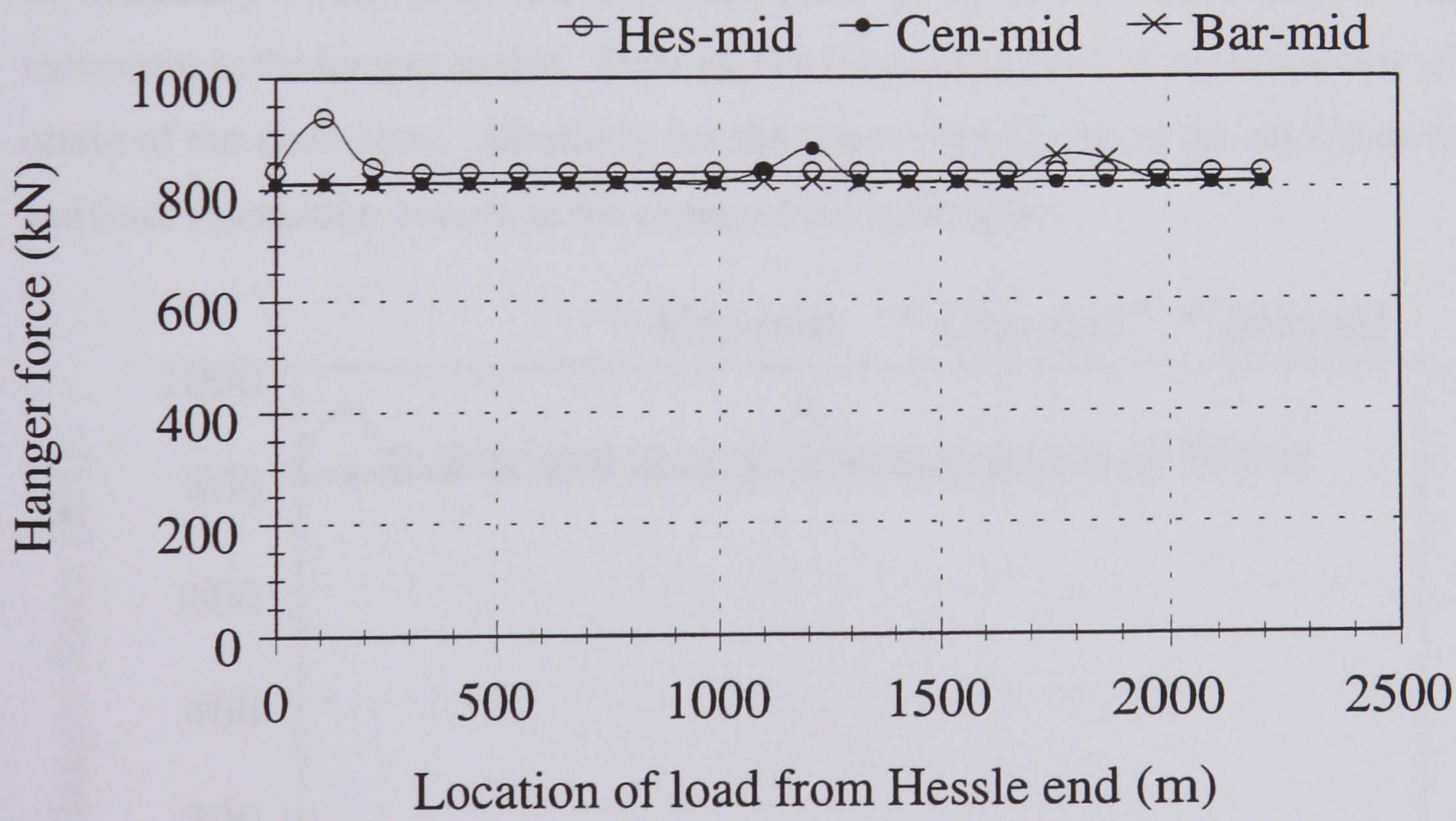

Figure 11p: Hanger force on an element for the vertical hanger system model

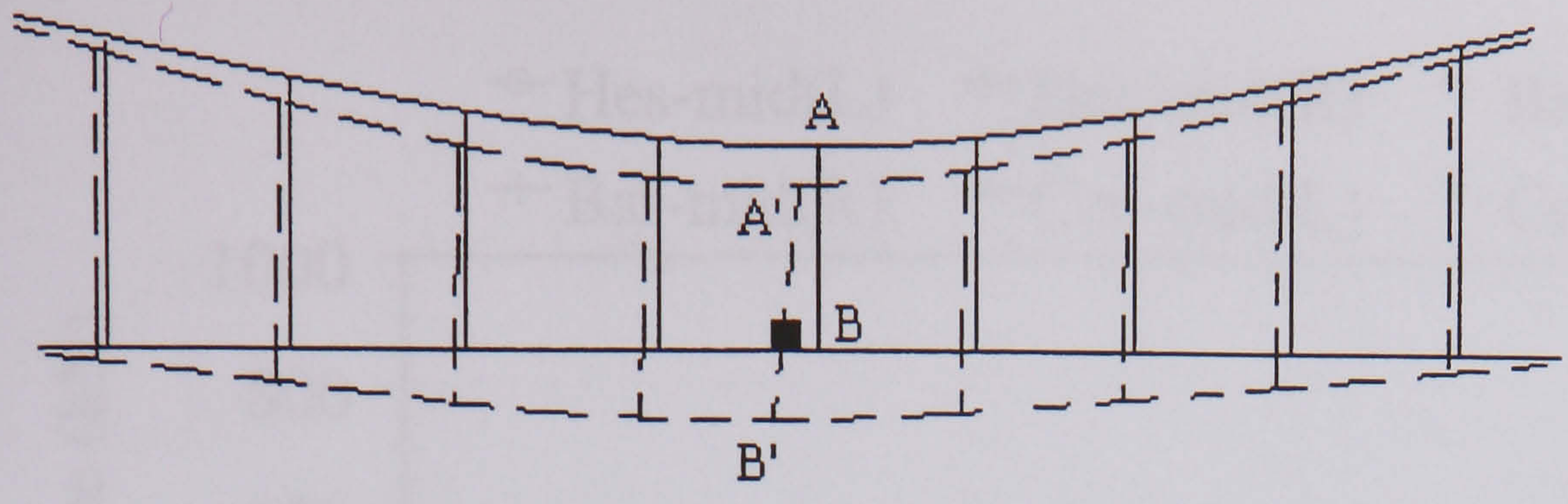

Figure 11p1: Vertical hanger system under point load condition

The above figure 11p1 shows the strain on the hangers due to the movement of the point load, where the shortening of the hangers is less likely related to its initial stage. Due to the displacement of the main cable and the deck, the hanger closer to the point load strained (from AB to A^1B^1) more than the others.

iii) Mod1 hanger system

For the Mod 1 hanger system model, the upper element gave a maximum hanger force fluctuation of 120 kN (refer Figure 11q1) at the centre of the main span. Again the flexibility of the deck and the main cable at the centre causes higher relative movement at the hanger nodes. Thus higher force and force fluctuation occurs at the centre of the main span. Similarly for the lower element again the maximum force and force fluctuation occurs at the centre of the main span.

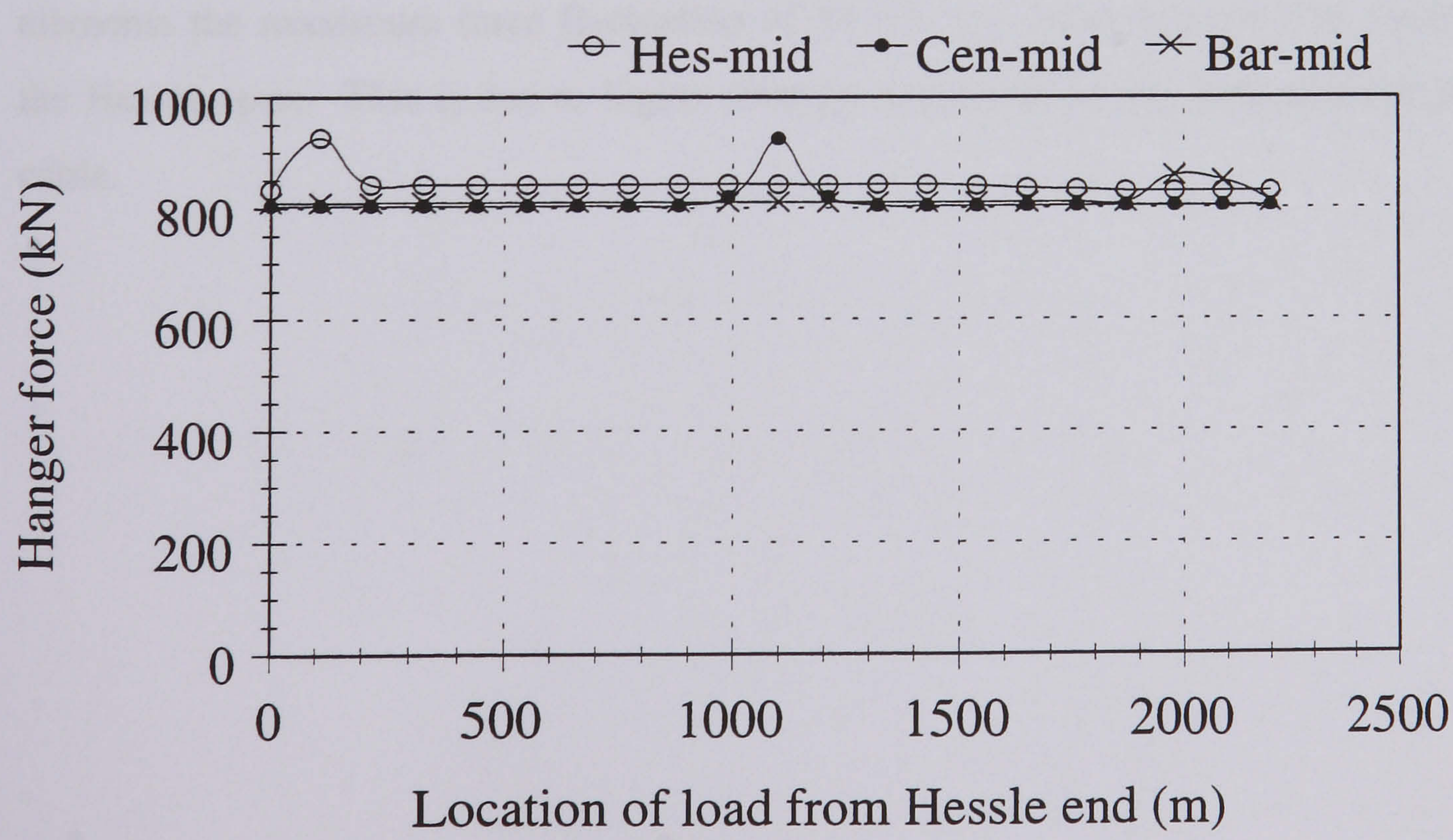

Figure 11q1: Mod 1 hanger model (upper element)

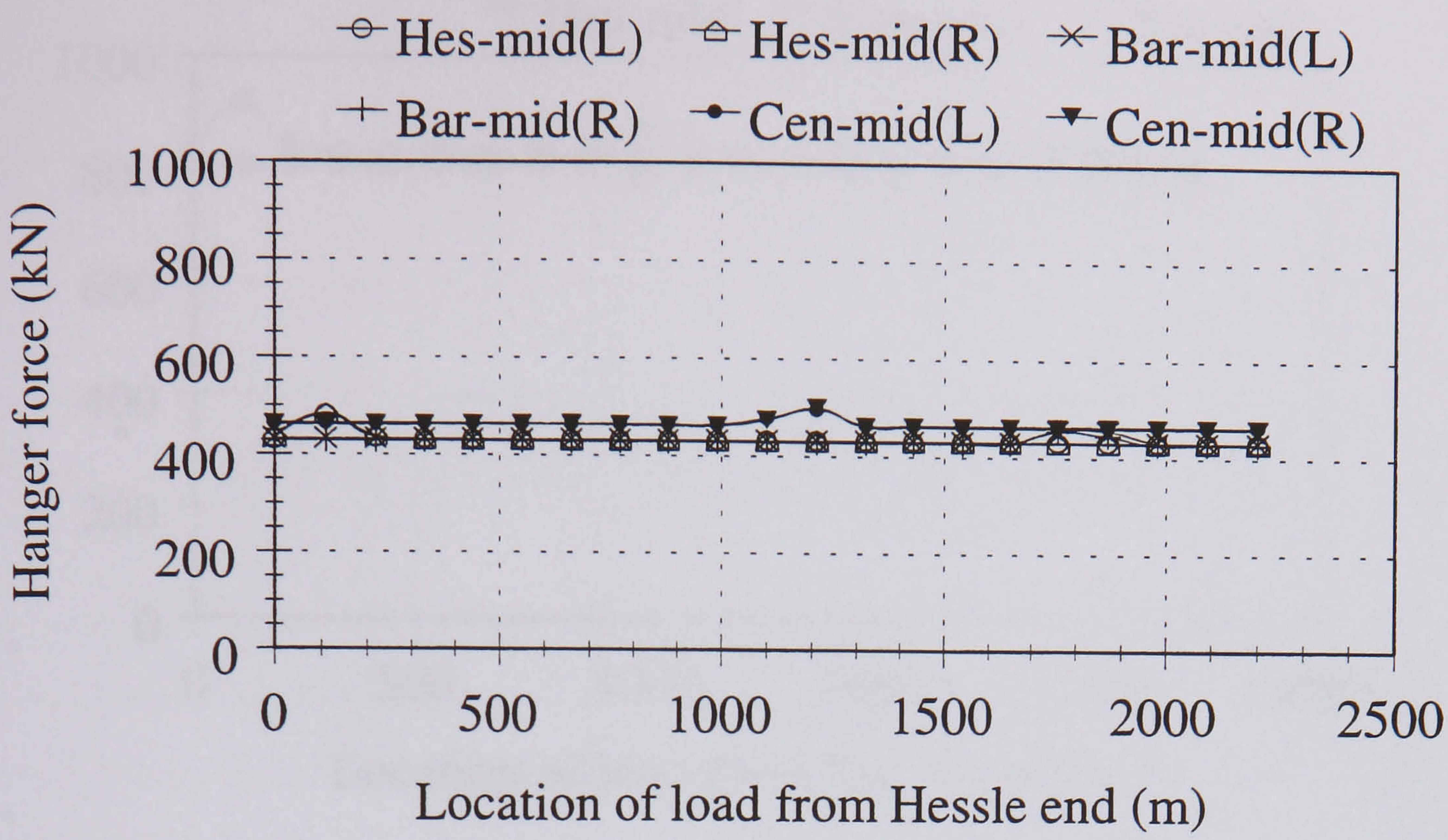

Figure 11q2: Mod 1 hanger model (lower element)

iv) Mod2 hanger system

For the Mod 2 hanger system model, the upper element gave the maximum hanger force fluctuation of 90 kN (refer Figure 11r1) at the centre of Hessle span-similar to the vertical hanger system model. Again as mentioned above (in section ii) the Hessle side hanger at the centre strained more than the other spans. At the lower elements the maximum force fluctuation of 58 kN was found again at the centre of the Hessle span. This is due to higher relative movement of the deck and the main cable.

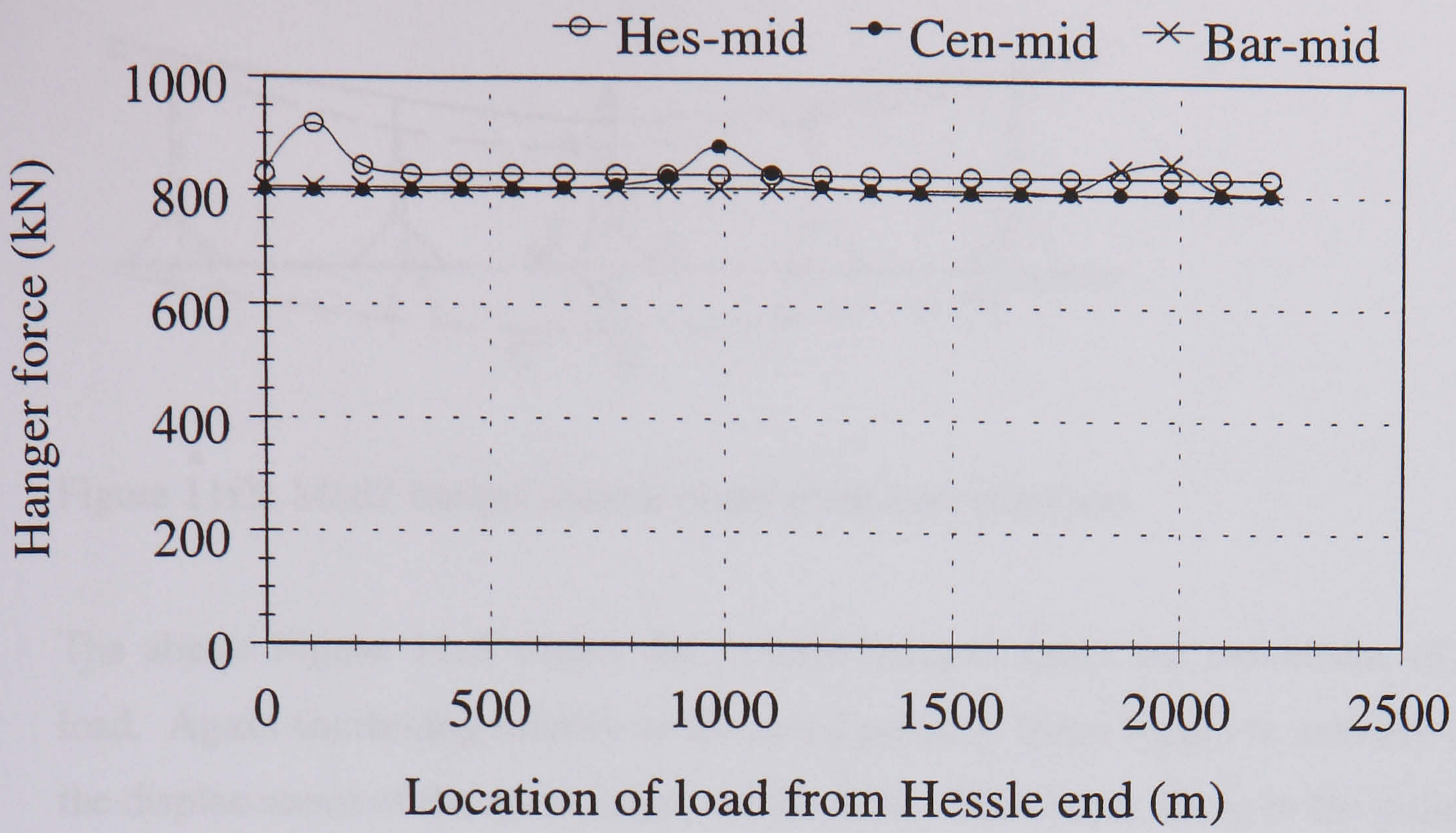

Figure 11r1: Mod 2 hanger model (upper element)

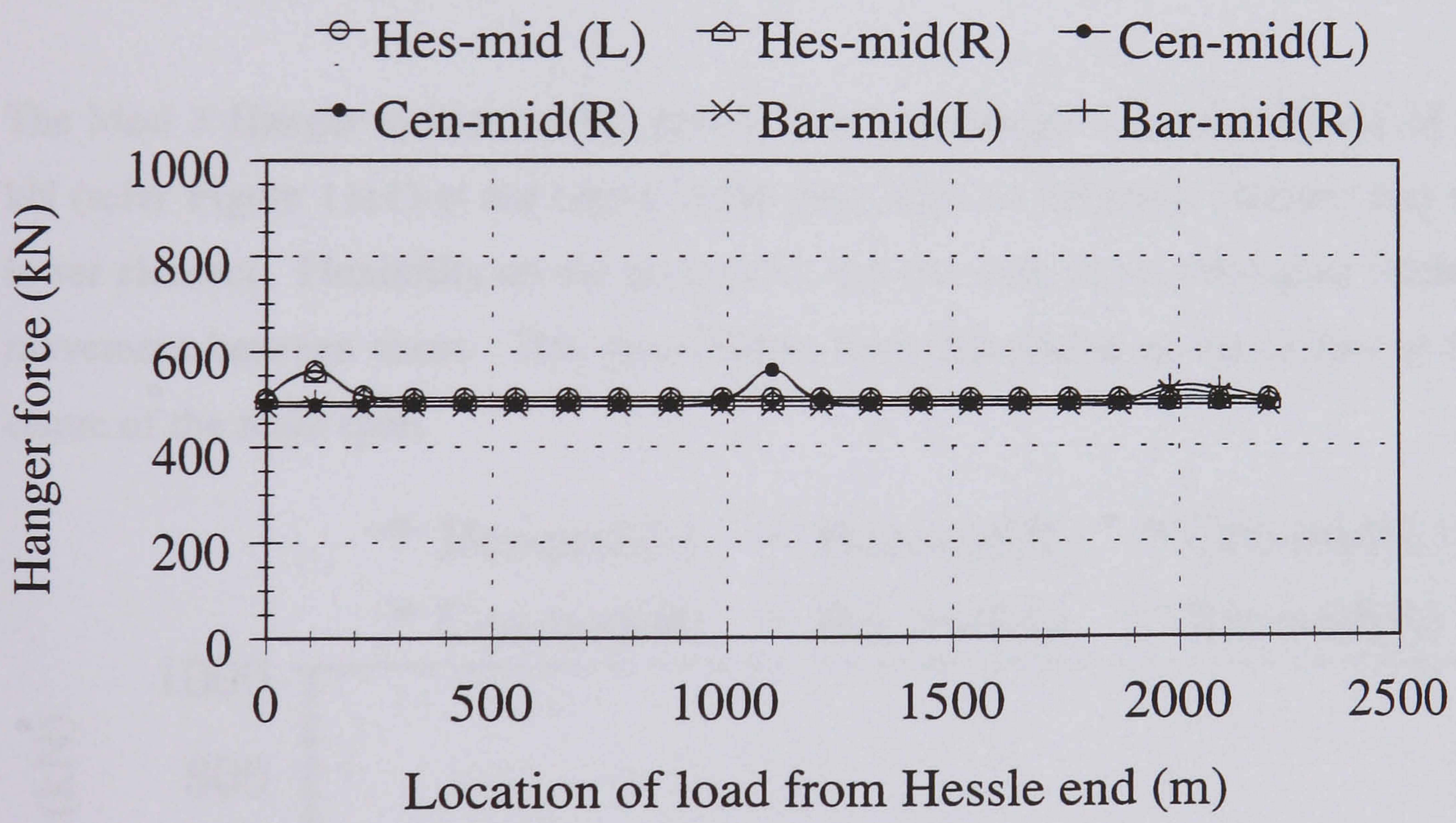

Figure 11r2: Mod 2 hanger model (lower element)

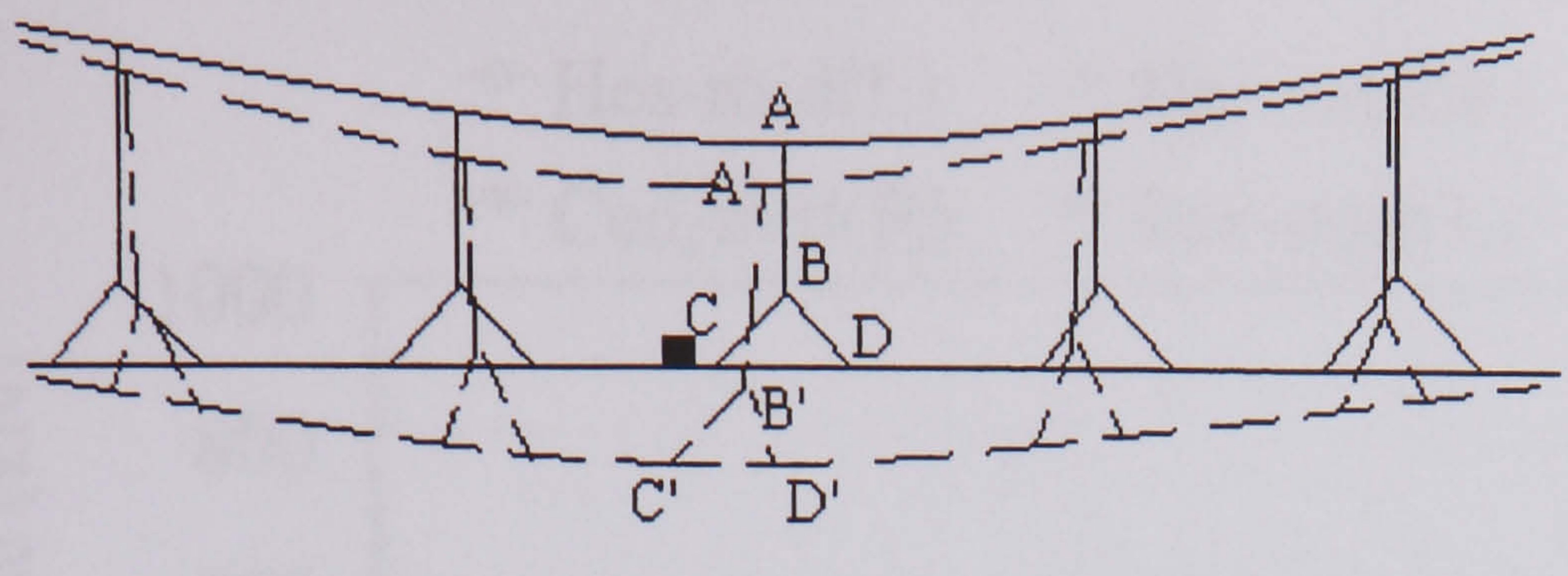

Figure 11r3: Mod2 hanger system under point load condition

The above Figure 11r3 shows the strained hangers under the movement of point load. Again shortening relative to the initial position of the hanger is unlikely due to the displacement of the main cable and the deck. The hanger closer to the point load strained (from ABCD to $A^1B^1C^1D^1$) more than the others.

v) Mod3 hanger system model

The Mod 3 Hanger system model gave a maximum hanger force fluctuation of 60 kN (refer Figure 11s1) at the centre of the main span on the upper element and the lower element. Flexibility on the main cable and the deck causes the higher relative movement between them. This gives higher force fluctuation on the hanger at the centre of the main span.

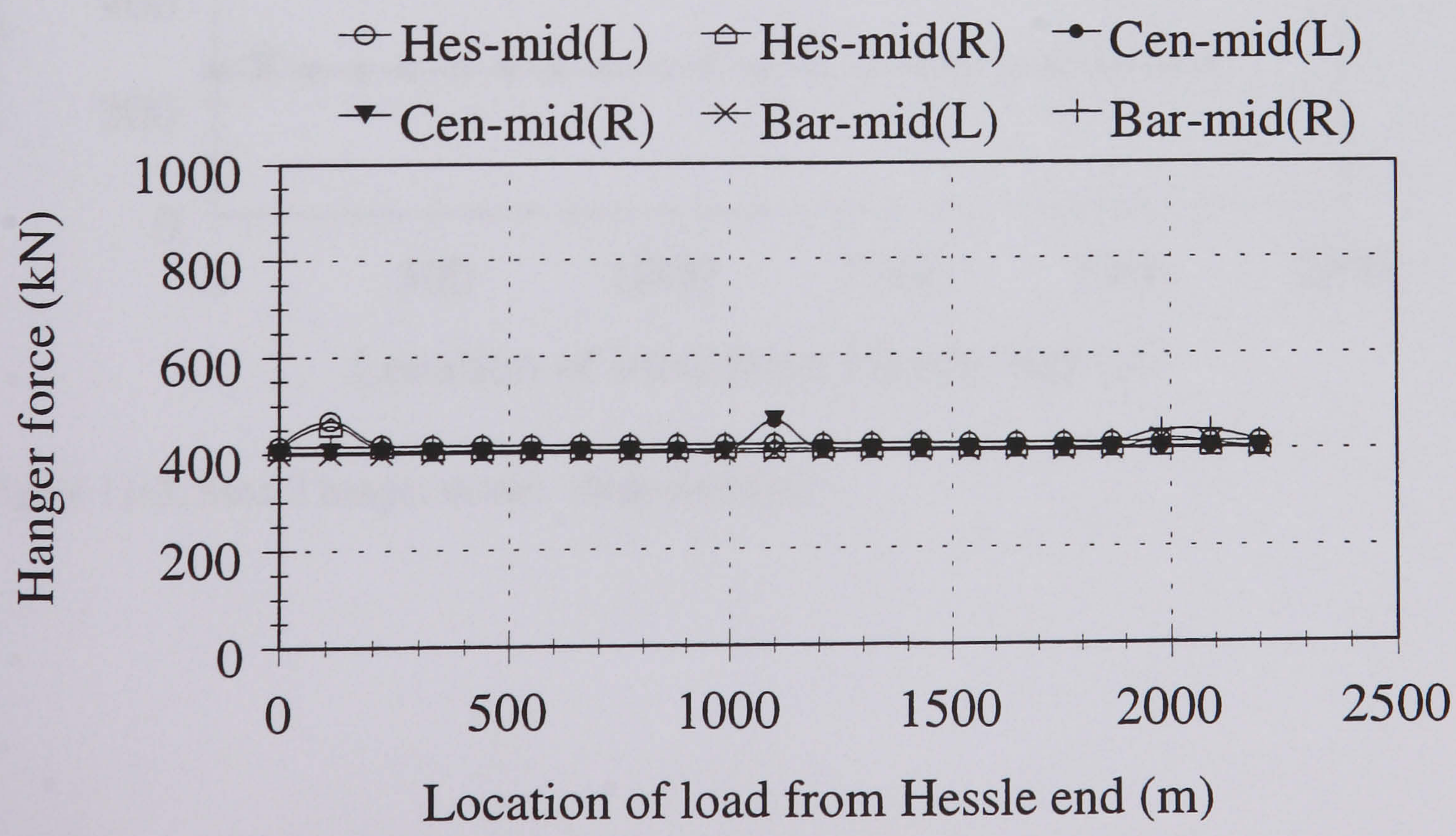

Figure 11s1: Mod 3 hanger model (upper element)

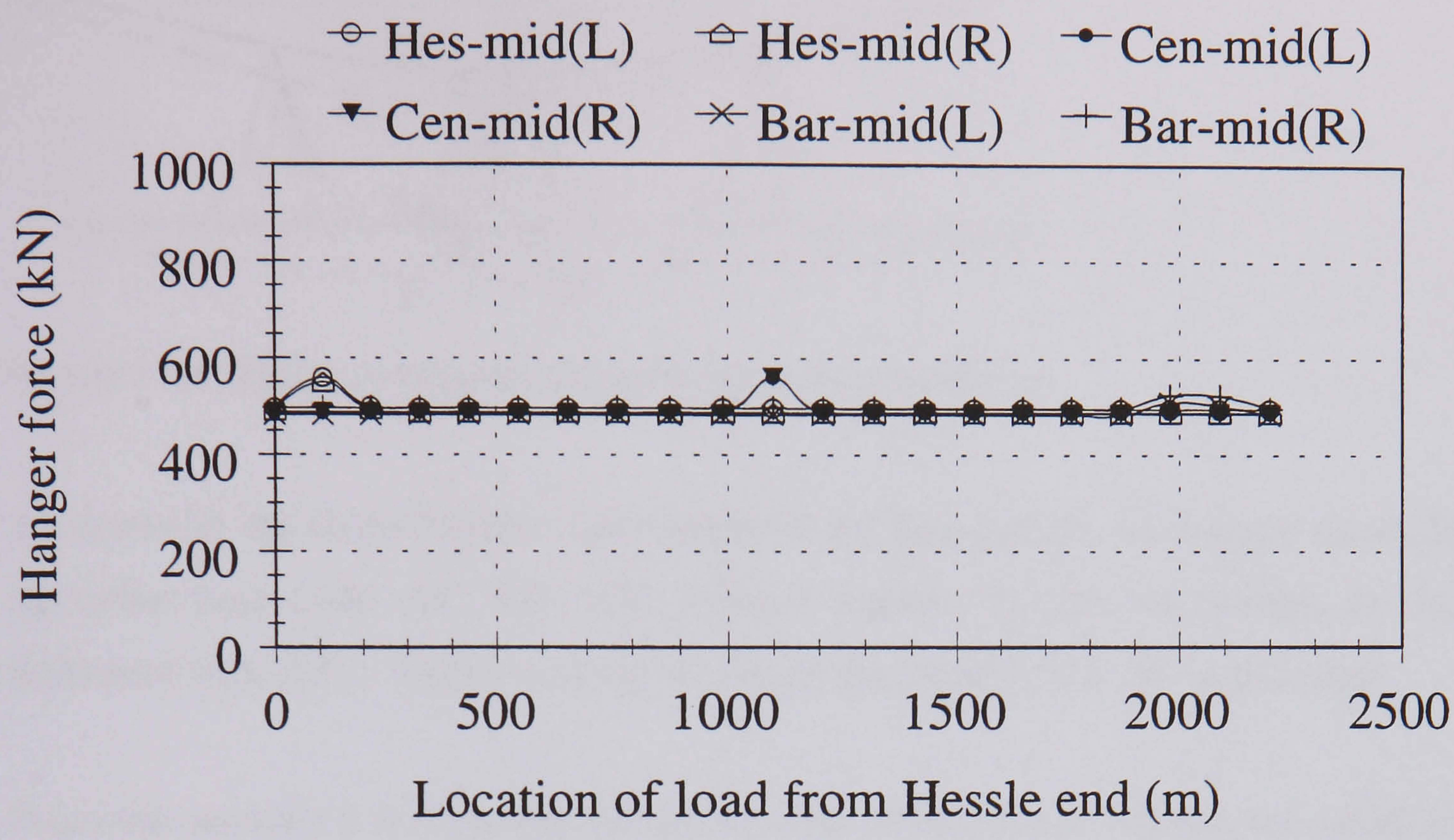

Figure 11s2: Mod 3 hanger model (lower element)

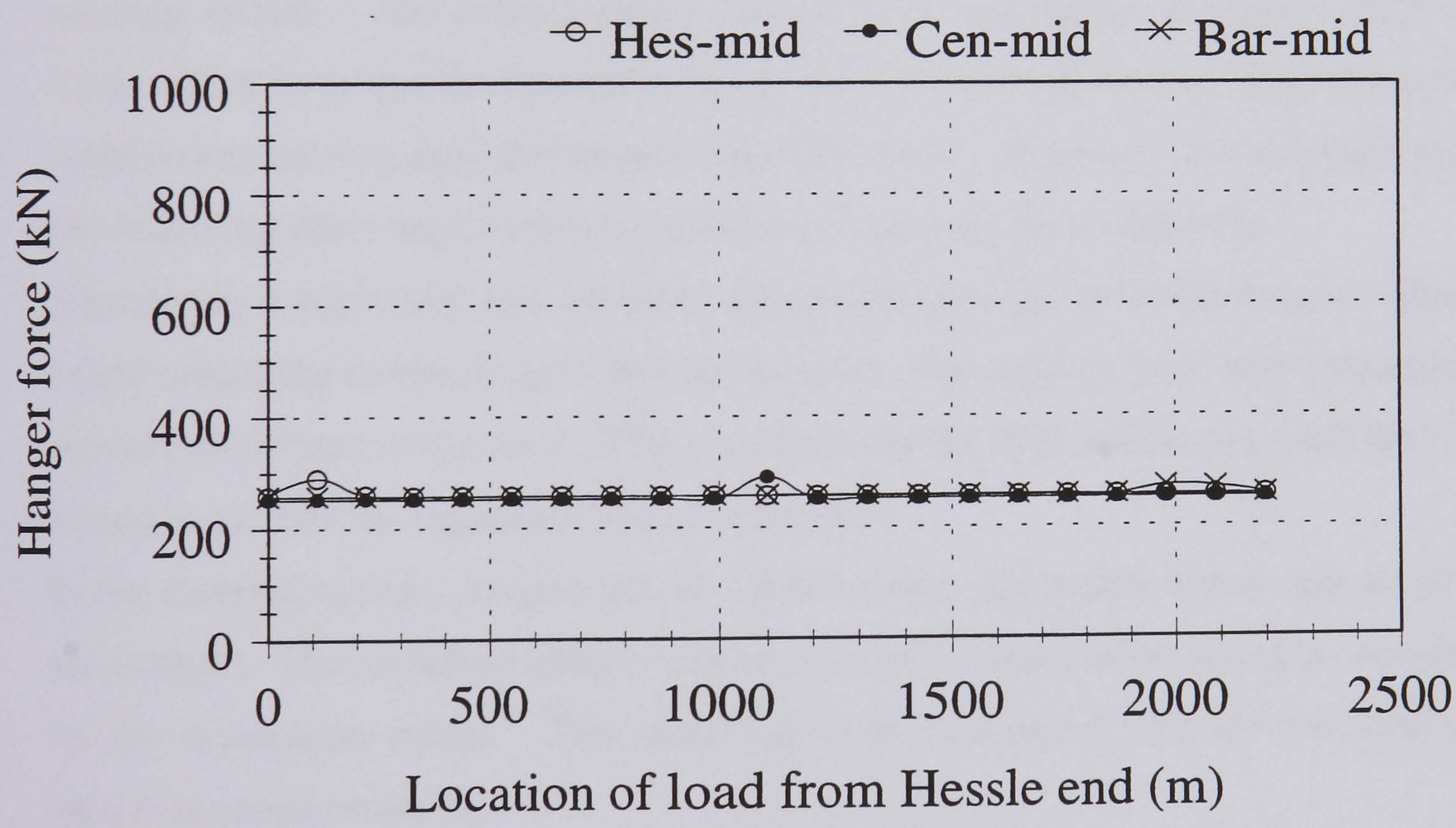

Figure 11s3: Mod 3 hanger model (link element)

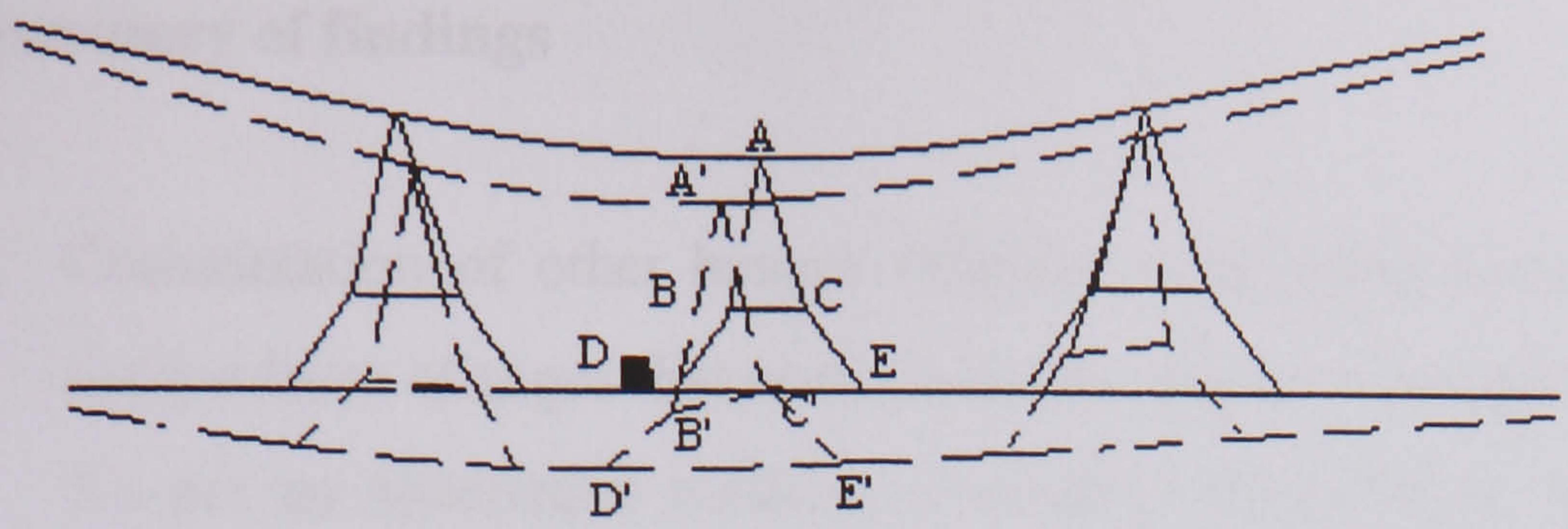

Figure 11s4: Mod3 system model under point load condition

As shown in the above Figure 11s4, unlike the existing system, the hangers closer to the point load (AB, AC, BD, CE) strained together by the introduction of the horizontal link (BC). There is no shortening of the hangers from the initial stage.

From this analysis it is clear that hanger systems other than the existing one could be more effective in minimising hanger load variation.

The hanger system showed that in Figure 11e (Mod3) is easily convertible from the existing system. The corresponding hanger forces are shown in Figures 11s1 to 11s3, which have less fluctuation of forces than the existing system. This is a good solution considering only the hanger force fluctuation. However, it is necessary that the following other requirements would have to be analysed extensively.

Introducing a horizontal link between adjacent hangers on the Mod3 hanger system might reduce the hanger length between the main cable and the deck, but could cause upward movement of the deck. This would change the deck profile and could lead to a need to modify the expansion joints on the deck.

In the existing system, hangers are designed to carry the tensile stress only as they are straight. The modified system creates additional compressive and shear stresses on the connection points. This issue has to be considered with the selection of hanger material property.

Increasing the cross section area of the deck (to increase the overall stiffness of the structure) might increase the tension on the main cable, ending up with need for modification on the main cable and the anchorage chamber.

Summary of findings

- Consideration of other hanger systems is initiated because of the considerable hanger force changes that occur between adjacent hangers in the existing system. To get an alternative solution a number of different hanger systems such as vertical, vertical with inclined and inclined hangers with horizontal link were introduced.
- Except for the existing inclined hanger system the others give comparatively less change in forces between adjacent hangers.
- Vertical defection at mid and quarter of the main span due to a moving heavy lorry load (120 tonnes) for all the different hanger system models are the same due to same effective cross sectional area and hanger initial strain value.
- Natural frequency values and mode shapes have been compared between each model. The existing inclined hanger systems have higher vertical and torsional natural frequency values. This reflects that the inclined system has a comparatively higher stiffness value than others.
- The main cable force does not show any significant change along the bridge due to the introduction of different hanger systems.
- Under uniformly distributed loaded condition (BSALL, dead or wind) the existing system shows a very high change of hanger forces along the bridge compared with the other systems. In fact the changes of hanger forces on the other systems are comparatively negligible.
- Hangers at Hessle, Barton and central main span for a moving lorry load show a relatively high fluctuation of forces for the existing system. Similarly hangers for the existing system at other places produces a force fluctuation with the moving lorry load. Comparatively other hanger systems produce very low fluctuation of forces.
- Among the suggested systems (vertical, mod1, mod2 and mod3), the mod3 hanger system (with the introduction of horizontal link) is the more feasible to change from the existing system.
- Compared with these suggested systems the fluctuations of forces are low for the mod3 hanger system under the uniformly distributed load and the point load

conditions. This system is considered as the quickest to incorporate and needs less material and manpower than the others.

- Most of the newly built suspension bridge structures have vertical hanger systems in place. Comparatively low fluctuation of hanger forces and easy installation are the main reasons. Changing the existing hanger system of the Humber Bridge to vertical hanger system would cause high consumption of material and manpower. Closure of the bridge for a long period would be unavoidable.
- Extra caution is needed (for the mod3 hanger system) at the connection point where the horizontal link is joining the hangers from the adjacent brackets. In addition to the tensile stress, compressive stresses are also possible at these points so that the material properties of the hanger would have to be reassessed.
- Introduction of this new mod3 hanger system might change the main cable and the deck profile as the hanger length between the main cable and the deck changes (due to the introduction of horizontal link). As a result, the behaviour of the expansion joints on the deck would have to be reassessed.

Chapter 12

Conclusions & Future Work

i) Conclusions

1. Three finite element models have been developed as part of this research and demonstrated as being capable of making accurate predictions of the structural behaviour of the Humber Bridge.
2. Through the analysis of these models it is possible to develop predictive tools enabling bridge owners to maximise their income by maintaining the bridge in an in-service state whilst maintenance/repair work is carried out. For example hanger removal can be done without affecting the day to day traffic.
3. Of the three models, the 2-D plate formulation model is appropriate to situations in which it is preferable to analyse the symmetrical loading condition and the necessity of only vertical mode shapes and associated natural frequency values. Also it will save computer-running time. The only limitation is, if hangers start to slacken they act as compressive members as the spar element which is representing the hanger does not have the tension only capability.
4. Of the three models, the 3-D plate formulation model is appropriate to situations in which it allows symmetrical and asymmetrical loading, and produces vertical and laterals mode shapes and associated natural frequency values. As the element representing the hanger has tension only capability, it will detect the slack hangers and make them ineffective.
5. Of the three models, the 3-D box formulation model is appropriate to situations where it will accommodate symmetrical and asymmetrical loading. In addition to that it will accommodate the wind load. Also it will produce torsional mode shapes and associated natural frequency values of the bridge accurately. Stress levels on the deck and on the stiffeners can be produced precisely for different load cases.
6. Each model may be analysed cost-effectively on a moderately powered PC and each is sufficiently user-friendly to enable the engineer to begin to use

them and understand the implications of any planned activity his duties may require.

7. The models created facilitate rapid structural appraisal with revised loading conditions after accidents. For example damage caused by a vehicle hitting the hanger bracket or a minor explosion on the edge of the carriageway might damage the hanger bracket and the hanger connections.

8. The models allow investigation of various "what if" scenarios, for example breakdown of a number of hangers during traffic flow. Models assist with decisions regarding traffic management in unusual circumstances as well as being an important maintenance tool. For example closure of a lane due to unavoidable circumstances.

9. Geometrically non-linear large deformation analysis has been adopted throughout the research. Comparison of results (deflection) between small deformation and large deformation analysis shows a measurable difference. This reflects the importance of non-linear large deformation analysis.

10. Five separate models (including the existing hanger system) were created with different hanger system styles to understand the difference of behaviour of the structure. Performance on the existing structure regarding hanger force was noted, which gave higher fluctuation of forces between adjacent hangers due to a moving load. For the uniformly distributed loading again changes in forces were found between adjacent hangers in the existing inclined hanger system model.

11. Alternative hanger systems were introduced where the fluctuation of forces between adjacent hangers due to a moving load and changes in hanger forces due to uniformly distributed loading were eliminated. The most feasible one can be selected out of the five models without the need for a long closure of the bridge.

12. The sensitiveness of each major component on the bridge structure was analysed with the influence of self-weight. Self-weight of the structure was selected as the major loading because the main load carrying component, the main cable carries 80 % of its design load. Also this loading condition gives a general view on component sensitiveness for a particular point load or uniformly distributed load.

13. The main cable and the deck are found to be the most sensitive structural components. These components easily change the profile of the main cable and the deck and subsequently they will change the behaviour on other components like hangers, towers and A-frames.

14. The diameter of the main cable is the most sensitive parameter. Decreasing the main cable diameter has 2.3 times higher effect on the deck and the main cable profile than increasing the main cable diameter by the same percentage of change.

15. The initial strain value of the main cable is the next sensitive parameter. Then comes the deck thickness (keeping the stiffness as constant) in the order of the most sensitive parameters.

16. Sensitivity rating based on the changing deck and the main cable profile can be given as follows:
    a) decreasing the diameter of the main cable is the most sensitive factor,
    b) then the changes of the initial strain value of the main cable,
    c) increasing the diameter of the main cable is next,
    d) and finally the deck thickness is the fourth sensitive factor.
    e) changes on the hanger and the tower parameters do not have much effect on the overall profiles.

17. The sensitivity rating based on the movement of the tower top depends on changing the profile of the main cable and the deck. Moving the main cable profile upward from its initial position gives outward movement of the tower tops from the main span. Consequently downward movement of the main cable profile from its initial position gives inward movement of the tower tops with respect to the main span. Changing hanger and tower parameters does not have any significant effect on tower top movements.

18. The sensitivity rating based on slack hangers again shows that the main cable diameter, the main cable initial strain value and the deck thickness (keep stiffness as constant) are the significant parameters to consider. Increasing or decreasing any one of these parameter values beyond 20 % from its initially assumed value starts to produce slack hangers.

19. The hanger initial strain, followed by the hanger diameter are the less sensitive parameters to consider with regard to the response of the main cable, the deck and the tower top movement.

20. The tower cross sectional area and the stiffness of the tower are the least sensitive parameters under the assumed self-weight condition.

21. Models have been validated under dead load condition where acceptable deflected profiles were obtained. Under the same dead load condition the main cable and the hanger forces at key locations were compared with the Humber Bridge designer's calculation report. The results show that the models coincide well with the designer's predictions.

22. The first load test (single lorry load, displacement measurement on the site) gives the same pattern of displacement vs. time curves at the middle and quarter span location of the main span for the measured and FE analysis results. Adjusting the applied lorry load from 170 tonnes to 120 tonnes on the model produces the same magnitude of deformation as the field measurements. This gives confidence that the passage of the single lorry load was 120 tonnes.

23. The second load test (passage of five 32 tonnes lorry load, GPS measurements) gives very close agreement on deflection vs. time curves at three locations including mid and quarter of the main span and the mid of the Barton span. This gives confidence on distribution of stiffness and masses along the bridge structure.

24. The natural frequency values and the associated mode shapes give good correlation between measured and FE analysis results. The vertical, lateral and torsional mode shapes and the natural frequency values on the field measurements compared well with the corresponding FE analysis results. This confirms the vertical, lateral and torsional stiffness on the structure are modelled well. In addition it also confirms the mass distribution along the structure.

25. Models have been used to assess the structure under different critical loading conditions, for example extreme wind, traffic and temperature loading conditions. In addition to that, the models can be used as a traffic management tool where any maintenance work can be done with greater confidence.

26. Some specified load cases were created according to the Humber Bridge Board's requirement to assess the A-frame capabilities. Load cases includes revised BSALL asymmetric (alternative lane loaded and/or alternative span

loaded) loading and concentrated loading (HB loading: 180 tonnes) to create maximum tensile and compressive forces on the A-frame members.

27. The reviewed loading (BSALL) condition has been applied to the bridge model with wind, temperature and HB loading and the structural components have been assessed, and the stability of the structure ensured.

28. There were no slack hangers found under revised BSALL loading condition and also all the forces are well within the design limit.

29. As in the original design, the wind and temperature loads are applied to the bridge model and the forces and displacements were found; these values are within the expected limits.

30. To assess the A-frame members, specified load cases were applied to get the maximum compressive and tensile forces according to BSALL uniformly distributed loaded condition and combination of BSALL and BD37/88 HB loaded condition. Results are found to be well within the design limit.

31. Removal of hangers was analysed with a number of loading situations such as with traffic HA and HB loading, wind and temperature. The stability of the structure was determined for a maximum possible removal of hangers.

32. The maximum possible number of hanger removals was found with an all-span loaded BSALL case. To get a failure envelope, the hanger carrying the maximum force was removed, and then the adjacent hanger which carried the current maximum force was removed. The results indicate that a maximum of two hangers can be removed anywhere in the bridge structure still ensuring its safety under the mentioned all span loaded BSALL condition.

33. The existing hanger system gives considerable hanger force changes (fluctuation) between adjacent hangers with uniformly distributed loading and point-loaded conditions.

34. To get an alternative solution a number of different hanger systems such as vertical, vertical with inclined and inclined hangers with horizontal link, were introduced. Except for the inclined hanger system (which is the one in use) the others give comparatively less change in forces (fluctuation) between adjacent hangers.

35. Vertical deflection at mid and quarter of the main span due to a moving heavy lorry load (120 tonnes) for all different hanger system models are the

same due to the hangers having the same effective cross sectional area and hanger initial strain value.

36. Natural frequency values and mode shapes have been compared with each model. The inclined hanger system has higher vertical and torsional natural frequency values. This reflects that the inclined system has comparatively higher stiffness value than the others.

37. The main cable force does not undergo significant change along the bridge due to the introduction of a different hanger system. Self-weight of the structure is predominant to decide the magnitude of the main cable force.

38. Under uniformly distributed loaded condition (BSALL, dead or wind) the existing system shows a very high change of hanger forces along the bridge compared with the other systems. The changes of hanger forces on the other systems are comparatively negligible.

39. Hangers at the middle of each span for a moving lorry load produce relatively high fluctuation of forces for the existing system. Similarly hangers along the bridge in other places also produces force fluctuation with the moving lorry load. Comparatively, alternative hanger (except the existing one) systems produce very low fluctuation of forces for the moving lorry load.

40. Among the suggested systems, the mod3 hanger system, which has the introduction of a horizontal link, is more feasible to change from the existing system. It needs less pre-arrangement on the site and can be done with less or no bridge closure period of time.

41. Compared with these suggested systems the changes of hanger forces are low for the mod3 hanger system under uniformly distributed load and point load conditions. Extra caution is needed (for the mod3 hanger system) at the connection point where the horizontal link is joining the hangers from the adjacent brackets. In addition to the tensile stress, compressive stresses are also possible at these points so that the material properties of the hanger have to be reassessed.

42. Introduction of this new mod3 hanger system might change the main cable and the deck profile as the hanger length between the main cable and the deck changes (due to the introduction of a horizontal link). Also the behaviour of the expansion joints on the deck would have to be reassessed.

ii) Future work

Continuous monitoring of the traffic intensity for finding the revised BSALL condition is extremely important. From Figure 11i, the present minimum hanger force value due to a full span BSALL loaded condition is 11 kN. Increasing the BSALL value in the future or the traffic intensity will decrease the minimum hanger force value. This reduction of hanger force will end up with slacking of hangers at the middle of the main span region. This slacking gives a potentially adverse effect to the lifetime of the hanger and the hanger bracket. A hanger becoming slack can lead to localised bending, which would cause compressive stress on that location and might lead to failure. Possible lane restriction may need to be applied in the future depending on the increase of the traffic intensity.

Alternatively the previously mentioned mod3 hanger system styles could be introduced. Assurances have to be made in connection with the hanger material property as compressive stress may occur at the connection point. The profiles of the deck and main cable have to be considered due to possible changes of hanger length.

Passage of the increased concentrated point load on the existing system will increase the fluctuation of the hanger force. As mentioned before this will give adverse lifetime effect to the hangers and the hanger brackets. Again the previously mentioned modified hanger system (mod3) is appropriate to resolve this problem.

Fatigue lifetime of the hangers and the hanger brackets has to be analysed. As hangers undergo fluctuation of forces this would be useful research. This research can be done with the expected percentage of increment of the BSALL value over a number of years. Also an increasing percentage of heavy vehicles passing has to be considered.

To understand the local effect on the deck, forced vibration analysis due to vehicle movement (engine vibration, bouncing movement, etc.) has to be considered. This will lead to analysis the deck behaviour with respect to fatigue.

References

Ammann O, et. al. (1941) March, The Failure of the Tacoma Narrows Bridge, *Report to the Federal Works Agency*, USA.

ANSYS (1995), *User's Manual for Revision 5.0*, Swanson Analysis Systems inc., Houston, U.S.A.

Atkinson RJ and Southwell RV (1939), On the problem of stiffened suspension bridges and its treatment by relaxation methods, *Journal of Institute of Civil Engineers*, Vol. 11.

Bleich F, McCullough CB, Rosecranz R and Vincent GS (1950), The Mathematical Theory of Vibration in Suspension Bridges, *Bureau of Public Roads*, Washington, USA.

Brown CJ, Karuna R, Ashkenazi V, Robert GW, Evans RA (1999) February, Monitoring of structures using the Global Positioning System, *Proceeding of the Institute of Civil Engineers UK, Structures and Buildings*, Vol 134.

Brownjohn JMW, Dumanoglu AA, Severn RT, Taylor CA (1986), Ambient vibration survey of the Humber Suspension Bridge, Report No: UBCE-EE-86-2, Department of Civil Engineering, University of Bristol.

Brownjohn JMW, Bocciolone M, Curami A, Falco M and Zasso A (1994), "Humber Bridge full-scale measurement campaigns 1990-1991", *Journal of Wind Engineering and Industrial Aerodynamics*, Vol. 52.

BS 153, Part 3A (1954), Loading code for the steel girder bridges.

BS 5400, Part 2 (1978), Loading code for the steel, concrete and composite bridges.

Burdet, OL and Corhay S (1995) August, Dynamic load testing of Swiss bridges, *IABSE Symposium Extending the Life span of Structures*, San Francisco, USA.

Correspondence (1997), Thoughts on the structural efficiency of cable-stayed and catenary suspension bridges, *The Structural Engineer*, Vol 75/ No19.

CP3, Chapter V, Part 2 (1972), Code for the wind loading on structures.

Croll JGA (1997), Thoughts on the structural efficiency of cable-stayed and catenary suspension bridges, *The Structural Engineer*, Vol 75/ No10.

Departmental Standard BD 37/88 (1989), Loads for Highway bridges, The Department of Transport, Highways and Traffic.

Dredge J (1843), Mathematical demonstration of the principles of Dredge's patent iron bridges, Mechanics Magazine.

Eurocode 1 (1995) March, Basis of design and actions on structures – Part 3: Traffic loads on bridges.

Fairhurst & Partners and Humber Bridge Board, (1995) April, Structural assessment of the Humber Bridge, (internal).

Farquharson FB (1949), Aerodynamic Stability of Suspension Bridges, Bulletin 116, University of Washington, USA.

Fisher D (1982) 5 September, Design and construction of the Humber Bridge, Physics Education, No: 17, Institute of Physics Publishing Ltd., UK.

Frazer RA and Scruton CA (1952), Summarized Account of the Severn Bridge Aerodynamic Investigation, H.M.S.O.

French MJ (1994), On the minimum volume of material in temperature-compensating devices, *Journal of Mechanical Engineering Science*, ImechE.

Geographical Journal (1942) August, The Indian Geographical Society, India.

Gimsing NJ (1983), Cable supported bridges, concept and design, John Wiley & Sons, New York, USA.

Goller R (1965) October, The Legacy of 'Galloping Gertie' 25 Years After, Civil Engineering.

Homberg H (1982) 15 April, The case against inclined hangers, *New Civil Engineer.*

Humber Bridge Board (1973), Document of Cable and Suspended Structure, Tender drawings (internal).

Humber Bridge Board (1971), Design Data (internal).

Koughan J (1996) August, The Collapse of the Tacoma Narrows Bridge, Evaluation of Competing Theories of its Demise, and the Effects of the Disaster of Succeeding Bridge Designs, Department of Mechanical Engineering, The University of Texas at Austin, USA.

Maxwell JC (1964), Scientific papers, Vol. 2, Cambridge University press, UK.

Melan J (1888), Theorie der eisernen Bogenbrucken und der Hangerbrucken, Handbuch der Ingenieurwissenschaften, Leipzig, 2nd edition. (Theories of Iron Arched Bridges and Hanging Bridges, Manual of Engineering Sciences).

Melan J (1906), Theorie der eisernen Bogenbrucken und der Hangerbrucken, Handbuch der Ingenieurwissenschaften, Leipzig, 3rd edition.

Millar MA and Al-Khalili MA (1988), Suspension bridge inclined hangers, *Structural Engineering Review*, Chapman & Hall Ltd.

Moaveni S (1999), Finite element analysis- Theory and application with ANSYS, Prentice-Hall, Inc., New Jersey, USA.

Moisseiff IS and Lienhard, F (1932), Suspension Bridges under the action of lateral forces, *Proceeding of American Society of Civil Engineers.*

Mott MacDonald (1997), Review of the BSALL on the Humber Bridge structural elements, The Humber Bridge Board (internal).

NAFEMS (1992), A finite element primer, NAFEMS, Glasgow, UK.

Navier (1823), Memoire sur les ponts suspendus, Societes savantes toulouse asso., France. (Memories of Suspension Bridges).

News (1982) 15 April, Research backs hanger corrosion theory, *New Civil Engineer.*

News (1982) 18 November, Severn report lists wide ranging weaknesses, *New Civil Engineer.*

News (1982) 3 November, Severn fears grow with 'sudden collapse' warning, *New Civil Engineer.*

Pippard AJS and Baker JF (1936), The analysis of Engineering Structures, 1st edition, Edward Arnold (Publishers) Ltd., London, UK.

Pugsley A (1958), The theory of suspension bridges, Edward Arnold (Publishers) Ltd., London, UK.

Rankine WJM (1858), A Manual of applied mechanics, 3rd edition, Charles Griffin & Co, London, UK.

Robins WF (1948), The story of the bridge, Cornish Bros. Publishers, Birmingham, UK.

Ross S, et. al. (1984), Tacoma Narrows, 1940, Construction Disasters, 1st edition, McGraw-Hill Book Company, New York, U.S.A.

Scanlan R and Jones N (1990), A Minimum Design Methodology for Evaluating Bridge Flutter and Buffeting Response, *Journal of Wind Engineering and Industrial Aerodynamics*, Vol. 36.

Schlager N (1994), Tacoma Narrows Bridge Collapse, When Technology Fails: Significant Technological Disasters, Accidents, and Failures of the Twentieth Centruy, First Edition, Detroit: Gale Research Publishers.

Sibly P and Walker A (1977) May, Structural Accidents and Their Causes, *Proceedings of the Institution of Civil Engineers*, vol. 62, Part 1.

Southwell RV (1940), Relaxation Methods in Engineering Science, Oxford University press, UK.

Steinman DB (1913), Suspension Bridges and Cantilevers, D. Van Nostrand Publishers.

Stephen GA, Brownjohn JMW and Taylor CA (1993), "Measurements of static and dynamic displacement from visual monitoring of the Humber Bridge", *Engineering Structures*, Vol.15/No 3.

The Humber Bridge Board (1981), Engineering The Humber Bridge, Hillingdon Press, Uxbridge.

The Humber Bridge Board (2001), Traffic & Toll Information, Web page for the Humber Bridge.

Timoshenko S (1928), The Stiffness of Suspension Bridges, *Proceeding of American Society of Civil Engineers*.

Timoshenko SP (1943) March, Theory of suspension bridges, *Journal of the Franklin Institute*, Vol. 235/No 3.

Bibliography

Abdul-Gaffer AM (1994) 12-15 October, Seismic behaviour of Cable-stayed and Suspension bridges, Cable stayed and suspension bridge, *International conference A.I.P.C.- F.I.P*, Deauville, France.

Arzoumanidis SG and Bieniek MP (1985), Finite element analysis of suspension bridges, *Computer & Structures*, Vol. 21/No 6.

Beard S (1995) March, Tsing Ma bridge, Hong Kong, *Structural Engineering International.*

Buchholdt H (1997), Structural dynamics for engineers, Thomas Telford Publication, London, UK.

Das PC (1997), Safety of bridges, Thomas Telford Publication, London, UK.

Encyclopaedia Britannica (2001).

Farrar CR and Duffey TA (1995) August, Evaluation of a bridge using simplified finite element modelling, *IABSE Symposium Extending the Life span of Structures*, San Francisco,USA.

Gimsing NJ (1987) November, Parametric studies of the cable stayed bridges with extreme spans, *International conference on cable stayed bridges*, Bangkok, Thailand.

Gimsing NJ (1999), Cable-Stayed Bridges - Past, Present and Future, *IABSE Conference*, Malmoe.

Gimsing NJ (1994) 12-15 October, Suspension bridges with very long spans, Cable stayed and suspension bridge, *International conference A.I.P.C.- F.I.P*, Deauville, France.

Hitchings D (1992), A finite element dynamic primer, NAFEMS, Glasgow, UK.

Hobbs, HR (2000) January, Puente Duarte Suspension Bridge Strengthening, *The Structural Engineer*, Vol 78/ No 1.

Homberg H (1964), Progress in German steel bridge construction, Report on steel congress of the high authority of the European Economic Community.

Karoumi R (1999), Some modeling aspects in the non-linear finite element analysis of cable supported bridges, *Computer and Structures*, Vol.71.

Kazama K, Yamada H and Miyata T (1995), Wind resistant design for long span suspension bridges, *Journal of Wind Engineering and Industrial Aerodynamics*, Vol. 54/55.

Ketchum MA and Cheng KM (1994) 12-15 October, Seismic analysis and behaviour of three major western-U.S. suspension bridges, Cable stayed and suspension bridge, *International conference A.I.P.C.- F.I.P*, Deauville, France.

Ko JM, Ni YQ and Chan THT (2000), Feasibility of damage detection of Tsing Ma Bridge using vibration measurements, *Proceedings of SPIE - The International Society for Optical Engineering*, v 3995, p 370-381.

Larsen SV and Gimsing NJ (1994) 12-15 October, Static and dynamic behaviour of cable supported bridge with small-width-to span ratios, Cable stayed and suspension bridge, *International conference A.I.P.C.- F.I.P*, Deauville, France.

Maguire J (1994) 12-15 October, Validation of structural models, Cable stayed and suspension bridge, *International conference A.I.P.C.- F.I.P*, Deauville, France.

Mason P, Kumar A (1994) 12-15 October, Large deflection analysis of clifton suspension bridge, Cable stayed and suspension bridge, *International conference A.I.P.C.- F.I.P*, Deauville, France.

Mehrkar-Asl S and Brookes CL (1996) July, Load testing in bridge assessment, *Joint IstructE/City University International seminar*, City University, London, UK.

Morisset A (1994) 12-15 October, Large displacement analysis applied to cable-stayed and suspension bridges, Cable stayed and suspension bridge, *International conference A.I.P.C.- F.I.P*, Deauville, France.

Ohshima H Sato K and Watanane N (1984) March, Structural analysis of suspension bridges, *Journal of Engineering Mechanics*, Vol. 110/No 3.

Paolo C, Giulio N and Aldo R (2000) December, Preliminary design of very long-span suspension bridges, *Engineering Structures*, v 22, n 12, p 1699-1706.

Paultre P and Proulx J (1997) January, Dynamic testing of large-scale structures, *Structural Engineering International.*

Pritchard B (1997), Bridge modification 2- Stronger and safer bridges, Thomas Telford Publication, London, UK.

Roberts GP and Pearson AJ (1996), Dynamic monitoring as a tool for long span bridges, *Bridge Management 3*, Published by E & FN Spon.

Saafan SA (1965) August, Theoretical analysis of suspension bridges, *Journal of the Structural division*, Proceeding of American Society of Civil Engineers.

Semper A (1993), A Mathematical Model for Suspension Bridge Vibration, *Mathematical Computer Modeling*, Vol 18/No 11.

Shun-ichi N (2000) December, GPS measurement of wind-induced suspension bridge girder displacements, *Journal of Structural Engineering*, v 126, n 12, 1413-1419.

Taly N (1998), Design of modern highway bridges, The McGraw-Hill companies, Inc.

Ulstrup CC (1995) September, Rating and preliminary analysis of suspension bridges, *Journal of Structural Engineering*, Vol. 119/No 9.

Ventura CE, Felber AJ, Prion HGL, Taylor PR and Selst AV (1995) August, Dynamic characteristics of Port Mann bridge by modal testing, *IABSE Symposium Extending the Life span of Structures*, San Francisco, USA.

Wahab MA and Roeck GD (1997) April, Effect of temperature on dynamic system parameters of a highway bridge, *Structural Engineering International.*

Yozo F, Masanobu M, Satoshi O and Masahiro T (2000), Monitoring system of the Akashi Kaikyo Bridge and displacement measurement using GPS, *The International Society for Optical Engineering*, v 3995, p 229-236.

Zhang QW, Chang CC and Chang TYP (2000) July, Finite element model updating for structures with parametric constraints, *Earthquake Engineering and Structural Dynamics*, v 29, n 7, 927-944.

Zienkiewicz OC (1986), The finite element method, 3rd edition, McGraw-Hill book company Ltd., UK.

Appendices

Appendix 1

Comparison of material efficiency

a) Classical approach

Classical approach (Croll, 1997) and Maxwell's Lemma approach (Correspondence, 1996) are followed to compare the material efficiency of the suspension and cable-stayed bridges.

i) Suspension Bridge

Suspension bridge is considered first with the main span length of l with the tower height of h above the ground level and the hanger spacing of s, as shown in Figure 1A1.

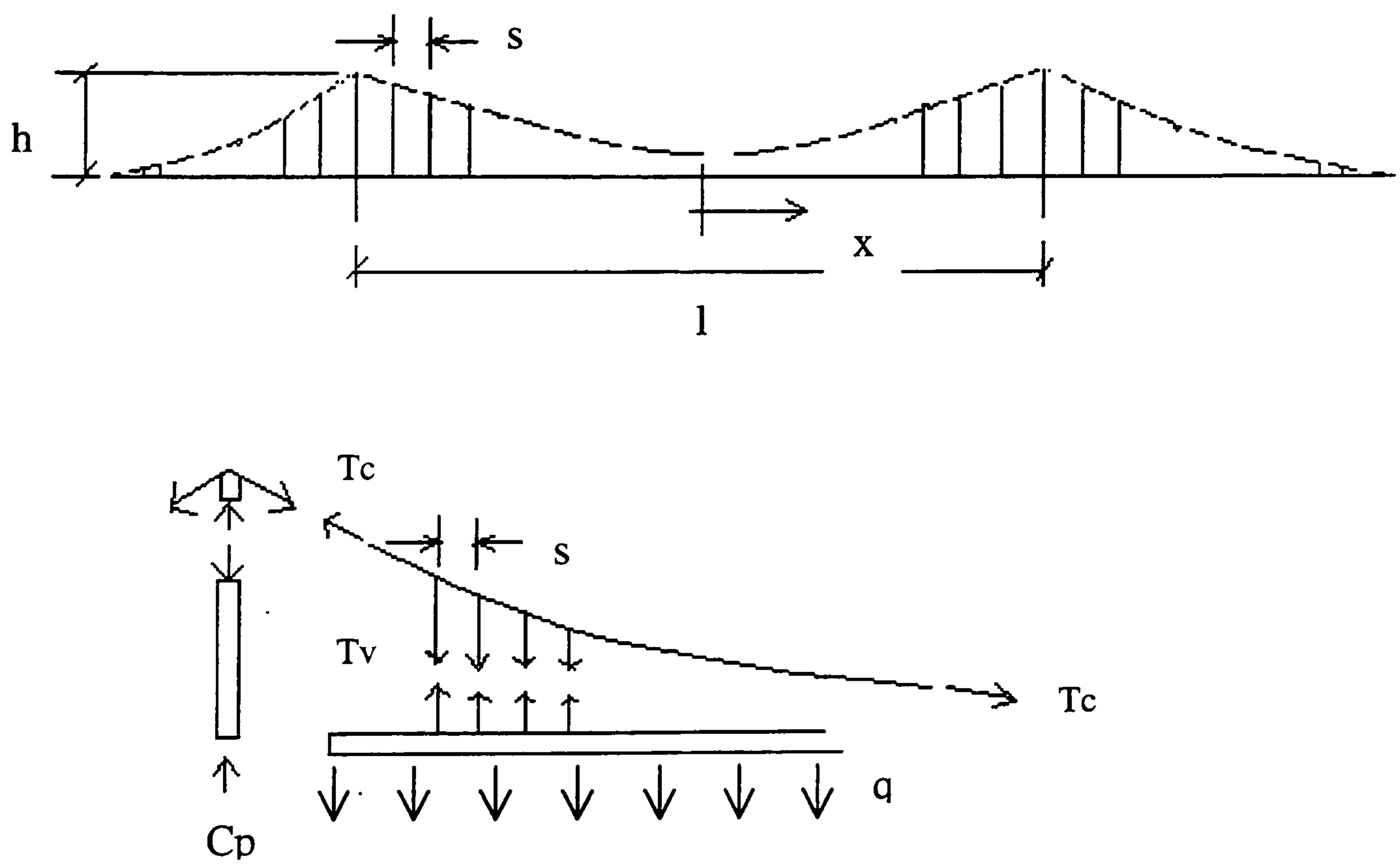

Figure 1A1

The tension on the hanger is Tv, given by $Tv = sq$ and it is reasonable to consider the area under the parabolic main cable has the uniform tension field of q.

Volume of vertical hanger cable for tower height above deck h, spacing between hangers s, uniformly distributed loading intensity of q and steel characteristic tensile strength σt given by the equation $Vv = \frac{1}{3} hl \frac{q}{\sigma t}$.

The tension on the main cable at a point x can be given as,

$Tc(x) = \left(\frac{ql^2}{8h}\right)\left(1+\left(\frac{8hx}{l^2}\right)^2\right)^{\frac{1}{2}}$. And the volume of steel required can be given with an integration of cross sectional area $A(x)$ with ds, $Vc = \int_{\frac{-l}{2}}^{\frac{l}{2}} A(x).ds$,

where $A(x) = Tc(x)/\sigma t$.

So that the volume of main cable after integration, $Vc = \frac{ql^3}{8h\sigma t}\left(1+\frac{16}{3}\left(\frac{h}{l}\right)^2\right)$

Each tower has the compressive force of $ql/2$, compressive strength σc, the volume above the deck level (since it same for both bridge below the deck level) can be given as

$$Vt = 2\frac{ql}{2\sigma c}h$$

So that the Volume of tower for a characteristic strength of σc, $Vt = \frac{qlh}{\sigma c}$

This gives a total primary steel volume for a suspension bridge of

$$Vsus = \left(\frac{qhl}{\sigma t}\right)\left[\frac{1}{3}+\left(\frac{2}{3}+\frac{1}{8}\left(\frac{l}{h}\right)^2\right)+\frac{\sigma t}{\sigma c}\right]$$

ii) Cable-stayed Bridge

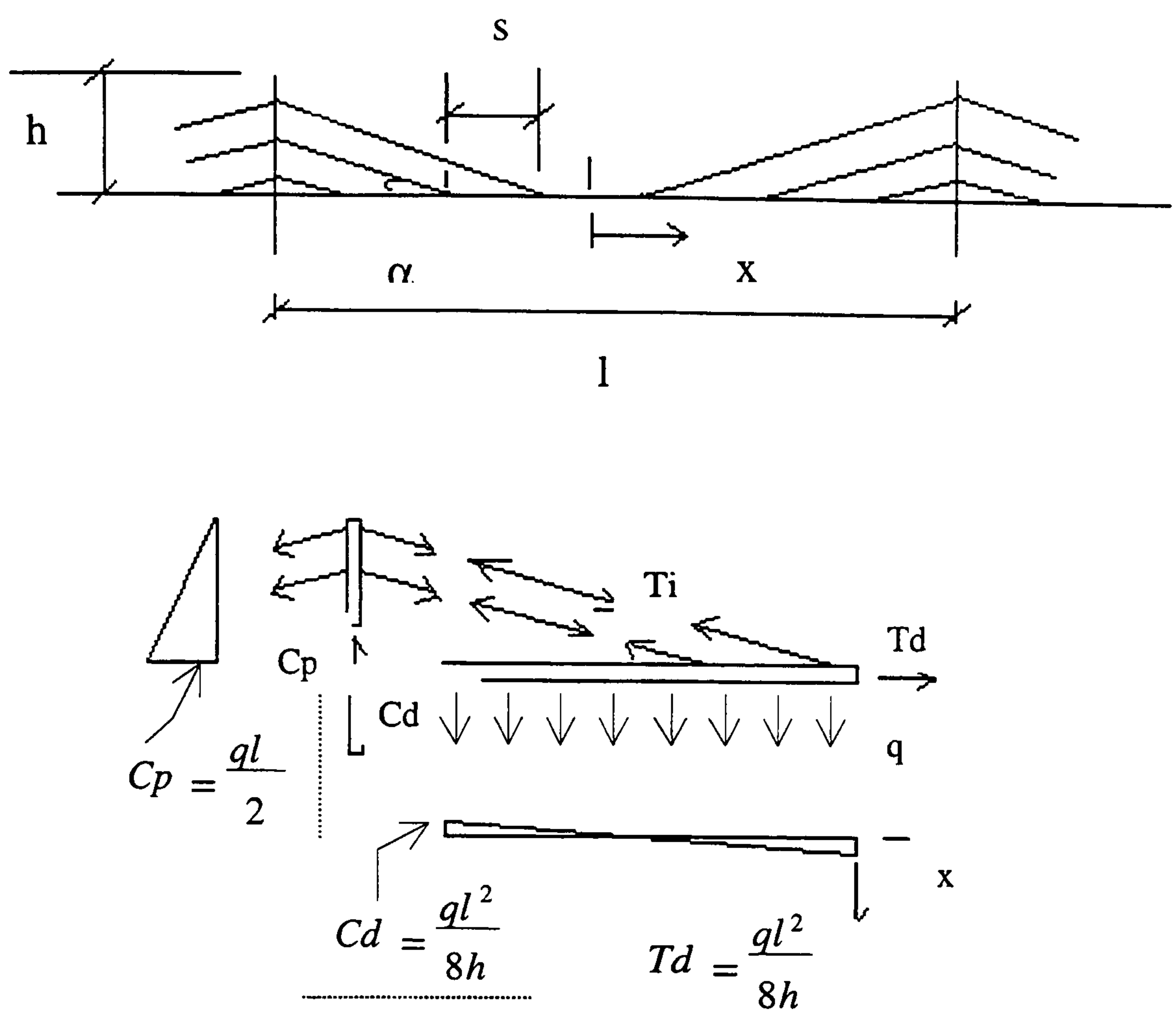

Figure 1A2

The cable-stayed bridge is considered as like the suspension bridge with the main span length of l and the tower height above the deck is h. Parallel inclined hangers are arranged at a horizontal spacing of s, as shown in Figure 1A2.

As shown in the above figure within half of the span ($l/2$), the horizontal component is given by $Ti \cos\alpha$, where $Ti = qs/\sin\alpha$. Solving this bring the tensile and compressive forces on the deck Td and Cd equals to $ql^2/8h$.

For a cable-stayed bridge keeping the same overall dimensions, with parallel inclined hangers at horizontal spacing of s and angle of inclination α, the volume of inclined cable $Vi = \frac{1}{2}(hl)\left(\frac{q}{\sigma t \sin^2 \alpha}\right)$

The deck tension for the range of $0<x<l/4$ can be given as, $Td = \frac{ql^2}{8h}\left(1 - 4\frac{x}{l}\right)$

The deck compression for the range of $l/4<x<l/2$ can be give as, $Cd = \frac{ql^2}{8h}\left(4\frac{x}{l}-1\right)$

Volume of the deck can be found with $Vd = \int A(x).ds$, where $A(x) = Tc(x)/\sigma t$ for the range of $0<x<l/4$ and $A(x) = Tc(x)/\sigma c$ for the range of $l/4<x<l/2$.

So that the material required to develop these primary tensile and compressive forces on the deck, $Vd = \frac{ql^3}{32h}\left(\frac{5}{\sigma t}+\frac{1}{\sigma c}\right)$

Each tower has the average compression force of $ql/2$

So that the average cross section area of the tower is given by $\frac{ql/2}{\sigma c}$

Compression steel volume required for tower $Vp = \frac{qlh}{2\sigma c}$

So, total volume of steel required for cable-stayed bridge

$$Vcab = \frac{qhl}{\sigma t}\left[\frac{1}{2\sin^2\alpha}+\frac{1}{32}\left(\frac{l}{h}\right)^2\left(5+\frac{\sigma t}{\sigma c}\right)+\frac{1}{2}\left(\frac{\sigma t}{\sigma c}\right)\right]$$

When compare the material efficiency (total volume of steel) of both bridges with the assumption of $\sigma c = \frac{2}{3}\sigma t$, the equations can be simplified in the following forms.

$$Vsus = \left(\frac{qhl}{\sigma t}\right)\left[\frac{5}{2}+\left(\frac{1}{8}\left(\frac{l}{h}\right)^2\right)\right]$$

$$Vcab = \left(\frac{qhl}{\sigma t}\right)\left[\frac{5}{4}+\left(\frac{13}{64}\left(\frac{l}{h}\right)^2\right)\right]$$

This can be further simplified as

$$\frac{Vsus}{Vcab} = 1+\frac{80-5(l/h)^2}{80+13(l/h)^2}$$

From the above equations it can be concluded that, if $h < l/4$ the suspension bridge is more efficient where the volume of suspension bridge ($Vsub$) reduces. And if $h > l/4$ cable-stayed bridge is more efficient where the volume of cable stayed bridge ($Vcab$) reduces.

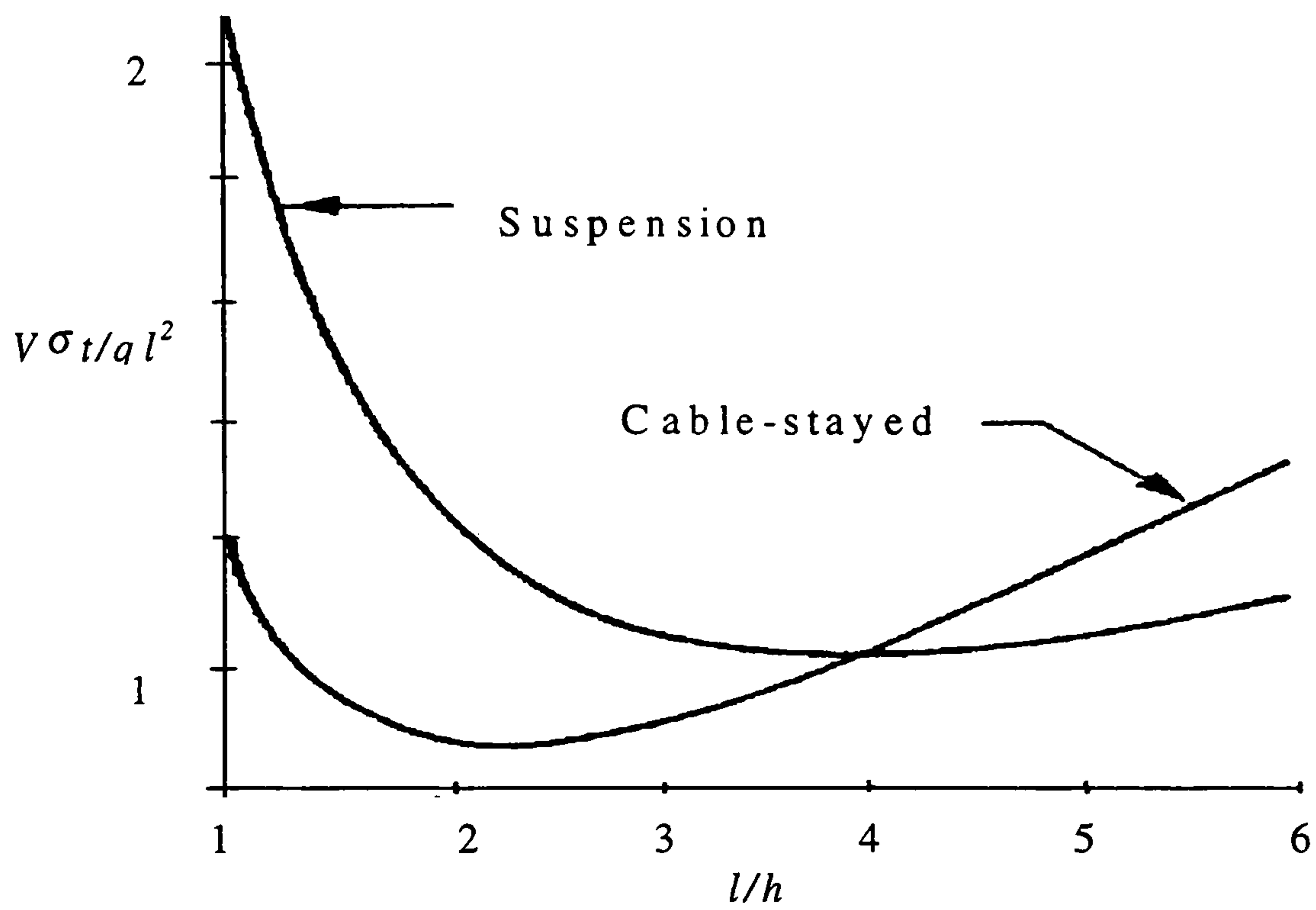

Figure 1A3

The intersection point of both curves at the value of 4 is shown in Figure 1A3 in non-dimensional form for a graph of $V\sigma t/ql^2$ Vs l/h. For a constant tower height h, suspension bridge is economical for longer span cases and the cable-stayed bridge is economical for shorter span cases. Also for the cable-stayed bridge the minimum volume occurs at l/h value of 2.4 and for the suspension bridge this occurs at the value of 4.5.

b) Maxwell's Lemma approach

Maxwell's Lemma approach (Correspondence, 1996) to compare the material energy. Normalized expressions where the equations are divided by ql^2 for the comparison.

PERC of suspension bridge is given by h/l

PERT of suspension bridge is given by $h/l + l/8h$

PERC of cable-stayed bridge is given by $h/_{2l} + l/_{32h}$

PERT of cable-stayed bridge is given by $h/_{2l} + 5l/_{32h}$

The PER for the suspension bridge and the cable-stayed bridge are same, which is given by PERT – PERC, the value is $l/_{8h}$.

The intersection value of the curves is given by equating the PERC (or PERT) of the suspension bridge and the cable-stayed bridge.

It gives $h/_{2l} = l/_{32h}$, hence $l = 4h$ like the intersection value in Figure A3.

To get the minimum material used, the total (PERC + PERT) of the suspension bridge and the cable stayed bridge has to be differentiated with respect to $l/_{h}$.

For the suspension bridge it gives $l/_{h}$ value of 4 and for the cable-stayed bridge it gives the value of 2.3. These values are closer to the values from the classical approach.

Appendix 2

Example on Initial Strain

The following example explains the term "initial strain" in Ansys with the spar (link) elements. A parabolic cable is hanging from its both ends placed at the same level. The main cable is assumed as flexible where no stiffness is included. The horizontal deck is simply supported at its both ends and connected to the main cable at a number of places through vertical hangers, refer Figure 2A1. Diameter of the main cable, cross-section of the deck and the diameter of the hangers are same as the corresponding Humber Bridge components.

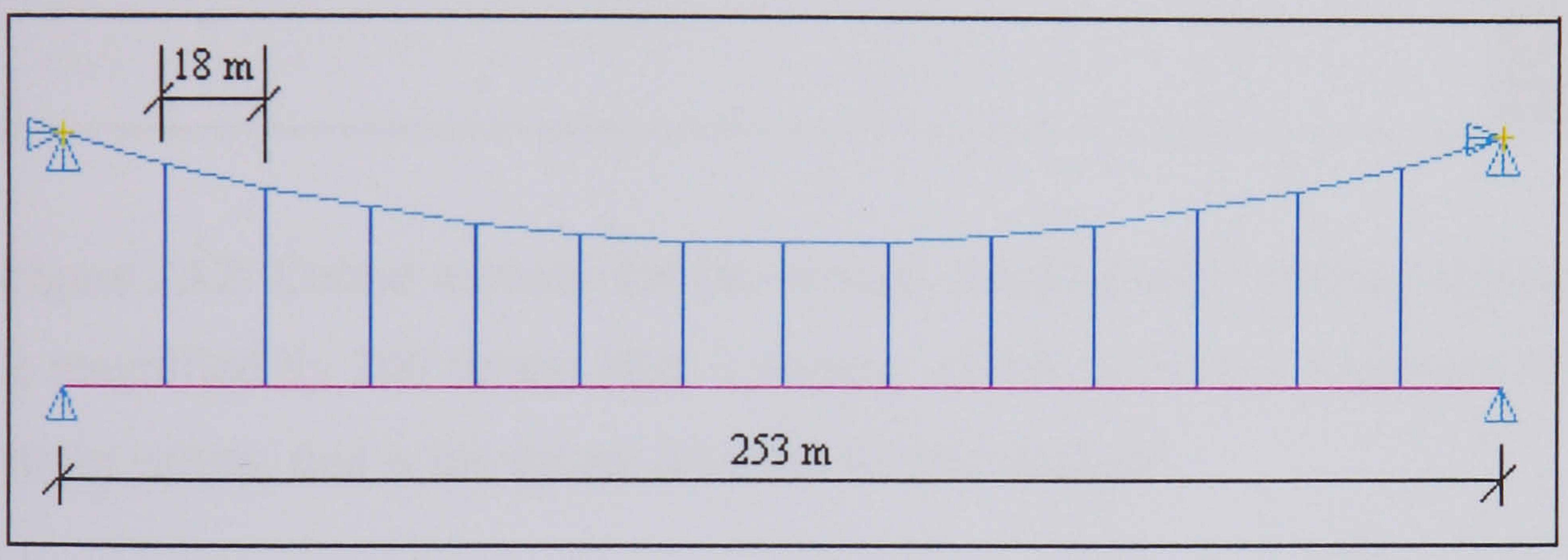

Figure 2A1: Sample model with vertical hangers

This structure will not be stable without the initial strain for the main cable and the hangers. Co-ordinates of the initial geometry are taken related to the as-built structure. So that the structure under self-weight has to follow the same profile as the main cable and the deck. In this respect, the initial strain values of the main cable and the hanger are determined through a number of trial and error iterations. Because these initial strain values highly influence the profile of the main cable and the deck. It is impossible to obtain zero deviation from the as built structure in terms of deflection of the profiles and member forces. Always small inaccuracies on results are possible due to minor adjustment on initial strain values.

Figure 2A2 shows the deformed and undeformed shape of the structure under self-weight condition. This deformed shape is for the initial strain value of 0.00035 for the main cable and 0.0014 for the hanger. The maximum vertical downward deflections of 12 mm at the quarter of the main cable and 4.2 mm at the quarter of the deck were obtained. Similarly the vertical downward deflection of 8.4 mm at the middle of the main cable and 3.4 mm at the middle of the deck were obtained. These deflection values are negligible compared with the span length of 253 m of the structure.

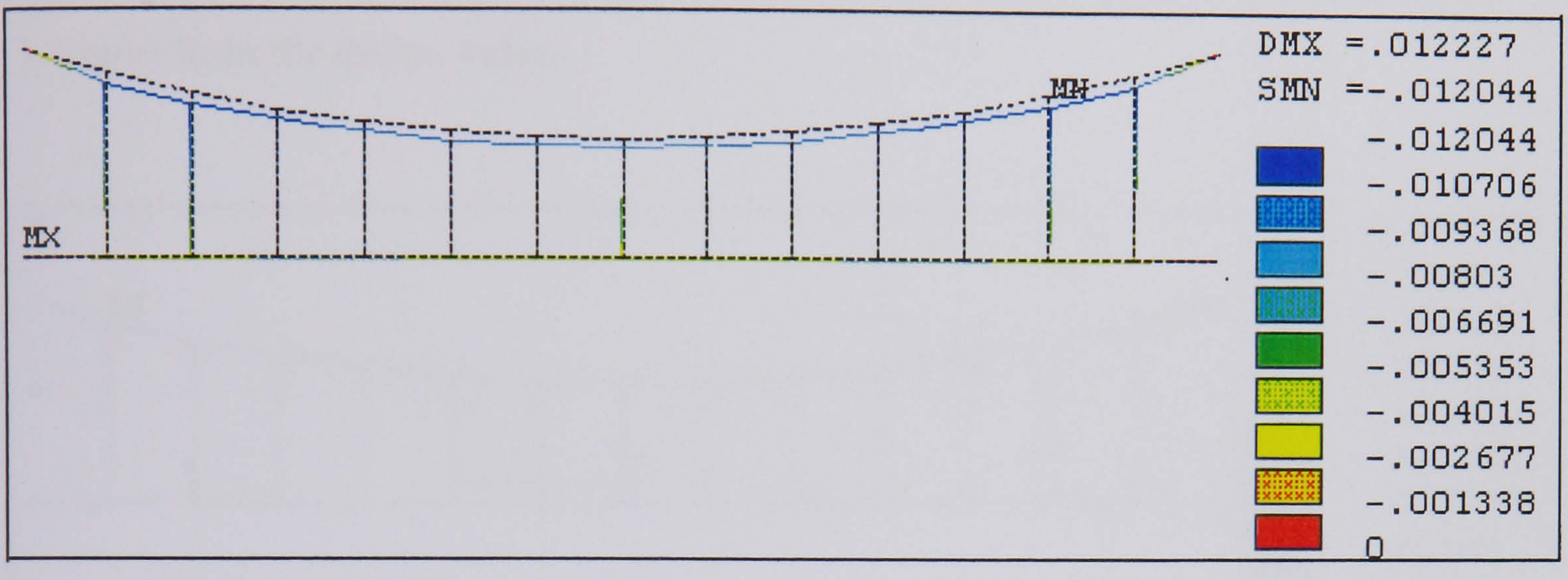

Figure 2A2: Colour contour for the vertical displacement (vertical displacement (m) is magnified by 200 times) after a number of trial and error iterations for the initial strain values, this is the datum level for further analysis.

This deformed shape (under self-weight load) will be taken as the datum level for further analysis. These initial strain values applied to the main cable and the hanger are compatible with the deformed shape of the structure. The found initial strain values for the main cable and the hanger through the trial and error iterations are fixed for the model structure. These values have to be changed only if any changes on the profile (datum level) of the main cable and the deck of the structure (under self-weight condition).

Increasing and decreasing values (say 10 %) of the initial strains to the main cable were applied to show the effect of the initial strain value of the main cable over the profile of the main cable and the deck. Where the initial strain value of the hanger was kept as constant.

Figure 2A3 shows the effect of the main cable and the deck profile with the increases of main cable strain value by 10 %. The present initial strain value is 0.000385, the deformed and undeformed shape of the structure was found still under the same self-weight condition. Increasing the initial strain on the main cable increases the axial (pulling) tensile force. This effect moves the main cable and the deck profile upwards. Now the vertical displacement at the middle of the main cable is 15.5 mm, which is 23.9 mm (15.5 mm + 8.4 mm) from the datum value. Similarly the vertical displacement at the middle of the deck is 20.5 mm, which is 23.9 mm (20.5 mm + 3.4 mm) from the datum value.

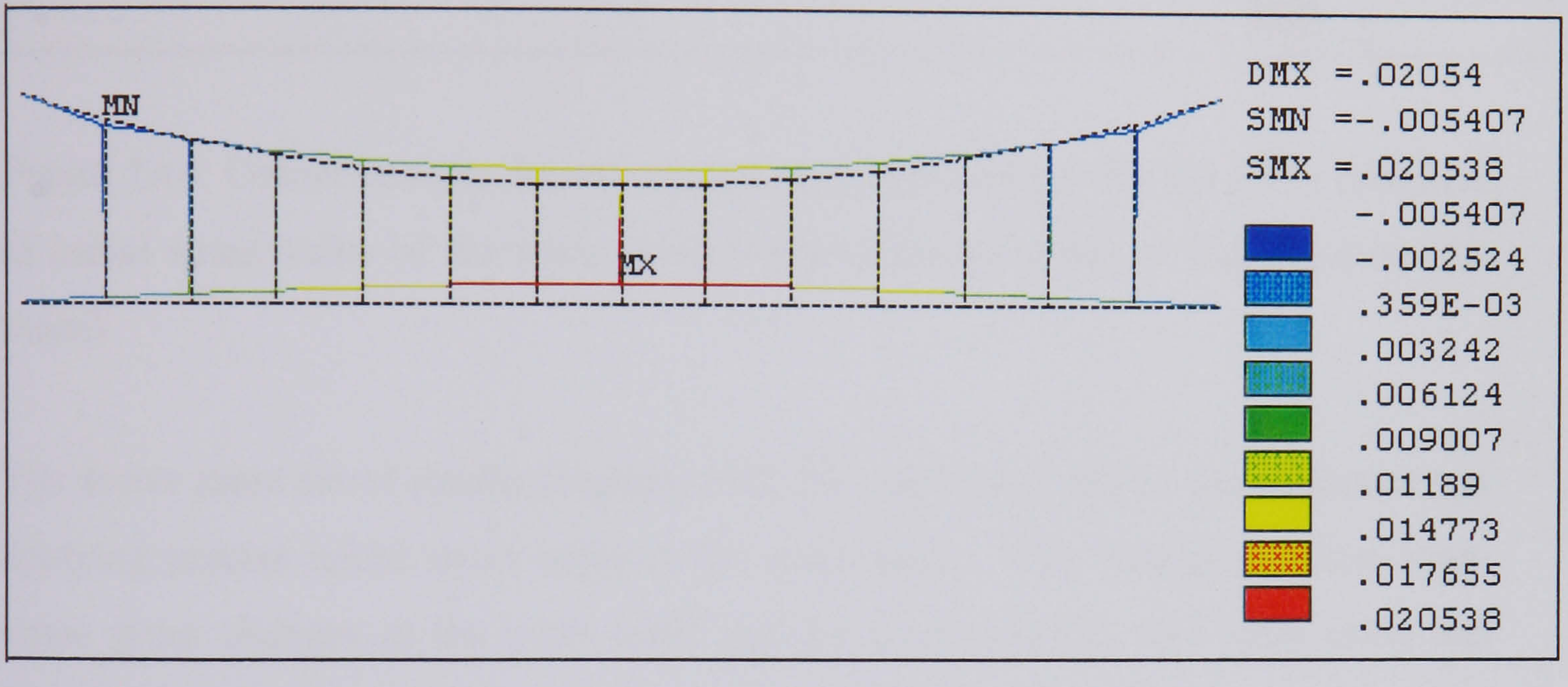

Figure 2A3: Colour contour for the vertical displacement (m) for the 10 % increment of initial strain value of the main cable (vertical displacement is magnified by 200 times)

As previously, Figure 2A4 shows the deformed and undeformed shape of the structure with the 10 % reduction of the initial strain value of the main cable from the initially assumed value. The present initial strain value is 0.000315, where the structure is still analysed under self-weight condition. Reduction of initial strain reduces the axial pulling force hence the main cable and the deck move downwards. The centre of the main cable moves vertically downward by 32.4 mm, which is 24 mm (32.4 mm – 8.4 mm) from the datum level. Similarly the centre of the deck moves vertically downward by 27.3 mm, which is 23.9 mm (27.3 mm – 3.4 mm) from the datum level.

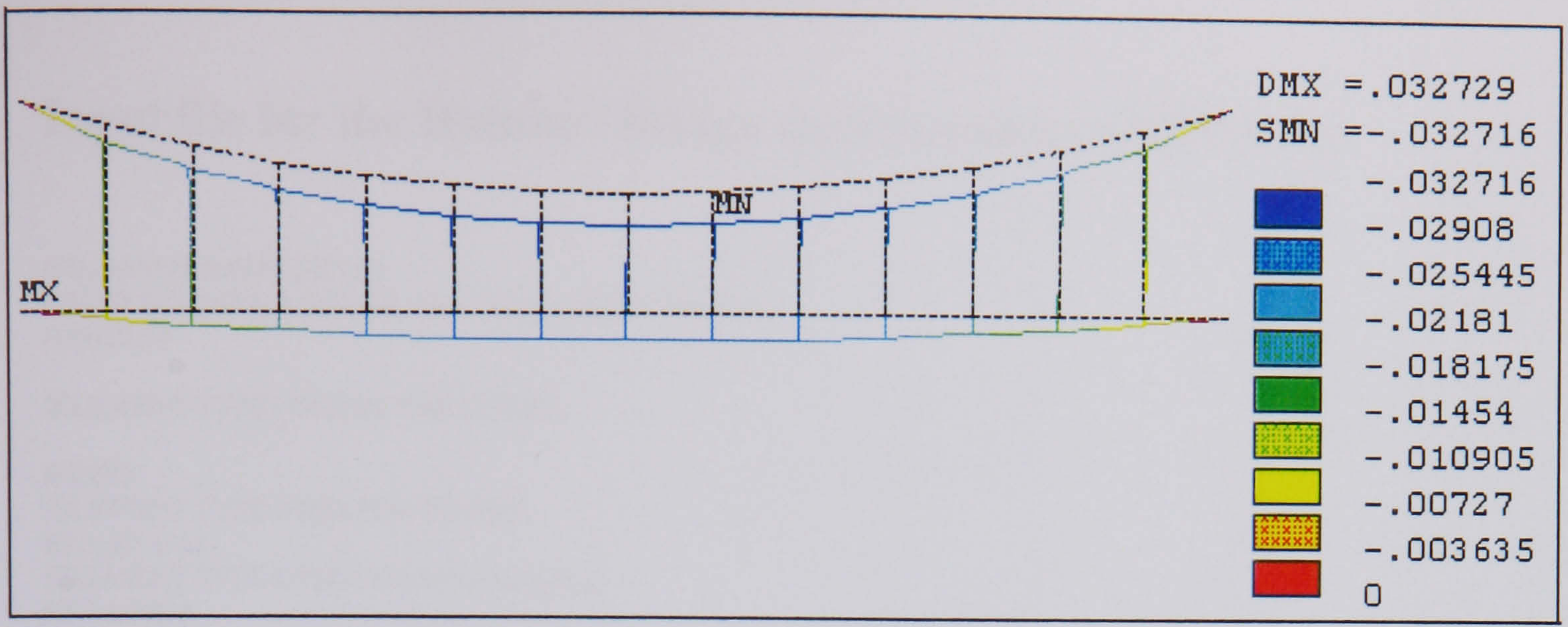

Figure 2A4: Colour contour for the vertical displacement (m) for the 10 % reduction of initial strain value of the main cable (vertical displacement is magnified by 200 times)

The above three set of results (Figures 2A2, 2A3 and 2A4) shows the importance in applying precise initial strain value to the main cable. This change in initial strain value gives changes in the main cable and the deck profiles, and main cable and hanger forces. Also it gives changing reaction forces on the supports.

Changes in the initial strain value by an amount either increment or reduction on the main cable gives force changes on the main cable by the same amount (either increment or reduction). This effect moves the main cable and the deck profile by the same amount either upward or downward.

As this is the datum level for further analysis, it can be concluded that the application of precise initial strain values is important through a number of trial and error iterations.

Similarly changing the initial strain values of the hangers (keeping the initial strain value of the main cable as constant) give changes in the main cable and the deck profiles, and changes in the hanger forces.

Appendix 3

Input file for the Humber Bridge detail model (ANSYS 5.3)

```
/FILNAM,HUMBERDET3D
/TITLE,3-D DETAIL MODEL OF THE HUMBER BRIDGE
/UNITS,SI

!ELEMENT TYPE USED IN THE MODEL

/PREP7
!ELEMENT TYPE USED FOR TOWER
ET,1,BEAM4
!ELEMENT TYPE USED FOR MAIN CABLE
ET,2,LINK8
!ELEMENT TYPE USED FOR FOOT PATH SUPPORT BEAM
ET,3,BEAM4
!ELEMENT TYPE USED FOR HANGER
ET,4,LINK10
!ELEMENT TYPE USED FOR FOOT PATH LONGITUDINAL BEAM
ET,5,BEAM4
!ELEMENT TYPE USED FOR DECK
ET,6,SHELL63
!ELEMENT TYPE USED FOR A-FRAME
ET,7,BEAM44
!ELEMENT TYPE USED FOR VERTICAL BEAM ON A-FRAME
ET,8,BEAM44
!ELEMENT TYPE USED FOR BEAM ROUND THE STIFFENER
ET,9,BEAM4

!GEOMETRICAL PROPERTIES USED IN THE MODEL

!REAL CONSTANTS USED FOR TOWER
R,1,18.237,30.223,36.049,4.790,4.228
R,2,19.365,42.677,44.516,4.970,4.705
R,3,22.823,56.582,60.769,5.300,5.115
R,4,26.929,76.574,79.951,5.635,5.540
R,5,28.15,95.288,96.140,5.90,5.875
R,6,16.000,30.21,23.33,4.00,4.500
R,7,18.000,30.38,24,4.000,4.500
R,8,26.8,45.45,156.93,8.000,4.000
!REAL CONSTANT FOR FOOT PATH SUPPORT BEAM
R,11,0.0069,0.00009,0.00002,0.083,0.083
!REAL CONSTANT FOR FOOT PATH LONGITUDINAL BEAM
R,12,.0074,.000028,.0000098,0.086,0.086
!REAL CONSTANTS USED FOR HANGERS
R,25,0.418E-2,0.304E-2
R,26,0.209E-2,0.304E-2
R,10,0.209E-2,0.140E-2
!REAL CONSTANTS USED FOR DECK
R,31,0.0116,0.0116,0.0116,0.0116,,,
RMORE,178.5,0.1337,0.0253
R,32,0.0205,0.0205,0.0205,0.0205,,,
RMORE,148.5,0.2097,0.0623
R,33,0.0109,0.0109,0.0109,0.0109,,,
RMORE,230.6,0.122,0.036
R,34,0.00707,0.00707,0.00707,0.00707,,,
RMORE,167.8,0.1186,0.0124
R,37,0.0113,0.0113,0.0113,0.0113,,,
RMORE,174.8,0.1356,0.0234
!REAL CONSTANTS USED FOR MAIN CABLE
R,20,0.2935,0.289E-2
R,21,0.2935,0.289E-2
R,22,0.2935,0.289E-2
R,23,0.2935,0.289E-2
R,24,0.3092,0.289E-2
R,30,0.3092,0.289E-2
!REAL CONSTANTS USED FOR A-FRAME
R,29,0.3E-1,7.46E-5,7.46E-5,0.173,0.173
```

```
!REAL CONSTANT USED FOR STIFFENER BEAM
R,38,0.0253,0.0316,0.000014,0.159,0.159
!REAL CONSTANT FOR VERTICAL A-FRAME BEAM
R,39,0.06,0.0018,0.0018,0.245,0.245

!MATERIAL PROPERTIES USED IN THE MODEL

!MATERIAL PROPERTIES USED FOR HANGER(HESSLE)
MP,EX,1,0.142196E12
MP,NUXY,1,0.3
MP,ALPX,1,0.12E-4
MP,DENS,1,8995.22
!MATERIAL PROPERTIES USED FOR HANGER(MIDDLE)
MP,EX,9,0.142196E12
MP,NUXY,9,0.3
MP,ALPX,9,0.12E-4
MP,DENS,9,9473.68
!MATERIAL PROPERTIES USED FOR HANGER(BARTON)
MP,EX,10,0.142196E12
MP,NUXY,10,0.3
MP,ALPX,10,0.12E-4
MP,DENS,10,9186.6
!MATERIAL PROPERTIES USED FOR TOWER
MP,EX,2,0.2809E11
MP,NUXY,2,0.2
MP,ALPX,2,0.12E-4
MP,DENS,2,2400
!MATERIAL PROPERTIES USED FOR DECK(HESSLE)
MP,EX,4,0.200E12
MP,NUXY,4,0.3
MP,ALPX,4,0.12E-4
MP,DENS,4,8115.8
!MATERIAL PROPERTIES USED FOR DECK(MIDDLE)
MP,EX,7,0.200E12
MP,NUXY,7,0.3
MP,ALPX,7,0.12E-4
MP,DENS,7,8007
!MATERIAL PROPERTIES USED FOR DECK(BARTON)
MP,EX,8,0.200E12
MP,NUXY,8,0.3
MP,ALPX,8,0.12E-4
MP,DENS,8,8091
!MATERIAL PROPERTIES USED FOR MAIN CABLE(HESSLE)
MP,EX,5,0.187895E12
MP,NUXY,5,0.3
MP,ALPX,5,0.12E-4
MP,DENS,5,8166.24
!MATERIAL PROPERTIES USED FOR MAIN CABLE(MIDDLE)
MP,EX,11,0.187895E12
MP,NUXY,11,0.3
MP,ALPX,11,0.12E-4
MP,DENS,11,8218.06
!MATERIAL PROPERTIES USED FOR MAIN CABLE(BARTON)
MP,EX,12,0.187895E12
MP,NUXY,12,0.3
MP,ALPX,12,0.12E-4
MP,DENS,12,8207.84
!MATERIAL PROPERTIES USED FOR A-FRAME
MP,EX,6,0.200E12
MP,NUXY,6,0.3
MP,ALPX,6,0.12E-4
MP,DENS,6,7940.7
!MATERIAL PROPERTIES USED FOR FOOT PATH SUPPORT BEAM
MP,EX,13,0.200E12
MP,NUXY,13,0.3
MP,ALPX,13,0.12E-4
MP,DENS,13,7940.7
!MATERIAL PROPERTIES USED FOR FOOT PATH LONGITUDINAL BEAM
MP,EX,14,0.200E12
MP,NUXY,14,0.3
MP,ALPX,14,0.12E-4
MP,DENS,14,7940.7
```

```
!CONNECTING INPUT FILES

!INPUTTING HESSLE SIDE DECK
/INPUT,AD-L2
!INPUTTING BARTON SIDE DECK
/INPUT,AD-R2
!INPUTTING MAIN SPAN DECK
/INPUT,AD-M2
!INPUTTING HESSLE SIDE DECK DIAPHRAGM (STIFFENER)
/INPUT,STIFF-LL
!INPUTTING BARTON SIDE DECK DIAPHRAGM (STIFFENER)
/INPUT,STIFF-RR
!INPUTTING MAIN SPAN DECK DIAPHRAGM (STIFFENER)
/INPUT,STIFF-MM
!INPUTTING END DECK (HESSLE SIDE)
/INPUT,P111
!INPUTTING END DECK (HESSLE TOWER)
/INPUT,P222
!INPUTTING END DECK (BARTON TOWER)
/INPUT,P333
!INPUTTING END DECK (BARTON SIDE)
/INPUT,P444
!INPUTTING THE MAIN CABLE
/INPUT,AD-CA
!INPUTTING THE HANGER
/INPUT,DETHR2,DAT
!INPUTTING THE FOOTPATH BEAM
/INPUT,BEAM
!INPUTTING THE TOWER
/INPUT,ALT-T
!INPUTTING THE DECK DIAPHRAGM (STIFFENER) AT HESSLE AND BARTON TOWER
/INPUT,EXTRA
NUMMRG,NODE,0.02
/VIEW,1,-1,1,1
EPLOT
```

!INPUT FILE FOR THE HESSLE SIDE DECK

```
/prep7

*dim,x0,,17
*dim,y0,,17
*dim,z0,,17
*dim,q,,16

X0(1)=-279.10
x0(2)=-272.138
x0(3)=-256.125
x0(4)=-242.55
x0(5)=-224.45
x0(6)=-206.35
x0(7)=-188.25
x0(8)=-170.15
x0(9)=-152.05
x0(10)=-133.95
x0(11)=-115.85
x0(12)=-97.75
x0(13)=-79.65
x0(14)=-61.55
x0(15)=-43.45
x0(16)=-25.35
x0(17)=-7.25

Y0(1)=-131.107
y0(2)=-131.011
y0(3)=-130.790
y0(4)=-130.607
y0(5)=-130.355
y0(6)=-130.103
y0(7)=-129.852
y0(8)=-129.600
y0(9)=-129.348
y0(10)=-129.097
```

```
y0(11)=-128.845
y0(12)=-128.594
y0(13)=-128.342
y0(14)=-128.091
y0(15)=-127.839
y0(16)=-127.588
y0(17)=-127.337

z0(1)=0
z0(2)=0
z0(3)=0
z0(4)=0
z0(5)=0
z0(6)=0
z0(7)=0
z0(8)=0
z0(9)=0
z0(10)=0
z0(11)=0
z0(12)=0
z0(13)=0
z0(14)=0
z0(15)=0
z0(16)=0
Z0(17)=0

numstr,kp,1
numstr,line,1
numstr,area,1
k0=1
l0=0
A0=0

NL=0
NW=1
NW1=2
NT=1
NB=1
NA=2
NF=1

*do,i,1,16

*set,q(i),x0(i+1)-x0(i)

!*if,q(i),lt,4.525,then
*set,ns,0
*set,ns1,0
*set,ns2,0
*set,ns3,0
*set,ns4,0
*set,ns5,0

!CREATING THE KEYPOINTS

K,k0+0,0.00+x0(i),0.0045+y0(i),7.40+z0(i)
!K,k0+1,0.00+x0(i),2.127+y0(i),2.113+z0(i)
K,k0+2,0.00+x0(i),2.971+y0(i),0.00+z0(i)
K,k0+3,0.00+x0(i),4.311+y0(i),1.90+z0(i)
K,k0+4,0.00+x0(i),4.494+y0(i),11.00+z0(i)
K,k0+5,0.00+x0(i),2.971+y0(i),-3.25+z0(i)
K,k0+6,0.00+x0(i),0.0045+y0(i),14.6+z0(i)
K,k0+7,0.00+x0(i),2.971+y0(i),22.00+z0(i)
K,k0+8,0.00+x0(i),4.311+y0(i),20.10+z0(i)
K,k0+9,0.00+x0(i),2.971+y0(i),25.25+z0(i)
!K,k0+10,0.00+x0(i),2.127+y0(i),19.90+z0(i)
K,k0+24,0.00+x0(i),4.383383+y0(i),5.5+z0(i)
K,k0+25,0.00+x0(i),4.383383+y0(i),16.5+z0(i)
K,k0+26,0.00+x0(i),0.0045+y0(i),11.00+z0(i)
!--------------------------------
K,k0+11,q(i)+x0(i),0.0045+y0(i+1),14.6+z0(i)
K,k0+12,q(i)+x0(i),2.971+y0(i+1),22.00+z0(i)
K,k0+13,q(i)+x0(i),4.494+y0(i+1),11.00+z0(i)
K,k0+14,q(i)+x0(i),4.311+y0(i+1),20.10+z0(i)
!K,k0+15,q(i)+x0(i),2.127+y0(i+1),19.90+z0(i)
```

```
K,k0+16,q(i)+x0(i),2.971+y0(i+1),25.25+z0(i)
K,k0+17,q(i)+x0(i),0.0045+y0(i+1),7.40+z0(i)
!K,k0+18,q(i)+x0(i),2.127+y0(i+1),2.113+z0(i)
K,k0+19,q(i)+x0(i),2.971+y0(i+1),0.00+z0(i)
K,k0+20,q(i)+x0(i),4.311+y0(i+1),1.90+z0(i)
K,k0+21,q(i)+x0(i),2.971+y0(i+1),-3.25+z0(i)
K,k0+22,q(i)+x0(i),4.383383+y0(i+1),5.5+z0(i)
K,k0+23,q(i)+x0(i),4.383383+y0(i+1),16.5+z0(i)
K,k0+27,q(i)+x0(i),0.0045+y0(i+1),11.00+z0(i)
!-----------------------------------

!CREATING THE CORRESPONDING LINES

L,k0+8,k0+25,NW
L,k0+24,k0+3,NW
L,k0+3,k0+2,NT
L,k0+2,k0+0,NW1
L,k0+26,k0+6,NB
L,k0+6,k0+7,NW1
L,k0+7,k0+8,NT
L,k0+2,k0+5,NF
L,k0+7,k0+9,NF
L,k0+23,k0+13,NW
L,k0+13,k0+22,NW
L,k0+20,k0+19,NT
L,k0+19,k0+17,NW1
L,k0+17,k0+27,NB
L,k0+11,k0+12,NW1
L,k0+12,k0+14,NT
L,k0+19,k0+21,NF
L,k0+12,k0+16,NF
L,k0+8,k0+14,NL
L,k0+4,k0+13,NL
L,k0+3,k0+20,NL
L,k0+2,k0+19,NL
L,k0+0,k0+17,NL
L,k0+6,k0+11,NL
L,k0+7,k0+12,NL

L,k0+5,k0+21,NL
L,k0+9,k0+16,NL

L,k0+23,k0+14,NW
L,k0+20,k0+22,NW
L,k0+4,k0+24,NW
L,k0+4,k0+25,NW
L,k0+25,k0+23,NL
L,k0+24,k0+22,NL
L,k0+26,k0+27,NL
L,k0+0,k0+26,NB
L,k0+27,k0+11,NB

TYPE,5
MAT,14
REAL,12
ESIZE,5
LSEL,,,,L0+26,L0+27,1
LMESH,ALL
ALLSEL

!CREATING THE CORRESPONDING AREAS & AREA MESHING

!BOTTOM PLATE
AL,L0+34,L0+35,L0+23,L0+14
AL,L0+24,L0+5,L0+34,L0+36
AL,L0+23,L0+4,L0+22,L0+13
AL,L0+25,L0+6,L0+24,L0+15

TYPE,6
MAT,4
REAL,31
ESIZE,5
ASEL,,,,A0+1,A0+4,1
AMESH,ALL
ALLSEL
```

```
!SIDE PLATE
AL,L0+21,L0+3,L0+22,L0+12
AL,L0+25,L0+7,L0+19,L0+16

TYPE,6
MAT,4
REAL,37
ESIZE,5
ASEL,,,,A0+5,A0+6,1
AMESH,ALL
ALLSEL

!TOP PLATE
AL,L0+19,L0+1,L0+32,L0+28
AL,L0+31,L0+20,L0+10,L0+32
AL,L0+33,L0+2,L0+21,L0+29
AL,L0+20,L0+30,L0+33,L0+11

TYPE,6
MAT,4
REAL,32
ESIZE,5
ASEL,,,,A0+7,A0+10,1
AMESH,ALL
ALLSEL

!FOOT PATH
AL,L0+22,L0+8,L0+26,L0+17
AL,L0+27,L0+9,L0+25,L0+18

TYPE,6
MAT,4
REAL,33
ESIZE,5
ASEL,,,,A0+11,A0+12,1
AMESH,ALL
ALLSEL

!*endif
*set,k0,k0+28
*set,l0,l0+36
*set,A0,A0+12

*enddo
```

!INPUT FILE FOR THE BARTON SIDE DECK

```
/prep7

x0=
y0=
z0=
q=

*dim,x0,,34
*dim,y0,,34
*dim,z0,,34
*dim,q,,33

x0(1)=1419.05
x0(2)=1437.15
x0(3)=1455.25
x0(4)=1473.35
x0(5)=1491.45
x0(6)=1509.55
x0(7)=1527.65
x0(8)=1545.75
x0(9)=1563.85
x0(10)=1581.95
x0(11)=1600.05
x0(12)=1618.15
x0(13)=1636.25
x0(14)=1654.35
```

```
x0(15)=1672.45
x0(16)=1690.55
x0(17)=1708.65
x0(18)=1726.75
x0(19)=1744.85
x0(20)=1762.95
x0(21)=1781.05
x0(22)=1799.219
x0(23)=1817.25
x0(24)=1818.717
x0(25)=1834.119
x0(26)=1837.938
x0(27)=1850.965
x0(28)=1857.281
x0(29)=1867.890
x0(30)=1880.600
x0(31)=1898.700
x0(32)=1916.800
x0(33)=1933.375
X0(34)=1940.900
!-------------------------
y0(1)=-127.330
y0(2)=-127.596
y0(3)=-127.877
y0(4)=-128.173
y0(5)=-128.484
y0(6)=-128.810
y0(7)=-129.151
y0(8)=-129.507
y0(9)=-129.878
y0(10)=-130.264
y0(11)=-130.665
y0(12)=-131.081
y0(13)=-131.512
y0(14)=-131.958
y0(15)=-132.419
y0(16)=-132.895
y0(17)=-133.386
y0(18)=-133.892
y0(19)=-134.413
y0(20)=-134.949
y0(21)=-135.500
y0(22)=-136.072
y0(23)=-136.648
y0(24)=-136.695
y0(25)=-137.203
y0(26)=-137.334
y0(27)=-137.770
y0(28)=-137.986
y0(29)=-138.353
y0(30)=-138.800
y0(31)=-139.466
y0(32)=-140.132
y0(33)=-140.742
Y0(34)=-141.019
!------------------------
z0(1)=0
z0(2)=0
z0(3)=0
z0(4)=0
z0(5)=0
z0(6)=0
z0(7)=0
z0(8)=0
z0(9)=0
z0(10)=0
z0(11)=0
z0(12)=0
z0(13)=0
z0(14)=0
z0(15)=0
z0(16)=0
z0(17)=0
z0(18)=0
z0(19)=0
```

```
z0(20)=0
z0(21)=0
z0(22)=0
z0(23)=0
z0(24)=0
z0(25)=0
z0(26)=0
z0(27)=0
z0(28)=0
z0(29)=0
z0(30)=0
z0(31)=0
z0(32)=0
z0(33)=0
Z0(34)=0

numstr,kp,449
numstr,line,577
numstr,area,193
k0=449
l0=576
A0=192

NL=0
NW=1
NW1=2
NT=1
NB=1
NA=2
NF=1

*do,i,1,33
*set,q(i),x0(i+1)-x0(i)

!*if,q(i),lt,4.525,then
*set,ns,0
*set,ns1,0
*set,ns2,0
*set,ns3,0
*set,ns4,0
*set,ns5,0

!CREATING THE KEYPOINTS

K,k0+0,0.00+x0(i),0.0045+y0(i),7.40+z0(i)
!K,k0+1,0.00+x0(i),2.127+y0(i),2.113+z0(i)
K,k0+2,0.00+x0(i),2.971+y0(i),0.00+z0(i)
K,k0+3,0.00+x0(i),4.311+y0(i),1.90+z0(i)
K,k0+4,0.00+x0(i),4.494+y0(i),11.00+z0(i)
K,k0+5,0.00+x0(i),2.971+y0(i),-3.25+z0(i)
K,k0+6,0.00+x0(i),0.0045+y0(i),14.6+z0(i)
K,k0+7,0.00+x0(i),2.971+y0(i),22.00+z0(i)
K,k0+8,0.00+x0(i),4.311+y0(i),20.10+z0(i)
K,k0+9,0.00+x0(i),2.971+y0(i),25.25+z0(i)
!K,k0+10,0.00+x0(i),2.127+y0(i),19.90+z0(i)
K,k0+24,0.00+x0(i),4.383383+y0(i),5.5+z0(i)
K,k0+25,0.00+x0(i),4.383383+y0(i),16.5+z0(i)
K,k0+26,0.00+x0(i),0.0045+y0(i),11.00+z0(i)
!--------------------------------
K,k0+11,q(i)+x0(i),0.0045+y0(i+1),14.6+z0(i)
K,k0+12,q(i)+x0(i),2.971+y0(i+1),22.00+z0(i)
K,k0+13,q(i)+x0(i),4.494+y0(i+1),11.00+z0(i)
K,k0+14,q(i)+x0(i),4.311+y0(i+1),20.10+z0(i)
!K,k0+15,q(i)+x0(i),2.127+y0(i+1),19.90+z0(i)
K,k0+16,q(i)+x0(i),2.971+y0(i+1),25.25+z0(i)
K,k0+17,q(i)+x0(i),0.0045+y0(i+1),7.40+z0(i)
!K,k0+18,q(i)+x0(i),2.127+y0(i+1),2.113+z0(i)
K,k0+19,q(i)+x0(i),2.971+y0(i+1),0.00+z0(i)
K,k0+20,q(i)+x0(i),4.311+y0(i+1),1.90+z0(i)
K,k0+21,q(i)+x0(i),2.971+y0(i+1),-3.25+z0(i)
K,k0+22,q(i)+x0(i),4.383383+y0(i+1),5.5+z0(i)
K,k0+23,q(i)+x0(i),4.383383+y0(i+1),16.5+z0(i)
K,k0+27,q(i)+x0(i),0.0045+y0(i+1),11.00+z0(i)
!-----------------------------------
```

!CREATING THE CORRESPONDING LINES

```
L,k0+8,k0+25,NW
L,k0+24,k0+3,NW
L,k0+3,k0+2,NT
L,k0+2,k0+0,NW1
L,k0+26,k0+6,NB
L,k0+6,k0+7,NW1
L,k0+7,k0+8,NT
L,k0+2,k0+5,NF
L,k0+7,k0+9,NF
L,k0+23,k0+13,NW
L,k0+13,k0+22,NW
L,k0+20,k0+19,NT
L,k0+19,k0+17,NW1
L,k0+17,k0+27,NB
L,k0+11,k0+12,NW1
L,k0+12,k0+14,NT
L,k0+19,k0+21,NF
L,k0+12,k0+16,NF
L,k0+8,k0+14,NL
L,k0+4,k0+13,NL
L,k0+3,k0+20,NL
L,k0+2,k0+19,NL
L,k0+0,k0+17,NL
L,k0+6,k0+11,NL
L,k0+7,k0+12,NL

L,k0+5,k0+21,NL
L,k0+9,k0+16,NL

L,k0+23,k0+14,NW
L,k0+20,k0+22,NW
L,k0+4,k0+24,NW
L,k0+4,k0+25,NW
L,k0+25,k0+23,NL
L,k0+24,k0+22,NL
L,k0+26,k0+27,NL
L,k0+0,k0+26,NB
L,k0+27,k0+11,NB

TYPE,5
MAT,14
REAL,12
ESIZE,5
LSEL,,,,L0+26,L0+27,1
LMESH,ALL
ALLSEL
```

!CREATING THE CORRESPONDING AREAS & AREA MESHING

```
!BOTTOM PLATE
AL,L0+34,L0+35,L0+23,L0+14
AL,L0+24,L0+5,L0+34,L0+36
AL,L0+23,L0+4,L0+22,L0+13
AL,L0+25,L0+6,L0+24,L0+15

TYPE,6
MAT,8
REAL,31
ESIZE,5
ASEL,,,,A0+1,A0+4,1
AMESH,ALL
ALLSEL

!SIDE PLATE
AL,L0+21,L0+3,L0+22,L0+12
AL,L0+25,L0+7,L0+19,L0+16

TYPE,6
MAT,8
REAL,37
ESIZE,5
ASEL,,,,A0+5,A0+6,1
AMESH,ALL
```

```
ALLSEL

!TOP PLATE
AL,L0+19,L0+1,L0+32,L0+28
AL,L0+31,L0+20,L0+10,L0+32
AL,L0+33,L0+2,L0+21,L0+29
AL,L0+20,L0+30,L0+33,L0+11

TYPE,6
MAT,8
REAL,32
ESIZE,5
ASEL,,,,A0+7,A0+10,1
AMESH,ALL
ALLSEL

!FOOT PATH
AL,L0+22,L0+8,L0+26,L0+17
AL,L0+27,L0+9,L0+25,L0+18

TYPE,6
MAT,8
REAL,33
ESIZE,5
ASEL,,,,A0+11,A0+12,1
AMESH,ALL
ALLSEL

!*endif
*set,k0,k0+28
*set,l0,l0+36
*set,A0,A0+12

*enddo
```

!INPUT FILE FOR THE MAIN SPAN DECK

```
/prep7

x0=
y0=
z0=
q=

*dim,x0,,106
*dim,y0,,106
*dim,z0,,106
*dim,q,,105

x0(1)=9.05
x0(2)=27.15
x0(3)=45.25
x0(4)=63.35
x0(5)=81.45
x0(6)=99.55
x0(7)=117.65
x0(8)=135.75
x0(9)=153.85
x0(10)=171.95
x0(11)=190.05
x0(12)=208.15
x0(13)=226.25
x0(14)=244.35
x0(15)=262.45
x0(16)=280.55
x0(17)=298.65
x0(18)=316.75
x0(19)=334.85
x0(20)=352.95
x0(21)=371.05
x0(22)=389.15
x0(23)=407.25
x0(24)=425.35
x0(25)=443.45
```

x0(26)=461.33
x0(27)=462.73
x0(28)=478.44
x0(29)=481.75
x0(30)=495.325
x0(31)=500.69
x0(32)=512.88
x0(33)=519.57
x0(34)=530.21
x0(35)=538.37
x0(36)=547.42
x0(37)=557.08
x0(38)=565.10
x0(39)=575.74
x0(40)=582.65
x0(41)=594.32
x0(42)=600.27
x0(43)=612.83
x0(44)=617.97
x0(45)=631.26
x0(46)=635.74
x0(47)=649.315
x0(48)=653.58
x0(49)=667.90
x0(50)=671.50
x0(51)=686.11
x0(52)=689.49
x0(53)=704.24
x0(54)=707.56
x0(55)=722.31
x0(56)=725.69
x0(57)=740.30
x0(58)=743.90
x0(59)=758.21
x0(60)=762.18
x0(61)=775.755
x0(62)=780.28
x0(63)=793.83
x0(64)=798.97
x0(65)=811.53
x0(66)=817.48
x0(67)=829.15
x0(68)=836.05
x0(69)=846.70
x0(70)=854.71
x0(71)=863.76
x0(72)=873.43
x0(73)=881.58
x0(74)=892.23
x0(75)=898.91
x0(76)=911.10
x0(77)=915.625
x0(78)=930.05
x0(79)=933.36
x0(80)=949.07
x0(81)=950.47
x0(82)=968.30
x0(83)=986.40
x0(84)=1004.5
x0(85)=1022.6
x0(86)=1040.7
x0(87)=1058.8
x0(88)=1076.9
x0(89)=1095.0
x0(90)=1113.1
x0(91)=1131.2
x0(92)=1149.3
x0(93)=1167.4
x0(94)=1185.5
x0(95)=1203.6
x0(96)=1221.7
x0(97)=1239.8
x0(98)=1257.9
x0(99)=1276.0
x0(100)=1294.1

x0(101)=1312.2
x0(102)=1330.3
x0(103)=1348.4
x0(104)=1366.5
x0(105)=1384.6
x0(106)=1402.7

y0(1)=-127.101
y0(2)=-126.861
y0(3)=-126.431
y0(4)=-126.381
y0(5)=-126.161
y0(6)=-125.941
y0(7)=-125.731
y0(8)=-125.521
y0(9)=-125.321
y0(10)=-125.121
y0(11)=-124.941
y0(12)=-124.761
y0(13)=-124.581
y0(14)=-124.411
y0(15)=-124.251
y0(16)=-124.101
y0(17)=-123.961
y0(18)=-123.811
y0(19)=-123.671
y0(20)=-123.541
y0(21)=-123.421
y0(22)=-123.301
y0(23)=-123.191
y0(24)=-123.091
y0(25)=-122.991
y0(26)=-122.901
y0(27)=-122.901
y0(28)=-122.821
y0(29)=-122.811
y0(30)=-122.751
y0(31)=-122.731
y0(32)=-122.681
y0(33)=-122.661
y0(34)=-122.621
y0(35)=-122.591
y0(36)=-122.561
y0(37)=-122.531
y0(38)=-122.511
y0(39)=-122.481
y0(40)=-122.461
y0(41)=-122.441
y0(42)=-122.421
y0(43)=-122.401
y0(44)=-122.391
y0(45)=-122.371
y0(46)=-122.361
y0(47)=-122.341
y0(48)=-122.341
y0(49)=-122.331
y0(50)=-122.321
y0(51)=-122.321
y0(52)=-122.321
y0(53)=-122.311
y0(54)=-122.311
y0(55)=-122.321
y0(56)=-122.321
y0(57)=-122.321
y0(58)=-122.331
y0(59)=-122.341
y0(60)=-122.341
y0(61)=-122.361
y0(62)=-122.371
y0(63)=-122.391
y0(64)=-122.401
y0(65)=-122.421
y0(66)=-122.441
y0(67)=-122.461
y0(68)=-122.481

y0(69)=-122.511
y0(70)=-122.531
y0(71)=-122.561
y0(72)=-122.591
y0(73)=-122.621
y0(74)=-122.661
y0(75)=-122.681
y0(76)=-122.731
y0(77)=-122.751
y0(78)=-122.811
y0(79)=-122.821
y0(80)=-122.901
y0(81)=-122.901
y0(82)=-122.991
y0(83)=-123.091
y0(84)=-123.191
y0(85)=-123.301
y0(86)=-123.421
y0(87)=-123.541
y0(88)=-123.671
y0(89)=-123.811
y0(90)=-123.961
y0(91)=-124.101
y0(92)=-124.251
y0(93)=-124.411
y0(94)=-124.581
y0(95)=-124.761
y0(96)=-124.941
y0(97)=-125.121
y0(98)=-125.321
y0(99)=-125.521
y0(100)=-125.731
y0(101)=-125.941
y0(102)=-126.161
y0(103)=-126.381
y0(104)=-126.431
y0(105)=-126.861
y0(106)=-127.101

z0(1)=0
z0(2)=0
z0(3)=0
z0(4)=0
z0(5)=0
z0(6)=0
z0(7)=0
z0(8)=0
z0(9)=0
z0(10)=0
z0(11)=0
z0(12)=0
z0(13)=0
z0(14)=0
z0(15)=0
z0(16)=0
z0(17)=0
z0(18)=0
z0(19)=0
z0(20)=0
z0(21)=0
z0(22)=0
z0(23)=0
z0(24)=0
z0(25)=0
z0(26)=0
z0(27)=0
z0(28)=0
z0(29)=0
z0(30)=0
z0(31)=0
z0(32)=0
z0(33)=0
z0(34)=0
z0(35)=0
z0(36)=0

```
z0(37)=0
z0(38)=0
z0(39)=0
z0(40)=0
z0(41)=0
z0(42)=0
z0(43)=0
z0(44)=0
z0(45)=0
z0(46)=0
z0(47)=0
z0(48)=0
z0(49)=0
z0(50)=0
z0(51)=0
z0(52)=0
z0(53)=0
z0(54)=0
z0(55)=0
z0(56)=0
z0(57)=0
z0(58)=0
z0(59)=0
z0(60)=0
z0(61)=0
z0(62)=0
z0(63)=0
z0(64)=0
z0(65)=0
z0(66)=0
z0(67)=0
z0(68)=0
z0(69)=0
z0(70)=0
z0(71)=0
z0(72)=0
z0(73)=0
z0(74)=0
z0(75)=0
z0(76)=0
z0(77)=0
z0(78)=0
z0(79)=0
z0(80)=0
z0(81)=0
z0(82)=0
z0(83)=0
z0(84)=0
z0(85)=0
z0(86)=0
z0(87)=0
z0(88)=0
z0(89)=0
z0(90)=0
z0(91)=0
z0(92)=0
z0(93)=0
z0(94)=0
z0(95)=0
z0(96)=0
z0(97)=0
z0(98)=0
z0(99)=0
z0(100)=0
z0(101)=0
z0(102)=0
z0(103)=0
z0(104)=0
z0(105)=0
z0(106)=0

numstr,kp,1373
numstr,line,1765
numstr,area,589
k0=1373
```

```
I0=1764
A0=588

NL=0
NW=1
NW1=2
NT=1
NB=1
NA=2
NF=1

*do,i,1,105
*set,q(i),x0(i+1)-x0(i)

!*if,q(i),lt,4.525,then
*set,ns,0
*set,ns1,0
*set,ns2,0
*set,ns3,0
*set,ns4,0
*set,ns5,0

!CREATING THE KEYPOINTS

K,k0+0,0.00+x0(i),0.0045+y0(i),7.40+z0(i)
!K,k0+1,0.00+x0(i),2.127+y0(i),2.113+z0(i)
K,k0+2,0.00+x0(i),2.971+y0(i),0.00+z0(i)
K,k0+3,0.00+x0(i),4.311+y0(i),1.90+z0(i)
K,k0+4,0.00+x0(i),4.494+y0(i),11.00+z0(i)
K,k0+5,0.00+x0(i),2.971+y0(i),-3.25+z0(i)
K,k0+6,0.00+x0(i),0.0045+y0(i),14.6+z0(i)
K,k0+7,0.00+x0(i),2.971+y0(i),22.00+z0(i)
K,k0+8,0.00+x0(i),4.311+y0(i),20.10+z0(i)
K,k0+9,0.00+x0(i),2.971+y0(i),25.25+z0(i)
!K,k0+10,0.00+x0(i),2.127+y0(i),19.90+z0(i)
K,k0+24,0.00+x0(i),4.383383+y0(i),5.5+z0(i)
K,k0+25,0.00+x0(i),4.383383+y0(i),16.5+z0(i)
K,k0+26,0.00+x0(i),0.0045+y0(i),11.00+z0(i)
!--------------------------------
K,k0+11,q(i)+x0(i),0.0045+y0(i+1),14.6+z0(i)
K,k0+12,q(i)+x0(i),2.971+y0(i+1),22.00+z0(i)
K,k0+13,q(i)+x0(i),4.494+y0(i+1),11.00+z0(i)
K,k0+14,q(i)+x0(i),4.311+y0(i+1),20.10+z0(i)
!K,k0+15,q(i)+x0(i),2.127+y0(i+1),19.90+z0(i)
K,k0+16,q(i)+x0(i),2.971+y0(i+1),25.25+z0(i)
K,k0+17,q(i)+x0(i),0.0045+y0(i+1),7.40+z0(i)
!K,k0+18,q(i)+x0(i),2.127+y0(i+1),2.113+z0(i)
K,k0+19,q(i)+x0(i),2.971+y0(i+1),0.00+z0(i)
K,k0+20,q(i)+x0(i),4.311+y0(i+1),1.90+z0(i)
K,k0+21,q(i)+x0(i),2.971+y0(i+1),-3.25+z0(i)
K,k0+22,q(i)+x0(i),4.383383+y0(i+1),5.5+z0(i)
K,k0+23,q(i)+x0(i),4.383383+y0(i+1),16.5+z0(i)
K,k0+27,q(i)+x0(i),0.0045+y0(i+1),11.00+z0(i)
!-----------------------------------

!CREATING THE CORRESPONDING LINES

L,k0+8,k0+25,NW
L,k0+24,k0+3,NW
L,k0+3,k0+2,NT
L,k0+2,k0+0,NW1
L,k0+26,k0+6,NB
L,k0+6,k0+7,NW1
L,k0+7,k0+8,NT
L,k0+2,k0+5,NF
L,k0+7,k0+9,NF
L,k0+23,k0+13,NW
L,k0+13,k0+22,NW
L,k0+20,k0+19,NT
L,k0+19,k0+17,NW1
L,k0+17,k0+27,NB
L,k0+11,k0+12,NW1
L,k0+12,k0+14,NT
L,k0+19,k0+21,NF
L,k0+12,k0+16,NF
```

```
L,k0+8,k0+14,NL
L,k0+4,k0+13,NL
L,k0+3,k0+20,NL
L,k0+2,k0+19,NL
L,k0+0,k0+17,NL
L,k0+6,k0+11,NL
L,k0+7,k0+12,NL

L,k0+5,k0+21,NL
L,k0+9,k0+16,NL

L,k0+23,k0+14,NW
L,k0+20,k0+22,NW
L,k0+4,k0+24,NW
L,k0+4,k0+25,NW
L,k0+25,k0+23,NL
L,k0+24,k0+22,NL
L,k0+26,k0+27,NL
L,k0+0,k0+26,NB
L,k0+27,k0+11,NB

TYPE,5
MAT,14
REAL,12
ESIZE,5
LSEL,,,,L0+26,L0+27,1
LMESH,ALL
ALLSEL

!CREATING THE CORRESPONDING AREAS & AREA MESHING

!BOTTOM PLATE
AL,L0+34,L0+35,L0+23,L0+14
AL,L0+24,L0+5,L0+34,L0+36
AL,L0+23,L0+4,L0+22,L0+13
AL,L0+25,L0+6,L0+24,L0+15

TYPE,6
MAT,7
REAL,31
ESIZE,5
ASEL,,,,A0+1,A0+4,1
AMESH,ALL
ALLSEL

!SIDE PLATE
AL,L0+21,L0+3,L0+22,L0+12
AL,L0+25,L0+7,L0+19,L0+16

TYPE,6
MAT,7
REAL,37
ESIZE,5
ASEL,,,,A0+5,A0+6,1
AMESH,ALL
ALLSEL

!TOP PLATE
AL,L0+19,L0+1,L0+32,L0+28
AL,L0+31,L0+20,L0+10,L0+32
AL,L0+33,L0+2,L0+21,L0+29
AL,L0+20,L0+30,L0+33,L0+11

TYPE,6
MAT,7
REAL,32
ESIZE,5
ASEL,,,,A0+7,A0+10,1
AMESH,ALL
ALLSEL

!FOOT PATH
AL,L0+22,L0+8,L0+26,L0+17
AL,L0+27,L0+9,L0+25,L0+18
```

```
TYPE,6
MAT,7
REAL,33
ESIZE,5
ASEL,,,,A0+11,A0+12,1
AMESH,ALL
ALLSEL

!*endif
*set,k0,k0+28
*set,l0,l0+36
*set,A0,A0+12

*enddo
```

!INPUT FILE FOR THE HESSLE SIDE DECK DIAPHRAGM (STIFFENER)

```
/prep7

x0=
y0=
z0=

*dim,x0,,62
*dim,y0,,62
*dim,z0,,62

X0(  1  )=  -279.1
X0(  2  )=  -275.62
X0(  3  )=  -272.14
X0(  4  )=  -268.13
X0(  5  )=  -264.13
X0(  6  )=  -260.13
X0(  7  )=  -256.13
X0(  8  )=  -251.6
X0(  9  )=  -247.08
X0(  10  )=  -242.55
X0(  11  )=  -238.03
X0(  12  )=  -233.5
X0(  13  )=  -228.98
X0(  14  )=  -224.45
X0(  15  )=  -219.93
X0(  16  )=  -215.4
X0(  17  )=  -210.88
X0(  18  )=  -206.35
X0(  19  )=  -201.83
X0(  20  )=  -197.3
X0(  21  )=  -192.78
X0(  22  )=  -188.25
X0(  23  )=  -183.73
X0(  24  )=  -179.2
X0(  25  )=  -174.68
X0(  26  )=  -170.15
X0(  27  )=  -165.63
X0(  28  )=  -161.1
X0(  29  )=  -156.58
X0(  30  )=  -152.05
X0(  31  )=  -147.53
X0(  32  )=  -143
X0(  33  )=  -138.48
X0(  34  )=  -133.95
X0(  35  )=  -129.43
X0(  36  )=  -124.9
X0(  37  )=  -120.38
X0(  38  )=  -115.85
X0(  39  )=  -111.32
X0(  40  )=  -106.8
X0(  41  )=  -102.28
X0(  42  )=  -97.75
X0(  43  )=  -93.225
X0(  44  )=  -88.7
X0(  45  )=  -84.175
X0(  46  )=  -79.65
X0(  47  )=  -75.125
```

X0(	48	)=	-70.6
X0(	49	)=	-66.075
X0(	50	)=	-61.55
X0(	51	)=	-57.025
X0(	52	)=	-52.5
X0(	53	)=	-47.975
X0(	54	)=	-43.45
X0(	55	)=	-38.925
X0(	56	)=	-34.4
X0(	57	)=	-29.875
X0(	58	)=	-25.35
X0(	59	)=	-20.825
X0(	60	)=	-16.3
X0(	61	)=	-11.775
X0(	62	)=	-7.25

Y0(	1	)=	-131.1
Y0(	2	)=	-131.05
Y0(	3	)=	-131.01
Y0(	4	)=	-130.95
Y0(	5	)=	-130.9
Y0(	6	)=	-130.84
Y0(	7	)=	-130.79
Y0(	8	)=	-130.72
Y0(	9	)=	-130.66
Y0(	10	)=	-130.6
Y0(	11	)=	-130.54
Y0(	12	)=	-130.48
Y0(	13	)=	-130.41
Y0(	14	)=	-130.35
Y0(	15	)=	-130.29
Y0(	16	)=	-130.22
Y0(	17	)=	-130.16
Y0(	18	)=	-130.1
Y0(	19	)=	-130.04
Y0(	20	)=	-129.97
Y0(	21	)=	-129.91
Y0(	22	)=	-129.85
Y0(	23	)=	-129.78
Y0(	24	)=	-129.72
Y0(	25	)=	-129.66
Y0(	26	)=	-129.6
Y0(	27	)=	-129.53
Y0(	28	)=	-129.47
Y0(	29	)=	-129.41
Y0(	30	)=	-129.34
Y0(	31	)=	-129.28
Y0(	32	)=	-129.22
Y0(	33	)=	-129.16
Y0(	34	)=	-129.09
Y0(	35	)=	-129.03
Y0(	36	)=	-128.97
Y0(	37	)=	-128.9
Y0(	38	)=	-128.84
Y0(	39	)=	-128.78
Y0(	40	)=	-128.71
Y0(	41	)=	-128.65
Y0(	42	)=	-128.59
Y0(	43	)=	-128.53
Y0(	44	)=	-128.46
Y0(	45	)=	-128.4
Y0(	46	)=	-128.34
Y0(	47	)=	-128.27
Y0(	48	)=	-128.21
Y0(	49	)=	-128.15
Y0(	50	)=	-128.09
Y0(	51	)=	-128.02
Y0(	52	)=	-127.96
Y0(	53	)=	-127.9
Y0(	54	)=	-127.83
Y0(	55	)=	-127.77
Y0(	56	)=	-127.71
Y0(	57	)=	-127.65
Y0(	58	)=	-127.58
Y0(	59	)=	-127.52

```
Y0(  60  )=  -127.46
Y0(  61  )=  -127.4
Y0(  62  )=  -127.33

Z0(  1  )=  0
Z0(  2  )=  0
Z0(  3  )=  0
Z0(  4  )=  0
Z0(  5  )=  0
Z0(  6  )=  0
Z0(  7  )=  0
Z0(  8  )=  0
Z0(  9  )=  0
Z0(  10  )=  0
Z0(  11  )=  0
Z0(  12  )=  0
Z0(  13  )=  0
Z0(  14  )=  0
Z0(  15  )=  0
Z0(  16  )=  0
Z0(  17  )=  0
Z0(  18  )=  0
Z0(  19  )=  0
Z0(  20  )=  0
Z0(  21  )=  0
Z0(  22  )=  0
Z0(  23  )=  0
Z0(  24  )=  0
Z0(  25  )=  0
Z0(  26  )=  0
Z0(  27  )=  0
Z0(  28  )=  0
Z0(  29  )=  0
Z0(  30  )=  0
Z0(  31  )=  0
Z0(  32  )=  0
Z0(  33  )=  0
Z0(  34  )=  0
Z0(  35  )=  0
Z0(  36  )=  0
Z0(  37  )=  0
Z0(  38  )=  0
Z0(  39  )=  0
Z0(  40  )=  0
Z0(  41  )=  0
Z0(  42  )=  0
Z0(  43  )=  0
Z0(  44  )=  0
Z0(  45  )=  0
Z0(  46  )=  0
Z0(  47  )=  0
Z0(  48  )=  0
Z0(  49  )=  0
Z0(  50  )=  0
Z0(  51  )=  0
Z0(  52  )=  0
Z0(  53  )=  0
Z0(  54  )=  0
Z0(  55  )=  0
Z0(  56  )=  0
Z0(  57  )=  0
Z0(  58  )=  0
Z0(  59  )=  0
Z0(  60  )=  0
Z0(  61  )=  0
Z0(  62  )=  0

numstr,kp,4313
numstr,line,5545
numstr,area,1849
k0=4313
l0=5544
A0=1848

NL=0
```

```
NW=1
NW1=2
NT=1
NB=1
NA=2
NF=1

*do,i,1,62

!CREATING THE KEYPOINTS

!stiffner 1
K,k0+1,x0(i),0.0045+y0(i),7.40+z0(i)
K,k0+2,x0(i),0.0045+y0(i),14.6+z0(i)
K,k0+3,x0(i),2.971+y0(i),0.00+z0(i)
K,k0+4,x0(i),4.311+y0(i),1.90+z0(i)
K,k0+5,x0(i),4.494+y0(i),11.00+z0(i)
K,k0+6,x0(i),2.971+y0(i),22.00+z0(i)
K,k0+7,x0(i),2.971+y0(i),-3.25+z0(i)
K,k0+8,x0(i),4.311+y0(i),20.10+z0(i)
K,k0+9,x0(i),2.971+y0(i),25.25+z0(i)
K,k0+10,x0(i),4.383383+y0(i),5.5+z0(i)
K,k0+11,x0(i),4.383383+y0(i),16.5+z0(i)
K,k0+12,x0(i),0.0045+y0(i),11.00+z0(i)
K,k0+13,x0(i),2.207+y0(i),20.1+z0(i)
K,k0+14,x0(i),2.207+y0(i),1.90+z0(i)

!CREATING THE CORRESPONDING LINES

!STIFF 1
L,k0+11,k0+5,NW
L,k0+4,k0+10,NW
L,k0+4,k0+3,NT
L,k0+3,k0+1,NW1
L,k0+1,k0+12,NB
L,k0+2,k0+6,NW1
L,k0+6,k0+8,NT
L,k0+3,k0+7,NF
L,k0+6,k0+9,NF
L,k0+5,k0+10,NW
L,k0+11,k0+8,NW
L,k0+2,k0+12,NW

L,k0+1,k0+10,NA
L,k0+2,k0+11,NA
L,k0+12,k0+5,NA
L,k0+13,k0+9,NA
L,k0+14,k0+7,NA

!CREATING THE CORRESPONDING AREAS & AREA MESHING

!STIFFNER 1
!AL,l0+56,l0+57,l0+58

AL,l0+6,l0+7,l0+11,l0+14
AL,l0+12,l0+14,l0+1,l0+15
AL,l0+5,l0+15,l0+10,l0+13
AL,l0+4,l0+13,l0+2,l0+3

!AL,l0+59,l0+60,l0+61

TYPE,6
MAT,4
REAL,34
ESIZE,5
!ASEL,,,,A0+25,A0+30,1
ASEL,,,,A0+1,A0+4,1
AMESH,ALL
ALLSEL

!TYPE,3
!MAT,13
!REAL,11
!ESIZE,5
!LSEL,,,,L0+16,L0+17,1
```

```
!LMESH,ALL
!ALLSEL

TYPE,9
MAT,14
REAL,38
ESIZE,,1
LSEL,,,,L0+1,L0+12,1
LMESH,ALL
ALLSEL

!*endif
*set,k0,K0+14
*set,L0,L0+17
*set,A0,A0+4
*enddo
```

!INPUT FILE FOR THE BARTON SIDE DECK DIAPHRAGM (STIFFENER)

```
/prep7

x0=
y0=
z0=

*dim,x0,,119
*dim,y0,,119
*dim,z0,,119

X0(  1  )=  1419.1
X0(  2  )=  1423.6
X0(  3  )=  1428.1
X0(  4  )=  1432.6
X0(  5  )=  1437.1
X0(  6  )=  1441.7
X0(  7  )=  1446.2
X0(  8  )=  1450.7
X0(  9  )=  1455.3
X0(  10  )=  1459.8
X0(  11  )=  1464.3
X0(  12  )=  1468.8
X0(  13  )=  1473.4
X0(  14  )=  1477.9
X0(  15  )=  1482.4
X0(  16  )=  1486.9
X0(  17  )=  1491.5
X0(  18  )=  1496
X0(  19  )=  1500.5
X0(  20  )=  1505
X0(  21  )=  1509.6
X0(  22  )=  1514.1
X0(  23  )=  1518.6
X0(  24  )=  1523.1
X0(  25  )=  1527.6
X0(  26  )=  1532.2
X0(  27  )=  1536.7
X0(  28  )=  1541.2
X0(  29  )=  1545.8
X0(  30  )=  1550.3
X0(  31  )=  1554.8
X0(  32  )=  1559.3
X0(  33  )=  1563.9
X0(  34  )=  1568.4
X0(  35  )=  1572.9
X0(  36  )=  1577.4
X0(  37  )=  1582
X0(  38  )=  1586.5
X0(  39  )=  1591
X0(  40  )=  1595.5
X0(  41  )=  1600.1
X0(  42  )=  1604.6
X0(  43  )=  1609.1
X0(  44  )=  1613.6
X0(  45  )=  1618.1
```

X0(	46	)=	1622.7
X0(	47	)=	1627.2
X0(	48	)=	1631.7
X0(	49	)=	1636.3
X0(	50	)=	1640.8
X0(	51	)=	1645.3
X0(	52	)=	1649.8
X0(	53	)=	1654.4
X0(	54	)=	1658.9
X0(	55	)=	1663.4
X0(	56	)=	1667.9
X0(	57	)=	1672.5
X0(	58	)=	1677
X0(	59	)=	1681.5
X0(	60	)=	1686
X0(	61	)=	1690.6
X0(	62	)=	1695.1
X0(	63	)=	1699.6
X0(	64	)=	1704.1
X0(	65	)=	1708.7
X0(	66	)=	1713.2
X0(	67	)=	1717.7
X0(	68	)=	1722.2
X0(	69	)=	1726.8
X0(	70	)=	1731.3
X0(	71	)=	1735.8
X0(	72	)=	1740.3
X0(	73	)=	1744.9
X0(	74	)=	1749.4
X0(	75	)=	1753.9
X0(	76	)=	1758.4
X0(	77	)=	1763
X0(	78	)=	1767.5
X0(	79	)=	1772
X0(	80	)=	1776.5
X0(	81	)=	1781.1
X0(	82	)=	1785.6
X0(	83	)=	1790.1
X0(	84	)=	1794.7
X0(	85	)=	1799.2
X0(	86	)=	1803.7
X0(	87	)=	1808.2
X0(	88	)=	1812.7
X0(	89	)=	1817.3
X0(	90	)=	1822.6
X0(	91	)=	1826.4
X0(	92	)=	1830.3
X0(	93	)=	1834.1
X0(	94	)=	1837.9
X0(	95	)=	1842.3
X0(	96	)=	1846.6
X0(	97	)=	1851
X0(	98	)=	1854.1
X0(	99	)=	1857.3
X0(	100	)=	1860.8
X0(	101	)=	1864.4
X0(	102	)=	1867.9
X0(	103	)=	1872.1
X0(	104	)=	1876.4
X0(	105	)=	1880.6
X0(	106	)=	1885.1
X0(	107	)=	1889.7
X0(	108	)=	1894.2
X0(	109	)=	1898.7
X0(	110	)=	1903.2
X0(	111	)=	1907.8
X0(	112	)=	1912.3
X0(	113	)=	1916.8
X0(	114	)=	1920.9
X0(	115	)=	1925.1
X0(	116	)=	1929.2
X0(	117	)=	1933.4
X0(	118	)=	1937.1
X0(	119	)=	1940.9

Y0(	1	)=	-127.33
Y0(	2	)=	-127.39
Y0(	3	)=	-127.46
Y0(	4	)=	-127.53
Y0(	5	)=	-127.59
Y0(	6	)=	-127.66
Y0(	7	)=	-127.73
Y0(	8	)=	-127.8
Y0(	9	)=	-127.87
Y0(	10	)=	-127.95
Y0(	11	)=	-128.02
Y0(	12	)=	-128.09
Y0(	13	)=	-128.17
Y0(	14	)=	-128.25
Y0(	15	)=	-128.32
Y0(	16	)=	-128.4
Y0(	17	)=	-128.48
Y0(	18	)=	-128.56
Y0(	19	)=	-128.64
Y0(	20	)=	-128.72
Y0(	21	)=	-128.81
Y0(	22	)=	-128.89
Y0(	23	)=	-128.98
Y0(	24	)=	-129.06
Y0(	25	)=	-129.15
Y0(	26	)=	-129.24
Y0(	27	)=	-129.32
Y0(	28	)=	-129.41
Y0(	29	)=	-129.5
Y0(	30	)=	-129.6
Y0(	31	)=	-129.69
Y0(	32	)=	-129.78
Y0(	33	)=	-129.87
Y0(	34	)=	-129.97
Y0(	35	)=	-130.07
Y0(	36	)=	-130.16
Y0(	37	)=	-130.26
Y0(	38	)=	-130.36
Y0(	39	)=	-130.46
Y0(	40	)=	-130.56
Y0(	41	)=	-130.66
Y0(	42	)=	-130.76
Y0(	43	)=	-130.87
Y0(	44	)=	-130.97
Y0(	45	)=	-131.08
Y0(	46	)=	-131.18
Y0(	47	)=	-131.29
Y0(	48	)=	-131.4
Y0(	49	)=	-131.51
Y0(	50	)=	-131.62
Y0(	51	)=	-131.73
Y0(	52	)=	-131.84
Y0(	53	)=	-131.95
Y0(	54	)=	-132.07
Y0(	55	)=	-132.18
Y0(	56	)=	-132.3
Y0(	57	)=	-132.41
Y0(	58	)=	-132.53
Y0(	59	)=	-132.65
Y0(	60	)=	-132.77
Y0(	61	)=	-132.89
Y0(	62	)=	-133.01
Y0(	63	)=	-133.14
Y0(	64	)=	-133.26
Y0(	65	)=	-133.38
Y0(	66	)=	-133.51
Y0(	67	)=	-133.63
Y0(	68	)=	-133.76
Y0(	69	)=	-133.89
Y0(	70	)=	-134.02
Y0(	71	)=	-134.15
Y0(	72	)=	-134.28
Y0(	73	)=	-134.41
Y0(	74	)=	-134.54
Y0(	75	)=	-134.68

Y0(76)= -134.81
Y0(77)= -134.94
Y0(78)= -135.08
Y0(79)= -135.22
Y0(80)= -135.36
Y0(81)= -135.5
Y0(82)= -135.64
Y0(83)= -135.78
Y0(84)= -135.92
Y0(85)= -136.07
Y0(86)= -136.21
Y0(87)= -136.36
Y0(88)= -136.5
Y0(89)= -136.64
Y0(90)= -136.82
Y0(91)= -136.94
Y0(92)= -137.07
Y0(93)= -137.2
Y0(94)= -137.33
Y0(95)= -137.47
Y0(96)= -137.62
Y0(97)= -137.77
Y0(98)= -137.87
Y0(99)= -137.98
Y0(100)= -138.1
Y0(101)= -138.23
Y0(102)= -138.35
Y0(103)= -138.5
Y0(104)= -138.65
Y0(105)= -138.8
Y0(106)= -138.96
Y0(107)= -139.13
Y0(108)= -139.3
Y0(109)= -139.46
Y0(110)= -139.63
Y0(111)= -139.79
Y0(112)= -139.96
Y0(113)= -140.13
Y0(114)= -140.28
Y0(115)= -140.43
Y0(116)= -140.58
Y0(117)= -140.74
Y0(118)= -140.88
Y0(119)= -141.01

Z0(1)= 0
Z0(2)= 0
Z0(3)= 0
Z0(4)= 0
Z0(5)= 0
Z0(6)= 0
Z0(7)= 0
Z0(8)= 0
Z0(9)= 0
Z0(10)= 0
Z0(11)= 0
Z0(12)= 0
Z0(13)= 0
Z0(14)= 0
Z0(15)= 0
Z0(16)= 0
Z0(17)= 0
Z0(18)= 0
Z0(19)= 0
Z0(20)= 0
Z0(21)= 0
Z0(22)= 0
Z0(23)= 0
Z0(24)= 0
Z0(25)= 0
Z0(26)= 0
Z0(27)= 0
Z0(28)= 0
Z0(29)= 0
Z0(30)= 0

Z0(	31	)=	0
Z0(	32	)=	0
Z0(	33	)=	0
Z0(	34	)=	0
Z0(	35	)=	0
Z0(	36	)=	0
Z0(	37	)=	0
Z0(	38	)=	0
Z0(	39	)=	0
Z0(	40	)=	0
Z0(	41	)=	0
Z0(	42	)=	0
Z0(	43	)=	0
Z0(	44	)=	0
Z0(	45	)=	0
Z0(	46	)=	0
Z0(	47	)=	0
Z0(	48	)=	0
Z0(	49	)=	0
Z0(	50	)=	0
Z0(	51	)=	0
Z0(	52	)=	0
Z0(	53	)=	0
Z0(	54	)=	0
Z0(	55	)=	0
Z0(	56	)=	0
Z0(	57	)=	0
Z0(	58	)=	0
Z0(	59	)=	0
Z0(	60	)=	0
Z0(	61	)=	0
Z0(	62	)=	0
Z0(	63	)=	0
Z0(	64	)=	0
Z0(	65	)=	0
Z0(	66	)=	0
Z0(	67	)=	0
Z0(	68	)=	0
Z0(	69	)=	0
Z0(	70	)=	0
Z0(	71	)=	0
Z0(	72	)=	0
Z0(	73	)=	0
Z0(	74	)=	0
Z0(	75	)=	0
Z0(	76	)=	0
Z0(	77	)=	0
Z0(	78	)=	0
Z0(	79	)=	0
Z0(	80	)=	0
Z0(	81	)=	0
Z0(	82	)=	0
Z0(	83	)=	0
Z0(	84	)=	0
Z0(	85	)=	0
Z0(	86	)=	0
Z0(	87	)=	0
Z0(	88	)=	0
Z0(	89	)=	0
Z0(	90	)=	0
Z0(	91	)=	0
Z0(	92	)=	0
Z0(	93	)=	0
Z0(	94	)=	0
Z0(	95	)=	0
Z0(	96	)=	0
Z0(	97	)=	0
Z0(	98	)=	0
Z0(	99	)=	0
Z0(	100	)=	0
Z0(	101	)=	0
Z0(	102	)=	0
Z0(	103	)=	0
Z0(	104	)=	0
Z0(	105	)=	0

```
ZO(   106   )=   0
ZO(   107   )=   0
ZO(   108   )=   0
ZO(   109   )=   0
ZO(   110   )=   0
ZO(   111   )=   0
ZO(   112   )=   0
ZO(   113   )=   0
ZO(   114   )=   0
ZO(   115   )=   0
ZO(   116   )=   0
ZO(   117   )=   0
ZO(   118   )=   0
ZO(   119   )=   0

numstr,kp,5182
numstr,line,6599
numstr,area,2097
k0=5182
l0=6598
A0=2096

NL=0
NW=1
NW1=2
NT=1
NB=1
NA=2
NF=1

*do,i,1,119

!CREATING THE KEYPOINTS

!stiffner 1
K,k0+1,x0(i),0.0045+y0(i),7.40+z0(i)
K,k0+2,x0(i),0.0045+y0(i),14.6+z0(i)
K,k0+3,x0(i),2.971+y0(i),0.00+z0(i)
K,k0+4,x0(i),4.311+y0(i),1.90+z0(i)
K,k0+5,x0(i),4.494+y0(i),11.00+z0(i)
K,k0+6,x0(i),2.971+y0(i),22.00+z0(i)
K,k0+7,x0(i),2.971+y0(i),-3.25+z0(i)
K,k0+8,x0(i),4.311+y0(i),20.10+z0(i)
K,k0+9,x0(i),2.971+y0(i),25.25+z0(i)
K,k0+10,x0(i),4.383383+y0(i),5.5+z0(i)
K,k0+11,x0(i),4.383383+y0(i),16.5+z0(i)
K,k0+12,x0(i),0.0045+y0(i),11.00+z0(i)

K,k0+13,x0(i),2.207+y0(i),20.1+z0(i)
K,k0+14,x0(i),2.207+y0(i),1.90+z0(i)

!CREATING THE CORRESPONDING LINES

!STIFF 1
L,k0+11,k0+5,NW
L,k0+4,k0+10,NW
L,k0+4,k0+3,NT
L,k0+3,k0+1,NW1
L,k0+1,k0+12,NB
L,k0+2,k0+6,NW1
L,k0+6,k0+8,NT
L,k0+3,k0+7,NF
L,k0+6,k0+9,NF
L,k0+5,k0+10,NW
L,k0+11,k0+8,NW
L,k0+2,k0+12,NW
L,k0+1,k0+10,NA
L,k0+2,k0+11,NA
L,k0+12,k0+5,NA
L,k0+13,k0+9,NA
L,k0+14,k0+7,NA

!CREATING THE CORRESPONDING AREAS & AREA MESHING

!STIFFNER 1
```

```
!AL,l0+56,l0+57,l0+58

AL,l0+6,l0+7,l0+11,l0+14
AL,l0+12,l0+14,l0+1,l0+15
AL,l0+5,l0+15,l0+10,l0+13
AL,l0+4,l0+13,l0+2,l0+3

!AL,l0+59,l0+60,l0+61

TYPE,6
MAT,8
REAL,34
ESIZE,5
!ASEL,,,,A0+25,A0+30,1
ASEL,,,,A0+1,A0+4,1
AMESH,ALL
ALLSEL

!TYPE,3
!MAT,13
!REAL,11
!ESIZE,5
!LSEL,,,,L0+16,L0+17,1
!LMESH,ALL
!ALLSEL

TYPE,9
MAT,14
REAL,38
ESIZE,,1
LSEL,,,,L0+1,L0+12,1
LMESH,ALL
ALLSEL

!*endif
*set,k0,K0+14
*set,L0,L0+17
*set,A0,A0+4
*enddo
```

!INPUT FILE FOR THE MAIN SPAN DECK

```
/prep7

x0=
y0=
z0=

*dim,x0,,316
*dim,y0,,316
*dim,z0,,316

X0(  1  )=  9.05
X0(  2  )=  13.575
X0(  3  )=  18.1
X0(  4  )=  22.625
X0(  5  )=  27.15
X0(  6  )=  31.675
X0(  7  )=  36.2
X0(  8  )=  40.725
X0(  9  )=  45.25
X0(  10  )=  49.775
X0(  11  )=  54.3
X0(  12  )=  58.825
X0(  13  )=  63.35
X0(  14  )=  67.875
X0(  15  )=  72.4
X0(  16  )=  76.925
X0(  17  )=  81.45
X0(  18  )=  85.975
X0(  19  )=  90.5
X0(  20  )=  95.025
X0(  21  )=  99.55
X0(  22  )=  104.07
```

X0(	23	)=	108.6
X0(	24	)=	113.13
X0(	25	)=	117.65
X0(	26	)=	122.18
X0(	27	)=	126.7
X0(	28	)=	131.23
X0(	29	)=	135.75
X0(	30	)=	140.28
X0(	31	)=	144.8
X0(	32	)=	149.33
X0(	33	)=	153.85
X0(	34	)=	158.38
X0(	35	)=	162.9
X0(	36	)=	167.43
X0(	37	)=	171.95
X0(	38	)=	176.48
X0(	39	)=	181
X0(	40	)=	185.53
X0(	41	)=	190.05
X0(	42	)=	194.58
X0(	43	)=	199.1
X0(	44	)=	203.63
X0(	45	)=	208.15
X0(	46	)=	212.68
X0(	47	)=	217.2
X0(	48	)=	221.73
X0(	49	)=	226.25
X0(	50	)=	230.78
X0(	51	)=	235.3
X0(	52	)=	239.83
X0(	53	)=	244.35
X0(	54	)=	248.88
X0(	55	)=	253.4
X0(	56	)=	257.92
X0(	57	)=	262.45
X0(	58	)=	266.97
X0(	59	)=	271.5
X0(	60	)=	276.03
X0(	61	)=	280.55
X0(	62	)=	285.08
X0(	63	)=	289.6
X0(	64	)=	294.13
X0(	65	)=	298.65
X0(	66	)=	303.18
X0(	67	)=	307.7
X0(	68	)=	312.23
X0(	69	)=	316.75
X0(	70	)=	321.27
X0(	71	)=	325.8
X0(	72	)=	330.33
X0(	73	)=	334.85
X0(	74	)=	339.38
X0(	75	)=	343.9
X0(	76	)=	348.42
X0(	77	)=	352.95
X0(	78	)=	357.48
X0(	79	)=	362
X0(	80	)=	366.53
X0(	81	)=	371.05
X0(	82	)=	375.58
X0(	83	)=	380.1
X0(	84	)=	384.63
X0(	85	)=	389.15
X0(	86	)=	393.68
X0(	87	)=	398.2
X0(	88	)=	402.73
X0(	89	)=	407.25
X0(	90	)=	411.78
X0(	91	)=	416.3
X0(	92	)=	420.83
X0(	93	)=	425.35
X0(	94	)=	429.88
X0(	95	)=	434.4
X0(	96	)=	438.92
X0(	97	)=	443.45

X0(	98	)=	447.92
X0(	99	)=	452.39
X0(	100	)=	456.86
X0(	101	)=	461.33
X0(	102	)=	466.66
X0(	103	)=	470.59
X0(	104	)=	474.51
X0(	105	)=	478.44
X0(	106	)=	481.75
X0(	107	)=	486.28
X0(	108	)=	490.8
X0(	109	)=	495.33
X0(	110	)=	500.69
X0(	111	)=	504.75
X0(	112	)=	508.82
X0(	113	)=	512.88
X0(	114	)=	516.23
X0(	115	)=	519.57
X0(	116	)=	523.12
X0(	117	)=	526.66
X0(	118	)=	530.21
X0(	119	)=	534.29
X0(	120	)=	538.37
X0(	121	)=	542.9
X0(	122	)=	547.42
X0(	123	)=	552.25
X0(	124	)=	557.08
X0(	125	)=	561.09
X0(	126	)=	565.1
X0(	127	)=	568.65
X0(	128	)=	572.19
X0(	129	)=	575.74
X0(	130	)=	579.19
X0(	131	)=	582.65
X0(	132	)=	586.54
X0(	133	)=	590.43
X0(	134	)=	594.32
X0(	135	)=	600.27
X0(	136	)=	604.46
X0(	137	)=	608.64
X0(	138	)=	612.83
X0(	139	)=	617.97
X0(	140	)=	622.4
X0(	141	)=	626.83
X0(	142	)=	631.26
X0(	143	)=	635.74
X0(	144	)=	640.27
X0(	145	)=	644.79
X0(	146	)=	649.31
X0(	147	)=	653.58
X0(	148	)=	658.35
X0(	149	)=	663.13
X0(	150	)=	667.9
X0(	151	)=	671.5
X0(	152	)=	676.37
X0(	153	)=	681.24
X0(	154	)=	686.11
X0(	155	)=	689.49
X0(	156	)=	694.41
X0(	157	)=	699.32
X0(	158	)=	704.24
X0(	159	)=	707.56
X0(	160	)=	712.48
X0(	161	)=	717.39
X0(	162	)=	722.31
X0(	163	)=	725.69
X0(	164	)=	730.56
X0(	165	)=	735.43
X0(	166	)=	740.3
X0(	167	)=	743.9
X0(	168	)=	748.67
X0(	169	)=	753.44
X0(	170	)=	758.21
X0(	171	)=	762.18
X0(	172	)=	766.71

X0(	173	)=	771.23
X0(	174	)=	775.76
X0(	175	)=	780.28
X0(	176	)=	784.8
X0(	177	)=	789.31
X0(	178	)=	793.83
X0(	179	)=	798.97
X0(	180	)=	803.16
X0(	181	)=	807.34
X0(	182	)=	811.53
X0(	183	)=	817.48
X0(	184	)=	821.37
X0(	185	)=	825.26
X0(	186	)=	829.15
X0(	187	)=	832.6
X0(	188	)=	836.05
X0(	189	)=	839.6
X0(	190	)=	843.15
X0(	191	)=	846.7
X0(	192	)=	850.71
X0(	193	)=	854.71
X0(	194	)=	859.24
X0(	195	)=	863.76
X0(	196	)=	868.6
X0(	197	)=	873.43
X0(	198	)=	877.51
X0(	199	)=	881.58
X0(	200	)=	885.13
X0(	201	)=	888.68
X0(	202	)=	892.23
X0(	203	)=	895.57
X0(	204	)=	898.91
X0(	205	)=	902.97
X0(	206	)=	907.04
X0(	207	)=	911.1
X0(	208	)=	915.63
X0(	209	)=	920.43
X0(	210	)=	925.24
X0(	211	)=	930.05
X0(	212	)=	933.36
X0(	213	)=	937.29
X0(	214	)=	941.21
X0(	215	)=	945.14
X0(	216	)=	950.47
X0(	217	)=	954.93
X0(	218	)=	959.39
X0(	219	)=	963.84
X0(	220	)=	968.3
X0(	221	)=	972.83
X0(	222	)=	977.35
X0(	223	)=	981.88
X0(	224	)=	986.4
X0(	225	)=	990.93
X0(	226	)=	995.45
X0(	227	)=	999.98
X0(	228	)=	1004.5
X0(	229	)=	1009
X0(	230	)=	1013.6
X0(	231	)=	1018.1
X0(	232	)=	1022.6
X0(	233	)=	1027.1
X0(	234	)=	1031.7
X0(	235	)=	1036.2
X0(	236	)=	1040.7
X0(	237	)=	1045.2
X0(	238	)=	1049.8
X0(	239	)=	1054.3
X0(	240	)=	1058.8
X0(	241	)=	1063.3
X0(	242	)=	1067.9
X0(	243	)=	1072.4
X0(	244	)=	1076.9
X0(	245	)=	1081.4
X0(	246	)=	1086
X0(	247	)=	1090.5

X0(	248	)=	1095
X0(	249	)=	1099.5
X0(	250	)=	1104.1
X0(	251	)=	1108.6
X0(	252	)=	1113.1
X0(	253	)=	1117.6
X0(	254	)=	1122.2
X0(	255	)=	1126.7
X0(	256	)=	1131.2
X0(	257	)=	1135.7
X0(	258	)=	1140.3
X0(	259	)=	1144.8
X0(	260	)=	1149.3
X0(	261	)=	1153.8
X0(	262	)=	1158.4
X0(	263	)=	1162.9
X0(	264	)=	1167.4
X0(	265	)=	1171.9
X0(	266	)=	1176.5
X0(	267	)=	1181
X0(	268	)=	1185.5
X0(	269	)=	1190
X0(	270	)=	1194.6
X0(	271	)=	1199.1
X0(	272	)=	1203.6
X0(	273	)=	1208.1
X0(	274	)=	1212.7
X0(	275	)=	1217.2
X0(	276	)=	1221.7
X0(	277	)=	1226.2
X0(	278	)=	1230.8
X0(	279	)=	1235.3
X0(	280	)=	1239.8
X0(	281	)=	1244.3
X0(	282	)=	1248.9
X0(	283	)=	1253.4
X0(	284	)=	1257.9
X0(	285	)=	1262.4
X0(	286	)=	1267
X0(	287	)=	1271.5
X0(	288	)=	1276
X0(	289	)=	1280.5
X0(	290	)=	1285.1
X0(	291	)=	1289.6
X0(	292	)=	1294.1
X0(	293	)=	1298.6
X0(	294	)=	1303.2
X0(	295	)=	1307.7
X0(	296	)=	1312.2
X0(	297	)=	1316.7
X0(	298	)=	1321.3
X0(	299	)=	1325.8
X0(	300	)=	1330.3
X0(	301	)=	1334.8
X0(	302	)=	1339.4
X0(	303	)=	1343.9
X0(	304	)=	1348.4
X0(	305	)=	1352.9
X0(	306	)=	1357.5
X0(	307	)=	1362
X0(	308	)=	1366.5
X0(	309	)=	1371
X0(	310	)=	1375.6
X0(	311	)=	1380.1
X0(	312	)=	1384.6
X0(	313	)=	1389.1
X0(	314	)=	1393.7
X0(	315	)=	1398.2
X0(	316	)=	1402.7

Y0(	1	)=	-127.101
Y0(	2	)=	-127.041
Y0(	3	)=	-126.981
Y0(	4	)=	-126.921
Y0(	5	)=	-126.861

Y0(	6	)=	-126.751
Y0(	7	)=	-126.641
Y0(	8	)=	-126.531
Y0(	9	)=	-126.431
Y0(	10	)=	-126.411
Y0(	11	)=	-126.401
Y0(	12	)=	-126.391
Y0(	13	)=	-126.381
Y0(	14	)=	-126.321
Y0(	15	)=	-126.271
Y0(	16	)=	-126.211
Y0(	17	)=	-126.161
Y0(	18	)=	-126.101
Y0(	19	)=	-126.051
Y0(	20	)=	-125.991
Y0(	21	)=	-125.941
Y0(	22	)=	-125.881
Y0(	23	)=	-125.831
Y0(	24	)=	-125.781
Y0(	25	)=	-125.731
Y0(	26	)=	-125.671
Y0(	27	)=	-125.621
Y0(	28	)=	-125.571
Y0(	29	)=	-125.521
Y0(	30	)=	-125.471
Y0(	31	)=	-125.421
Y0(	32	)=	-125.371
Y0(	33	)=	-125.321
Y0(	34	)=	-125.271
Y0(	35	)=	-125.221
Y0(	36	)=	-125.171
Y0(	37	)=	-125.121
Y0(	38	)=	-125.071
Y0(	39	)=	-125.031
Y0(	40	)=	-124.981
Y0(	41	)=	-124.941
Y0(	42	)=	-124.891
Y0(	43	)=	-124.851
Y0(	44	)=	-124.801
Y0(	45	)=	-124.761
Y0(	46	)=	-124.711
Y0(	47	)=	-124.671
Y0(	48	)=	-124.621
Y0(	49	)=	-124.581
Y0(	50	)=	-124.531
Y0(	51	)=	-124.491
Y0(	52	)=	-124.451
Y0(	53	)=	-124.411
Y0(	54	)=	-124.371
Y0(	55	)=	-124.331
Y0(	56	)=	-124.291
Y0(	57	)=	-124.251
Y0(	58	)=	-124.211
Y0(	59	)=	-124.171
Y0(	60	)=	-124.131
Y0(	61	)=	-124.101
Y0(	62	)=	-124.061
Y0(	63	)=	-124.031
Y0(	64	)=	-123.991
Y0(	65	)=	-123.961
Y0(	66	)=	-123.921
Y0(	67	)=	-123.881
Y0(	68	)=	-123.841
Y0(	69	)=	-123.811
Y0(	70	)=	-123.771
Y0(	71	)=	-123.741
Y0(	72	)=	-123.701
Y0(	73	)=	-123.671
Y0(	74	)=	-123.631
Y0(	75	)=	-123.601
Y0(	76	)=	-123.571
Y0(	77	)=	-123.541
Y0(	78	)=	-123.511
Y0(	79	)=	-123.481
Y0(	80	)=	-123.451

Y0(	81	)=	-123.421
Y0(	82	)=	-123.391
Y0(	83	)=	-123.361
Y0(	84	)=	-123.331
Y0(	85	)=	-123.301
Y0(	86	)=	-123.271
Y0(	87	)=	-123.241
Y0(	88	)=	-123.211
Y0(	89	)=	-123.191
Y0(	90	)=	-123.161
Y0(	91	)=	-123.141
Y0(	92	)=	-123.111
Y0(	93	)=	-123.091
Y0(	94	)=	-123.061
Y0(	95	)=	-123.041
Y0(	96	)=	-123.011
Y0(	97	)=	-122.991
Y0(	98	)=	-122.961
Y0(	99	)=	-122.941
Y0(	100	)=	-122.921
Y0(	101	)=	-122.901
Y0(	102	)=	-122.881
Y0(	103	)=	-122.861
Y0(	104	)=	-122.841
Y0(	105	)=	-122.821
Y0(	106	)=	-122.811
Y0(	107	)=	-122.791
Y0(	108	)=	-122.771
Y0(	109	)=	-122.751
Y0(	110	)=	-122.731
Y0(	111	)=	-122.711
Y0(	112	)=	-122.691
Y0(	113	)=	-122.681
Y0(	114	)=	-122.671
Y0(	115	)=	-122.661
Y0(	116	)=	-122.641
Y0(	117	)=	-122.631
Y0(	118	)=	-122.621
Y0(	119	)=	-122.601
Y0(	120	)=	-122.591
Y0(	121	)=	-122.571
Y0(	122	)=	-122.561
Y0(	123	)=	-122.541
Y0(	124	)=	-122.531
Y0(	125	)=	-122.521
Y0(	126	)=	-122.511
Y0(	127	)=	-122.501
Y0(	128	)=	-122.491
Y0(	129	)=	-122.481
Y0(	130	)=	-122.471
Y0(	131	)=	-122.461
Y0(	132	)=	-122.451
Y0(	133	)=	-122.441
Y0(	134	)=	-122.441
Y0(	135	)=	-122.421
Y0(	136	)=	-122.411
Y0(	137	)=	-122.401
Y0(	138	)=	-122.401
Y0(	139	)=	-122.391
Y0(	140	)=	-122.381
Y0(	141	)=	-122.371
Y0(	142	)=	-122.371
Y0(	143	)=	-122.361
Y0(	144	)=	-122.351
Y0(	145	)=	-122.341
Y0(	146	)=	-122.341
Y0(	147	)=	-122.341
Y0(	148	)=	-122.331
Y0(	149	)=	-122.331
Y0(	150	)=	-122.331
Y0(	151	)=	-122.321
Y0(	152	)=	-122.321
Y0(	153	)=	-122.321
Y0(	154	)=	-122.321
Y0(	155	)=	-122.321

Y0(	156	)=	-122.311
Y0(	157	)=	-122.311
Y0(	158	)=	-122.311
Y0(	159	)=	-122.311
Y0(	160	)=	-122.311
Y0(	161	)=	-122.311
Y0(	162	)=	-122.321
Y0(	163	)=	-122.321
Y0(	164	)=	-122.321
Y0(	165	)=	-122.321
Y0(	166	)=	-122.321
Y0(	167	)=	-122.331
Y0(	168	)=	-122.331
Y0(	169	)=	-122.331
Y0(	170	)=	-122.341
Y0(	171	)=	-122.341
Y0(	172	)=	-122.341
Y0(	173	)=	-122.351
Y0(	174	)=	-122.361
Y0(	175	)=	-122.371
Y0(	176	)=	-122.371
Y0(	177	)=	-122.381
Y0(	178	)=	-122.391
Y0(	179	)=	-122.401
Y0(	180	)=	-122.401
Y0(	181	)=	-122.411
Y0(	182	)=	-122.421
Y0(	183	)=	-122.441
Y0(	184	)=	-122.441
Y0(	185	)=	-122.451
Y0(	186	)=	-122.461
Y0(	187	)=	-122.471
Y0(	188	)=	-122.481
Y0(	189	)=	-122.491
Y0(	190	)=	-122.501
Y0(	191	)=	-122.511
Y0(	192	)=	-122.521
Y0(	193	)=	-122.531
Y0(	194	)=	-122.541
Y0(	195	)=	-122.561
Y0(	196	)=	-122.571
Y0(	197	)=	-122.591
Y0(	198	)=	-122.601
Y0(	199	)=	-122.621
Y0(	200	)=	-122.631
Y0(	201	)=	-122.641
Y0(	202	)=	-122.661
Y0(	203	)=	-122.671
Y0(	204	)=	-122.681
Y0(	205	)=	-122.691
Y0(	206	)=	-122.711
Y0(	207	)=	-122.731
Y0(	208	)=	-122.751
Y0(	209	)=	-122.771
Y0(	210	)=	-122.791
Y0(	211	)=	-122.811
Y0(	212	)=	-122.821
Y0(	213	)=	-122.841
Y0(	214	)=	-122.861
Y0(	215	)=	-122.881
Y0(	216	)=	-122.901
Y0(	217	)=	-122.921
Y0(	218	)=	-122.941
Y0(	219	)=	-122.961
Y0(	220	)=	-122.991
Y0(	221	)=	-123.011
Y0(	222	)=	-123.041
Y0(	223	)=	-123.061
Y0(	224	)=	-123.091
Y0(	225	)=	-123.111
Y0(	226	)=	-123.141
Y0(	227	)=	-123.161
Y0(	228	)=	-123.191
Y0(	229	)=	-123.211
Y0(	230	)=	-123.241

Y0(	231	)=	-123.271
Y0(	232	)=	-123.301
Y0(	233	)=	-123.331
Y0(	234	)=	-123.361
Y0(	235	)=	-123.391
Y0(	236	)=	-123.421
Y0(	237	)=	-123.451
Y0(	238	)=	-123.481
Y0(	239	)=	-123.511
Y0(	240	)=	-123.541
Y0(	241	)=	-123.571
Y0(	242	)=	-123.601
Y0(	243	)=	-123.631
Y0(	244	)=	-123.671
Y0(	245	)=	-123.701
Y0(	246	)=	-123.741
Y0(	247	)=	-123.771
Y0(	248	)=	-123.811
Y0(	249	)=	-123.841
Y0(	250	)=	-123.881
Y0(	251	)=	-123.921
Y0(	252	)=	-123.961
Y0(	253	)=	-123.991
Y0(	254	)=	-124.031
Y0(	255	)=	-124.061
Y0(	256	)=	-124.101
Y0(	257	)=	-124.131
Y0(	258	)=	-124.171
Y0(	259	)=	-124.211
Y0(	260	)=	-124.251
Y0(	261	)=	-124.291
Y0(	262	)=	-124.331
Y0(	263	)=	-124.371
Y0(	264	)=	-124.411
Y0(	265	)=	-124.451
Y0(	266	)=	-124.491
Y0(	267	)=	-124.531
Y0(	268	)=	-124.581
Y0(	269	)=	-124.621
Y0(	270	)=	-124.671
Y0(	271	)=	-124.711
Y0(	272	)=	-124.761
Y0(	273	)=	-124.801
Y0(	274	)=	-124.851
Y0(	275	)=	-124.891
Y0(	276	)=	-124.941
Y0(	277	)=	-124.981
Y0(	278	)=	-125.031
Y0(	279	)=	-125.071
Y0(	280	)=	-125.121
Y0(	281	)=	-125.171
Y0(	282	)=	-125.221
Y0(	283	)=	-125.271
Y0(	284	)=	-125.321
Y0(	285	)=	-125.371
Y0(	286	)=	-125.421
Y0(	287	)=	-125.471
Y0(	288	)=	-125.521
Y0(	289	)=	-125.571
Y0(	290	)=	-125.621
Y0(	291	)=	-125.671
Y0(	292	)=	-125.731
Y0(	293	)=	-125.781
Y0(	294	)=	-125.831
Y0(	295	)=	-125.881
Y0(	296	)=	-125.941
Y0(	297	)=	-125.991
Y0(	298	)=	-126.051
Y0(	299	)=	-126.101
Y0(	300	)=	-126.161
Y0(	301	)=	-126.211
Y0(	302	)=	-126.271
Y0(	303	)=	-126.321
Y0(	304	)=	-126.381
Y0(	305	)=	-126.391

Y0(	306	)=	-126.401
Y0(	307	)=	-126.411
Y0(	308	)=	-126.431
Y0(	309	)=	-126.531
Y0(	310	)=	-126.641
Y0(	311	)=	-126.751
Y0(	312	)=	-126.861
Y0(	313	)=	-126.921
Y0(	314	)=	-126.981
Y0(	315	)=	-127.041
Y0(	316	)=	-127.101

Z0(	1	)=	0
Z0(	2	)=	0
Z0(	3	)=	0
Z0(	4	)=	0
Z0(	5	)=	0
Z0(	6	)=	0
Z0(	7	)=	0
Z0(	8	)=	0
Z0(	9	)=	0
Z0(	10	)=	0
Z0(	11	)=	0
Z0(	12	)=	0
Z0(	13	)=	0
Z0(	14	)=	0
Z0(	15	)=	0
Z0(	16	)=	0
Z0(	17	)=	0
Z0(	18	)=	0
Z0(	19	)=	0
Z0(	20	)=	0
Z0(	21	)=	0
Z0(	22	)=	0
Z0(	23	)=	0
Z0(	24	)=	0
Z0(	25	)=	0
Z0(	26	)=	0
Z0(	27	)=	0
Z0(	28	)=	0
Z0(	29	)=	0
Z0(	30	)=	0
Z0(	31	)=	0
Z0(	32	)=	0
Z0(	33	)=	0
Z0(	34	)=	0
Z0(	35	)=	0
Z0(	36	)=	0
Z0(	37	)=	0
Z0(	38	)=	0
Z0(	39	)=	0
Z0(	40	)=	0
Z0(	41	)=	0
Z0(	42	)=	0
Z0(	43	)=	0
Z0(	44	)=	0
Z0(	45	)=	0
Z0(	46	)=	0
Z0(	47	)=	0
Z0(	48	)=	0
Z0(	49	)=	0
Z0(	50	)=	0
Z0(	51	)=	0
Z0(	52	)=	0
Z0(	53	)=	0
Z0(	54	)=	0
Z0(	55	)=	0
Z0(	56	)=	0
Z0(	57	)=	0
Z0(	58	)=	0
Z0(	59	)=	0
Z0(	60	)=	0
Z0(	61	)=	0
Z0(	62	)=	0

Z0(	63	)=	0
Z0(	64	)=	0
Z0(	65	)=	0
Z0(	66	)=	0
Z0(	67	)=	0
Z0(	68	)=	0
Z0(	69	)=	0
Z0(	70	)=	0
Z0(	71	)=	0
Z0(	72	)=	0
Z0(	73	)=	0
Z0(	74	)=	0
Z0(	75	)=	0
Z0(	76	)=	0
Z0(	77	)=	0
Z0(	78	)=	0
Z0(	79	)=	0
Z0(	80	)=	0
Z0(	81	)=	0
Z0(	82	)=	0
Z0(	83	)=	0
Z0(	84	)=	0
Z0(	85	)=	0
Z0(	86	)=	0
Z0(	87	)=	0
Z0(	88	)=	0
Z0(	89	)=	0
Z0(	90	)=	0
Z0(	91	)=	0
Z0(	92	)=	0
Z0(	93	)=	0
Z0(	94	)=	0
Z0(	95	)=	0
Z0(	96	)=	0
Z0(	97	)=	0
Z0(	98	)=	0
Z0(	99	)=	0
Z0(	100	)=	0
Z0(	101	)=	0
Z0(	102	)=	0
Z0(	103	)=	0
Z0(	104	)=	0
Z0(	105	)=	0
Z0(	106	)=	0
Z0(	107	)=	0
Z0(	108	)=	0
Z0(	109	)=	0
Z0(	110	)=	0
Z0(	111	)=	0
Z0(	112	)=	0
Z0(	113	)=	0
Z0(	114	)=	0
Z0(	115	)=	0
Z0(	116	)=	0
Z0(	117	)=	0
Z0(	118	)=	0
Z0(	119	)=	0
Z0(	120	)=	0
Z0(	121	)=	0
Z0(	122	)=	0
Z0(	123	)=	0
Z0(	124	)=	0
Z0(	125	)=	0
Z0(	126	)=	0
Z0(	127	)=	0
Z0(	128	)=	0
Z0(	129	)=	0
Z0(	130	)=	0
Z0(	131	)=	0
Z0(	132	)=	0
Z0(	133	)=	0
Z0(	134	)=	0
Z0(	135	)=	0
Z0(	136	)=	0
Z0(	137	)=	0

Z0(	138	)=	0
Z0(	139	)=	0
Z0(	140	)=	0
Z0(	141	)=	0
Z0(	142	)=	0
Z0(	143	)=	0
Z0(	144	)=	0
Z0(	145	)=	0
Z0(	146	)=	0
Z0(	147	)=	0
Z0(	148	)=	0
Z0(	149	)=	0
Z0(	150	)=	0
Z0(	151	)=	0
Z0(	152	)=	0
Z0(	153	)=	0
Z0(	154	)=	0
Z0(	155	)=	0
Z0(	156	)=	0
Z0(	157	)=	0
Z0(	158	)=	0
Z0(	159	)=	0
Z0(	160	)=	0
Z0(	161	)=	0
Z0(	162	)=	0
Z0(	163	)=	0
Z0(	164	)=	0
Z0(	165	)=	0
Z0(	166	)=	0
Z0(	167	)=	0
Z0(	168	)=	0
Z0(	169	)=	0
Z0(	170	)=	0
Z0(	171	)=	0
Z0(	172	)=	0
Z0(	173	)=	0
Z0(	174	)=	0
Z0(	175	)=	0
Z0(	176	)=	0
Z0(	177	)=	0
Z0(	178	)=	0
Z0(	179	)=	0
Z0(	180	)=	0
Z0(	181	)=	0
Z0(	182	)=	0
Z0(	183	)=	0
Z0(	184	)=	0
Z0(	185	)=	0
Z0(	186	)=	0
Z0(	187	)=	0
Z0(	188	)=	0
Z0(	189	)=	0
Z0(	190	)=	0
Z0(	191	)=	0
Z0(	192	)=	0
Z0(	193	)=	0
Z0(	194	)=	0
Z0(	195	)=	0
Z0(	196	)=	0
Z0(	197	)=	0
Z0(	198	)=	0
Z0(	199	)=	0
Z0(	200	)=	0
Z0(	201	)=	0
Z0(	202	)=	0
Z0(	203	)=	0
Z0(	204	)=	0
Z0(	205	)=	0
Z0(	206	)=	0
Z0(	207	)=	0
Z0(	208	)=	0
Z0(	209	)=	0
Z0(	210	)=	0
Z0(	211	)=	0
Z0(	212	)=	0

Z0(	213	)=	0
Z0(	214	)=	0
Z0(	215	)=	0
Z0(	216	)=	0
Z0(	217	)=	0
Z0(	218	)=	0
Z0(	219	)=	0
Z0(	220	)=	0
Z0(	221	)=	0
Z0(	222	)=	0
Z0(	223	)=	0
Z0(	224	)=	0
Z0(	225	)=	0
Z0(	226	)=	0
Z0(	227	)=	0
Z0(	228	)=	0
Z0(	229	)=	0
Z0(	230	)=	0
Z0(	231	)=	0
Z0(	232	)=	0
Z0(	233	)=	0
Z0(	234	)=	0
Z0(	235	)=	0
Z0(	236	)=	0
Z0(	237	)=	0
Z0(	238	)=	0
Z0(	239	)=	0
Z0(	240	)=	0
Z0(	241	)=	0
Z0(	242	)=	0
Z0(	243	)=	0
Z0(	244	)=	0
Z0(	245	)=	0
Z0(	246	)=	0
Z0(	247	)=	0
Z0(	248	)=	0
Z0(	249	)=	0
Z0(	250	)=	0
Z0(	251	)=	0
Z0(	252	)=	0
Z0(	253	)=	0
Z0(	254	)=	0
Z0(	255	)=	0
Z0(	256	)=	0
Z0(	257	)=	0
Z0(	258	)=	0
Z0(	259	)=	0
Z0(	260	)=	0
Z0(	261	)=	0
Z0(	262	)=	0
Z0(	263	)=	0
Z0(	264	)=	0
Z0(	265	)=	0
Z0(	266	)=	0
Z0(	267	)=	0
Z0(	268	)=	0
Z0(	269	)=	0
Z0(	270	)=	0
Z0(	271	)=	0
Z0(	272	)=	0
Z0(	273	)=	0
Z0(	274	)=	0
Z0(	275	)=	0
Z0(	276	)=	0
Z0(	277	)=	0
Z0(	278	)=	0
Z0(	279	)=	0
Z0(	280	)=	0
Z0(	281	)=	0
Z0(	282	)=	0
Z0(	283	)=	0
Z0(	284	)=	0
Z0(	285	)=	0
Z0(	286	)=	0
Z0(	287	)=	0

```
Z0(  288  )=  0
Z0(  289  )=  0
Z0(  290  )=  0
Z0(  291  )=  0
Z0(  292  )=  0
Z0(  293  )=  0
Z0(  294  )=  0
Z0(  295  )=  0
Z0(  296  )=  0
Z0(  297  )=  0
Z0(  298  )=  0
Z0(  299  )=  0
Z0(  300  )=  0
Z0(  301  )=  0
Z0(  302  )=  0
Z0(  303  )=  0
Z0(  304  )=  0
Z0(  305  )=  0
Z0(  306  )=  0
Z0(  307  )=  0
Z0(  308  )=  0
Z0(  309  )=  0
Z0(  310  )=  0
Z0(  311  )=  0
Z0(  312  )=  0
Z0(  313  )=  0
Z0(  314  )=  0
Z0(  315  )=  0
Z0(  316  )=  0

numstr,kp,6849
numstr,line,8622
numstr,area,2573
k0=6849
l0=8621
A0=2572

NL=0
NW=1
NW1=2
NT=1
NB=1
NA=2
NF=1

*do,i,1,316

!CREATING THE KEYPOINTS

!stiffner 1
K,k0+1,x0(i),0.0045+y0(i),7.40+z0(i)
K,k0+2,x0(i),0.0045+y0(i),14.6+z0(i)
K,k0+3,x0(i),2.971+y0(i),0.00+z0(i)
K,k0+4,x0(i),4.311+y0(i),1.90+z0(i)
K,k0+5,x0(i),4.494+y0(i),11.00+z0(i)
K,k0+6,x0(i),2.971+y0(i),22.00+z0(i)
K,k0+7,x0(i),2.971+y0(i),-3.25+z0(i)
K,k0+8,x0(i),4.311+y0(i),20.10+z0(i)
K,k0+9,x0(i),2.971+y0(i),25.25+z0(i)
K,k0+10,x0(i),4.383383+y0(i),5.5+z0(i)
K,k0+11,x0(i),4.383383+y0(i),16.5+z0(i)
K,k0+12,x0(i),0.0045+y0(i),11.00+z0(i)

K,k0+13,x0(i),2.207+y0(i),20.1+z0(i)
K,k0+14,x0(i),2.207+y0(i),1.90+z0(i)

!CREATING THE CORRESPONDING LINES

!STIFF 1
L,k0+11,k0+5,NW
L,k0+4,k0+10,NW
L,k0+4,k0+3,NT
L,k0+3,k0+1,NW1
L,k0+1,k0+12,NB
L,k0+2,k0+6,NW1
```

```
L,k0+6,k0+8,NT
L,k0+3,k0+7,NF
L,k0+6,k0+9,NF
L,k0+5,k0+10,NW
L,k0+11,k0+8,NW
L,k0+2,k0+12,NW

L,k0+1,k0+10,NA
L,k0+2,k0+11,NA
L,k0+12,k0+5,NA
L,k0+13,k0+9,NA
L,k0+14,k0+7,NA

!CREATING THE CORRESPONDING AREAS & AREA MESHING

!STIFFNER 1
!AL,l0+56,l0+57,l0+58

AL,l0+6,l0+7,l0+11,l0+14
AL,l0+12,l0+14,l0+1,l0+15
AL,l0+5,l0+15,l0+10,l0+13
AL,l0+4,l0+13,l0+2,l0+3

!AL,l0+59,l0+60,l0+61

TYPE,6
MAT,7
REAL,34
ESIZE,5
!ASEL,,,,A0+25,A0+30,1
ASEL,,,,A0+1,A0+4,1
AMESH,ALL
ALLSEL

!TYPE,3
!MAT,13
!REAL,11
!ESIZE,5
!LSEL,,,,L0+16,L0+17,1
!LMESH,ALL
!ALLSEL

TYPE,9
MAT,14
REAL,38
ESIZE,,1
LSEL,,,,L0+1,L0+12,1
LMESH,ALL
ALLSEL

!*endif
*set,k0,K0+14
*set,L0,L0+17
*set,A0,A0+4
*enddo


!INPUT FILE FOR THE END DECK (HESSLE SIDE)

/prep7

x0=
y0=
z0=
q=

*dim,x0,,2
*dim,y0,,2
*dim,z0,,1
*dim,q,,1

X0(1)=0.00
X0(2)=-7.25
Y0(1)=-127.215
Y0(2)=-127.337
```

```
Z0(1)=0.00

numstr,kp,11274
numstr,line,13994
numstr,area,3837

k0=11274
l0=13993
A0=3836

*do,i,1,1
*set,q(i),x0(i+1)-x0(i)

*if,q,lt,9.05,then

!CREATING THE KEYPOINTS

K,k0+0,0.00+x0(i),0.0045+y0(i),7.40+z0(i)
K,k0+1,0.00+x0(i),2.127+y0(i),2.1+z0(i)
K,k0+2,0.00+x0(i),2.971+y0(i),0.00+z0(i)
K,k0+3,0.00+x0(i),4.311+y0(i),1.90+z0(i)
K,k0+4,0.00+x0(i),4.494+y0(i),11.00+z0(i)
K,k0+5,0.00+x0(i),2.971+y0(i),-3.25+z0(i)
K,k0+6,0.00+x0(i),0.0045+y0(i),14.6+z0(i)
K,k0+7,0.00+x0(i),2.971+y0(i),22.00+z0(i)
K,k0+8,0.00+x0(i),4.311+y0(i),20.10+z0(i)
K,k0+9,0.00+x0(i),2.971+y0(i),25.25+z0(i)
K,k0+10,0.00+x0(i),2.127+y0(i),19.90+z0(i)
K,k0+24,0.00+x0(i),4.383383+y0(i),5.5+z0(i)
K,k0+25,0.00+x0(i),4.383383+y0(i),16.5+z0(i)
K,k0+26,0.00+x0(i),0.0045+y0(i),11.00+z0(i)
!--------------------------------
K,k0+11,q(i)+x0(i),0.0045+y0(i+1),14.6+z0(i)
K,k0+12,q(i)+x0(i),2.971+y0(i+1),22.00+z0(i)
K,k0+13,q(i)+x0(i),4.494+y0(i+1),11.00+z0(i)
K,k0+14,q(i)+x0(i),4.311+y0(i+1),20.10+z0(i)
K,k0+15,q(i)+x0(i),2.127+y0(i+1),19.90+z0(i)
K,k0+16,q(i)+x0(i),2.971+y0(i+1),25.25+z0(i)
K,k0+17,q(i)+x0(i),0.0045+y0(i+1),7.40+z0(i)
K,k0+18,q(i)+x0(i),2.127+y0(i+1),2.1+z0(i)
K,k0+19,q(i)+x0(i),2.971+y0(i+1),0.00+z0(i)
K,k0+20,q(i)+x0(i),4.311+y0(i+1),1.90+z0(i)
K,k0+21,q(i)+x0(i),2.971+y0(i+1),-3.25+z0(i)
K,k0+22,q(i)+x0(i),4.383383+y0(i+1),5.5+z0(i)
K,k0+23,q(i)+x0(i),4.383383+y0(i+1),16.5+z0(i)
K,k0+27,q(i)+x0(i),0.0045+y0(i+1),11.00+z0(i)
!-----------------------------------
!stiffner 1
K,k0+28,-2.725+x0(i),0.0045+y0(i)-2.725*(y0(i+1)-y0(i))/q(i),7.40+z0(i)
K,k0+29,-2.725+x0(i),0.0045+y0(i)-2.725*(y0(i+1)-y0(i))/q(i),14.6+z0(i)
K,k0+30,-2.725+x0(i),2.127+y0(i)-2.725*(y0(i+1)-y0(i))/q(i),2.1+z0(i)
K,k0+31,-2.725+x0(i),2.971+y0(i)-2.725*(y0(i+1)-y0(i))/q(i),0.00+z0(i)
K,k0+32,-2.725+x0(i),4.311+y0(i)-2.725*(y0(i+1)-y0(i))/q(i),1.90+z0(i)
K,k0+33,-2.725+x0(i),4.494+y0(i)-2.725*(y0(i+1)-y0(i))/q(i),11.00+z0(i)
K,k0+34,-2.725+x0(i),2.971+y0(i)-2.725*(y0(i+1)-y0(i))/q(i),22.00+z0(i)
K,k0+35,-2.725+x0(i),2.971+y0(i)-2.725*(y0(i+1)-y0(i))/q(i),-3.25+z0(i)
K,k0+36,-2.725+x0(i),4.311+y0(i)-2.725*(y0(i+1)-y0(i))/q(i),20.10+z0(i)
K,k0+37,-2.725+x0(i),2.127+y0(i)-2.725*(y0(i+1)-y0(i))/q(i),19.90+z0(i)
K,k0+38,-2.725+x0(i),2.971+y0(i)-2.725*(y0(i+1)-y0(i))/q(i),25.25+z0(i)
K,k0+39,-2.725+x0(i),4.383383+y0(i)-2.725*(y0(i+1)-y0(i))/q(i),5.5+z0(i)
K,k0+40,-2.725+x0(i),4.383383+y0(i)-2.725*(y0(i+1)-y0(i))/q(i),16.5+z0(i)
K,k0+41,-2.725+x0(i),0.0045+y0(i)-2.725*(y0(i+1)-y0(i))/q(i),11.00+z0(i)

NL=0
NW=1
NW1=2
NT=1
NB=1
NA=2

!CREATING THE CORRESPONDING LINES

L,k0+8,k0+25,NW
L,k0+24,k0+3,NW
L,k0+3,k0+2,NT
```

```
L,k0+2,k0+0,NW1

L,k0+26,k0+6,NB
L,k0+6,k0+7,NW1

L,k0+7,k0+8,NT
L,k0+23,k0+13,NW
L,k0+13,k0+22,NW
L,k0+20,k0+19,NT
L,k0+19,k0+17,NW1

L,k0+17,k0+27,NB
L,k0+11,k0+12,NW1

L,k0+12,k0+14,NT
L,k0+36,k0+14,NL
L,k0+8,k0+36,NL
L,k0+33,k0+13,NL
L,k0+4,k0+33,NL
L,k0+32,k0+20,NL
L,k0+32,k0+3,NL
L,k0+31,k0+19,NL
L,k0+2,k0+31,NL
L,k0+28,k0+17,NL
L,k0+0,k0+28,NL
L,k0+29,k0+11,NL
L,k0+6,k0+29,NL
L,k0+34,k0+12,NL
L,k0+7,k0+34,NL
L,k0+23,k0+14,NW
L,k0+22,k0+20,NW
L,k0+4,k0+24,NW
L,k0+4,k0+25,NW
L,k0+40,k0+23,NL
L,k0+25,k0+40,NL
L,k0+39,k0+22,NL
L,k0+24,k0+39,NL
L,k0+27,k0+41,NL
L,k0+41,k0+26,NL
L,k0+0,k0+26,NB
L,k0+27,k0+11,NB

!STIFF 1
L,k0+40,k0+33,NW
L,k0+32,k0+39,NW
L,k0+32,k0+31,NT
L,k0+31,k0+28,NW1
L,k0+28,k0+41,NB
L,k0+29,k0+34,NW1
L,k0+34,k0+36,NT
L,k0+33,k0+39,NW
L,k0+40,k0+36,NW
L,k0+29,k0+41,NW
L,k0+28,k0+39,NA
L,k0+29,k0+40,NA
L,k0+41,k0+33,NA

!CREATING THE CORRESPONDING AREAS & AREA MESHING

AL,L0+3,L0+22,L0+43,L0+20
AL,L0+43,L0+21,L0+10,L0+19
AL,L0+7,L0+16,L0+47,L0+28
AL,L0+47,L0+15,L0+14,L0+27
TYPE,6
MAT,4
REAL,37
ESIZE,5
ASEL,,,,A0+1,A0+4,1
AMESH,ALL
ALLSEL

AL,L0+2,L0+20,L0+42,L0+36

AL,L0+19,L0+30,L0+35,L0+42
AL,L0+31,L0+36,L0+48,L0+18
```

```
AL,L0+48,L0+35,L0+9,L0+17

AL,L0+18,L0+32,L0+34,L0+41

AL,L0+41,L0+17,L0+8,L0+33
AL,L0+1,L0+34,L0+49,L0+16

AL,L0+29,L0+33,L0+49,L0+15

TYPE,6
MAT,4
REAL,32
ESIZE,5
ASEL,,,,A0+5,A0+12,1
AMESH,ALL
ALLSEL
!-------------------
AL,L0+4,L0+22,L0+44,L0+24
AL,L0+44,L0+21,L0+11,L0+23
AL,L0+6,L0+26,L0+46,L0+28
AL,L0+46,L0+25,L0+13,L0+27
AL,L0+39,L0+24,L0+45,L0+38
AL,L0+45,L0+23,L0+12,L0+37
AL,L0+5,L0+38,L0+50,L0+26
AL,L0+50,L0+37,L0+40,L0+25

TYPE,6
MAT,4
REAL,31
ESIZE,5
ASEL,,,,A0+13,A0+20,1
AMESH,ALL
ALLSEL
!---------------

AL,L0+51,L0+42,L0+43,L0+44
AL,L0+53,L0+48,L0+51,L0+45
AL,L0+53,L0+50,L0+52,L0+41
AL,L0+52,L0+49,L0+47,L0+46

TYPE,6
MAT,4
REAL,34
ESIZE,5
ASEL,,,,A0+21,A0+24,1
AMESH,ALL
ALLSEL

!ROUND BEAM ON STIFFNERS AND TOWER ENDS
TYPE,9
REAL,38
MAT,14
LSEL,,,,L0+1,L0+7,1
LSEL,A,,,L0+31,L0+32,1
LSEL,A,,,L0+39
LSEL,A,,,L0+41,L0+50,1
LMESH,ALL
ALLSEL

*endif

*enddo
```

!INPUT FILE FOR THE END DECK (HESSLE TOWER)

```
/prep7

x0=
y0=
z0=
q=

*dim,x0,,2
*dim,y0,,2
```

```
*dim,z0,,1
*dim,q,,1

X0(1)=1.8
X0(2)=9.05
Y0(1)=-127.215
Y0(2)=-127.101
Z0(1)=0

numstr,kp,11316
numstr,line,14047
numstr,area,3861

k0=11316
l0=14046
A0=3860

*do,i,1,1
*set,q(i),x0(i+1)-x0(i)

*if,q,lt,9.05,then

!CREATING THE KEYPOINTS

K,k0+0,0.00+x0(i),0.0045+y0(i),7.40+z0(i)
K,k0+1,0.00+x0(i),2.127+y0(i),2.1+z0(i)
K,k0+2,0.00+x0(i),2.971+y0(i),0.00+z0(i)
K,k0+3,0.00+x0(i),4.311+y0(i),1.90+z0(i)
K,k0+4,0.00+x0(i),4.494+y0(i),11.00+z0(i)
K,k0+5,0.00+x0(i),2.971+y0(i),-3.25+z0(i)
K,k0+6,0.00+x0(i),0.0045+y0(i),14.6+z0(i)
K,k0+7,0.00+x0(i),2.971+y0(i),22.00+z0(i)
K,k0+8,0.00+x0(i),4.311+y0(i),20.10+z0(i)
K,k0+9,0.00+x0(i),2.971+y0(i),25.25+z0(i)
K,k0+10,0.00+x0(i),2.127+y0(i),19.90+z0(i)
K,k0+24,0.00+x0(i),4.383383+y0(i),5.5+z0(i)
K,k0+25,0.00+x0(i),4.383383+y0(i),16.5+z0(i)
K,k0+26,0.00+x0(i),0.0045+y0(i),11.00+z0(i)
!--------------------------------
K,k0+11,q(i)+x0(i),0.0045+y0(i+1),14.6+z0(i)
K,k0+12,q(i)+x0(i),2.971+y0(i+1),22.00+z0(i)
K,k0+13,q(i)+x0(i),4.494+y0(i+1),11.00+z0(i)
K,k0+14,q(i)+x0(i),4.311+y0(i+1),20.10+z0(i)
K,k0+15,q(i)+x0(i),2.127+y0(i+1),19.90+z0(i)
K,k0+16,q(i)+x0(i),2.971+y0(i+1),25.25+z0(i)
K,k0+17,q(i)+x0(i),0.0045+y0(i+1),7.40+z0(i)
K,k0+18,q(i)+x0(i),2.127+y0(i+1),2.1+z0(i)
K,k0+19,q(i)+x0(i),2.971+y0(i+1),0.00+z0(i)
K,k0+20,q(i)+x0(i),4.311+y0(i+1),1.90+z0(i)
K,k0+21,q(i)+x0(i),2.971+y0(i+1),-3.25+z0(i)
K,k0+22,q(i)+x0(i),4.383383+y0(i+1),5.5+z0(i)
K,k0+23,q(i)+x0(i),4.383383+y0(i+1),16.5+z0(i)
K,k0+27,q(i)+x0(i),0.0045+y0(i+1),11.00+z0(i)
!-----------------------------------
!stiffner 1
K,k0+28,2.725+x0(i),0.0045+y0(i)+2.725*(y0(i+1)-y0(i))/q(i),7.40+z0(i)
K,k0+29,2.725+x0(i),0.0045+y0(i)+2.725*(y0(i+1)-y0(i))/q(i),14.6+z0(i)
K,k0+30,2.725+x0(i),2.127+y0(i)+2.725*(y0(i+1)-y0(i))/q(i),2.1+z0(i)
K,k0+31,2.725+x0(i),2.971+y0(i)+2.725*(y0(i+1)-y0(i))/q(i),0.00+z0(i)
K,k0+32,2.725+x0(i),4.311+y0(i)+2.725*(y0(i+1)-y0(i))/q(i),1.90+z0(i)
K,k0+33,2.725+x0(i),4.494+y0(i)+2.725*(y0(i+1)-y0(i))/q(i),11.00+z0(i)
K,k0+34,2.725+x0(i),2.971+y0(i)+2.725*(y0(i+1)-y0(i))/q(i),22.00+z0(i)
K,k0+35,2.725+x0(i),2.971+y0(i)+2.725*(y0(i+1)-y0(i))/q(i),-3.25+z0(i)
K,k0+36,2.725+x0(i),4.311+y0(i)+2.725*(y0(i+1)-y0(i))/q(i),20.10+z0(i)
K,k0+37,2.725+x0(i),2.127+y0(i)+2.725*(y0(i+1)-y0(i))/q(i),19.90+z0(i)
K,k0+38,2.725+x0(i),2.971+y0(i)+2.725*(y0(i+1)-y0(i))/q(i),25.25+z0(i)
K,k0+39,2.725+x0(i),4.383383+y0(i)+2.725*(y0(i+1)-y0(i))/q(i),5.5+z0(i)
K,k0+40,2.725+x0(i),4.383383+y0(i)+2.725*(y0(i+1)-y0(i))/q(i),16.5+z0(i)
K,k0+41,2.725+x0(i),0.0045+y0(i)+2.725*(y0(i+1)-y0(i))/q(i),11.00+z0(i)

NL=0
NW=1
NW1=2
NT=1
NB=1
```

```
NA=2

!CREATING THE CORRESPONDING LINES

L,k0+8,k0+25,NW
L,k0+24,k0+3,NW
L,k0+3,k0+2,NT
L,k0+2,k0+0,NW1

L,k0+26,k0+6,NB
L,k0+6,k0+7,NW1

L,k0+7,k0+8,NT
L,k0+23,k0+13,NW
L,k0+13,k0+22,NW
L,k0+20,k0+19,NT
L,k0+19,k0+17,NW1

L,k0+17,k0+27,NB
L,k0+11,k0+12,NW1

L,k0+12,k0+14,NT
L,k0+36,k0+14,NL
L,k0+8,k0+36,NL
L,k0+33,k0+13,NL
L,k0+4,k0+33,NL
L,k0+32,k0+20,NL
L,k0+32,k0+3,NL
L,k0+31,k0+19,NL
L,k0+2,k0+31,NL
L,k0+28,k0+17,NL
L,k0+0,k0+28,NL
L,k0+29,k0+11,NL
L,k0+6,k0+29,NL
L,k0+34,k0+12,NL
L,k0+7,k0+34,NL
L,k0+23,k0+14,NW
L,k0+22,k0+20,NW
L,k0+4,k0+24,NW
L,k0+4,k0+25,NW
L,k0+40,k0+23,NL
L,k0+25,k0+40,NL
L,k0+39,k0+22,NL
L,k0+24,k0+39,NL
L,k0+27,k0+41,NL
L,k0+41,k0+26,NL
L,k0+0,k0+26,NB
L,k0+27,k0+11,NB

!STIFF 1
L,k0+40,k0+33,NW
L,k0+32,k0+39,NW
L,k0+32,k0+31,NT
L,k0+31,k0+28,NW1
L,k0+28,k0+41,NB
L,k0+29,k0+34,NW1
L,k0+34,k0+36,NT
L,k0+33,k0+39,NW
L,k0+40,k0+36,NW
L,k0+29,k0+41,NW
L,k0+28,k0+39,NA
L,k0+29,k0+40,NA
L,k0+41,k0+33,NA

!CREATING THE CORRESPONDING AREAS & AREA MESHING

AL,L0+43,L0+22,L0+3,L0+20
AL,L0+19,L0+10,L0+21,L0+43
AL,L0+28,L0+47,L0+16,L0+7
AL,L0+27,L0+14,L0+15,L0+47

TYPE,6
MAT,7
REAL,37
ESIZE,5
```

```
ASEL,,,,A0+1,A0+4,1
AMESH,ALL
ALLSEL

AL,L0+36,L0+42,L0+20,L0+2
AL,L0+42,L0+35,L0+30,L0+19
AL,L0+18,L0+48,L0+36,L0+31
AL,L0+17,L0+9,L0+35,L0+48
AL,L0+32,L0+34,L0+41,L0+18
AL,L0+33,L0+8,L0+17,L0+41
AL,L0+16,L0+49,L0+34,L0+1
AL,L0+49,L0+15,L0+29,L0+33

TYPE,6
MAT,7
REAL,32
ESIZE,5
ASEL,,,,A0+5,A0+12,1
AMESH,ALL
ALLSEL
!-------------------
AL,L0+4,L0+22,L0+44,L0+24
AL,L0+44,L0+21,L0+11,L0+23
AL,L0+6,L0+26,L0+46,L0+28
AL,L0+46,L0+25,L0+13,L0+27
AL,L0+39,L0+24,L0+45,L0+38
AL,L0+45,L0+23,L0+12,L0+37
AL,L0+5,L0+38,L0+50,L0+26
AL,L0+50,L0+37,L0+40,L0+25

TYPE,6
MAT,7
REAL,31
ESIZE,5
ASEL,,,,A0+13,A0+20,1
AMESH,ALL
ALLSEL
!---------------

AL,L0+51,L0+42,L0+43,L0+44
AL,L0+53,L0+48,L0+51,L0+45
AL,L0+53,L0+50,L0+52,L0+41
AL,L0+52,L0+49,L0+47,L0+46

TYPE,6
MAT,7
REAL,34
ESIZE,5
ASEL,,,,A0+21,A0+24,1
AMESH,ALL
ALLSEL

!ROUND BEAM ON STIFFNERS AND TOWER ENDS
TYPE,9
REAL,38
MAT,14
LSEL,,,,L0+1,L0+7,1
LSEL,A,,,L0+31,L0+32,1
LSEL,A,,,L0+39
LSEL,A,,,L0+41,L0+50,1
LMESH,ALL
ALLSEL

*endif

*enddo
```

!INPUT FILE FOR THE END DECK (BARTON TOWER)

```
/prep7

x0=
y0=
z0=
```

```
q=

*dim,x0,,2
*dim,y0,,2
*dim,z0,,1
*dim,q,,1

X0(1)=1402.7
X0(2)=1410.0
Y0(1)=-127.101
Y0(2)=-127.215
Z0(1)=0

numstr,kp,11358
numstr,line,14100
numstr,area,3885

k0=11358
l0=14099
A0=3884

*do,i,1,1
*set,q(i),x0(i+1)-x0(i)

*if,q,lt,9.05,then

!CREATING THE KEYPOINTS

K,k0+0,0.00+x0(i),0.0045+y0(i),7.40+z0(i)
K,k0+1,0.00+x0(i),2.127+y0(i),2.1+z0(i)
K,k0+2,0.00+x0(i),2.971+y0(i),0.00+z0(i)
K,k0+3,0.00+x0(i),4.311+y0(i),1.90+z0(i)
K,k0+4,0.00+x0(i),4.494+y0(i),11.00+z0(i)
K,k0+5,0.00+x0(i),2.971+y0(i),-3.25+z0(i)
K,k0+6,0.00+x0(i),0.0045+y0(i),14.6+z0(i)
K,k0+7,0.00+x0(i),2.971+y0(i),22.00+z0(i)
K,k0+8,0.00+x0(i),4.311+y0(i),20.10+z0(i)
K,k0+9,0.00+x0(i),2.971+y0(i),25.25+z0(i)
K,k0+10,0.00+x0(i),2.127+y0(i),19.90+z0(i)
K,k0+24,0.00+x0(i),4.383383+y0(i),5.5+z0(i)
K,k0+25,0.00+x0(i),4.383383+y0(i),16.5+z0(i)
K,k0+26,0.00+x0(i),0.0045+y0(i),11.00+z0(i)
!--------------------------------
K,k0+11,q(i)+x0(i),0.0045+y0(i+1),14.6+z0(i)
K,k0+12,q(i)+x0(i),2.971+y0(i+1),22.00+z0(i)
K,k0+13,q(i)+x0(i),4.494+y0(i+1),11.00+z0(i)
K,k0+14,q(i)+x0(i),4.311+y0(i+1),20.10+z0(i)
K,k0+15,q(i)+x0(i),2.127+y0(i+1),19.90+z0(i)
K,k0+16,q(i)+x0(i),2.971+y0(i+1),25.25+z0(i)
K,k0+17,q(i)+x0(i),0.0045+y0(i+1),7.40+z0(i)
K,k0+18,q(i)+x0(i),2.127+y0(i+1),2.1+z0(i)
K,k0+19,q(i)+x0(i),2.971+y0(i+1),0.00+z0(i)
K,k0+20,q(i)+x0(i),4.311+y0(i+1),1.90+z0(i)
K,k0+21,q(i)+x0(i),2.971+y0(i+1),-3.25+z0(i)
K,k0+22,q(i)+x0(i),4.383383+y0(i+1),5.5+z0(i)
K,k0+23,q(i)+x0(i),4.383383+y0(i+1),16.5+z0(i)
K,k0+27,q(i)+x0(i),0.0045+y0(i+1),11.00+z0(i)
!-----------------------------------
!stiffner 1
K,k0+28,4.525+x0(i),0.0045+y0(i)+4.525*(y0(i+1)-y0(i))/q(i),7.40+z0(i)
K,k0+29,4.525+x0(i),0.0045+y0(i)+4.525*(y0(i+1)-y0(i))/q(i),14.6+z0(i)
K,k0+30,4.525+x0(i),2.127+y0(i)+4.525*(y0(i+1)-y0(i))/q(i),2.1+z0(i)
K,k0+31,4.525+x0(i),2.971+y0(i)+4.525*(y0(i+1)-y0(i))/q(i),0.00+z0(i)
K,k0+32,4.525+x0(i),4.311+y0(i)+4.525*(y0(i+1)-y0(i))/q(i),1.90+z0(i)
K,k0+33,4.525+x0(i),4.494+y0(i)+4.525*(y0(i+1)-y0(i))/q(i),11.00+z0(i)
K,k0+34,4.525+x0(i),2.971+y0(i)+4.525*(y0(i+1)-y0(i))/q(i),22.00+z0(i)
K,k0+35,4.525+x0(i),2.971+y0(i)+4.525*(y0(i+1)-y0(i))/q(i),-3.25+z0(i)
K,k0+36,4.525+x0(i),4.311+y0(i)+4.525*(y0(i+1)-y0(i))/q(i),20.10+z0(i)
K,k0+37,4.525+x0(i),2.127+y0(i)+4.525*(y0(i+1)-y0(i))/q(i),19.90+z0(i)
K,k0+38,4.525+x0(i),2.971+y0(i)+4.525*(y0(i+1)-y0(i))/q(i),25.25+z0(i)
K,k0+39,4.525+x0(i),4.383383+y0(i)+4.525*(y0(i+1)-y0(i))/q(i),5.5+z0(i)
K,k0+40,4.525+x0(i),4.383383+y0(i)+4.525*(y0(i+1)-y0(i))/q(i),16.5+z0(i)
K,k0+41,4.525+x0(i),0.0045+y0(i)+4.525*(y0(i+1)-y0(i))/q(i),11.00+z0(i)

NL=0
```

```
NW=1
NW1=2
NT=1
NB=1
NA=2

!CREATING THE CORRESPONDING LINES

L,k0+8,k0+25,NW
L,k0+24,k0+3,NW
L,k0+3,k0+2,NT
L,k0+2,k0+0,NW1

L,k0+26,k0+6,NB
L,k0+6,k0+7,NW1

L,k0+7,k0+8,NT
L,k0+23,k0+13,NW
L,k0+13,k0+22,NW
L,k0+20,k0+19,NT
L,k0+19,k0+17,NW1

L,k0+17,k0+27,NB
L,k0+11,k0+12,NW1

L,k0+12,k0+14,NT
L,k0+36,k0+14,NL
L,k0+8,k0+36,NL
L,k0+33,k0+13,NL
L,k0+4,k0+33,NL
L,k0+32,k0+20,NL
L,k0+32,k0+3,NL
L,k0+31,k0+19,NL
L,k0+2,k0+31,NL
L,k0+28,k0+17,NL
L,k0+0,k0+28,NL
L,k0+29,k0+11,NL
L,k0+6,k0+29,NL
L,k0+34,k0+12,NL
L,k0+7,k0+34,NL
L,k0+23,k0+14,NW
L,k0+22,k0+20,NW
L,k0+4,k0+24,NW
L,k0+4,k0+25,NW
L,k0+40,k0+23,NL
L,k0+25,k0+40,NL
L,k0+39,k0+22,NL
L,k0+24,k0+39,NL
L,k0+27,k0+41,NL
L,k0+41,k0+26,NL
L,k0+0,k0+26,NB
L,k0+27,k0+11,NB

!STIFF 1
L,k0+40,k0+33,NW
L,k0+32,k0+39,NW
L,k0+32,k0+31,NT
L,k0+31,k0+28,NW1
L,k0+28,k0+41,NB
L,k0+29,k0+34,NW1
L,k0+34,k0+36,NT
L,k0+33,k0+39,NW
L,k0+40,k0+36,NW
L,k0+29,k0+41,NW
L,k0+28,k0+39,NA
L,k0+29,k0+40,NA
L,k0+41,k0+33,NA

!CREATING THE CORRESPONDING AREAS & AREA MESHING

!SIDE PLATE
AL,L0+43,L0+20,L0+3,L0+22
AL,L0+19,L0+10,L0+21,L0+43
AL,L0+28,L0+47,L0+16,L0+7
AL,L0+27,L0+14,L0+15,L0+47
```

```
TYPE,6
MAT,7
REAL,37
ESIZE,5
ASEL,,,,A0+1,A0+4,1
AMESH,ALL
ALLSEL

!TOP PLATE
AL,L0+20,L0+2,L0+36,L0+42
AL,L0+42,L0+19,L0+30,L0+35
AL,L0+18,L0+48,L0+36,L0+31
AL,L0+17,L0+9,L0+35,L0+48
AL,L0+32,L0+34,L0+41,L0+18
AL,L0+33,L0+41,L0+17,L0+8
AL,L0+16,L0+49,L0+34,L0+1
AL,L0+49,L0+33,L0+29,L0+15

TYPE,6
MAT,7
REAL,32
ESIZE,5
ASEL,,,,A0+5,A0+12,1
AMESH,ALL
ALLSEL
!-------------------
AL,L0+4,L0+22,L0+44,L0+24
AL,L0+44,L0+21,L0+11,L0+23
AL,L0+6,L0+26,L0+46,L0+28
AL,L0+46,L0+25,L0+13,L0+27
AL,L0+39,L0+24,L0+45,L0+38
AL,L0+45,L0+23,L0+12,L0+37
AL,L0+5,L0+38,L0+50,L0+26
AL,L0+50,L0+37,L0+40,L0+25

TYPE,6
MAT,7
REAL,31
ESIZE,5
ASEL,,,,A0+13,A0+20,1
AMESH,ALL
ALLSEL
!---------------

AL,L0+51,L0+42,L0+43,L0+44
AL,L0+53,L0+48,L0+51,L0+45
AL,L0+53,L0+50,L0+52,L0+41
AL,L0+52,L0+49,L0+47,L0+46

TYPE,6
MAT,7
REAL,34
ESIZE,5
ASEL,,,,A0+21,A0+24,1
AMESH,ALL
ALLSEL

!ROUND BEAM ON STIFFNERS AND TOWER ENDS
TYPE,9
REAL,38
MAT,14
LSEL,,,,L0+8,L0+14,1
LSEL,A,,,L0+29,L0+30,1
LSEL,A,,,L0+40
LSEL,A,,,L0+41,L0+50,1
LMESH,ALL
ALLSEL

*endif

*enddo
```

!INPUT FILE FOR THE END DECK (BARTON SIDE)

```
/prep7

x0=
y0=
z0=
q=

*dim,x0,,2
*dim,y0,,2
*dim,z0,,1
*dim,q,,1

X0(1)=1411.8
X0(2)=1419.05
Y0(1)=-127.215
Y0(2)=-127.330
Z0(1)=0

numstr,kp,11400
numstr,line,14153
numstr,area,3909

k0=11400
l0=14152
A0=3908

*do,i,1,1
*set,q(i),x0(i+1)-x0(i)

*if,q,lt,8.55,then

!CREATING THE KEYPOINTS

K,k0+0,0.00+x0(i),0.0045+y0(i),7.40+z0(i)
K,k0+1,0.00+x0(i),2.127+y0(i),2.1+z0(i)
K,k0+2,0.00+x0(i),2.971+y0(i),0.00+z0(i)
K,k0+3,0.00+x0(i),4.311+y0(i),1.90+z0(i)
K,k0+4,0.00+x0(i),4.494+y0(i),11.00+z0(i)
K,k0+5,0.00+x0(i),2.971+y0(i),-3.25+z0(i)
K,k0+6,0.00+x0(i),0.0045+y0(i),14.6+z0(i)
K,k0+7,0.00+x0(i),2.971+y0(i),22.00+z0(i)
K,k0+8,0.00+x0(i),4.311+y0(i),20.10+z0(i)
K,k0+9,0.00+x0(i),2.971+y0(i),25.25+z0(i)
K,k0+10,0.00+x0(i),2.127+y0(i),19.90+z0(i)
K,k0+24,0.00+x0(i),4.383383+y0(i),5.5+z0(i)
K,k0+25,0.00+x0(i),4.383383+y0(i),16.5+z0(i)
K,k0+26,0.00+x0(i),0.0045+y0(i),11.00+z0(i)
!--------------------------------
K,k0+11,q(i)+x0(i),0.0045+y0(i+1),14.6+z0(i)
K,k0+12,q(i)+x0(i),2.971+y0(i+1),22.00+z0(i)
K,k0+13,q(i)+x0(i),4.494+y0(i+1),11.00+z0(i)
K,k0+14,q(i)+x0(i),4.311+y0(i+1),20.10+z0(i)
K,k0+15,q(i)+x0(i),2.127+y0(i+1),19.90+z0(i)
K,k0+16,q(i)+x0(i),2.971+y0(i+1),25.25+z0(i)
K,k0+17,q(i)+x0(i),0.0045+y0(i+1),7.40+z0(i)
K,k0+18,q(i)+x0(i),2.127+y0(i+1),2.1+z0(i)
K,k0+19,q(i)+x0(i),2.971+y0(i+1),0.00+z0(i)
K,k0+20,q(i)+x0(i),4.311+y0(i+1),1.90+z0(i)
K,k0+21,q(i)+x0(i),2.971+y0(i+1),-3.25+z0(i)
K,k0+22,q(i)+x0(i),4.383383+y0(i+1),5.5+z0(i)
K,k0+23,q(i)+x0(i),4.383383+y0(i+1),16.5+z0(i)
K,k0+27,q(i)+x0(i),0.0045+y0(i+1),11.00+z0(i)
!-----------------------------------
!stiffner 1
K,k0+28,2.725+x0(i),0.0045+y0(i)+2.725*(y0(i+1)-y0(i))/q(i),7.40+z0(i)
K,k0+29,2.725+x0(i),0.0045+y0(i)+2.725*(y0(i+1)-y0(i))/q(i),14.6+z0(i)
K,k0+30,2.725+x0(i),2.127+y0(i)+2.725*(y0(i+1)-y0(i))/q(i),2.1+z0(i)
K,k0+31,2.725+x0(i),2.971+y0(i)+2.725*(y0(i+1)-y0(i))/q(i),0.00+z0(i)
K,k0+32,2.725+x0(i),4.311+y0(i)+2.725*(y0(i+1)-y0(i))/q(i),1.90+z0(i)
K,k0+33,2.725+x0(i),4.494+y0(i)+2.725*(y0(i+1)-y0(i))/q(i),11.00+z0(i)
```

```
K,k0+34,2.725+x0(i),2.971+y0(i)+2.725*(y0(i+1)-y0(i))/q(i),22.00+z0(i)
K,k0+35,2.725+x0(i),2.971+y0(i)+2.725*(y0(i+1)-y0(i))/q(i),-3.25+z0(i)
K,k0+36,2.725+x0(i),4.311+y0(i)+2.725*(y0(i+1)-y0(i))/q(i),20.10+z0(i)
K,k0+37,2.725+x0(i),2.127+y0(i)+2.725*(y0(i+1)-y0(i))/q(i),19.90+z0(i)
K,k0+38,2.725+x0(i),2.971+y0(i)+2.725*(y0(i+1)-y0(i))/q(i),25.25+z0(i)
K,k0+39,2.725+x0(i),4.383383+y0(i)+2.725*(y0(i+1)-y0(i))/q(i),5.5+z0(i)
K,k0+40,2.725+x0(i),4.383383+y0(i)+2.725*(y0(i+1)-y0(i))/q(i),16.5+z0(i)
K,k0+41,2.725+x0(i),0.0045+y0(i)+2.725*(y0(i+1)-y0(i))/q(i),11.00+z0(i)

NL=0
NW=1
NW1=2
NT=1
NB=1
NA=2

!CREATING THE CORRESPONDING LINES

L,k0+8,k0+25,NW
L,k0+24,k0+3,NW
L,k0+3,k0+2,NT
L,k0+2,k0+0,NW1

L,k0+26,k0+6,NB
L,k0+6,k0+7,NW1

L,k0+7,k0+8,NT
L,k0+23,k0+13,NW
L,k0+13,k0+22,NW
L,k0+20,k0+19,NT
L,k0+19,k0+17,NW1

L,k0+17,k0+27,NB
L,k0+11,k0+12,NW1

L,k0+12,k0+14,NT
L,k0+36,k0+14,NL
L,k0+8,k0+36,NL
L,k0+33,k0+13,NL
L,k0+4,k0+33,NL
L,k0+32,k0+20,NL
L,k0+32,k0+3,NL
L,k0+31,k0+19,NL
L,k0+2,k0+31,NL
L,k0+28,k0+17,NL
L,k0+0,k0+28,NL
L,k0+29,k0+11,NL
L,k0+6,k0+29,NL
L,k0+34,k0+12,NL
L,k0+7,k0+34,NL
L,k0+23,k0+14,NW
L,k0+22,k0+20,NW
L,k0+4,k0+24,NW
L,k0+4,k0+25,NW
L,k0+40,k0+23,NL
L,k0+25,k0+40,NL
L,k0+39,k0+22,NL
L,k0+24,k0+39,NL
L,k0+27,k0+41,NL
L,k0+41,k0+26,NL
L,k0+0,k0+26,NB
L,k0+27,k0+11,NB

!STIFF 1
L,k0+40,k0+33,NW
L,k0+32,k0+39,NW
L,k0+32,k0+31,NT
L,k0+31,k0+28,NW1
L,k0+28,k0+41,NB
L,k0+29,k0+34,NW1
L,k0+34,k0+36,NT
L,k0+33,k0+39,NW
L,k0+40,k0+36,NW
L,k0+29,k0+41,NW
L,k0+28,k0+39,NA
```

```
L,k0+29,k0+40,NA
L,k0+41,k0+33,NA

!CREATING THE CORRESPONDING AREAS & AREA MESHING

!SIDE PLATE
AL,L0+43,L0+20,L0+3,L0+22
AL,L0+19,L0+10,L0+21,L0+43
AL,L0+28,L0+47,L0+16,L0+7
AL,L0+27,L0+14,L0+15,L0+47
TYPE,6
MAT,8
REAL,37
ESIZE,5
ASEL,,,,A0+1,A0+4,1
AMESH,ALL
ALLSEL

!TOP PLATE
AL,L0+20,L0+2,L0+36,L0+42
AL,L0+42,L0+19,L0+30,L0+35
AL,L0+18,L0+48,L0+36,L0+31
AL,L0+17,L0+9,L0+35,L0+48
AL,L0+32,L0+34,L0+41,L0+18
AL,L0+33,L0+41,L0+17,L0+8
AL,L0+16,L0+49,L0+34,L0+1
AL,L0+49,L0+33,L0+29,L0+15

TYPE,6
MAT,8
REAL,32
ESIZE,5
ASEL,,,,A0+5,A0+12,1
AMESH,ALL
ALLSEL
!-------------------
AL,L0+4,L0+22,L0+44,L0+24
AL,L0+44,L0+21,L0+11,L0+23
AL,L0+6,L0+26,L0+46,L0+28
AL,L0+46,L0+25,L0+13,L0+27
AL,L0+39,L0+24,L0+45,L0+38
AL,L0+45,L0+23,L0+12,L0+37
AL,L0+5,L0+38,L0+50,L0+26
AL,L0+50,L0+37,L0+40,L0+25

TYPE,6
MAT,8
REAL,31
ESIZE,5
ASEL,,,,A0+13,A0+20,1
AMESH,ALL
ALLSEL
!---------------

AL,L0+51,L0+42,L0+43,L0+44
AL,L0+53,L0+48,L0+51,L0+45
AL,L0+53,L0+50,L0+52,L0+41
AL,L0+52,L0+49,L0+47,L0+46

TYPE,6
MAT,8
REAL,34
ESIZE,5
ASEL,,,,A0+21,A0+24,1
AMESH,ALL
ALLSEL

!ROUND BEAM ON STIFFNERS AND TOWER ENDS
TYPE,9
REAL,38
MAT,14
LSEL,,,,L0+1,L0+7,1
LSEL,A,,,L0+31,L0+32,1
LSEL,A,,,L0+39
LSEL,A,,,L0+41,L0+50,1
```

```
LMESH,ALL
ALLSEL
*endif
*enddo
```

!INPUT FILE FOR THE MAIN CABLE

```
/PREP7

!CREATING THE KEYPOINTS

!main cable span
k,11815,.9,-.296,0
k,11816,1410.9,-.296,0
k,11817,18.1,-5.965,0
k,11818,36.2,-11.716,0
k,11819,54.3,-17.309,0
k,11820,72.4,-22.744,0
k,11821,90.5,-28.022,0
k,11822,108.6,-33.142,0
k,11823,126.7,-38.106,0
k,11824,144.8,-42.913,0
k,11825,162.9,-47.564,0
k,11826,181.0,-52.060,0
k,11827,199.1,-56.400,0
k,11828,217.2,-60.585,0
k,11829,235.3,-64.616,0
k,11830,253.4,-68.491,0
k,11831,271.5,-72.213,0
k,11832,289.6,-75.781,0
k,11833,307.7,-79.195,0
k,11834,325.8,-82.455,0
k,11835,343.9,-85.563,0
k,11836,362.0,-88.517,0
k,11837,380.1,-91.319,0
k,11838,398.2,-93.968,0
k,11839,416.3,-96.464,0
k,11840,434.4,-98.809,0
k,11841,452.5,-101.001,0
k,11842,470.6,-103.041,0
k,11843,488.7,-104.930,0
k,11844,506.8,-106.670,0
k,11845,524.9,-108.252,0
k,11846,543.0,-109.686,0
k,11847,561.1,-110.969,0
k,11848,579.2,-112.101,0
k,11849,597.3,-113.081,0
k,11850,615.4,-113.910,0
k,11851,633.5,-114.590,0
k,11852,651.6,-115.117,0
k,11853,669.7,-115.494,0
k,11854,687.8,-115.720,0
k,11855,705.9,-115.796,0

k,11856,1393.7,-5.965,0
k,11857,1375.6,-11.716,0
k,11858,1357.5,-17.309,0
k,11859,1339.4,-22.744,0
k,11860,1321.3,-28.022,0
k,11861,1303.2,-33.142,0
k,11862,1285.1,-38.106,0
k,11863,1267.0,-42.913,0
k,11864,1248.9,-47.564,0
k,11865,1230.8,-52.060,0
k,11866,1212.7,-56.400,0
k,11867,1194.6,-60.585,0
k,11868,1176.5,-64.616,0
k,11869,1158.4,-68.491,0
k,11870,1140.3,-72.213,0
k,11871,1122.2,-75.781,0
k,11872,1104.1,-79.195,0
k,11873,1086.0,-82.455,0
k,11874,1067.9,-85.563,0
k,11875,1049.8,-88.517,0
```

```
k,11876,1031.7,-91.319,0
k,11877,1013.6,-93.968,0
k,11878,995.5,-96.464,0
k,11879,977.4,-98.809,0
k,11880,959.3,-101.001,0
k,11881,941.2,-103.041,0
k,11882,923.1,-104.930,0
k,11883,905.0,-106.670,0
k,11884,886.9,-108.252,0
k,11885,868.8,-109.686,0
k,11886,850.7,-110.969,0
k,11887,832.6,-112.101,0
k,11888,814.5,-113.081,0
k,11889,796.4,-113.911,0
k,11890,778.3,-114.590,0
k,11891,760.2,-115.117,0
k,11892,742.1,-115.494,0
k,11893,724.0,-115.721,0

!hessle span cable
k,11894,-233.5,-107.8710,0
k,11895,-215.4,-100.5270,0
k,11896,-197.3,-93.0192,0
k,11897,-179.2,-85.3562,0
k,11898,-161.1,-77.5420,0
k,11899,-143.0,-69.5610,0
k,11900,-124.9,-61.4210,0
k,11901,-106.8,-53.1190,0
k,11902,-88.7,-44.6550,0
k,11903,-70.6,-36.0236,0
k,11904,-52.5,-27.2420,0
k,11905,-34.4,-18.2900,0
k,11906,-16.3,-9.1750,0
k,11907,-310.643,-141.557,0
k,11908,-292.9,-130.896,0
k,11909,-272.138,-123.006,0
k,11910,-256.125,-116.815,0

!barton span cable
k,11911,1880.6,-126.6107,0
k,11912,1862.5,-123.6794,0
k,11913,1844.4,-120.5789,0
k,11914,1826.3,-117.3273,0
k,11915,1808.2,-113.9254,0
k,11916,1790.1,-110.3725,0
k,11917,1772.0,-106.6671,0
k,11918,1753.9,-102.8084,0
k,11919,1735.8,-98.7961,0
k,11920,1717.7,-94.6437,0
k,11921,1699.6,-90.3232,0
k,11922,1681.5,-85.8484,0
k,11923,1663.4,-81.2194,0
k,11924,1645.3,-76.4361,0
k,11925,1627.2,-71.4979,0
k,11926,1609.1,-66.4042,0
k,11927,1591.0,-61.1551,0
k,11928,1572.9,-55.7501,0
k,11929,1554.8,-50.1849,0
k,11930,1536.7,-44.4713,0
k,11931,1518.6,-38.5961,0
k,11932,1500.5,-32.5730,0
k,11933,1482.4,-26.3770,0
k,11934,1464.3,-20.0230,0
k,11935,1446.2,-13.5100,0
k,11936,1428.1,-6.8390,0
k,11937,1972.443,-147.737,0
k,11938,1954.7,-137.076,0
k,11939,1933.38,-134.3276,0
k,11940,1916.8,-132.0457,0
k,11941,1898.7,-129.4064,0
!-------------------------
k,11942,.9,-.296,22
k,11943,1410.9,-.296,22
k,11944,18.1,-5.965,22
k,11945,36.2,-11.716,22
```

k,11946,54.3,-17.309,22
k,11947,72.4,-22.744,22
k,11948,90.5,-28.022,22
k,11949,108.6,-33.142,22
k,11950,126.7,-38.106,22
k,11951,144.8,-42.913,22
k,11952,162.9,-47.564,22
k,11953,181.0,-52.060,22
k,11954,199.1,-56.400,22
k,11955,217.2,-60.585,22
k,11956,235.3,-64.616,22
k,11957,253.4,-68.491,22
k,11958,271.5,-72.213,22
k,11959,289.6,-75.781,22
k,11960,307.7,-79.195,22
k,11961,325.8,-82.455,22
k,11962,343.9,-85.563,22
k,11963,362.0,-88.517,22
k,11964,380.1,-91.319,22
k,11965,398.2,-93.968,22
k,11966,416.3,-96.464,22
k,11967,434.4,-98.809,22
k,11968,452.5,-101.001,22
k,11969,470.6,-103.041,22
k,11970,488.7,-104.930,22
k,11971,506.8,-106.670,22
k,11972,524.9,-108.252,22
k,11973,543.0,-109.686,22
k,11974,561.1,-110.969,22
k,11975,579.2,-112.101,22
k,11976,597.3,-113.081,22
k,11977,615.4,-113.910,22
k,11978,633.5,-114.590,22
k,11979,651.6,-115.117,22
k,11980,669.7,-115.494,22
k,11981,687.8,-115.720,22
k,11982,705.9,-115.796,22
k,11983,1393.7,-5.965,22
k,11984,1375.6,-11.716,22
k,11985,1357.5,-17.309,22
k,11986,1339.4,-22.744,22
k,11987,1321.3,-28.022,22
k,11988,1303.2,-33.142,22
k,11989,1285.1,-38.106,22
k,11990,1267.0,-42.913,22
k,11991,1248.9,-47.564,22
k,11992,1230.8,-52.060,22
k,11993,1212.7,-56.400,22
k,11994,1194.6,-60.585,22
k,11995,1176.5,-64.616,22
k,11996,1158.4,-68.491,22
k,11997,1140.3,-72.213,22
k,11998,1122.2,-75.781,22
k,11999,1104.1,-79.195,22
k,12000,1086.0,-82.455,22
k,12001,1067.9,-85.563,22
k,12002,1049.8,-88.517,22
k,12003,1031.7,-91.319,22
k,12004,1013.6,-93.968,22
k,12005,995.5,-96.464,22
k,12006,977.4,-98.809,22
k,12007,959.3,-101.001,22
k,12008,941.2,-103.041,22
k,12009,923.1,-104.930,22
k,12010,905.0,-106.670,22
k,12011,886.9,-108.252,22
k,12012,868.8,-109.686,22
k,12013,850.7,-110.969,22
k,12014,832.6,-112.101,22
k,12015,814.5,-113.081,22
k,12016,796.4,-113.911,22
k,12017,778.3,-114.590,22
k,12018,760.2,-115.117,22
k,12019,742.1,-115.494,22
k,12020,724.0,-115.721,22

```
k,12021,-233.5,-107.871,22
k,12022,-215.4,-100.527,22
k,12023,-197.3,-93.0192,22
k,12024,-179.2,-85.3562,22
k,12025,-161.1,-77.542,22
k,12026,-143.0,-69.561,22
k,12027,-124.9,-61.421,22
k,12028,-106.8,-53.119,22
k,12029,-88.7,-44.655,22
k,12030,-70.6,-36.0236,22
k,12031,-52.5,-27.242,22
k,12032,-34.4,-18.290,22
k,12033,-16.3,-9.175,22
k,12034,-310.643,-141.557,22
k,12035,-292.9,-130.896,22
k,12036,-272.138,-123.006,22
k,12037,-256.125,-116.815,22
k,12038,1880.6,-126.6107,22
k,12039,1862.5,-123.6794,22
k,12040,1844.4,-120.5789,22
k,12041,1826.3,-117.3273,22
k,12042,1808.2,-113.9254,22
k,12043,1790.1,-110.3725,22
k,12044,1772.0,-106.6671,22
k,12045,1753.9,-102.8084,22
k,12046,1735.8,-98.7961,22
k,12047,1717.7,-94.6437,22
k,12048,1699.6,-90.3232,22
k,12049,1681.5,-85.8484,22
k,12050,1663.4,-81.2194,22
k,12051,1645.3,-76.4361,22
k,12052,1627.2,-71.4979,22
k,12053,1609.1,-66.4042,22
k,12054,1591.0,-61.1551,22
k,12055,1572.9,-55.7501,22
k,12056,1554.8,-50.1849,22
k,12057,1536.7,-44.4713,22
k,12058,1518.6,-38.5961,22
k,12059,1500.5,-32.573,22
k,12060,1482.4,-26.377,22
k,12061,1464.3,-20.023,22
k,12062,1446.2,-13.51,22
k,12063,1428.1,-6.839,22
k,12064,1972.443,-147.737,22
k,12065,1954.7,-137.076,22
k,12066,1933.38,-134.3276,22
k,12067,1916.8,-132.0457,22
k,12068,1898.7,-129.4064,22

!CREATING THE CORRESPONDING LINES & LINE MESHING

!----------HESSLE SIDE MAIN CABLE-------------
ESIZE,,1
!NUMSTR,LINE,13472
NUMSTR,LINE,19700
L,11907,11908
L,11908,11909
L,11909,11910
L,11910,11894
L,11894,11895
L,11895,11896
L,11896,11897
L,11897,11898
REAL,24
TYPE,2
MAT,5
!LSEL,,,,13472,13479,1
LSEL,,,,19700,19707,1
LMESH,ALL
!---------------------------
!NUMSTR,LINE,13480
NUMSTR,LINE,19708
L,11898,11899
L,11899,11900
L,11900,11901
```

```
L,11901,11902
L,11902,11903
L,11903,11904
L,11904,11905
L,11905,11906
L,11906,11815
REAL,24
TYPE,2
MAT,5
!LSEL,,,,13480,13488,1
LSEL,,,,19708,19716,1
LMESH,ALL
!------------------
!NUMSTR,LINE,13489
NUMSTR,LINE,19717
L,12034,12035
L,12035,12036
L,12036,12037
L,12037,12021
L,12021,12022
L,12022,12023
L,12023,12024
REAL,30
TYPE,2
MAT,5
!LSEL,,,,13489,13495,1
LSEL,,,,19717,19723,1
LMESH,ALL
!--------------------
!NUMSTR,LINE,13496
NUMSTR,LINE,19724
L,12024,12025
L,12025,12026
L,12026,12027
L,12027,12028
L,12028,12029
L,12029,12030
L,12030,12031
L,12031,12032
L,12032,12033
L,12033,11942
REAL,30
TYPE,2
MAT,5
!LSEL,,,,13496,13505,1
LSEL,,,,19724,19733,1
LMESH,ALL

!--------BARTON SIDE MAIN CABLE---------

!NUMSTR,LINE,13506
NUMSTR,LINE,19734
L,11937,11938
L,11938,11939
L,11939,11940
L,11940,11941
L,11941,11911
L,11911,11912
L,11912,11913
L,11913,11914
L,11914,11915
L,11915,11916
L,11916,11917
L,11917,11918
L,11918,11919
L,11919,11920
L,11920,11921
L,11921,11922
L,11922,11923
L,11923,11924
L,11924,11925
L,11925,11926
REAL,20
TYPE,2
MAT,12
```

```
!LSEL,,,,13506,13525,1
LSEL,,,,19734,19753,1
LMESH,ALL
!-----------------------
!NUMSTR,LINE,13526
NUMSTR,LINE,19754
L,11926,11927
L,11927,11928
L,11928,11929
L,11929,11930
L,11930,11931
L,11931,11932
L,11932,11933
L,11933,11934
L,11934,11935
L,11935,11936
L,11936,11816
REAL,20
TYPE,2
MAT,12
!LSEL,,,,13526,13536,1
LSEL,,,,19754,19764,1
LMESH,ALL
!---------------------------
!NUMSTR,LINE,13537
NUMSTR,LINE,19765
L,12064,12065
L,12065,12066
L,12066,12067
L,12067,12068
L,12068,12038
L,12038,12039
L,12039,12040
L,12040,12041
L,12041,12042
L,12042,12043
L,12043,12044
L,12044,12045
L,12045,12046
L,12046,12047
L,12047,12048
L,12048,12049
L,12049,12050
L,12050,12051
L,12051,12052
L,12052,12053
REAL,20
TYPE,2
MAT,12
!LSEL,,,,13537,13556,1
LSEL,,,,19765,19784,1
LMESH,ALL
!------------------------
!NUMSTR,LINE,13557
NUMSTR,LINE,19785
L,12053,12054
L,12054,12055
L,12055,12056
L,12056,12057
L,12057,12058
L,12058,12059
L,12059,12060
L,12060,12061
L,12061,12062
L,12062,12063
L,12063,11943
REAL,20
TYPE,2
MAT,12
!LSEL,,,,13557,13567,1
LSEL,,,,19785,19795,1
LMESH,ALL

!---------MIDDLE MAIN CABLE------------
!NUMSTR,LINE,13568
```

```
NUMSTR,LINE,19796
L,11815,11817
L,11817,11818
L,11818,11819
L,11819,11820
L,11820,11821
REAL,21
TYPE,2
MAT,11
!LSEL,,,,13568,13572,1
LSEL,,,,19796,19800,1
LMESH,ALL
!------------------------
!NUMSTR,LINE,13573
NUMSTR,LINE,19801
L,11821,11822
L,11822,11823
L,11823,11824
L,11824,11825
L,11825,11826
L,11826,11827
L,11827,11828
L,11828,11829
L,11829,11830
L,11830,11831
L,11831,11832
L,11832,11833
L,11833,11834
L,11834,11835
L,11835,11836
L,11836,11837
L,11837,11838
L,11838,11839
L,11839,11840
L,11840,11841
L,11841,11842
REAL,22
TYPE,2
MAT,11
!LSEL,,,,13573,13593,1
LSEL,,,,19801,19821,1
LMESH,ALL
!--------------------------
!NUMSTR,LINE,13594
NUMSTR,LINE,19822
L,11842,11843
L,11843,11844
L,11844,11845
L,11845,11846
L,11846,11847
L,11847,11848
L,11848,11849
L,11849,11850
L,11850,11851
L,11851,11852
L,11852,11853
L,11853,11854
L,11854,11855
REAL,23
TYPE,2
MAT,11
!LSEL,,,,13594,13606,1
LSEL,,,,19822,19834,1
LMESH,ALL
!-----------------------------
!NUMSTR,LINE,13607
NUMSTR,LINE,19835
L,11855,11893
L,11893,11892
L,11892,11891
L,11891,11890
L,11890,11889
L,11889,11888
L,11888,11887
L,11887,11886
```

```
L,11886,11885
L,11885,11884
L,11884,11883
L,11883,11882
L,11882,11881
REAL,23
TYPE,2
MAT,11
!LSEL,,,,13607,13619,1
LSEL,,,,19835,19847,1
LMESH,ALL
!---------------------------
!NUMSTR,LINE,13620
NUMSTR,LINE,19848
L,11881,11880
L,11880,11879
L,11879,11878
L,11878,11877
L,11877,11876
L,11876,11875
L,11875,11874
L,11874,11873
L,11873,11872
L,11872,11871
L,11871,11870
L,11870,11869
L,11869,11868
L,11868,11867
L,11867,11866
L,11866,11865
L,11865,11864
L,11864,11863
L,11863,11862
L,11862,11861
L,11861,11860
REAL,22
TYPE,2
MAT,11
!LSEL,,,,13620,13640,1
LSEL,,,,19848,19868,1
LMESH,ALL
!----------------------------
!NUMSTR,LINE,13641
NUMSTR,LINE,19869
L,11860,11859
L,11859,11858
L,11858,11857
L,11857,11856
L,11856,11816
REAL,21
TYPE,2
MAT,11
!LSEL,,,,13641,13645,1
LSEL,,,,19869,19873,1
LMESH,ALL
!----------------------------
!NUMSTR,LINE,13646
NUMSTR,LINE,19874
L,11943,11983
L,11983,11984
L,11984,11985
L,11985,11986
L,11986,11987
REAL,21
TYPE,2
MAT,11
!LSEL,,,,13646,13650,1
LSEL,,,,19874,19878,1
LMESH,ALL
!----------------------------
!NUMSTR,LINE,13651
NUMSTR,LINE,19879
L,11987,11988
L,11988,11989
L,11989,11990
```

```
L,11990,11991
L,11991,11992
L,11992,11993
L,11993,11994
L,11994,11995
L,11995,11996
L,11996,11997
L,11997,11998
L,11998,11999
L,11999,12000
L,12000,12001
L,12001,12002
L,12002,12003
L,12003,12004
L,12004,12005
L,12005,12006
L,12006,12007
L,12007,12008
REAL,22
TYPE,2
MAT,11
!LSEL,,,,13651,13671,1
LSEL,,,,19879,19899,1
LMESH,ALL
!------------------------------
!NUMSTR,LINE,13672
NUMSTR,LINE,19900
L,12008,12009
L,12009,12010
L,12010,12011
L,12011,12012
L,12012,12013
L,12013,12014
L,12014,12015
L,12015,12016
L,12016,12017
L,12017,12018
L,12018,12019
L,12019,12020
REAL,23
TYPE,2
MAT,11
!LSEL,,,,13672,13683,1
LSEL,,,,19900,19911,1
LMESH,ALL
!------------------------------
!NUMSTR,LINE,13684
NUMSTR,LINE,19912
L,12020,11982
L,11982,11981
L,11981,11980
L,11980,11979
L,11979,11978
L,11978,11977
L,11977,11976
L,11976,11975
L,11975,11974
L,11974,11973
L,11973,11972
L,11972,11971
L,11971,11970
L,11970,11969
REAL,23
TYPE,2
MAT,11
!LSEL,,,,13684,13697,1
LSEL,,,,19912,19925,1
LMESH,ALL
!----------------------------
!NUMSTR,LINE,13698
NUMSTR,LINE,19926
L,11969,11968
L,11968,11967
L,11967,11966
L,11966,11965
```

```
L,11965,11964
L,11964,11963
L,11963,11962
L,11962,11961
L,11961,11960
L,11960,11959
L,11959,11958
L,11958,11957
L,11957,11956
L,11956,11955
L,11955,11954
L,11954,11953
L,11953,11952
L,11952,11951
L,11951,11950
L,11950,11949
L,11949,11948
REAL,22
TYPE,2
MAT,11
!LSEL,,,,13698,13718,1
LSEL,,,,19926,19946,1
LMESH,ALL
!---------------------------
!NUMSTR,LINE,13719
NUMSTR,LINE,19947
L,11948,11947
L,11947,11946
L,11946,11945
L,11945,11944
L,11944,11942
REAL,21
TYPE,2
MAT,11
!LSEL,,,,13719,13723,1
LSEL,,,,19947,19951,1
LMESH,ALL
ALLSEL

!INPUT FILE FOR THE HANGER

/PREP7

!CREATING THE CORRESPONDING LINES & LINE MESHING

!HASSLE SIDE HANGER ELEMENTS

NUMSTR,LINE,20000
L,KP(-272.138,-123.006,0),KP(-272.138,-128.04,0.00),1
!----------------------------------------------------
L,KP(-272.138,-123.006,22),KP(-272.138,-128.04,22.0),1

L,KP(-256.125,-116.815,0),KP(-256.125,-127.819,0.00),1
!---------------------------------------------
L,KP(-256.125,-116.815,22),KP(-256.125,-127.819,22.0),1
TYPE,4
MAT,1
REAL,25
LSEL,S,,,20000,20003
LMESH,ALL
LSEL,ALL
ALLSEL

NUMSTR,LINE,20004
L,KP(-16.3,-9.1750,0),KP(-7.25,-124.366,0.00),1
!---------------------------------------------
L,KP(-16.3,-9.1750,22),KP(-7.2500,-124.366,22.0),1
TYPE,4
MAT,1
REAL,26
LSEL,S,,,20004,20005
LMESH,ALL
LSEL,ALL
ALLSEL
```

```
NUMSTR,LINE,20006
L,KP(-233.5,-107.8710,0),KP(-242.55,-127.636,0.00),1
L,KP(-233.5,-107.8710,0),KP(-224.45,-127.384,0.00),1
L,KP(-215.4,-100.5270,0),KP(-206.35,-127.132,0.00),1
L,KP(-197.3,-93.0192,0),KP(-188.25,-126.881,0.00),1
L,KP(-179.2,-85.3562,0),KP(-170.15,-126.629,0.00),1
L,KP(-161.1,-77.5420,0),KP(-152.05,-126.377,0.00),1
L,KP(-143.0,-69.5610,0),KP(-133.95,-126.126,0.00),1
L,KP(-124.9,-61.4210,0),KP(-115.85,-125.874,0.00),1
L,KP(-106.8,-53.1190,0),KP(-97.750,-125.623,0.00),1
L,KP(-88.7,-44.6550,0),KP(-79.650,-125.371,0.00),1
L,KP(-70.6,-36.0236,0),KP(-61.550,-125.120,0.00),1
L,KP(-52.5,-27.2420,0),KP(-43.450,-124.868,0.00),1
L,KP(-34.4,-18.2900,0),KP(-25.350,-124.617,0.00),1
L,KP(-215.4,-100.5270,0),KP(-224.45,-127.384,0.00),1
L,KP(-197.3,-93.0192,0),KP(-206.35,-127.132,0.00),1
L,KP(-179.2,-85.3562,0),KP(-188.25,-126.881,0.00),1
L,KP(-161.1,-77.5420,0),KP(-170.15,-126.629,0.00),1
L,KP(-143.0,-69.5610,0),KP(-152.05,-126.377,0.00),1
L,KP(-124.9,-61.4210,0),KP(-133.95,-126.126,0.00),1
L,KP(-106.8,-53.1190,0),KP(-115.85,-125.874,0.00),1
L,KP(-88.7,-44.6550,0),KP(-97.750,-125.623,0.00),1
L,KP(-70.6,-36.0236,0),KP(-79.650,-125.371,0.00),1
L,KP(-52.5,-27.2420,0),KP(-61.550,-125.120,0.00),1
L,KP(-34.4,-18.2900,0),KP(-43.450,-124.868,0.00),1
L,KP(-16.3,-9.1750,0),KP(-25.350,-124.617,0.00),1
!------------------------------------------------
L,KP(-233.5,-107.8710,22),KP(-242.55,-127.636,22.0),1
L,KP(-215.4,-100.5270,22),KP(-206.35,-127.132,22.0),1
L,KP(-197.3,-93.0192,22),KP(-188.25,-126.881,22.0),1
L,KP(-179.2,-85.3562,22),KP(-170.15,-126.629,22.0),1
L,KP(-161.1,-77.5420,22),KP(-152.05,-126.377,22.0),1
L,KP(-143.0,-69.5610,22),KP(-133.95,-126.126,22.0),1
L,KP(-124.9,-61.4210,22),KP(-115.85,-125.874,22.0),1
L,KP(-106.8,-53.1190,22),KP(-97.750,-125.623,22.0),1
L,KP(-88.7,-44.6550,22),KP(-79.650,-125.371,22.0),1
L,KP(-70.6,-36.0236,22),KP(-61.550,-125.120,22.0),1
L,KP(-52.5,-27.2420,22),KP(-43.450,-124.868,22.0),1
L,KP(-34.4,-18.2900,22),KP(-25.350,-124.617,22.0),1
L,KP(-233.5,-107.8710,22),KP(-224.45,-127.384,22.0),1
L,KP(-215.4,-100.5270,22),KP(-224.45,-127.384,22.0),1
L,KP(-197.3,-93.0192,22),KP(-206.35,-127.132,22.0),1
L,KP(-179.2,-85.3562,22),KP(-188.25,-126.881,22.0),1
L,KP(-161.1,-77.5420,22),KP(-170.15,-126.629,22.0),1
L,KP(-143.0,-69.5610,22),KP(-152.05,-126.377,22.0),1
L,KP(-124.9,-61.4210,22),KP(-133.95,-126.126,22.0),1
L,KP(-106.8,-53.1190,22),KP(-115.85,-125.874,22.0),1
L,KP(-88.7,-44.6550,22),KP(-97.750,-125.623,22.0),1
L,KP(-70.6,-36.0236,22),KP(-79.650,-125.371,22.0),1
L,KP(-52.5,-27.2420,22),KP(-61.550,-125.120,22.0),1
L,KP(-34.4,-18.2900,22),KP(-43.450,-124.868,22.0),1
L,KP(-16.3,-9.1750,22),KP(-25.35,-124.617,22.0),1
TYPE,4
MAT,1
REAL,10
LSEL,S,,,20006,20055
LMESH,ALL
LSEL,ALL
ALLSEL

!BARTON SIDE HANGER ELEMENTS

NUMSTR,LINE,20056
L,KP(1428.1,-6.8390,0),KP(1419.05,-124.359,0.00),1
!--------------------------------------------
L,KP(1428.1,-6.8390,22),KP(1419.05,-124.359,22.0),1
TYPE,4
MAT,10
REAL,26
LSEL,S,,,20056,20057
LMESH,ALL
LSEL,ALL
ALLSEL
```

```
NUMSTR,LINE,20058
L,KP(1933.38,-134.3276,0),KP(1933.375,-137.771,0.00),1
L,KP(1916.8,-132.0457,0),KP(1916.8,-137.161,0.00),1
L,KP(1898.7,-129.4064,0),KP(1898.7,-136.495,0.00),1
L,KP(1880.6,-126.6107,0),KP(1880.6,-135.829,0.00),1
!-------------------------------------------
L,KP(1933.38,-134.3276,22),KP(1933.375,-137.771,22.0),1
L,KP(1916.8,-132.0457,22),KP(1916.8,-137.161,22.0),1
L,KP(1898.7,-129.4064,22),KP(1898.7,-136.495,22.0),1
L,KP(1880.6,-126.6107,22),KP(1880.6,-135.829,22.0),1
TYPE,4
MAT,10
REAL,25
LSEL,S,,,20058,20065
LMESH,ALL
LSEL,ALL
ALLSEL

NUMSTR,LINE,20066
L,KP(1428.1,-6.8390,0),KP(1437.15,-124.625,0.00),1
L,KP(1446.2,-13.5100,0),KP(1455.25,-124.906,0.00),1
L,KP(1464.3,-20.0230,0),KP(1473.35,-125.202,0.00),1
L,KP(1482.4,-26.3770,0),KP(1491.45,-125.513,0.00),1
L,KP(1500.5,-32.5730,0),KP(1509.55,-125.839,0.00),1
L,KP(1518.6,-38.5961,0),KP(1527.65,-126.18,0.00),1
L,KP(1536.7,-44.4713,0),KP(1545.75,-126.536,0.00),1
L,KP(1554.8,-50.1849,0),KP(1563.85,-126.907,0.00),1
L,KP(1844.4,-120.5789,0),KP(1850.965,-134.799,0.00),1
L,KP(1826.3,-117.3273,0.00),KP(1818.717,-133.724,0.00),1
L,KP(1862.5,-123.6794,0),KP(1857.281,-135.015,0.00),1
L,KP(1862.5,-123.6794,0),KP(1867.89,-135.382,0.00),1
L,KP(1844.4,-120.5789,0),KP(1837.938,-134.363,0.00),1
L,KP(1808.2,-113.9254,0),KP(1799.219,-133.101,0.00),1
L,KP(1790.1,-110.3725,0.00),KP(1781.05,-132.529,0.00),1
L,KP(1772.0,-106.6671,0),KP(1762.95,-131.978,0.00),1
L,KP(1753.9,-102.8084,0),KP(1744.85,-131.442,0.00),1
L,KP(1735.8,-98.7961,0),KP(1726.75,-130.921,0.00),1
L,KP(1717.7,-94.6437,0),KP(1708.65,-130.415,0.00),1
L,KP(1699.6,-90.3232,0),KP(1690.55,-129.924,0.00),1
L,KP(1681.5,-85.8484,0),KP(1672.45,-129.448,0.00),1
L,KP(1663.4,-81.2194,0),KP(1654.35,-128.987,0.00),1
L,KP(1645.3,-76.4361,0),KP(1636.25,-128.541,0.00),1
L,KP(1627.2,-71.4979,0),KP(1618.15,-128.110,0.00),1
L,KP(1609.1,-66.4042,0),KP(1600.05,-127.694,0.00),1
L,KP(1591.0,-61.1551,0),KP(1581.95,-127.293,0.00),1
L,KP(1572.9,-55.7501,0),KP(1563.85,-126.907,0.00),1
L,KP(1554.8,-50.1849,0),KP(1545.75,-126.536,0.00),1
L,KP(1536.7,-44.4713,0),KP(1527.65,-126.180,0.00),1
L,KP(1518.6,-38.5961,0),KP(1509.55,-125.839,0.00),1
L,KP(1500.5,-32.5730,0),KP(1491.45,-125.513,0.00),1
L,KP(1482.4,-26.3770,0),KP(1473.35,-125.202,0.00),1
L,KP(1464.3,-20.0230,0),KP(1455.25,-124.906,0.00),1
L,KP(1446.2,-13.5100,0),KP(1437.15,-124.625,0.00),1
L,KP(1826.3,-117.3273,0),KP(1834.119,-134.232,0.00),1
L,KP(1808.2,-113.9254,0),KP(1817.25,-133.677,0.00),1
L,KP(1790.1,-110.3725,0),KP(1799.219,-133.101,0.00),1
L,KP(1772.0,-106.6671,0),KP(1781.05,-132.529,0.00),1
L,KP(1753.9,-102.8084,0),KP(1762.95,-131.978,0.00),1
L,KP(1735.8,-98.7961,0),KP(1744.85,-131.442,0.00),1
L,KP(1717.7,-94.6437,0),KP(1726.75,-130.921,0.00),1
L,KP(1699.6,-90.3232,0),KP(1708.65,-130.415,0.00),1
L,KP(1681.5,-85.8484,0),KP(1690.55,-129.924,0.00),1
L,KP(1663.4,-81.2194,0),KP(1672.45,-129.448,0.00),1
L,KP(1645.3,-76.4361,0),KP(1654.35,-128.987,0.00),1
L,KP(1627.2,-71.4979,0),KP(1636.25,-128.541,0.00),1
L,KP(1609.1,-66.4042,0),KP(1618.15,-128.110,0.00),1
L,KP(1591.0,-61.1551,0),KP(1600.05,-127.694,0.00),1
L,KP(1572.9,-55.7501,0),KP(1581.95,-127.293,0.00),1
!---------------------------------------------------
L,KP(1826.3,-117.3273,22),KP(1818.717,-133.724,22.0),1
L,KP(1790.1,-110.3725,22),KP(1781.05,-132.529,22.0),1
L,KP(1772.0,-106.6671,22),KP(1762.95,-131.978,22.0),1
L,KP(1753.9,-102.8084,22),KP(1744.85,-131.442,22.0),1
L,KP(1735.8,-98.7961,22),KP(1726.75,-130.921,22.0),1
L,KP(1717.7,-94.6437,22),KP(1708.65,-130.415,22.0),1
```

```
L,KP(1699.6,-90.3232,22),KP(1690.55,-129.924,22.0),1
L,KP(1681.5,-85.8484,22),KP(1672.45,-129.448,22.0),1
L,KP(1663.4,-81.2194,22),KP(1654.35,-128.987,22.0),1
L,KP(1645.3,-76.4361,22),KP(1636.25,-128.541,22.0),1
L,KP(1627.2,-71.4979,22),KP(1618.15,-128.110,22.0),1
L,KP(1609.1,-66.4042,22),KP(1600.05,-127.694,22.0),1
L,KP(1591.0,-61.1551,22),KP(1581.95,-127.293,22.0),1
L,KP(1572.9,-55.7501,22),KP(1563.85,-126.907,22.0),1
L,KP(1554.8,-50.1849,22),KP(1545.75,-126.536,22.0),1
L,KP(1536.7,-44.4713,22),KP(1527.65,-126.180,22.0),1
L,KP(1518.6,-38.5961,22),KP(1509.55,-125.839,22.0),1
L,KP(1500.5,-32.5730,22),KP(1491.45,-125.513,22.0),1
L,KP(1482.4,-26.3770,22),KP(1473.35,-125.202,22.0),1
L,KP(1464.3,-20.0230,22),KP(1455.25,-124.906,22.0),1
L,KP(1446.2,-13.5100,22),KP(1437.15,-124.625,22.0),1
L,KP(1826.3,-117.3273,22),KP(1834.119,-134.232,22.0),1
L,KP(1808.2,-113.9254,22),KP(1817.25,-133.677,22.0),1
L,KP(1790.1,-110.3725,22),KP(1799.219,-133.101,22.0),1
L,KP(1772.0,-106.6671,22),KP(1781.05,-132.529,22.0),1
L,KP(1753.9,-102.8084,22),KP(1762.95,-131.978,22.0),1
L,KP(1735.8,-98.7961,22),KP(1744.85,-131.442,22.0),1
L,KP(1717.7,-94.6437,22),KP(1726.75,-130.921,22.0),1
L,KP(1699.6,-90.3232,22),KP(1708.65,-130.415,22.0),1
L,KP(1681.5,-85.8484,22),KP(1690.55,-129.924,22.0),1
L,KP(1663.4,-81.2194,22),KP(1672.45,-129.448,22.0),1
L,KP(1645.3,-76.4361,22),KP(1654.35,-128.987,22.0),1
L,KP(1627.2,-71.4979,22),KP(1636.25,-128.541,22.0),1
L,KP(1609.1,-66.4042,22),KP(1618.15,-128.110,22.0),1
L,KP(1591.0,-61.1551,22),KP(1600.05,-127.694,22.0),1
L,KP(1572.9,-55.7501,22),KP(1581.95,-127.293,22.0),1
L,KP(1862.5,-123.6794,22),KP(1857.281,-135.015,22.0),1
L,KP(1862.5,-123.6794,22),KP(1867.89,-135.382,22.0),1
L,KP(1844.4,-120.5789,22),KP(1837.938,-134.363,22.0),1
L,KP(1844.4,-120.5789,22),KP(1850.965,-134.799,22.0),1
L,KP(1428.1,-6.8390,22),KP(1437.15,-124.625,22.0),1
L,KP(1446.2,-13.5100,22),KP(1455.25,-124.906,22.0),1
L,KP(1464.3,-20.0230,22),KP(1473.35,-125.202,22.0),1
L,KP(1482.4,-26.3770,22),KP(1491.45,-125.513,22.0),1
L,KP(1500.5,-32.5730,22),KP(1509.55,-125.839,22.0),1
L,KP(1518.6,-38.5961,22),KP(1527.65,-126.18,22.0),1
L,KP(1536.7,-44.4713,22),KP(1545.75,-126.536,22.0),1
L,KP(1554.8,-50.1849,22),KP(1563.85,-126.907,22.0),1
L,KP(1808.2,-113.9254,22),KP(1799.219,-133.101,22.0),1
TYPE,4
MAT,10
REAL,10
LSEL,S,,,20066,20163
LMESH,ALL
ALLSEL

!MAIN SPAN HANGER ELEMENTS

NUMSTR,LINE,20164

L,KP(18.099,-5.964,0),KP(9.05,-124.13,0.00),1
L,KP(18.099,-5.964,22),KP(9.05,-124.13,22.0),1

L,KP(1393.7,-5.964,22),KP(1402.7,-124.13,22.0),1
L,KP(1393.7,-5.964,0),KP(1402.7,-124.13,0.00),1

TYPE,4
MAT,9
REAL,26
LSEL,S,,,20164,20167
LMESH,ALL
LSEL,ALL
ALLSEL

NUMSTR,LINE,20168

L,KP(18.099,-5.964,0),KP(27.15,-123.89,0.00),1
L,KP(36.199,-11.715,0),KP(27.15,-123.89,0.00),1
L,KP(36.199,-11.715,0),KP(45.25,-123.46,0.00),1
L,KP(54.299,-17.308,0),KP(45.25,-123.46,0.00),1
L,KP(54.299,-17.308,0),KP(63.35,-123.41,0.00),1
```

```
L,KP(72.399,-22.743,0),KP(63.35,-123.41,0.00),1
L,KP(72.399,-22.743,0),KP(81.45,-123.19,0.00),1
L,KP(90.499,-28.021,0),KP(81.45,-123.19,0.00),1
L,KP(90.499,-28.021,0),KP(99.55,-122.97,0.00),1
L,KP(108.6,-33.141,0),KP(99.55,-122.97,0.00),1
L,KP(108.6,-33.141,0),KP(117.65,-122.76,0.00),1
L,KP(126.7,-38.105,0),KP(117.65,-122.76,0.00),1
L,KP(126.7,-38.105,0),KP(135.75,-122.55,0.00),1
L,KP(144.8,-42.913,0),KP(135.75,-122.55,0.00),1
L,KP(144.8,-42.913,0),KP(153.85,-122.35,0.00),1
L,KP(162.9,-47.564,0),KP(153.85,-122.35,0.00),1
L,KP(162.9,-47.564,0),KP(171.95,-122.15,0.00),1
L,KP(181.0,-52.059,0),KP(171.95,-122.15,0.00),1
L,KP(181.0,-52.059,0),KP(190.05,-121.97,0.00),1
L,KP(199.1,-56.4,0),KP(190.05,-121.97,0.00),1
L,KP(199.1,-56.4,0),KP(208.15,-121.79,0.00),1
L,KP(217.2,-60.585,0),KP(208.15,-121.79,0.00),1
L,KP(217.2,-60.585,0),KP(226.25,-121.61,0.00),1
L,KP(235.3,-64.615,0),KP(226.25,-121.61,0.00),1
L,KP(235.3,-64.615,0),KP(244.35,-121.44,0.00),1
L,KP(253.4,-68.491,0),KP(244.35,-121.44,0.00),1
L,KP(253.4,-68.491,0),KP(262.45,-121.28,0.00),1
L,KP(271.5,-72.213,0),KP(262.45,-121.28,0.00),1
L,KP(271.5,-72.213,0),KP(280.55,-121.13,0.00),1
L,KP(289.6,-75.78,0),KP(280.55,-121.13,0.00),1
L,KP(289.6,-75.78,0),KP(298.65,-120.99,0.00),1
L,KP(307.7,-79.194,0),KP(298.65,-120.99,0.00),1
L,KP(307.7,-79.194,0),KP(316.75,-120.84,0.00),1
L,KP(325.8,-82.455,0),KP(316.75,-120.84,0.00),1
L,KP(325.8,-82.455,0),KP(334.85,-120.70,0.00),1
L,KP(343.9,-85.562,0),KP(334.85,-120.70,0.00),1
L,KP(343.9,-85.562,0),KP(352.95,-120.57,0.00),1
L,KP(362.0,-88.517,0),KP(352.95,-120.57,0.00),1
L,KP(362.0,-88.517,0),KP(371.05,-120.45,0.00),1
L,KP(380.1,-91.318,0),KP(371.05,-120.45,0.00),1
L,KP(380.1,-91.318,0),KP(389.15,-120.33,0.00),1
L,KP(398.2,-93.967,0),KP(389.15,-120.33,0.00),1
L,KP(398.2,-93.967,0),KP(407.25,-120.22,0.00),1
L,KP(416.3,-96.464,0),KP(407.25,-120.22,0.00),1
L,KP(416.3,-96.464,0),KP(425.35,-120.12,0.00),1
L,KP(434.4,-98.808,0),KP(425.35,-120.12,0.00),1
L,KP(434.4,-98.808,0),KP(443.45,-120.02,0.00),1
L,KP(452.5,-101.0,0),KP(461.33,-119.93,0.00),1
L,KP(470.6,-103.04,0),KP(462.73,-119.93,0.00),1
L,KP(470.6,-103.04,0),KP(478.44,-119.85,0.00),1
L,KP(488.7,-104.93,0),KP(481.75,-119.84,0.00),1
L,KP(488.7,-104.93,0),KP(495.325,-119.78,0.00),1
L,KP(506.8,-106.67,0),KP(500.69,-119.76,0.00),1
L,KP(506.8,-106.67,0),KP(512.88,-119.71,0.00),1
L,KP(524.9,-108.25,0),KP(519.57,-119.69,0.00),1
L,KP(524.9,-108.25,0),KP(530.21,-119.65,0.00),1
L,KP(1375.6,-11.715,0),KP(1384.6,-123.89,0.00),1
L,KP(1393.7,-5.964,0),KP(1384.6,-123.89,0.00),1
L,KP(1375.6,-11.715,0),KP(1366.5,-123.46,0.00),1
L,KP(1357.5,-17.308,0),KP(1366.5,-123.46,0.00),1
L,KP(1357.5,-17.308,0),KP(1348.4,-123.41,0.00),1
L,KP(1339.4,-22.743,0),KP(1348.4,-123.41,0.00),1
L,KP(1339.4,-22.743,0),KP(1330.3,-123.19,0.00),1
L,KP(1321.3,-28.021,0),KP(1330.3,-123.19,0.00),1
L,KP(1321.3,-28.021,0),KP(1312.2,-122.97,0.00),1
L,KP(1303.2,-33.141,0),KP(1312.2,-122.97,0.00),1
L,KP(1303.2,-33.141,0),KP(1294.1,-122.76,0.00),1
L,KP(1285.1,-38.105,0),KP(1294.1,-122.76,0.00),1
L,KP(1285.1,-38.105,0),KP(1276.0,-122.55,0.00),1
L,KP(1267.0,-42.913,0),KP(1276.0,-122.55,0.00),1
L,KP(1267.0,-42.913,0),KP(1257.9,-122.35,0.00),1
L,KP(1248.9,-47.564,0),KP(1257.9,-122.35,0.00),1
L,KP(1248.9,-47.564,0),KP(1239.8,-122.15,0.00),1
L,KP(1230.8,-52.059,0),KP(1239.8,-122.15,0.00),1
L,KP(1230.8,-52.059,0),KP(1221.7,-121.97,0.00),1
L,KP(1212.7,-56.4,0),KP(1221.7,-121.97,0.00),1
L,KP(1212.7,-56.4,0),KP(1203.6,-121.79,0.00),1
L,KP(1194.6,-60.585,0),KP(1203.6,-121.79,0.00),1
L,KP(1194.6,-60.585,0),KP(1185.5,-121.61,0.00),1
L,KP(1176.5,-64.615,0),KP(1185.5,-121.61,0.00),1
```

```
L,KP(1176.5,-64.615,0),KP(1167.4,-121.44,0.00),1
L,KP(1158.4,-68.491,0),KP(1167.4,-121.44,0.00),1
L,KP(1158.4,-68.491,0),KP(1149.3,-121.28,0.00),1
L,KP(1140.3,-72.213,0),KP(1149.3,-121.28,0.00),1
L,KP(1140.3,-72.213,0),KP(1131.2,-121.13,0.00),1
L,KP(1122.2,-75.78,0),KP(1131.2,-121.13,0.00),1
L,KP(1122.2,-75.78,0),KP(1113.1,-120.99,0.00),1
L,KP(1104.1,-79.194,0),KP(1113.1,-120.99,0.00),1
L,KP(1104.1,-79.194,0),KP(1095.0,-120.84,0.00),1
L,KP(1086.0,-82.455,0),KP(1095.0,-120.84,0.00),1
L,KP(1086.0,-82.455,0),KP(1076.9,-120.70,0.00),1
L,KP(1067.9,-85.562,0),KP(1076.9,-120.70,0.00),1
L,KP(1067.9,-85.562,0),KP(1058.8,-120.57,0.00),1
L,KP(1049.8,-88.517,0),KP(1058.8,-120.57,0.00),1
L,KP(1049.8,-88.517,0),KP(1040.7,-120.45,0.00),1
L,KP(1031.7,-91.318,0),KP(1040.7,-120.45,0.00),1
L,KP(1031.7,-91.318,0),KP(1022.6,-120.33,0.00),1
L,KP(1013.6,-93.967,0),KP(1022.6,-120.33,0.00),1
L,KP(1013.6,-93.967,0),KP(1004.5,-120.22,0.00),1
L,KP(995.5,-96.464,0),KP(1004.5,-120.22,0.00),1
L,KP(995.5,-96.464,0),KP(986.40,-120.12,0.00),1
L,KP(977.4,-98.808,0),KP(986.40,-120.12,0.00),1
L,KP(959.3,-101.0,0),KP(968.30,-120.02,0.00),1
L,KP(959.3,-101.0,0),KP(950.47,-119.93,0.00),1
L,KP(941.2,-103.04,0),KP(949.07,-119.93,0.00),1
L,KP(941.2,-103.04,0),KP(933.36,-119.85,0.00),1
L,KP(923.1,-104.93,0),KP(930.05,-119.84,0.00),1
L,KP(923.1,-104.93,0),KP(915.625,-119.78,0.00),1
L,KP(905.0,-106.67,0),KP(911.10,-119.76,0.00),1
L,KP(905.0,-106.67,0),KP(898.91,-119.71,0.00),1
L,KP(886.9,-108.25,0),KP(892.23,-119.69,0.00),1
L,KP(886.9,-108.25,0),KP(881.58,-119.65,0.00),1
L,KP(868.8,-109.69,0),KP(873.43,-119.62,0.00),1
L,KP(868.8,-109.69,0),KP(863.76,-119.59,0.00),1
L,KP(850.7,-110.97,0),KP(854.71,-119.56,0.00),1
L,KP(850.7,-110.97,0),KP(846.70,-119.54,0.00),1
L,KP(832.6,-112.1,0),KP(836.05,-119.51,0.00),1
L,KP(832.6,-112.1,0),KP(829.15,-119.49,0.00),1
L,KP(814.5,-113.08,0),KP(817.48,-119.47,0.00),1
L,KP(814.5,-113.08,0),KP(811.53,-119.45,0.00),1
L,KP(796.4,-113.91,0),KP(798.97,-119.43,0.00),1
L,KP(796.4,-113.91,0),KP(793.83,-119.42,0.00),1
L,KP(778.3,-114.59,0),KP(780.28,-119.40,0.00),1
L,KP(778.3,-114.59,0),KP(775.755,-119.39,0.00),1
L,KP(18.099,-5.964,22),KP(27.150,-123.89,22.0),1
L,KP(36.199,-11.715,22),KP(27.150,-123.89,22.0),1
L,KP(36.199,-11.715,22),KP(45.250,-123.46,22.0),1
L,KP(54.299,-17.308,22),KP(45.250,-123.46,22.0),1
L,KP(54.299,-17.308,22),KP(63.350,-123.41,22.0),1
L,KP(72.399,-22.743,22),KP(63.350,-123.41,22.0),1
L,KP(72.399,-22.743,22),KP(81.450,-123.19,22.0),1
L,KP(90.499,-28.021,22),KP(81.450,-123.19,22.0),1
L,KP(90.499,-28.021,22),KP(99.550,-122.97,22.0),1
L,KP(108.6,-33.141,22),KP(99.550,-122.97,22.0),1
L,KP(108.6,-33.141,22),KP(117.65,-122.76,22.0),1
L,KP(126.7,-38.105,22),KP(117.65,-122.76,22.0),1
L,KP(126.7,-38.105,22),KP(135.75,-122.55,22.0),1
L,KP(144.8,-42.913,22),KP(135.75,-122.55,22.0),1
L,KP(144.8,-42.913,22),KP(153.85,-122.35,22.0),1
L,KP(162.9,-47.564,22),KP(153.85,-122.35,22.0),1
L,KP(162.9,-47.564,22),KP(171.95,-122.15,22.0),1
L,KP(181.0,-52.059,22),KP(171.95,-122.15,22.0),1
L,KP(181.0,-52.059,22),KP(190.05,-121.97,22.0),1
L,KP(199.1,-56.4,22),KP(190.05,-121.97,22.0),1
L,KP(199.1,-56.4,22),KP(208.15,-121.79,22.0),1
L,KP(217.2,-60.585,22),KP(208.15,-121.79,22.0),1
L,KP(217.2,-60.585,22),KP(226.25,-121.61,22.0),1
L,KP(235.3,-64.615,22),KP(226.25,-121.61,22.0),1
L,KP(235.3,-64.615,22),KP(244.35,-121.44,22.0),1
L,KP(253.4,-68.491,22),KP(244.35,-121.44,22.0),1
L,KP(253.4,-68.491,22),KP(262.45,-121.28,22.0),1
L,KP(271.5,-72.213,22),KP(262.45,-121.28,22.0),1
L,KP(271.5,-72.213,22),KP(280.55,-121.13,22.0),1
L,KP(289.6,-75.78,22),KP(280.55,-121.13,22.0),1
L,KP(289.6,-75.78,22),KP(298.65,-120.99,22.0),1
```

```
L,KP(307.7,-79.194,22),KP(298.65,-120.99,22.0),1
L,KP(307.7,-79.194,22),KP(316.75,-120.84,22.0),1
L,KP(325.8,-82.455,22),KP(316.75,-120.84,22.0),1
L,KP(325.8,-82.455,22),KP(334.85,-120.70,22.0),1
L,KP(343.9,-85.562,22),KP(334.85,-120.70,22.0),1
L,KP(343.9,-85.562,22),KP(352.95,-120.57,22.0),1
L,KP(362.0,-88.517,22),KP(352.95,-120.57,22.0),1
L,KP(362.0,-88.517,22),KP(371.05,-120.45,22.0),1
L,KP(380.1,-91.318,22),KP(371.05,-120.45,22.0),1
L,KP(380.1,-91.318,22),KP(389.15,-120.33,22.0),1
L,KP(398.2,-93.967,22),KP(389.15,-120.33,22.0),1
L,KP(398.2,-93.967,22),KP(407.25,-120.22,22.0),1
L,KP(416.3,-96.464,22),KP(407.25,-120.22,22.0),1
L,KP(416.3,-96.464,22),KP(425.35,-120.12,22.0),1
L,KP(434.4,-98.808,22),KP(425.35,-120.12,22.0),1
L,KP(434.4,-98.808,22),KP(443.45,-120.02,22.0),1
L,KP(452.5,-101.0,22),KP(461.33,-119.93,22.0),1
L,KP(470.6,-103.04,22),KP(462.73,-119.93,22.0),1
L,KP(470.6,-103.04,22),KP(478.44,-119.85,22.0),1
L,KP(488.7,-104.93,22),KP(481.75,-119.84,22.0),1
L,KP(488.7,-104.93,22),KP(495.325,-119.78,22.0),1
L,KP(506.8,-106.67,22),KP(500.69,-119.76,22.0),1
L,KP(506.8,-106.67,22),KP(512.88,-119.71,22.0),1
L,KP(524.9,-108.25,22),KP(519.57,-119.69,22.0),1
L,KP(524.9,-108.25,22),KP(530.21,-119.65,22.0),1
L,KP(1393.7,-5.964,22),KP(1384.6,-123.89,22.0),1
L,KP(1375.6,-11.715,22),KP(1384.6,-123.89,22.0),1
L,KP(1375.6,-11.715,22),KP(1366.5,-123.46,22.0),1
L,KP(1357.5,-17.308,22),KP(1366.5,-123.46,22.0),1
L,KP(1357.5,-17.308,22),KP(1348.4,-123.41,22.0),1
L,KP(1339.4,-22.743,22),KP(1348.4,-123.41,22.0),1
L,KP(1339.4,-22.743,22),KP(1330.3,-123.19,22.0),1
L,KP(1321.3,-28.021,22),KP(1330.3,-123.19,22.0),1
L,KP(1321.3,-28.021,22),KP(1312.2,-122.97,22.0),1
L,KP(1303.2,-33.141,22),KP(1312.2,-122.97,22.0),1
L,KP(1303.2,-33.141,22),KP(1294.1,-122.76,22.0),1
L,KP(1285.1,-38.105,22),KP(1294.1,-122.76,22.0),1
L,KP(1285.1,-38.105,22),KP(1276.0,-122.55,22.0),1
L,KP(1267.0,-42.913,22),KP(1276.0,-122.55,22.0),1
L,KP(1267.0,-42.913,22),KP(1257.9,-122.35,22.0),1
L,KP(1248.9,-47.564,22),KP(1257.9,-122.35,22.0),1
L,KP(1248.9,-47.564,22),KP(1239.8,-122.15,22.0),1
L,KP(1230.8,-52.059,22),KP(1239.8,-122.15,22.0),1
L,KP(1230.8,-52.059,22),KP(1221.7,-121.97,22.0),1
L,KP(1212.7,-56.4,22),KP(1221.7,-121.97,22.0),1
L,KP(1212.7,-56.4,22),KP(1203.6,-121.79,22.0),1
L,KP(1194.6,-60.585,22),KP(1203.6,-121.79,22.0),1
L,KP(1194.6,-60.585,22),KP(1185.5,-121.61,22.0),1
L,KP(1176.5,-64.615,22),KP(1185.5,-121.61,22.0),1
L,KP(1176.5,-64.615,22),KP(1167.4,-121.44,22.0),1
L,KP(1158.4,-68.491,22),KP(1167.4,-121.44,22.0),1
L,KP(1158.4,-68.491,22),KP(1149.3,-121.28,22.0),1
L,KP(1140.3,-72.213,22),KP(1149.3,-121.28,22.0),1
L,KP(1140.3,-72.213,22),KP(1131.2,-121.13,22.0),1
L,KP(1122.2,-75.78,22),KP(1131.2,-121.13,22.0),1
L,KP(1122.2,-75.78,22),KP(1113.1,-120.99,22.0),1
L,KP(1104.1,-79.194,22),KP(1113.1,-120.99,22.0),1
L,KP(1104.1,-79.194,22),KP(1095.0,-120.84,22.0),1
L,KP(1086.0,-82.455,22),KP(1095.0,-120.84,22.0),1
L,KP(1086.0,-82.455,22),KP(1076.9,-120.70,22.0),1
L,KP(1067.9,-85.562,22),KP(1076.9,-120.70,22.0),1
L,KP(1067.9,-85.562,22),KP(1058.8,-120.57,22.0),1
L,KP(1049.8,-88.517,22),KP(1058.8,-120.57,22.0),1
L,KP(1049.8,-88.517,22),KP(1040.7,-120.45,22.0),1
L,KP(1031.7,-91.318,22),KP(1040.7,-120.45,22.0),1
L,KP(1031.7,-91.318,22),KP(1022.6,-120.33,22.0),1
L,KP(1013.6,-93.967,22),KP(1022.6,-120.33,22.0),1
L,KP(1013.6,-93.967,22),KP(1004.5,-120.22,22.0),1
L,KP(995.5,-96.464,22),KP(1004.5,-120.22,22.0),1
L,KP(995.5,-96.464,22),KP(986.40,-120.12,22.0),1
L,KP(977.4,-98.808,22),KP(986.40,-120.12,22.0),1
L,KP(959.3,-101.0,22),KP(968.30,-120.02,22.0),1
L,KP(959.3,-101.0,22),KP(950.47,-119.93,22.0),1
L,KP(941.2,-103.04,22),KP(949.07,-119.93,22.0),1
L,KP(941.2,-103.04,22),KP(933.36,-119.85,22.0),1
```

```
L,KP(923.1,-104.93,22),KP(930.05,-119.84,22.0),1
L,KP(923.1,-104.93,22),KP(915.625,-119.78,22.0),1
L,KP(905.0,-106.67,22),KP(911.10,-119.76,22.0),1
L,KP(905.0,-106.67,22),KP(898.91,-119.71,22.0),1
L,KP(886.9,-108.25,22),KP(892.23,-119.69,22.0),1
L,KP(886.9,-108.25,22),KP(881.58,-119.65,22.0),1
L,KP(868.8,-109.69,22),KP(873.43,-119.62,22.0),1
L,KP(868.8,-109.69,22),KP(863.76,-119.59,22.0),1
L,KP(850.7,-110.97,22),KP(854.71,-119.56,22.0),1
L,KP(850.7,-110.97,22),KP(846.70,-119.54,22.0),1
L,KP(832.6,-112.1,22),KP(836.05,-119.51,22.0),1
L,KP(832.6,-112.1,22),KP(829.15,-119.49,22.0),1
L,KP(814.5,-113.08,22),KP(817.48,-119.47,22.0),1
L,KP(814.5,-113.08,22),KP(811.53,-119.45,22.0),1
L,KP(796.4,-113.91,22),KP(798.97,-119.43,22.0),1
L,KP(796.4,-113.91,22),KP(793.83,-119.42,22.0),1
L,KP(778.3,-114.59,22),KP(780.28,-119.40,22.0),1
L,KP(778.3,-114.59,22),KP(775.755,-119.39,22.0),1
L,KP(543.0,-109.69,0),KP(538.37,-119.62,0.00),1
L,KP(543.0,-109.69,22),KP(538.37,-119.62,22.0),1
L,KP(543.0,-109.69,0),KP(547.42,-119.59,0.00),1
L,KP(561.1,-110.97,0),KP(557.08,-119.56,0.00),1
L,KP(561.1,-110.97,0),KP(565.10,-119.54,0.00),1
L,KP(579.2,-112.1,0),KP(575.74,-119.51,0.00),1
L,KP(579.2,-112.1,0),KP(582.65,-119.49,0.00),1
L,KP(597.3,-113.08,0),KP(594.32,-119.47,0.00),1
L,KP(597.3,-113.08,0),KP(600.27,-119.45,0.00),1
L,KP(615.4,-113.91,0),KP(612.83,-119.43,0.00),1
L,KP(615.4,-113.91,0),KP(617.97,-119.42,0.00),1
L,KP(633.5,-114.59,0),KP(631.26,-119.40,0.00),1
L,KP(633.5,-114.59,0),KP(635.74,-119.39,0.00),1
L,KP(651.6,-115.12,0),KP(649.315,-119.37,0.00),1
L,KP(651.6,-115.12,0),KP(653.58,-119.37,0.00),1
L,KP(669.7,-115.49,0),KP(667.90,-119.36,0.00),1
L,KP(669.7,-115.49,0),KP(671.50,-119.35,0.00),1
L,KP(687.8,-115.72,0),KP(686.11,-119.35,0.00),1
L,KP(687.8,-115.72,0),KP(689.49,-119.35,0.00),1
L,KP(705.9,-115.8,0),KP(704.24,-119.34,0.00),1
L,KP(760.2,-115.12,0),KP(762.18,-119.37,0.00),1
L,KP(760.2,-115.12,0),KP(758.21,-119.37,0.00),1
L,KP(742.1,-115.49,0),KP(743.90,-119.36,0.00),1
L,KP(742.1,-115.49,0),KP(740.30,-119.35,0.00),1
L,KP(724.0,-115.72,0),KP(725.69,-119.35,0.00),1
L,KP(724.0,-115.72,0),KP(722.31,-119.35,0.00),1
L,KP(705.9,-115.8,0),KP(707.56,-119.34,0.00),1
L,KP(543.0,-109.69,22),KP(547.42,-119.59,22.0),1
L,KP(561.1,-110.97,22),KP(557.08,-119.56,22.0),1
L,KP(561.1,-110.97,22),KP(565.10,-119.54,22.0),1
L,KP(579.2,-112.1,22),KP(575.74,-119.51,22.0),1
L,KP(579.2,-112.1,22),KP(582.65,-119.49,22.0),1
L,KP(597.3,-113.08,22),KP(594.32,-119.47,22.0),1
L,KP(597.3,-113.08,22),KP(600.27,-119.45,22.0),1
L,KP(615.4,-113.91,22),KP(612.83,-119.43,22.0),1
L,KP(615.4,-113.91,22),KP(617.97,-119.42,22.0),1
L,KP(633.5,-114.59,22),KP(631.26,-119.40,22.0),1
L,KP(633.5,-114.59,22),KP(635.74,-119.39,22.0),1
L,KP(651.6,-115.12,22),KP(649.315,-119.37,22.0),1
L,KP(651.6,-115.12,22),KP(653.58,-119.37,22.0),1
L,KP(669.7,-115.49,22),KP(667.90,-119.36,22.0),1
L,KP(669.7,-115.49,22),KP(671.50,-119.35,22.0),1
L,KP(687.8,-115.72,22),KP(686.11,-119.35,22.0),1
L,KP(687.8,-115.72,22),KP(689.49,-119.35,22.0),1
L,KP(705.9,-115.8,22),KP(704.24,-119.34,22.0),1
L,KP(760.2,-115.12,22),KP(762.18,-119.37,22.0),1
L,KP(760.2,-115.12,22),KP(758.21,-119.37,22.0),1
L,KP(742.1,-115.49,22),KP(743.90,-119.36,22.0),1
L,KP(742.1,-115.49,22),KP(740.30,-119.35,22.0),1
L,KP(724.0,-115.72,22),KP(725.69,-119.35,22.0),1
L,KP(724.0,-115.72,22),KP(722.31,-119.35,22.0),1
L,KP(705.9,-115.8,22),KP(707.56,-119.34,22.0),1
L,KP(977.4,-98.808,0),KP(968.30,-120.02,0.00),1
L,KP(452.5,-101.0,0),KP(443.45,-120.02,0.00),1
L,KP(452.5,-101.0,22),KP(443.45,-120.02,22.0),1
L,KP(977.4,-98.808,22),KP(968.30,-120.02,22.0),1
```

```
TYPE,4
MAT,9
REAL,10
LSEL,S,,,20168,20471
LMESH,ALL
LSEL,ALL
ALLSEL
```

!INPUT FILE FOR THE FOOTPATH BEAM

```
/PREP7

!CREATING KEYPOINTS

NX=1
K,12090,-279.1,-126.73,5.1
K,12091,-279.1,-126.73,16.9
K,12092,0,-122.84,5.1
K,12093,0,-122.84,16.9
K,12094,1.8,-122.84,5.1
K,12095,1.8,-122.84,16.9
K,12096,1410,-122.84,5.1
K,12097,1410,-122.84,16.9
K,12098,1411.8,-122.84,5.1
K,12099,1411.8,-122.84,16.9
K,12100,1940.9,-136.65,5.1
K,12101,1940.9,-136.65,16.9

NUMSTR,LINE,20605
!CREATING THE CORRESPONDING LINES & LINE MESHING

L,4,12090,NX
L,12090,25,NX
L,26,12091,NX
L,12091,9,NX

L,11277,12092,NX
L,12092,11298,NX
L,11299,12093,NX
L,12093,11282,NX

L,11319,12094,NX
L,12094,11340,NX
L,11341,12095,NX
L,12095,11324,NX

L,11378,12096,NX
L,12096,11380,NX
L,11381,12097,NX
L,12097,11372,NX

L,11403,12098,NX
L,12098,11424,NX
L,11425,12099,NX
L,12099,11408,NX

L,1359,12101,NX
L,12101,1368,NX
L,1365,12100,NX
L,12100,1367,NX

MAT,14
TYPE,5
REAL,12
ESIZE,,1
LSEL,S,,,20605,20628,1
LMESH,ALL
ALLSEL

!INPUT FILE FOR THE TOWER & A-FRAME (VERTICAL & TRIANGULAR MEMBERS)

!FOR THE TOWER

/PREP7
```

```
!CREATING KEYPOINTS

K,11669,0.9,-152.576,0
K,11670,0.9,-128.726,0
K,11671,0.9,-88.176,0
K,11672,0.9,-48.376,0
K,11673,0.9,-8.576,0
K,11676,0.9,-152.576,22
K,11677,0.9,-128.726,22
K,11678,0.9,-88.176,22
K,11679,0.9,-48.376,22
K,11680,0.9,-8.576,22
K,11681,1410.9,-8.576,0
K,11682,1410.9,-48.376,0
K,11683,1410.9,-88.176,0
K,11684,1410.9,-128.726,0
K,11685,1410.9,-152.576,0
K,11686,1410.9,-8.576,22
K,11687,1410.9,-48.376,22
K,11688,1410.9,-88.176,22
K,11689,1410.9,-128.726,22
K,11690,1410.9,-152.576,22
K,11694,0.9,-128.726,11.0
K,11697,1410.9,-128.726,11.0

!CREATING THE CORRESPONDING LINES & LINE MESHING

!--------------------------
TYPE,1
MAT,2
REAL,5
ESIZE,,1
numstr,line,20514
L,11669,11670
L,11676,11677
L,11685,11684
L,11690,11689
LSEL,S,,,20514,20517,1
LMESH,ALL
!--------------------------------
TYPE,1
MAT,2
REAL,4
ESIZE,,1
L,11670,11671
L,11677,11678
L,11684,11683
L,11689,11688
LSEL,S,,,20518,20521,1
LMESH,ALL
!-------------------------
TYPE,1
MAT,2
REAL,3
ESIZE,,1
L,11671,11672
L,11678,11679
L,11683,11682
L,11688,11687
LSEL,S,,,20522,20525,1
LMESH,ALL
!-------------------------
TYPE,1
MAT,2
REAL,2
ESIZE,,1
L,11672,11673
L,11679,11680
L,11682,11681
L,11687,11686
LSEL,S,,,20526,20529,1
LMESH,ALL
!-------------------------
TYPE,1
```

```
MAT,2
REAL,1
ESIZE,,1
L,11673,KP(0.9,-0.296,0)
L,11680,KP(0.9,-0.296,22)
L,11681,KP(1410.9,-0.296,0)
L,11686,KP(1410.9,-0.296,22)
LSEL,S,,,20530,20533,1
LMESH,ALL
!----------------------
TYPE,1
MAT,2
REAL,8
ESIZE,,1
L,11670,11677
L,11684,11689
LSEL,S,,,20534,20535,1
LMESH,ALL
!--------------------------
TYPE,1
MAT,2
REAL,7
ESIZE,,1
L,11671,11678
L,11672,11679
L,11683,11688
L,11682,11687
LSEL,S,,,20536,20539,1
LMESH,ALL
!---------------------------
TYPE,1
MAT,2
REAL,6
ESIZE,,1
L,11673,11680
L,11681,11686
LSEL,S,,,20540,20541,1
LMESH,ALL
ALLSEL
```

!INPUT DATA FOR A-FRAME & SPLAY SADDLE

!CREATING KEYPOINTS

```
!K,10707,-272.14,-128.04,-5.5
!K,10708,-272.14,-128.04,-16.5
!K,10709,1933.4,-137.70,-5.5
!K,10710,1933.4,-137.70,-16.5
!---------------------------
K,11725,0,-126.03,3.45
K,11726,0,-126.03,6.75
K,11727,1.8,-126.91,3.45
K,11728,1.8,-126.91,6.75
K,11729,1410,-126.03,3.45
K,11730,1410,-126.03,6.75
K,11731,1411.8,-126.91,3.45
K,11732,1411.8,-126.91,6.75
K,11733,0,-126.03,15.25
K,11734,0,-126.03,18.55
K,11735,1.8,-126.91,15.25
K,11736,1.8,-126.91,18.55
K,11737,1410,-126.03,15.25
K,11738,1410,-126.03,18.55
K,11739,1411.8,-126.91,15.25
K,11740,1411.8,-126.91,18.55
!-------------------------
!K,10741,0,-124.25,-5.5
!K,11742,1.8,-124.25,-5.5
!K,11743,0,-124.25,-16.5
!K,11744,1.8,-124.25,-16.5
!K,11745,1410,-124.25,-5.5
!K,11746,1411.8,-124.25,-5.5
!K,11747,1410,-124.25,-16.5
!K,11748,1411.8,-124.25,-16.5
```

```
!-----------------------------
K,11749,-290.909,-134.996,-1.4
K,11750,-290.909,-134.996,1.4
K,11751,-290.909,-134.996,20.6
K,11752,-290.909,-134.996,23.4
K,11753,1953.205,-141.382,-1.4
K,11754,1953.205,-141.382,1.4
K,11755,1953.205,-141.382,20.6
K,11756,1953.205,-141.382,23.4
K,11757,-279.1,-130.3,3.7
K,11758,-279.1,-130.3,6.5
K,11759,-279.1,-130.3,15.5
K,11760,-279.1,-130.3,18.3
K,11761,1940.9,-140.22,3.7
K,11762,1940.9,-140.22,6.5
K,11763,1940.9,-140.22,15.5
K,11764,1940.9,-140.22,18.3

K,12070,-279.1,-127.03,5.1
K,12071,-279.1,-127.03,16.9
K,12072,1940.9,-136.95,5.1
K,12073,1940.9,-136.95,16.9
K,12074,0.0000,-123.14,5.1
K,12075,0.0000,-123.14,16.9
K,12076,1.8000,-123.14,5.1
K,12077,1.8000,-123.14,16.9
K,12078,1410.0,-123.14,5.1
K,12079,1410.0,-123.14,16.9
K,12080,1411.8,-123.14,5.1
K,12081,1411.8,-123.14,16.9

!-------------------------------

!CREATING THE CORRESPONDING LINES & LINE MESHING

NUMSTR,LINE,20542
ET,7,LINK8
TYPE,7
MAT,6
REAL,29
ESIZE,,1

L,11749,KP(-292.9,-130.896,0)
L,11750,KP(-292.9,-130.896,0)
L,11749,11750
L,11751,KP(-292.9,-130.896,22)
L,11752,KP(-292.9,-130.896,22)
L,11751,11752
L,11757,12070
L,11758,12070
L,11757,11758
L,11759,12071
L,11760,12071
L,11759,11760
!------------------------
L,11753,KP(1954.7,-137.076,0)
L,11754,KP(1954.7,-137.076,0)
L,11753,11754
L,11755,KP(1954.7,-137.076,22)
L,11756,KP(1954.7,-137.076,22)
L,11755,11756
L,11761,12072
L,11762,12072
L,11761,11762
L,11763,12073
L,11764,12073
L,11763,11764
!--------------------------
L,11725,12074
L,11726,12074
L,11725,11726
L,11727,12076
L,11728,12076
L,11727,11728
L,11733,12075
```

```
L,11734,12075
L,11733,11734
L,11735,12077
L,11736,12077
L,11735,11736
!--------------------------------
L,11729,12078
L,11730,12078
L,11729,11730
L,11731,12080
L,11732,12080
L,11731,11732
L,11737,12079
L,11738,12079
L,11737,11738
L,11739,12081
L,11740,12081
L,11739,11740

LSEL,S,,,20542,20589,1
LMESH,ALL
ALLSEL
!--------------------------------

NUMSTR,LINE,20590
TYPE,8
MAT,6
REAL,39
ESIZE,,1

L,12070,KP(-279.1,-126.73,5.1)
L,12071,KP(-279.1,-126.73,16.9)
L,12072,KP(1940.9,-136.65,5.1)
L,12073,KP(1940.9,-136.65,16.9)
L,12074,KP(0.00,-122.84,5.1)
L,12076,KP(1.8,-122.84,5.1)
L,12075,KP(0.00,-122.84,16.9)
L,12077,KP(1.8,-122.84,16.9)
L,12078,KP(1410.0,-122.84,5.1)
L,12080,KP(1411.8,-122.84,5.1)
L,12079,KP(1410.0,-122.84,16.9)
L,12081,KP(1411.8,-122.84,16.9)

LSEL,S,,,20590,20601,1
LMESH,ALL
ALLSEL

NUMMRG,NODE,.1
```

!COUPLING OF A-FRAME BASE WITH TOWER CROSS-BEAM

```
CP,1,UX,18061,18108,18111,18110,18113
CP,NEXT,UY,18061,18108,18111,18110,18113
CP,NEXT,UZ,18061,18108,18111,18110,18113
CP,NEXT,ROTX,18061,18108,18111,18110,18113
CP,NEXT,ROTY,18061,18108,18111,18110,18113
CP,NEXT,ROTZ,18061,18108,18111,18110,18113

CP,NEXT,UX,18063,18114,18117,18116,18119
CP,NEXT,UY,18063,18114,18117,18116,18119
CP,NEXT,UZ,18063,18114,18117,18116,18119
CP,NEXT,ROTX,18063,18114,18117,18116,18119
CP,NEXT,ROTY,18063,18114,18117,18116,18119
CP,NEXT,ROTZ,18063,18114,18117,18116,18119

CP,NEXT,UX,18057,18096,18099,18098,18101
CP,NEXT,UY,18057,18096,18099,18098,18101
CP,NEXT,UZ,18057,18096,18099,18098,18101
CP,NEXT,ROTX,18057,18096,18099,18098,18101
CP,NEXT,ROTY,18057,18096,18099,18098,18101
CP,NEXT,ROTZ,18057,18096,18099,18098,18101

CP,NEXT,UX,18059,18102,18105,18104,18107
CP,NEXT,UY,18059,18102,18105,18104,18107
```

```
CP,NEXT,UZ,18059,18102,18105,18104,18107
CP,NEXT,ROTX,18059,18102,18105,18104,18107
CP,NEXT,ROTY,18059,18102,18105,18104,18107
CP,NEXT,ROTZ,18059,18102,18105,18104,18107

EPLOT

!INPUT FILE FOR THE DECK DIAPHRAGM (STIFFENER) AT HESSLE AND BARTON TOWER

/PREP7

!CREATING KEYPOINTS

!BARTON TOWER BARTON SIDE
k,12200,1411.8,-127.21,14.6
k,12201,1411.8,-125.72,18.3
k,12202,1411.8,-124.24,22.0
k,12203,1411.8,-122.90,20.1
k,12204,1411.8,-122.83,16.5
k,12205,1411.8,-122.72,11.0
k,12206,1411.8,-122.83,5.50
k,12207,1411.8,-122.90,1.90
k,12208,1411.8,-124.24,0.00
k,12209,1411.8,-125.72,3.70
k,12210,1411.8,-127.21,7.40
k,12211,1411.8,-127.21,11.0

!BARTON TOWER MAIN SIDE
k,12212,1410.0,-127.21,7.40
k,12213,1410.0,-125.73,3.70
k,12214,1410.0,-124.24,0.00
k,12215,1410.0,-122.90,1.90
k,12216,1410.0,-122.83,5.50
k,12217,1410.0,-122.72,11.0
k,12218,1410.0,-122.83,16.5
k,12219,1410.0,-122.90,20.1
k,12220,1410.0,-124.24,22.0
k,12221,1410.0,-125.73,18.3
k,12222,1410.0,-127.21,14.6
k,12223,1410.0,-127.21,11.0

!HESSLE TOWER HESSLE SIDE
k,12224,0.00,-127.20,7.40
k,12225,0.00,-125.71,3.70
k,12226,0.00,-124.23,0.00
k,12227,0.00,-122.89,1.90
k,12228,0.00,-122.82,5.50
k,12229,0.00,-122.71,11.0
k,12230,0.00,-122.82,16.5
k,12231,0.00,-122.89,20.1
k,12232,0.00,-124.23,22.0
k,12233,0.00,-125.71,18.3
k,12234,0.00,-127.20,14.6
k,12235,0.00,-127.20,11.0

!HESSLE TOWER MAIN SIDE

k,12236,1.80,-127.21,14.6
k,12237,1.80,-125.72,18.3
k,12238,1.80,-124.24,22.0
k,12239,1.80,-122.90,20.1
k,12240,1.80,-122.83,16.5
k,12241,1.80,-122.72,11.0
k,12242,1.80,-122.83,5.50
k,12243,1.80,-122.90,1.90
k,12244,1.80,-124.24,0.00
k,12245,1.80,-125.72,3.70
k,12246,1.80,-127.21,7.40
k,12247,1.80,-127.21,11.0

!CREATING THE CORRESPONDING AREAS & AREA MESHING

NUMSTR,AREA,3950
A,12200,12201,12202,12203,12204,12205,12206,12207,12208,12209,12210,12211
TYPE,6
```

```
MAT,8
REAL,34
ESIZE,2.5
ASEL,,,,3950
AMESH,ALL
ALLSEL

A,12224,12224,12226,12227,12228,12229,12230,12231,12232,12233,12234,12235
TYPE,6
MAT,4
REAL,34
ESIZE,2.5
ASEL,,,,3951
AMESH,ALL
ALLSEL

A,12236,12237,12238,12239,12240,12241,12242,12243,12244,12245,12246,12247
A,12212,12213,12214,12215,12216,12217,12218,12219,12220,12221,12222,12223
TYPE,6
MAT,7
REAL,34
ESIZE,2.5
ASEL,,,,3952,3953,1
AMESH,ALL
ALLSEL
```

Appendix 4

Wind load file for the detail model

```
/SOLU
ANTYPE,STATIC
SSTIF,ON
NLGEOM,ON
NEQIT,25
BFUNIF,TEMP,20
TREF,20

DK, 11907,ALL, 0.00
DK, 12034,ALL, 0.00

DK, 11749,ALL, 0.00
DK, 11750,ALL, 0.00
DK, 11751,ALL, 0.00
DK, 11752,ALL, 0.00
DK, 11757,ALL, 0.00
DK, 11758,ALL, 0.00
DK, 11759,ALL, 0.00
DK, 11760,ALL, 0.00

DK, 12064,ALL, 0.00
DK, 11937,ALL, 0.00

DK, 11755,ALL, 0.00
DK, 11756,ALL, 0.00
DK, 11753,ALL, 0.00
DK, 11754,ALL, 0.00
DK, 11761,ALL, 0.00
DK, 11762,ALL, 0.00
DK, 11763,ALL, 0.00
DK, 11764,ALL, 0.00
DK, 11690,ALL, 0.00
DK, 11685,ALL, 0.00
DK, 11676,ALL, 0.00
DK, 11669,ALL, 0.00

DK, 11908,UZ, 0.00
DK, 12035,UZ, 0.00
DK, 11938,UZ, 0.00
DK, 12065,UZ, 0.00

DK, 12101,UZ, 0.00
DK, 12073,UZ, 0.00
DK, 12100,UZ, 0.00
DK, 12072,UZ, 0.00
DK, 12091,UZ, 0.00
DK, 12071,UZ, 0.00
DK, 12090,UZ, 0.00
DK, 12070,UZ, 0.00

DK, 12101,ROTX, 0.00
DK, 12073,ROTX, 0.00
DK, 12100,ROTX, 0.00
DK, 12072,ROTX, 0.00
DK, 12091,ROTX, 0.00
DK, 12071,ROTX, 0.00
DK, 12090,ROTX, 0.00
DK, 12070,ROTX, 0.00

DK, 12101,ROTY, 0.00
DK, 12073,ROTY, 0.00
DK, 12100,ROTY, 0.00
DK, 12072,ROTY, 0.00
DK, 12091,ROTY, 0.00
```

```
DK, 12071,ROTY , 0.00
DK, 12090,ROTY , 0.00
DK, 12070,ROTY , 0.00

DK, 12093,UZ , 0.00
DK, 12075,UZ , 0.00
DK, 12095,UZ , 0.00
DK, 12077,UZ , 0.00
DK, 12092,UZ , 0.00
DK, 12074,UZ , 0.00
DK, 12094,UZ , 0.00
DK, 12076,UZ , 0.00
DK, 12097,UZ , 0.00
DK, 12079,UZ , 0.00
DK, 12099,UZ , 0.00
DK, 12081,UZ , 0.00
DK, 12096,UZ , 0.00
DK, 12078,UZ , 0.00
DK, 12098,UZ , 0.00
DK, 12080,UZ , 0.00

DK, 12090,ROTX,0.00
DK, 12091,ROTX,0.00
DK, 12092,ROTX,0.00
DK, 12093,ROTX,0.00
DK, 12094,ROTX,0.00
DK, 12095,ROTX,0.00
DK, 12096,ROTX,0.00
DK, 12097,ROTX,0.00
DK, 12098,ROTX,0.00
DK, 12099,ROTX,0.00
DK, 12100,ROTX,0.00
DK, 12101,ROTX,0.00

DK, 12074,ROTX,0.00
DK, 12076,ROTX,0.00
DK, 12075,ROTX,0.00
DK, 12077,ROTX,0.00
DK, 12078,ROTX,0.00
DK, 12080,ROTX,0.00
DK, 12079,ROTX,0.00
DK, 12081,ROTX,0.00
DK, 12070,ROTX,0.00
DK, 12071,ROTX,0.00
DK, 12072,ROTX,0.00
DK, 12073,ROTX,0.00

DK, 12090,ROTY,0.00
DK, 12091,ROTY,0.00
DK, 12092,ROTY,0.00
DK, 12093,ROTY,0.00
DK, 12094,ROTY,0.00
DK, 12095,ROTY,0.00
DK, 12096,ROTY,0.00
DK, 12097,ROTY,0.00
DK, 12098,ROTY,0.00
DK, 12099,ROTY,0.00
DK, 12100,ROTY,0.00
DK, 12101,ROTY,0.00

DK, 12074,ROTY,0.00
DK, 12076,ROTY,0.00
DK, 12075,ROTY,0.00
DK, 12077,ROTY,0.00
DK, 12078,ROTY,0.00
DK, 12080,ROTY,0.00
DK, 12079,ROTY,0.00
DK, 12081,ROTY,0.00
DK, 12070,ROTY,0.00
DK, 12071,ROTY,0.00
DK, 12072,ROTY,0.00
DK, 12073,ROTY,0.00

DTRAN
```

```
ACEL,,9.81

!------------------------------------------
!WIND FORCES ON THE DECK

!DUE TO WIND LIFTING FORCE
ESEL,S,REAL,,33
ESEL,A,REAL,,32
ESEL,A,REAL,,37
NSLE,S
SFE,ALL,2,PRES,,388.36
ALLSEL
!-------------------------------------
!DUE TO WIND DRAG FORCE ON THE TOP PLATE
NSEL,S,LOC,Z,-0.1,2
NSEL,R,LOC,X,-279.2,1941
ESLN,,1
ESEL,R,REAL,,37
SFE,ALL,2,PRES,,741.9
ALLSEL

!DUE TO WIND DRAG FORCE ON THE SIDE PLATE
NSEL,S,LOC,Z,-0.1,7.5
NSEL,R,LOC,X,-279.2,1941
ESLN,,1
ESEL,R,REAL,,31
SFE,ALL,2,PRES,,-741.9
ALLSEL

SFEDELE,12555,ALL,ALL
SFEDELE,12556,ALL,ALL
SFEDELE,12557,ALL,ALL
SFEDELE,12558,ALL,ALL

SFE,12555,1,PRES,,-741.9
SFE,12556,1,PRES,,-741.9
SFE,12557,1,PRES,,-741.9
SFE,12558,1,PRES,,-741.9
ALLSEL

!-------------------------------------
!WIND FORCE ON THE MAIN CABLE
NSEL,S,LOC,Z,-0.1,0.1
ESLN,,1
ESEL,U,TYPE,,1
ESEL,U,TYPE,,4
NSLE,S
F,ALL,FZ,28766.1
ALLSEL

NSEL,S,LOC,Z,21.9,22.1
ESLN,,1
ESEL,U,TYPE,,1
ESEL,U,TYPE,,4
NSLE,S
F,ALL,FZ,28766.1
ALLSEL
!----------------------------------------
!WIND FORCE ON THE TOWER
NSEL,S,LOC,Z,0
ESLN,,1
ESEL,U,TYPE,,2
ESEL,U,TYPE,,4
NSLE,S
SFBEAM,ALL,1,PRES,-22255.3
ALLSEL

SOLVE
```

Appendix 5

Publications from this research

1) Brown CJ, Karuna R, Ashkenazi V, Robert GW, Evans RA (1999) February, Monitoring of structures using the Global Positioning System, *Proceeding of the Institute of Civil Engineers UK, Structures and Buildings*, Vol 134.

2) Karuna R, Yao MS, Brown CJ, Evans RA (1998) August, Modelling and Analysis of the Humber Bridge, *Journal of the International Association for Shell and Spatial Structures*, Vol 39.

3) Karuna R, Yao MS, Brown CJ, Evans RA (1998) September, In-Service Modelling of the Humber Bridge, Long-Span and High-Rise Structures, *IABSE Symposium*, Kobe, Japan.

4) Karuna R, Yao MS, Brown CJ, Evans RA (1998) July, Modelling the Behaviour of the Humber Bridge, *Mechanics in design' 98*, The Nottingham Trent University, Nottingham, UK.

5) Karuna R, Yao MS, Brown CJ, Evans RA (1997) August, Behaviour of the Humber Bridge, *7th International Conference on Computing in Civil and Building Engineering*, Korea.

6) Roberts GW, Dodson AH, Ashkenazi, V, Brown CJ, Karuna R, Evans RA (1999) October, The use of Kinematics GPS and Finite Element Modeling for the Deformation Measurements of the Humber Bridge, *3rd European Symposium on Global Navigation Satellite Systems GNSS'99*, Genoa, Italy.

7) Roberts GW, Dodson AH, Ashkenazi, V, Brown CJ, Karuna R, Evans RA (1999) September, Comparison of GPS Measurements and Finite Element Modelling for Deformation Measurements of the Humber Bridge, *Proceeding of the ION-GPS-99*,

The 12th International Technical Meeting of the Satellite Division of the Institute of Navigation, Nashville, USA.

8) Roberts GW, Dodson AH, Ashkenazi, V, Brown CJ, Karuna R, Evans RA (2000), Monitoring the Height Deflections of the Humber Bridge by GPS, GLONASS and Finite Element Modelling, *IAG Symposia Geodesy Beyond 2000*, Springer-Verlag, Vol 121, Schwarz (ed), ISBN 3-540-67002-5, Berlin.

9) Karuna R, Yao MS, Brown CJ, Evans RA (1997) October, Case Study on Humber Bridge F.E. Modelling, *ANSYS UK User Conference*, ANSYS Europe, Reading, UK.